BENEFICIAL MICROBES AND THE INTERCONNECTION BETWEEN CROP MINERAL NUTRITION AND INDUCED SYSTEMIC RESISTANCE

EDITED BY: Carlos Lucena, Sabine Dagmar Zimmermann, Ricardo Aroca and Jianfei Wang

PUBLISHED IN: Frontiers in Plant Science

frontiers Research Topics

ISSN 1664-8714
ISBN 978-2-88974-086-4
DOI 10.3389/978-2-88974-086-4

About Frontiers

Frontiers is more than just an open-access publisher of scholarly articles: it is a pioneering approach to the world of academia, radically improving the way scholarly research is managed. The grand vision of Frontiers is a world where all people have an equal opportunity to seek, share and generate knowledge. Frontiers provides immediate and permanent online open access to all its publications, but this alone is not enough to realize our grand goals.

Frontiers Journal Series

The Frontiers Journal Series is a multi-tier and interdisciplinary set of open-access, online journals, promising a paradigm shift from the current review, selection and dissemination processes in academic publishing. All Frontiers journals are driven by researchers for researchers; therefore, they constitute a service to the scholarly community. At the same time, the Frontiers Journal Series operates on a revolutionary invention, the tiered publishing system, initially addressing specific communities of scholars, and gradually climbing up to broader public understanding, thus serving the interests of the lay society, too.

Dedication to Quality

Each Frontiers article is a landmark of the highest quality, thanks to genuinely collaborative interactions between authors and review editors, who include some of the world's best academicians. Research must be certified by peers before entering a stream of knowledge that may eventually reach the public - and shape society; therefore, Frontiers only applies the most rigorous and unbiased reviews.
Frontiers revolutionizes research publishing by freely delivering the most outstanding research, evaluated with no bias from both the academic and social point of view. By applying the most advanced information technologies, Frontiers is catapulting scholarly publishing into a new generation.

What are Frontiers Research Topics?

Frontiers Research Topics are very popular trademarks of the Frontiers Journals Series: they are collections of at least ten articles, all centered on a particular subject. With their unique mix of varied contributions from Original Research to Review Articles, Frontiers Research Topics unify the most influential researchers, the latest key findings and historical advances in a hot research area! Find out more on how to host your own Frontiers Research Topic or contribute to one as an author by contacting the Frontiers Editorial Office: frontiersin.org/about/contact

BENEFICIAL MICROBES AND THE INTERCONNECTION BETWEEN CROP MINERAL NUTRITION AND INDUCED SYSTEMIC RESISTANCE

Topic Editors:
Carlos Lucena, University of Cordoba, Spain
Sabine Dagmar Zimmermann, Délégation Languedoc Roussillon (CNRS), France
Ricardo Aroca, Experimental Station of Zaidín, Spanish National Research Council (CSIC), Spain
Jianfei Wang, Anhui University of Science and Technology, China

Citation: Lucena, C., Zimmermann, S. D., Aroca, R., Wang, J., eds. (2022). Beneficial Microbes and The Interconnection Between Crop Mineral Nutrition and Induced Systemic Resistance. Lausanne: Frontiers Media SA. doi: 10.3389/978-2-88974-086-4

Table of Contents

frontiers in Plant Science

EDITORIAL
published: 29 November 2021
doi: 10.3389/fpls.2021.790616

Editorial: Beneficial Microbes and the Interconnection Between Crop Mineral Nutrition and Induced Systemic Resistance

Carlos Lucena[1], Sabine Dagmar Zimmermann[2]*, Jianfei Wang[3]* and Ricardo Aroca[4]**

[1] Departamento de Agronomía (DAUCO-María de Maeztu Unit of Excellence), Universidad de Córdoba, Córdoba, Spain, [2] BPMP, CNRS, INRAE, Institut Agro, Université de Montpellier, Montpellier, France, [3] Anhui University of Science and Technology, Huainan, China, [4] Departamento de Microbiología del Suelo y Sistemas Simbióticos, Estación Experimental del Zaidín (CSIC), Granada, Spain

Keywords: nutrient deficiency, ISR eliciting microbes, crops, soil, microbial consortia

Editorial on the Research Topic

Beneficial Microbes and the Interconnection Between Crop Mineral Nutrition and Induced Systemic Resistance

To cope with nutrient deficiencies, plants develop morphological and physiological responses, mainly in their roots, aimed to facilitate nutrient acquisition (Lucena et al., 2018). In the last years, it has been found that some rhizosphere microbes can induce physiological and morphological responses in roots of dicot plants similar to the ones induced by plants under nutrient deficiencies (Verbon et al., 2017). Remarkably, these rhizosphere microbes are also capable of eliciting the induced systemic resistance (ISR) against pathogens and insects (Pieterse et al., 2014; Verbon et al., 2017). This observation suggests that both processes (ISR and nutrient deficiency responses) are closely interconnected thus opening new possibilities for optimizing the management of the rhizosphere microbiota for improving mineral nutrition and health (Zamioudis et al., 2015; Verbon et al., 2017, 2019). However, the nodes of convergence between the two processes remain unclear (Romera et al., 2019). Elucidating the main nodes of interconnection between the pathways regulating microbe-elicited ISR and mineral uptake is critical for optimizing the use of plant mutualistic microbes in agriculture. The Research Topic updates latest findings related to the roles of ISR eliciting microbes in crops. It includes 12 original articles and one review, eight articles are related to beneficial microbes as biocontrol effectors inducing disease resistance and growth promotion of their hosts (Cueva-Yesquén et al.; La Spada et al.; Qu et al.; Qin et al.; Tseng et al.; Yu et al.; Zhou et al.; Zhu et al.), two articles concern growth promotion under abiotic stress (Tseng et al.; Yuan et al.), two others are linked to reduced chemical fertilization or soil property changes (Cardoso et al.; Wang et al.), and one to the role of N_2 fixing bacteria (Kordi et al.). The review is related to the special role of mycorrhizal fungi on orchid seed germination (Zhao et al.).

Regarding the role of diverse microorganisms as biocontrol effectors, a variability of physiological and molecular mechanisms has been observed. The tight link between beneficial effects of microorganisms on plant growth by improved nutrition and defense priming through systematic enhancement of resistance against below-ground and above pathogens or insect herbivores has been described for arbuscular mycorrhizal (AM) fungi as mycorrhiza-induced resistance (MIR) (Cameron et al., 2013). Such interactions might be dependent on abiotic factors and mediated by jasmonic acid (JA) signaling. This interconnection between *Plantago lanceolate* with the AM fungus *Funneliformis mosseae* and the herbivore *Mamestra brassica* was studied by

OPEN ACCESS

Edited and reviewed by:
Jonathan Michael Plett, Western Sydney University, Australia

****Correspondence:***
Carlos Lucena
b42lulec@uco.es
Sabine Dagmar Zimmermann
sabine.zimmermann@cnrs.fr
Jianfei Wang
jfwang1@aliyun.com
Ricardo Aroca
raroca@eez.csic.es

Specialty section:
This article was submitted to Plant Symbiotic Interactions, a section of the journal Frontiers in Plant Science

Received: *07 October 2021*
Accepted: *05 November 2021*
Published: *29 November 2021*

Citation:
Lucena C, Zimmermann SD, Wang J and Aroca R (2021) Editorial: Beneficial Microbes and the Interconnection Between Crop Mineral Nutrition and Induced Systemic Resistance. Front. Plant Sci. 12:790616. doi: 10.3389/fpls.2021.790616

Qu et al.. Surprisingly, in contrast to tomato (Rivero et al., 2021), they reported in their specific case a repression of JA-mediated defense by AM fungi, underlining the complexity of the studied model under their selected conditions (symbiotic and pathogen partners, age of plants, light, soil P, JA treatments). Mycoparasitic *Trichoderma* fungi have been used as biocontrol agents (Guzmán-Guzmán et al., 2019). La Spada et al. demonstrated that two selected *Trichoderma* strains (*T. asperellum* and *T. atroviride*) promoted tomato growth and reduced the disease severity caused by the oomycete *Phytophthora nicotianae*. Genetic patterns of the components of the experimental model tomato–*Trichoderma* spp.–*P. nicotianae* were differentially modified. Both counteract the challenge of infections by modulating the expression of crinkler, necrosis-inducing *Phytophthora* protein 1, and cellulose-binding elicitor lectin pathogenic effectors involved in plant defense mechanisms. Tseng et al. isolated a new endophytic fungus (a *Trichoderma* strain) from the leaves of a deciduous wood tree *Leucas aspera*. When applied to *Arabidopsis thaliana* and *Nicotiana attenuata*, this fungus colonized their roots thereby strongly promoting the initial plant growth in soil. The fungus showed predatory capability on the pathogenic fungus *Alternaria brassicicola*. Colonized *A. thaliana* plants displayed lower *A. brassicicola* spread in roots and shoots, while AM formation in *N. attenuata* was not affected by the *Trichoderma* strain.

Plant growth promoting bacteria (PGPB) living as endophytes display several beneficial traits as improving nutrient bioavailability, interfering with hormone levels, or protection against abiotic and biotic stress (de Souza et al., 2015; Kumar et al., 2020) thus leading also to better plant growth, development, and resistance. Cueva-Yesquén et al. isolated and analyzed such culturable bacterial endophytes from passionflower (*Passiflora incarnata*) by phenotypic and genotypic approaches and confirmed finally the probiotic effect of some of them by evaluating their capacity to boost germination and growth of another plant, namely of the Cape gooseberry (*Physalis peruviana*). In another study, in the context of rhizobacteria-mediated defense, Zhu et al. reported that the PGPB *Pseudomonas fluorescens* could increase the resistance of cucumber plants against infection by *Botrytis cinerea*. *Pseudomonas* bacteria have been used before as biocontrol effectors in different plant species (Kupferschmied et al., 2013; De Vrieze et al., 2020) and different mechanisms were proposed. Here, the authors found by RNA-sequencing that the improved defense would be linked to the expression of polyamine-associated and defense-related genes. Zhou et al. demonstrated the ability of the rhizobacterial strain *Bacillus subtilis* SL18r to trigger ISR in tomato plants against the foliar pathogen *Botrytis cinerea*. The authors reported that the long non-coding RNAs (lncRNAs) were involved in the mediation of the rhizobacteria-primed ISR processes in plants by a comparative transcriptome analysis between non-inoculated and SL18r-inoculated plants. Postharvest strawberry is susceptible to gray mold disease caused by *B. cinerea*. Yu et al. found that inoculation with *Bacillus cereus* diminished disease severity by modulating salicylic acid (SA) pathway as revealed by transcriptomic analysis, and enhancing antioxidant activity of strawberry fruits. Finally, the cotton seedling response to *Bacillus circulans* GN03 was explored by Qin et al. showing a remarkably enhanced growth promotion as well as disease resistance. GN03 inoculation altered the microbiota in and around the plant roots. At the physiological and molecular level, the authors observed a significant accumulation of growth-related (indole acetic acid (IAA), gibberellic acid (GA), and brassinosteroids) and disease resistance-related hormones (SA, JA), an up-regulated expression of phytohormone synthesis-related genes (EDS1, AOC1, BES1, GA20ox), of an auxin transporter gene (Aux1), and of disease-resistance genes (NPR1, PR1).

Regarding abiotic stress, it is well-known that PGPB enhance salt tolerance of plants by several mechanisms (Kumar et al., 2020), one of them might be the production of some organic compounds. One of these compounds are phenazines, a class of diffusible, heterocyclic compounds harboring substitutions of various functional groups on the core of the phenazine ring structure. Thus, Yuan et al. demonstrated with *Pseudomonas chlororaphis* defective or overproducing strains, that phenazine production improved the efficiency in increasing wheat salt tolerance. The fungal *Trichoderma* strain isolated by Tseng et al. acting as biocontrol effector (see above) could grow on high NaCl or mannitol concentrations and improved salt tolerance of colonized *A. thaliana*.

With respect to soil nutrient conditions, results obtained by Cardoso et al. showed the potential ability of the PGPB strain *Bacillus cereus* UFRABC40 to promote the growth performance of coconut seedlings under decreased application of inorganic fertilizers. Seedling treatments by 100% chemical fertilizer NPK or 50% NPK together with *B. cereus* indicated that the inoculation increased phytohormone levels (IAA, GA) and leaf gas exchange (by assimilation of CO_2, stomatal conductance to water vapor, transpiration and instantaneous carboxylation efficiency). Furthermore, growth parameters and macro- and micronutrient levels were improved. More generally, Wang et al. found a change of bacterial diversity and community together with soil properties and plant functioning during long-term grassland restoration and recovery. The observed changes in soil microbial community were tightly linked to the presence of increased soil C and N substrates due to plant growth and diversity. However, whether these bacterial changes improved growth and tolerance of plants to facilitate the recovery of the analyzed grassland ecosystem remains to be further studied.

Finally, the use of N_2 fixing bacteria in the field to increase essential oil (EO) quantity and quality of sweet basil was explored by Kordi et al.. These authors found that application of free living N_2 fixing bacteria *Azospirillum brasilense* and *Azotobacter chroococcum* together with 50% of regular chemical fertilizer enhanced EO quantity and quality, more than when intercropped with maize plants.

The review concerns orchids being among the most endangered in the plant kingdom. Lack of endosperm in their seeds renders orchids to depend on nutrients provided by orchid mycorrhizal fungi (OMF) for seed

germination and seedling formation in the wild (Li et al., 2021). Zhao et al. presented a new technology using seed germination-promoting OMF coming from roots or seeds of orchid plants to be used for reintroduction of orchids in their natural habitat.

In conclusion, this Research Topic, by putting together different beneficial and nutritional aspects affected by a diversity of microorganisms, tries to pave the way for future research about their role in plant mineral nutrition linked to ISR aiming finally in their better use and involvement in a more sustainable and environmentally friendly agriculture.

AUTHOR CONTRIBUTIONS

RA, SZ, and CL reviewed and summarized the articles of the Topic. CL wrote the draft. All authors revised and validated the final manuscript.

ACKNOWLEDGMENTS

The Topic Editors are grateful to all authors who contributed to this Research Topic, to the Reviewers for evaluating their work, and to the Frontiers editorial staff for their guidance and production assistance.

REFERENCES

Cameron, D. D., Neal, A. L., van Wees, S. C., and Ton, J. (2013). Mycorrhiza-induced resistance: more than the sum of its parts? *Trends Plant Sci.* 18, 539–545. doi: 10.1016/j.tplants.2013.06.004

de Souza, R., Ambrosini, A., and Passaglia, L. M. (2015). Plant growth-promoting bacteria as inoculants in agricultural soils. *Genet. Mol. Biol.* 38, 401–419. doi: 10.1590/S1415-475738420150053

De Vrieze, M., Varadarajan, A. R., Schneeberger, K., Bailly, A., Rohr, R. P., Ahrens, C. H., et al. (2020). Linking comparative genomics of nine potato-associated *Pseudomonas* isolates with their differing biocontrol potential against late blight. *Front. Microbiol.* 11:857. doi: 10.3389/fmicb.2020.00857

Guzmán-Guzmán, P., Porras-Troncoso, M. D., Olmedo-Monfil, V., and Herrera-Estrella, A. (2019). Trichoderma species: versatile plant symbionts. *Phytopathology* 109, 6–16. doi: 10.1094/PHYTO-07-18-0218-RVW

Kumar, A., Singh, S., Gaurav, A. K., Srivastava, S., and Verma, J. P. (2020). Plant growth-promoting bacteria: biological tools for the mitigation of salinity stress in plants. *Front. Microbiol.* 11:1216. doi: 10.3389/fmicb.2020.01216

Kupferschmied, P., Maurhofer, M., and Keel, C. (2013). Promise for plant pest control: root-associated pseudomonads with insecticidal activities. *Front. Plant Sci.* 4:287. doi: 10.3389/fpls.2013.00287

Li, T., Yang, W., Wu, S., Selosse, M.-A., and Gao, J. (2021). Progress and prospects of mycorrhizal fungal diversity in orchids. *Front. Plant Sci.* 12:646325. doi: 10.3389/fpls.2021.646325

Lucena, C., Porras, R., Romera, F. J., Alcántara, E., García, M. J., and Pérez-Vicente, R. (2018). Similarities and differences in the acquisition of Fe and P by dicot plants. *Agronomy* 8:148. doi: 10.3390/agronomy8080148

Pieterse, C. M. J., Zamioudis, C., Berendsen, R. L., Weller, D. M., Van Wees, S. C. M., and Bakker, P. A. H. M. (2014). Induced systemic resistance by beneficial microbes. *Annu. Rev. Phytopathol.* 52, 347–375. doi: 10.1146/annurev-phyto-082712-102340

Rivero, J., Lidoy, J., Llopis-Giménez, Á., Herrero, S., Flors, V., and Pozo, M. J. (2021). Mycorrhizal symbiosis primes the accumulation of antiherbivore compounds and enhances herbivore mortality in tomato. *J. Exp. Bot.* 72, 5038–5050. doi: 10.1093/jxb/erab171

Romera, F. J., García, M. J., Lucena, C., Martínez-Medina, A., Aparicio, M. A., Ramos, J., et al. (2019). Induced systemic resistance (ISR) and Fe deficiency responses in dicot plants. *Front. Plant Sci.* 10:287. doi: 10.3389/fpls.2019.00287

Verbon, E. H., Trapet, P. L., Kruijs, S., Temple-Boyer-Dury, C., Rouwenhorst, T. G., and Pieterse, C. M. J. (2019). Rhizobacteria-mediated activation of the Fe deficiency response in Arabidopsis roots: Impact on Fe status and signaling. *Front. Plant Sci.* 10:909. doi: 10.3389/fpls.2019.00909

Verbon, E. H., Trapet, P. L., Stringlis, I. A., Kruijs, S., Bakker, P. A. H. M., and Pieterse, C. M. J. (2017). Iron and immunity. *Annu. Rev. Phytopathol.* 55, 355–375. doi: 10.1146/annurev-phyto-080516-035537

Zamioudis, C., Korteland, J., Van Pelt, J. A., van Hamersveld, M., Dombrowski, N., Bai, Y., et al. (2015). Rhizobacterial volatiles and photosynthesis-related signals coordinate MYB72 expression in Arabidopsis roots during onset of induced systemic resistance and iron-deficiency responses. *Plant J.* 84, 309–322. doi: 10.1111/tpj.12995

Conflict of Interest: The authors declare that the research was conducted in the absence of any commercial or financial relationships that could be construed as a potential conflict of interest.

Publisher's Note: All claims expressed in this article are solely those of the authors and do not necessarily represent those of their affiliated organizations, or those of the publisher, the editors and the reviewers. Any product that may be evaluated in this article, or claim that may be made by its manufacturer, is not guaranteed or endorsed by the publisher.

frontiers in Plant Science

ORIGINAL RESEARCH
published: 29 September 2020
doi: 10.3389/fpls.2020.575314

Phenazine-Producing Rhizobacteria Promote Plant Growth and Reduce Redox and Osmotic Stress in Wheat Seedlings Under Saline Conditions

Peiguo Yuan[1], *Huiqiao Pan*[1,2], *Emily N. Boak*[1], *Leland S. Pierson III*[3] *and Elizabeth A. Pierson*[1,2,3*]

[1] Department of Horticultural Sciences, Texas A&M University, College Station, TX, United States, [2] Molecular and Environmental Plant Sciences Program, Texas A&M University, College Station, TX, United States, [3] Department of Plant Pathology and Microbiology, Texas A&M University, College Station, TX, United States

OPEN ACCESS

Edited by:
Jianfei Wang,
Anhui University of Science and Technology, China

Reviewed by:
Hassan Etesami,
University of Tehran, Iran
Collin M. Timm,
Johns Hopkins University, United States
Sheng Qin,
Jiangsu Normal University, China

***Correspondence:**
Elizabeth A. Pierson
eapierson@tamu.edu

Specialty section:
This article was submitted to Plant Symbiotic Interactions, a section of the journal Frontiers in Plant Science

Received: *23 June 2020*
Accepted: *01 September 2020*
Published: *29 September 2020*

Citation:
Yuan P, Pan H, Boak EN, Pierson LS III and Pierson EA (2020) Phenazine-Producing Rhizobacteria Promote Plant Growth and Reduce Redox and Osmotic Stress in Wheat Seedlings Under Saline Conditions. Front. Plant Sci. 11:575314. doi: 10.3389/fpls.2020.575314

Application of plant growth promoting bacteria may induce plant salt stress tolerance, however the underpinning microbial and plant mechanisms remain poorly understood. In the present study, the specific role of phenazine production by rhizosphere-colonizing *Pseudomonas* in mediating the inhibitory effects of salinity on wheat seed germination and seedling growth in four different varieties was investigated using *Pseudomonas chlororaphis* 30-84 (wild type) and isogenic derivatives deficient or enhanced in phenazine production. The results showed that varieties differed in how they responded to the salt stress treatment and the benefits derived from colonization by *P. chlororaphis* 30-84. In all varieties, the salt stress treatment significantly reduced seed germination, and in seedlings, reduced relative water content, increased reactive oxygen species (ROS) levels in leaves, and in three of four varieties, reduced shoot and root production compared to the no salt stress treatment. Inoculation of seeds with *Pseudomonas chlororaphis* 30-84 wild type or derivatives promoted salt-stress tolerance in seedlings of the four commercial winter wheat varieties tested, but the salt-stress tolerance phenotype was not entirely due to phenazine production. For example, all *P. chlororaphis* derivatives (including the phenazine-producing mutant) significantly improved relative water content in two varieties, Iba and CV 1, for which the salt stress treatment had a large impact. Importantly, all *P. chlororaphis* derivatives enabled the salt inhibited wheat varieties studied to maintain above ground productivity in saline conditions. However, only phenazine-producing derivatives enhanced the shoot or root growth of seedlings of all varieties under nonsaline conditions. Notably, ROS accumulation was reduced, and antioxidant enzyme (catalase) activity enhanced in the leaves of seedlings grown in saline conditions that were seed-treated with phenazine-producing *P. chlororaphis* derivatives as compared to noninoculated seedlings. The results demonstrate the capacity of *P. chlororaphis* to improve salt tolerance in wheat

seedlings by promoting plant growth and reducing osmotic stress and a role for bacterial phenazine production in reducing redox stress.

Keywords: salt stress, plant growth promoting rhizobacteria, wheat, phenazine, reactive oxygen species, plant-microbe interaction

INTRODUCTION

Increasing soil salinity is a worldwide problem that is detrimental to plant growth, crop production, food security, and the livelihoods of farmers. Recent global estimates suggest that soil salinity affects almost one billion ha of arable land (Shrivastava and Kumar, 2015; Shahid et al., 2018) and causes billions of dollars in crop yield losses annually (Qadir et al., 2014; Abiala et al., 2018). Saline soils are defined as having an electrical conductivity of the saturation extract (ECe) greater than 4 dS/m (approximately 40 mM NaCl) at 25°C (Richards, 1954), and at this ECe, yields of most crops are reduced, although many crops exhibit yield reductions at lower values (Munns, 2005). Under severe salinity (ECe > 16dS/m, ~160 mM NaCl), average yields of most agronomically important crops such as rice, wheat, maize, sorghum, sugarcane, potato, sugar beet soybean and sweet potato, are reduced by 50% (Panta et al., 2014). For instance, wheat stressed at 100–175 mM NaCl showed delayed floral initiation and significant reduction in spikelet number, resulting in poor grain yields (Munns and Rawson, 1999). In addition to ion type and salt concentration, soil type, plant species (or varieties), plant developmental stage, stress distribution, cultivation system and weather conditions are strong determinants of the impacts of salt stress on plants (Morton et al., 2019).

Salinity impairs plant growth and development *via* a combination of factors including osmotic stress, nutrient deficiency, ion toxicity, and oxidative stress (Farooq et al., 2015; Isayenkov and Maathuis, 2019). Due to the high osmotic potential of saline soil water, plants are less efficient in absorbing water and nutrients, but may have excessive uptake of sodium (Na^+) and chloride (Cl^-) ions. Due to ion competition, plant deficiencies of several nutrients (Ca^{2+}, K^+, Mg^{2+}, and NO_3^-) and nutritional imbalances may occur. Salt stress also causes an imbalance in the production of reactive oxygen species (ROS) and antioxidant defense compounds so accumulation of ROS is typical. These factors lead to poor germination, closure of stomata, inhibition of leaf cell expansion, reduced rates of transpiration, photosynthesis, and other metabolic processes, retarded plant growth and development, leaf senescence, reduction in productivity, and ultimately loss of yield (Yuan et al., 2018a; Morton et al., 2019; Zelm et al., 2020).

Plants have evolved diverse mechanisms to tolerate salinity but primarily do so *via* ion avoidance and exclusion and osmotic and tissue tolerance (Farooq et al., 2015; Reddy et al., 2017). Ion exclusion occurs in roots *via* mechanisms affecting ion uptake and transport but includes Na^+ export from the xylem back into the soil. Salt stress avoidance *via* ion exclusion may be improved by the production of barriers to ion uptake, including suberization of the exo- and endodermis and increasing root cap development and border cell and mucilage production (Munns and Tester, 2008; Hawes et al., 2016). Osmotic salinity tolerance occurs when the plant can maintain water use efficiency *via* regulation of stomatal conductance and leaf expansion, similar to drought stress tolerance. Osmotic tolerance is regulated by phytohormones and long-distance signaling mechanisms (Chinnusamy et al., 2006). For example, salt-stressed plants may synthesize phytohormones such as abscisic acid (ABA) leading to stomatal closure to promote water use efficiency (Younis et al., 2003; Zhu, 2016). Tissue tolerance involves sequestration of Na^+ in vacuoles, synthesis of compatible solutes, and production of enzymes catalyzing detoxification of ROS. Plants may accumulate compatible solutes such as proline, soluble sugars, glycine betaine, organic acids, trehalose and other osmolytes, to alleviate the osmotic stress at the cellular level (Liang et al., 2018). They may upregulate ROS scavenging enzymes such as superoxide dismutase, peroxidase and catalase to mitigate secondary oxidative stress under salt conditions (Yuan et al., 2018b; Zelm et al., 2020). The relative importance of stress tolerance mechanisms varies among crops and varieties, and knowledge of salt tolerance mechanisms is essential for the development and management of salt tolerant crops (Morton et al., 2019; Zelm et al., 2020).

Increasingly the use of plant-associated microorganisms, especially rhizosphere-colonizing and endophytic bacteria and fungi, is being studied as a rapid and cost-effective strategy to augment the development of stress tolerant crop varieties (Nadeem et al., 2014; Shrivastava and Kumar, 2015; Numan et al., 2018). It is well established that phytobiome members, especially rhizosphere and root dwellers, can play important roles in mediating abiotic stresses tolerance *via* promotion of plant growth, enhancement of nutrient availability, disease control, and modulation of plant abiotic stress signaling and response pathways (Yang et al., 2009; Hardoim et al., 2015; Reinhold-Hurek et al., 2015; de Vries et al., 2020). With regard to salinity, previous studies focused on plant growth-promoting rhizobacteria (PGPR) showed that they may alleviate salinity induced osmotic stress, nutrient deficiency, oxidative stress, and ion toxicity *via* the production of bioactive compounds and modifications to the rhizosphere environment. For example, PGPR were shown to alleviate salt stress *via* the production or metabolism of phytohormones triggering osmotic responses; the production of siderophores, phosphate solubilizing compounds, and other traits important for improved nutritional status; the production of antioxidants involved in ROS degradation and management of redox stress; and the production of an exopolysaccharide (EPS) matrix, which

improves soil structure, increases soil water retention, and reduces available Na^+ (Shrivastava and Kumar, 2015; Numan et al., 2018; Xiong et al., 2019).

Previous studies showed that phenazine-producing pseudomonads have diverse growth promoting capabilities. Phenazines are a class of diffusible, heterocyclic compounds each having substitution of various functional groups on the core phenazine ring structure (Mavrodi et al., 2001; Mavrodi et al., 2006; Biessy and Filion, 2018). Phenazines were shown to inhibit a diversity of plant pathogens and suppress the plant diseases they cause (Thomashow and Weller, 1988; Chin-A-Woeng et al., 2001; Pierson and Pierson, 2010; Cezairliyan et al., 2013; Zhou et al., 2016; Yu et al., 2018b). Phenazine production is important for the rhizosphere competence of producers (Mazzola et al., 1992; Chin-A-Woeng et al., 2003), contributes to biofilm formation *via* extracellular matrix production (Maddula et al., 2006; Maddula et al., 2008; Das et al., 2015; Wang et al., 2016), and may alter the availability of metals or other nutrients (Wang et al., 2011). Phenazines are redox active metabolites that have been studied extensively due largely to their capacity to generate host-damaging ROS (Mavrodi et al., 2001; Price-Whelan et al., 2006). Studies have shown that pseudomonads having genes required for phenazine production are prevalent in the rhizospheres of wheat grown under dryland production in Washington (Mavrodi et al., 2012) or grown in soils from dryland production fields in Texas (Mahmoudi, 2017). Recently, Mahmoudi et al. (2019) demonstrated that bacterial phenazine production contributed to plant drought-stress tolerance using *P. chlororaphis* 30-84 and isogenic derivative strains of *Pseudomonas chlororaphis* 30-84 deficient or enhanced in phenazine production compared to the wild type (Yu et al., 2018a). In that study, production of phenazines by *P. chlororaphis* 30-84 promoted drought-stress tolerance and resilience to repeated cycles of water deficit in seedlings of the winter wheat variety TAM 112. This was due in part to enhanced root system development that contributed to seedling survival and the drought-stress tolerance phenotype. Additionally, seedlings treated with phenazine-producing strains, especially the enhanced producer, managed osmotic stress better during the drought (as evident from shoot relative water content) and had less leaf tissue mortality and greater recovery after the drought than seedlings treated with no-inoculum controls. Recently, we showed that bacterial phenazine production in the rhizosphere contributed to the management of drought associated redox stress in the leaves (in prep). This led us to hypothesize that bacterial phenazine production may induce systemic tolerance of drought and other abiotic stresses such as salt stress that require osmotic and ROS stress management. Currently nothing is known regarding whether microbial phenazine production contributes to salt stress management.

In the present study, we explored this hypothesis using the same isogenic derivative strains of *Pseudomonas chlororaphis* 30-84 deficient or enhanced in phenazine production from the previous drought study. As in the previous study, the focus was on bacterially mediated improvements in stress tolerance during seedling establishment because this is often the most vulnerable stage and may greatly impact crop stand and yield (Liao et al., 2006). In addition to plant productivity under salt stress, we measured relative water content, and ROS accumulation and antioxidant enzyme activity in leaves following salt stress as indicators of osmotic stress tolerance and redox homeostasis. The use of phenazine deficient and overproducing strains enabled us to investigate whether microbial phenazine production in the rhizosphere was associated with improvements in any of these plant stress tolerance responses. We included TAM 112 (used in the previous drought study) and three additional commercial winter wheat varieties selected and widely used for dryland production in Texas, where phenazine-producing bacteria may be isolated. Because little is known regarding the salt tolerance of these wheat varieties, we used border cell production as a preliminary screen to select varieties that potentially varied in salt stress tolerance.

METHODS

Bacterial Strains and Culture Conditions

Bacterial strains used in this study are shown in **Table 1**. A spontaneous rifampicin-resistant derivative of *Pseudomonas chlororaphis* subsp. *aureofaciens* 30-84 was used and is hereafter referred to as wild type (30-84 WT). A derivative of 30-84 WT with enhanced phenazine production (30-84 Enh) was obtained by removing a 90-bp sequence in the 5' end untranslated region (5′-UTR) of *phzX*, the first gene in the phenazine biosynthetic operon, as described previously (Yu et al., 2018a). A phenazine deficient mutant (30-84 ZN) (Wood et al., 1997), was employed as a phenazine-deficient control. 30-84 WT and its derivatives were grown in Luria-Bertani medium (LB) medium containing 5 g of NaCl per liter, pH 7 (Lennox, 1955) at 28°C, with rapid agitation (200 rpm). Antibiotics were used where appropriate at the following concentrations: gentamicin (Gm) at 50 μg/ml and rifampicin (Rif) at 100 μg/ml.

Root Border Cell Production

Seeds of 20 winter wheat varieties were provided by Xuejin Dong, Texas A&M AgriLife Research, Uvalde, Texas and included 10 commercial varieties from the Oklahoma State University and Texas A&M University breeding programs and 10 proprietary commercial varieties recommended and widely used for dryland production in the Texas High Plains and Texas Rolling Plains. These varieties vary in development and their drought tolerance and disease and insect resistance (**Supplementary Table 1**).

TABLE 1 | Bacterial strains used in this study.

Strain	Description[a]	Reference or source
P. chlororaphis		
30-84 WT	PCA^+, 2-OH-PCA^+, 2-OH-PHZ^+, Rif^R, Wild type	
30-84 Enh	PCA^+, 2-OH-PCA^+, 2-OH-PHZ^+, Rif^R, 90bp deletion at the 5'UTR of *phzX*	Yu et al., 2018b
30-84 ZN	Phz^-, *phzB*::*lacZ*, Rif^R	Wood et al., 1997

[a] *Rif^R = rifampin resistance.*

Wheats seeds of each variety were surface sterilized and germinated within germination paper (10 seeds/paper) and maintained in the dark (28°C) for two days, as described previously (Mahmoudi et al., 2019). Uniformly sized seedlings were selected for border cells counts. The root tips from the primary root and two seminal roots were excised and incubated separately in 100 µl sterilized water with gently shaking for 10 min to release border cell from root. The border cells were collected, transferred to a hemocytometer, and counted using light microscopy (100 X). Data are reported as the average for the three root tips from five seedlings per wheat variety across three independent experiments.

Bacterial Growth and Phenazine Production Under Salt Stress Treatment

Inoculum of each of strain was prepared by growing them separately overnight in LB broth. Cells were collected *via* centrifugation (after being washed with sterile water) and resuspended in LB, and then cell densities were adjusted to a standard optical density (OD_{620} = 1.0). The cultures were used to inoculate (1:50 ratio) the nonstressed control (no additional salt) or saline growth medium. Saline conditions were generated by the addition of NaCl (0%, 0.5%, 1.25%, 2.5%, 5%, and 10%, w/v, e.g., 85, 210, 425, 850, and 1,700 mM NaCl) to LB medium. This concentration gradient produced saline conditions similar to or exceeding (by ~10 X) the concentration measured in the saturation extracts from soil classified as saline to severely saline (~40–160 mM). At 12 and 24 h bacteria populations were quantified by spectroscopy (OD_{620}) and then phenazines were extracted and quantified by spectroscopy (OD_{367}, standardized to cell density) as described previously (Maddula et al., 2008; Wang et al., 2016). Briefly, cell cultures were acidified and phenazines were extracted in benzene, benzene was removed *via* evaporation, and phenazines were resuspended on 0.1 N NaOH.

Effect of Bacterial Inoculation on Wheat Seed Germination Under Salt Stress Treatment

The experiment consisted of 2 × 2 factorial design: seeds of each variety treated with 30-84 WT or receiving no inoculum × exposure to the salt stress or no salt stress treatments. Inoculum of 30-84 WT was prepared as above. After 6 h, cells were pelleted, washed, and then cell densities were standardized to OD_{620} = 0.8 (≈ 10^8 colony forming units/cfu) in 0.5% methylcellulose solution.

Wheats seeds of each variety were surface sterilized as described previously (Mahmoudi et al., 2019). Surface-sterilized seeds were submerged either in bacterial inoculum (room temperature, 10 min) or 0.5% methylcellulose solution (no-inoculum control) and then air dried (~3 h). For each treatment, 10 air dried seed were spaced apart on petri dishes on germination paper (three replicate plates/treatment). Seeds receiving a salt treatment were watered with 200mM NaCl or 120mM NaCl (5 ml), whereas nonsalt stressed seeds were treated with the same volume of sterile distilled water. These concentrations were selected because they bracket the concentration measured in the saturation extracts from soil classified as severely saline (160 mM). Three replicate petri dishes/treatment were placed in the dark at 28°C and germination percentage was measured after 3 days.

Effect of Bacterial Inoculation on Wheat Seedling Growth Under Salt Stress

Four wheat varieties were selected for further testing: Iba, commercial variety CV 1, TAM 112 and TAM 113. For each variety, a 4 × 2 experimental design was used: seeds treated with either 30-84 WT, the phenazine-deficient mutant 30-84 ZN, or the phenazine-overproducing derivative 30-84 Enh, or no inoculum x salt stress or no stress treatments.

Wheats seeds of each variety were surface sterilized as above, placed onto germination paper, and maintained in the dark (28°C) for two days. Germinated seedlings that were uniform in growth were selected and treated with bacterial inoculum or methylcellulose (no inoculum control) as described above. Seedlings were grown separately in plastic tubes (Ray Leach Cone-tainers, 2.5-cm diameter × 16.5-cm long) containing steam sterilized (two times at 121°C for 1 h with a 24-h pause) planting medium (MetroMix 366, Sungro, Agawam, MA). Plants were grown for 7 days under well-watered (no salt) conditions (25°C, 16:8 light dark cycle, 150–170 μE^{-1} m^{-1} s^{-1}, water twice weekly with 10 ml distilled water). After 7 days, the seedlings received either a salt stress treatment (10 ml of 200 mM NaCl, twice weekly) or no salt (10 ml distilled water). This concentration was selected because it is slightly above the concentration measured in the saturation extracts from soil classified severely saline (160 mM). After 3 weeks, seedlings were harvested, and roots were washed to remove adhering planting medium. Bacterial population sizes were determined from a random sample of replicates *via* serial dilution plating on LB agar supplemented with rifampicin. Shoot and root fresh weight (FW), turgid weight (TW, saturated leaf weight after 24 h), and dry weight (DW, 12 h at 65° C) were measured and shoot measurements were used to calculate relative water content as described previously (Mahmoudi et al., 2019). Productivity indices were calculated by standardizing shoot or root DW biomass to the DW shoot or root biomass of the no salt control, respectively. Data are from three independent experiments with five replicates seedlings/treatment.

Effect of Bacterial Inoculation on ROS Accumulation and Antioxidant Enzyme Activity in Leaves

Hydrogen peroxide (H_2O_2) detection was performed *in situ* using a 3,3′-diaminobenzidine (DAB) staining method as described previously (Daudi and O'Brien, 2012). For all inoculation x stress treatments, three fully expanded leaves (third leaves) from separate wheat plants were obtained 2-week post salt stress treatment. Leaves were immediately vacuum-infiltrated with DAB (Sigma) staining solution (1 mg/ml DAB, 10mM Na_2HPO_4 and 0.05% Tween-20, pH 7.4) and incubated in the dark (3 h, gentle agitation). Leaves were fixed and chlorophyll destained using several washes with a 1:3:1 mixture of lactic acid: ethanol:glycerol (65°C, 6 h), mounted in Tris/glycerol, and examined under a dissecting microscope (1.5X) for the presence of reddish-brown precipitate.

Antioxidant enzyme (catalase) activity was measured in three fully expanded leaves taken from separate wheat plants 1-week post salt stress treatment based on previous methods (Kar and Mishra, 1976). Immediately after harvested, leaves were stored at –80°C. Samples were ground in liquid N_2; 0.5 g of the grounded sample was homogenized in 1 ml PBS (pH 7.4) solution with protease inhibitor. The catalase (CAT) activity of the samples was quantified using spectrophotometry (NanoVue Plus, GE Healthcare, Piscata, NJ) to measure the decomposition of H_2O_2 over 10 min (as the decrease in absorbance at 240 nm). Data are from three independent experiments with three replicates/treatment (i.e., leaves taken from separate plants).

Statistical Analyses

For ROS staining and catalase activity, measurements were made on three leaves from separate plants/treatment/experiment and the experiment was replicated independently three times. Data were analyzed by variety using a two-way ANOVA and Tukey's test for multiple comparisons ($P < 0.05$, N=9). For border cell counts, data are reported as the average for the three root tips from five seedlings per wheat variety across three independent experiments. For germination rates, data are the average and standard error of the percentage of 10 seeds that germinated in three replicates. Root and shoot productivity and relative water content measurements were made on five seedlings/treatment/experiment and experiments were replicated three times. Productivity data were analyzed by variety using a one-way ANOVA and Dunnett's test for comparison to the control ($P < 0.05$, N=15) using Real Statistics in Excel (http://www.real-statistics.com). Relative water content was analyzed using ANOVA as above. For bacterial growth and phenazine production, there were three replicates/treatment and three independent experiments were performed, and data were analyzed using ANOVA as above. Data were examined graphically to ensure they met the assumptions of the ANOVA.

RESULTS

Root Border Cell Production

In the absence of any varietal information on salt stress tolerance, we prescreened 20 winter wheat varieties for potential salt sensitivity based on root border cell production, given the potential for mucilage secreted by border cells to contribute to salt tolerance. The lowest border cell producing varieties (~2,000/root tips) were TAM 304, Iba, and a commercial variety (CV 1) (**Supplementary Table 1; Supplementary Figure 1**). The highest border cell producing varieties were the drought tolerant varieties TAM 112 and Duster (~5,000/root tips). In an effort to obtain a spectrum of potential susceptibilities to salinity among varieties, based on these observations varieties Iba and CV 1 were included in the subsequent experiments as potentially salt sensitive varieties. TAM 112 used in a previous drought study (Mahmoudi et al., 2019) and TAM 113 (also a high border cell producer) were included as potentially more salt/stress tolerant varieties.

Effect of Bacterial Inoculation on Wheat Seedling Growth Under Salt Stress

The effects of bacterial seed-inoculation on growth was measured by comparing seedlings of Iba, CV 1, TAM 112 and TAM 113 receiving no inoculum or inoculum comprised of 30-84 ZN, 30-84 WT, or 30-84 Enh grown in salt or no salt treatments. Prior to the application of salt stress treatment, all seedlings were grown 7 days without salt treatment and several replicate plants were sacrificed for bacterial population measurements *via* serial dilution. Bacterial populations of all three strains on all four varieties achieved populations greater than or equal to 10^7 cfu/g dry weight root.

The wheat varieties varied in their response to the salt stress treatment in terms of cumulative above and below ground productivity and relative water content (RWC) of the above ground tissue (**Table 2; Supplementary Figure 2**). For example, compared to the no salt stress/no inoculum control, shoot productivity and root productivity of all salt-stressed/noninoculated varieties were reduced to 45%–63% (shoot) and 28%–44% (root) for varieties Iba, CV 1, and TAM 112. However, TAM 113 maintained shoot and root productivity at a level that was not significantly different from the no salt control. Salinity caused osmotic stress in all four varieties as evident from the drop in RWC compared to the nonstressed control plants, however in TAM 112 and TAM 113 the reduction was less (RWC = 66%) than observed for IBA and CV 1 (RWC < 40%).

In the no salt stress condition, seed treatment with 30-84 Enh promoted above ground growth of Iba and CV 1 and below ground growth of TAM 112 and TAM 113. However, the growth promoting effect on TAM 113 was not dependent on phenazine production as 30-84ZN also promoted plant growth. Under salt-stressed conditions, seed treatment with 30-84 WT, 30-84 Enh or 30-84ZN enabled seedlings of most varieties to maintain shoot productivity equivalent to the no stress/no inoculum control, however for TAM 112 growth promotion occurred only when plants were treated with phenazine producing bacteria. Under the salt stress condition, seed treatment with 30-84 WT, 30-84 Enh or 30-84 ZN enabled TAM 113 to maintain root productivity. These data indicate that seed treatment with *P. chlororaphis* 30-84 plays a role in promoting growth and helping seedlings tolerate salt stress, but the requirement for phenazine production depends on wheat variety.

Effect of Bacterial Inoculation on ROS Accumulation and Antioxidant Enzyme Activity in Leaves

The effect of seed inoculation with 30-84 ZN, 30-84 WT, or 30-84 Enh on ROS (H_2O_2) accumulation in seedling leaves was measured using three fully expanded leaves (third leaves) from separate wheat plants collected two-weeks post salt stress treatment (**Figure 1**). Under the no salt condition, almost no ROS accumulation was observed in the leaves obtained from any of the four wheat varieties and all seed-inoculation treatments (data not shown). For seedlings grown in the salt treatment, the leaves of CV 1 and Iba obtained from noninoculated

TABLE 2 | Productivity and Relative Water Content of seedlings grown under no salt or salt stress conditions treated with or without bacterial inoculum.

Variety Control/ Stress Treatment	Inoculation Treatment*	Percent Productivity Shoot (P < 0.05)**	Percent Productivity Root (P < 0.05)	Relative Water Content***
Iba				
No Salt	**No Inoculum**	**100**	**100**	89 ± 4 a
	30-84 ZN	93	107	94 ± 1 a
	30-84 WT	124	108	90 ± 2 a
	30-84 Enh	157 **+**	114	91 ± 3 a
Salt	No Inoculum	48 **-**	28 **-**	38 ± 7 c
	30-84 ZN	79	28 **-**	67 ± 5 b
	30-84 WT	79	32 **-**	63 ± 9 b
	30-84 Enh	100	38 **-**	73 ± 5 b
CV 1				
No Salt	**No Inoculum**	**100**	**100**	92 ± 4 a
	30-84 ZN	118	99	88 ± 1 a
	30-84 WT	166 **+**	107	88 ± 2 a
	30-84 Enh	170 **+**	111	91 ± 3 a
Salt	No Inoculum	63 **-**	30 **-**	36 ± 7 c
	30-84 ZN	89	29 **-**	63 ± 5 b
	30-84 WT	96	34 **-**	70 ± 9 b
	30-84 Enh	115	47 **-**	79 ± 5 b
TAM 112				
No Salt	**No Inoculum**	**100**	**100**	92 ± 11 a
	30-84 ZN	102	107	91 ± 8 a
	30-84 WT	100	107	99 ± 8 a
	30-84 Enh	122	130 **+**	93 ± 8 a
Salt	No Inoculum	45 **-**	44 **-**	66 ± 7 b
	30-84 ZN	67 **-**	44 **-**	66 ± 3 b
	30-84 WT	71	56 **-**	72 ± 8 b
	30-84 Enh	92	56 **-**	79 ± 13 ab
TAM 113				
No Salt	**No Inoculum**	**100**	**100**	92 ± 3 a
	30-84 ZN	102	139 **+**	99 ± 2 a
	30-84 WT	106	138 **+**	98 ± 4 a
	30-84 Enh	108	138 **+**	94 ± 5 a
Salt	No Inoculum	93	66 ± 9 b	
	30-84 ZN	81	82	76 ± 5 b
	30-84 WT	100	125	77 ± 9 b
	30-84 Enh	104	115	82 ± 6 b

**Three-day old seedlings received either no inoculum (methylcellulose control) or 30-84 ZN, 30-84 WT, or 30-84 Enh inoculum and were grown for one week without stress. Plants then received no salt stress (control) or a salt stress treatment (200 mM NaCl) for 3 weeks and dry weight biomass of shoots and roots were measured. Data are from three independent experiments with five replicates seedlings/variety/treatment.*

*** Productivity is expressed as the shoot or root dry weight biomass standardized to the shoot or root dry weight biomass of the no salt/no inoculum control (bold), respectively. Productivity measurements were analyzed by variety using a one-way ANOVA and Dunnett's test for comparison to the control (P < 0.05, N=15). + and – indicate whether the productivity is significantly greater or less than the control, respectively.*

**** Means and standard deviations of the relative water content of the above ground tissue were compared by variety using a two-way ANOVA and Tukey's test for multiple comparisons (P < 0.05, N=3) and letters indicate significant differences.*

seedlings or seedlings seed-inoculated with 30-84 ZN displayed high levels of ROS stress, whereas TAM 112 and TAM 113 leaf ROS accumulation was lower. In all varieties, seed-inoculation with 30-84 WT and especially 30-84 Enh resulted in little ROS accumulation in the leaves of seedlings when grown in the salt treatment. These observations indicated that seed-inoculation of wheat with 30-84 WT or 30-84 Enh reduced ROS accumulation as compared to noninoculated seedlings, in the salt stress treatment.

Catalase activity was significantly greater in seedlings grown in the salt stress treatment compared to the nonstressed treatment (200–475 U/g versus ≤ 150 U/g, respectively, **Figure 2**). Moreover, in the salt stress treatment catalase activity was significantly higher in Iba and CV 1 leaves from plants seed-inoculated with 30-84 WT or 30-84 Enh (400–500 U/g) compared to the noninoculated control, whereas for TAM 112 and TAM 113 differences were less obvious. These observations suggest that seed-inoculation of plants with 30-84 WT or 30-84 Enh enhanced catalase enzyme activity in the leaves of wheat seedlings grown in the salt stress condition, consistent with the reduction in leaf ROS accumulation we observed.

Effect of Bacterial Inoculation on Wheat Seed Germination Under Salt Stress Treatment

Percent germination rates of seeds of 20 winter wheat varieties with and without bacterial inoculum and with and without salt treatment were compared. Seeds from the different wheat varieties were either treated with 30-84 WT or received no inoculum (methylcellulose control) and either watered with distilled water or solutions containing 200 mM or 120 mM NaCl solution. After 3 days, average germination rates of all 20 varieties in the no salt stress treatment, whether receiving no inoculum or 30-84 WT inoculum were 95% ± 1% and 96% ± 1%, respectively. No seeds germinated from the 200 mM treatment. For the 120 mM treatment, average germination rates of all wheat varieties were markedly reduced and ranged from 33%–70% with or without bacterial inoculum (**Supplementary Table 1**). Several of the varieties including Iba and CV 1, and TAM 304 had germination rates in the 30-45% range under saline conditions (e.g., 37% ± 3%, 43% ± 3%, 33% ± 8%, respectively), however inoculation of seeds with 30-84 WT improved germination of both Iba and CV 1, but not TAM 304 (53% ± 8%, 63% ± 8%, and 47% ± 8%, respectively). At the high end of the spectrum, under saline conditions the germination percentages of the widely used drought tolerant TAM 112, TAM 113, and Duster were 63% ± 3%, 47% ± 8%, and 70% ± 6%, respectively and were not improved by inoculation with 30-84 WT (63% ± 8%, 40% ± 5%, and 70% ± 6%), indicating seed inoculation with 30-84 WT mediated saline inhibition of germination in some, but not all varieties.

Bacterial Growth and Phenazine Production Under Salt Stress Treatment

To determine the extent to which salt concentration affects bacterial growth and phenazine production, 30-84 WT and derivatives deficient (30-84 ZN) or enhanced (30-84 Enh) in phenazine production were grown in LB media amended with no NaCl or different concentrations of NaCl (0.5%, 1.25%, 2.5%, 5%, and 10%, w/v, e.g. 85–1,700 mM), and bacterial populations and phenazine production was quantified at 12 and 24 h (**Figure 3**). Because phenazine production is regulated *via* quorum sensing in a cell density-dependent manner, it was important to consider the

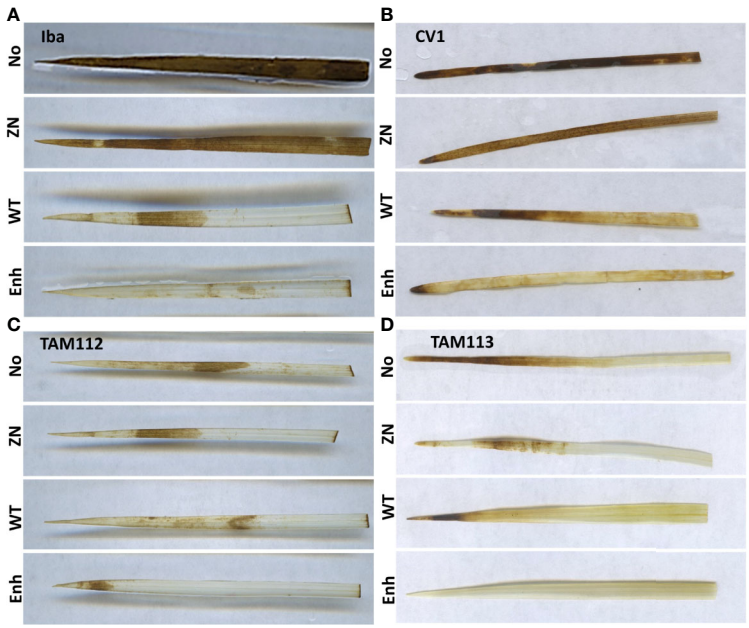

FIGURE 1 | The effect of no inoculum or inoculation with 30-84 ZN, 30-84 WT, or 30-84 Enh (top to bottom, NO, ZN, WT, Enh, respectively) on reactive oxygen species (ROS) accumulation in leaves obtained from seedlings of different wheat varieties grown under the salt stress condition. **(A)** Iba, **(B)** CV 1, **(C)** TAM 112, and **(D)** TAM 113. Seeds were treated with either no inoculum (methylcellulose) or 30-84 ZN, 30-84 WT or 30-84 Enh and grown one week without stress. Then plants were exposed to salt stress (200mM NaCl). DAB staining revealed ROS accumulation in fully expanded leaves (third leaves) from three separate wheat plants/variety/experiment in three separate experiments. Representative images are shown.

effects of salt on population density. Cell densities of 30-84 WT and 30-84 Enh when grown in the lowest salt concentrations (0.5 to 2.5%, e.g. ≤ 425 mM) were only slightly different from the no-salt treatment, however phenazine production by 30-84 WT was reduced at 2.5%, but not at 1.25% (~210 mM). Compared to the no salt control, at the 5% salt concentration (850 mM) bacterial growth and phenazine production were significantly reduced. None of the derivatives grew in 10% NaCl. These data suggest that when *P. chlororaphis* 30-84 is grown in saline conditions similar to those measured in the saturation extracts from soil classified as saline to severely saline (~40–160 mM), bacterial growth and phenazine production are not substantially impaired.

DISCUSSION

This study demonstrated that the four wheat varieties examined responded differently to the salt stress treatment and the benefits derived from colonization by *P. chlororaphis* 30-84. In all varieties, the salt stress treatment reduced seed germination rates. In seedlings of the four varieties tested, salt stress reduced shoot water content, increased reactive oxygen species levels in leaves, and in three of four varieties, reduced shoot and root production compared to the no salt stress treatment. It was interesting that TAM 113 seedlings were able to maintain biomass production in the salt treatment despite experiencing osmotic stress (RWC=66%), indicating seedlings of this variety may be less susceptible to growth inhibition at this level of salinity. Also, root border cell production turned out to be a somewhat good predictor of salinity tolerance, although our sample size was small, and more validation is required. Iba and CV 1, which produce 60% fewer border cells than TAM 112, experienced greater leaf redox stress, significant reductions in relative water content under saline conditions, and reduced germination rates under saline conditions. They also gained significant improvements in these traits with bacterial inoculation. Previous work showed that in responses to metal ions such as aluminum, copper, lead, cadmium, mercury, arsenic, and iron mucilage from border cells of various crops including cotton, cereals, and legumes expands to trap metal ions in a concentration-dependent manner and when border cells are removed, plants experience greater heavy metal toxicity (reviewed in Hawes et al., 2016). Although not specifically addressed in this study, potential roles for border cells in helping plants protect themselves from salt ions and improving plant responses to the activities of stress-mediating microbes deserves further consideration.

The most striking finding of our study was the association between bacterial phenazine production in the rhizosphere and enhanced catalase activity and redox stress management in the leaves in all four varieties. *P. chlororaphis* 30-84 produces several phenazines, but only two in significant abundance: phenazine-1-carboxylic acid (PCA) and 2-hydroxy-PCA (2-OH-PCA). It is well established that salt stress causes the accumulation ROS such as $O_2^{\cdot-}$, H_2O_2, and ·OH in leaves, leading to cytoplasmic and nuclear

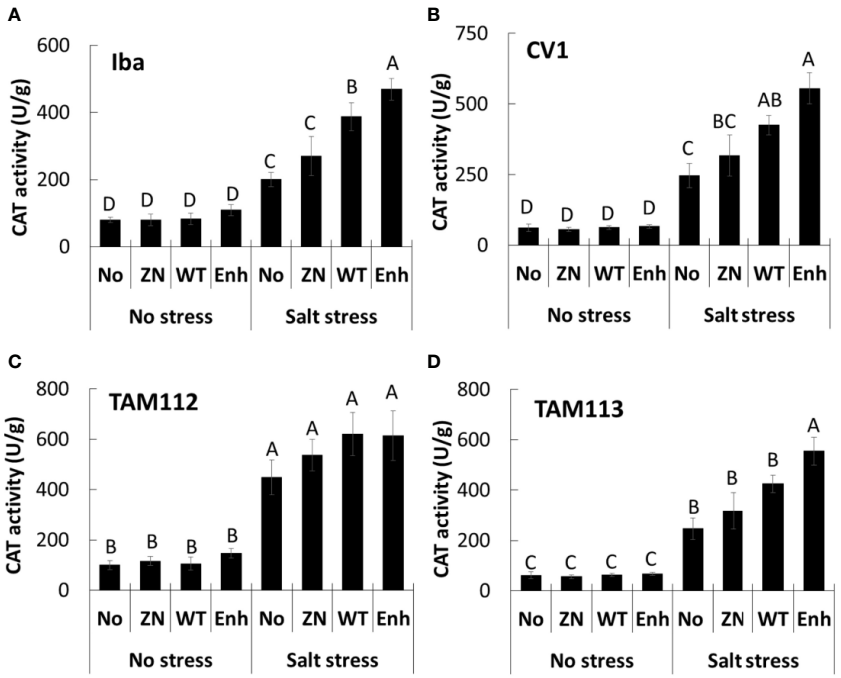

FIGURE 2 | The effect of no inoculum or inoculation with 30-84 ZN, 30-84 WT, or 30-84 Enh on catalase enzyme activity in leaves obtained from seedlings of different wheat varieties in no salt and salt stress treatments. **(A)** Iba, **(B)** CV 1, **(C)** TAM 112, and **(D)** TAM 113. Seeds were treated with either no inoculum (methylcellulose) or 30-84 ZN, 30-84 WT, or 30-84 Enh and grown one week without stress and the received either a salt stress (200mM NaCl) or no salt stress. Catalase activity was measured in fully expanded leaves (third leaves) from three different wheat plants/variety/experiment in three separate experiments. Data are the means and standard errors. Data were analyzed by variety using a two-way ANOVA and Tukey's test for multiple comparisons ($P < 0.05$, N=9) and letters indicate significant differences.

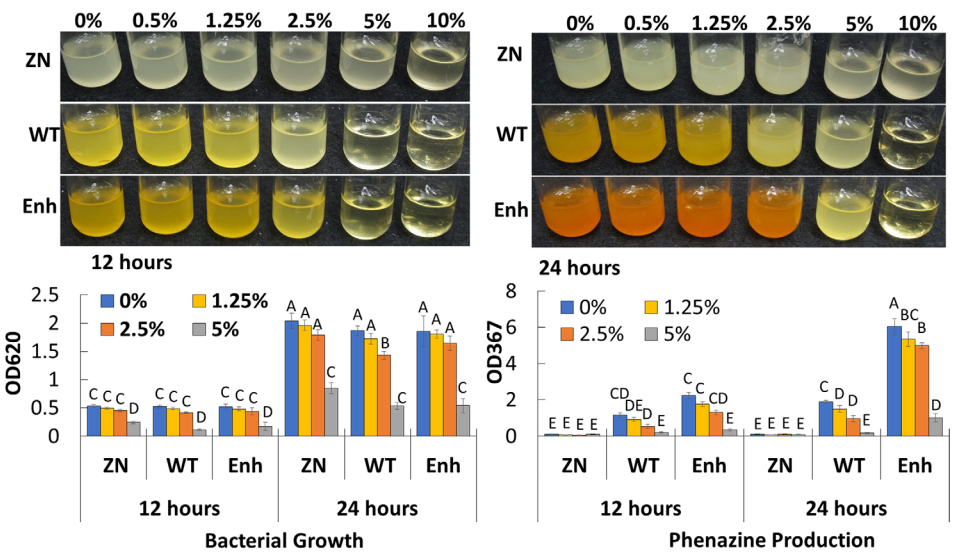

FIGURE 3 | Growth and phenazine production of *P. chlororaphis* 30-84 WT and derivatives under increasing salt concentrations. Bacterial populations and phenazine production for 30-84WT, 30-84ZN, and 30-84 Enh were measured after 12 and 24 h in Luria-Bertani medium (LB) amended with different salt concentrations (0%, 0.5%, 1.25%, 2.5%, 5%, and 10% NaCl, w/v, e.g., 85, 210, 425, 850, and 1,700 mM NaCl). Bacterial populations and phenazine production were quantified spectrophotometrically (OD_{620} and OD_{367}, respectively) and means and standard errors are shown. Data were analyzed using a two-way ANOVA and Tukey's test for multiple comparisons ($P < 0.05$, N=3) and letters indicate significant differences.

membrane peroxidation (Zhu, 2016; Yuan et al., 2017; Yuan et al., 2018c). Moreover, cellular redox state serves as a sensor of environmental changes that impose oxidative stress, and plants have efficient ROS scavenging systems to avoid ROS accumulation to maintain cellular homeostasis (Zhu, 2016). Previous studies showed that under saline conditions PGPR may augment plant ROS scavenging systems *via* transcriptional induction of genes encoding plant antioxidant enzymes such as ascorbate peroxidase (APX), superoxide dismutase (SOD), peroxidase (POD), catalase (CAT), and glutathione peroxidase (GPX) (Bharti et al., 2016). In the present study under saline conditions, microscopic observation of DAB-staining in leaves revealed that ROS accumulation was located on the cell membranes and in apoplasts of leaf cells (**Figure 1**). However, inoculation of seedlings with phenazine-producing *P. chlororaphis* 30-84 visibly diminished H_2O_2 accumulation in all varieties and significantly promoted catalase activity in leaves of Iba and CV 1, especially plants treated with 30-84 Enh as compared to plants treated with 30-84 ZN or receiving no inoculum. Recently using the same staining protocol, we found that seed inoculation of TAM 112 with 30-84 WT or 30-84 Enh, but not 30-84 ZN, also visibly diminished H_2O_2 accumulation in the leaves of drought stressed seedlings. These observations suggest that bacterial phenazine production promotes tolerance of drought and salt stress in wheat seedlings in part through the modulation of ROS-mediated signaling pathways, although the precise mechanism needs further study. As indicated from previous work showing the broad transcriptomic consequences associated with the lack or overexpression of phenazines (Wang et al., 2016), it is reasonable that the microbial mechanisms underlying these results may be more complex and not solely due to the phenazines.

Previous studies showed that in addition to suppression of seedling disease, PGPR contribute to growth promotion and salt stress tolerance directly and indirectly *via* the production of bioactive compounds and modifications to the rhizosphere environment *via* extensive biofilm formation, respectively (Yang et al., 2009). For example, PGPR are known to enhance germination rates, improve nutrient status, and alleviate salt stress in wheat seedlings *via* the production of: indole acetic acid (IAA), which mediates lateral branching, resulting in increased fine root length, surface area, tip number, and water and primary nutrient uptake (Ramadoss et al., 2013; Egamberdieva et al., 2015); the enzyme 1-aminocyclopropane-1-carboxylate (ACC)-deaminase, involved in the degradation of the ethylene precursor ACC, resulting in improved root growth and stress tolerance (Bal et al., 2013); antioxidant enzymes such as catalase involved in ROS degradation and management of redox stress (Jha and Subramanian, 2014); siderophores and phosphate solubilizing compounds and other undetermined traits important for improved nutritional status (Nadeem et al., 2014; Rajkumar et al., 2017); and EPS matrix, which helps improve soil structure, increase soil water retention, and reduce the available Na^+ (Naseem and Bano, 2014; Banerjee et al., 2019). *P. chlororaphis* 30-84 (including 30-84ZN) produces some of these bioactive compounds, including IAA, ACC-deaminase, pyoverdine class siderophores, and antioxidants (Mahmoudi et al., 2019). It is likely these contributed to the effects of both phenazine-producing and nonproducing strains on growth promotion and osmotic tolerance in seedlings. An interesting question is whether the production of these bioactive compounds is correlated with phenazine production, thus contributing to the beneficial effects associated with phenazine production. Previous research showed that IAA production by 30-84ZN was higher than by 30-84WT in static floating biofilms, whereas the expression of genes encoding ACC-deaminase were similar in both strains, and the genes encoding pyoverdine biosynthesis and catalase and other enzymes involved in redox stress management were expressed at higher levels in 30-84WT than 30-84ZN, although production of these enzymes or compounds were not measured (Wang et al., 2016). In addition to the production of bioactive compounds, *P. chlororaphis* 30-84 makes substantial EPS matrix, which could serve to buffer the plant to some extent from the saline environment. Consistent with other phenazine-producing strains, biofilm development is partially dependent on phenazine production (Wang et al., 2016; Letourneau et al., 2018).

Previous studies demonstrated inhibitory effects of NaCl on phenazine production as observed in this study (Girard and Rigali, 2011). Thus, we were interested in whether phenazines would be produced when the strains were exposed to the salinity conditions used in our plant assays. For *P. chlororaphis* 30-84, these effects were only observed at extremely high salt concentrations (425-850 mM) that are unlikely to occur in saline soil water. These observations suggest that it is unlikely that the production of phenazines was diminished in the saline treatment, but further testing is warranted.

In summary, the results of our study using phenazine deficient and overexpressing derivatives as seed-inoculants demonstrate that phenazine-producing rhizobacteria promote plant growth and reduce redox and osmotic stress in seedlings grown in saline conditions, and that the reduction in redox stress is associated with phenazine production. These findings indicate a critical starting point for investigating the mechanisms underlying the relationship between phenazine production by rhizosphere-colonizing bacteria and plant stress tolerance, and ongoing work is focused on how bacterial phenazine production alters plant signaling pathways involved in redox homeostasis. Results from the present study, together with those from previous studies (Yu et al., 2018b; Mahmoudi et al., 2019), demonstrate the potential for phenazine-producing strains prevalent in dryland wheat production areas to suppress plant diseases and promote drought and salt stress tolerance in wheat seedlings. These studies also suggest that breeding wheat for effective recruitment and response to native phenazine-producing bacteria could be a viable approach for improving wheat stress tolerance.

DATA AVAILABILITY STATEMENT

The datasets generated during this study are available on request to the corresponding author.

AUTHOR CONTRIBUTIONS

PY, LP, and EP designed the experiments. PY and EB carried out the experiments and generated original data, with technical advice from HP. PY and EP performed the data analysis. PY, EB, HP, LP, and EP contributed to the interpretation of results, and PY, HP, and EP contributed to the first draft of the manuscript. EP provided project supervision, and EP and HP provided major contribution to the final draft. All authors contributed to the article and approved the submitted version.

FUNDING

This research was funded in part by support to EP from DOE-Office of Energy Efficiency and Renewable Energy Award DE-EE0007104 and the College of Agriculture and Life Sciences.

ACKNOWLEDGMENTS

We thank current and former members of the Pierson research group including Julien Levy, Jun Myoung Yu, Tessa Mahmoudi, and Eric Olivier Tiembo. We are also grateful to Xuejun Dong and Shuyu Liu for providing seeds of wheat varieties from their breeding programs and for helpful discussions. We also thank Jackie Rudd and Michael Kolomiets for helpful discussions and Hisashi Kiowa for assistance with and use of the microscope and other scientific equipment.

SUPPLEMENTARY MATERIAL

The Supplementary Material for this article can be found online at: https://www.frontiersin.org/articles/10.3389/fpls.2020.575314/full#supplementary-material

REFERENCES

Abiala, M. A., Abdelrahman, M., Burritt, D. J., and Tran, L.-S. P. (2018). Salt stress tolerance mechanisms and potential applications of legumes for sustainable reclamation of salt-degraded soils. *Land Degradation Dev.* 29, 3812–3822. doi: 10.1002/ldr.3095

Bal, H. B., Nayak, L., Das, S., and Adhya, T. K. (2013). Isolation of ACC deaminase producing PGPR from rice rhizosphere and evaluating their plant growth promoting activity under salt stress. *Plant Soil* 366, 93–105. doi: 10.1007/s11104-012-1402-5

Banerjee, A., Sarkar, S., Cuadros-Orellana, S., and Bandopadhyay, R. (2019). "Exopolysaccharides and biofilms in mitigating salinity stress: the biotechnological potential of halophilic and soil-inhabiting PGPR microorganisms," in *Microorganisms in Saline Environments: Strategies and Functions. Soil Biology,* vol 56. Eds. B. Giri and A. Varma (Cham: Springer). doi: 10.1007/978-3-030-18975-4_6

Bharti, N., Pandey, S. S., Barnawal, D., Patel, V. K., and Kalra, A. (2016). Plant growth promoting rhizobacteria *Dietzia natronolimnaea* modulates the expression of stress responsive genes providing protection of wheat from salinity stress. *Sci. Rep.* 6, 34768. doi: 10.1038/srep34768

Biessy, A., and Filion, M. (2018). Phenazines in plant-beneficial *Pseudomonas* spp.: biosynthesis, regulation, function and genomics. *Environ. Microbiol.* 20, 3905–3917. doi: 10.1111/1462-2920.14395

Cezairliyan, B., Vinayavekhin, N., Grenfell-Lee, D., Yuen, G. J., Saghatelian, A., and Ausubel, F. M. (2013). Identification of *Pseudomonas aeruginosa* phenazines that kill *Caenorhabditis elegans*. *PloS Pathog.* 9, e1003101. doi: 10.1371/journal.ppat.1003101

Chin-A-Woeng, T. F. C., Thomas-Oates, J. E., Lugtenberg, B. J. J., and Bloemberg, G. V. (2001). Introduction of the *phzH* gene of *Pseudomonas chlororaphis* PCL1391 extends the range of biocontrol ability of phenazine-1-carboxylic acid-producing *Pseudomonas* spp. strains. *Mol. Plant-Microbe Interact.* 14, 1006–1015. doi: 10.1094/MPMI.2001.14.8.1006

Chin-A-Woeng, T. F. C., Bloemberg, G. V., and Lugtenberg, B. J. J. (2003). Phenazines and their role in biocontrol by *Pseudomonas* bacteria. *New Phytol.* 157, 503–523. doi: 10.1046/j.1469-8137.2003.00686.x

Chinnusamy, V., Zhu, J., and Zhu, J.-K. (2006). "Salt Stress signaling and mechanisms of plant salt tolerance," in *JK Setlow (ed) Genetic Engineering: Principles and Methods* (Boston, MA: Springer US). doi: 10.1007/0-387-25856-6_9

Das, T., Kutty, S. K., Tavallaie, R., Ibugo, A. I., Panchompoo, J., Sehar, S., et al. (2015). Phenazine virulence factor binding to extracellular DNA is important for *Pseudomonas aeruginosa* biofilm formation. *Sci. Rep.* 5, 8398. doi: 10.1038/srep08398

Daudi, A., and O'Brien, J. A. (2012). Detection of hydrogen peroxide by DAB staining in *Arabidopsis* leaves. *Bio-protocol* 2, e263. doi: 10.21769/BioProtoc.263

de Vries, F. T., Griffiths, R. I., Knight, C. G., Nicolitch, O., and Williams, A. (2020). Harnessing rhizosphere microbiomes for drought-resilient crop production. *Science* 368, 270–274. doi: 10.1126/science.aaz5192

Egamberdieva, D., Jabborova, D., and Hashem, A. (2015). *Pseudomonas* induces salinity tolerance in cotton (*Gossypium hirsutum*) and resistance to *Fusarium* root rot through the modulation of indole-3-acetic acid. *Saudi J. Biol. Sci.* 22, 773–779. doi: 10.1016/j.sjbs.2015.04.019

Farooq, M., Hussain, M., Wakeel, A., and Siddique, K. H. M. (2015). Salt stress in maize: effects, resistance mechanisms, and management. A review. *Agron. Sustain. Dev.* 35, 461–481. doi: 10.1007/s13593-015-0287-0

Girard, G., and Rigali, S. (2011). Role of the phenazine-inducing protein Pip in stress resistance of *Pseudomonas chlororaphis*. *Microbiology* 157, 398–407. doi: 10.1099/mic.0.043075-0

Hardoim, P. R., van Overbeek, L. S., Berg, G., Pirttilä, A. M., Compant, S., Campisano, A., et al. (2015). The hidden world within plants: ecological and evolutionary considerations for defining functioning of microbial endophytes. *Microbiol. Mol. Biol. Rev.* 79, 293–320. doi: 10.1128/mmbr.00050-14

Hawes, M. C., McLain, J., Ramirez-Andreotta, M., Curlango-Rivera, G., Flores-Lara, Y., and Brigham, L. A. (2016). Extracellular trapping of soil contaminants by root border cells: new insights into plant defense. *Agronomy* 6, 5. doi: 10.3390/agronomy6010005

Isayenkov, S. V., and Maathuis, F. J. M. (2019). Plant salinity stress: many unanswered questions remain. *Front. Plant Sci.* 10, 80. doi: 10.3389/fpls.2019.00080

Jha, Y., and Subramanian, R. B. (2014). PGPR regulate caspase-like activity, programmed cell death, and antioxidant enzyme activity in paddy under salinity. *Physiol. Mol. Biol. Plants* 20, 201–207. doi: 10.1007/s12298-014-0224-8

Kar, M., and Mishra, D. (1976). Catalase, peroxidase, and polyphenoloxidase activities during rice leaf senescence. *Plant Physiol.* 57, 315–319. doi: 10.1104/pp.57.2.315

Lennox, E. S. (1955). Transduction of linked genetic characters of the host by bacteriophage P1. *Virology* 1, 190–206. doi: 10.1016/0042-6822(55)90016-7

Letourneau, M., Marshall, M., Cliff, J., Bonsall, R., Dohnalkova, A., Mavrodi, D., et al. (2018). Phenazine-1-carboxylic acid and soil moisture influence biofilm development and turnover of rhizobacterial biomass on wheat root surfaces. *Environ. Microbiol.* 20, 2178–2194. doi: 10.1111/1462-2920.14244

Liang, W., Ma, X., Wan, P., and Liu, L. (2018). Plant salt-tolerance mechanism: A review. *Biochem. Biophys. Res. Commun.* 495, 286–291. doi: 10.1016/j.bbrc.2017.11.043

Liao, M., Palta, J. A., and Fillery, I. R. P. (2006). Root characteristics of vigorous wheat improve early nitrogen uptake. *Aust. J. Agric. Res.* 57, 1097–1107. doi: 10.1071/AR05439

Maddula, V. S. R. K., Zhang, Z., Pierson, E. A., and Pierson, L. S. (2006). Quorum sensing and phenazines are involved in biofilm formation by *Pseudomonas chlororaphis (aureofaciens)* strain 30-84. *Microbial Ecol.* 52, 289–301. doi: 10.1007/s00248-006-9064-6

Maddula, V. S. R. K., Pierson, E. A., and Pierson, L. S. (2008). Altering the ratio of phenazines in *Pseudomonas chlororaphis (aureofaciens)* strain 30-84: effects on biofilm formation and pathogen inhibition. *J. Bacteriol.* 190, 2759–2766. doi: 10.1128/jb.01587-07

Mahmoudi, T. R., Yu, J. M., Liu, S., Pierson, L. S., and Pierson, E. A. (2019). Drought-stress tolerance in wheat seedlings conferred by phenazine-producing rhizobacteria. *Front. Microbiol.* 10, 1590. doi: 10.3389/fmicb.2019.01590

Mahmoudi, T. R. (2017). *Bacterially Mediated Water Stress Tolerance in Wheat Conferred by Phenazine-Producing Rhizobacteria. Master's thesis* (Texas: Texas A&M University). Available at: https://oaktrust.library.tamu.edu/handle/1969.1/173201.

Mavrodi, D. V., Bonsall, R. F., Delaney, S. M., Soule, M. J., Phillips, G., and Thomashow, L. S. (2001). Functional analysis of genes for biosynthesis of pyocyanin and phenazine-1-carboxamide from *Pseudomonas aeruginosa* PAO1. *J. Bacteriol.* 183, 6454–6465. doi: 10.1128/jb.183.21.6454-6465.2001

Mavrodi, D. V., Blankenfeldt, W., and Thomashow, L. S. (2006). Phenazine compounds in Fluorescent *Pseudomonas* Spp. biosynthesis and regulation. *Annu. Rev. Phytopathol.* 44, 417–445. doi: 10.1146/annurev.phyto.44.013106.145710

Mavrodi, D. V., Mavrodi, O. V., Parejko, J. A., Bonsall, R. F., Kwak, Y.-S., Paulitz, T. C., et al. (2012). Accumulation of the antibiotic phenazine-1-carboxylic acid in the rhizosphere of dryland cereals. *Appl. Environ. Microbiol.* 78, 804–812. doi: 10.1128/aem.06784-11

Mazzola, M., Cook, R. J., Thomashow, L. S., Weller, D. M., and Pierson, L. S. (1992). Contribution of phenazine antibiotic biosynthesis to the ecological competence of fluorescent pseudomonads in soil habitats. *Appl. Environ. Microbiol.* 58, 2616–2624. doi: 10.1128/AEM.58.8.2616-2624.1992

Morton, M. J. L., Awlia, M., Al-Tamimi, N., Saade, S., Pailles, Y., Negrão, S., et al. (2019). Salt stress under the scalpel – dissecting the genetics of salt tolerance. *Plant J.* 97, 148–163. doi: 10.1111/tpj.14189

Munns, R., and Rawson, H. M. (1999). Effect of salinity on salt accumulation and reproductive development in the apical meristem of wheat and barley. *Funct. Plant Biol.* 26, 459–464. doi: 10.1071/PP99049

Munns, R., and Tester, M. (2008). Mechanisms of salinity tolerance. *Annu. Rev. Plant Biol.* 59, 651–681. doi: 10.1146/annurev.arplant.59.032607.092911

Munns, R. (2005). Genes and salt tolerance: bringing them together. *New Phytol.* 167, 645–663. doi: 10.1111/j.1469-8137.2005.01487.x

Nadeem, S. M., Ahmad, M., Zahir, Z. A., Javaid, A., and Ashraf, M. (2014). The role of mycorrhizae and plant growth promoting rhizobacteria (PGPR) in improving crop productivity under stressful environments. *Biotechnol. Adv.* 32, 429–448. doi: 10.1016/j.biotechadv.2013.12.005

Naseem, H., and Bano, A. (2014). Role of plant growth-promoting rhizobacteria and their exopolysaccharide in drought tolerance of maize. *J. Plant Interact.* 9, 689–701. doi: 10.1080/17429145.2014.902125

Numan, M., Bashir, S., Khan, Y., Mumtaz, R., Shinwari, Z. K., Khan, A. L., et al. (2018). Plant growth promoting bacteria as an alternative strategy for salt tolerance in plants: A review. *Microbiol. Res.* 209, 21–32. doi: 10.1016/j.micres.2018.02.003

Panta, S., Flowers, T., Lane, P., Doyle, R., Haros, G., and Shabala, S. (2014). Halophyte agriculture: success stories. *Environ. Exp. Bot.* 107, 71–83. doi: 10.1016/j.envexpbot.2014.05.006

Pierson, L. S., and Pierson, E. A. (2010). Metabolism and function of phenazines in bacteria: impacts on the behavior of bacteria in the environment and biotechnological processes. *Appl. Microbiol. Biotechnol.* 86, 1659–1670. doi: 10.1007/s00253-010-2509-3

Price-Whelan, A., Dietrich, L. E. P., and Newman, D. K. (2006). Rethinking 'secondary' metabolism: physiological roles for phenazine antibiotics. *Nat. Chem. Biol.* 2, 71–78. doi: 10.1038/nchembio764

Qadir, M., Quillérou, E., Nangia, V., Murtaza, G., Singh, M., Thomas, R. J., et al. (2014). Economics of salt-induced land degradation and restoration. *Natural Resour. Forum* 38, 282–295. doi: 10.1111/1477-8947.12054

Rajkumar, M., Bruno, L. B., and Banu, J. R. (2017). Alleviation of environmental stress in plants: The role of beneficial *Pseudomonas* spp. *Crit. Rev. Environ. Sci. Technol.* 47 (6), 372–407. doi: 10.1080/10643389.2017.1318619

Ramadoss, D., Lakkineni, V. K., Bose, P., Ali, S., and Annapurna, K. (2013). Mitigation of salt stress in wheat seedlings by halotolerant bacteria isolated from saline habitats. *SpringerPlus* 2, 6. doi: 10.1186/2193-1801-2-6

Reddy, I. N. B. L., Kim, B.-K., Yoon, I.-S., Kim, K.-H., and Kwon, T.-R. (2017). Salt tolerance in rice: focus on mechanisms and approaches. *Rice Sci.* 24, 123–144. doi: 10.1016/j.rsci.2016.09.004

Reinhold-Hurek, B., Bünger, W., Burbano, C. S., Sabale, M., and Hurek, T. (2015). Roots shaping their microbiome: global hotspots for microbial activity. *Annu. Rev. Phytopathol.* 53, 403–424. doi: 10.1146/annurev-phyto-082712-102342

Richards, L. A. (1954). "Diagnosis and improvement of saline alkali soils.". in *US Department of Agriculture, Hand Book 60.* (Washington, D. C.: U. S. Government Printing Office), pp. 160.

Shahid, S. A., Zaman, M., and Heng, L. (2018). "Soil salinity: historical perspectives and a world overview of the problem," in *Guideline for salinity assessment, mitigation and adaptation using nuclear and related techniques*. Eds. M. Zaman, S. A. Shahid and L. Heng (Cham: Springer International Publishing).

Shrivastava, P., and Kumar, R. (2015). Soil salinity: A serious environmental issue and plant growth promoting bacteria as one of the tools for its alleviation. *Saudi J. Biol. Sci.* 22, 123–131. doi: 10.1016/j.sjbs.2014.12.001

Thomashow, L. S., and Weller, D. M. (1988). Role of a phenazine antibiotic from *Pseudomonas fluorescens* in biological control of *Gaeumannomyces graminis var. tritici*. *J. Bacteriol.* 170, 3499–3508. doi: 10.1128/jb.170.8.3499-3508.1988

Wang, Y., Wilks, J. C., Danhorn, T., Ramos, I., Croal, L., and Newman, D. K. (2011). Phenazine-1-carboxylic acid promotes bacterial biofilm development via ferrous iron acquisition. *J. Bacteriol.* 193,14, 3606–3617. doi: 10.1128/JB.00396-11

Wang, D., Yu, J. M., Dorosky, R. J., Pierson, L. S. III, and Pierson, E. A. (2016). The phenazine 2-hydroxy-phenazine-1-carboxylic acid promotes extracellular DNA release and has broad transcriptomic consequences in *Pseudomonas chlororaphis* 30–84. *PloS One* 11, e0148003. doi: 10.1371/journal.pone.0148003

Wood, D. W., Gong, F., Daykin, M. M., Williams, P., and Pierson, L. S.,. 3. (1997). N-acyl-homoserine lactone-mediated regulation of phenazine gene expression by *Pseudomonas aureofaciens* 30-84 in the wheat rhizosphere. *J. Bacteriol.* 179, 7663–7670. doi: 10.1128/jb.179.24.7663-7670.1997

Xiong, Y.-W., Gong, Y., Li, X.-W., Chen, P., Ju, X.-Y., Zhang, C.-M., et al. (2019). Enhancement of growth and salt tolerance of tomato seedlings by a natural halotolerant actinobacterium *Glutamicibacter halophytocola* KLBMP 5180 isolated from a coastal halophyte. *Plant Soil* 445, 307–322. doi: 10.1007/s11104-019-04310-8

Yang, J., Kloepper, J. W., and Ryu, C. M. (2009). Rhizosphere bacteria help plants tolerate abiotic stress. *Trends Plant Sci.* 14, 1–4. doi: 10.1016/j.tplants.2008.10.004

Younis, M. E., El-Shahaby, O. A., Alla, M. M. N., and El-Bastawisy, Z. M. (2003). Kinetin alleviates the influence of waterlogging and salinity on growth and affects the production of plant growth regulators in *Vigna sinensis* and *Zea mays*. *Agronomie* 23, 277–285. doi: 10.1051/agro:2003010

Yu, J. M., Wang, D., Pierson, L. S. III, and Pierson, E. A. (2018a). Effect of Producing Different Phenazines on Bacterial Fitness and Biological Control in *Pseudomonas chlororaphis* 30-84. *Plant Pathol. J.* 34 (1), 30–84. doi: 10.5423/PPJ.FT.12.2017.0277

Yu, J. M., Wang, D., Ries, T. R., Pierson, L. S. III, and Pierson, E. A. (2018b). An upstream sequence modulates phenazine production at the level of transcription and translation in the biological control strain *Pseudomonas chlororaphis* 30-84. *PLoS ONE* 13 (2), e0193063. doi: 10.1371/journal.pone.0193063

Yuan, P., Jauregui, E., Du, L., Tanaka, K., and Poovaiah, B. W. (2017). Calcium signatures and signaling events orchestrate plant–microbe interactions. *Curr. Opin. Plant Biol.* 38, 173–183. doi: 10.1016/j.pbi.2017.06.003

Yuan, P., Du, L., and Poovaiah, B. (2018a). Ca2+/Calmodulin-dependent AtSR1/CAMTA3 plays critical roles in balancing plant growth and immunity. *Int. J. Mol. Sci.* 19, 1764. doi: 10.3390/ijms19061764

Yuan, P., Tanaka, K., Du, L., and Poovaiah, B. W. (2018b). Calcium signaling in plant autoimmunity: a guard model for AtSR1/CAMTA3-mediated immune response. *Mol. Plant* 11, 637–639. doi: 10.1016/j.molp.2018.02.014

Yuan, P., Yang, T., and Poovaiah, B. W. (2018c). Calcium signaling-mediated plant response to cold stress. *Int. J. Mol. Sci.* 19, 3896. doi: 10.3390/ijms19123896

Zelm, Ev, Zhang, Y., and Testerink, C. (2020). Salt tolerance mechanisms of plants. *Annu. Rev. Plant Biol.* 71, 403–433. doi: 10.1146/annurev-arplant-050718-100005

Zhou, L., Jiang, H.-X., Sun, S., Yang, D.-D., Jin, K.-M., Zhang, W., et al. (2016). Biotechnological potential of a rhizosphere *Pseudomonas aeruginosa* strain producing phenazine-1-carboxylic acid and phenazine-1-carboxamide. *World J. Microbiol. Biotechnol.* 32, 50. doi: 10.1007/s11274-015-1987-y

Zhu, J.-K. (2016). Abiotic stress signaling and responses in plants. *Cell* 167, 313–324. doi: 10.1016/j.cell.2016.08.029

Conflict of Interest: The authors declare that the research was conducted in the absence of any commercial or financial relationships that could be construed as a potential conflict of interest.

frontiers in Plant Science

ORIGINAL RESEARCH
published: 04 November 2020
doi: 10.3389/fpls.2020.583539

Trichoderma Counteracts the Challenge of *Phytophthora nicotianae* Infections on Tomato by Modulating Plant Defense Mechanisms and the Expression of Crinkler, Necrosis-Inducing *Phytophthora* Protein 1, and Cellulose-Binding Elicitor Lectin Pathogenic Effectors

Federico La Spada[1], Claudia Stracquadanio[1,2], Mario Riolo[1,2,3], Antonella Pane[1] and Santa Olga Cacciola[1]**

[1] Department of Agriculture, Food and Environment (Di3A), University of Catania, Catania, Italy, [2] Department of Agriculture, University Mediterranea of Reggio Calabria, Reggio Calabria, Italy, [3] Council for Agricultural Research and Agricultural Economy Analysis, Research Centre for Olive, Citrus and Tree Fruit-Rende CS (CREA-OFA), Rende, Italy

OPEN ACCESS

Edited by:
Katharina Pawlowski,
Stockholm University, Sweden

Reviewed by:
Carlos Lucena,
University of Córdoba, Spain
Jianfei Wang,
Anhui University of Science and Technology, China

***Correspondence:**
Antonella Pane
apane@unict.it
Santa Olga Cacciola
olga.cacciola@unict.it

Specialty section:
This article was submitted to Plant Symbiotic Interactions, a section of the journal Frontiers in Plant Science

Received: 15 July 2020
Accepted: 06 October 2020
Published: 04 November 2020

Citation:
La Spada F, Stracquadanio C, Riolo M, Pane A and Cacciola SO (2020) Trichoderma Counteracts the Challenge of Phytophthora nicotianae Infections on Tomato by Modulating Plant Defense Mechanisms and the Expression of Crinkler, Necrosis-Inducing Phytophthora Protein 1, and Cellulose-Binding Elicitor Lectin Pathogenic Effectors. Front. Plant Sci. 11:583539. doi: 10.3389/fpls.2020.583539

Decoding the mechanisms of plant defense against plant pathogens in a scenario where antagonistic activity and the plant growth-promoting effects of useful organisms intervene simultaneously is a new frontier of plant pathology. Here, we demonstrated that (i) two selected strains of *Trichoderma asperellum* and *Trichoderma atroviride* promoted tomato (*Solanum lycopersicum*) growth and reduced the severity of disease caused by the oomycete *Phytophthora nicotianae* and (ii) the genetic patterns of the components of the experimental model system tomato–*Trichoderma* spp.–*P. nicotianae* were differentially expressed. The beneficial effects in both the promotion of the growth of host plant and the biological control of the pathogen by two selected strains of different *Trichoderma* species were tested both *in planta* and *in vitro*. In both respects, *T. atroviride* demonstrated to be more effective than *T. asperellum*. Additionally, the simultaneous transcriptional reprogramming of several plant defense-related genes, pathogen effectors, and mycoparasitism-related genes in tomato, *P. nicotianae*, and *Trichoderma* spp., respectively, was evaluated during the three-component interaction. Results support the hypothesis that *Trichoderma* spp. elicit the expression of plant defense-related genes. As expected, a mycoparasitism-related gene was significantly up-regulated in *Trichoderma*-colonizing tomato plants infected by *P. nicotianae*. Finally, a marked up-regulation of the genes encoding two necrosis-inducing effectors was observed in *P. nicotianae* infecting tomato plants colonized by *Trichoderma*. In conclusion, this study is a contribution toward understanding the genetic pathways

related with the ability of *Trichoderma* spp. to counteract the challenge of *P. nicotianae* infections on tomato. Additionally, the experiments revealed the beneficial effects in the tomato growth promotion of a new *T. atroviride* strain and its good antagonistic effectiveness in the biological control of root and crown rot incited by *P. nicotianae*, confirming that *Trichoderma* spp. can be a powerful tool in integrated pest management strategies of *Phytophthora* diseases of horticultural crops.

Keywords: gene expression, antagonism, *Trichoderma asperellum*, *Trichoderma atroviride*, biological control, root rot, crown rot

INTRODUCTION

In the last years, the biological control agents of plant pathogens, also known as antagonists, have inspired several research projects and the development of new strategies in the management of plant diseases (Ghazanfar et al., 2018).

The use of antagonistic microorganisms in plant protection is a low-risk practice for human health; moreover, the combination of these organisms with reduced levels of fungicides promotes a degree of disease suppression similar to that achieved with treatment using fungicide at normal doses (Monte, 2001; Benítez et al., 2004; Gilardi et al., 2020).

Among plant pathogens, phytopathogenic soil-borne fungi and oomycetes stand out since they are a threat to plant productivity on a global scale for a broad range of crops (Erwin and Ribeiro, 1996; Benítez et al., 2004; Mammella et al., 2011; Cacciola and Gullino, 2019).

The majority of applications of antagonistic microorganisms in the control of soil-borne plant diseases caused by fungal and oomycete pathogens have been conducted by selected strains of *Trichoderma* species (Benítez et al., 2004; Woo et al., 2014; Guzmán-Guzmán et al., 2019). The high effectiveness of *Trichoderma* spp. as biological control agents is due to both their antagonistic activity (Benítez et al., 2004) and the efficiency of these organisms in promoting plant growth and defense mechanisms (Harman et al., 2004; Verma et al., 2007; Shoresh et al., 2010; Singh and Islam, 2010; Tucci et al., 2011). The antagonistic activity of *Trichoderma* spp. can be considered the final result of different mechanisms, direct and indirect, acting synergistically to achieve disease control (Howell, 2003; Benítez et al., 2004). The indirect mechanisms include the competition for nutrients and space and the ability to produce metabolites that either inhibit spore germination, kill the cells (antibiosis), or modify the pH of rhizosphere. The direct interaction between antagonist and pathogen, usually indicated as mycoparasitism, includes both physical contact and the synthesis of hydrolytic enzymes, toxic compounds, and/or antibiotics that act synergistically to kill the pathogen (Benítez et al., 2004). Among hydrolytic enzymes, chitinases are the most relevant in mycoparasitism (Carsolio et al., 1994; Osorio-Hernández et al., 2016). High levels of these enzymes produced by *Trichoderma* spp. have been positively correlated with the inhibition in the growth of both fungi and oomycetes (Osorio-Hernández et al., 2016).

The colonization of the rhizosphere by *Trichoderma* spp. also produces direct positive effects on plants, promoting their growth and activating their defense mechanisms. It is well known that the interaction with microorganisms triggers two main defense mechanisms in plants that protect them against the infection (Shoresh et al., 2005). The first is known as systemic acquired resistance (SAR); this mechanism, which is considered to be triggered by local infection, can provide long-term resistance throughout the plant to subsequent infection by different pathogens. It is correlated with the synthesis of pathogenesis-related (PR) proteins, which is mediated by the up-regulation of genes encoding enzymes involved in the biosynthesis of salicylic acid (SA) (Zhang et al., 2010). The second mechanism, known as induced systemic resistance (ISR) and initially described in plants colonized by non-pathogenic rhizobacteria (Segarra et al., 2007), is correlated with the synthesis of jasmonic acid (JA) and ethylene (ET), which are mediated by the transcription factors MYC2 and ERF (Shoresh et al., 2005). This kind of resistance induces a primed state which enhances defense gene expression in the plant upon subsequent pathogen attack (Segarra et al., 2007). Since *Trichoderma* spp. are able to activate both kinds of resistances, the current hypothesis is that plants initially perceive their root colonization as a potential pathogen attack and then react with the activation of ISR mechanisms (Shoresh et al., 2005; Tucci et al., 2011).

Plant defensive mechanisms also comprise the synthesis of protective molecules acting directly against the pathogen; these include plant defensins, a family of small cationic peptides widely distributed among all plant families (Cui et al., 2018). These antimicrobial peptides proved to be very effective in the inhibition on the growth of pathogens (Lay and Anderson, 2005; Seo et al., 2014). Antifungal defensins have been identified in radish (Terras et al., 1992), pea (Mendenhall and Hodge, 1998; Almeida et al., 2000; Lobo et al., 2007; Gonçalves et al., 2012), and tomato (Cui et al., 2018). The sequencing of the whole genome of tomato (Sato et al., 2012) makes this plant a good model system for the study of plant-microorganisms interaction (Cui et al., 2018). With more than 75,000 ha, tomato is the most widely cultivated vegetable crop in Italy (ISTAT, 2020). Globally, among horticultural products, tomato ranks third for volumes of production–after potato and sweet potato–and first in terms of processing volumes (Brasesco et al., 2019). Tomato is susceptible to numerous diseases (Jones et al., 2016), among which root and crown rot incited by *Phytophthora* species represent one of the most important causes of yield losses (Erwin and Ribeiro, 1996; Jones et al., 2016). Several *Phytophthora* spp., including *Phytophthora capsici*, *Phytophthora cryptogea*, *Phytophthora drechsleri*, *Phytophthora infestans*, and

Phytophthora nicotianae, have been reported to infect tomato worldwide (Pane et al., 2000; Jones et al., 2016). In Italy, *P. nicotianae* is the main species associated with the disease (Garibaldi and Gullino, 2010). *P. nicotianae* is worldwide recognized as one of the most devastating oomycete plant pathogens with a very broad host range of more than 255 plant species, including model plants such as *Nicotiana tabacum* and *Arabidopsis thaliana* (Kamoun et al., 2015; Panabières et al., 2016). The progress in the knowledge of the genomics of *P. nicotianae* makes it a suitable model to understand the molecular basis of pathogenesis of oomycete plant pathogens (Meng et al., 2014).

Plant pathogens secrete arsenals of proteins (effectors) that enable parasitic infection and reproduction (Birch et al., 2006; Stassen and Van den Ackerveken, 2011). Plants recognize the initial pathogen-associated molecular pattern (PAMPs) signals and activate pattern-triggered immunity (PTI) to counteract the further colonization by the pathogen. Successful pathogens have developed wide effector repertoires that not only function directly as toxins to induce plant cell death but can also suppress PTI and trigger susceptibility of the plant (Jones and Dangl, 2006). *Phytophthora* species also secrete a large array of effectors during infection of the plant hosts (Stam et al., 2013). Effectors of several species of *Phytophthora* have been identified (Chepsergon et al., 2020; McGowan et al., 2020). Among these, the *Crinkler* (CRN) proteins are a family of effectors that cause necrosis in the cells of the host and also induce further intracellular effectors that target the host nucleus during infection (Stam et al., 2013). The necrosis-inducing *Phytophthora* protein 1 (NPP1) is another important *Phytophthora* effector which has been associated with the induction of necrosis in parsley, *A. thaliana*, and potato (Fellbrich et al., 2002; Gijzen and Nürnberger, 2006). After artificial infiltration, this protein has also been observed to induce the transcription of PR-genes in *A. thaliana* leaves (Fellbrich et al., 2002). An additional important group of effectors includes cell wall glycoproteins named cellulose-binding elicitor lectin (CBEL); they have been found localized in the inner and outer layers of the *Phytophthora* mycelium cell walls and are present in close contact with the host cell during infection (Séjalon et al., 1995). Previous studies carried out on tobacco demonstrated that artificial infiltration with CBEL results in local necrosis of the infiltrated area and the induction of an array of defense responses (Séjalon-Delmas et al., 1997).

As a consequence of the restrictions in the use of synthetic fungicides due to their toxicity to humans and animals as well as to their environmental impact, there has been growing interest in alternative approaches to chemical control of *P. nicotianae*, including the application of biocontrol agents (Singh and Islam, 2010; Gilardi et al., 2014a,b). Although the genomics of the infection process of host plants by *Phytophthora* spp. as well as the plant root colonization process and the mycoparasitism of fungal pathogens by *Trichoderma* spp. has been extensively investigated (Kubicek et al., 2011; Atanasova et al., 2013; Meng et al., 2014; Crutcher et al., 2015; Guzmán-Guzmán et al., 2017; Köhl et al., 2019; Morán-Diez et al., 2019; Ramírez-Valdespino et al., 2019; Chepsergon et al., 2020; Pachauri et al., 2020; Wang et al., 2020), there is limited information on the complex interaction of plant-beneficial antagonistic microorganism-pathogen, as analyzed in a comprehensive experimental workflow considering together physiological effects, metabolic pathways, and genes involved in this tripartite interaction (**Figure 1**).

To gain a better understanding of the events involved in the plant-microorganisms interaction, this study focuses on (i) the evaluation of the ability of two selected strains of *Trichoderma asperellum* and *Trichoderma atroviride* to promote the growth of *Solanum lycopersicum* and control root and crown rot incited by *P. nicotianae* and (ii) the identification of the main differentially expressed genes and metabolic pathways activated as a consequence of tripartite interaction in the experimental system tomato–*Trichoderma* spp.–*P. nicotianae*.

MATERIALS AND METHODS

Fungal Isolates

The pathogen *P. nicotianae*, strain Ph_nic, was sourced from roots of a symptomatic plant of a local cultivar of *S. lycopersicum* in a nursery in Sicily. For the isolation, infected roots were firstly separated from the stem of the plant and washed with distilled water; then, washed roots were blotted dry and plated on selective PARPNH V8-agar (Jung et al., 2019) and examined

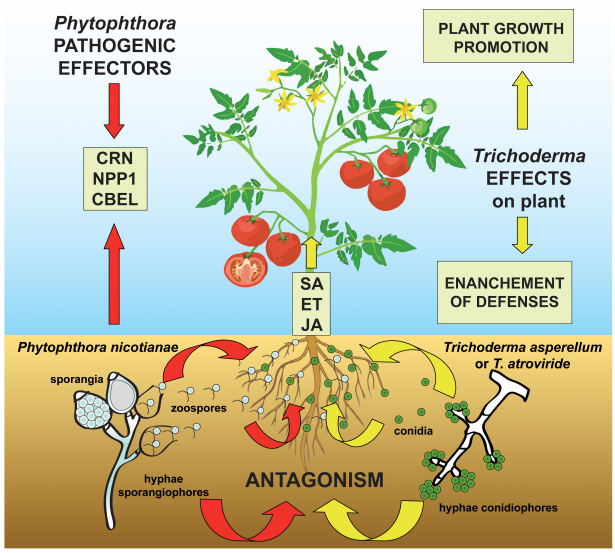

FIGURE 1 | Proposed model for the three-way system plant-pathogen-antagonist showing how *Trichoderma* species can modulate the molecular signaling in the challenge between the oomycete pathogen *Phytophthora nicotianae* and the host plant tomato. The colonization of the tomato rhizosphere by *Trichoderma* spp. triggers both growth promotional effects and plant defense mechanisms by the elicitation of salicylic acid (SA)-, ethylene (ET)-, and jasmonic acid (JA)-dependent processes. At the same time, the *P. nicotianae*-parasitic infection process is mediated by the secretion of pathogenic effectors (including *Crinkler*–CRN–proteins, the necrosis-inducing *Phytophthora* protein 1–NPP1, and cellulose-binding elicitor lectin–CBEL–glycoproteins) which act to suppress the ET- and JA-plant response and whose synthesis is modified by the antagonistic interaction with *Trichoderma* spp.

under a stereomicroscope for the presence of *Phytophthora*-like coenocytic hyphae after 48 h of incubation at 28°C in the dark. Then, pieces cut from the advancing margins of the colony were sub-cultured on V8-agar Petri dishes and incubated at 28°C in the dark for a week. Purified cultures were finally obtained by single hyphal culture on V8-agar.

The antagonist *T. asperellum* strain IMI393899 (Puglisi et al., 2012; Cacciola et al., 2015), previously identified as *Trichoderma harzianum*, belonged to the collection of the Molecular Plant Pathology Laboratory (MPPL); Department of Agriculture, Food, and Environment (Di3A); University of Catania, while the *T. atroviride*, isolate TS, was obtained from the parasitized basidiocarp of a specimen of *Ganoderma lucidum* collected in Apulia (southern Italy). For the isolation of *T. atroviride*, infected tissues from the parasitized basidiocarp of *G. lucidum* were excised in 5-mm fragments, disinfected with 1% NaClO for 2 min, rinsed in sterile distilled water, and plated on Potato Dextrose Agar (PDA) amended with streptomycin sulfate at the concentration of 0.25 g/l. After 24 h of incubation at 25°C in the dark, growing colonies were sub-cultured on PDA plates. Purified cultures were finally obtained by single spore culture on PDA medium.

Molecular Identification of Fungal and Oomycete Isolates

The identification of the isolates of *P. nicotianae* and *T. atroviride* was carried out by the amplification and analysis of the internal transcribed spacer (ITS) regions of the ribosomal DNA (rDNA). In this study, the DNA was extracted by using PowerPlant® Pro DNA Isolation Kit following the manufacturer's instructions. The amplifications of the ITS regions of the rDNA of *Phytophthora* and *Trichoderma* isolates were performed by using the *Taq* DNA polymerase, recombinant (Invitrogen™) with the universal primer pairs ITS-6 (5′-GAAGGTGAAGTCGTAACAAGG-3′) (Cooke et al., 2000) and ITS-4 (5′-TCCTCCGCTTATTGATATGC-3′) (White et al., 1990) and ITS-5 (5′-GGAAGTAAAAGTCGTAACAAGG-3′) (White et al., 1990) and ITS-4, respectively. The PCR amplifications were carried out in a 25-μl reaction mix containing PCR buffer (1×), dNTP mix (0.2 mM), MgCl2 (1.5 mM), forward and reverse primers (0.5 μM each), *Taq* DNA polymerase (1 U), and 100 ng of DNA. The thermocycler conditions were as follows: 94°C for 3 min; followed by 35 cycles of 94°C for 30 s, 55°C for 30 s, and 72°C for 30 s; and then 72°C for 10 min. Obtained amplicons were detected in 1% agarose gel and sequenced in both directions by an external service (Macrogen). Obtained sequences were analyzed by using FinchTV v.1.4.0[1]. For species identification, blast searches in GenBank[2] were performed.

Two representative isolates, namely, Ph_nic (*P. nicotianae*) and TS (*T. atroviride*), were randomly selected for further experimentations. *T. asperellum* strain IMI393899 had been previously identified (Puglisi et al., 2012; Cacciola et al., 2015) with the same procedure used for *T. atroviride* and stored in the collection of MPPL, Di3A.

[1]https://digitalworldbiology.com/FinchTV

[2]http://www.ncbi.nlm.nih.gov/BLAST/

Treatment of Tomato Plants With *Trichoderma* Strains

In order to investigate the plant growth-promoting effect and induction of resistance to the pathogen infection by the symbiotic interaction with *Trichoderma* spp., tomato plants were grown in association with the selected *Trichoderma* strains at the root system.

The *Trichoderma*-tomato interaction was established in accordance with the method described by Tucci et al. (2011). Seeds of *S. lycopersicum* cv. Cuor di bue (Vilmorin Italia S.R.L., Funo, Bologna, Italy) were sterilized in 2% NaClO for 20 min, rinsed in sterile distilled water, and incubated in a conidial suspension (10^6 conidia/ml) of either IMI393899 or TS; control seeds were suspended in water. Both treated and control seeds were air dried for 24 h and then sown in sterilized universal soil (©Cifo Srl, Giorgio di Piano, Bologna, Italy) in 40-well polystyrene trays and maintained in a growth chamber at 23°C, 80% relative humidity, and a photoperiod of 16 h of light and 8 h of dark. After 22 days, seedlings were transplanted in 200-cm^3 plastic pots in sterilized universal soil. The positive-root colonization by *Trichoderma* was verified by re-isolation on PDA from roots of additional tomato control plants; the identity of the purified cultures of the *Trichoderma* strains was confirmed by PCR amplification and sequencing of their ITS region. These tomato plants will be called "*Trichoderma*-treated plants" in the text.

Growth Promotion of Tomato Plants

Twenty-two-day-old tomato seedlings were grown with either strain IMI393899 of *T. asperellum* or strain TS of *T. atroviride*, which colonized the root systems and were grown for 12 weeks in a growth chamber at 23°C, 80% relative humidity, and a photoperiod of 16 h of light and 8 h of dark. Untreated seedlings (controls) were grown in the same conditions. A normal weekly irrigation was also provided.

The experimental set-up consisted of three treatments with 10 repetitions each: (i) untreated tomato plants (controls), (ii) tomato plants grown with *T. asperellum* strain IMI393899, and (iii) tomato plants grown with *T. atroviride* strain TS.

The promotion of the plant growth of "*Trichoderma*-treated plants" was then evaluated as follows: (i) weekly stem growth rate (cm/week), (ii) seedling total length, (iii) fresh root weight, and (iv) length at the end of the test (i.e., 12 weeks after the transplanting). All data were analyzed by using one-way ANOVA followed by Tukey's honestly significant difference (HSD) test as a *post hoc* test (R software). Differences at $P \leq 0.05$ were considered significant.

At the end of the test, *T. asperellum* strain IMI393899 and *T. atroviride* strain TS were re-isolated from roots of tomato plants from the respective treatments and then sequenced.

Biological Control of *Phytophthora nicotianae*

In vitro Antagonistic Ability

The selected strains of *T. asperellum* and *T. atroviride* were screened for their ability to inhibit the mycelial growth (%) of

P. nicotianae strain Ph_nic by *in vitro* dual culture assays. The formula applied was as follows:

$$\text{Inhibition of growth } (\%) = \left(\frac{X - Y}{X}\right) \cdot 100$$

where,

X = growth of pathogen alone without antagonist (control) and

Y = growth of pathogen along with the antagonist.

The dual culture test was carried out in 90-mm Petri dishes with 20 ml of PDA by placing 5-mm diameter agar plugs of the pathogen and antagonists taken from the margin of 1-week-old colonies grown on V8-agar and PDA, respectively. The dual culture was set by placing the pathogen and the antagonist 4 cm apart from each other. Furthermore, since the daily radial growth rate of the *P. nicotianae* strain Ph_nic was significantly lower than that of *Trichoderma* isolates, *P. nicotianae* was plated 72 h before the *Trichoderma* sp. Single cultures of the pathogen were used as control. Plates were incubated at 28°C in the dark, and radial mycelial growth was measured when *P. nicotianae* mycelium of control cultures covered the whole Petri dishes (namely, 13 days after incubation). Overall, the experimental set-up consisted of the following three treatments (including controls) made of 10 replicates each: (i) *P. nicotianae* isolate Ph_nic, (ii) *P. nicotianae* isolate Ph_nic + *T. asperellum* strain IMI393899, and (iii) *P. nicotianae* isolate Ph_nic + *T. atroviride* strain TS.

Data from the inhibition of the growth (%) of *P. nicotianae* 13 days from the beginning of the trial were analyzed by using one-way ANOVA followed by Tukey's HSD test as a *post hoc* test (R software). Differences at $P \leq 0.05$ were considered significant.

In planta Antagonistic Ability

The *in planta* antagonistic ability of *T. asperellum* strain IMI393899 and *T. atroviride* strain TS toward *P. nicotianae*, strain Ph_nic, was demonstrated on tomato plants in a soil infestation test. Inoculum consisted of 12-day-old culture of the isolate Ph_nic grown at 25°C in a 750-ml jar containing 140 ml autoclaved V8-juice broth (200 ml/l juice and 800 ml/l distilled water amended with 3 g/l CaCO3) (Jung et al., 1996) and 170 ml of millet seeds. This experimental trial was carried out in two different steps which included a double treatment with the *Trichoderma* strains.

First Step

For the test, 4-month-old potted plants of *S. lycopersicum* cv. Cuor di bue, grown in sterilized universal soil with either *T. asperellum* strain IMI393899 or *T. atroviride* strain TS, in association with the root system ("*Trichoderma*-treated tomato seedlings"), were transplanted into 1,000-cm^3 pots filled with a mixture of sterilized soil and the inoculum of Ph_nic prepared as described above (20 cm^2 of inoculum per 1,000 cm^3 of potting mixture). Untreated plants (controls) were not grown in association with *Trichoderma* strains; they were transplanted into pots filled with a mixture of sterilized soil and non-infested millet seed/V8-juice medium at the same rate.

Second Step

After transplanting, additional 100 ml of a conidial suspension (10^6 conidia/ml) from *T. asperellum* IMI393899 and *T. atroviride* TS were provided to each plant from respective *Trichoderma* pre-treatment. All plants were then irrigated and maintained in a growth chamber at 23°C, 80% relative humidity, and a photoperiodic lighting of 16 h of light and 8 h of dark; a normal irrigation was also provided twice per week.

Overall, the experimental assay consisted of the following six treatments: (i) untreated tomato plants transplanted in a non-infested potting mixture (NI-PM); (ii) untreated tomato plants inoculated with infested potting mixture (I-PM); (iii) tomato plants treated with *T. asperellum* strain IMI393899 and transplanted in NI-PM; (iv) tomato plants treated with *T. asperellum* strain IMI393899 and transplanted in I-PM; (v) tomato plants treated with *T. atroviride* strain TS and transplanted in NI-PM; and (vi) tomato plants treated with *T. atroviride* strain TS and transplanted in I-PM. Each treatment included 10 replicates. The test was considered completed when plants of treatment (ii) showed severe symptoms of decay (i.e., 15 days after inoculation).

Plant damage was assessed on the basis of three different parameters: (i) wilting severity, visually evaluated in accordance with the empirical scale reported by Engelbrecht et al. (2007); (ii) fresh root weight; and (iii) fresh root length; the last two parameters were determined by separating the root system from the rest of the plant. The empirical scale used to rate the severity of wilting included the following values: 1 = normal (not wilted)–no signs of wilting or drought stress; 2 = slightly wilted–slight leaf angle changes but no folding, rolling, or changes in leaf surface structure; 3 = wilted–strong leaf angle change or protrusion of veins on the leaf surface but no cell death; 4 = severely wilted–very strong change of leaf angle or protrusion of veins on the leaf surface with initial necrosis; 5 = nearly dead–most leaves necrotic, some young leaves still green near the midrib, and leaf angles mostly near 0; 6 = dead–all above-ground parts dead.

At the end of the test, *T. asperellum* strain IMI393899, *T. atroviride* strain TS, and *P. nicotianae* isolate Ph_nic were re-isolated from plants of respective treatments and their identity was confirmed by PCR amplification and sequencing of their ITS region.

Data were analyzed by using one-way ANOVA followed by Tukey's HSD test as a *post hoc* test (R software). Differences at $P \leq 0.05$ were considered significant.

Gene Expression in the Three-Way System Tomato–*Trichoderma* spp.–*Phytophthora nicotianae* Assay

Fungal Isolates

Trichoderma asperellum strain IMI393899 and *T. atroviride* strain TS were cultured on PDA for 7 days at 25°C, while *P. nicotianae* isolate Ph_nic was cultured in Petri dishes on V8-agar for 1 week at 28°C in the dark.

Tomato Plants

Tomato seeds (*S. lycopersicum* cv. Cuor di bue–Vilmorin Italia S.R.L., Funo, Bologna, Italy) were sterilized in 2% NaClO for 20 min, rinsed in sterile distilled water, and sown in an alveolar tray containing sterile vermiculite soaked in a nutrient solution (NS) prepared in accordance with Guérin et al. (2014) and Lebreton et al. (2018) with the following modifications: fertilizer 20-20-20 (Asso di Fiori-Cifo, S. Giorgio di Piano, Bologna, Italy) (0.1634 g/l), $MgSO_4 \times 7H_2O$ (0.15 g/l), FeNa-EDTA (40 mg/l). Trays were kept for 3 days in the dark at 23°C and 80% relative humidity; then, seedlings were transferred to a photoperiodic lighting (16 h of light:8 h of dark) and kept at the same temperature conditions and relative humidity for 30 days. Moreover, 30 ml of NS were provided once a week to renew the content of mineral salts; tomato plantlets were also watered twice a week. Seedlings were then transferred into plastic tubes containing 30 ml of NS.

Trichoderma spp. Colonization Assay

Thirty-day-old tomato seedlings growing in the aforementioned plastic tubes were treated with 300 μl of a suspension of germinated conidia (100 conidia/ml) of *T. asperellum* strain IMI393899 and *T. atroviride* strain TS. The suspension of germinated conidia of *Trichoderma* spp. was prepared as reported in Yedidia et al. (1999) with the following modifications: two flasks containing 100 ml each of a synthetic medium consisting of the aforementioned NS amended with 15 g/l of sucrose were autoclaved and then inoculated with 1 ml of conidial suspension (10^6 conidia/ml) of each *Trichoderma* obtained from 7-day-old cultures grown on PDA medium; flasks were then shaken at 150 rpm for 24 h at 25°C to allow spore germination; after 24 h, tubes containing tomato seedlings were inoculated with 300 μl of the suspension of germinated conidia. Controls were inoculated with the NS amended with 15 g/l of sucrose.

Phytophthora nicotianae Infection Assay

Forty-eight hours after the treatment with *Trichoderma* spp., tomato seedlings were inoculated with zoospores of *P. nicotianae* (concentration: 100 zoospores/ml). *P. nicotianae* inoculum was prepared as follows: mycelial plugs from a 7-day-old culture of *P. nicotianae* grown on V8-agar were flooded with 20 ml of sterile distilled water and incubated at 25°C for 48 h under a constant fluorescent light. Zoospores were released in sterile distilled water by mature sporangia by placing mycelial plugs at 6°C for 1 h followed by another hour at 25°C. Zoospore concentration was measured by using a hemocytometer. Controls were inoculated with sterile distilled water.

Experimental Assay

Overall, the experimental assay consisted of the following six treatments: (i) untreated tomato seedlings; (ii) untreated tomato seedlings inoculated with *P. nicotianae* isolate Ph_nic; (iii) "*Trichoderma*-treated tomato seedlings" with *T. asperellum* strain IMI393899; (iv) "*Trichoderma*-treated tomato seedlings" with *T. atroviride* strain TS; (v) "*Trichoderma*-treated tomato seedlings" with *T. asperellum* strain IMI393899 and inoculated with *P. nicotianae* Ph_nic; and (vi) "*Trichoderma*-treated tomato seedlings" with *T. atroviride* strain TS and inoculated with *P. nicotianae* isolate Ph_nic. Each treatment was made up of six replicates. The test was considered completed (7 days after the inoculation of *P. nicotianae*) when seedlings of treatment (ii) showed severe symptoms of disease.

At the end of the test, seedlings from each treatment were collected and immediately frozen in liquid nitrogen and stored at −80°C. At the end of the test, *T. asperellum* strain IMI393899, *T. atroviride* strain TS, and *P. nicotianae* isolate Ph_nic were re-isolated and then sequenced, from additional seedlings from respective treatments.

RNA Isolation From Colonized Tomato Seedlings and cDNA Synthesis

Total RNA was extracted by using RNeasy Plant Mini Kit (Qiagen, Hilden, Germany) from frozen stem and roots from tomato seedlings (100 mg) ground to a fine powder with liquid nitrogen, following the protocol of the manufacturer and treated with TURBO DNA-free™ Kit. RNA concentration was then adjusted to 200 ng/μl, and its quality was verified by performing a denaturing RNA electrophoresis gel in TAE agarose (Masek et al., 2005). Reverse transcription was performed by using High-Capacity cDNA Reverse Transcription Kit (Applied Biosystems™, Foster City, CA, United States) following the manufacturer's instructions.

Selection of Genes and Development of Specific Primers

Several genes from tomato, *Trichoderma* spp., and *P. nicotianae* involved in the tripartite interaction plant-antagonist-pathogen were selected (**Supplementary Table S1**). Both housekeeping and target genes from tomato and *P. nicotianae* were selected from previous studies (Tucci et al., 2011; Cui et al., 2018; Dalio et al., 2018). An NCBI nucleotide database[3] search was carried out to select specific sequences from both endochitinase and housekeeping genes in *Trichoderma* spp. In order to obtain the highest primer specificity, sequences of genes LOC101262163, PR1b1, TomLoxA, SlyDF2, PpCRN4, PpCBEL4, PpNPP1.1, PpNPP1.3, PpNPP1.4, EF-1α, chi42, Gp_dh_N, and CHI18-5 (**Supplementary Table S1**) were directly derived from the respective genomic region as reported in the GenBank "whole genome shotgun sequencing project" of the respective organism (GenBank accession numbers: AEKE00000000.3–Tomato; MBGH00000000.1–*T. asperellum*; ABDG00000000.2–*T. atroviride*; AVGE00000000.1–*P. nicotianae*), and respective primer pairs were designed by using the Primer BLAST NCBI tool[4]; specificity of all selected primers was tested both by *in silico* (by using the Primer BLAST NCBI tool) and PCR amplification and sequencing of the target region.

Quantitative Real-Time PCR Analysis of Gene Expression

Amplifications were performed by using the iCycler iQ™ Real-Time PCR Detection System (Bio-Rad). Reactions were

[3]https://www.ncbi.nlm.nih.gov/nucleotide/

[4]https://www.ncbi.nlm.nih.gov/tools/primer-blast/

performed in a total volume of 20 µl by mixing 10 ng of cDNA with 1 µl of 10 µM of each primer and 10 µl of PowerUp™ SYBR™ Green Master Mix (2×) (Applied Biosystems). Quantitative real-time PCR (qRT-PCR) experiments were carried out in triplicate. The thermo-cycling conditions were 2 min at 50°C (UDG activation) and 2 min at 95°C (Dual-Lock™ DNA polymerase) followed by 40 cycles of two steps: 95°C for 15 s (denaturation) and 59°C or 60°C (annealing/extension) for 1 min. The quantification of gene expression was carried out by using the $2^{-\Delta\Delta Ct}$ method (Livak and Schmittgen, 2001). For each organism involved in the experiments, calibrator samples were represented by six replicates of the following: (i) untreated tomato seedling control samples and 7-day-old cultures of (ii) *P. nicotianae* isolate Ph_nic, (iii) *T. asperellum* strain IMI393899, and (iv) *T. atroviride* strain TS grown on NS-agarized medium (16 g/l of agar) amended with 15 g/l of sucrose.

The PCR efficiency was checked by standard curve Ct values vs. log (cDNA dilution). Curves were constructed by serial 10-fold dilution of cDNA for each primer pair; linear equations, determination coefficients (R^2), and reaction efficiencies are given in **Supplementary Table S2**.

Data on gene expression were analyzed by using one-way ANOVA followed by Dunnett's multiple comparisons test by using R software. Differences at $P \leq 0.05$ were considered significant.

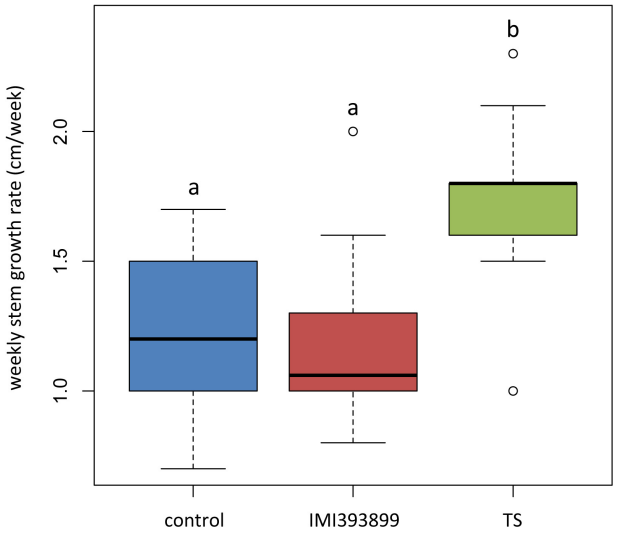

FIGURE 2 | Effects of *Trichoderma asperellum* IMI393899 and *Trichoderma atroviride* TS treatments on the growth of *Solanum lycopersicum* cv. Cuor di bue seedlings. Weekly stem growth rate. Open and gray circles represent outliers and mean value data, respectively. Values sharing same letters are not statistically different according to Tukey's honestly significant difference (HSD) test ($P \leq 0.05$).

RESULTS

Growth Promotion Assay

Results from growth promotion test showed that the growth of plants treated with *T. atroviride* strain TS was significantly stimulated compared with *T. asperellum* IMI393899-treated plants and untreated control plants (**Figure 2**). Overall, the weekly shoot growth of plants treated with *T. atroviride* strain TS was on average ca. 0.5 cm more than both the untreated and *T. asperellum*-treated plants, while the weekly shoot growth of *T. asperellum*-treated plants did not differ statistically from the untreated control (**Figure 2**).

The same attitude in growth promotion was also confirmed by values of root length and fresh weight (**Figures 3A,B**). Overall, the treatment with *T. asperellum* IMI393899 reduced the growth of the root system of the plants, while plants treated with *T. atroviride* strain TS did not differ from the untreated control. The same trend was also observed for the total length of seedlings (**Figure 4**).

Biological Control of *Phytophthora nicotianae*

In vitro Antagonistic Ability

Results from dual culture trial showed that both *Trichoderma*-tested isolates had an antagonistic effect on the growth of *P. nicotianae* (**Table 1**). In particular, the *T. atroviride* strain TS was more effective and inhibited the *P. nicotianae* growth by 63.50%, while *T. asperellum* strain IMI393899 inhibited the growth of *P. nicotianae* by 58.77% (differences between means were significant).

In planta Antagonistic Ability

At the end of the trial, both untreated plants and plants treated with *Trichoderma* spp. and transplanted into non-infested potting mixture (NI-PM), namely, those from treatments (i), (iii), and (v), were substantially asymptomatic showing a mean rating of wilting of 1.60, 1.60, and 1.30, respectively (**Figure 5**) (differences among means were not significant). They also showed a healthy root system, with the only exception of plants treated with *T. asperellum* IMI393899 that showed a statistically significant reduction of fresh weight and length compared with untreated controls (**Figures 6A,B**).

Plants inoculated with infested potting mixture (I-PM) showed severe symptoms of wilting (**Figure 5**) and a substantial reduction of root system (**Figures 6A,B**). However, the treatment with *T. atroviride* TS and *T. asperellum* IMI393899, with 40 and 60% of plant mortality, respectively, significantly reduced the mortality over untreated control plants (90% of mortality). Similarly, plants treated with *T. atroviride* TS and *T. asperellum* IMI393899 showed significant higher values of fresh root weight and length than untreated controls. However, overall, *T. atroviride* TS was more effective than *T. asperellum* IMI393899 in preventing root rot (**Figures 6A,B**).

Gene Expression Levels in the Tripartite Interaction Tomato–*Trichoderma* spp.–*Phytophthora nicotianae*

Differences in the Expression of Tomato Defense-Related Genes

The defense mechanisms activated by tomato plants upon the simultaneous colonization of the root system by a root pathogen

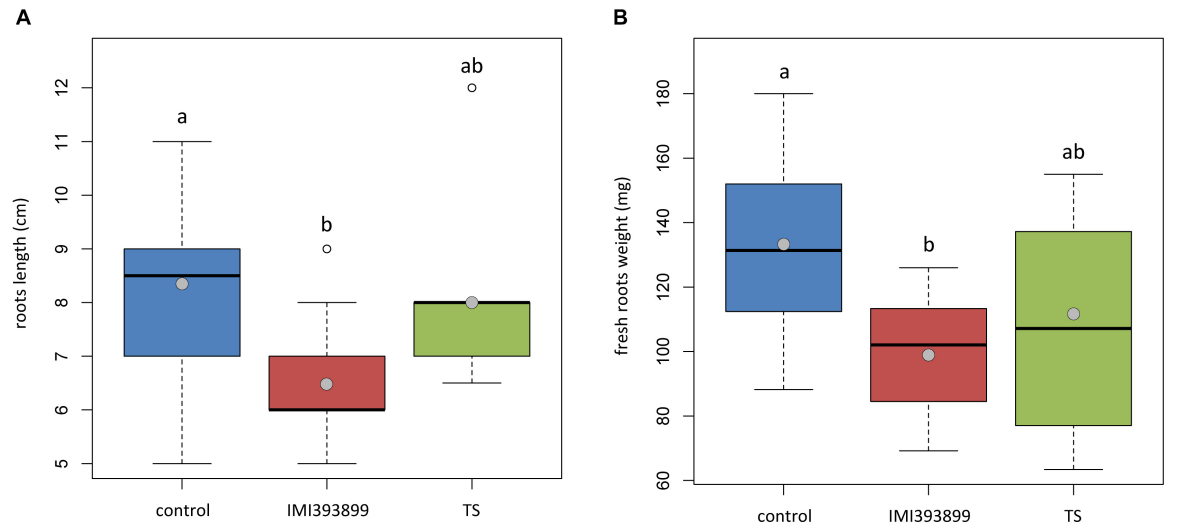

FIGURE 3 | Effects of *Trichoderma asperellum* IMI393899 and *Trichoderma atroviride* TS treatments on the growth of *Solanum lycopersicum* cv. Cuor di bue seedlings. **(A)** Stem length and **(B)** fresh root weight at the end of the test. Open and gray circles represent outliers and mean value data, respectively. Values sharing same letters are not statistically different according to Tukey's honestly significant difference (HSD) test ($P \leq 0.05$).

(*P. nicotianae*) and biocontrol agents (*Trichoderma* spp.) were evaluated on the basis of the expression of genes involved in the main plant defense pathways, namely, SA (i.e., PR proteins–*PR1b1* and *PR-P2*-encoding genes), JA (i.e., lipoxygenases enzymes–*TomLoxC* and *TomLoxA*-encoding genes), and a tomato plant defensin protein (i.e., *SlyDF2*-encoding gene) usually strongly involved in the tomato-*Phytophthora* sp. infection process (Cui et al., 2018; **Figure 7**).

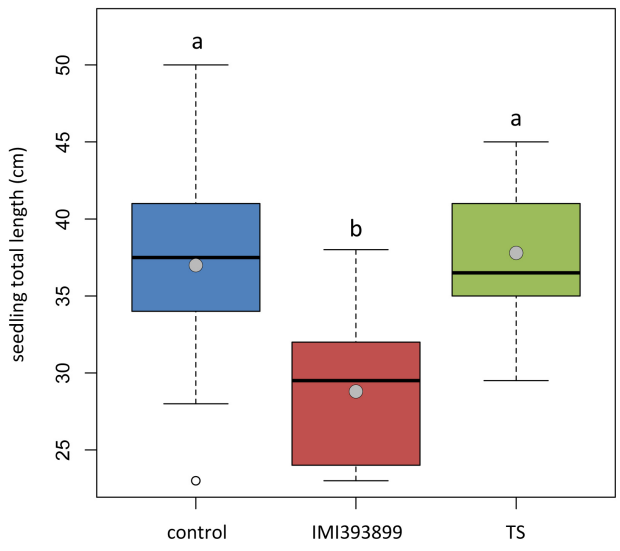

FIGURE 4 | Effects of *Trichoderma asperellum* IMI393899 and *Trichoderma atroviride* TS treatments on the growth of *Solanum lycopersicum* cv. Cuor di bue seedlings. Seedling total length at the end of the test. Open and gray circles represent outliers and mean value data, respectively. Values sharing same letters are not statistically different according to Tukey's honestly significant difference (HSD) test ($P \leq 0.05$).

Statistically significant reprogramming in the gene expression was observed for *PR1b1*, *PR-P2*, and *SlyDF2* in treatments that included the inoculation with the pathogen. PR1b1 was up-regulated in treatments (ii) (i.e., untreated tomato seedlings inoculated with *P. nicotianae* isolate Ph_nic) and (vi) (i.e., tomato seedlings treated with *T. atroviride* strain TS and inoculated with *P. nicotianae* isolate Ph_nic). *PR-P2* was strongly up-regulated in treatment (ii), while showed a lower up-regulation in treatments (v) (i.e., tomato seedlings treated with *T. asperellum* strain IMI393899 and inoculated with *P. nicotianae* Ph_nic) and (vi). Similarly, the tomato defensin *SlyDF2* was up-regulated only in treatments (ii), (v), and (vi). Both lipoxygenase-encoding genes (i.e., *TomLoxC* and *TomLoxA*) were expressed at similar levels in all treatments.

Differences in the Expression of *Phytophthora nicotianae* Pathogenic Effectors

The effector expression of *P. nicotianae* was evaluated as differences in the relative expression levels of effector genes from different families: CRinkling and Necrosis effector PpCRN4; CBEL PpCBEL4; and three different members of the NEP1-like necrosis-inducing proteins PpNPP1.1, PpNPP1.3, and PpNPP1.4 (**Figure 8**).

Statistically significant differences were observed in the levels of all the effectors; both the *PpCRN4* and *PpCBEL4* genes were up-regulated only in untreated and inoculated seedlings [i.e., treatment (ii)], while were normally expressed on seedlings inoculated with the pathogen after being treated with TS of *T. atroviride* and IMI393899 of *T. asperellum* [i.e., treatments (v) and (vi), respectively]. Referring to the necrosis-inducing *Phytophthora* protein-encoding genes, *PpNPP1.1* showed a strong up-regulation in treatments (v), "*Trichoderma*-treated

TABLE 1 | *In vitro* antagonistic ability of *Trichoderma asperellum IMI393899* and *Trichoderma atroviride* test strains against *Phytophthora nicotianae* isolate Ph_nic.

Treatments	Mean mycelial radius of *P. nicotianae* (cm) ± standard deviations (SD)	Mean mycelial radius of *Trichoderma* sp. (cm) ± (SD)	Mean% of inhibition in growth ± (SD)
Trichoderma asperellum strain IMI393899	1.48 ± 0.10	2.50 ± 0.10	58.77 ± 2.80 a
Trichoderma atroviride strain TS	1.31 ± 0.08	2.69 ± 0,08	63.50 ± 1.93 b
Phytophthora nicotianae isolate Ph_nic	3.59 ± 0.00	–	–

In the fourth column, values with different letters are statistically different according to Tukey's honestly significant difference (HSD) test ($P \leq 0.05$).

seedlings" with IMI393899 and inoculated with Ph_nic, and (vi), tomato seedlings treated with *T. atroviride* strain TS and inoculated with *P. nicotianae* isolate Ph_nic. On the contrary, *PpNPP1.3* was down-regulated in treatment (ii) and up-regulated in treatments (v) and (vi). Finally, *PpNPP1.4* was down-regulated in untreated seedlings and in treatment (v), "*Trichoderma*-treated seedlings" with IMI393899 and inoculated with Ph_nic.

Differences in the Expression of *Trichoderma* Antagonistic-Related Gene

The mycoparasitism of both *Trichoderma* test strains was assessed based on the differential expression of gene encoding for chitinases (i.e., *CHI18-5*-encoding gene for *T. atroviride*; *chi42*-encoding gene for *T. asperellum*). As expected, both *Trichoderma* strains up-regulated the respective selected endochitinase-encoding gene exclusively in the treatment with *Phytophthora*-inoculated seedlings (**Figure 9**).

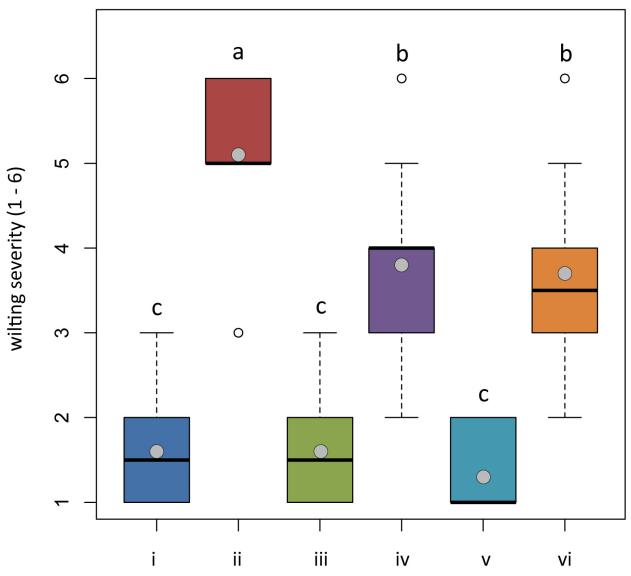

FIGURE 5 | *In planta* antagonistic effectiveness of *Trichoderma* test strains against *Phytophthora nicotianae*. Wilting severity of 4-month-old *Solanum lycopersicum* cv. Cuor di bue developed from the following: (i) untreated tomato plants transplanted in a non-infested potting mixture (NI-PM); (ii) untreated tomato plants inoculated with infested potting mixture (I-PM); (iii) tomato plants treated with *Trichoderma asperellum* strain IMI393899 and transplanted in NI-PM; (iv) tomato plants treated with *T. asperellum* strain IMI393899 and transplanted in I-PM; (v) tomato plants treated with *Trichoderma atroviride* strain TS and transplanted in NI-PM; and (vi) tomato plants treated with *T. atroviride* strain TS and transplanted in I-PM. Open and gray circles represent outliers and mean value data, respectively. Values sharing same letters are not statistically different according to Tukey's honestly significant difference (HSD) test ($P \leq 0.05$).

DISCUSSION

This study provides a comprehensive assessment of physiological and molecular mechanisms involved in the complex three-way plant-antagonist-pathogen interaction. Firstly, the effectiveness in the promotion of growth of the model plant *S. lycopersicum* cv. Cuor di bue by two selected strains of *T. asperellum* and *T. atroviride* was compared. Previous studies revealed that different cultivated lines of tomato have a differential response in the promotion of growth by commercial strains of *Trichoderma* spp. (Tucci et al., 2011); the strains *T. atroviride* P1 and *T. harzianum* T22 induced statistically significant improvements in the development of the stem only in one and two (respectively) out of four different tomato lines (i.e., Corbarino, TA209, M82, and SM36), compared with untreated controls. A similar trend was also observed in the root weight with also a significant decrement for one variety (i.e., M82) treated with *T. harzianum* T22 (Tucci et al., 2011). In general, our results indicated that between the two *Trichoderma* species, only *T. atroviride* was significantly able to promote the weekly growth rate of the tomato cv. Cuor di bue. This result confirms the variability of the effects induced by *Trichoderma* spp. in the promotion of the growth of different tomato varieties. In order to acquire a complete evaluation of the antagonistic activity of the selected *T. asperellum* IMI393899 and *T. atroviride* TS strains against the *P. nicotianae* Ph_nic isolate virulent toward tomato seedlings, in this study, a dual culture test and an *in planta* antagonistic trial were carried out. Various *Trichoderma* spp., including *T. harzianum*, *Trichoderma viride*, *Trichoderma virens*, *T. asperellum*, *Trichoderma gamsii*, *Trichoderma longibrachiatum*, and *T. atroviride*, showed a good antagonistic activity both *in vitro* and *in vivo* against several soil-borne fungal pathogens (Smith, 1990; Al-mughrabi, 2008; Mastouri et al., 2010; Singh and Islam, 2010; Haggag and El-Gamal, 2012; Widmer, 2014; Yao et al., 2015; Ghazanfar et al., 2018). Results obtained here from *in vitro* tests show that both *Trichoderma* spp. tested strongly inhibited the growth of *P. nicotianae* isolate Ph_nic, with a more marked inhibition by *T. atroviride* TS over *T. asperellum* IMI393899. Similarly, the *in planta* antagonistic trial showed that *T. atroviride* TS was more effective than *T. asperellum* IMI393899 in the reduction of disease severity, even if none of them provided a

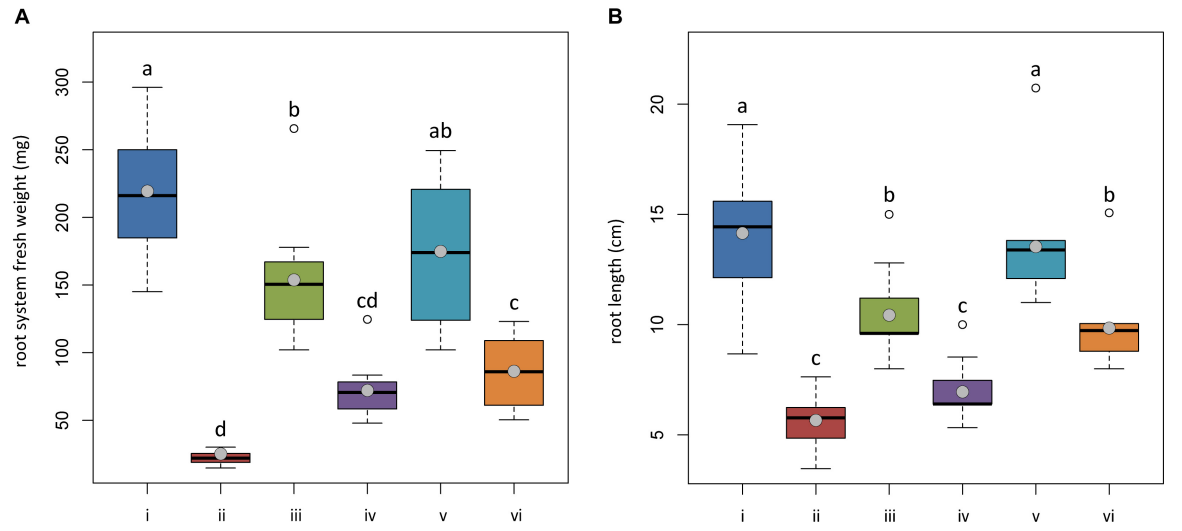

FIGURE 6 | *In planta* antagonistic effectiveness of *Trichoderma* test strains against *Phytophthora nicotianae*. **(A)** Fresh root weight and **(B)** length of 4-month-old *Solanum lycopersicum* cv. Cuor di bue developed from the following: (i) untreated tomato plants transplanted in a non-infested potting mixture (NI-PM); (ii) untreated tomato plants inoculated with infested potting mixture (I-PM); (iii) tomato plants treated with *Trichoderma asperellum* strain IMI393899 and transplanted in NI-PM; (iv) tomato plants treated with *T. asperellum* strain IMI393899 and transplanted in I-PM; (v) tomato plants treated with *Trichoderma atroviride* strain TS and transplanted in NI-PM; (vi) tomato plants treated with *T. atroviride* strain TS and transplanted in I-PM. Open and gray circles represent outliers and mean value data, respectively. Values sharing same letters are not statistically different according to Tukey's honestly significant difference (HSD) test ($P \leq 0.05$).

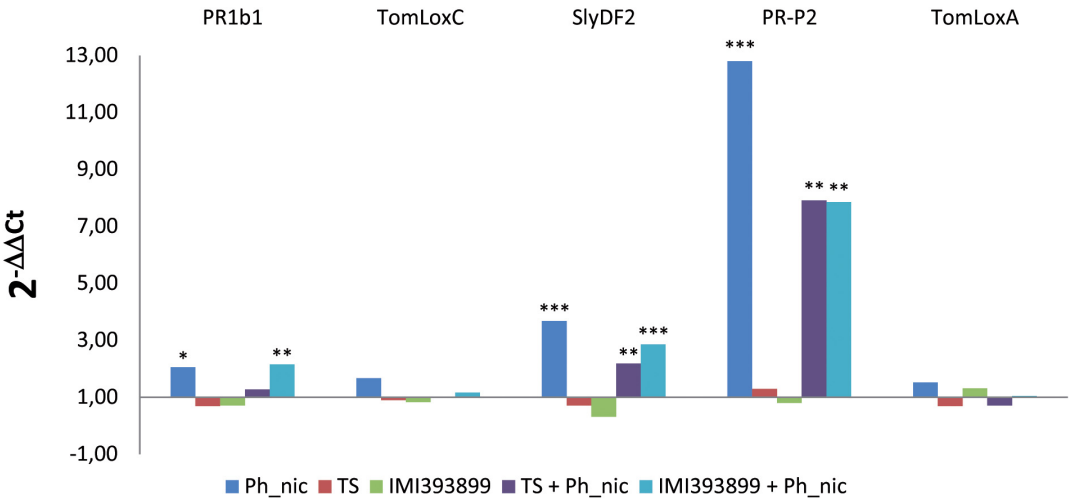

FIGURE 7 | Differences in the expression levels of PR1b, TomLoxC, SlyDF2, PR-P2, and TomLoxA-encoding genes (GenBank accession numbers: Y08804.1, U37839.1, NM_001346524.1, X58548.1 and U09026.1, respectively) from 7-day-old *Trichoderma*-treated or non-treated *Solanum lycopersicum* cv. Cuor di bue seedlings inoculated or non-inoculated with *Phytophthora nicotianae*. Columns with asterisks are statistically different according to Dunnett's test (*$P < 0.05$, **$P < 0.01$, ***$P < 0.001$), compared to their calibrator.

complete control of the disease. These results are in agreement with those obtained in other similar pathogen-plant systems. Positive *in vitro* and *in planta* effectiveness by *Trichoderma* spp. was reported against virulent *Phytophthora* strains from pepper (Ezziyyani et al., 2017) and potato (Al-mughrabi, 2008). In accordance with previous studies, our results confirm that selected strains from *Trichoderma* spp. can represent a valid support in the integrated pest management strategies of *Phytophthora* diseases.

Decrypting the genetic pathways of plant defense mechanisms to counteract the plethora of effectors deployed by pathogens to develop the infection, concomitant with both the antagonistic activity and the growth-promoting effects of plant beneficial organisms, nowadays represents one of the main topics of modern plant pathology. Many studies have already investigated the modulation of the expression of protective molecules, pathogenic metabolites, and mucolytic enzymes in plants, pathogens, and antagonists, respectively, during a simplified

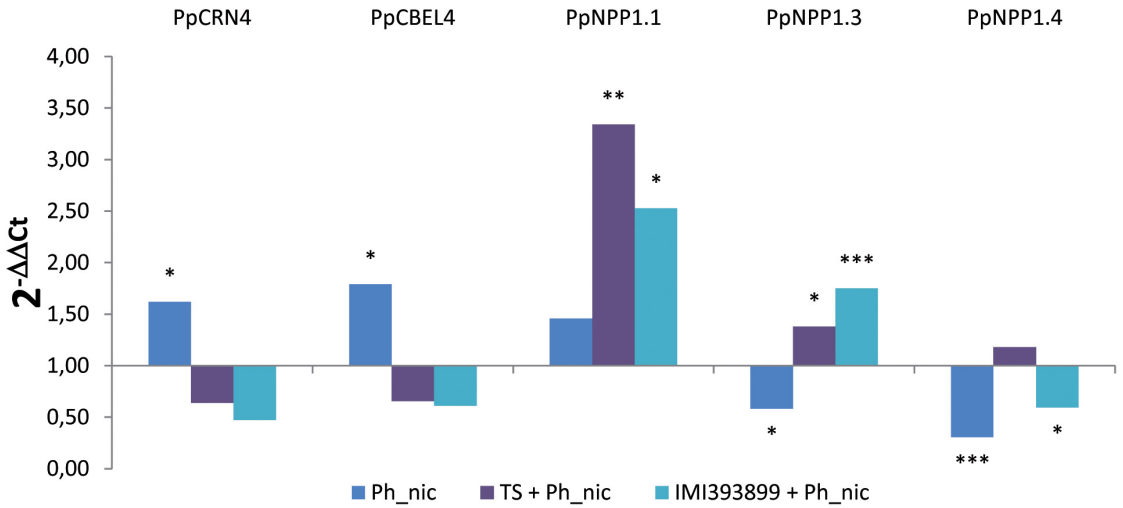

FIGURE 8 | Differences in the expression levels of PpCRN4, PpCBEL4, PpNPP1.1, PpNPP1.3, and PpNPP1.4-encoding genes (GenBank accession numbers: ETM55095.1, ETM43740.1, ETM52620.1, ETM39327.1 and ETM36738.1, respectively) in *Phytophthora nicotianae* isolate Ph_nic from 7-day-old *Trichoderma*-treated or non-treated *Solanum lycopersicum* cv. Cuor di bue *P. nicotianae*-inoculated seedlings. Columns with asterisks are statistically different according to Dunnett's test (*$P < 0.05$, **$P < 0.01$, ***$P < 0.001$), compared to their calibrator.

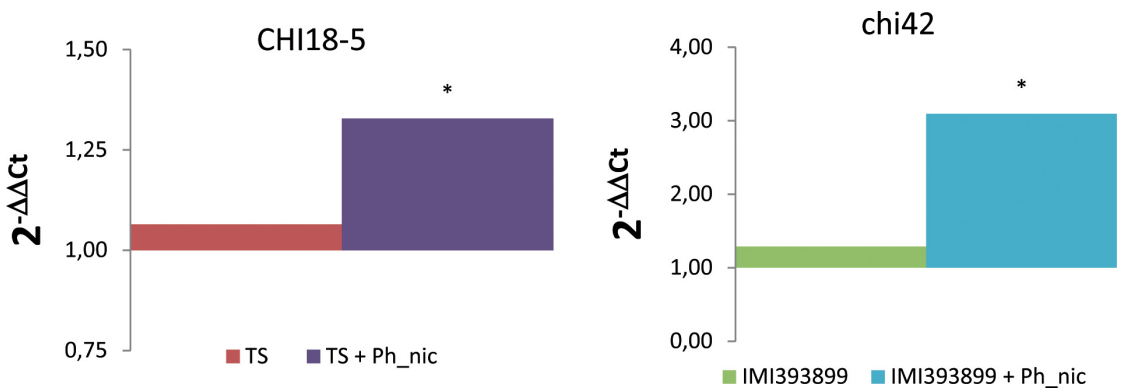

FIGURE 9 | Differences in the expression levels of CHI18-5 (GenBank accession number: XM_014088210) and *chi42* (GenBank accession number: HM191684.1)-encoding genes, respectively, in *Trichoderma atroviride* strain TS (on the left) and *Trichoderma asperellum* strain IMI393899 (on the right) from 7-day-old *Phytophthora nicotianae*-inoculated or non-inoculated *Solanum lycopersicum* cv. Cuor di bue *Trichoderma*-treated seedlings. Columns with asterisks are statistically different according to Dunnett's test (*$P < 0.05$), compared to their calibrator.

two-way interaction (i.e., plant-antagonist, plant-pathogen, and antagonist-pathogen) (Carsolio et al., 1994; Tucci et al., 2011; Dalio et al., 2018). However, this compartmentalized approach does not clarify how the real mutual and simultaneous three-way interaction between the main actors involved in the biological control can reprogram their respective metabolic responses. In the present study, it has been investigated how the mutual gene-induced metabolic response of *S. lycopersicum* cv. Cuor di bue, *P. nicotianae*, and *Trichoderma* spp. is modified under the influence of the infection by the pathogen as well as of both the mycoparasitic and plant-beneficial activity of the antagonistic beneficial microorganism. To this aim, the modulation of the genetic pathways related with SA-dependent SAR (PR1b1 and PR-P2), ISR (TomLoxC and TomLoxA), and antifungal defensins (SlyDF2)-encoding genes were evaluated in tomato plants under *P. nicotianae* infection and the simultaneous *Trichoderma* spp. root colonization. The expression levels were compared with both *Trichoderma*-untreated–*P. nicotianae*-inoculated and *Trichoderma*-treated–*P. nicotianae*-non-inoculated tomato plants.

Among (SA)-dependent SAR and ISR-related genes, a statistically significant increment of transcripts was observed only in *PR1b1* and *PR-P2* transcript levels, while both analyzed *TomLoxC* and *TomLoxA* were normally expressed in all treatments. Previous studies have already demonstrated a significant variability between different *Trichoderma*-treated tomato varieties, including a widespread normal expression, in the levels of PR and ISR-related genes (Tucci et al., 2011). Considering also that root colonization by *Trichoderma* spp. activates only transiently the expression of defense-related genes

(Yedidia et al., 1999, 2003; Shoresh et al., 2005; Segarra et al., 2009), results obtained here contribute to support the hypothesis that the colonization of roots by *Trichoderma* spp. could markedly take place only during the first phases of the interaction and then run out after a short time. Interestingly, the PR protein-encoding gene PR-P2 was activated more strongly in *Phytophthora*-inoculated and *Trichoderma*-untreated plants over treated and inoculated ones. The *PR-P2* is a PR4-encoding gene induced both by SA and wounding (Tornero et al., 1997; Bertini et al., 2003; Tucci et al., 2011). The expression of PR protein-encoding genes in *Trichoderma*-treated and pathogen-inoculated plants seems to be a mechanism characterized by a high spectrum of responses (Shoresh et al., 2005). A decreasing trend in the expression of PR-encoding genes was reported from different lines of tomato after the inoculation with *Botrytis cinerea* (Tucci et al., 2011); at the same time, proteomic studies on levels of PR proteins in *Trichoderma*-treated plants reported increments in pepper under *P. capsici* infection (Ezziyyani et al., 2017), in cucumber and maize (inoculated with *Pythium ultimum* and *Colletotrichum graminicola*, respectively) (Harman et al., 2004), and decrements in bean under leaf infection by *B. cinerea* and *Rhizoctonia solani* (Marra et al., 2006). By comparing the results obtained here with previous studies, it could then be speculated that the promotion of plant defenses by *Trichoderma* spp. is a mechanism affected by a variability of factors that could depend both on plant species and pathogens.

Additional significant increments of transcripts were observed in the levels of the tomato defensin SlyDF2-encoding gene. In this study, the evaluated tomato defensin gene was up-regulated only in *Phytophthora*-inoculated plants, including both *Trichoderma*-treated and untreated ones, while it was slightly down-regulated in *Trichoderma*-treated plants which did not receive *Phytophthora* inoculum. Plant defensins play a crucial role in the resistance of plants to pathogens (Penninckx et al., 1996). Antifungal activities were reported for several plant defensins, including RsAFP1 and RsAFP2 from radish (Terras et al., 1992), MsDef1 and MtDef4 from *Medicago* spp. (Gao et al., 2000), NaD1 from tobacco (Lay et al., 2003a,b), and Psd1 from pea (Almeida et al., 2000). However, in the last few years, the research has been mainly focused on the study of the potentiality of transgenic up-regulating defensin plants in the protection from fungal infections (Breen et al., 2015), resulting in a significant lack of knowledge about the modulation in the induction of defensins *in planta* under the pathogen/antagonist interaction. Results obtained here from the two-way interactions *Trichoderma*-tomato and *Phytophthora*-tomato agree with previous studies which described the induction of plant defensins by *Trichoderma* spp. in *A. thaliana* (Poveda et al., 2019) and the modulation of plant defensins by *Phytophthora* infection in tomato plants (Cui et al., 2018), respectively. However, the expression levels of defensins in tomato plants under the simultaneous *Trichoderma* root colonization and *Phytophthora* infection were not previously reported. In this study, the generalized reduction in the expression levels of the SlyDF2-encoding gene in *Trichoderma*-treated and *Phytophthora*-inoculated tomato plants over the untreated and *Phytophthora*-inoculated ones make it possible to speculate that the presence of *Trichoderma* control agents could reduce the intensity of this particular plant response.

In this study, the modulation of the transcription levels of the *P. nicotianae* genes encoding the effectors PpCRN4, PpCBEL4, PpNPP1.1, PpNPP1.3, and PpNPP1.4 was evaluated in *Phytophthora*-inoculated and *Trichoderma*-treated tomato plants and compared with untreated controls. Even though the role of *Phytophthora* effectors in the plant-pathogen interaction was previously reported (Séjalon et al., 1995; Séjalon-Delmas et al., 1997; Fellbrich et al., 2002; Gijzen and Nürnberger, 2006; Stam et al., 2013), this is the first study where the modulation of *P. nicotianae* effectors in a three-way tomato–*Trichoderma* spp.–*Phytophthora* system has been evaluated.

Interestingly, in this study, among NPP1-encoding genes, a marked up-regulation was observed in the levels of *PnNPP1.1* and *PnNPP1.3* of *P. nicotianae* from *Trichoderma*-treated tomato plants over the untreated controls. The *P. nicotianae* necrosis-inducing *Phytophthora* protein 1 (NPP1) has been associated with the induction of necrosis in parsley and *A. thaliana* (Fellbrich et al., 2002), and a significant up-regulation of NPP1-encoding genes was reported for *P. nicotianae* during the infection of *Citrus sunki* and *Poncirus trifoliata* (Dalio et al., 2018). By comparing the expression levels from *Trichoderma*-untreated and -treated tomato plants, it could be speculated, therefore, that the antagonistic activity of *Trichoderma* spp. toward *P. nicotianae* could hamper the infection process of the plant, resulting in an up-regulation of the transcripts in this particular genetic pathway, which, in principle, should weaken the plant defenses, making the invasion of the host possible.

In this study, the *PpCRN4* and *PpCBEL4* genes showed both a generalized down-regulation in *Trichoderma*-treated tomato plants over the untreated ones. *PpCRN4* is a gene encoding a clinker (CRN) protein, while *PpCBEL4* encodes a cell wall glycoprotein named CBEL (Dalio et al., 2018). Both groups of effectors (i.e., CRN and CBEL) induce necrosis in plant tissue (Séjalon-Delmas et al., 1997; Stam et al., 2013). Dalio et al. (2018) observed that 3 days after inoculation, the expression levels of the *P. nicotianae PpCRN4*-encoding gene manifested differences that depended on the host plant, as the gene down-regulated and normally expressed by the pathogen in *C. sunki* and *P. trifoliata*, respectively. In the same plant-pathogen systems, *PpCBEL4*-encoding gene was up-regulated both in *C. sunki* and *P. trifoliata*. As already observed by other authors (Woo et al., 2006), the different response in the expression level of the pathogenic effectors of *P. nicotianae* could be explained by the great variety of molecular weapons of *Trichoderma* spp. These mechanisms can be activated in different combinations or at different steps of the infection process; they can be also triggered depending on the pathogen they are confronting or the plant they are colonizing. In particular, the up-regulation of *PnNPP1.1* and *PnNPP1.3* pathogenic effectors could be a response of *P. nicotianae* to the induction of the plant resistance mechanisms by *Trichoderma* spp. An analogous pattern has been already demonstrated by Marra et al. (2006) who observed, using a proteomic approach, an over production of the superoxide dismutase by *B. cinerea* in the three-way system *B. cinerea*-bean-*Trichoderma*. Conversely, the down-regulation of *PpCRN4* and *PpCBEL4* in *P. nicotianae* in

the presence of *Trichoderma* spp. could be due to the antagonistic interaction between the microorganisms as well as the result of the enhancement of specific plant defenses by *Trichoderma* spp., which, in turn, could trigger in tomato plants a response similar to that constitutively activated by *C. sunki* plants infected by *P. nicotianae* (Dalio et al., 2018), thus determining the down-regulation of the *PpCRN4* gene. However, these pathogen genetic responses deserve to be further investigated.

Finally, in accordance with other authors (Osorio-Hernández et al., 2016), in this study, the level of endochitinase from both *T. asperellum* and *T. atroviride* was higher in *Trichoderma*-treated and *Phytophthora*-inoculated plants over the non-inoculated ones.

CONCLUSION

This study provides the basis for understanding the complex and often unpredictable genetic interactions in a tripartite system, plant/beneficial organism/pathogen, instead of two, plant/pathogen, as in most systems studied so far. The experimental approach, including the individual components of the system, the host plant tomato, the oomycete *P. nicotianae*, i.e., the challenging pathogen, and the beneficial fungus *Trichoderma*, in all possible two-way combinations and the comparison with the three-way combinations made it possible to confirm or verify genetic mechanisms involved in the host-pathogen, host-growth-promoting beneficial organism, and pathogen-antagonistic beneficial organism interactions. Moreover, a better insight on how reciprocal interactions are modulated in more complex systems has been obtained. In particular, in this tripartite system, it was observed the simultaneous transcriptional reprogramming of plant defense-related genes, pathogen effectors, and mycoparasitism-related genes. Results support the hypothesis that *Trichoderma* spp. elicit the expression of plant defense-related genes and, as expected, a mycoparasitism-related gene was significantly up-regulated in *Trichoderma*-colonizing tomato plants infected by *P. nicotianae*.

Moreover, for the first time, it was observed that the *Trichoderma* treatment of tomato plants induced a marked up-regulation of the *P. nicotianae* pathogenic effectors *PnNPP1.1* and *PnNPP1.3* and, at the same time, a slight down-regulation of *PpCRN4* and *PpCBEL4*.

The findings that both the two- and three-way interactions vary with different *Trichoderma* species and the selection of a *T. atroviride* strain showing both a direct antagonistic activity against *P. nicotianae* and a growth-promoting effect on tomato plants are other interesting achievements of this study that have practical implications in the development and design of sustainable disease management strategies based on the application of biocontrol agents.

DATA AVAILABILITY STATEMENT

The datasets presented in this study can be found in online repositories. The names of the repository/repositories and accession number(s) can be found in the article/ **Supplementary Material**.

AUTHOR CONTRIBUTIONS

SOC, FLS, and AP conceptualized the study, analyzed the results, and reviewed and edited the draft. FLS, CS, and MR did the investigation and formal analysis and performed the experiments. SOC and AP were responsible for funding acquisition and supervised the study. FLS wrote the original draft. All authors reviewed the manuscript.

FUNDING

This study was funded by grant awarded to SOC by MIUR–FFABR 2017 (n°. 5A725192051) and to AP and SOC by the University of Catania–Program n°. 5A722192134: "Emergent Pests and Pathogens and Relative Sustainable Management Strategies (DIFESA)." FLS was supported by a Ph.D. fellowship funded by "PON Ricerca e Innovazione" 2014–2020 (CCI 2014IT16M2OP005).

ACKNOWLEDGMENTS

We wish to thank Prof. Sophien Kamoun for his encouragement and helpful suggestions and Dr. Rossella Labarile for her technical advice and useful discussions. We are grateful to Mrs. Ann Davies for the English revision.

SUPPLEMENTARY MATERIAL

The Supplementary Material for this article can be found online at: https://www.frontiersin.org/articles/10.3389/fpls.2020.583539/full#supplementary-material

REFERENCES

Almeida, M. S., Cabral, K. M. S., Zingali, R. B., and Kurtenbach, E. (2000). Characterization of two novel defense peptides from pea (*Pisum sativum*) seeds. *Archiv. Biochem. Biophys.* 378, 278–286. doi: 10.1006/abbi.2000.1824

Al-mughrabi, K. (2008). Biological control of *Phytophthora infestans* of potatoes using *Trichoderma atroviride*. *Pest Technol.* 2, 104–108.

Atanasova, L., Crom, S. Le, Gruber, S., Coulpier, F., Seidl-Seiboth, V., Kubicek, C. P., et al. (2013). Comparative transcriptomics reveals different strategies of *Trichoderma mycoparasitism*. *BMC Genom.* 14:121. doi: 10.1186/1471-2164-14-121

Benítez, T., Rincón, A. M., Limón, M. C., and Codón, A. C. (2004). Biocontrol mechanisms of *Trichoderma* strains. *Intern. Microbiol.* 7, 249–260. doi: 10.2436/im.v7i4.9480

Bertini, L., Leonardi, L., Caporale, C., Tucci, M., Cascone, N., Di Berardino, I., et al. (2003). Pathogen-responsive wheat PR4 genes are induced by activators of systemic acquired resistance and wounding. *Plant Sci.* 164, 1067–1078. doi: 10.1016/S0168-9452(03)00112-2

Birch, P. R. J., Rehmany, A. P., Pritchard, L., Kamoun, S., and Beynon, J. L. (2006). Trafficking arms: oomycete effectors enter host plant cells. *Trends Microbiol.* 14, 8–11. doi: 10.1016/j.tim.2005.11.007

Brasesco, F., Asgedom, D., and Casari, G. (2019). *Strategic Analysis and Intervention Plan for Fresh and Industrial Tomato in the Agro-Commodities Procurement Zone of the Pilot Integrated Agro-Industrial Park in Central-Eastern Oromia, Ethiopia*. Addis Ababa: FAO.

Breen, S., Solomon, P. S., Bedon, F., and Vincent, D. (2015). Surveying the potential of secreted antimicrobial peptides to enhance plant disease resistance. *Front. Plant Sci.* 6:900. doi: 10.3389/fpls.2015.00900

Cacciola, S. O., and Gullino, M. L. (2019). Emerging and re-emerging fungus and oomycete soil-borne plant diseases in Italy. *Phytopathol. Med.* 58, 451–472. doi: 10.14601/PHYTO-10756

Cacciola, S. O., Puglisi, I., Faedda, R., Sanzaro, V., Pane, A., Lo Piero, A. R., et al. (2015). Cadmium induces cadmium-tolerant gene expression in the filamentous fungus *Trichoderma harzianum*. *Mol. Biol. Rep.* 42, 1559–1570. doi: 10.1007/s11033-015-3924-4

Carsolio, C., Gutiérrez, A., Jiménez, B., Van Montagu, M., and Herrera-Estrella, A. (1994). Characterization of ech-42, a *Trichoderma harzianum* endochitinase gene expressed during mycoparasitism. *Proc. Natl. Acad. Sci. U.S.A.* 91, 10903–10907. doi: 10.1073/pnas.91.23.10903

Chepsergon, J., Motaung, T. E., Bellieny-Rabelo, D., and Moleleki, L. N. (2020). Organize, don't agonize: strategic success of *Phytophthora* species. *Microorganisms* 8:917. doi: 10.3390/microorganisms8060917

Cooke, D. E. L., Drenth, A., Duncan, J. M., Wagels, G., and Brasier, C. M. (2000). A molecular phylogeny of *Phytophthora* and related oomycetes. *Fungal Genet. Biol.* 30, 17–32. doi: 10.1006/fgbi.2000.1202

Crutcher, F. K., Moran-Diez, M. E., Ding, S., Liu, J., Horwitz, B. A., Mukherjee, P. K., et al. (2015). A paralog of the proteinaceous elicitor SM1 is involved in colonization of maize roots by *Trichoderma virens*. *Fungal Biol.* 119, 476–486. doi: 10.1016/j.funbio.2015.01.004

Cui, J., Jiang, N., Meng, J., Hou, X., Yang, G., and Luan, Y. (2018). Identification and characterization of defensin genes conferring *Phytophthora infestans* resistance in tomato. *Physiol. Mol. Plant Pathol.* 103, 28–35. doi: 10.1016/J.PMPP.2018.04.003

Dalio, R. J. D., Máximo, H. J., Oliveira, T. S., Azevedo, T., de, M., Felizatti, H. L., et al. (2018). molecular basis of *Citrus sunki* susceptibility and *Poncirus trifoliata* resistance upon *Phytophthora parasitica* attack. *Mol. Plant Microb. Interact.* 31, 386–398. doi: 10.1094/MPMI-05-17-0112-FI

Engelbrecht, B. M. J., Tyree, M. T., and Kursar, T. A. (2007). Visual assessment of wilting as a measure of leaf water potential and seedling drought survival. *J. Trop. Ecol.* 23, 497–500. doi: 10.1017/S026646740700421X

Erwin, D. C., and Ribeiro, O. K. (1996). *Phytophthora Diseases Worldwide*. St. Paul, MI: American Phytopathological Society.

Ezziyyani, M., Hamdache, A., Egea-Gilabert, C., Requena, M. E., Candela, M. E., and Mater, J. (2017). Production of Pathogenesis-Related proteins during the induction of resistance to *Phytophthora capsici* in pepper plants treated with *Burkholderia cepacia* and *Trichoderma harzianum* in combination compatible. *J. Mater. Environ. Sci.* 8, 4785–4795.

Fellbrich, G., Romanski, A., Varet, A., Blume, B., Brunner, F., Engelhardt, S., et al. (2002). NPP1, a *Phytophthora* -associated trigger of plant defense in parsley and *Arabidopsis*. *Plant J.* 32, 375–390. doi: 10.1046/j.1365-313X.2002.01454.x

Gao, A. G., Hakimi, S. M., Mittanck, C. A., Wu, Y., Woerner, B. M., Stark, D. M., et al. (2000). Fungal pathogen protection in potato by expression of a plant defensin peptide. *Nat. Biotechnol.* 18, 1307–1310. doi: 10.1038/82436

Garibaldi, A., and Gullino, M. L. (2010). Emerging soilborne diseases of horticultural crops and new trends in their management. *Acta Hortic.* 883, 37–48. doi: 10.17660/actahortic.2010.883.2

Ghazanfar, M. U., Raza, M., Raza, W., and Qamar, M. I. (2018). *Trichoderma* as potential biocontrol agent, its exploitation in agriculture: a review. *Plant Protect.* 2, 109–135.

Gijzen, M., and Nürnberger, T. (2006). Nep1-like proteins from plant pathogens: recruitment and diversification of the NPP1 domain across taxa. *Phytochemistry* 67, 1800–1807. doi: 10.1016/j.phytochem.2005.12.008

Gilardi, G., Demarchi, S., Gullino, M. L., and Garibaldi, A. (2014a). Control of *Phytophthora nicotianae* of tomato by using non-conventional strategies. *Acta Hortic.* 8, 325–330. doi: 10.17660/ActaHortic.2014.1044.42

Gilardi, G., Demarchi, S., Gullino, M. L., and Garibaldi, A. (2014b). Managing *Phytophthora* crown and root rot on tomato by pre-plant treatments with biocontrol agents, resistance inducers, organic and mineral fertilizers under nursery conditions. *Phytopathol. Med.* 53, 205–215. doi: 10.14601/Phytopathol_Mediterr-12361

Gilardi, G., Pugliese, M., Gullino, M. L., and Garibaldi, A. (2020). Effect of biocontrol agents and potassium phosphite against *Phytophthora* crown rot, caused by *Phytophthora capsici*, on zucchini in a closed soilless system. *Sci. Hortic.* 265:207. doi: 10.1016/j.scienta.2020.109207

Gonçalves, S., Teixeira, A., Abade, J., De Medeiros, L. N., Kurtenbach, E., and Santos, N. C. (2012). Evaluation of the membrane lipid selectivity of the pea defensin Psd1. *Biochim. Biophys. Acta Biomembr.* 1818, 1420–1426. doi: 10.1016/j.bbamem.2012.02.012

Guérin, V., Lebreton, A., Phytologie, D., and De Laval, U. (2014). A zoospore inoculation method with *Phytophthora sojae* to assess the prophylactic role of silicon on soybean cultivars. *Plant Dis.* 98, 1632–1638. doi: 10.1094/PDIS-01-14-0102-RE

Guzmán-Guzmán, P., Alemán-Duarte, M. I., Delaye, L., Herrera-Estrella, A., and Olmedo-Monfil, V. (2017). Identification of effector-like proteins in *Trichoderma* spp. and role of a hydrophobin in the plant-fungus interaction and mycoparasitism. *BMC Genet.* 18:16. doi: 10.1186/s12863-017-0481-y

Guzmán-Guzmán, P., Porras-Troncoso, M. D., Olmedo-Monfil, V., and Herrera-Estrella, A. (2019). *Trichoderma* species: versatile plant symbionts. *Phytopathology* 109, 6–16. doi: 10.1094/PHYTO-07-18-0218-RVW

Haggag, H., and El-Gamal, G. (2012). In vitro study on *Fusarium solani* and *Rhizoctonia solani* isolates causing the damping off and root rot diseases in tomatoes. *Nat. Sci.* 10, 16–25.

Harman, G. E., Howell, C. R., Viterbo, A., Chet, I., and Lorito, M. (2004). *Trichoderma* species — opportunistic, avirulent plant symbionts. *Nat. Rev. Microbiol.* 2, 43–56. doi: 10.1038/nrmicro797

Howell, C. R. (2003). Mechanisms employed by *Trichoderma* species in the biological control of plant diseases: the history and evolution of current concepts. *Plant Dis.* 87, 4–10. doi: 10.1094/PDIS.2003.87.1.4

ISTAT (2020). *Istat.it Agriculture*. Available online at: https://www.istat.it/en/agriculture?data-and-indicators (accessed January 22, 2020).

Jones, J. B., Zitter, T. A., Momol, T. M., and Miller, S. A. (2016). *Compendium of Tomato Diseases and Pests*, 2nd Edn, Saint Paul, MI: American Phytopathological Society.

Jones, J. D. G., and Dangl, J. L. (2006). The plant immune system. *Nature* 444, 323–329. doi: 10.1038/nature05286

Jung, T., Blaschke, H., and Neumann, P. (1996). Isolation, identification and pathogenicity of *Phytophthora* species from declining oak stands. *Eur. J. For. Pathol.* 26, 253–272. doi: 10.1111/j.1439-0329.1996.tb00846.x

Jung, T., La Spada, F., Pane, A., Aloi, F., Evoli, M., Horta Jung, M., et al. (2019). Diversity and distribution of *Phytophthora* species in protected natural areas in Sicily. *Forests* 10:259. doi: 10.3390/f10030259

Kamoun, S., Furzer, O., Jones, J. D. G., Judelson, H. S., Ali, G. S., Dalio, R. J. D., et al. (2015). The Top 10 oomycete pathogens in molecular plant pathology. *Mol. Plant Pathol.* 16, 413–434. doi: 10.1111/mpp.12190

Köhl, J., Kolnaar, R., and Ravensberg, W. J. (2019). Mode of action of microbial biological control agents against plant diseases: relevance beyond efficacy. *Front. Plant Sci.* 10:845. doi: 10.3389/fpls.2019.00845

Kubicek, C. P., Herrera-Estrella, A., Seidl-Seiboth, V., Martinez, D. A., Druzhinina, I. S., Thon, M., et al. (2011). Comparative genome sequence analysis underscores mycoparasitism as the ancestral life style of *Trichoderma*. *Genome Biol.* 12:R40. doi: 10.1186/gb-2011-12-4-r40

Lay, F., and Anderson, M. (2005). Defensins - components of the innate immune system in plants. *Curr. Protein Pept. Sci.* 6:29. doi: 10.2174/1389203053027575

Lay, F. T., Brugliera, F., and Anderson, M. A. (2003a). Isolation and properties of floral defensins from ornamental tobacco and petunia. *Plant Physiol.* 131:26. doi: 10.1104/pp.102.016626

Lay, F. T., Schirra, H. J., Scanlon, M. J., Anderson, M. A., and Craik, D. J. (2003b). The three-dimensional solution structure of NaD1, a new floral defensin from *Nicotiana alata* and its application to a homology model of the crop defense protein alfAFP. *J. Mol. Biol.* 325, 175–188. doi: 10.1016/S0022-2836(02)01103-8

Lebreton, A., Labbé, C., De Ronne, M., Xue, A. G., Marchand, G., and Bélanger, R. R. (2018). Development of a simple hydroponic assay to study vertical and

horizontal resistance of soybean and pathotypes of *Phytophthora sojae*. *Plant Dis.* 102, 114–123. doi: 10.1094/PDIS-04-17-0586-RE

Livak, K. J., and Schmittgen, T. D. (2001). Analysis of relative gene expression data using real-time quantitative PCR and the 2-ΔΔCT method. *Methods* 25, 402–408. doi: 10.1006/meth.2001.1262

Lobo, D. S., Pereira, I. B., Fragel-Madeira, L., Medeiros, L. N., Cabral, L. M., Faria, J., et al. (2007). Antifungal *Pisum sativum* defensin 1 interacts with *Neurospora crassa* cyclin F related to the cell cycle. *Biochemistry* 46, 987–996. doi: 10.1021/bi061441j

Mammella, M. A., Cacciola, S. O., Martin, F., and Schena, L. (2011). Genetic characterization of *Phytophthora nicotianae* by the analysis of polymorphic regions of the mitochondrial DNA. *Fungal Biol.* 115, 432–442. doi: 10.1016/j.funbio.2011.02.018

Marra, R., Ambrosino, P., Carbone, V., Vinale, F., Woo, S. L., Ruocco, M., et al. (2006). Study of the three-way interaction between *Trichoderma atroviride*, plant and fungal pathogens by using a proteomic approach. *Curr. Genet.* 50, 307–321. doi: 10.1007/s00294-006-0091-0

Masek, T., Vopalensky, V., Suchomelova, P., and Pospisek, M. (2005). Denaturing RNA electrophoresis in TAE agarose gels. *Analyt. Biochem.* 336, 46–50. doi: 10.1016/J.AB.2004.09.010

Mastouri, F., Björkman, T., and Harman, G. E. (2010). Seed treatment with *Trichoderma harzianum* alleviates biotic, abiotic, and physiological stresses in germinating seeds and seedlings. *Phytopathology* 100, 1213–1221. doi: 10.1094/PHYTO-03-10-0091

McGowan, J., O'hanlon, R., Owens, R. A., and Fitzpatrick, D. A. (2020). Comparative genomic and proteomic analyses of three widespread *Phytophthora* species: *Phytophthora chlamydospora*, *Phytophthora gonapodyides* and *Phytophthora pseudosyringae*. *Microorganisms* 8:653. doi: 10.3390/microorganisms8050653

Mendenhall, M. D., and Hodge, A. E. (1998). Regulation of Cdc28 cyclin-dependent protein kinase activity during the cell cycle of the yeast *Saccharomyces cerevisiae*. *Microbiol. Mol. Biol. Rev.* 62, 1191–1243.

Meng, Y., Zhang, Q., Ding, W., and Shan, W. (2014). *Phytophthora parasitica*: a model oomycete plant pathogen. *Mycology* 5, 43–51. doi: 10.1080/21501203.2014.917734

Monte, E. (2001). Understanding *Trichoderma*: between biotechnology and microbial ecology. *Intern. Microbiol.* 4, 1–4. doi: 10.1007/s101230100001

Morán-Diez, M. E., Carrero-Carrón, I., Belén Rubio, M., Jiménez-Díaz, R. M., Monte, E., and Hermosa, R. (2019). *Transcriptomic* analysis of *Trichoderma atroviride* overgrowing plant-wilting verticillium dahliae reveals the role of a new m14 metallocarboxypeptidase CPA1 in biocontrol. *Front. Microbiol.* 10:1120. doi: 10.3389/fmicb.2019.01120

Osorio-Hernández, E., Hernández-Morales, J., Conde-Martínez, V., Michel-Aceves, A. C., Lopez-Santillan, J. A., and Torres-Castillo, J. A. (2016). In vitro activities of *Trichoderma* species against *Phytophthora parasitica* and *Fusarium oxysporum*. *Afr. J. Microbiol. Res.* 10, 521–527. doi: 10.5897/ajmr2016.7958

Pachauri, S., Sherkhane, P. D., Kumar, V., and Mukherjee, P. K. (2020). Whole genome sequencing reveals major deletions in the genome of M7, a gamma ray-induced mutant of *Trichoderma virens* that is repressed in conidiation, secondary metabolism, and *Mycoparasitism*. *Front. Microbiol.* 11:1030. doi: 10.3389/fmicb.2020.01030

Panabières, F., Ali, G. S., Allagui, M. B., Dalio, R. J. D., Gudmestad, N. C., Kuhn, M. L., et al. (2016). *Phytophthora nicotianae* diseases worldwide: new knowledge of a long-recognised pathogen. *Phytopathol. Med.* 55, 20–40. doi: 10.14601/Phytopathol_Mediterr-16423

Pane, A., Agosteo, G. E., and Cacciola, S. O. (2000). *Phytophthora* species causing crown and root rot of tomato in southern Italy. *EPPO Bull.* 30, 251–255. doi: 10.1111/j.1365-2338.2000.tb00890.x

Penninckx, I. A. M. A., Eggermont, K., Terras, F. R. G., Thomma, B. P. H. J., De Samblanx, G. W., Buchala, A., et al. (1996). Pathogen-induced systemic activation of a plant defensin gene in *Arabidopsis* follows a salicylic acid-independent pathway. *Plant Cell* 8, 2309–2323. doi: 10.2307/3870470

Poveda, J., Hermosa, R., Monte, E., and Nicolás, C. (2019). *Trichoderma harzianum* favours the access of *Arbuscular mycorrhizal* fungi to non-host *Brassicaceae* roots and increases plant productivity. *Sci. Rep.* 9:11650. doi: 10.1038/s41598-019-48269-z

Puglisi, I., Faedda, R., Sanzaro, V., Lo Piero, A. R., Petrone, G., and Cacciola, S. O. (2012). Identification of differentially expressed genes in response to mercury I and II stress in *Trichoderma harzianum*. *Gene* 506, 325–330. doi: 10.1016/j.gene.2012.06.091

Ramírez-Valdespino, C. A., Casas-Flores, S., and Olmedo-Monfil, V. (2019). *Trichoderma* as a model to study effector-like molecules. *Front. Microbiol.* 10:1030. doi: 10.3389/pmic.2019.01030

Sato, S., Tabata, S., Hirakawa, H., Asamizu, E., Shirasawa, K., Isobe, S., et al. (2012). The tomato genome sequence provides insights into fleshy fruit evolution. *Nature* 485, 635–641. doi: 10.1038/nature11119

Segarra, G., Casanova, E., Bellido, D., Odena, M. A., Oliveira, E., and Trillas, I. (2007). Proteome, salicylic acid, and jasmonic acid changes in cucumber plants inoculated with *Trichoderma asperellum* strain T34. *Proteomics* 7, 3943–3952. doi: 10.1002/pmic.200700173

Segarra, G., Van Der Ent, S., Trillas, I., and Pieterse, C. M. J. (2009). MYB72, a node of convergence in induced systemic resistance triggered by a fungal and a bacterial beneficial microbe. *Plant Biol.* 11, 90–96. doi: 10.1111/j.1438-8677.2008.00162.x

Séjalon, N., Dargent, R., Villalba, F., Bottin, A., Rickauer, M., and Esquerré-Tugayé, M. T. (1995). Characterization of a cell-surface antigen isolated from the plant pathogen *Phytophthora parasitica* var. *nicotianae*. *Can. J. Bot.* 73, 1104–1108. doi: 10.1139/b95-365

Séjalon-Delmas, N., Villalba Mateos, F., Bottin, A., Rickauer, M., Dargent, R., and Esquerré-Tugayé, M. T. (1997). Purification, elicitor activity, and cell wall localization of a glycoprotein from *Phytophthora parasitica* var. *nicotianae*, a fungal pathogen of tobacco. *Phytopathology* 87, 899–909. doi: 10.1094/PHYTO.1997.87.9.899

Seo, H. H., Park, S., Park, S., Oh, B. J., Back, K., Han, O., et al. (2014). Overexpression of a defensin enhances resistance to a fruit-specific anthracnose fungus in pepper. *PLoS One* 9:e97936. doi: 10.1371/journal.pone.0097936

Shoresh, M., Harman, G. E., and Mastouri, F. (2010). Induced systemic resistance and plant responses to fungal biocontrol agents. *Annu. Rev. Phytopathol.* 48, 21–43. doi: 10.1146/annurev-phyto-073009-114450

Shoresh, M., Yedidia, I., and Chet, I. (2005). Involvement of jasmonic acid/ethylene signaling pathway in the systemic resistance induced in cucumber by *Trichoderma asperellum* T203. *Phytopathology* 95, 76–84. doi: 10.1094/PHYTO-95-76

Singh, A., and Islam, M. N. (2010). In vitro evaluation of *Trichoderma* spp. against *Phytophthora nicotianae*. *Intern. J. Exper. Agric.* 1, 1923–7766.

Smith, V. L. (1990). Potential for biological control of *Phytophthora* root and crown rots of apple by *Trichoderma* and *Gliocladium* spp. *Phytopathology* 80, 880–885. doi: 10.1094/phyto-80-880

Stam, R., Jupe, J., Howden, A. J. M., Morris, J. A., Boevink, P. C., Hedley, P. E., et al. (2013). Identification and characterisation CRN effectors in *Phytophthora capsici* shows modularity and functional diversity. *PLoS One* 8:e59517. doi: 10.1371/journal.pone.0059517

Stassen, J. H. M., and Van den Ackerveken, G. (2011). How do oomycete effectors interfere with plant life? *Curr. Opin. Plant Biol.* 14, 407–414. doi: 10.1016/j.pbi.2011.05.002

Terras, F. R. G., Schoofs, H. M. E., De Bolle, M. F. C., Van Leuven, F., Rees, S. B., Vanderleyden, J., et al. (1992). Analysis of two novel classes of plant antifungal proteins from radish (*Raphanus sativus* L.) seeds. *J. Biol. Chem.* 267, 15301–15309.

Tornero, P., Gadea, J., Conejero, V., and Vera, P. (1997). Two PR-1 genes from tomato are differentially regulated and reveal a novel mode of expression for a pathogenesis-related gene during the hypersensitive response and development. *Mol. Plant Microb. Interact.* 10, 624–634. doi: 10.1094/MPMI.1997.10.5.624

Tucci, M., Ruocco, M., De Masi, L., De Palma, M., and Lorito, M. (2011). The beneficial effect of *Trichoderma* spp. on tomato is modulated by the plant genotype. *Mol. Plant Pathol.* 12, 341–354. doi: 10.1111/j.1364-3703.2010.00674.x

Verma, M., Brar, S. K., Tyagi, R. D., Surampalli, R. Y., and Valéro, J. R. (2007). Antagonistic fungi, *Trichoderma* spp.: panoply of biological control. *Biochem. Eng. J.* 37, 1–20. doi: 10.1016/J.BEJ.2007.05.012

Wang, K., Der Borrego, E. J., Kenerley, C. M., and Kolomiets, M. V. (2020). Oxylipins other than jasmonic acid are xylem-resident signals regulating systemic resistance induced by *Trichoderma virens* in Maize. *Plant Cell* 32, 166–185. doi: 10.1105/tpc.19.00487

White, T. J., Bruns, T., Lee, S., and Taylor, J. W. (1990). "Amplification and direct sequencing of fungal ribosomal RNA genes for phylogenetics," in *PCR*

Protocols: a Guide to Methods and Applications, eds M. A. Innis, D. H. Gelfand, J. J. Sninsky, and T. J. White (San Diego, CA: Academic Press Inc), 315–322.

Widmer, T. L. (2014). Screening *Trichoderma* species for biological control activity against *Phytophthora ramorum* in soil. *Biol. Control* 79, 43–48. doi: 10.1016/j.biocontrol.2014.08.003

Woo, S. L., Ruocco, M., Vinale, F., Nigro, M., Marra, R., Lombardi, N., et al. (2014). *Trichoderma*-based products and their widespread use in agriculture. *Open Mycol. J.* 8, 71–126. doi: 10.2174/1874437001408010071

Woo, S. L., Scala, F., Ruocco, M., and Lorito, M. (2006). The molecular biology of the interactions between *Trichoderma* spp., Phytopathogenic Fungi, and Plants. *Phytopathology* 96, 181–185. doi: 10.1094/PHYTO-96-0181

Yao, Y., Li, Y., Chen, Z., Zheng, B., Zhang, L., Niu, B., et al. (2015). Biological control of potato late blight using isolates of *Trichoderma*. *Am. J. Potato Res.* 93, 33–42. doi: 10.1007/s12230-015-9475-3

Yedidia, I., Benhamou, N., and Chet, I. (1999). Induction of defense responses in cucumber plants (*Cucumis sativus* L.) by the biocontrol agent *Trichoderma harzianum*. *Appl. Environ. Microbiol.* 65, 1061–1070.

Yedidia, I., Shoresh, M., Kerem, Z., Benhamou, N., Kapulnik, Y., and Chet, I. (2003). Concomitant induction of systemic resistance to *Pseudomonas syringae* pv. *lachrymans* in cucumber by *Trichoderma asperellum* (T-203) and accumulation of *Phytoalexins*. *Appl. Environ. Microbiol.* 69, 7343–7353. doi: 10.1128/AEM.69.12.7343-7353.2003

Zhang, Y., Xu, S., Ding, P., Wang, D., Cheng, Y. T., He, J., et al. (2010). Control of salicylic acid synthesis and systemic acquired resistance by two members of a plant-specific family of transcription factors. *Proc. Natl. Acad. Sci. U.S.A.* 107, 18220–18225. doi: 10.1073/pnas.1005225107

Conflict of Interest: The authors declare that the research was conducted in the absence of any commercial or financial relationships that could be construed as a potential conflict of interest.

frontiers in Plant Science

ORIGINAL RESEARCH
published: 03 December 2020
doi: 10.3389/fpls.2020.573670

An Endophytic *Trichoderma* Strain Promotes Growth of Its Hosts and Defends Against Pathogen Attack

*Yu-Heng Tseng[1], Hamid Rouina[1], Karin Groten[2], Pijakala Rajani[3], Alexandra C. U. Furch[1], Michael Reichelt[2], Ian T. Baldwin[2], Karaba N. Nataraja[4], Ramanan Uma Shaanker[3] and Ralf Oelmüller[1,3]**

[1] Department of Plant Physiology, Matthias Schleiden Institute of Genetics, Bioinformatics and Molecular Botany, Friedrich-Schiller-University Jena, Jena, Germany, [2] Department of Molecular Ecology, Max-Planck-Institute for Chemical Ecology, Jena, Germany, [3] School of Ecology and Conservation, University of Agricultural Sciences, Gandhi Krishi Vigyana Kendra (GKVK), Bengaluru, India, [4] Department of Crop Physiology, University of Agricultural Sciences, Gandhi Krishi Vigyana Kendra (GKVK), Bengaluru, India

OPEN ACCESS

Edited by:
Sabine Dagmar Zimmermann, Délégation Languedoc Roussillon (CNRS), France

Reviewed by:
Marc Knight, Durham University, United Kingdom
Justin Lee, Leibniz-Institut für Pflanzenbiochemie (IPB), Germany

***Correspondence:**
Ralf Oelmüller
b7oera@uni-jena.de

Specialty section:
This article was submitted to Plant Symbiotic Interactions, a section of the journal Frontiers in Plant Science

Received: *17 June 2020*
Accepted: *02 November 2020*
Published: *03 December 2020*

Citation:
Tseng Y-H, Rouina H, Groten K, Rajani P, Furch ACU, Reichelt M, Baldwin IT, Nataraja KN, Uma Shaanker R and Oelmüller R (2020) An Endophytic Trichoderma Strain Promotes Growth of Its Hosts and Defends Against Pathogen Attack. Front. Plant Sci. 11:573670. doi: 10.3389/fpls.2020.573670

Plants host numerous endophytic microbes which promote plant performance, in particular under stress. A new endophytic fungus was isolated from the leaves of a deciduous wood tree *Leucas aspera.* Morphological inspection and multilocus phylogeny identified the fungus as a new *Trichoderma* strain. If applied to *Arabidopsis thaliana* and *Nicotiana attenuata*, it mainly colonizes their roots and strongly promotes initial growth of the plants on soil. The fungus grows on high NaCl or mannitol concentrations, and shows predatory capability on the pathogenic fungus *Alternaria brassicicola*. Colonized *Arabidopsis* plants tolerate higher salt stress and show lower *A. brassicicola* spread in roots and shoots, while arbuscular mycorrhiza formation in *N. attenuata* is not affected by the *Trichoderma* strain. These beneficial features of the novel *Trichoderma* strain are important prerequisites for agricultural applications.

Keywords: *Trichoderma*, plant beneficial endophyte, growth promotion, pathogen protection, hormone induction

INTRODUCTION

Trichoderma species are versatile filamentous ascomycetes which are found in nearly all environments. They live in soil, grow on wood as saprophytes, or feed on fungi, plants, animals and insects as parasites (Carsolio et al., 1994; Gautheret et al., 1995; Furukawa et al., 1998; El-Katatny et al., 2000; Rocha-Ramirez et al., 2002; Druzhinina et al., 2011; Li et al., 2013; Mukherjee et al., 2014; Li Destri Nicosia et al., 2015; Berini et al., 2016; Druzhinina and Kubicek, 2016; Rosmana et al., 2016; Karlsson et al., 2017). Various *Trichoderma* species were shown to protect plants against pathogenic fungi, such as *Rhizoctonia solani* (Grosch et al., 2007; Zhang and Zhuang, 2020). Therefore, they are commonly used as bio-control agents in agriculture, with more than 250 commercial *Trichoderma*-based bio-fungicides registered world-wide (Woo et al., 2014). Apart from being used as bio-fungicide, *Trichoderma* species also stimulate plant growth (Lee et al., 2016)

and nutrient uptake under nutrient deficient conditions (Li et al., 2015), often in combination with better stress tolerance of crop plants (Studholme et al., 2013). Other species, such as *T. pleuroti* (CBS124387) and *T. pleuroticola* (CBS124383) cause green mold disease in oyster mushroom (*Pleurotus ostreatus*) farms (Park et al., 2006).

Most of the investigated *Trichoderma* species colonize either the root surface, or live as endophytes inside root tissues (Samolski et al., 2012; Ruano-Rosa et al., 2016). However, some species were also isolated from the aerial parts of the plants (Bailey and Melnick, 2013). In response, plants often activate defense mechanisms including the biosynthesis of the defense-related phytohormones salicylic acid (SA), jasmonic acid (JA), ethylene (ET) or abscisic acid (ABA) (Contreras-Cornejo et al., 2009; Hermosa et al., 2012; Sivakumaran et al., 2016; Checker et al., 2018). The phytohormones regulate two types of induced resistance in plants, namely, SA-dependent systemic acquired resistance (SAR) and JA/ET-dependent induced systemic resistance (ISR). The signaling events induced by *Trichoderma* species often result in elevated SA and JA levels in different parts of the plant (Martínez-Medina et al., 2013; Leonetti et al., 2017).

In this study, we wanted to find out if the novel endophytic *Trichoderma* strain isolated from the leaves of *Leucas aspera* also interacts with other plant species (*Arabidopsis*, *Nicotiana attenuata*) and has beneficial effects in terms of plant growth and alleviation of abiotic and biotic stress. We could show that, although the strain is phylogenetically related to mushroom-infecting *T. pleuroti* and *T. pleuroticola*, it efficiently colonizes the roots of the two plant species, strongly promotes their growth on soil during early development and protects them against systemic *A. brassicicola* spread, while mycorrhiza formation in *N. attenuata* appears not to be affected. We also evaluated if phytohormones might be involved in the plant-fungus interaction.

MATERIALS AND METHODS

Growth Medium and Conditions for Seedlings

Seeds of wild-type *A. thaliana* (ecotype Columbia-0) were surface-sterilized for 8 min in sterilizing solution containing lauryl sarcosine (1%) and Clorix cleaner (23%). Surface-sterilized seeds were washed with sterilized water eight times and placed on Petri dishes with MS medium supplemented with 0.3% gelrite (Murashige and Skoog, 1962). After cold treatment at 4°C for 48–72 h, plates were incubated at 22°C under long day conditions (16 h light/8 h dark; 80 μmol m^{-2} s^{-1}).

Nicotiana attenuata Torr. ex S. Watson seeds of the 31st generation of an inbred accession originally collected from southwestern Utah were used for all experiments mentioned for this species. Seeds were germinated after surface sterilization and treatment with liquid smoke (1:50 dilution; House of Herbs, Passaic, NY, United States) and 1 mM of gibberellic acid (GA_3; Duchefa-Biochemie, The Netherlands) on agar plates containing Gamborg's B5 medium as previously described in Krügel et al. (2002). Seeds were kept in a growth chamber under a day/night cycle of 16 h (26–28°C)/8 h (24–26°C).

Growth of Fungi and Spore Collection

Based on our previous screen for plant growth-promoting fungi in a field station in India, the new *Trichoderma* strain was selected for detailed characterization. It was isolated from the leaves of *Leucas aspera* (Wild.) Link (family: *Lamiaceae*), a widely distributed medicinal plant reported for its antifungal, antioxidant, antimicrobial and cytotoxic activities (Prajapati et al., 2010; Rajani et al., 2020). The *Trichoderma* strain was grown on Petri dishes with Kaefer medium (KM) or Potato-Dextrose-Agar (PDA) medium, pH 6.5, at 23°C in the dark (Bains and Tewari, 1987; Hill and Käfer, 2001). *Alternaria brassicicola* was grown on Potato-Dextrose-Agar (PDA) medium, pH 6.5, 23°C in the dark (Bains and Tewari, 1987). We did not observe any difference of the fungal performance on the two media. Two additional pathogens, *Fusarium brachygibbosum* and *Alternaria* spp. isolate Utah 10, native to the natural habitat of *N. attenuata* isolated in a previous study (Luu et al., 2015), were grown on PDA medium at 26°C in the dark.

For spore collection, sterilized 0.01% Tween 20 solution was poured onto plates with fungi which were grown for less than 2 weeks. Spores were scratched from the agar surface and dispersed in 0.01% Tween 20. The resulting spore suspension was filtered through two layers of nylon membrane (75 μm pore size, Sefar AG, Switzerland), pelleted and washed with sterile distilled water. The *A. brassicicola* spore concentration was determined in a hemocytometer, while the *Trichoderma* spore concentration was determined by $O.D._{600\ nm}$ measurements using a spectrometer (BioSpectrometer® basic, Eppendorf, Germany).

For co-cultivation experiments with *N. attenuata*, the *Trichoderma* strain was cultivated on PDA plates. Spores of 7–14 day-old cultures were dislodged from the surface with sterile distilled water containing 0.01% Triton X-100. The resulting solution was diluted with distilled water to an $O.D._{600\ nm}$ of 0.250–0.350.

Co-cultivation of *A. thaliana* and *N. attenuata* With *Trichoderma*

Co-cultivation of *A. thaliana* and fungi was performed according to Johnson et al. (2011) with modifications. A plug (5 mm diameter) from a KM plate containing the fungus or a control plug without the fungus was put on a fresh plate with solid plant nutrient medium (PNM), which contained a layer of a nylon membrane (pore size 75 μm) on the agar surface. The plates were incubated at 23°C for 7 days. Unless specified, four 10 day-old *A. thaliana* seedlings of equal size were transferred to the plates. They were incubated at 22°C under long day conditions (16 h light/8 h dark; 80 μmol m^{-2} s^{-1}).

For co-cultivation of *A. thaliana* with *Trichoderma* on soil, 1 kg of soil was suspended in 5 L of distilled water overnight. The liquid was removed by filtration and the soil was autoclaved twice. 200 g of the soil was transferred to magenta boxes for co-cultivation assays. The soil was inoculated with a 5 mm plug of KM medium with or without *Trichoderma* 3 cm below the soil

surface in the center of the box. 10 day-old *Arabidopsis* seedlings were transferred to the soil, and the boxes were kept at 22°C under long day conditions (16 h light/8 h dark; 80 μmol m^{-2} s^{-1}) for 4 weeks.

Co-cultivation of *N. attenuata* with *Trichoderma* was performed in Petri dishes and on soil. For experiments in Petri dishes, sterilized seeds treated with liquid smoke (1:50 dilution; House of Herbs, Passaic, NY, United States) and GA (1 mM GA_3; Duchefa-Biochemie, The Netherlands) were incubated for 1 h with a highly diluted spore and hyphae solution before transfer to GB5 medium (see Santhanam et al., 2019 for experimental details). In a second set-up, liquid smoke-and GA-treated seeds were germinated on GB5 medium for 7 days before they were transferred in a circle with 10 seedlings to a new plate. Immediately after transfer roots either received 10 μL sterile distilled water or the same amount of spore solution ($O.D._{600\ nm}$ = 0.2653). One day later an Agar plug of *Alternaria* spp. Utah 10 was placed in the middle of the plate. Inoculated seedlings were kept at 26°C and 14 h light and 10 h dark cycle for 16 days.

For pot experiments on soil, *Trichoderma* treated seedlings and controls were transferred to pots and cultivated in a Snijders Chamber with a 16 h light/8 h dark cycle at 65% relative humidity.

To study the effect of *Trichoderma* strain on arbuscular mycorrhizal fungi (AMF), *N. attenuata* seedlings were transferred to Teku pots with sand 10 days after germination, and transferred to 10% of the commercial inoculum (BiomycVital, which contains AMF spores and tiny pieces of roots/hyphae in expanded clay)[1] after another 12 days. Upon transfer, half of the plants received a *Trichoderma* spore solution, while control plants received the same amount of distilled water. Plants were watered with hydroponics solution containing 0.05 mM P. Roots were collected for further analysis 8 weeks after transfer.

Nucleic Acid Isolation, Primers, and PCR and Sequencing

Arabidopsis root and fungal tissue were ground in liquid nitrogen, and DNA extraction was performed according to Doyle (1990). RNA from AMF-colonized *N. attenuata* roots was extracted with the LiCl method according to Kistner and Matamoros (2005). RNA samples were treated with DNAse removal kit (Ambion, Thermo Fisher Scientific, Germany) according to the manufacturer's instructions and reverse transcribed with Superscript II (Invitrogen, Thermo Fisher Scientific, Germany) and Oligo-dT.

The primer pairs for amplifying the *TEF1* (translation elongation factor 1-alpha) and *RPB2* (RNA polymerase II subunit 2) genes from *Trichoderma* are: TEF1-F: 5′-CATCGAGAAGTTCGAGAAGG-3′; TEF1-R: 5′-AACTTGCAG GCAATGTGG-3′; RPB2-F: 5′-TGGGGWGAYCARAARAAGG-3′; RPB2-R: 5′-CATRATGACSGAATCTTCCTGGT-3′. Each 20 μL PCR reaction contains 2 μL of 10× DreamTaq Buffer (Thermo Fisher Scientific, Germany), 0.2 mM dNTP, 1.0 μM forward/reverse primer, 100 ng genomic DNA template and 1U of DreamTaq DNA Polymerase (Thermo Fisher Scientific, Germany). The reaction was performed in a thermal cycler (Applied Biosystems SimpliAmp Thermal Cycler, Thermo Fischer Scientific, Germany). The initial denaturation step was set at 95°C for 3 min, followed by 30 cycles of denaturation at 95°C for 30 s, annealing at 55°C (*TEF1*) or 62°C (*RPB2*) for 30 s, and extension at 72°C for 30 s. The final extension step was set at 72°C for 10 min. The PCR products from at least two independent PCR runs were purified by NucleoSpin Gel and PCR Clean-up kit (Macherey-Nagel, Germany). Purified PCR products were sent to Eurofins Genomics for Sanger sequencing. Consensus sequence of *TEF1* and *RPB2* was deposited to Genbank with accession numbers MT591352 and MT602550, respectively.

To quantify the colonization of *Trichoderma* under various salt concentrations, *Trichoderma TEF1* and *A. thaliana RPS* (AT1G34030) were detected by qPCR with the following primers: TEF-qF: 5′-TCAAGTCCGTTGAGATGCAC-3′; TEF-qR: 5′-CGTTCTTGACGTTGAAACCA-3′; RPS-qF: 5′- GT CTCCAATGCCCTTGACAT-3′; RPS-qR: 5′-TCTTTCCTCTGCGACCAGTT-3′.

For qPCR analysis of AMF colonization of *N. attenuata* roots, qPCR reactions were performed on Mx3005P qPCR system (Stratagene, Santa Clara, CA, United States) with Takyon Sybr Green No ROX kit (Eurogentec, Belgium). Primers for *NaRAM1*, *NaPT4*, and *Rhizophagus irregularis tubulin* are from Wang et al. (2018a). Primers for *NaEF1* are from Wang et al. (2018b). Primers for *RPB2* of *Trichoderma* are: RPB2-qF: 5′-AGACGTCCATGATCTGCATGAC-3′; RPB2-qR: 5′-TGTCTTGGTCTTGAGTCGCTTG-3′

The genes for *A. thaliana Ubiquitin 5*, *N. attenuata Elongation Factor 1 alpha* (*NaEF1,* Wang et al., 2018b) and *A. brassicicola Cutinase 1* were used to monitor *A. brassicicola* infection in root tissue. The primer pairs for qPCR analysis are: AtUBQ5-qF: 5′-GACGCTTCATCTCGTCC-3′; AtUBQ5-qR: 5′-GTAAACGTAGGTGAGTCCA-3′; AbCUT1-qF: 5′-GACCGAGGAAGCTCAGATGC-3′; AbCUT1-qR: 5′-GCCTGGGATCTTGGAATGC-3′.

Multilocus Phylogenetic Analysis

The nucleotide sequences of *TEF1* and *RPB2* from 55 *Trichoderma* species and an outgroup species, *Nectria eustromatica*, were retrieved from the NCBI Nucleotide public database. The *TEF1* and *RPB2* sequences of the new *Trichoderma* strain were obtained from the PCR products. *TEF1* and *RPB2* genes from the same species were concatenated for combined analysis. In total, 56 concatenated sequences were subjected to alignment using MAFFT v7 online at https://mafft.cbrc.jp/alignment/server (Katoh et al., 2019), with G-INS-i parameters and a scoring matrix of "1PAM/κ = 2" for nucleotide sequences. The resulting alignment was inspected and selected for conserved blocks using Gblocks version 0.91b (Castresana, 2000).

Maximum likelihood analysis was conducted using RaxML-NG v.0.9.0 through web service at https://raxml-ng.vital-it.ch (Kozlov et al., 2019). Using the GTR+FO+G4m model, 2000 distinct ML tree were searched and bootstrapped with 100 replicates. For maximum parsimony analysis,

[1] www.biomyc.de

PAUP 4.0a166 was utilized (Swofford, 2002). Heuristic search of 100 replicates was performed with random addition of sequence, and tree bisection-reconnection (TBR) as the branch-swapping algorithm (steepest decent and MulTrees option not in effect). All characters were weighted equally, and gaps were treated as missing character. Bootstrap of 1,000 replicates was undertaken with Maxtrees set as 5,000.

The Bayesian analysis was conducted using MrBayes v3.2.7a (Huelsenbeck and Ronquist, 2001; Ronquist and Huelsenbeck, 2003). The evolutionary model was set to the general time-reversible model (GTR; Tavare, 1986), and the nucleotide variation rate set to inverse gamma distribution (Yang, 1993). Two simultaneous and independent Markov chain Monte Carlo (mcmc) analyses was run to generate 1 million generations each, while they were sampled for every 10 generations to determine the posterior probability (Geyer, 1991). From the resulting 100,000 sampled trees, the first 25% of them were discarded, and the remaining 75,000 trees were summarized to produce the consensus tree.

The Maximum likelihood boostrap proportions (MLBP), Maximum parsimony bootstrap proportions (MPBP), as well as the Bayesian inference posterior probability (BIPP) from each analysis were combined to the phylogenetic tree from the RAxML analysis using TreeGraph2.15.0–887 beta (Stöver and Müller, 2010). The final tree was created with FigTree v1.4.4 (Rambaut, 2018). The accession numbers of the individual genes are provided in **Supplementary Table 1**.

Histological Staining and Microscopy

Roots of *A. thaliana* co-cultivated with the *Trichoderma* strain for 2 or 7 days were collected and immersed in Wheat Germ Agglutinin, Alexa Fluor^{TM} 488 Conjugate (Thermo Fisher Scientific, Germany) for 10 min in dark. Immersed samples were taken out from the staining solution and placed on a glass slide. Water was applied to the slide to wash away excess staining solution and the slide was covered with a cover slip for microscopic inspection with Axio Imager.M2 (Zeiss Microscopy GmbH, Germany). The bright field and fluorescent images were recorded with a monochromatic camera Axiocam 503 mono (Zeiss Microscopy GmbH, Germany). Digital images were processed with the ZEN software (Zeiss Microscopy GmbH, Germany).

For confocal imaging of root colonization, *A. thaliana* roots co-cultivated with *Trichoderma* for 2 days were stained with Wheat Germ Agglutinin, Alexa Fluor^{TM}488 Conjugate and RH414 [N-(3-Triethylammoniumpropyl)-4-(4-(4-(Diethylamino)phenyl)Butadienyl)Pyridinium Dibromide; Thermo Fischer Scientific, Germany] with the method described above. Samples were imaged using an LSM 880 microscope (Zeiss Microscopy GmbH, Germany) with the 488 nm laser line of an argon multiline laser (11.5 mW). Images were taken with a 40× objective (Plan-Apochromat 40×/0.8). Lambda stacks were created using the 32 channel GaAsP detector followed by Linear Unmixing with the ZEN software. Z-stacks were taken from specific areas of the sample and Maximum Intensity Projections were produced with the ZEN software.

Phytohormone Analyses by LC-MS/MS

Sixteen seedlings from control and co-cultured plates were harvested and separated into root and shoot samples. Mycelium of the *Trichoderma* strain grown on KM plates was harvested for phytohormone analysis.

Fifty to one hundred thirty milligrams of fresh tissue were extracted and homogenized in 1.5 mL methanol containing 60 ng D4-SA (Santa Cruz Biotechnology, United States), 60 ng D6-JA (HPC Standards GmbH, Germany), 60 ng D6-ABA (Santa Cruz Biotechnology, United States), 12 ng D6-JA-Ile (HPC Standards GmbH), and D5-indole-acetic acid (D5-IAA, OlChemIm s.r.o., Olomouc, Czech Republic) as internal standards. Samples were agitated on a horizontal shaker at room temperature for 10 min. The homogenate was mixed for 30 min and centrifuged at 13,000 rpm for 20 min at 4°C and the supernatant was collected. The homogenate was re-extracted with 500 μL methanol, mixed and centrifuged and the supernatants were pooled. The combined extracts were evaporated under reduced pressure at 30°C and dissolved in 500 μL methanol.

Phytohormone analysis was performed by LC-MS/MS as in Heyer et al. (2018) on an Agilent 1260 series HPLC system (Agilent Technologies) with the modification that a tandem mass spectrometer QTRAP 6500 (SCIEX, Darmstadt, Germany) was used. Since we observed that both the D6-labeled JA and D6-labeled JA-Ile standards (HPC Standards GmbH, Cunnersdorf, Germany) contained 40% of the corresponding D5-labeled compounds, the sum of the peak areas of the D5- and D6-compounds was used for quantification. Details of the instrument parameters and response factors for quantification can be found in **Supplementary Table 2**.

Indole-acetic acid was quantified using the same LC-MS/MS system with the same chromatographic conditions but with positive mode ionization with an ion spray voltage at 5,500 eV. Multiple reaction monitoring (MRM) was used to monitor analyte parent ion → product ion fragmentations as follows: m/z 176 →130 [collision energy (CE) 19 V; declustering potential (DP) 31 V] for indole-acetic acid (IAA); m/z 181 →133 + m/z 181 →134 + m/z 181 →135 (CE 19 V; DP 31 V) for D5-indole-acetic acid.

Quantification of Mycelial Growth, AMF Colonization, and 11-Carboxyblumenol Levels

Plates with mycelia were scanned with an Epson scanner (Perfection V600 Photo, Epson, Germany), and the files imported into ImageJ (Schindelin et al., 2012). Mycelial coverage on each plate was delineated using a free-hand selection tool and measured with the built-in "Measure" function.

AMF colonization was determined by the "magnified intersections method" described in detail by McGonigle et al. (1990). In brief, roots were cut in about 1 cm pieces and we counted the fungal structures of 150 intersections per sample after staining with Trypan Blue.

For determination of AMF colonization marker 11-carboxyblumenol, three leaf disks per AMF inoculated of the first and second stem leaf were harvested 6 and 8 weeks after

AMF inoculation. 11-Carboxyblumenol levels were determined as markers of arbuscule colonization and quantified following the protocol of Wang et al. (2018a).

Statistical Tests

Statistical tests were performed using R studio version 1.1.463 with R version 3.4.4. Figures were plotted using Python 3.7.4 and arranged with LibreOffice Draw 5.1.6.2.

RESULTS

Morphological and Phylogenetic Analysis of the New *Trichoderma* Strain

The *Trichoderma* strain was isolated from leaves of *Leucas aspera* (Wild.) Link. We selected this strain for further analysis because we observed in preliminary field experiments that it promotes growth of several crop species. Its morphology shows typical characteristics of *Trichoderma* species of the *harzianum* clade. On KM plates, the hyphae cover the entire Petri dish from a single plug (5 mm in diameter) in 3–4 days (**Supplementary Figure 1A**). During the first 3 days after transfer to a new plate, the hyphae extended and formed conidiophores at the tip of hyphal branches. The conidia grew, replicated, and aggregated at the tip of a conidiophore (**Supplementary Figure 1B**). After 7 days, mature conidia developed as sphere-like structure composed of numerous individual conidia (**Supplementary Figure 1C**). The hyphal cell shrank after the conidia were fully developed. This allowed them to detach from the hyphae (**Supplementary Figure 1D**). The fully matured conidia displayed a green color (**Supplementary Figure 1E**).

Phylogenetic analysis based on Maximum likelihood, Maximum Parsimony and Bayesian Inference of phylogeny uncovered that the isolated *Trichoderma* strain belongs to the *harzianum* clade (**Figure 1**), closely related to *T. confertum* TC62 and *T. confertum* TC139, two strains recently isolated from the soil 2,000 m above sea level in Tibet (Chen and Zhuang, 2017). The multilocus sequence analysis also indicated that the strain is closely related to *T. pleuroti* and *T. pleuroticola*, but less compared to *T. confertum*. In summary, according to the three different analysis methods, the isolated fungus is most probably a new *Trichoderma* strain closely related to *T. confertum*.

The New *Trichoderma* Strain Colonizes *Arabidopsis* and *Nicotiana* Roots and Promotes Plant Growth

To characterize the endophytic lifestyle of the new strain, and to check which organ of the plant can be colonized by the fungus, it was co-cultivated with the model species, *Arabidopsis thaliana*. Two days after co-cultivation, hyphae were already detectable on the surface of the roots (**Figures 2A,C**). Light and confocal microscopy showed that hyphae also invaded into the root hair (**Figures 2B,D–G** and **Supplementary Movie 1**). Seven days after co-cultivation, the *Arabidopsis* roots were highly colonized, and conidiophores were found at the tip of the root hair, although not every root hair contained hyphae or conidiophore (**Figures 2H–K**). Close inspections revealed that the conidiophores derived from the hyphae in the root hairs. Under these co-cultivation conditions without stress, the aerial parts of the plant were not colonized.

When *Arabidopsis* plants were co-cultivated on soil in the greenhouse, the germination rate and the performance of the young seedlings were not affected by the fungus. However, we observed a strong initial growth-promoting effect of the fungus on 4-week old *Arabidopsis* plants, since colonized plants were almost twice as large as the uncolonized controls (**Figures 3A,B**). Root colonization by the *Trichoderma* strain was confirmed by microscopy (**Supplementary Figure 2**). During later stages, the growth difference between colonized and uncolonized plants became less and during flowering time, the growth-stimulating effect of the fungus was barely visible. The number and size of seeds was not significantly different for plants grown with or without the fungus (data not shown). This indicates that the fungus promotes plant growth during early stages of development.

Growth promotion was also observed for the model plant *N. attenuata* (cf. also below). We observed the same colonization efficiencies as described above for *Arabidopsis* seedlings. Also, the germination rates were similar for inoculated and non-inoculated seeds, and all seedlings were healthy. Similar to *Arabidopsis*, we observed a stimulatory effect of the fungus on *N. attenuata* growth after 4 weeks on soil, when both the rosette diameter and root biomass were larger (**Figures 3C,D**). Comparable to *Arabidopsis*, the growth-stimulating effect disappeared during later stages of development. However, we observed a clear difference in the response of the two hosts on agar plates during early seedling's development, where root and shoot development can be monitored in more details. With fungal inoculation, the shoots and roots of 12-day-old *Arabidopsis* seedlings were bigger in the presence of the fungus (see **Figure 5**), while 12-day-old colonized *N. attenuata* had significantly shorter shoots and roots than the uncolonized controls (**Figure 3E**). We also observed more root hairs beneath the root-shoot junction, where roots are in contact with the fungus (**Figure 3F**). These effects were not observed for the roots of *Arabidopsis* seedlings. In conclusion, the fungus has different effects on the early development of the seedlings on agar medium.

The New *Trichoderma* Strain Is Tolerant Against 100 mM Salt and Mild Salt Conditions Promote the Interaction With the Host on Synthetic Medium

Plant growth promoting fungi and bacteria often also improve the stress tolerance of plants (Qin et al., 2016). Therefore, we first tested if the fungus itself is tolerant against salt and mannitol (osmotic) stress. Fungal growth was not altered on 100 mM NaCl compared to control plates without salt. At 300 mM NaCl, the mycelial growth was reduced by about 50%. At 1 M NaCl, only slowly growing mycelia could be detected after 10 days, and no growth was detectable on 3 M NaCl (**Figure 4A** and **Supplementary Figures 3A–G**). Increasing mannitol concentrations did not inhibit mycelial

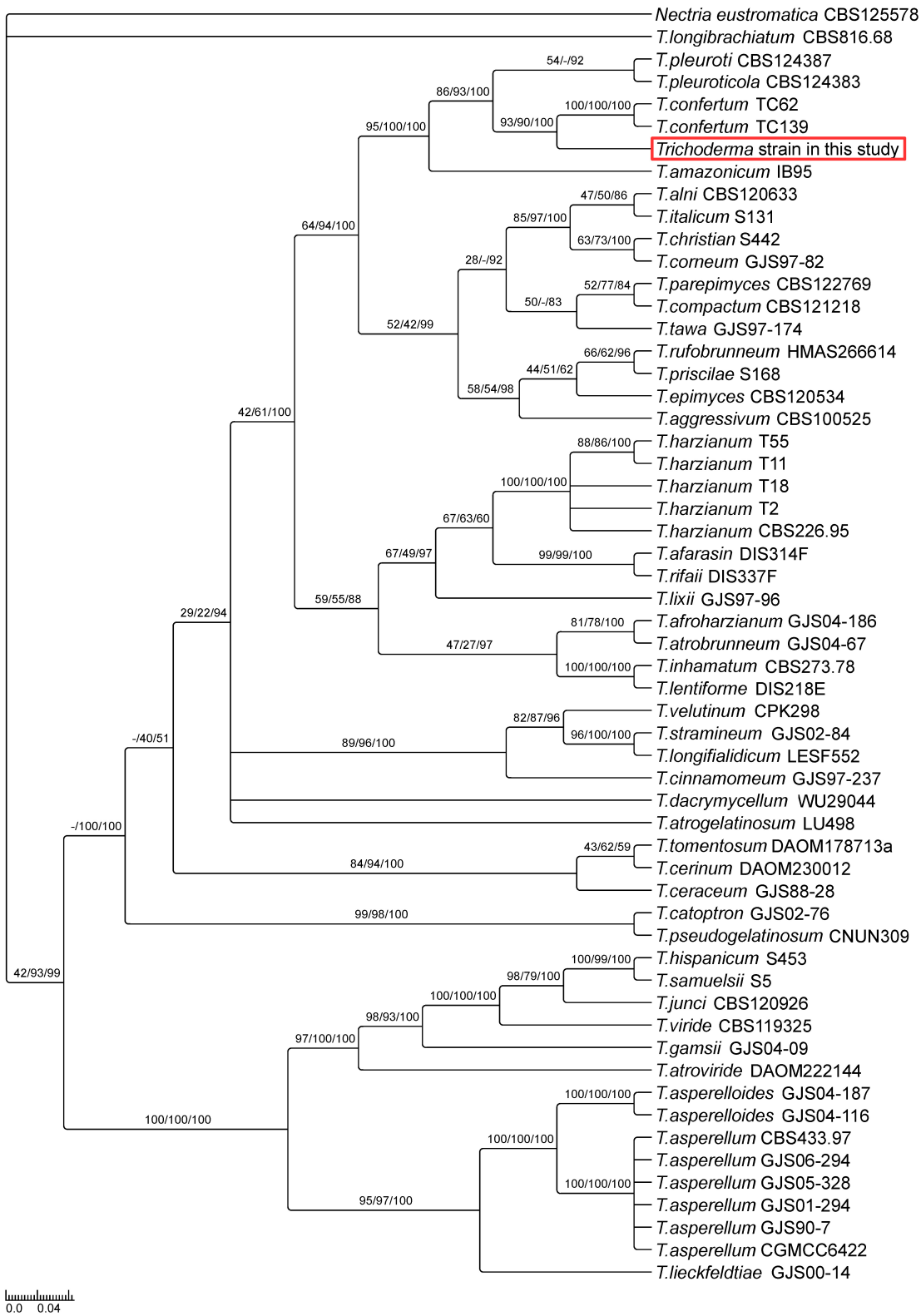

FIGURE 1 | Phylogeny of selected *Trichoderma* species suggests a new *Trichoderma* strain closely related to *T. confertum*. The phylogenetic tree is based on combined analysis of *TEF1* and *RPB2* genes using Bayesian inference of phylogeny. Maximum likelihood bootstrap values (MLBP, left), maximum parsimony bootstrap values (MPBP, center) and Bayesian inference posterior probabilities (BIPP, right) are shown at each node. *Nectria eustromatica* was used as outgroup.

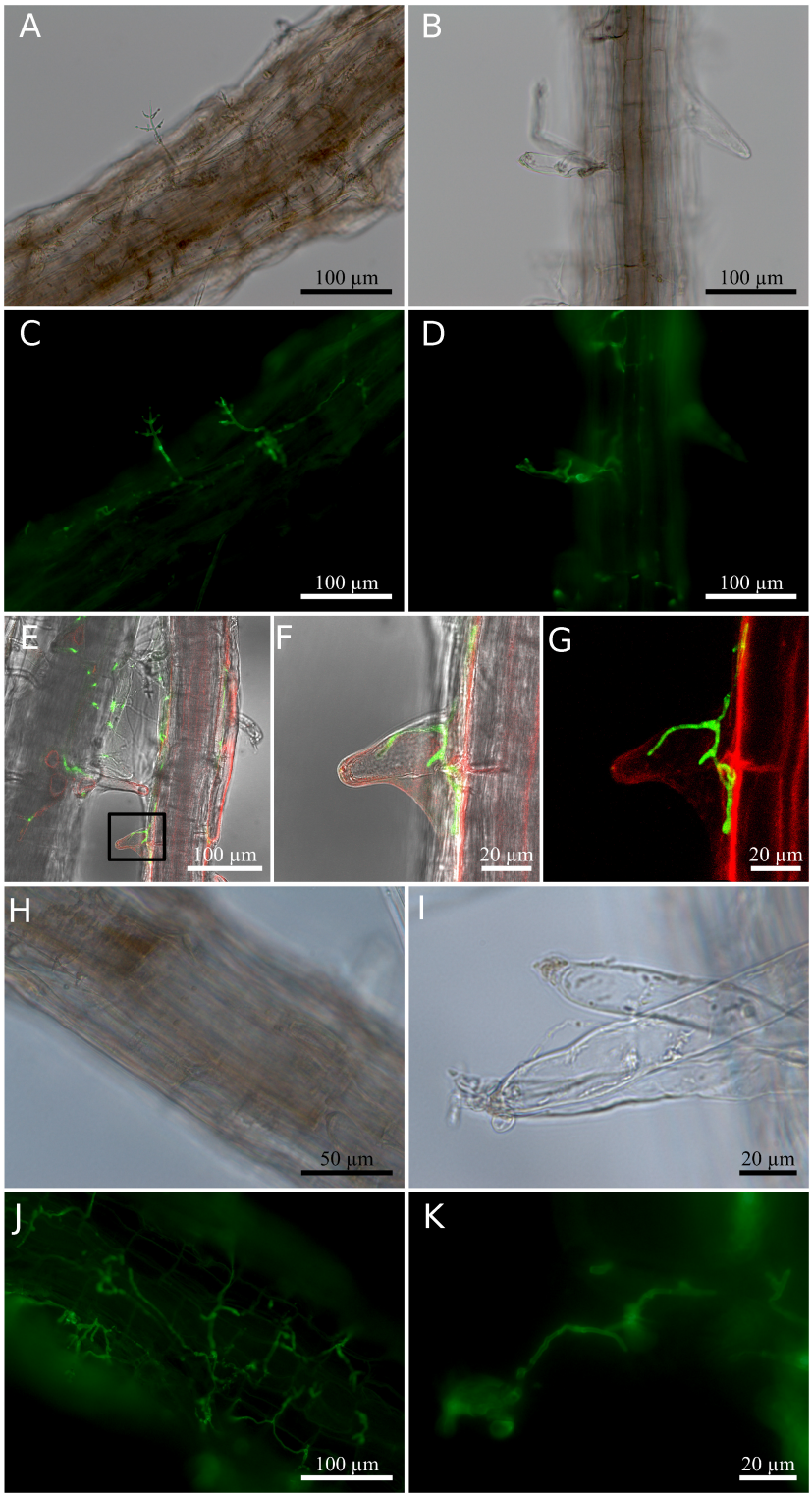

FIGURE 2 | Root colonization of *Arabidopsis thaliana* by *Trichoderma*. **(A–D)** Co-cultivation for 2 days. **(A,B)** Bright field; **(C,D)** fluorescence of fungal stain. **(E)** Confocal images of hyphae inside root hair observed 2 days after co-cultivation. **(F)** Magnified view of the region enclosed by the small box in **(E)**. **(G)** Fluorescence signal indicating hyphae (green) and plant cell plasma membrane (red) in **(F)**. **(H–K)** Co-cultivation for 7 days. **(H,I)** Bright field; **(J,K)** fluorescence of fungal stain. Colonized root tissues were stained with WGA Alexa Fluor™ 488 conjugate to detect the presence of the fungus, and RH414 was used to visualize the plant plasma membrane. The image shown for the confocal microscopy was chosen from three individual roots of three biological replicates.

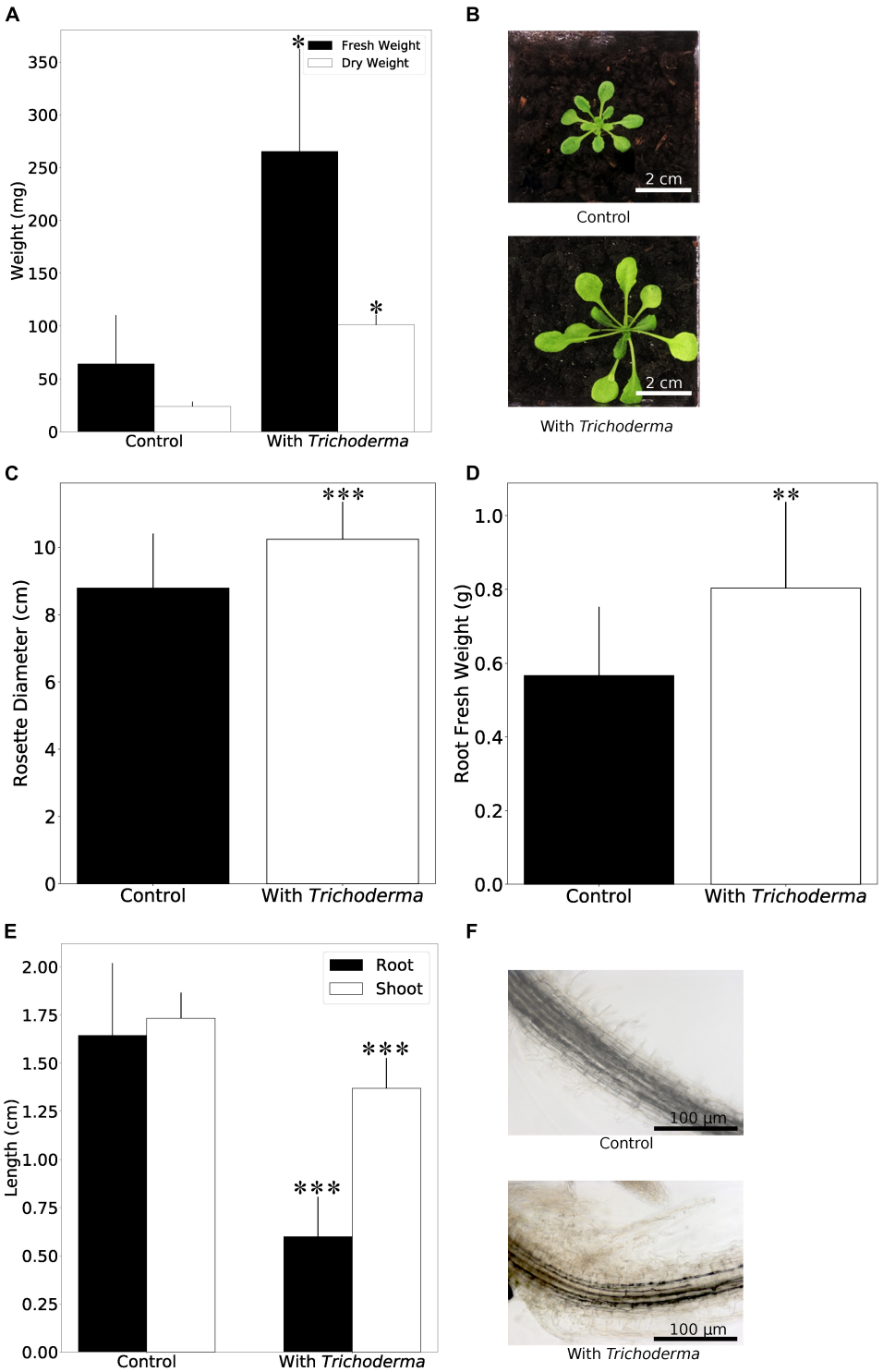

FIGURE 3 | Plant growth performance is influenced by *Trichoderma* colonization. **(A)** Fresh and dry weights of *A. thaliana* grown on soil with or without *Trichoderma* after 4 weeks. Error bars represent SEs from three independent biological replicates, each with four seedlings. Statistical significance was determined by Welch Two Sample *t*-test (*$P < 0.05$). **(B)** Growth promotion on *A. thaliana* on soil after 4 weeks. **(C,D)** Rosette diameter **(C)** and root fresh weight **(D)** of *N. attenuata* inoculated with or without *Trichoderma* on soil after 4 weeks. Error bars represent SDs from 39 independent biological replicates for shoots and 18 replicates for roots. Statistical significance was determined by Welch Two Sample *t*-test (**$P < 0.01$; ***$P < 0.001$). **(E)** Shoot and root lengths of *N. attenuata* 12 days after co-cultivation with *Trichoderma* (spore solution $O.D._{600\ nm} = 0.0135$) or without *Trichoderma* on Petri dishes. Error bars represent SDs from 10 biological replicates. Statistical significance was determined by Welch Two Sample *t*-test (***$P < 0.001$). **(F)** Microscopy of *N. attenuata* roots 12 days on Petri dishes with or without *Trichoderma*.

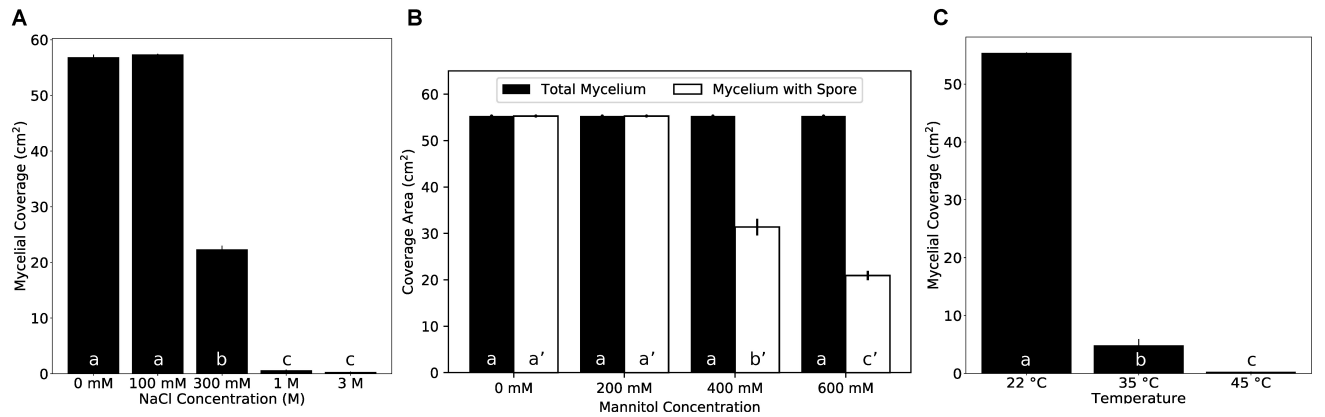

FIGURE 4 | Growth of the *Trichoderma* strain under various conditions on KM plates. **(A)** Fungal growth on different NaCl concentrations. **(B)** Fungal growth on different mannitol concentrations. **(C)** Fungal growth at different temperatures. Error bars represent SEs from three independent biological replicates. Statistical significance was determined by Tukey's HSD test with $P < 0.05$, and is indicated by different lower-case letters.

growth, although the production of conidia was reduced on media with >400 mM mannitol (**Figure 4B** and **Supplementary Figures 3H–K**). Also high temperature strongly impaired growth of the fungus (**Figure 4C** and **Supplementary Figures 3L–N**).

The ability of the fungus to survive 1 M NaCl intrigued us to find out if salt influences the growth stimulating effect of its host. Unlike on soil, when seedlings were grown on solid PNM medium without addition of NaCl for 5 days, we observed only a small increase in growth and biomass production of the *Arabidopsis* seedlings in the presence of the fungus. However, application of 50 mM NaCl to the medium strongly promoted growth and biomass production (**Figures 5A,B**; supported by *post-hoc* analysis shown in **Supplementary Table 3**). This was accompanied by a stronger root colonization (**Figure 5C**). In particular, the lateral roots of the host were massively colonized and the fungus produced large amounts of conidiospores, compared to those on medium without NaCl. On 100 mM and higher NaCl concentrations, the growth of the uncolonized plants was gradually reduced, and growth of *Trichoderma*-colonized roots was not stimulated any more (**Figure 5A** and **Supplementary Figure 4**). Closer inspections uncovered that roots were even more colonized, and the hyphae also appeared on the surface of the areal parts. They were not only detectable at and around the hypocotyl (**Supplementary Figure 4**) but also on the leaf surface (data not shown). In summary, apparently, the fungus colonizes preferentially the roots. Low NaCl concentrations promoted root colonization and stimulated plant growth, while higher salt concentrations forced the fungus to invade the aerial parts which was associated with a loss of the benefits to the host.

The New *Trichoderma* Strain Inhibits Growth of *Alternaria* and Protects *Arabidopsis* and *Nicotiana* Against *Alternaria* Infection

One of the prominent traits of *Trichoderma* species in the *harzianum* clade is their potential to act as bio-control agent. After 8 days of co-cultivation of *Alternaria brassicicola* with the *Trichoderma* strain on PDA plates, the mycelial coverage of *A. brassicicola* was reduced by 73% and *Trichoderma* hyphae grew on top of the *A. brassicicola* mycelial lawn (**Figures 6A–C**). To rule out that faster growth of *Trichoderma* restricts *A. brassicicola* growth, *Trichoderma* was added to an agar plate with a 7-day old *A. brassicicola* culture (**Figure 6D**). After additional 7 days of co-cultivation, *Trichoderma* hyphae and spores were again observed on top of the *A. brassicicola* mycelial lawn (**Figure 6E**). This supports active predation of *A. brassicicola* by the new *Trichoderma* strain (Druzhinina et al., 2018).

We further tested *Fusarium brachygibbosum and Alternaria* spp. *Utah isolate 10*, two fungal species previously characterized as a native pathogen for *N. attenuta* (Luu et al., 2015), and co-cultivated them with *Trichoderma*. Growth of *Trichoderma* was much faster than that of the two other species, but *F. brachygibbosum* clearly stopped further growth of *Trichoderma* when hyphae of the two fungi met, while *Alternaria* spp. was overgrown by *Trichoderma* after 3½ weeks of co-cultivation (**Figures 6F,G**).

To test if the *Trichoderma* strain also protects plants from *Alternaria* infection, *Arabidopsis* seedlings were first exposed to *A. brassicicola* (A) or *Trichoderma* (T) or were mock-treated (C) and then transferred to plates with either *A. brassicicola* or *Trichoderma* for additional 7 days. As expected, the highest amount of *A. brassicicola* DNA was detected in seedlings which were exposed to *A. brassicicola* only (**Figure 7A**). Roots which were exposed to *Trichoderma* either before or after *A. brassicicola* treatment (A-T) contained less DNA of the fungal pathogen. Furthermore, the seedlings were better protected against *A. brassicicola* when they were already colonized by *Trichoderma* before pathogen infection (**Figure 7A** and **Supplementary Figure 5A**). Similar results were observed for *N. attenuata* and *Alternaria* (**Supplementary Figure 5B**). This demonstrates that the *Trichoderma* strain restricts growth of the pathogen in roots of its host plant.

To investigate whether *Trichoderma* also protects the leaves against *A. brassicicola* infection, 500 colony forming units (CFU)

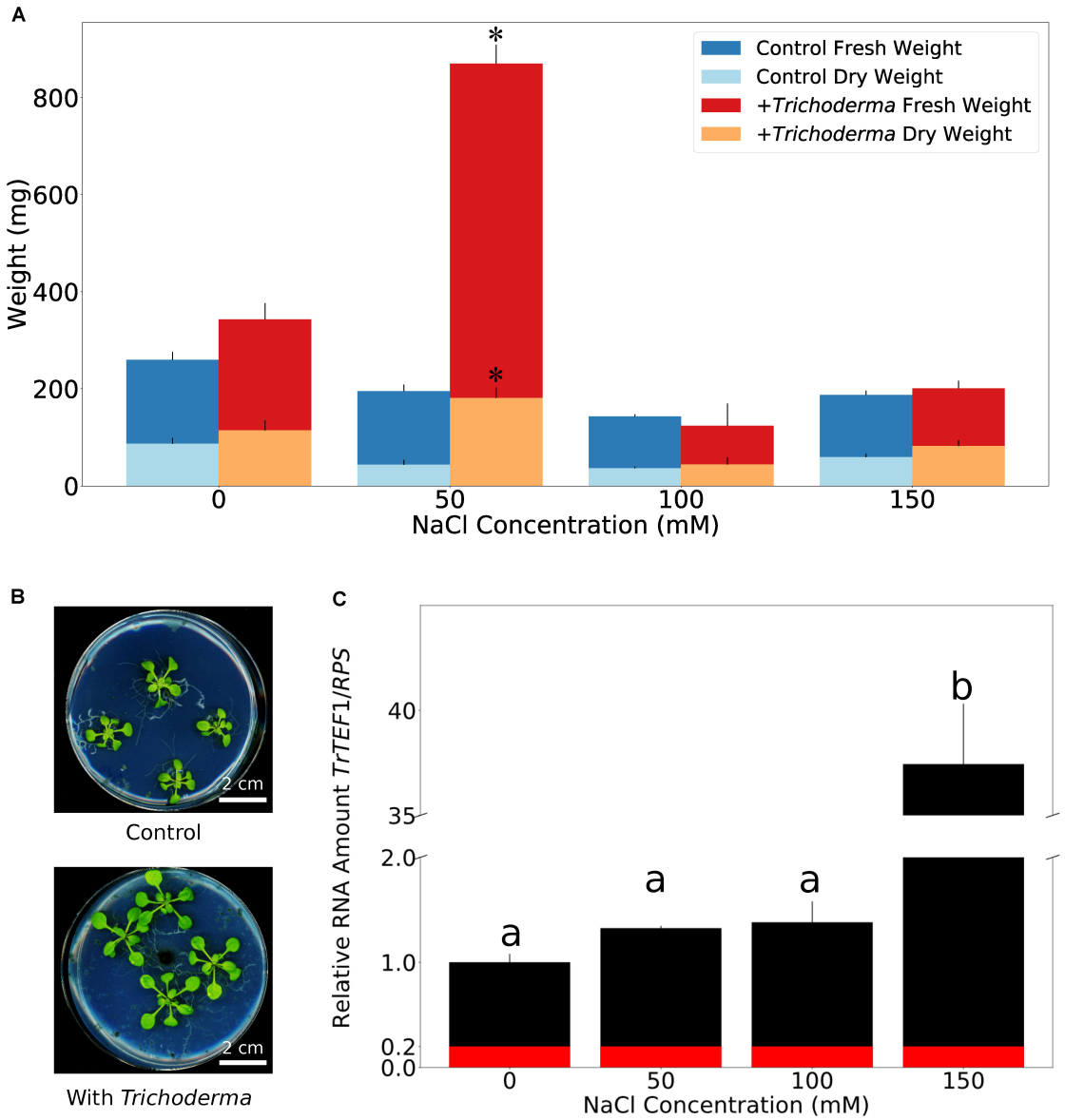

FIGURE 5 | Mild salt condition optimizes fungal colonization and plant growth performance on synthetic medium. **(A)** Fresh and dry weights of *A. thaliana* co-cultivated with or without *Trichoderma* on PNM medium with 0–150 mM NaCl for 5 days. Error bars represent SEs from three independent biological replicates, each with four seedlings. Statistical significance was determined by 2-Way ANOVA. *Post-hoc* analysis between all groups was further carried out by Tukey HSD test with $P < 0.05$, and is shown in **Supplementary Table 3**. Asterisks indicate significant difference in fresh/dry weight of seedlings grown on 50 mM NaCl with or without *Trichoderma*. **(B)** Growth phenotype of *A. thaliana* on PNM medium with 50 mM NaCl 5 days after co-cultivation with or without *Trichoderma*. **(C)** Quantification of *Trichoderma* root colonization on *A. thaliana* on PNM medium with 0–150 mM NaCl by qPCR. *TrTEF1*: *Trichoderma TEF1*; *RPS*: *A. thaliana* ribosomal protein S13/S18 family. Error bars represent SEs from three independent biological replicates, each with four seedlings. Statistical significance was determined by Tukey's HSD test with $P < 0.05$, and is indicated by different lower-case letters. Red color represents average background value referred from samples without *Trichoderma*.

of an *A. brassicicola* spore suspension were applied to the leaves of *Arabidopsis* seedlings which were either co-cultivated with the symbiont or mock-treated for 7 days. Four days later, the necrotic zone on the leaves of co-cultivated plants was significantly smaller compared to the non-colonized controls (**Figure 7B**). Taken together, *Trichoderma* restricts spread of *Alternaria* in both roots and shoots.

Mycorrhiza Formation Is Not Affected by the New *Trichoderma* Strain in *N. attenuata*

Restriction of *Alternaria* growth by the new *Trichoderma* strain indicated a putative use for bioprotection. However, agricultural application requires that other beneficial fungi, such as arbuscular mycorrhizal fungi (AMF) are not affected by the

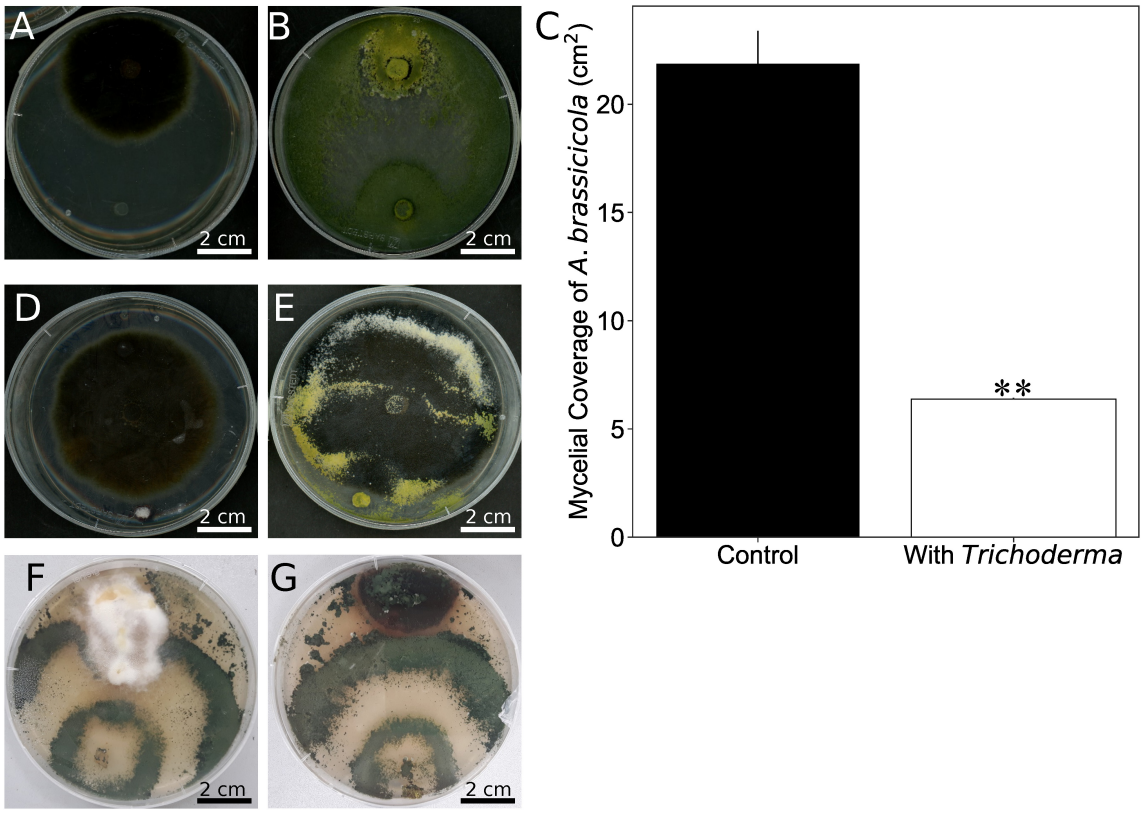

FIGURE 6 | *Trichoderma* inhibits growth of *Alternaria brassicicola*. **(A,B)** A plug of *A. brassicicola* was applied to the upper side of the PDA plate. A plug of KM agar **(A)** or the *Trichoderma* strain **(B)** was put to the lower side of the plate before co-cultivation for 8 days. **(C)** Quantification of *A. brassicicola* mycelial coverage from **(A,B)**. Error bars represent SDs from three independent biological replicates. Statistical significance was determined by Welch Two Sample *t*-test (**$P < 0.01$). **(D)** An agar plug with *Trichoderma* was placed on a PDA plate which contained 7-day old *A. brassicicola* culture. **(E)** Seven days after the plug with *Trichoderma* was placed in **(D)**. **(F,G)** Co-cultivation of *Trichoderma* with the native *N. attenuata* pathogens *Fusarium brachygibbosum* **(F)** or *Alternaria* spp. strain Utah 10 **(G)**.

Trichoderma strain. As *Arabidopsis* is a non-mycorrhizal species, we used the well-established *N. attenuata* system (Groten et al., 2015). *N. attenuata* plants grown on soil in the greenhouse were simultaneously inoculated with AMF and *Trichoderma*. Microscopic observations of the roots and qPCR analyses with fungus-specific markers clearly indicate that AMF and *Trichoderma* colonize the roots and propagate, without inhibiting each other (**Figures 8A,B**). In addition, the amounts of 11-carboxyblumenol, a marker for AMF root colonization (Wang et al., 2018a), did not differ between *Trichoderma*-inoculated and non-inoculated samples (**Figure 8C**). 11-Carboxyblumenol levels were also similar when plants were pre-inoculated with AMF and after 6 weeks co-cultured with *Trichoderma* (data not shown). These results suggest that AMF colonization is not affected by the new *Trichoderma* strain in *N. attenuata*.

The *Trichoderma* Strain Alters Phytohormone Levels in *Arabidopsis* Roots and Shoots

Beneficial plant-microbe interactions often result in altered phytohormone levels, which may lead to better fitness of the host upon pathogen attack but can also influence root colonization due to an altered plant immune system (Jacobs et al., 2011). In mycelial cultures, we detected only trace amounts of auxin (indole-acetic acid, IAA) and SA (**Figure 9A**). However, SA in *Trichoderma*-colonized seedlings were significantly reduced in roots and increased in shoots compared to controls (**Figure 9B**). Metabolites related to the biosynthesis and degradation of JA as well as ABA and IAA also showed some minor changes after *Trichoderma* colonization, but compared to SA, these changes were rather weak (**Figures 9C,D** and **Supplementary Figure 6**). Overall, it appears that the fungus does not produce high hormone levels itself influencing plant performance, but the fungus may activate SA-dependent resistance responses in the plant.

DISCUSSION

In this study, a new endophytic *Trichoderma* strain is described. It belongs to the *harzianum* clade, closely related to *T. confertum, T. pleuroti* and *T. pleuroticola*. It survives under salt and osmotic stress, and possesses a strong capability to reduce *A. brassicicola* growth. The hyphae colonize the root surface and are found in root hairs of *A. thaliana*. Infection assays showed reduced

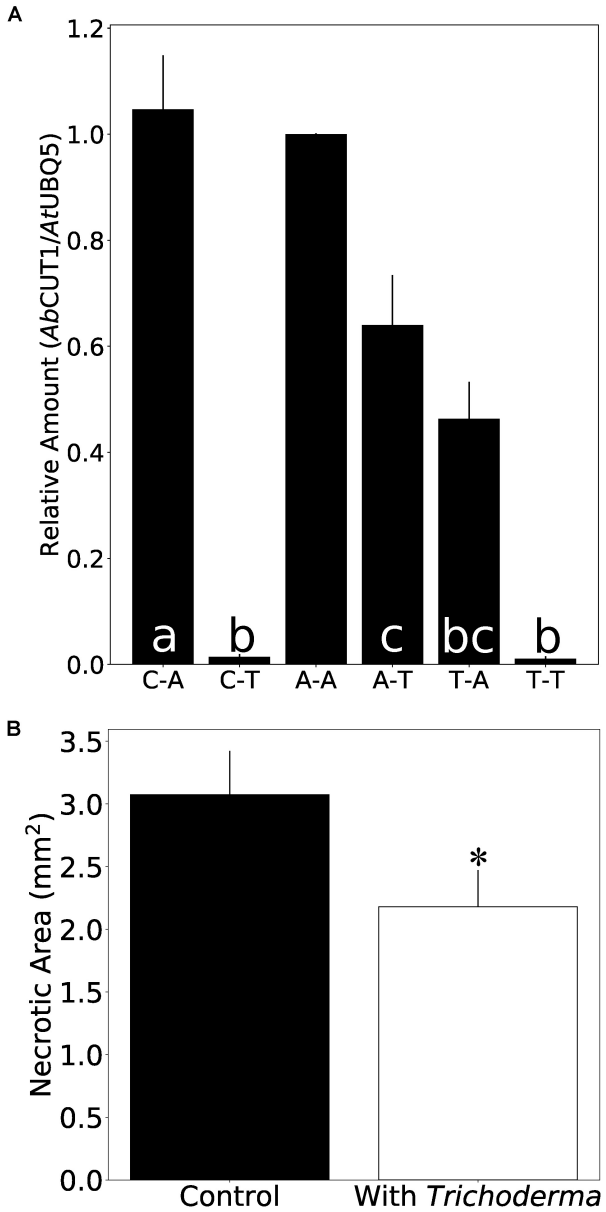

FIGURE 7 | *Trichoderma* protects *Arabidopsis* seedlings against *A. brassicicola* infection. **(A)** Amount of *A. brassicicola CUT1* DNA relative to *A. thaliana UBQ5* DNA in root tissue. C-A: co-cultivation with control plug for 7 days, then co-cultivation with *A. brassicicola* for another 7 days. C-T: co-cultivation with control plug for 7 days, then co-cultivation with *Trichoderma* for another 7 days. A-A: co-cultivation with *A. brassicicola* for 7 days, then co-cultivation with *A. brassicicola* for another 7 days. A-T: co-cultivation with *A. brassicicola* for 7 days, then co-cultivation with *Trichoderma* for another 7 days. T-A: co-cultivation with *Trichoderma* for 7 days, then co-cultivation with *A. brassicicola* for another 7 days. T-T: co-cultivation with *Trichoderma* for 7 days, then co-cultivation with *Trichoderma* for another 7 days. Values from qPCR experiment were normalized to A-A. Error bars represent SEs from three independent biological replicates, each with 6–9 seedlings. Statistical significance was determined by Tukey's HSD test with $P < 0.05$, and is indicated by different lower-case letters. **(B)** Necrosis area on leaflets infected by *A. brassicicola.* Error bars represent SEs from 35 independent biological replicates. Statistical significance was determined by Welch Two Sample *t*-test (*$P < 0.05$).

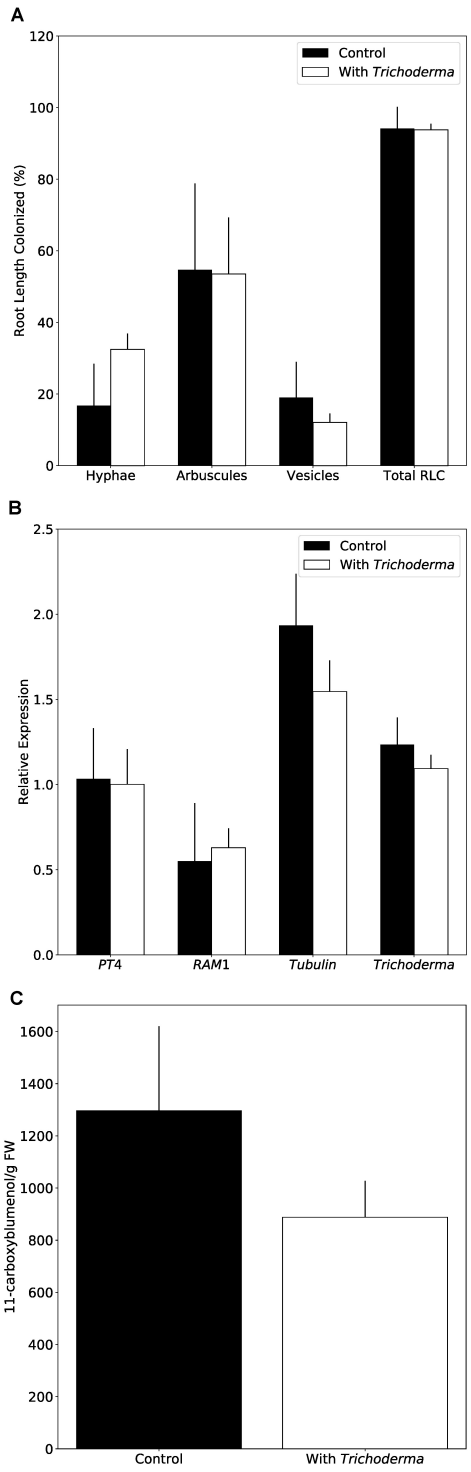

FIGURE 8 | *Trichoderma* does not interfere with mycorrhiza formation on *N. attenuata*. **(A)** AMF colonization 8 weeks after inoculation with or without *Trichoderma* and AMF simultaneously. Error bars represent SEs from three independent biological replicates. Statistical significance was determined by Welch Two Sample *t*-test between control and co-culture treatments and was not significantly different. RLC, Root length colonization. **(B)** AMF marker gene expression determined by qPCR. *PT4*, Phosphate transporter 4; *RAM1*,

(Continued)

FIGURE 8 | Continued
Reduced Arbuscular Mycorrhization 1; *Tubulin*, *Tubulin* gene of *R. irregularis; Trichoderma, RPB2* of *Trichoderma*. Relative expression was normalized to *N. attenuata* elongation factor 1-α. Error bars represent SEs from three to five independent biological replicates. Statistical significance was determined by Welch Two Sample *t*-test between control and co-culture treatments, and was not significantly different. **(C)** 11-Carboxyblumenol level in *N. attenuata* roots 8 weeks after inoculation of AMF, with or without *Trichoderma*. Error bars represent SEs from five to six independent biological replicates. Statistical significance was determined by Welch Two Sample *t*-test between control and co-culture treatments; no significant differences were found.

A. brassicicola spread in roots and shoots of *Trichoderma*-colonized *Arabidopsis* plants, while mycorrhiza formation is not affected in *N. attenuata*. These observations are important for potential application of the endophyte as bio-control agent, and for the development of more effective and versatile bio-control agents.

Numerous *Trichoderma* species have been reported to stimulate plant growth (Contreras-Cornejo et al., 2009; González-Pérez et al., 2018), and *T. atroviride* and *T. virens* have been shown to promote root hair development (Contreras-Cornejo et al., 2015; González-Pérez et al., 2018). Our results highlight the importance of the growth conditions for the investigations of the symbiotic interactions with the new *Trichoderma* strain. Most importantly, as long as the symbionts grow in soil, we observe growth promotion during early phases of the development in the two tested host species. However, the growth stimulating effect of the fungus was barely or not detectable at all on agar plates, as long as no NaCl is added. A possible scenario could be that the fungus requires low concentrations of NaCl for growth and thus root colonization. If the salt concentration in the medium is too high, the fungus helps the plant by stimulating osmolyte production and Na^+ elimination through root exudates (Contreras-Cornejo et al., 2014). We demonstrate that the fungus also tries to escape from the stress by growing on the plant material, since the roots become more colonized with increased salt concentrations. Ultimately, hyphae can also be detected in the aerial parts of the plant, which occurs only when the stress around the roots is high. We assume that the extensive fungal propagation triggers the plant defense machinery to restrict fungal growth and consequently may reduce the host´s investment into growth. While our experiment focusses on the role of NaCl for the symbiosis, there are apparently other growth-stimulating factors in soil. A comparative analysis of the different growth conditions established in this study may help to elucidate critical parameters with agricultural relevance.

Root Colonization Alters Root Architecture

The new *Trichoderma* strain not only colonizes the root surface, but also penetrates into the root epidermis and resides in the root hairs (**Figures 2E–G** and **Supplementary Movie 1**). To the best of our knowledge, this is a new colonization strategy for *Trichoderma* species and demonstrates that the fungus can also live as endophyte. This finding is further supported by the fact that the fungus was originally isolated from the leaf cells of a tree. Although *Trichoderma* species have been often reported to colonize plant roots (López-Bucio et al., 2015; Ruano-Rosa et al., 2016), the invasion of hyphae into root cells might indicate a closer symbiosis compared to other *Trichoderma* strains and species. Reprogramming of root development, inhibition of root growth and stimulating root branching is a typical feature of AMF (Bonfante and Genre, 2010), but also observed for *Trichoderma*-colonized *Arabidopsis* roots (e.g., Contreras-Cornejo et al., 2015). Similar to AMF associations, the endophyte might contribute to nutrient and water uptake and allow the plants to reduce their root sizes. Further studies are needed to support this hypothesis. Additionally, an increase in the number of root hairs may lead to a larger surface area for fungal attachment. Its close phylogenetic relationship to *Trichoderma* species which grow preferentially on mushrooms also demonstrates that minor changes in the *Trichoderma* genomes allow major changes, enlargements or alterations in their host range or preference.

The New *Trichoderma* Strain Has Potential as New Bio-Control Agent

The infection assays with *A. brassicicola* show effective protection of *Arabidopsis* roots and shoots by *Trichoderma*. Interestingly, the beneficial fungus also restricted growth of *A. brassicicola* in the roots, when the roots were already infected by the pathogen (**Figure 7A**, A-T vs. C-T). This is consistent with the plate experiments in which *Trichoderma* actively predated *A. brassicicola*. Propagation of the pathogen in the leaves is also restricted when the roots are colonized by *Trichoderma*. Different local and systemic plant immune responses against various pathogens in *Alternaria*-colonized hosts have been reported, however, a general strategy for *Trichoderma* species is not apparent (Busby et al., 2016; Rai and Agarkar, 2016). Apparently, systemic signals travel from the roots to the leaves, and this is reflected by elevated SA levels in the leaves of *Trichoderma*-colonized seedlings even before they are exposed to the pathogen (**Figure 9B**). The higher SA levels in the leaves might indicate that the new *Trichoderma* strain has the ability to induce SAR. The low or undetectable levels of the defense-related hormones in the mycelium suggest that they are not of fungal origin.

Another feature of this new strain is its ability to sustain beneficial microbe interaction with plants. Although pathogen progression in root tissue is hindered by the new *Trichoderma* strain, the presence of the fungus does not interfere with AMF colonization. Recently, Metwally and Al-Amri (2020) showed an interactive role of *Trichoderma viride* and AMF on growth and pigment content of onion plants, however, due to the small number of AMF—*Trichoderma*–host plant combinations that have been investigated so far, general conclusions on those tripartite interactions are not possible (cf. Szczałba et al., 2019). Those studies are important for a successful bio-control agent, as *Trichoderma* species are also competitors of beneficial microbes (Sood et al., 2020), which could impair plant growth or yield.

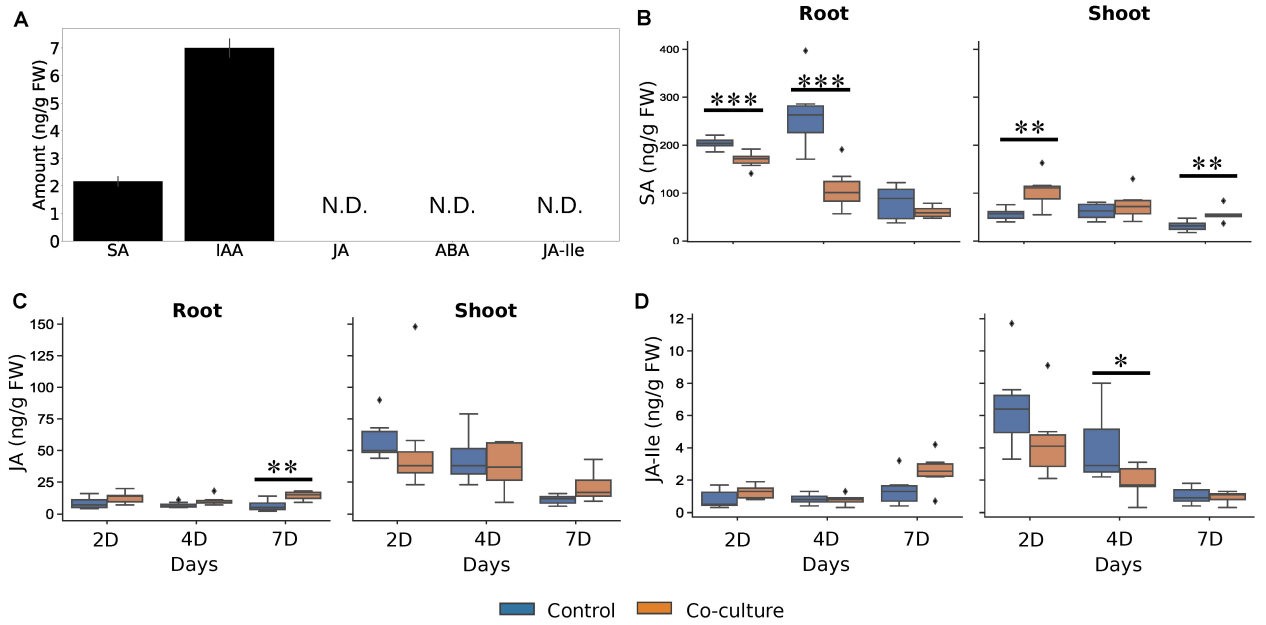

FIGURE 9 | *Trichoderma* facilitates the allocation of phytohormones in *A. thaliana*. **(A)** Phytohormone levels in *Trichoderma* mycelium. Error bars represent the SEs from six independent biological replicates. N.D., not detected. **(B–D)** SA **(B)**, JA **(C)**, and JA-Ile **(D)** levels from control and co-cultured seedlings in roots and shoots 2, 4, and 7 days after co-cultivation. Statistical significance was determined by Welch Two Sample *t*-test between control and co-culture treatments (**P* < 0.05; ***P* < 0.01; ****P* < 0.001). At least 6 biological replicates were used for measurement, each with 16 seedlings. ABA, abscisic acid; IAA, indole-3-acetic acid; SA, salicylic acid; JA, jasmonic acid; JA-Ile, jasmonoyl-isoleucine conjugate. The diamond shape in the figure represent outliers, which the data points exceed 1.5 times of the inter-quartile range from the 75th percentiles, or lower than 1.5 times of the inter-quartile range from the 25th percentiles. The inter-quartile range is the range between 25th and 75th percentiles.

CONCLUSION

In conclusion, the new *Trichoderma* strain might be a useful tool as bio-control agent, since it stimulates the plant immune system against pathogen infection, but at the same time does not interfere with other beneficial microbial interactions, such as mycorrhizal formation. Its growth promoting ability in soil provides additional benefit in agricultural application. Furthermore, the experimental set-up allows us to address further questions to understand the role of this fungus on plant performance, especially why the fungus is successful in promoting plant growth in soil but not on minimal medium, and how it influences the balance between growth and stress responses under different environmental conditions.

DATA AVAILABILITY STATEMENT

The datasets generated for this study can be found in the online repositories. The names of the repository/repositories and accession number(s) can be found in the article/**Supplementary Material**.

AUTHOR CONTRIBUTIONS

Y-HT organized the project, performed the experiments, collected the samples and data, analyzed the results, plotted the figures, and wrote up the study. HR performed the soil and salt experiments on *Arabidopsis*. KG performed the experiments on *Nicotiana*. PR isolated the *Trichoderma* strain. AF assisted in the microscopy. MR measured the phytohormones. IB, KN, RU, and RO edited the manuscript. RO organized the project and wrote up the study. All authors contributed to the article and approved the submitted version.

FUNDING

The work was supported by the CRC1127.

ACKNOWLEDGMENTS

We thank Veit Grabe from the Max Planck Institute for Chemical Ecology, Jena, for his assistance on confocal microscopy.

SUPPLEMENTARY MATERIAL

The Supplementary Material for this article can be found online at: https://www.frontiersin.org/articles/10.3389/fpls.2020.573670/full#supplementary-material

REFERENCES

Bailey, B. A., and Melnick, R. L. (2013). "The endophytic *Trichoderma*," in *Trichoderma: Biology and Applications*, eds P. K. Mukherjee, B. K. Horwitz, U. S. Singh, M. Mukherjee, and M. Schmoll (Wallingford: CAB International), 152–172. doi: 10.1079/9781780642475.0000

Bains, P. S., and Tewari, J. P. (1987). Purification, chemical characterization and host-specificity of the toxin produced by *Alternaria brassicae*. *Physiol. Mol. Plant Pathol.* 30, 259–271. doi: 10.1016/0885-5765(87)90039-7

Berini, F., Caccia, S., Franzetti, E., Congiu, T., Marinelli, F., Casartelli, M., et al. (2016). Effects of *Trichoderma viride* chitinases on the peritrophic matrix of *Lepidoptera*. *Pest Manag. Sci.* 72, 980–989. doi: 10.1002/ps.4078

Bonfante, P., and Genre, A. (2010). Mechanisms underlying beneficial plant–fungus interactions in mycorrhizal symbiosis. *Nat. Commun.* 1, 1–11. doi: 10.1038/ncomms1046

Busby, P. E., Ridout, M., and Newcombe, G. (2016). Fungal endophytes: modifiers of plant disease. *Plant Mol. Biol.* 90, 645–655. doi: 10.1007/s11103-015-0412-0

Carsolio, C., Gutiérrez, A., Jiménez, B., Van Montagu, M., and Herrera-Estrella, A. (1994). Characterization of ech-42, a *Trichoderma harzianum* endochitinase gene expressed during mycoparasitism. *Proc. Natl. Acad. Sci. U. S. A.* 91, 10903–10907. doi: 10.1073/pnas.91.23.10903

Castresana, J. (2000). Selection of conserved blocks from multiple alignments for their use in phylogenetic analysis. *Mol. Biol. Evol.* 17, 540–552. doi: 10.1093/oxfordjournals.molbev.a026334

Checker, V. G., Kushwaha, H. R., Kumari, P., and Yadav, S. (2018). "Role of phytohormones in plant defense: signaling and cross talk," in *Molecular Aspects of Plant-Pathogen Interaction*, eds A. Singh, and I. K. Singh (Singapore: Springer), 159–184. doi: 10.1007/978-981-10-7371-7_7

Chen, K., and Zhuang, W.-Y. (2017). Seven new species of *Trichoderma* from soil in China. *Mycosystema* 36, 1441–1462. doi: 10.13346/j.mycosystema.170134

Contreras-Cornejo, H. A., López-Bucio, J. S., Méndez-Bravo, A., Macías-Rodríguez, L., Ramos-Vega, M., Guevara-García, ÁA., et al. (2015). Mitogen-activated protein kinase 6 and ethylene and auxin signaling pathways are involved in *Arabidopsis* root-system architecture alterations by *Trichoderma atroviride*. *Mol. Plant-Microbe Interact.* 28, 701–710. doi: 10.1094/MPMI-01-15-0005-R

Contreras-Cornejo, H. A., Macías-Rodríguez, L., Alfaro-Cuevas, R., and López-Bucio, J. (2014). *Trichoderma* spp. improve growth of *Arabidopsis* seedlings under salt stress through enhanced root development, osmolite production, and Na+ elimination through root exudates. *Mol. Plant-Microbe Interact. MPMI* 27, 503–514. doi: 10.1094/MPMI-09-13-0265-R

Contreras-Cornejo, H. A., Macías-Rodríguez, L., Cortés-Penagos, C., and López-Bucio, J. (2009). *Trichoderma* virens, a plant beneficial fungus, enhances biomass production and promotes lateral root growth through an auxin-dependent mechanism in *Arabidopsis*. *Plant Physiol.* 149, 1579–1592. doi: 10.1104/pp.108.130369

Doyle, J. J. (1990). Isolation of plant DNA from fresh tissue. *Focus.* 12, 13–15.

Druzhinina, I. S., Chenthamara, K., Zhang, J., Atanasova, L., Yang, D., Miao, Y., et al. (2018). Massive lateral transfer of genes encoding plant cell wall-degrading enzymes to the mycoparasitic fungus *Trichoderma* from its plant-associated hosts. *PLoS Genet.* 14:e1007322. doi: 10.1371/journal.pgen.1007322

Druzhinina, I. S., and Kubicek, C. P. (eds) (2016). *Environmental and Microbial Relationships*, 3rd Edn. Berlin: Springer International Publishing, doi: 10.1007/978-3-319-29532-9

Druzhinina, I. S., Seidl-Seiboth, V., Herrera-Estrella, A., Horwitz, B. A., Kenerley, C. M., Monte, E., et al. (2011). *Trichoderma*: the genomics of opportunistic success. *Nat. Rev. Microbiol.* 9, 749–759. doi: 10.1038/nrmicro2637

El-Katatny, M., Somitsch, W., Robra, K., El-Katatny, M., and Gubitz, G. (2000). Production of chitinase and β-1,3-glucanase by *Trichoderma harzianum* for control of the phytopathogenic fungus. *Sclerotium rolfsii*. *Food Technol. Biotechnol.* 38, 173–180.

Furukawa, H., Kusne, S., Sutton, D. A., Manez, R., Carrau, R., Nichols, L., et al. (1998). Acute invasive sinusitis due to *Trichoderma longibrachiatum* in a liver and small bowel transplant recipient. *Clin. Infect. Dis. Off. Publ. Infect. Dis. Soc. Am.* 26, 487–489. doi: 10.1086/516317

Gautheret, A., Dromer, F., Bourhis, J. H., and Andremont, A. (1995). *Trichoderma pseudokoningii* as a cause of fatal infection in a bone marrow transplant recipient. *Clin. Infect. Dis. Off. Publ. Infect. Dis. Soc. Am.* 20, 1063–1064. doi: 10.1093/clinids/20.4.1063

Geyer, C. J. (1991). "Markov chain monte carlo maximum likelihood," in *Computing Science and Statistics: Proceedings of the 23rd Symposium on the Interface*, ed. E. M. Keramidas (Fairfax, VA: Interface Foundation), 156–163.

González-Pérez, E., Ortega-Amaro, M. A., Salazar-Badillo, F. B., Bautista, E., Douterlungne, D., and Jiménez-Bremont, J. F. (2018). The *Arabidopsis-Trichoderma* interaction reveals that the fungal growth medium is an important factor in plant growth induction. *Sci. Rep.* 8:16427. doi: 10.1038/s41598-018-34500-w

Grosch, R., Lottmann, J., Rehn, V. N. C., Rehn, K. G., Mendonça-Hagler, L., Smalla, K., et al. (2007). Analysis of antagonistic interactions between *Trichoderma* isolates from Brazilian weeds and the soil-borne pathogen *Rhizoctonia solani*. *J. Plant Dis. Prot.* 114, 167–175. doi: 10.1007/BF03356213

Groten, K., Nawaz, A., Nguyen, N. H. T., Santhanam, R., and Baldwin, I. T. (2015). Silencing a key gene of the common symbiosis pathway in *Nicotiana attenuata* specifically impairs arbuscular mycorrhizal infection without influencing the root-associated microbiome or plant growth. *Plant Cell Environ.* 38, 2398–2416. doi: 10.1111/pce.12561

Hermosa, R., Viterbo, A., Chet, I., and Monte, E. (2012). Plant-beneficial effects of *Trichoderma* and of its genes. *Microbiol. Read. Engl.* 158, 17–25. doi: 10.1099/mic.0.052274-0

Heyer, M., Reichelt, M., and Mithöfer, A. (2018). A holistic approach to analyze systemic jasmonate accumulation in individual leaves of *Arabidopsis* rosettes upon wounding. *Front. Plant Sci.* 9:1569. doi: 10.3389/fpls.2018.01569

Hill, T., and Käfer, E. (2001). Improved protocols for Aspergillus minimal medium: trace element and minimal medium salt stock solutions. *Fungal Genet Newsl* 48, 20–21. doi: 10.4148/1941-4765.1173

Huelsenbeck, J. P., and Ronquist, F. (2001). MRBAYES: bayesian inference of phylogenetic trees. *Bioinforma. Oxf. Engl.* 17, 754–755. doi: 10.1093/bioinformatics/17.8.754

Jacobs, S., Zechmann, B., Molitor, A., Trujillo, M., Petutschnig, E., Lipka, V., et al. (2011). Broad-spectrum suppression of innate immunity is required for colonization of *Arabidopsis* roots by the Fungus *Piriformospora indica*. *Plant Physiol.* 156, 726–740. doi: 10.1104/pp.111.176446

Johnson, J. M., Sherameti, I., Ludwig, A., Nongbri, P., Sun, C., Lou, B., et al. (2011). Protocols for *Arabidopsis thaliana* and *Piriformospora indica* co-cultivation – A model system to study plant beneficial traits. *Endocytobiosis Cell Res.* 21, 101–113.

Karlsson, M., Atanasova, L., Jensen, D., and Zeilinger, S. (2017). "Necrotrophic mycoparasites and their genomes," in *The Fungal Kingdom*, eds J. Heitman, B. Howlett, P. Crous, E. Stukenbrock, T. James, and N. Gow (Washington, DC: ASM Press), 1005-1026. doi: 10.1128/microbiolspec.FUNK-0016-2016

Katoh, K., Rozewicki, J., and Yamada, K. D. (2019). MAFFT online service: multiple sequence alignment, interactive sequence choice and visualization. *Brief. Bioinform.* 20, 1160–1166. doi: 10.1093/bib/bbx108

Kistner, C., and Matamoros, M. (2005). "RNA isolation using phase extraction and LiCl precipitation," in *Lotus Japonicus Handbook*, ed. A. J. Márquez (Berlin: Springer-Verlag), 123–124. doi: 10.1007/1-4020-3735-X_9

Kozlov, A. M., Darriba, D., Flouri, T., Morel, B., and Stamatakis, A. (2019). RAxML-NG: a fast, scalable and user-friendly tool for maximum likelihood phylogenetic inference. *Bioinforma. Oxf. Engl.* 35, 4453–4455. doi: 10.1093/bioinformatics/btz305

Krügel, T., Lim, M., Gase, K., Halitschke, R., and Baldwin, I. T. (2002). Agrobacterium-mediated transformation of *Nicotiana attenuata*, a model ecological expression system. *Chemoecology* 12, 177–183. doi: 10.1007/PL00012666

Lee, S., Yap, M., Behringer, G., Hung, R., and Bennett, J. W. (2016). Volatile organic compounds emitted by *Trichoderma* species mediate plant growth. *Fungal Biol. Biotechnol.* 3:7. doi: 10.1186/s40694-016-0025-7

Leonetti, P., Zonno, M. C., Molinari, S., and Altomare, C. (2017). Induction of SA-signaling pathway and ethylene biosynthesis in *Trichoderma harzianum*-treated tomato plants after infection of the root-knot nematode Meloidogyne incognita. *Plant Cell Rep.* 36, 621–631. doi: 10.1007/s00299-017-2109-0

Li, R.-X., Cai, F., Pang, G., Shen, Q.-R., Li, R., and Chen, W. (2015). Solubilisation of phosphate and micronutrients by *Trichoderma harzianum* and its relationship with the promotion of tomato plant growth. *PloS One* 10:e0130081. doi: 10.1371/journal.pone.0130081

Li, Y., Fu, K., Gao, S., Wu, Q., Fan, L., Li, Y., et al. (2013). Impact on bacterial community in midguts of the Asian corn borer larvae by transgenic *Trichoderma* strain overexpressing a heterologous chit42 gene with chitin-binding domain. *PloS One* 8:e55555. doi: 10.1371/journal.pone.0055555

Li Destri Nicosia, M. G., Mosca, S., Mercurio, R., and Schena, L. (2015). Dieback of Pinus nigra seedlings caused by a strain of *Trichoderma viride*. *Plant Dis.* 99, 44–49. doi: 10.1094/PDIS-04-14-0433-RE

López-Bucio, J., Pelagio-Flores, R., and Herrera-Estrella, A. (2015). *Trichoderma* as biostimulant: exploiting the multilevel properties of a plant beneficial fungus. *Sci. Hortic.* 196, 109–123. doi: 10.1016/j.scienta.2015.08.043

Luu, V. T., Schuck, S., Kim, S.-G., Weinhold, A., and Baldwin, I. T. (2015). Jasmonic acid signalling mediates resistance of the wild tobacco *Nicotiana attenuata* to its native *Fusarium*, but not Alternaria, fungal pathogens. *Plant Cell Environ.* 38, 572–584. doi: 10.1111/pce.12416

Martínez-Medina, A., Fernández, I., Sánchez-Guzmán, M. J., Jung, S. C., Pascual, J. A., and Pozo, M. J. (2013). Deciphering the hormonal signalling network behind the systemic resistance induced by *Trichoderma harzianum* in tomato. *Front. Plant Sci.* 4:206. doi: 10.3389/fpls.2013.00206

McGonigle, T. P., Miller, M. H., Evans, D. G., Fairchild, G. L., and Swan, J. A. (1990). A new method which gives an objective measure of colonization of roots by vesicular—arbuscular mycorrhizal fungi. *New Phytol.* 115, 495–501. doi: 10.1111/j.1469-8137.1990.tb00476.x

Metwally, R. A., and Al-Amri, S. M. (2020). Individual and interactive role of *Trichoderma viride* and arbuscular mycorrhizal fungi on growth and pigment content of onion plants. *Lett. Appl. Microbiol.* 70, 79–86. doi: 10.1111/lam.13246

Mukherjee, A. K., Sampath Kumar, A., Kranthi, S., and Mukherjee, P. K. (2014). Biocontrol potential of three novel *Trichoderma* strains: isolation, evaluation and formulation. *3 Biotech* 4, 275–281. doi: 10.1007/s13205-013-0150-4

Murashige, T., and Skoog, F. (1962). A revised medium for rapid growth and bio assays with tobacco tissue cultures. *Physiol. Plant.* 15, 473–497. doi: 10.1111/j.1399-3054.1962.tb08052.x

Park, M. S., Bae, K. S., and Yu, S. H. (2006). Two new species of *Trichoderma* associated with green mold of oyster mushroom cultivation in Korea. *Mycobiology* 34, 111–113. doi: 10.4489/MYCO.2006.34.3.111

Prajapati, M. S., Patel, J. B., Modi, K., and Shah, M. B. (2010). Leucas aspera: a review. *Pharmacogn. Rev.* 4, 85–87. doi: 10.4103/0973-7847.65330

Qin, Y., Druzhinina, I. S., Pan, X., and Yuan, Z. (2016). Microbially mediated plant salt tolerance and microbiome-based solutions for saline agriculture. *Biotechnol. Adv.* 34, 1245–1259. doi: 10.1016/j.biotechadv.2016.08.005

Rai, M., and Agarkar, G. (2016). Plant–fungal interactions: what triggers the fungi to switch among lifestyles? *Crit. Rev. Microbiol.* 42, 428–438. doi: 10.3109/1040841X.2014.958052

Rajani, P., Rajasekaran, C., Vasanthakumari, M. M., Olsson, S. B., Ravikanth, G., Uma Shaanker, R., et al. (2020). Inhibition of plant pathogenic fungi by endophytic *Trichoderma* spp. through mycoparasitism and volatile organic compounds. *Microbiol. Res* 242:126595. doi: 10.1016/j.micres.2020.126595

Rambaut, A. (2018). *FigTree*. Available at: http://tree.bio.ed.ac.uk/software/figtree/ (accessed June 11, 2020).

Rocha-Ramirez, V., Omero, C., Chet, I., Horwitz, B. A., and Herrera-Estrella, A. (2002). *Trichoderma atroviride* G-protein alpha-subunit gene tga1 is involved in mycoparasitic coiling and conidiation. *Eukaryot. Cell* 1, 594–605. doi: 10.1128/ec.1.4.594-605.2002

Ronquist, F., and Huelsenbeck, J. (2003). MRBAYES 3: bayesian phylogenetic inference under mixed models. *Bioinforma. Oxf. Engl.* 19, 1572–1574. doi: 10.1093/bioinformatics/btg180

Rosmana, A., Nasaruddin, N., Hendarto, H., Hakkar, A. A., and Agriansyah, N. (2016). Endophytic association of *Trichoderma asperellum* within *Theobroma cacao* suppresses vascular streak dieback incidence and promotes side graft growth. *Mycobiology* 44, 180–186. doi: 10.5941/MYCO.2016.44.3.180

Ruano-Rosa, D., Prieto, P., Rincón, A., Gómez Rodríguez, M. V., Valderrama, R., Barroso, J., et al. (2016). Fate of *Trichoderma harzianum* in the olive rhizosphere: time course of the root colonization process and interaction with the fungal pathogen *Verticillium dahliae*. *BioControl* 61, 269–282. doi: 10.1007/s10526-015-9706-z

Samolski, I., Rincón, A. M., Pinzón, L. M., Viterbo, A., and Monte, E. (2012). The qid74 gene from *Trichoderma harzianum* has a role in root architecture and plant biofertilization. *Microbiol. Read. Engl.* 158, 129–138. doi: 10.1099/mic.0.053140-0

Santhanam, R., Menezes, R. C., Grabe, V., Li, D., Baldwin, I. T., and Groten, K. (2019). A suite of complementary biocontrol traits allows a native consortium of root-associated bacteria to protect their host plant from a fungal sudden-wilt disease. *Mol. Ecol.* 28, 1154–1169. doi: 10.1111/mec.15012

Schindelin, J., Arganda-Carreras, I., Frise, E., Kaynig, V., Longair, M., Pietzsch, T., et al. (2012). Fiji: an open-source platform for biological-image analysis. *Nat. Methods* 9, 676–682. doi: 10.1038/nmeth.2019

Sivakumaran, A., Akinyemi, A., Mandon, J., Cristescu, S. M., Hall, M. A., Harren, F. J. M., et al. (2016). ABA suppresses *Botrytis cinerea* elicited NO production in tomato to influence H2O2 generation and increase host susceptibility. *Front. Plant Sci.* 7:709. doi: 10.3389/fpls.2016.00709

Sood, M., Kapoor, D., Kumar, V., Sheteiwy, M. S., Ramakrishnan, M., Landi, M., et al. (2020). *Trichoderma*: the "secrets" of a multitalented biocontrol agent. *Plants Basel Switz.* 9:762. doi: 10.3390/plants9060762

Stöver, B. C., and Müller, K. F. (2010). TreeGraph 2: combining and visualizing evidence from different phylogenetic analyses. *BMC Bioinformatics* 11:7. doi: 10.1186/1471-2105-11-7

Studholme, D. J., Harris, B., Le Cocq, K., Winsbury, R., Perera, V., Ryder, L., et al. (2013). Investigating the beneficial traits of *Trichoderma* hamatum GD12 for sustainable agriculture-insights from genomics. *Front. Plant Sci.* 4:258. doi: 10.3389/fpls.2013.00258

Swofford, D. (2002). *PAUP*. Phylogenetic Analysis Using Parsimony (*and Other Methods). Version 4.0b10*. doi: 10.1111/j.0014-3820.2002.tb00191.x

Szczałba, M., Kopta, T., Gąstoł, M., and Sękara, A. (2019). Comprehensive insight into arbuscular mycorrhizal fungi, *Trichoderma* spp. and plant multilevel interactions with emphasis on biostimulation of horticultural crops. *J. Appl. Microbiol.* 127, 630–647. doi: 10.1111/jam.14247

Tavare, S. (1986). Some probabilistic and statistical problems on the analysis of DNA sequences. *Lect. Math. Life Sci.* 17, 57–86.

Wang, M., Schäfer, M., Li, D., Halitschke, R., Dong, C., McGale, E., et al. (2018a). Blumenols as shoot markers of root symbiosis with arbuscular mycorrhizal fungi. *eLife* 7:e37093. doi: 10.7554/eLife.37093

Wang, M., Wilde, J., Baldwin, I. T., and Groten, K. (2018b). *Nicotiana attenuata*'s capacity to interact with arbuscular mycorrhiza alters its competitive ability and elicits major changes in the leaf transcriptome. *J. Integr. Plant Biol.* 60, 242–261. doi: 10.1111/jipb.12609

Woo, S. L., Ruocco, M., Vinale, F., Nigro, M., Marra, R., Lombardi, N., et al. (2014). *Trichoderma*-based products and their widespread use in agriculture. *Open Mycol. J.* 8, 71–126. doi: 10.2174/1874437001408010071

Yang, Z. (1993). Maximum-likelihood estimation of phylogeny from DNA sequences when substitution rates differ over sites. *Mol. Biol. Evol.* 10, 1396–1401. doi: 10.1093/oxfordjournals.molbev.a040082

Zhang, Y., and Zhuang, W.-Y. (2020). *Trichoderma* brevicrassum strain TC967 with capacities of diminishing cucumber disease caused by *Rhizoctonia solani* and promoting plant growth. *Biol. Control* 142:104151. doi: 10.1016/j.biocontrol.2019.104151

Conflict of Interest: The authors declare that the research was conducted in the absence of any commercial or financial relationships that could be construed as a potential conflict of interest.

frontiers in Plant Science

ORIGINAL RESEARCH
published: 23 December 2020
doi: 10.3389/fpls.2020.610026

Intercropping System and N_2 Fixing Bacteria Can Increase Land Use Efficiency and Improve the Essential Oil Quantity and Quality of Sweet Basil (*Ocimum basilicum* L.)

Sajad Kordi[1], *Saeid Zehtab Salmasi*[1], *Jalil Shafagh Kolvanagh*[1], *Weria Weisany*[2]* *and Dennis A. Shannon*[3]

[1] Department of Ecophysiology, Faculty of Agriculture, University of Tabriz, Tabriz, Iran, [2] Department of Agriculture and Food Science, Science and Research Branch, Islamic Azad University, Tehran, Iran, [3] Department of Crop, Soil and Environmental Sciences, Auburn University, Auburn, AL, United States

Intercropping fodder plants with medicinal plants, in addition to enhancing productivity, can remarkably reduce the population of weeds, pests and diseases and for naturally meeting of livestock medicinal needs. Two experiments were conducted to evaluate biological yield, essential oil (EO) composition and yield of sweet basil (*Ocimum basilicum* L.) treated with N_2 fixing bacteria in additive intercropping with forage maize during the 2018 and 2019. Treatments were arranged in factorial split-plot-in time in randomized complete block design with three replications. The factors were 100% chemical fertilizer (N), N_2 fixing bacteria (*Azospirillum brasilense* and *Azotobacter chroococcum*), integration of N_2 fixing bacteria + 50% nitrogen chemical fertilizer and control. The cropping pattern factor included of sole cropping basil and the additive intercropping of maize + 25% basil, maize + 50% basil, maize + 75% basil, and maize + 100% basil. The results indicated that the highest essential oil yield (30.8 kg ha^{-1}) and essential oil percentage (0.75%) were obtained in sole cropping with *A. brasilense* and *A. chroococcum* + 50% chemical nitrogen fertilizer application in second harvest in 2019. In both cropping systems, the N_2 fixing bacteria application significantly increased fresh and dry yield and land equivalent ratio (LER) as compared to control plants. In both years of experiments could remarkably vary depending on type of treatment. In both years, eight constituents including methyl chavicol (17.24–51.28%), Z-citral (neral) (8.33–24.3%), geranial (10.2–31.3%), (E)-caryophyllene (1.05–5.64%), α-*trans*-bergamotene (0.53–1.7%), α-humulene (0.4–1.69%), germacrene-D (0.2–1.88%), and (Z)-α- bisabolene (1.16–3.86%) were the main constituents of EO. The highest content of methyl chavicol was found through sole cropping of sweet basil with nitrogen chemical fertilizer followed by sole cropping of sweet basil with an integration of *A. brasilense* and *A. chroococcum* + 50% nitrogen chemical fertilizer in 2018 and 2019. Intercropping system and N_2 fixing bacteria can be effective in reducing chemical fertilizer consumption and environmental pollution and achieving the sustainable agriculture goals.

Keywords: basil, cropping system, essential oil composition, fertilizer, integrated management

OPEN ACCESS

Edited by:
Sabine Dagmar Zimmermann, Délégation Languedoc Roussillon (CNRS), France

Reviewed by:
Yan Dong, Yunnan Agricultural University, China
Zoran Petar Zekovic, University of Novi Sad, Serbia

***Correspondence:**
Weria Weisany
weria.wisany@gmail.com

Specialty section:
This article was submitted to Plant Symbiotic Interactions, a section of the journal Frontiers in Plant Science

Received: *24 September 2020*
Accepted: *30 November 2020*
Published: *23 December 2020*

Citation:
Kordi S, Salmasi SZ, Kolvanagh JS, Weisany W and Shannon DA (2020) Intercropping System and N_2 Fixing Bacteria Can Increase Land Use Efficiency and Improve the Essential Oil Quantity and Quality of Sweet Basil (Ocimum basilicum L.). Front. Plant Sci. 11:610026. doi: 10.3389/fpls.2020.610026

INTRODUCTION

Since the green revolution and the introduction of fertilizer-consuming cultivars, the consumption of chemical fertilizers has been widely increased. Soil fertility improvement is mainly achieved through the use of chemical fertilizers, which their high consumption is a threat to environment and human health (Kordi, 2017). In this regard, some issues concerning soil like erosion, salinity, acidification, and decline in qualitative and quantitative properties of surface-area soils as well as other issues such as contaminating surface and groundwater, devastating biodiversity, reduced soil biological activities, and finally increasing cost of crop production are consequences of illogical using of chemical fertilizers (Kordi et al., 2017). Some conditions, such as climatic and nutrient factors suitable for plant growth, are the most important factors affecting growth of medicinal plants and their active components quantitatively and qualitatively (Street, 2012). Therefore, alternative sources of fertilizer and the use of organic fertilizers (e.g., N_2 fixing bacteria) are considered as sustainable agriculture options to improve soil quality in modern agriculture (Chen et al., 2014; Meena et al., 2015).

The utilization of bio-fertilizers (e.g., free-living N-fixing bacteria) is of particular importance in the agriculture sector due to their potential role in healthy food, improving crop yield, and decreasing greenhouse emissions (Ghilavizadeh et al., 2013; Raei et al., 2015). Raei et al. (2015) showed that the seeds of sweet basil inoculated with *Azospirillum* produced plants with higher fresh and dry weights, height, and more lateral branches as compared to controls. Ghilavizadeh et al. (2013) showed that inoculating the seeds of fennel with *Azotobacter* and *Azospirillum* could increase seed essential oil (EO) content.

In industrial agriculture, one of the major ways to increment livestock production is to utilization a diet having some cereal grains such as maize and barley, or silage plants and many types of concentrates containing dietary supplements and chemical content designed to stimulate animal growth and prevent diseases. The improper application of these compounds is associated with outbreaks of many metabolic diseases such as liver abscesses and acidosis in ruminants, and finally causes many problems (Kordi et al., 2017). Nowadays, these problems have led to organic crops production is considered as an option to decrement the negative effects of chemical fertilizers (Aguilera et al., 2013; Aires et al., 2013). In some countries where organic agriculture is practiced, emphasis has been placed on availability of some medicinal plants such as chicory (*Cichorium intybus* L.) and caraway (*Carum carvi* L.) in pasture that is grazed by livestock for naturally meeting their medicinal needs (Kordi et al., 2017). In this regard, "medicinal forage" idea was introduced. From the standpoint of forage value, although some medicinal plants fed solitarily to livestock have resulted in forage unpalatability or with high amounts of anti-nutritional compounds (such as coumarin, phenolic compounds, and prussic acid), intercropping with ordinary forage plants gives them high value as medicinal forage through efficient, scientific management (Kordi et al., 2017). Intercropping fodder plants with medicinal plants, in addition to enhancing productivity, can remarkably reduce the population of weeds, pests, and diseases and increase plant tolerance to biotic and abiotic stresses. By intercropping sweet basil with maize, Kordi (2017) obtained highest land equivalent ratio (LER) (1.566) with a combination of maize + 100% stands of basil and N_2 fixing bacteria.

Sweet basil (*Ocimum basilicum* L.) is an annual herbaceous plant in the Lamiaceae family, native to Asia, Africa, America, and the subtropics (Roman, 2012; Borloveanu, 2014). Many aromatic plants including basil are rich in secondary metabolites (Srivastava et al., 2014; Li et al., 2017). Having high commercial values, these secondary metabolites are exploited largely as flavors, fragrances and pharmaceuticals (Al-Maskri et al., 2011).

Many studies documented that EO of sweet basil have antifungal, insecticidal (Hossain et al., 2014a,b), antibacterial, and antioxidant (Karagözl et al., 2011) properties. The chemical composition of sweet basil EO depends on genetic, season, environmental factors, and the plant growth stage (Bilal et al., 2012). Padalia et al. (2014) has reported linalool, methyl chavicol, methyl eugenol, eugenol, and geraniol as dominant components in the basil EO. Since there is limited information about the suitability of medicinal plants especially sweet basil as intercrops in maize in Iran, therefore this study was conducted to evaluate biological yield, yield and chemical composition of sweet basil EO treated with nitrogen fertilizers (N_2 fixing bacteria, chemical and integrated) in additive intercropping with forage maize.

MATERIALS AND METHODS

Location and Plant Materials

This research was carried out in the Experimental Farm of Faculty of Agriculture, Lorestan University, Iran (33°29′N, 48°22′E and altitude 1,125 m), during 2017–2018 and 2018–2019 growing seasons. Weather conditions during the experimental period are shown in **Table 1**. Physicochemical properties of soil at the depth 0–40 cm are presented in **Table 2**. Different cropping patterns included: sole cropping pattern of sweet basil (80 plants per m^2), and the additive intercropping of sweet basil at 25% (20 sweet basil plants m^{-2}), 50% (40 sweet basil plants m^{-2}), 75% (60 sweet basil plants m^{-2}), and 100% basil (80 sweet basil plants m^{-2}) stand into maize at 10 plants m^{-2}. Crops seed were sown in plots whose area was 5 m^2, consisting of five 2-m rows spaced 50 cm apart. Both crops were planted on the same day in early May 2018 and 2019. The distance between plants on the row was 20 cm for maize (*Zea mays* L. cv. S.C. 704) and was 2.5, 3.3, 5, and 10 cm for different ratio of sweet basil, respectively. All plots were irrigated immediately after sowing and subsequent irrigations were performed every 5 days. Hand weeding was done as needed.

Experimental Design

The main experimental design of this study was a factorial experiment based on Randomized Complete Blocks Design with three replications. However, due to three harvest times in each season for basil plants, the basil traits except for fresh and dry yields (which were total yield of three harvests) were statistically analyzed based on factorial split-plot-in time experiment. Fertilization factor consisted of F_1: control (without

TABLE 1 | Khorramabad meteorological station monthly statistics in the experiment period in 2018 and 2019.

Month	Precipitation (mm)		Number of rainy days		Maximum temperature (°C)		Minimum temperature (°C)		Average temperature (°C)	
	2018	2019	2018	2019	2018	2019	2018	2019	2018	2019
Apr	51.4	86.9	8	9	20.9	21.2	5.2	6.1	13.2	13.7
May	14.5	22.8	5	8	28.2	29.4	10.5	10.7	19.4	20
Jun	0.2	2	1	2	34.8	37.3	14.6	15.6	24.7	26.4
Jul	0	0.2	0	1	40	40.2	19.3	20.4	29.6	30.2
Aug	0	0	0	0	40.5	41	19.4	20.4	30	30.7
Sep	0	17	0	1	36.9	36.2	15	17.4	25.6	26.8

TABLE 2 | Some physical and chemical properties of the soil of experimental area.

Year	Soil texture	Clay (%)	Silt (%)	Sand (%)	pH	EC (dS m^{-1})	Total N (%)	Available P (ppm)	Available K (ppm)
2018	Clay loam	32.16	42	25.84	7.17	0.459	0.302	8	390
2019	Clay loam	31.52	41.5	26.98	7.36	0.536	0.285	6	356

nitrogen fertilization); F_2: 100% chemical fertilizer (N); F_3: nitrogen-fixing bacteria (*Azospirillum brasilense* and *Azotobacter chroococcum*) and F_4: integration of nitrogen-fixing bacteria + 50% nitrogen chemical fertilizer. Cropping pattern factor included sole cropping of basil (I_1) and the additive intercropping of maize + 25% basil (I_2), maize + 50% basil (I_3), maize + 75% basil (I_4), and maize + 100% basil (I_5) (Kordi et al., 2017). Basil was harvested three times each season. The experiment was repeated at a different site in the second season.

Fertilizer and Microbial Inocula

According to soil test, 150 kg triple superphosphate ha^{-1} and 50 kg potassium sulfate ha^{-1} were applied before cultivation. In application of 100% chemical fertilizer (F_2), 375 kg N ha^{-1} was used as urea. The half of the nitrogen amount was added to F_2 and F_4 treatments (187.5 and 93.7 kg N ha^{-1}, respectively) with the last plow before sowing. The rest of the nitrogen was used in two stages: the eight-leaf stage of maize and before the start of tassel formation in the plots. The N_2 fixing bacteria were *Azospirillum brasilense* and *Azotobacter chroococcum* strains. Both strains of bacteria consisted of 10^8 CFU ml^{-1} inoculant which were provided from Mehr Asia Biotechnology Company, Tehran, Iran. Following cultivation, the seeds were completely soaked with the N_2 fixing bacteria and kept in the shade for half an hour in to dry and be ready for planting. The liquid N_2 fixing bacteria (*A. brasilense* and *A. chroococcum*) applied at 2 L ha^{-1} (Kordi et al., 2017).

Traits Measurement

The traits measured in this research included fresh and dry yields, EO percentage, chemical composition and yield of sweet basil EO.

Fresh and Dry Yields

The sweet basil was harvested three times each season in early flowering stage in July, August, and September. Samples of 1 m length were taken from the center of two rows located in middle of each plot. Plants were cut above ground and transferred into a lab to measure fresh weight. To measure dry weight, the samples were dried in an oven at 75°C for 72 h and then weighed. For determination of EO content, the aerial parts of sweet basil plants were dried naturally in the shade.

Essential Oil Isolation

Fifty grams of naturally dried aerial parts were sampled for analysis. Woody parts of plants were separated and then remainder parts hydro-distilled for 3.5 h by a Clevenger-type apparatus (Weisany et al., 2016a,b). The obtained EO was dehydrated using anhydrous sodium sulfate and stored in sealed vials at 4°C, until further analyses. To measure main constituents of EO, all treatments belonged to a given repetition were chosen in second harvest (Weisany et al., 2015).

Gas Chromatography-Mass Spectrometry (GC-MS)

The EO samples were analyzed in a gas chromatograph Agilent model 7890 using HP-5MS column (30 m × 0.25 mm, 0.25 μm in thickness). The oven temperature was programmed from 50°C (held for 2 min) and increased to 240°C at a rate of 3°C/min then 240–300°C at a rate of 15°C/min. The constant flow rate of helium as carrier gas was 1 mL/min. The mass spectra were recorded on electron ionization (EI) mode, with ionization energy of 70 eV. The temperature at the injection site was 290°C. The identification of chemical constituents was done based on the retention indices (calculated using from C8 to C20 alkanes) and through analyzing the mass spectra compared to a computer databank (Wiley 7 and Nist 62) (Adams, 2007; Carneiro et al., 2017).

Land Equivalent Ratio (LER)

Land equivalent ratio is an index for comparing and estimating the advantage of different methods of intercropping compared to monocropping. To calculate the LER, the intercrop yield of one culture is divided by the yield of the pure stand (Mead and Willey, 1980). In present research, seed weight is considered as yield parameter.

$$LER = (Yab/Ya) + (Yba/Yb)$$

TABLE 3 | Fresh and dry yield of maize and basil as affected by sole and intercropping systems in 2018 and 2019.

Cropping systems		Nitrogen sources	Fresh yield				Dry yield			
			2018		2019		2018		2019	
			Maize (Ton/ha)	Basil (kg/ha)	Maize (Ton/ha)	Basil (kg/ha)	Maize (Ton/ha)	Basil (kg/ha)	Maize (Ton/ha)	Basil (kg/ha)
	M10	F1	59 ± 2.63	–	64.1 ± 0.55	–	16.5 ± 0.73	–	17.9 ± 0.14	–
	M10	F2	74.8 ± 2.3	–	76.6 ± 0.91	–	20.6 ± 0.49	–	21.3 ± 0.52	–
	M10	F3	63.1 ± 1.93	–	70.7 ± 3.74	–	17.6 ± 0.26	–	19.7 ± 0.77	–
	M10	F4	68.8 ± 2.31	–	73.7 ± 1.01	–	19.4 ± 0.16	–	20.7 ± 0.12	–
Sole cropping	B80	F1	–	24,326 ± 399	–	22,920 ± 498	–	4,236 ± 59	–	3,995 ± 774
	B80	F2	–	36,529 ± 1,503	–	46,497 ± 1,206	–	6,327 ± 256	–	8,036 ± 208
	B80	F3	–	29,514 ± 1,239	–	30,867 ± 2,478	–	5,125 ± 214	–	5,356 ± 425
	B80	F4	–	37,259 ± 313	–	47,591 ± 1,403	–	6,451 ± 54	–	8,224 ± 240
Intercropping	M10/B20	F1	56.3 ± 4.36	7,769 ± 230	62.5 ± 3.54	7,183 ± 91	16 ± 0.94	1,335 ± 41	17.5 ± 1.47	1,231 ± 16
	M10/B20	F2	72.1 ± 1.82	8,909 ± 155	76.6 ± 2.76	8,649 ± 307	20.3 ± 0.4	1,530 ± 29	21.1 ± 0.39	1,484 ± 53
	M10/B20	F3	63.2 ± 2.54	8,986 ± 171	68.2 ± 2.66	8,295 ± 231	17.9 ± 0.93	1,541 ± 28	19.1 ± 0.84	1,424 ± 37
	M10/B20	F4	68 ± 4.3	9,178 ± 378	72.1 ± 1.47	8,913 ± 497	19.6 ± 0.39	1,574 ± 65	20.3 ± 0.57	1,529 ± 85
	M10/B40	F1	52.3 ± 2.52	11,307 ± 652	57.5 ± 2.92	10,371 ± 64	15.2 ± 0.44	1,938 ± 112	16.5 ± 0.43	1,778 ± 11
	M10/B40	F2	66.7 ± 1.01	14,977 ± 577	74.1 ± 1.98	15,649 ± 355	19.4 ± 0.04	2,568 ± 97	21.3 ± 0.33	2,683 ± 61
	M10/B40	F3	61.4 ± 4.05	13,722 ± 500	65.6 ± 1.85	14,235 ± 472	17.8 ± 0.5	2,352 ± 86	18.8 ± 0.57	2,440 ± 81
	M10/B40	F4	64.8 ± 3.3	15,161 ± 175	71.6 ± 1.53	16,191 ± 222	19 ± 0.56	2,600 ± 31	20.6 ± 0.33	2,777 ± 37
	M10/B60	F1	50 ± 3.10	13,688 ± 175	56.1 ± 2.84	13,761 ± 345	14.9 ± 0.19	2,347 ± 29	16.4 ± 0.86	2,360 ± 60
	M10/B60	F2	63.4 ± 4.1	20,311 ± 324	69.6 ± 1.39	22,702 ± 837	18.6 ± 1.14	3,484 ± 57	20.3 ± 2.48	3,892 ± 143
	M10/B60	F3	57 ± 3.8	17,779 ± 209	61.7 ± 4.5	19,631 ± 396	16.9 ± 0.55	3,048 ± 36	18 ± 1.24	3,365 ± 68
	M10/B60	F4	61.4 ± 0.89	20,960 ± 740	69.8 ± 2.07	22,829 ± 557	18.2 ± 0.27	3,593 ± 127	20.4 ± 0.27	3,915 ± 96
	M10/B80	F1	47.9 ± 0.38	16,524 ± 642	49.1 ± 1.14	15,720 ± 180	14.4 ± 0.37	2,833 ± 110	14.8 ± 0.27	2,697 ± 31
	M10/B80	F2	61.1 ± 0.67	23,248 ± 321	67.8 ± 3.32	25,476 ± 1,678	18.1 ± 0.24	3,986 ± 54	19.9 ± 1.1	4,367 ± 288
	M10/B80	F3	53.1 ± 3.82	20,044 ± 451	58.1 ± 1.89	21,260 ± 317	15.8 ± 0.97	3,438 ± 78	17.3 ± 0.42	3,646 ± 56
	M10/B80	F4	58.6 ± 1.82	23,407 ± 255	66.2 ± 3.45	25,888 ± 519	17.4 ± 0.22	4,013 ± 44	19.6 ± 0.89	4,438 ± 89

F1, control; F2, 100% chemical fertilizer (N); F3, Azospirillum brasilense and Azotobacter chroococcum; F4, integration of A. brasilense and A. chroococcum + 50% nitrogen chemical fertilizer.

where Ya and Yb are the sweet basil and maize yields in sole cropping and Yab and Yba are the yields of sweet basil and maize in intercropping, respectively. LER values >1 shows the superiority of intercropping system in environmental resources consumption for growth and production of plant compared to sole cropping, and when LER <1 resources are used more efficiently in monocropping than in intercropping system (Vandermeer, 1989).

Data Analysis

SAS and MSTATC softwares were applied to analysis of variance (ANOVA) and comparison of means, respectively. The mean data were compared using Duncan's multiple range test at $p \leq 0.05$. The graphs were drawn by Excel and error bars were assigned on the basis of standard deviation (SD).

RESULTS AND DISCUSSION

Fresh and Dry Yields of Basil

The result showed that the highest fresh and dry yields of sweet basil were obtained by sole cropping of sweet basil and using integration of *A. brasilense* and *A. chroococcum* + 50% nitrogen chemical fertilizer in second year of experiment (**Table 3**). Both years did not have the same effect on the mentioned traits, due to difference between climatic conditions in those periods, such that appropriate climate in early of second year caused plants to have a better establishment and growth consequently, led to more photosynthesis activities and yield. The higher fresh and dry yields in sole cropping of sweet basil can be attributed to the homogeneous environment in monoculture system (Amani-Machiani et al., 2018). This demonstrated that the interspecific competition in the sweet basil + forage maize intercropping system was higher than the intraspecific competition in sole cropping system (Xie and Kristensen, 2017; Amani-Machiani et al., 2018). On the other hand, the high competitive ability of forage maize compared to sweet basil in different intercropping patterns led to a significant decrement in sweet basil yield, likely due to shade from the maize. In a study, it was found that among different cropping patterns, higher fresh and dry yields of sweet basil were gained by its sole cropping relative to its intercropping with maize (Bagheri et al., 2014). Amani-Machiani et al. (2018) indicated that the peppermint biomass in intercropping with faba bean (*Vicia faba* L.) was significantly less than sole crop of peppermint. As nitrogen enhances plant's vegetative growth and

consequently improves its yield, accordingly the more nitrogen is used by plants, by impacting on physiological processes, increases photosynthesis activities and produces more assimilate, biomass, and eventually yield. Due to effects of *A. brasilense* and *A. chroococcum* on nitrogen fixing and secreting growth activator in comparison to control, the yield of sweet basil was significantly increased by application *A. brasilense* and *A. chroococcum* (Ghilavizadeh et al., 2013; Pešakovic et al., 2013).

Fresh and Dry Yields of Maize

The highest fresh and dry yields of maize were achieved in second year (**Table 3**). The effect of two growing seasons on these traits was not the same and the difference between the growing seasons was significant. Better climatic conditions in the beginning of the growing season provided suitable seedling establishment, photosynthesis and yield for maize plants in the second year.

The data presented in **Table 3** showed that among the different intercropping systems the highest fresh and dry yields of maize were obtained from sole cropping pattern. Among the different intercropping systems, sole cropping pattern in terms of dry yield of maize had no significant difference with maize + 25% basil treatment. Due to high plant density of basil intercropped with maize and competition for water and nutrients, the fresh and dry yields of maize in maize + 100% basil pattern was apparently decreased as compared to maize's monoculture. Best utilization of nutrients, moisture, space, and solar energy can be derived through mono cropping system (Aiyer, 1963). Bagheri et al. (2014) reported that fresh and dry weight of leaves, stem, and ear in sole culture of maize were more than intercrops. Increasing the proportions of sweet basil and/or borage decreased the weight of leaves, stem, and ear of maize. Higher yield of sole culture compared to intercrop may be due to minimal disruption of the plants habitat (Banik et al., 2006).

The highest and lowest fresh and dry yields of maize have shown by nitrogen chemical fertilizer and control (without-fertilizer) treatments, respectively (**Table 3**). Application of *A. brasilense* and *A. chroococcum* resulted in 12% extra dry yield of maize, compared with the control. It seems that application nitrogen fertilizer plays a significant role in increasing plant's vegetative growth and consequently paves the way for increasing the yield of forage corn. An increase in the rate of applied nitrogen and also its effect on physiological processes resulted in more photosynthesis, assimilation, dry matter and yield. In other words, due to nitrogen-fixing and the effects of nitrogen-fixing bacteria on secreting growth regulator as well as stimulating plant's growth, the forage corn's yield was increased through application of nitroxin biofertilizer as compared to control. The positive role of nitrogen on qualitative and quantitative traits of corn such as dry weight has been proved (Cox et al., 1993). In this respect, Nanda et al. (1995) also showed that inoculating corn's seeds with nitrogen-fixing bacteria under field conditions caused to increase the yield compared with different levels of nitrogen fertilizer. By 2-year planting two types of corn seeds in the field (i.e., the inoculated seeds with free living N-fixing bacteria and non-inoculated seeds as control group) under different treatments of consumption and non-consumption of nitrogen, Rohitashav et al. (1993) found that the yield of dry matter of forage was higher due to inoculation benefits. Hernandez et al. (1995) also reported that inoculating seeds with nitrogen-fixing bacteria enhanced the fresh weight of aerial parts of plant and the number of leaves per plant.

Content of Essential Oil (EO)

Intercropping forage maize + 100% basil with chemical nitrogen fertilizer resulted in the lowest content of EO (0.53%) while the highest (0.75%) was obtained by sole cropping of sweet basil with N_2 fixing bacteria of *A. brasilense* and *A. chroococcum* (**Figure 1**). Under sole cropping pattern, competition between sweet basil plants was reduced because the space needed for growth was increased. Thus, sole cropping pattern, as compared to intercropping pattern, adequately supplied light and soil resources to increase EO content in plants. Amaki et al. (2011) stated that amount of EO of sweet basil was affected by intensity of light, as EO was enhanced by excessive light. Figueiredo et al. (2008) stated that intense sunlight directly resulting in an increase in the EO of *O. basilicum*.

In a study by Nobahar and Pazoki (2010) on sweet basil, increasing the number of plants per area significantly reduced the content of EO. A reduction in plant density resulted in an increase in percentage of EO due to reduction in the level of plants' competition. However, in our study, there was not a significant difference in EO content between intercropping patterns (forage maize + 100% basil and forage maize + 50% basil) nourished by *A. brasilense* and *A. chroococcum* and sole cropping pattern of sweet basil nourished by *A. brasilense* and *A. chroococcum.* This showed that, in addition to producing more forage maize per area which is considered as a merit of cropping medicinal forage, the quality was not negatively affected by intercropping with maize when fertilized with N_2 fixing bacteria.

According to the results of this research, it seems that there is an inverse relationship between EO content of sweet basil and using nitrogen chemical fertilizer. The superiority of controls over other treatments, i.e., nitrogen chemical fertilizer and an integration of N_2 fixing bacteria + 50% nitrogen chemical fertilizer with high biological yield, is attributed to an increase in secondary metabolite under environmental stress and nutritional deficiency conditions. Nitrogen chemical fertilizer and an integration of N_2 fixing bacteria + 50% nitrogen chemical fertilizer adequately paved the way for plants to grow adequately through supplying nutritional resources. Khalediyan et al. (2020) stated that EO yield of *Ocimum basilicum and Satureja hortensis* was significantly increased due to N_2 fixing bacteria treatments compared to control plants.

The mean comparisons of cropping pattern × harvest showed that sole cropping of sweet basil in second harvest produced the highest content of EO (0.79%) while the lowest was recorded by intercropping forage maize + 100% basil at first harvest (0.56%) (**Figure 2**). Although all harvests were performed at identical growth stage, plants of second and third harvests generated more secondary metabolite due to abundant light and more photosynthesis activities. Jahan et al. (2013) stated that among all harvests, the first harvest of sweet basil produced lowest EO content. The mean comparisons of year of experiment × harvest showed that highest EO content (0.73%) was found in second

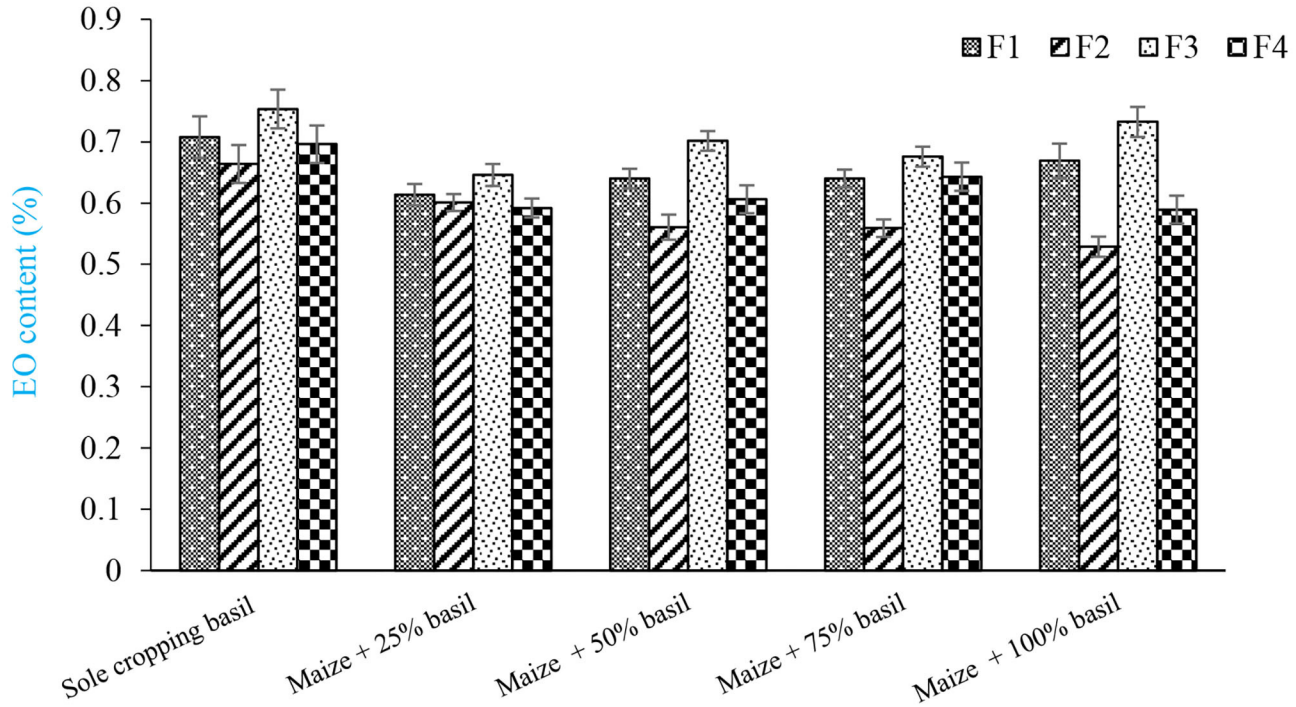

FIGURE 1 | Mean comparisons of interaction of cropping patterns and N_2 fixing bacteria on content of basil essential oil. F1, control; F2, 100% chemical fertilizer (N); F3, *Azospirillum brasilense* and *Azotobacter chroococcum*; F4, integration of *A. brasilense* and *A. chroococcum* + 50% nitrogen chemical fertilizer.

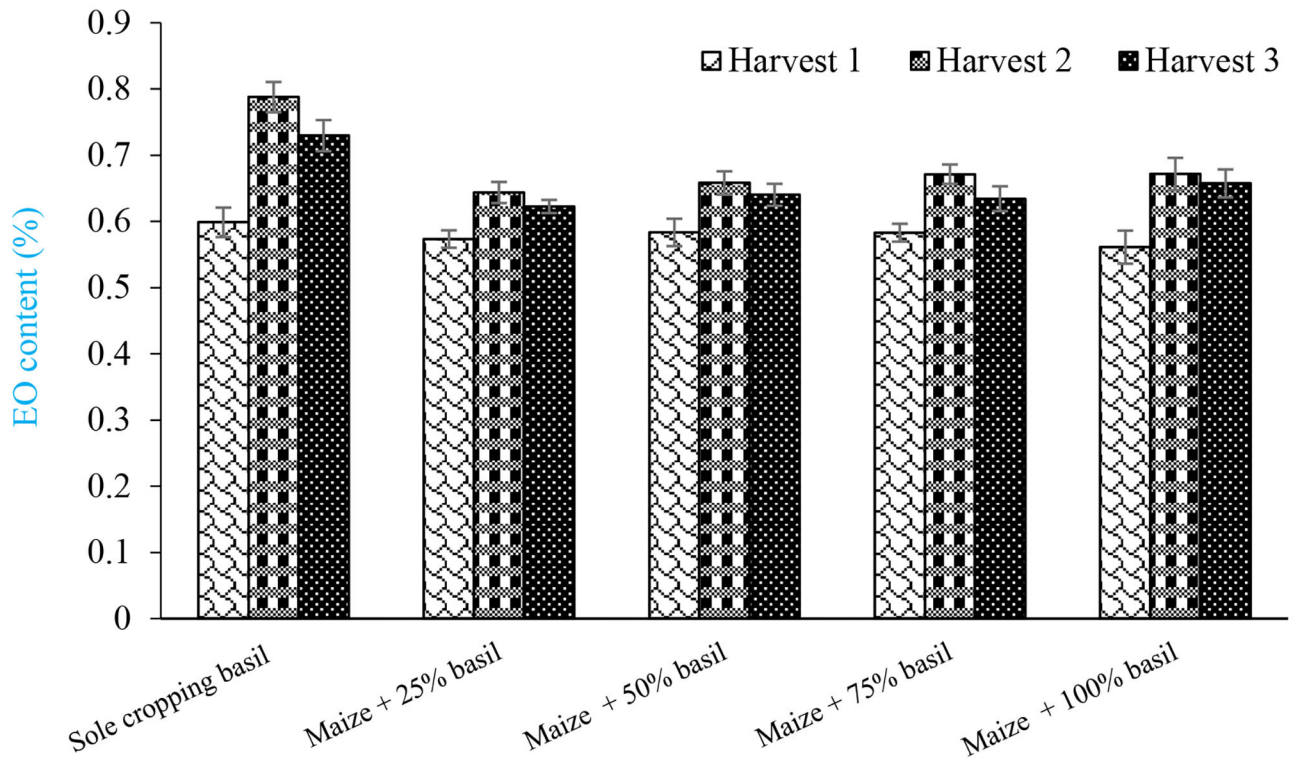

FIGURE 2 | Mean comparisons of interaction of cropping patterns and different harvest on content of basil essential oil.

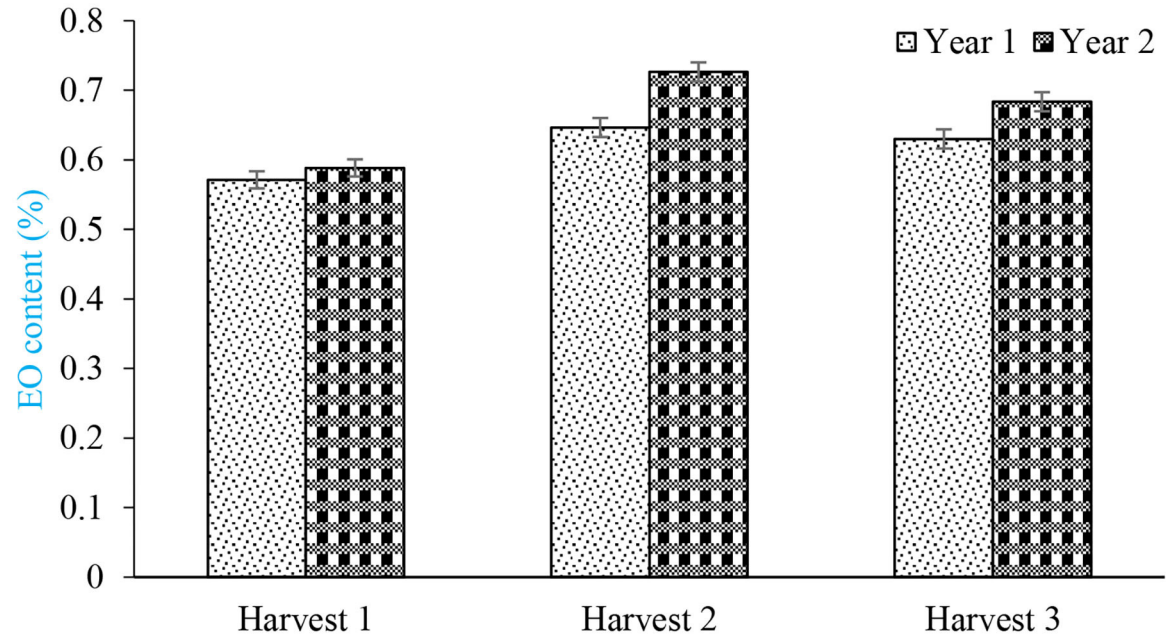

FIGURE 3 | Mean comparisons of interaction of different harvest and years of experiments on content of basil essential oil.

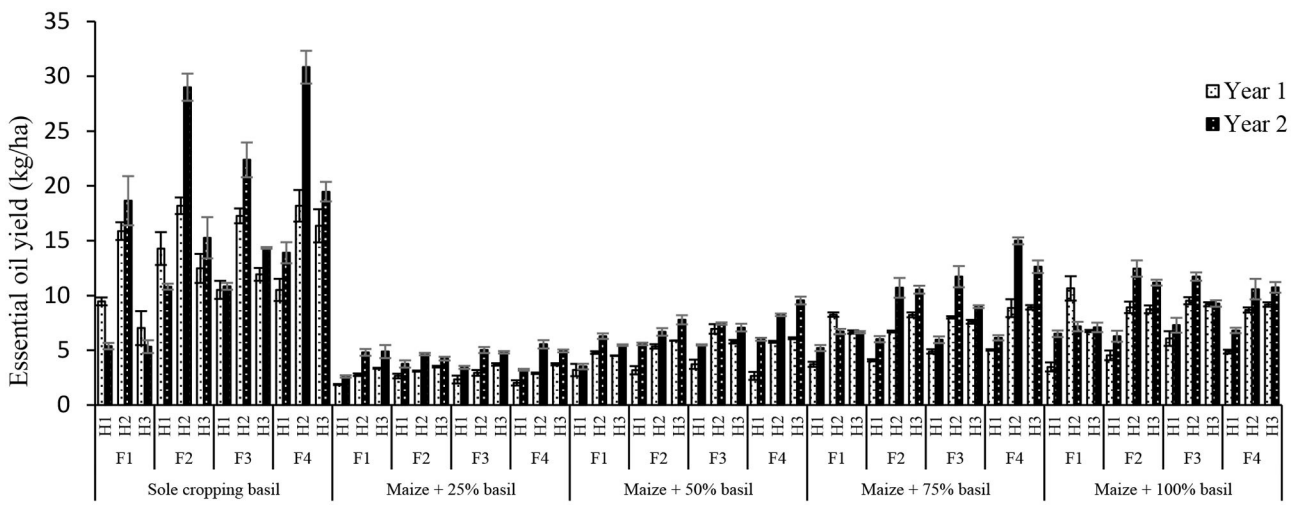

FIGURE 4 | Mean comparisons of interaction of cropping patterns and N_2 fixing bacteria in different harvest during two growing seasons on essential oil yield of basil. I1, I2, I3, I4, and I5: sole cropping of basil, the additive intercropping of maize + 25% basil, maize + 50% basil, maize + 75% basil and maize + 100% basil, respectively. F1, control; F2, 100% chemical fertilizer (N); F3, *Azospirillum brasilense* and *Azotobacter chroococcum*; F4, integration of *A. brasilense* and *A. chroococcum* + 50% nitrogen chemical fertilizer and H1, first harvest; H2, second harvest; and H3, third harvest.

harvest of second year (**Figure 3**). As the number of leaf and inflorescence in second year were higher than those of first year (unpublished data), and as well as more EO content of sweet basil is found in leaf and flower, it was expected that rate of EO content in second year to be higher than that of first one

Essential Oil Yield

The result revealed that highest yield of EO of sweet basil was achieved by sole cropping with application of N_2 fixing bacteria + 50% nitrogen chemical fertilizer in second harvest of second year (30.8 kg ha^{-1}) (**Figure 4**). Sole cropping yielded more EO than did other cropping practices due to lack of interspecific competition, lack of shade, and having sufficient space for extending vegetative organs in order to take advantage of available resources. These beneficial factors allowed plants to expand their height and lateral branches. In keeping with the direct relationship between light irradiation and EO production reported by Amaki et al. (2011), sole cropping provided abundant

light for plants to enhance their EO content in absence of shading other taller plants (maize).

A. brasilense and *A. chroococcum* and control (without-fertilizer) treatments gave higher EO content compared to nitrogen chemical fertilizers and integration of *A. brasilense* and *A. chroococcum* + 50% nitrogen chemical fertilizer. This reflected the fact that EO yield of sweet basil was highly affected by biological yield and less by EO content. In other words, the contribution of EO content to increased yield of EO per area was lower than that of in biological yield of crops. This experiment confirmed the hypothesis that application of nitrogen chemical fertilizer and integrated *A. brasilense* and *A. chroococcum* + 50% nitrogen chemical fertilizer could increase yield of EO of sweet basil, mainly due to increase in biological yield. The availability of nitrogen enhances the rate of photosynthesis and enables the plant to grow rapidly and produced significant biomass, which may increase accumulation of secondary metabolites, such as EO (Sifola and Barbieri, 2006). Kumari Gour et al. (2017) stated that highest EO yield of dill was gained by using an integrated treatment of *Azospirillum* and *Azotobacter* plus 75% urea.

As the EO content and biological yield in second harvest were higher than those at the other two harvests, it was expected that the EO yield in second harvest to be higher than that of the others. Among three harvests of sweet basil, Jahan et al. (2013) demonstrated that the highest and lowest EO yield was found in second and first harvests, respectively. It was also shown that intercropping soybean with peppermint promoted the production of peppermint's EO as compared to their sole cropping and the maximum and minimum EO content were obtained in intercropping ratio of 3:2 (1.74%) and sole cropping of peppermint (1.26%), respectively. Furthermore, the first harvest produced more EO compared to the second harvest (Amani-Machiani et al., 2018). Since there is a positive correlation between EO yield and biological yield, the EO yield increased with rising density level of sweet basil plants intercropped with maize. In this respect, the maximum EO yield was attained by applying forage maize + 75% basil as well as application of *A. brasilense* and *A. chroococcum* + 50% nitrogen chemical fertilizer.

EO Composition

In addition to quantity, the quality (in terms of type and number of constituents) of EO is also received great attentions while cultivation medicinal plants (**Figure 5**). The analysis of EO carried out on aerial organs of sweet basil in different treatments revealed the presence of 23–32 constituents (**Tables 4**, **5**). As some of detected constituents such as 1,8-cineol, terpinolene, α-cubebene, eugenol, β-cubebene, β-elemen, and α-zingiberene were not observed in all treatments but found in small quantities in some treatments, they were not presented in tables. In current research, the results revealed that the types of EO components of in both years of experiments could remarkably vary depending on type of treatment. In both years, eight constituents including methyl chavicol (17.24–51.28%), Z-citral (neral) (8.33–24.3%), geranial (10.2–31.3%), (E)-caryophyllene (1.05–5.64%), α-*trans*-bergamotene (0.53–1.7%), α-humulene (0.4–1.69%), germacrene-D (0.2–1.88%), and (Z)-α-bisabolene (1.16–3.86%) were the main constituents of EO. In order to monitor the change occurred in type and amount of EO's constituents, their relative contents in different treatments were carefully assayed. The highest amount of methyl chavicol in first (51.03%) and second (51.28%) years were achieved by sole cropping of sweet basil with nitrogen chemical fertilizer (**Tables 4**, **5**), while the lowest were obtained in first and second years (17.24 and 38.2%, respectively) by sole cropping of sweet basil without-fertilizer. In both years, the highest content of methyl chavicol was found through sole cropping of sweet basil with nitrogen chemical fertilizer followed by sole cropping of sweet basil with an integration of *A. brasilense* and *A. chroococcum* + 50% nitrogen chemical fertilizer. The availability of nitrogen in chemical fertilizer and also the lack of competition among plants of sweet basil under sole cropping seemingly increased methyl chavicol concentration compared to other treatments. Zheljazkov et al. (2008) stated that nitrogen markably changed the amount of linalool, eugenol, bornil acetate and eucalyptol of EO of sweet basil. They continued that application of more nitrogen increased methyl chavicol while it decreased linalool of EO. The highest content of Z-citral (neral) (24.3 and 16.6%), geranial (31.3 and 21.94%), and (E)-caryophyllene (5.64 and 3.27%) were observed by an intercropping of forage maize + 25% basil and without–fertilizer in first and second years of experiment, respectively. Likewise, the highest levels of α-humulene (1.69 and 1.4%), germacrene-D (1.88 and 0.65%) were found in intercropped forage maize + 100% basil without-fertilizer in first and second years of experiment, respectively (**Tables 4**, **5**). It appears that some factors like nutrient deficiency (especially nitrogen deficiency in the control without fertilizer) and level of plants competition over light and nutrient resources under intercropping pattern could be considered as factors stimulating more production of these constituents. Main constituents of EO are affected by diverse factors: water stress, salt stress, and nutrition deficiencies resulting in change in EO constituents (Barbieri et al., 2012; Ekren et al., 2012).

In the first year of the experiment, the highest amount of α-*trans*-bergamotene (1.38%) was achieved by intercropping forage maize + 25% basil and without-fertilizer treatment, but in second year, highest amount (1.7%) was obtained by intercropping forage maize + 100% basil and without-fertilizer treatment. Based on Nurzyńska-Wierdak et al. (2013), different levels of nitrogen was shown to have a significant effect on the main constituents in the EO of basil in such that the highest amount α-*trans*-bergamotene in sweet basil was found by lowest level of nitrogen. At first year of experiment, the highest content of (Z)-α-bisabolene (3.86%) was obtained by intercropping forage maize + 75% basil without-fertilizer, while its highest rate in second year was found by intercropping forage maize + 75% basil and applying *A. brasilense* and *A. chroococcum* N_2 fixing bacteria treatments (**Tables 4**, **5**). There are some reports on effects of intercropping patterns on quality and quantity of EO. Rajeswara Rao (2002) figured out that intercropping corn mint (*Mentha arvensis* L.) with tomato under different planting dates, in addition to achieving an acceptable corn mint yield, increased the constituents' quality of

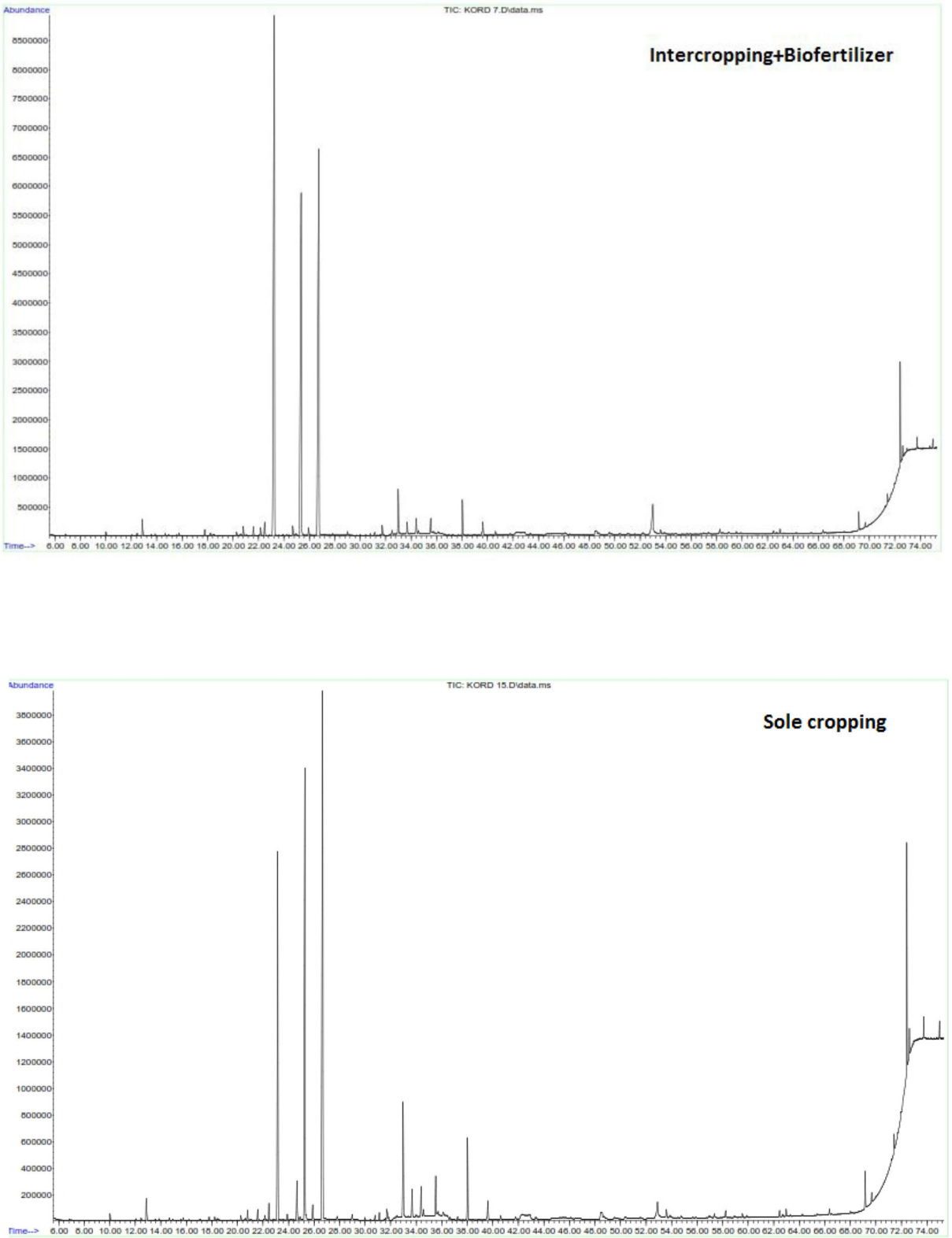

FIGURE 5 | *Ocimum basilicum* L. essential oil chromatogram carried out using a GC-MS. Essential oils were obtained from non-biofertilizer with *Azospirillum brasilense* and *Azotobacter chroococcum* application and sole and intercropped plants.

TABLE 4 | Essential oil constituents in basil grown with different sources of nitrogen under different patterns of cropping during 2018 growing season (expressed on relative percentage basis).

Compounds	Sole cropping of basil				Maize + 25% basil				Maize + 50% basil				Maize + 75% basil				Maize + 100% basil			
	F1	F2	F3	F4	F1	F2	F3	F4	F1	F2	F3	F4	F1	F2	F3	F4	F1	F2	F3	F4
α-Pinene	0.20	0.21	0.12	0.09	0.32	0.13	0.21	0.14	0.20	0.21	0.20	0.12	0.13	0.21	0.23	0.20	0.20	0.19	0.44	0.16
(Z)-3- Hexenyl acetate	0.05	0.10	0.16	0.10	0.03	0.06	0.13	0.06	0.06	0.13	0.09	0.14	0.11	0.12	0.08	0.11	0.12	0.13	0.09	0.12
Limonene	0.12	0.13	0.11	0.09	0.10	0.12	0.10	0.09	0.10	0.11	0.12	0.10	0.13	0.12	0.12	0.11	0.15	0.13	0.11	0.11
(E)-β- Ocimene	0.13	0.26	0.22	0.09	0.12	0.10	0.18	0.10	0.11	0.15	0.16	0.11	0.13	0.21	0.12	0.10	0.11	0.15	0.10	0.08
Fenchone	0.08	0.20	0.17	0.17	0.12	0.32	0.22	0.24	0.16	0.28	0.29	0.13	0.12	0.26	0.25	0.20	0.13	0.22	0.16	0.17
Rose furan epoxide	0.22	0.44	0.84	0.61	0.26	0.31	0.33	0.32	0.25	0.21	0.37	0.29	0.32	0.44	0.23	0.54	0.31	0.35	0.26	0.45
Methyl chavicol	**17.24**	**51.03**	**28.51**	**38.92**	**17.91**	**35.82**	**32.20**	**29.06**	**30.22**	**35.83**	**29.72**	**35.33**	**28.67**	**37.69**	**37.59**	**36.70**	**19.01**	**37.25**	**19.54**	**26.49**
Z-Geraniol (Nerol)	**0.21**	**0.68**	**0.83**	**0.57**	**1.91**	**0.70**	**1.53**	**0.44**	**0.58**	**1.27**	**0.79**	**2.32**	**2.27**	**1.93**	**0.37**	**1.19**	**2.02**	**2.60**	**1.37**	**2.51**
Z-Citral (Neral)	**21.47**	**13.92**	**22.85**	**15.77**	**24.30**	**19.07**	**21.84**	**18.46**	**21.85**	**21.84**	**22.66**	**19.42**	**22.00**	**20.11**	**20.88**	**19.70**	**19.17**	**18.46**	**20.12**	**19.60**
Geraniol	**0.85**	**0.23**	**0.34**	**0.25**	**0.76**	**0.29**	**0.81**	**0.32**	**0.85**	**0.54**	**0.40**	**0.76**	**1.02**	**0.80**	**0.42**	**0.49**	**0.82**	**1.04**	**0.50**	**0.83**
Geranial	**25.17**	**17.65**	**29.77**	**20.12**	**31.30**	**24.48**	**28.14**	**23.69**	**27.47**	**28.62**	**30.55**	**24.46**	**28.04**	**25.00**	**26.75**	**24.3**	**23.43**	**24.21**	**25.46**	**24.16**
Neryl acetate	0.17	0.38	0.73	0.24	0.26	0.15	0.19	0.18	0.21	0.17	0.15	0.34	0.36	0.23	0.18	0.55	0.39	0.35	0.22	0.51
α- Copaen	0.16	0.17	0.18	0.13	0.21	0.28	0.24	0.12	0.17	0.22	0.21	0.24	0.20	0.26	0.22	0.50	0.30	0.24	0.22	0.30
Geranyl acetate	0.09	0.09	0.22	–	–	0.09	0.40	0.06	0.06	0.10	0.49	0.10	0.15	0.10	0.30	0.20	0.16	0.08	0.10	0.18
Methyleugenol	0.11	0.46	0.18	0.25	0.24	0.31	0.19	0.20	0.32	0.20	0.16	0.18	0.13	0.25	0.20	0.42	0.17	0.19	0.17	0.24
(E)-Caryophyllene	**3.01**	**2.81**	**2.84**	**1.93**	**5.64**	**3.55**	**2.96**	**1.66**	**2.07**	**2.97**	**2.85**	**3.00**	**3.16**	**3.01**	**3.06**	**3.65**	**4.12**	**3.58**	**3.10**	**4.64**
α-trans-Bergamotene	**1.30**	**0.85**	**0.93**	**0.68**	**1.38**	**0.96**	**0.82**	**0.67**	**0.53**	**0.65**	**0.65**	**0.97**	**0.89**	**0.70**	**0.72**	**1.10**	**1.15**	**0.98**	**0.79**	**1.35**
α-Humulene	**1.55**	**1.23**	**1.35**	**0.86**	**1.50**	**1.11**	**0.92**	**0.57**	**0.70**	**0.75**	**0.96**	**0.98**	**0.97**	**1.08**	**1.02**	**1.50**	**1.69**	**1.17**	**1.03**	**1.62**
(E)- β-Farnesene	0.16	0.23	0.22	0.18	0.18	0.26	0.24	0.20	0.18	0.26	0.22	0.28	0.25	0.27	0.20	0.36	0.42	0.23	0.27	0.46
Germacrene-D	**1.50**	**0.82**	**0.70**	**0.50**	**1.87**	**1.20**	**1.29**	**0.55**	**0.61**	**0.48**	**1.03**	**1.32**	**1.28**	**1.36**	**0.68**	**1.70**	**1.88**	**1.44**	**1.00**	**1.85**
β-Bisabolene	0.10	0.13	–	0.10	0.09	0.11	0.05	0.15	0.09	0.15	0.09	0.14	0.12	0.16	0.09	0.20	0.18	0.20	0.13	0.23
(Z)-α- Bisabolene	**3.52**	**2.46**	**2.67**	**1.96**	**3.74**	**2.57**	**2.67**	**1.25**	**1.47**	**1.19**	**2.13**	**3.02**	**3.86**	**3.03**	**2.22**	**3.58**	**3.24**	**3.18**	**3.32**	**3.79**
Caryophyllene oxide	**0.35**	**0.84**	**1.23**	**0.58**	**1.05**	**1.02**	**0.72**	**0.85**	**0.86**	**0.73**	**0.65**	**0.74**	**0.57**	**1.11**	**1.10**	**1.10**	**0.75**	**0.68**	**0.91**	**1.04**
Humulene epoxide II	0.13	0.23	0.36	0.23	0.23	0.23	0.15	0.15	0.21	0.20	0.15	0.16	0.14	0.24	0.24	0.15	0.17	0.15	0.24	0.26

F1, control; F2, 100% chemical fertilizer (N); F3, Azospirillum brasilense and Azotobacter cerococcid; F4, integration of A. brasilense and A. chroococcum + 50% nitrogen chemical fertilizer. Bold values show significant increases between treatments.

TABLE 5 | Essential oil constituents in basil grown with different sources of nitrogen under different patterns of cropping during 2019 growing season (expressed on relative percentage basis).

Compounds	Sole cropping of basil				Maize + 25% basil				Maize + 50% basil				Maize + 75% basil				Maize + 100% basil			
	F1	F2	F3	F4	F1	F2	F3	F4	F1	F2	F3	F4	F1	F2	F3	F4	F1	F2	F3	F4
α-Pinene	0.08	0.09	0.07	0.09	0.13	0.08	0.10	0.12	0.08	0.10	0.11	0.10	0.06	0.21	0.13	0.15	0.08	0.15	0.19	0.14
(Z)-3- Hexenyl acetate	0.08	0.13	0.11	0.12	0.06	0.09	0.09	0.08	0.08	0.15	0.09	0.15	0.10	0.17	0.08	0.14	0.10	0.16	0.10	0.12
Limonene	0.10	0.09	0.10	0.10	0.09	0.08	0.08	0.08	0.12	0.07	0.08	0.08	0.10	0.08	0.10	0.09	0.12	0.10	0.12	0.10
(E)-β- Ocimene	–	–	–	–	–	–	–	–	–	–	–	–	–	–	–	–	–	–	–	–
Fenchone	0.10	0.19	0.28	0.18	0.11	0.25	0.29	0.20	0.12	0.24	0.23	0.20	0.16	0.20	0.21	0.22	0.12	0.18	0.20	0.20
Rose furan epoxide	0.58	0.34	0.45	0.47	0.31	0.30	0.37	0.32	0.20	0.31	0.40	0.22	0.19	0.28	0.35	0.18	0.19	0.25	0.38	0.20
Methyl chavicol	**38.20**	**51.28**	**46.32**	**50.46**	**39.20**	**40.23**	**45.55**	**43.10**	**44.20**	**41.20**	**42.40**	**42.38**	**43.50**	**43.52**	**47.60**	**49.15**	**39.29**	**40.10**	**41.40**	**38.80**
Z-Geraniol (Nerol)	**0.54**	**0.35**	**0.50**	**0.60**	**0.71**	**0.40**	**1.25**	**0.70**	**0.60**	**0.90**	**1.10**	**1.19**	**0.76**	**1.22**	**1.30**	**1.10**	**0.80**	**1.50**	**1.20**	**1.60**
Z-Citral (Neral)	**13.48**	**8.33**	**9.79**	**15.91**	**16.60**	**13.10**	**13.59**	**16.50**	**15.90**	**15.20**	**15.60**	**9.09**	**12.70**	**14.42**	**15.41**	**8.69**	**12.50**	**9.00**	**15.29**	**8.67**
Geraniol	**0.28**	**0.43**	**0.28**	**0.36**	**0.23**	**0.53**	**0.53**	**0.46**	**0.30**	**0.75**	**0.60**	**0.55**	**0.38**	**0.88**	**0.50**	**0.44**	**0.25**	**0.80**	**0.48**	**0.50**
Geranial	**17.35**	**10.67**	**12.90**	**15.00**	**21.94**	**17.20**	**18.47**	**17.20**	**18.90**	**18.02**	**18.50**	**13.69**	**17.40**	**16.94**	**17.30**	**13.33**	**16.90**	**15.10**	**20.76**	**10.20**
Neryl acetate	0.26	0.58	0.42	0.67	0.21	0.47	0.35	0.57	0.40	0.50	0.30	0.54	0.60	0.61	0.33	0.59	0.58	0.60	0.33	0.52
α- Copaen	0.58	0.20	0.25	0.28	0.39	0.26	0.27	0.25	0.30	0.20	0.25	0.13	0.34	0.25	0.21	0.25	0.35	0.23	0.21	0.22
Geranyl acetate	0.31	0.25	0.23	0.13	0.18	0.24	0.30	0.16	0.20	0.20	0.38	0.18	0.34	0.27	0.30	0.14	0.33	0.30	0.26	0.16
Methyleugenol	0.61	2.61	1.36	0.85	1.02	1.60	1.26	0.80	1.22	0.70	1.10	1.64	0.80	0.67	1.20	1.18	0.97	0.50	0.67	1.19
(E)-Caryophyllene	**2.57**	**1.10**	**2.06**	**1.48**	**3.27**	**1.82**	**1.93**	**1.05**	**2.95**	**1.73**	**2.02**	**2.71**	**3.08**	**1.13**	**2.75**	**1.57**	**3.15**	**1.84**	**2.76**	**2.45**
α-trans-Bergamotene	**1.46**	**0.62**	**1.16**	**1.06**	**1.05**	**0.60**	**0.88**	**0.81**	**0.91**	**0.95**	**0.84**	**0.71**	**1.60**	**1.13**	**1.25**	**0.94**	**1.70**	**1.20**	**1.29**	**1.17**
α-Humulene	**1.29**	**0.43**	**1.03**	**0.96**	**0.91**	**0.40**	**0.73**	**0.70**	**0.80**	**0.44**	**1.02**	**0.40**	**1.36**	**0.48**	**1.21**	**0.69**	**1.40**	**0.57**	**1.33**	**1.21**
(E)- β-Farnesene	0.25	0.24	0.24	0.16	0.25	0.27	0.26	0.19	0.27	0.27	0.24	0.19	0.30	0.30	0.30	0.19	0.35	0.30	0.34	0.24
Germacrene-D	0.21	0.36	0.23	0.35	0.27	0.38	0.29	0.40	0.26	0.20	0.25	0.27	0.60	0.44	0.55	0.50	0.65	0.47	0.60	0.60
β-Bisabolene	0.27	0.11	0.21	0.12	0.18	0.14	0.20	0.13	0.20	0.13	0.20	0.13	0.24	0.20	0.22	0.12	0.25	0.22	0.18	0.16
(Z)-α- Bisabolene	**3.33**	**1.48**	**2.52**	**2.96**	**2.86**	**1.52**	**1.94**	**1.35**	**2.31**	**1.16**	**1.80**	**1.25**	**3.46**	**1.96**	**3.50**	**2.13**	**3.11**	**2.40**	**3.45**	**2.38**
Caryophyllene oxide	**1.20**	**1.86**	**1.63**	**2.21**	**2.09**	**2.20**	**1.31**	**2.30**	**2.00**	**2.10**	**1.20**	**2.05**	**2.07**	**2.60**	**1.35**	**1.59**	**1.80**	**2.10**	**1.20**	**1.52**
Humulene epoxide II	0.76	0.57	0.60	1.59	0.36	0.50	0.41	0.88	0.40	0.56	0.31	0.79	0.49	0.50	0.30	0.45	0.30	0.44	0.45	0.48

F1, control; F2, 100% chemical fertilizer (N); F3, Azospirillum brasilense and Azotobacter chroococcum; F4, integration of A. brasilense and A. chroococcum + 50% nitrogen chemical fertilizer. Bold values show significant increases between treatments.

corn mint EO up to different extents such as menthol (73%), menthone (9.6%), isomenthone (4%), menthyl acetate (4%). Amani-Machiani et al. (2018) showed that the highest and lowest menthol, germacrene-D and (E)-caryophyllene were gained by intercropping peppermint with soybean and sole cropping of peppermint, respectively.

Compared to first year of experiment, all treatments gained markedly higher methyl chavicol in second year of experiment. By contrast, the rate of Z-citral (neral), geranial, germacrene-D and (E)-caryophyllene were higher in the first year of experiment. Although (E)-β-ocimene was observed in all treatments in the first year, it was not observed in second year. As the relative percentage of EO constituents usually changed (even) daily and it also was affected by a great deal of factors, it is expected that compositions fluctuated during both years of experiments, however the main constituents were identical in both years. The lowest content of main constituents in EO, except methyl chavicol, was observed in a cropping pattern in which nitrogen chemical fertilizer was employed. Thus, application of *A. brasilense* and *A. chroococcum* and an integration of N_2 fixing bacteria + 50% nitrogen chemical fertilizer is advisable to enhance the quality of EO. Plant growth-promoting bacteria (PGPB), as a growth stimulator, is able to change environmental conditions and constituents of EO with different mechanisms such as increasing nitrogen fixation and available nitrate, producing auxin and gibberellin, secreting antibiotics, and enhancing root growth and development as well as promoting water and nutrients uptake (Prasad et al., 2011; Santoro et al., 2011).

TABLE 6 | Land equivalent ratio (LER) in intercropping treatments of maize with sweet basil and N_2 fixing bacteria (2018 and 2019).

Treatments	2018	2019
Maize + 25% sweet basil-without fertilizer	1.28	1.17
Maize + 25% sweet basil+ chemical fertilizer	1.22	1.29
Maize + 25% sweet basil + *A. brasilense* and *A. chroococcum*	1.31	1.23
Maize + 25% sweet basil + *A. brasilense* and *A. chroococcum* + 50% chemical fertilizer	1.25	1.16
Maize + 50% sweet basil-without fertilizer	1.38	1.38
Maize + 50% sweet basil + chemical fertilizer	1.34	1.33
Maize + 50% sweet basil + *A. brasilense* and *A. chroococcum*	1.46	1.41
Maize + 50% sweet basil + *A. brasilense* and *A. chroococcum* + 50% chemical fertilizer	1.38	1.33
Maize + 75% sweet basil and control	1.46	1.52
Maize + 75% sweet basil + chemical fertilizer	1.45	1.43
Maize + 75% sweet basil + *A. brasilense* and *A. chroococcum*	1.55	1.54
Maize + 75% sweet basil + *A. brasilense* and *A. chroococcum* + 50% chemical fertilizer	1.49	1.46
Maize + 100% sweet basil-without fertilizer	1.54	1.52
Maize + 100% sweet basil +chemical fertilizer	1.51	1.47
Maize + 100% sweet basil + *A. brasilense* and *A. chroococcum*	1.56	1.56
Maize + 100% sweet basil + *A. brasilense* and *A. chroococcum* + 50% chemical fertilizer	1.52	1.48

Land Equivalent Ratio (LER)

As can be seen, in all treatments the LER values were higher than 1 (**Table 6**), which indicates advantage of intercropping relative to sole cropping. Meanwhile, N_2 fixing bacteria application significantly enhanced LER in both 2018 and 2019. The maximum LER (1.56) was achieved from maize + 100% sweet basil + N_2 fixing bacteria in 2018 and the minimum (1.17) in maize + 25% sweet basil + without fertilizer in 2019 (**Table 6**). The great efficiency of the intercropping systems found in the present research as supported by higher total LER is consistent with Baumann et al. (2001) findings, who attributed this phenomenon to the supplementary use of resources in plant production allowing an interspecific facilitation. Based on the findings of Hauggaard-Nielsen et al. (2003), the calculated LER demonstrated that plant growth resources were used from 27 to 31% more efficiently by intercrop than the sole crop. Khalediyan et al. (2020) indicated that LER, land utilization efficiency (LUE), relative value total (RVT) and time equivalent ratio (ATER) in intercropping were more than sole cropping.

CONCLUSION

The results of this research showed that the biological yield and EO yield of sweet basil intercropped with maize was enhanced as plant density was increased, such that among different intercropping patterns the maximum biological yield and EO yield were found in treatments with higher sweet basil plants density intercropped with maize. Compared to nitrogen chemical fertilizer, an integration of *A. brasilense* and *A. chroococcum* + 50% nitrogen chemical fertilizer showed an acceptable potential in terms of biological yield; and this treatment did not show a remarkable difference with nitrogen chemical fertilizer. The highest yield of EO was attained by applying *A. brasilense* and *A. chroococcum* + 50% nitrogen chemical fertilizer, although N_2 fixing bacteria and no-fertilizer treatments gave higher EO content than did nitrogen chemical fertilizer and *A. brasilense* and *A. chroococcum* + 50% nitrogen chemical fertilizer treatments, but nitrogen chemical fertilizer and an integration of *A. brasilense* and *A. chroococcum* + 50% chemical fertilizer treatments gave higher EO yield. This can be justified as EO yield was mainly affected by biological yield rather than EO content. As the lowest concentrations of main constituents of EO, except methyl chavicol, were obtained by a cropping pattern in which nitrogen chemical fertilizer was used, it is recommended to use the cropping pattern in which *A. brasilense* and *A. chroococcum* or an integration of *A. brasilense* and *A. chroococcum* + 50% nitrogen chemical fertilizer to be utilized. These treatments increased the quality and quantity of generated EO. Also, the highest contents of main EO constituents, except methyl chavicol, were obtained by intercropping; and this indicated an increase in content of most main EO constituents under

intercropping sweet basil with forage maize, as compared to its sole cropping.

DATA AVAILABILITY STATEMENT

The original contributions presented in the study are included in the article/supplementary material, further inquiries can be directed to the corresponding author.

AUTHOR CONTRIBUTIONS

SK, SS, JK, WW, and DS designed the study. SK, SS, and JK conducted the experiment and analyzed the data with support from WW and DS wrote the paper with contributions from all co-authors. All authors contributed to the article and approved the submitted version.

REFERENCES

Adams, R. P. (2007). *Identification of Essential Oil Components by Gas Chromatography/Mass Spectrometry, 4th Edn*. Carol Stream, IL: Allured Publishing Corporation.

Aguilera, E., Lassaletta, L., Sanz-Cobena, A., Garnier, J., and Vallejo, A. (2013). The potential of organic fertilizers and water management to reduce N_2O emissions in Mediterranean climate cropping systems: a review. *Agric. Ecosyst. Environ.* 164, 32–52. doi: 10.1016/j.agee.2012.09.006

Aires, A., Carvalho, R., Rosa, E. A. S., and Saavedra, M. J. (2013). Effects of agriculture production systems on nitrate and nitrite accumulation on baby-leaf salads. *Food. Sci. Nutr.* 1, 3–7. doi: 10.1002/fsn3.1

Aiyer, A. K. Y. N. (1963). *Principles of Crop Husbandry in India, 4th Edn*. Bangalore: Bangalore Press.

Al-Maskri, A. Y., Hanif, M. A., Al-Maskari, M. Y., Abraham, A. S., Al-Sabahi, J. N., and Al-Mantheri, O. (2011). Essential oil from *Ocimum basilicum* (Omani Basil): a desert crop. *Nat. Prod. Commun.* 6, 1487–1490. doi: 10.1177/1934578X1100601020

Amaki, W., Yamazaki, N., Ichimura, M., and Watanabe, H. (2011). Effects of light quality on the growth and essential oil content in sweet basil. *Acta. Hortic.* 907, 91–94. doi: 10.17660/ActaHortic.2011.907.9

Amani-Machiani, M., Javanmard, A., Morshedloo, M. R., and Maggi, F. (2018). Evaluation of yield, essential oil content and compositions of peppermint (*Mentha piperita* L.) intercropped with faba bean (*Vicia faba* L.). *J. Clean. Prod.* 171, 529–537. doi: 10.1016/j.jclepro.2017.10.062

Bagheri, M., Zaefarian, F., Bicharanlou, B., and Ghanizadeh, H. (2014). A study of intercropping of maize with sweet basil and borag. *Cercet. Agron. Mold.* 47, 13–28. doi: 10.2478/cerce-2014-0013

Banik, P., Midya, A., Sarkar, B. K., and Ghose, S. S. (2006). Wheat and chickpea intercropping systems in an additive series experiment: advantages and weed smothering. *Eur. J. Agron.* 24, 325–332. doi: 10.1016/j.eja.2005.10.010

Barbieri, G., Vallone, S., Orsini, F., Paradiso, R., De Pascale, S., Negre-Zakharov, F., et al. (2012). Stomatal density and metabolic determinants mediate salt stress adaptation and water use efficiency in basil (*Ocimum basilicum* L.). *J. Plant. Physiol.* 169, 1737–1746. doi: 10.1016/j.jplph.2012.07.001

Baumann, D. T., Bastiaans, L., and Kropff, M. J. (2001). Competition and rop performance in a leek-celery intercropping system. *Crop Sci.* 41, 764–774. doi: 10.2135/cropsci2001.413764x

Bilal, A., Jahan, N., Ahmed, A., Bilal, S. N., Habib, S., and Hajra, S. (2012). Phytochemical and pharmacological studies on *Ocimum basilicum* Linn–a review. *Int. J. Curr. Res. Rev.* 4, 73–83. doi: 10.31782/2231-2196

Borloveanu, M. (ed.). (2014). *Leacuri Mănăstiresti, 1st Edn. Terapii Pentru Trup si Suflet*. Bucuresti: Lumea Credintei.

Carneiro, N. S., Alves, C. C. F., Alves, J. M., Egea, M. B., Martins, C. H. G., Silva, T. S., et al. (2017). Chemical composition, antioxidant and antibacterial activities of essential oils from leaves and flowers of *Eugenia klotzchiana* Berg (*Myrtaceae*). *An. Acad. Bras. Cienc.* 89, 1907–1915. doi: 10.1590/0001-3765201720160652

Chen, X., Cui, Z., Fan, M., Vitousek, R., Zhao, M., Ma, W., et al. (2014). Producing more grain with lower environmental costs. *Nature* 514, 486–491. doi: 10.1038/nature13609

Cox, W. J., Kalonge, S., Cherney, D. J. R., and Reid, W. S. (1993). Growth, yield and quality of forage maize under different nitrogen management practices. *Agronomy J.* 85, 344–347. doi: 10.2134/agronj1993.00021962008500020033x

Ekren, S., Sönmez, C., Özcakal, E., Kurttas, Y. S. K., Bayram, E., and Gürgülü, H. (2012). The effect of different irrigation water levels on yield and quality characteristics of purple basil (*Ocimum basilicum* L.). *Agric. Water. Manage.* 109, 155–161. doi: 10.1016/j.agwat.2012.03.004

Figueiredo, A. C., Barroso, J. G., Pedro, L. G., and Scheffer, J. J. C. (2008). Factors affecting secondary metabolite production in plants: volatile components and essential oils. *Flavour. Fragr. J.* 23, 213–226. doi: 10.1002/ffj.1875

Ghilavizadeh, A., Darzi, M. T., and Haj Seyed Hadi, M. (2013). Effects of bio-fertilizer and plant density on essential oil content and yield traits of ajowan (*Carum copticum*), Middle-East. *J. Sci.* 14, 1508–1512.

Hauggaard-Nielsen, H., Ambus, P., and Jensen, E. S. (2003). The comparison of nitrogen use and leaching in sole cropped versus intercropped pea and barley. *Nutr. Cycl. Agroecosys.* 65, 289–300. doi: 10.1023/A:1022612528161

Hernandez, A. N., Hernandez, A., and Heydrich, M. (1995). Selection of rhizobacteria for use in maize cultivation. *Cultivar Tropicales* 6, 5–8.

Hossain, F., Follett, P., Vu, K. D., Salmieri, S., Senoussi, C., and Lacroix, M. (2014a). Radiosensitization of *Aspergillus niger* and *Penicillium chrysogenum* using basil essential oil and ionizing radiation for food. *Food. Control.* 45, 156–162. doi: 10.1016/j.foodcont.2014.04.022

Hossain, F., Lacroix, M., Salmieri, S., Vu, K., and Follett, P. A. (2014b). Basil oil fumigation increases radiation sensitivity in adult Sitophilus oryzae (*Coleoptera: Curculionidae*). *J. Stored. Prod. Res.* 59, 108–112. doi: 10.1016/j.jspr.2014.06.003

Jahan, M., Amiri, M. B., Dehghanipoor, F., and Tahami, M. K. (2013). Effects of biofertilizers and winter cover crops on essential oil production and some agroecological characteristics of basil (*Ocimum basilicum* L.) in a organic agrosystem. *J. Iranian. Agron. Res.* 10, 751–763.

Karagözl,ü, N., and Ergönül, B., Özcan, D. (2011). Determination of antimicrobial effect of mint and basil essential oils on survival of *E. coli* O157:H7 and *S. typhimurium* in fresh-cut lettuce and purslane. *Food. Control.* 22, 1851–1855. doi: 10.1016/j.foodcont.2011.04.025

Khalediyan, N., Weisany, W., and Schenk, P. M. (2020). Arbuscular mycorrhizae and rhizobacteria improve growth, nutritional status and essential oil production in Ocimum basilicum and Satureja hortensis. *Ind. Crop Prod.* 113163. doi: 10.1016/j.indcrop.2020.113163

Kordi, S. (2017). *Evaluation of quantitative and qualitative characteristics of forage maize (Zea mays* L.*) and sweet basil (Ocimum basilicum* L.*) under nitrogen fertilizers (biological, chemical and integrated) in additive intercropping* (Ph.D. thesis). Faculty of Agriculture, University of Tabriz, East Azerbaijan, Iran.

Kordi, S., Shafagh Kolvanagh, J., Zehtab Salmasi, S., and Daneshvar, M. (2017). Evaluation of yield and some physiological traits of forage corn affected by chemical and biological nitrogen fertilizers intercropped with sweet basil. *J. Cent. Eur. Agric.* 18, 477–493. doi: 10.5513/JCEA01/18.2.1921

Kumari Gour, K., Patel, A. M., Vyas, K. G., Sheshama, M. K., and Sharma, G. (2017). Effect of integrated nitrogen management on yield and quality characters of dill seed (*Anethum graveolens* L.) under north Gujarat agro-climatic condition. *Int. J. Chem. Stud.* 5, 953–956. doi: 10.20546/ijcmas.2017.612.300

Li, H., Ge, Y., Luo, Z., Zhou, Y., Zhang, X., Zhang, J., et al. (2017). Evaluation of the chemical composition, antioxidant and antiinflammatory activities of distillate and residue fractions of sweet basil essential oil. *J. Food. Sci. Technol.* 54, 1882–1890. doi: 10.1007/s13197-017-2620-x

Mead, R., and Willey, R. W. (1980). The concept of a land equivalent ratio and advantages in yields from intercropping. *Exp Agric.* 16, s217–228. doi: 10.1017/S0014479700010978

Meena, R. S., Meena, V. S., Meena, S. K., and Verma, J. P. (2015). The needs of healthy soils for a healthy world. *J. Clean. Prod.* 102, 560–561. doi: 10.1016/j.jclepro.2015.04.045

Nanda, S. S., Swain, K. C., Panda, S. C., Mohanty, A. K., and Alim, M. A. (1995). Effect of nitrogen and biofertilizers in fodder rainfed upland conditions of Orisa. *Curr. Agric. Res.* 8, 45–47.

Nobahar, A., and Pazoki, A. R. (2010). Effects of variety, planting pattern and plant density on essential oil percent and essential oil yield of basil (*Ocimum basilicum* L.). *Iranian. J. Agron. Plant. Breed.* 6, 81–92.

Nurzyńska-Wierdak, R., Borowski, B., Dzida, K., Zawiślak, G., and Kowalski, R. (2013). Essential oil composition of sweet basil cultivars as affected by nitrogen and potassium fertilization. *Turk. J. Agric. For.* 37, 427–436. doi: 10.3906/tar-1203-43

Padalia, R. C., Verma, R. S., Chauhan, A., Goswami, P., Chanotiya, C. S., Saroj, A., et al. (2014). Compositional variability and antifungal potentials of *Ocimum basilicum, O. tenuiflorum, O. gratissimum and O. kilimandscharicum* essential oils against *Rhizoctonia solani* and *Choanephora cucurbitarum*. *Nat. Prod. Commun.* 9, 1507–1510. doi: 10.1177/1934578X1400901026

Pešakovic, C. M., Karaklaji-Stajic, Z., Milenkovic, S., and Mitrovic, O. (2013). Biofertilizer affecting yield related characteristics of strawberry (*Fragaria* × *ananassa Duch.*) and soil micro-organisms. *Sci. Hort.* 150, 238–243. doi: 10.1016/j.scienta.2012.11.016

Prasad, A., Kumar, S., Khaliq, A., and Pandey, A. (2011). Heavy metals and arbuscular mycorrhizal (AM) fungi can alter the yield and chemical composition of volatile oil of sweet basil (*Ocimum basilicum* L.). *Biol. Fertil. Soil.* 47, 853–861. doi: 10.1007/s00374-011-0590-0

Raei, Y., Kordi, S., Ghanbari, F., Shayan, A. A., Shahkarami, G., and Fatahi, S. (2015). The effect of Azospirilium bacteria and salicylic acid effects on drought stress tolerance in *Ocimum basilicum* L. medicinal plant. *Adv. Bio. Res.* 6, 44–53.

Rajeswara Rao, B. R. (2002). Biomass yield, essential oil yield and essential oil composition of rose-scented geranium (*Pelargonium* species) as influenced by row spacings and intercropping with maize mint (*Mentha arvensis* L.*f. piperascens Malinv. ex Holmes*). *Ind. Crops. Prod.* 16, 133–144. doi: 10.1016/S0926-6690(02)00038-9

Rohitashav, S., Sood, B. K., Sharma, V. K., and Singh, R. (1993). Response of forage maize to Azotobacter inoculation and nitrogen. *Indian. J. Agron.* 38, 555–558.

Roman, G. V. (ed.). (2012). *Fitotehnie, 1st Edn, Plante Tehnice, Medicinale si Aromatice*. Bucuresti: Editura Universitară.

Santoro, M. V., Zygadlo, J., Giordano, W., and Banchio, E. (2011). Volatile organic compounds from rhizobacteria increase biosynthesis of essential oils and growth parameters in peppermint (*Mentha piperita* L.). *Plant Physiol. Biochem.* 49, 1177–1182. doi: 10.1016/j.plaphy.2011.07.016

Sifola, M. I., and Barbieri, G. (2006). Growth, yield and essential oil content of three cultivars of basil grown under different level of nitrogen in the field. *Sci. Hortic.* 108, 408–413. doi: 10.1016/j.scienta.2006.02.002

Srivastava, S., Cahill, D. M., Conlan, X. A., and Adholeya, A. (2014). A novel *in vitro* whole plant system for analysis of polyphenolics and their antioxidant potential in cultivars of *Ocimum basilicum*. *J. Agric. Food. Chem.* 62, 10064–10075. doi: 10.1021/jf502709e

Street, R. A. (2012). Heavy metals in medicinal plant products- an African perspective. *S. Afr. J. Bot.* 82, 67–74. doi: 10.1016/j.sajb.2012.07.013

Vandermeer, J. (1989). *The Ecology of Intercropping*. Cambridge: Cambridge University Press.

Weisany, W., Raei, Y., and Ghassemi-Golezani, K. (2016a). Funneliformis mosseae alters seed essential oil content and composition of dill in intercropping with common bean. *Ind. Crop Prod.* 79, 29–38. doi: 10.1016/j.indcrop.2015.10.041

Weisany, W., Raei, Y., and Pertot, I. (2015). Changes in the essential oil yield and composition of dill (*Anethum graveolens* L.) as response to arbuscular mycorrhiza colonization and cropping system. *Ind. Crop Prod.* 77, 295–306. doi: 10.1016/j.indcrop.2015.09.003

Weisany, W., Raei, Y., Zehtab-Salmasi, S., and Ghassemi-Golezani, K. (2016b). Arbuscular mycorrhizal fungi induced changes in rhizosphere, essential oil and mineral nutrients uptake in dill/common bean intercropping system Funneliformis mosseae improved nutrients uptake of intercropped plants. *Annal Appl Biol.* 169, 384–397. doi: 10.1111/aab.12309

Xie, Y., and Kristensen, H. L. (2017). Intercropping leek (*Allium porrum L.*) with dyer's woad (*Isatis tinctoria* L.) increases rooted zone and agro-ecosystem retention of nitrogen. *Eur. J. Agron.* 82, 21–32. doi: 10.1016/j.eja.2016.09.017

Zheljazkov, V. D., Cantrell, C. L., Ebelhar, M. W., Rowe, D. E., and Coker, C. (2008). Productivity, oil content, and oil composition of sweet basil as a function of nitrogen and sulfur fertilization. *Hort. Sci.* 43, 1415–1422. doi: 10.21273/HORTSCI.43.5.1415

Conflict of Interest: The authors declare that the research was conducted in the absence of any commercial or financial relationships that could be construed as a potential conflict of interest.

frontiers in Plant Science

ORIGINAL RESEARCH
published: 18 January 2021
doi: 10.3389/fpls.2020.621740

Multiple Plant Growth-Promotion Traits in Endophytic Bacteria Retrieved in the Vegetative Stage From Passionflower

Luis Gabriel Cueva-Yesquén[1,2], Marcela Cristina Goulart[1,2], Derlene Attili de Angelis[2], Marcos Nopper Alves[3] and Fabiana Fantinatti-Garboggini[1,2]*

[1]*Graduate Program in Genetics and Molecular Biology, Institute of Biology, University of Campinas, Campinas, Brazil,* [2]*Division of Microbial Resources, Research Center for Chemistry, Biology and Agriculture (CPQBA), University of Campinas, Paulínia, Brazil,* [3]*Division of Agrotechnology, Research Center for Chemistry, Biology and Agriculture (CPQBA), University of Campinas, Paulínia, Brazil*

OPEN ACCESS

Edited by:
Jianfei Wang,
Anhui University of Science and Technology, China

Reviewed by:
Erica Lumini,
National Research Council (CNR), Italy
Anna Poli,
University of Turin, Italy

***Correspondence:**
Luis Gabriel Cueva-Yesquén
luisg_cueva@yahoo.es

Specialty section:
This article was submitted to Plant Symbiotic Interactions, a section of the journal Frontiers in Plant Science

Received: *26 October 2020*
Accepted: *23 December 2020*
Published: *18 January 2021*

Citation:
Cueva-Yesquén LG, Goulart MC, Attili de Angelis D, Nopper Alves M and Fantinatti-Garboggini F (2021) Multiple Plant Growth-Promotion Traits in Endophytic Bacteria Retrieved in the Vegetative Stage From Passionflower. Front. Plant Sci. 11:621740. doi: 10.3389/fpls.2020.621740

Bacteria exhibiting beneficial traits like increasing the bioavailability of essential nutrients and modulating hormone levels in plants are known as plant growth promoting (PGP) bacteria. The occurrence of this specific group of bacteria in the endophytic environment may reflect the decisive role they play in a particular condition. This study aimed to determine the taxonomical diversity of the culturable bacterial endophytes, isolated in the vegetative stage of passionflower (*Passiflora incarnata*), and assess its potential to promote plant growth by phenotypic and genotypic approaches. The sequencing and phylogenetic analysis of the 16S rRNA gene allowed us to classify 58 bacterial endophytes into nine genera. *Bacillus* (70.7%) was the most dominant genus, followed by *Pseudomonas* (8.6%) and *Pantoea* (6.9%). A few isolates belonged to *Rhodococcus* and *Paenibacillus*, whereas the genera *Lysinibacillus*, *Microvirga*, *Xanthomonas*, and *Leclercia* were represented by only one isolate. The strains were tested for nitrogen fixation, phosphate solubilization, indole-acetic-acid synthesis, and siderophore production. Moreover, PGP related genes (*nifH*, *ipdC*, *asb*, and *AcPho*) were detected by PCR-based screening. Most of the isolates (94.8%) displayed a potential for at least one of the PGP traits tested by biochemical assays or PCR-based screening. Nine strains were selected based on results from both approaches and were evaluated for boosting the Cape gooseberry (*Physalis peruviana*) germination and growth. All tested isolates improved germination *in vitro*, and the majority (78%) increased growth parameters *in vivo*. The results suggested that most of culturable bacteria inhabiting *P. incarnata* in the vegetative stage could be used as probiotics for agricultural systems. Besides, their occurrence may be associated with specific physiological needs typical of this development stage.

Keywords: *Passiflora incarnata*, inoculant, Cape gooseberry, PGP bacteria, PGP genes

INTRODUCTION

Endophytes can be defined as microorganisms living inside the plant tissues without causing any apparent disease (Compant et al., 2010; Hardoim et al., 2015). They are mainly located in the extracellular fluids and, in some cases, inside the cells (Compant et al., 2010), where they may interact with each other and with the host to assemble a specific community in distinct compartments of the plant. The structure and composition of endophytic communities are determined by environment and plant-associated factors, such as the plant genotype, the developmental stage, phenology, and edaphic properties (Seghers et al., 2004; Van Overbeek and Van Elsas et al., 2008; de Silva et al., 2016; Goulart et al., 2019).

Endophytes are widely known for maintaining and boosting the plant health and development (Santoyo et al., 2016), while plants provide a complex niche constituted by specific abiotic and biotic factors supporting the endophytic colonization (McCully, 2001). However, due to different nutritional needs in different developmental stages, the physiology of plants varies across the life cycle. In the vegetative stage, the demand for essential nutrients, such as nitrogen, phosphorus, and iron, are often increased; however, these nutrients are poorly supplied or unavailable for plant uptake (López-Arredondo et al., 2013). Moreover, the role of indole-3-acetic acid (IAA) is so fundamental for vegetative growth that plants exhibit a higher capacity to synthesize this phytohormone during the vegetative stage (Ljung et al., 2001). Endophytic bacteria have been widely associated to mobilization of essential nutrients and synthesis of plant growth regulators (Santoyo et al., 2016). For example, various endophytic bacterial strains have shown beneficial traits, including nitrogen fixation, inorganic phosphorus solubilization, siderophores secretion, and IAA synthesis (Crowley, 2006; Gupta et al., 2012; Sharma et al., 2013; Glick, 2014). This specific group of bacteria is commonly known as plant growth promoting (PGP) bacteria. In general, it is thought that PGP bacteria can positively affect soil fertility and nutrient uptake in plants (Rashid et al., 2016; Bargaz et al., 2018; Kumar et al., 2020). These characteristics include them into plant probiotics, which promote the biological process directly related to plant development and protection (Bharti et al., 2017). The beneficial effect of probiotics on plants is reflected in the improvement of production and nutritional quality and the recovery of natural equilibrium in agro-ecosystems (Woo and Pepe, 2018).

Passionflower (*Passiflora incarnata*) is a tropical plant widely used as traditional herbal medicine. The phytochemical composition of passionflower includes mainly alkaloids and flavonoids, which support their therapeutic use to treat anxiety, nervousness, constipation, dyspepsia, and insomnia (Dhawan et al., 2001). These pharmacological properties allowed it to be included in the national pharmacopeias of France, Germany, and Switzerland. In addition, several *P. incarnata* derivative preparations have been manufactured and delivered as medicinal products and food supplements around the world (Miroddi et al., 2013). This plant has tendril-climbing stems and three-lobed leaves in its vegetative stage from December to January, and it blooms with showy and fragrant flowers from April to November (Fuentes et al., 2000). Passionflower occurs in sandy and well-drained soils, woods with low moisture and open areas (Miroddi et al., 2013). It is considered a "heavy feeder" plant since it needs a balanced fertilizer that supplies the macronutrients and micronutrients, which are often present in unavailable forms in the soil and have a critical role in its vegetative growth. Nevertheless, the pharmaceutical industry restricts the use of chemical fertilizer and pesticides in its culture, since they can compromise human food security (Björnberg et al., 2015). These conditions create a challenger scenario for passionflower culture.

The present knowledge of plant microbiome suggests that, when a plant host faces unfavorable conditions, it alters its physiological structure and consequently the plant-microbe and microbe-microbe interactions (Uroz et al., 2019). These changes can stimulate the recruitment and increase of beneficial microbes to meet plant physiological needs (Liu et al., 2020). Thus, the occurrence of microorganisms with traits related to essential nutrients acquisition and synthesis of growth regulators might suggest their role in the passionflower culture. We hypothesize that because of the environmental constraints and physiological needs in which *P. incarnata* is found, its associated microbiota contributes with beneficial functions for plant development. This study aims at determining the diversity of culturable endophytic bacteria retrieved from *P. incarnata* in the vegetative stage and at assessing their plant growth promotion traits.

MATERIALS AND METHODS

Bacterial Isolates From *Passiflora incarnata*

Fifty-eight endophytic bacteria, provided by the Microbial Resources Division of the Research Center for Chemistry, Biology and Agriculture (CPQBA), University of Campinas, were characterized in this study. These bacteria were isolated from leaf tissues in the vegetative stage of *P. incarnata* by Goulart et al. (2019). The passionflower leaves were collected in January 2015 from the Centroflora Group agricultural fields located at Botucatu, São Paulo, Brazil. The culture of *P. incarnata* in these fields is exempt from the application of any chemical fertilizers. Leaves were surface-sterilized and aseptically grounded in Phosphate Buffer Saline (PBS). Then, the suspensions were serially diluted to10^{-4}. Aliquots (100 µl) of each 10-fold dilution were plated in seven culture media including M9 minimal medium, Gause's synthetic agar, Tap Water Yeast Extract agar, Humic acid-Vitamin agar, Glycerol-asparagine agar, Chitin medium (Zhao et al., 2012), and 869 medium (Eevers et al., 2015). For this study, all isolates were sub-cultured in Trypticase Soy Agar (TSA) at 28°C for 48–96 h.

16S rRNA Gene Sequencing and Phylogenetic Analysis

The genomic DNA of bacteria was extracted according to a modified protocol of Van Soolingen et al. (1993). The 16S rRNA gene was partially amplified by PCR using the universal bacterial primers 10F (5'-AGAGTTTGATCCTGGCTCAG-3')

and 1501R (5'-AAGGAGGTGATCCAGCCGCA-3'; Lane, 1991). The PCR reaction was performed in 25 µl final volume containing dNTPs (0.2 mM each), 1X reaction buffer (20 mM Tris, pH 8.4), 1.5 mM $MgCl_2$, 0.5 µM each primer, 1 U of Taq DNA polymerase, and 10 ng of template DNA. The PCR cycling protocol consisted of an initial denaturation at 94°C for 4 min, followed by 32 cycles of 94°C for 1 min, 55°C for 1 min, and 72°C for 3 min, and a final extension at 72°C for 5 min. The PCR amplified products were run on a 1% (v/w) agarose gel stained with SYBR™ Safe (Thermo Fisher Scientific) and purified using the GFX™ PCR DNA Purification kit (GE Healthcare Life Sciences, Germany). Amplicons were sequenced by the Sanger method with BigDye Terminator v3.1 Cycle Sequencing Kit (Applied Biosystems Life Technologies) using the same primers of amplification and the internal primers 765F (5'-ATTAGATACCCTGGTAG-3') and 785R (5'-ACCAGGG TATCTAATCCTGT-3'). The sequencing cycling protocol consisted of an initial denaturation at 96°C for 1 min, followed by 30 cycles of 96°C for 15 s, 50°C for 15 s, and 60°C for 4 min. The reaction products were sequenced on an ABI3500XL Series (Applied Biosystems) sequencer. The sequences were assembled in contigs using BioEdit 7.2.6.1 software (Hall, 1999) and compared with the reference 16S rRNA gene sequences available in the EzBioCloud platform[1] (Yoon et al., 2017). Newly generated sequences were deposited in GenBank under accession numbers MG778707 to MG778907. The phylogenetically closest sequences were selected and used for subsequent phylogenetic analyses. The 16S rDNA sequences of the isolates and reference bacterial sequences were aligned using CLUSTAL W (Thompson et al., 1994), and the substitution model was determined with MODELTEST from MEGA X software (Tamura et al., 2013). The clustering was performed using the Neighbor-Joining algorithm, and evolutionary distances were computed with the Kimura two-parameter model. The support of nodes was estimated by bootstrapping with 1,000 replications (Felsenstein, 1985). The phylogenetic analysis resulting from MEGA X was exported in the Newick format to create a circular cladogram in iTOL[2] (Letunic and Bork, 2016).

Biochemical Assays for PGP Traits

Growth on N-Free Medium

The endophytic isolates were tested for their ability to fix or scavenge N using a nitrogen-free medium. Bacterial cultures were grown overnight at 30°C in Trypticase Soy Broth (TSB) medium, washed twice, and resuspended in PBS (pH 7.4). The bacterial concentration was adjusted for OD_{600} 0.5. A 30 µl aliquot of each bacterial suspension was inoculated into 10 ml vials containing 4 ml of semi-solid New Fabian broth (NFb) medium (Baldani et al., 1986) and incubated at 28°C. The bacterial growth was confirmed from 72 h incubation by forming a sub-surface pellicle on the culture medium. The diazotrophic potential was demonstrated through successive re-inoculations in NFb medium. The experiments were conducted in triplicate.

[1]https://www.ezbiocloud.net/
[2]http://itol.embl.de

Phosphate Solubilization

The ability of endophytic bacteria to solubilize inorganic phosphorous was evaluated according to Mehta and Nautiyal (2001). All bacterial isolates were first grown overnight at 30°C in TSB medium to obtain OD600 0.5. A 10 µl aliquot of each bacterial culture was inoculated in Petri dishes containing the solid National Botanical Research Institute's Phosphate (NBRIP) medium. The plates were incubated at 30°C for 15 days. The development of a transparent halo zone around the colony revealed the phosphate-solubilizing ability of the isolate. To estimate the phosphate-solubilizing ability quantitatively, the Solubilization Index (SI) was calculated as follows: SI = A/B, where A is the colony diameter + halo zone diameter, and B is the colony diameter (Edi-Premono, 1996).The isolates were grouped according to Silva Filho and Vidor (2000), in bacteria with low (SI < 2), intermediate (2 < SI < 3), and high (SI > 3) solubilization potential. The experiments were conducted in triplicate.

IAA-Like Compounds Production

Indole-3-acetic acid production was estimated by growing the isolates on a TSB medium containing 5 mM L-tryptophan, at 30°C in a rotary shaker at 150 rpm for 48 h in the dark. Bacterial cultures were centrifuged at 8,000 rpm for 15 min. An aliquot (1 ml) of supernatant was mixed with 2 ml of Salkowski reagent (0.5 M $FeCl_3.6H_2O$ in 35% $HClO_4$) and incubated in the dark for 30 min at room temperature (Tang and Bonner, 1948). The UV-Vis absorption spectra were measured spectrophotometrically at 530 nm. A standard curve with known concentrations (0.5–120 µg/ml) of IAA (Sigma-Aldrich) was used to determine the amount of IAA produced. The experiments were conducted in triplicate.

Siderophore Production

Siderophore production was determined qualitatively on Chrome Azurol S (CAS) supplemented Blue Agar plates (Schwyn and Neilands, 1987). The bacterial isolates were first grown overnight at 30°C in TSB medium to obtain OD_{600} 0.5. A 10 µl aliquot of each bacterial culture was inoculated onto a diffusion disc placed on the CAS-Blue Agar (Hussein and Joo, 2014). The diffusion disc method was used to avoid the toxic effect of Hexadecyltrimethylammonium (HDTMA; Chimwamurombe et al., 2016), responsible for the blue color of the medium. Plates were incubated for 72 h at 30°C and observed daily until a yellow orange halo was seen around the colony. The experiments were conducted in triplicate.

Detection of PGP Related Genes

A PCR based approach was applied to confirm and complement the information provided by biochemical assays or even to reveal new PGP potentials of bacteria. The ability to reduce atmospheric nitrogen was evaluated by amplifying the gene encoding for nitrogenase reductase *nifH*. For this purpose, a nested PCR protocol was performed using the primers *nifH* (forA) and *nifH* (reverse) for a first reaction and the primers *nifH* (forB) and *nifH* (reverse) in the second reaction (**Table 1**; Zehr and McReynolds, 1989).

TABLE 1 | Primers used to amplify genes associated with plant growth promotion.

Gene	Size of gene (pb)	Primer sequence (5'→3')	Amplicon (pb)	Reference
nifH	896	*forA*-GCIWTITAYGGNAARGGNGG *forB*-GGITGTGAYCCNAAVGCNGA *rever*-GCRTAIABNGCCATCATYTC	371	Zehr and Reynolds, 1989
ipdC	1,809	CAYTTGAAAACKCAMTATACTG AAGAATTTGYWKGCCGAATCT	1,715	Raddadi et al. (2008)
asb	1,685	GAGAATGGATTACAGAGGAT TTATGAACGAACAGCCACTT	1,685	Raddadi et al. (2008)
AcPho	828	AAGAGGGGCATTACCACTTTATTA CGCCTTCCCAATCRCCATACAT	734	Raddadi et al. (2008)

The PCR conditions were as indicated by Burgmann et al. (2004). Briefly, the first amplification was performed in a final volume of 25 µl, containing 10 ng of genomic DNA, 2 µM of each primer, 0.2 mM of each dNTP, 2 mM $MgCl_2$, 1 U of Taq Polymerase Recombinant (Invitrogen), and 1x of PCR buffer. The nested reaction was carried out with 1 µl of the PCR product added to a new mixture prepared as before. The annealing conditions were 30 s at 55° C and 30 s at 53° C for the first and second reactions, respectively. As a positive control, the gDNA of *Gluconacetobacter diazotrophicus* PAl 5, known for its nitrogen fixation activity, was used. The PCR products were separated by electrophoresis in a 1% (v/w) agarose gel stained with SYBR™ Safe (Thermo Fisher Scientific). The fragments with the expected size were sequenced and analyzed by BLASTX using "non-redundant" protein sequences database from NCBI. The matches with identity >80% were considered.

Indole-3-acetic acid production was screened by partial amplification of the *ipdC*, the gene encoding for indole-3-pyruvate (IPA) decarboxylase, the most important enzyme in the indole-3-pyruvic acid (IPyA) pathway. The IPyA is the pathway used by most beneficial bacteria (*Azospirillum*, *Bacillus*, *Bradyrhizobium*, *Enterobacter cloacae*, *Paenibacillus*, *Pseudomonas*, and *Rhizobium*; Spaepen and Vanderleyden, 2011). The ability to synthesize siderophores was assessed by partially amplifying the *asb* gene that encodes for petrobactin, a catechol-type siderophore commonly secreted by *Bacillus* spp. (Koppisch et al., 2008). To evaluate the potential of solubilizing phosphates, we amplified gene encoding for the acid phosphatase, an enzyme involved in the mineralization of most organic phosphorus compounds from soil (El-Sawah et al., 1993). PCR amplifications of *ipdC*, *asb*, and *AcPho* were conducted in all isolates using gene specific primers (**Table 1**) as described by Raddadi et al. (2008). The PCR reaction was performed in a final volume of 25 µl containing dNTPs (0.2 mM each), 1x reaction buffer (20 mM Tris, pH 8.4), 2.5 mM $MgCl_2$, 1.0 µM of each primer, 1 U of Taq DNA polymerase, and 50 ng of template DNA. The PCR cycling protocol consisted of an initial denaturation at 94°C for 2 min, followed by 30 cycles of 94°C for 1 min, 55°C (*asb* and *AcPho*) and 50°C (*ipdC*) for 45 s and 72°C for 2 min, followed by a final extension at 72°C for 5 min. The PCR amplified products were analyzed by 1% (v/w) agarose gel electrophoresis. The fragments with the correct size were sequenced and analyzed by BLASTX. The isolates with one or more PGP traits (by phenotypic and genotypic approaches) were intersected in an UpSet graphic using the Intervene platform (Khan and Mathelier, 2017).

Evaluation of Plant Growth Promotion *in vivo*

Effect on the Cape Gooseberry (*Physalis peruviana*) Germination

Cape gooseberry is a plant of economic importance which has gained recognition in the international market due to its nutritional value and versatility to be consumed. Seeds are the main propagation method in the Cape gooseberry culture, due to the high seed number per fruit (Puente et al., 2011). Based on the biochemical assays, nine bacterial isolates with multiple PGP traits (three or more) were selected and used to evaluate their effect on Cape gooseberry seedling vigor and germination. Seeds of *Physalis peruviana* were surface sterilized using a 3% sodium hypochlorite solution for 10 min, then washed five times with sterile distilled water for 3 min each. This plant genotype was obtained from the Collection of Medicinal Plants, at the Research Center for Chemistry, Biology and Agriculture (CPQBA), Brazil. The inocula were prepared by growing the selected isolates on TSB at 28°C for 20 h with shaking (150 rpm). Bacterial cells were harvested by centrifugation at 9,000 rpm for 10 min at 4°C, and each pellet was washed three times with the PBS solution. The pellets were suspended in the PBS solution and adjusted to 0.5 OD_{590}. Surface-sterilized seeds were dipped into bacterial inocula for 60 min and dried in a laminar flow bench at room temperature. Fifty seeds inoculated with each endophytic isolate were spread on two layers of moistened filter paper on the Petri plates. For the control treatment, 50 surface-sterilized seeds treated with sterilized PBS were also established. Inoculated and control plates were incubated in a light incubator (16 h in a day) at 28 ± 2°C for 10 days. To maintain sufficient moisture for germination, 1 ml of sterilized distilled water was added every 24 h. Germination was considered to occur once the radicles reached half of the seed length. The root and shoot length were measured after 10 days. The germination speed index (GSI) was calculated according to Maguire (1962) and sprouted seeds were counted 6, 8, and 10 days after test initiation. The experiment was carried out with three replicates.

Germination (%) = number of seeds germinated/ total number of seeds × 100

Vigor index = % germination × total plant length (mm)

Effect of Endophytic Bacteria on Cape Gooseberry Growth

The nine selected isolates were used to determine the growth promoting capability in Cape gooseberry plants. Surface-sterilized seeds were inoculated as described above with selected isolates. A set of seeds were treated with PBS (control treatment). Treated seeds were sown 1 cm deep in the commercial substrate (Tropstrato Hortaliças Mix, Brazil) contained in 108-plug trays. The substrate was autoclaved twice at 24 h intervals at 121°C and 15 psi for 30 min. After 15 days, germinated embryos were subjected to two additional inoculations. Bacterial suspensions, prepared according to "Effect on the Cape Gooseberry (*Physalis peruviana*) Germination" section, were applied to the plant base at 2 and 7 days after germination. Seedlings with similar growth status were selected from each treatment for further analysis. Plants were grown for 8 weeks in a net house, and seven plants (replicates) from each treatment were harvested for measuring the dry matter, root and shoot lengths, a and b chlorophyll, and macronutrients and micronutrients.

Statistical Analysis

A completely randomized design was used for pot experiments, with seven replications for each treatment. Arithmetic means and standard deviations were calculated. Significant differences were assessed by one-way analysis of variance (one-way ANOVA), *post-hoc* test Tukey HSD. ANOVA assumptions were revised by the equal variance test (Levene Median) and normality test (Kolmogorov-Smirnov and Lilliefors tests). All statistical analyses were performed in Sigma 12.0.

RESULTS

Phylogenetic Analysis of Bacterial Endophytic Isolates

The partial 16S rRNA gene sequencing from 58 bacteria provided sequences of sufficient length (mean length of 1,290 bp) to carry out the phylogenetic analysis. The sequences were submitted to the identify server of the EzBioCloud platform to recover the closest reference sequences. All sequences showed >99–100% similarity with reference sequences (**Supplementary Table S1**). The multiple sequence alignment in ClustalW generated 1,252 positions and it was used for constructing the phylogenetic tree (**Figure 1**), which showed well-supported clades and allowed to us determine the taxonomic affiliations of all isolates. However, sequences of EP178 and EP223 isolates did not group with any reference sequence. In a further phylogenetic analysis (**Supplementary Figure S1**), these sequences also formed a separated taxon supported by a high bootstrap value (100).

The phylogenetic analysis from 58 isolates allowed us to classify them into three phyla: Firmicutes, Proteobacteria, and Actinobacteria. The majority of the isolates (41/58) belong to the Firmicutes phylum, represented by Bacillaceae and Paenibacillaceae families. Proteobacteria was the second largest phylum (15/58) dominated by Enterobacteriaceae, Pseudomonadaceae, and Xanthomonadaceae. Bacteria belonging to the Actinobacteria phylum (2/58) were uniquely related to the Nocardiaceae family. The taxonomic affiliations of isolates, at the genera level, revealed that *Bacillus* (70.7%) was the dominant bacterial genus. Based on the tree topology, *Bacillus* sequences (marked in red color in **Figure 1**) formed six clades, one of them included sequences from 19 isolates (closely related to *Bacillus megaterium* and *Bacillus aryabhattai*). The EP206 isolate sequence clustered in the *Lysinibacillus* genus monophyletic group (marked in pink color). The *Paenibacillus* cluster (marked in green color) contained only two endophytic isolates (EP176 and EP212), which were distributed in two different clades. The second most abundant genus was *Pseudomonas* (8.6%), which was comprised of two clades (marked in light green), and their isolates were taxonomically associated to the species, *Pseudomonas cichorii* (EP220) and *Pseudomonas oryzihabitans* (EP201 and EP215), while the sequences of EP178 and EP223 grouped with *Pseudomonas* spp. Sequences from the *Pantoea* genus (marked in lilac color) formed three clades holding four endophytic isolates (EP200, EP204, EP205, and EP222). The others isolate belonging to Proteobacteria were distributed in the *Microvirga*, *Xanthomonas*, and *Leclercia* genera. The Actinobacteria strains (EP225 and EP208) were uniquely associated with the *Rhodococcus* genus and represented 3.4% of total bacterial endophytes.

Detection of PGP Traits

The ability of endophytic bacteria to improve plant growth was characterized by a phenotypic approach. The biochemical assays were addressed to reveal the potential of strains to favor essential nutrient acquisition (nitrogen, phosphates and iron) and to synthesize a plant growth regulator (indol acetic acid). The results obtained are presented in **Figure 2** (**Supplementary Table S2**). The assay on the semi-solid NFb medium allowed us to identify diazotrophic/N-scavenging strains. Twenty-six endophytic strains were able to grow in the N-free medium, forming a sub-surface pellicle, even after two successive inoculations. Most of the positive strains (92%) were related to the *Bacillus* genus, and only two (EP208 and EP225) belonged to *Rhodococcus*.

Thirty-three strains (56.9%) showed the ability to solubilize inorganic phosphates, $Ca_3(PO_4)_2$, on the solid NBRIP medium. The bacteria that formed a halo around the colony were considered positive for phosphate solubilization. From the positive strains, 18 were affiliated to the *Bacillus* genus, while *Pseudomonas* and *Pantoea* were represented by five and four, respectively. The SI was calculated for the halo-forming isolates and is shown in **Supplementary Table S2**. Based on this index, the best strain in solubilizing phosphate was EP223, which was assigned as *Pseudomonas* spp. Furthermore, *Pseudomonas* was the genus with the highest number of strains with high solubilization potential. At the same time, most

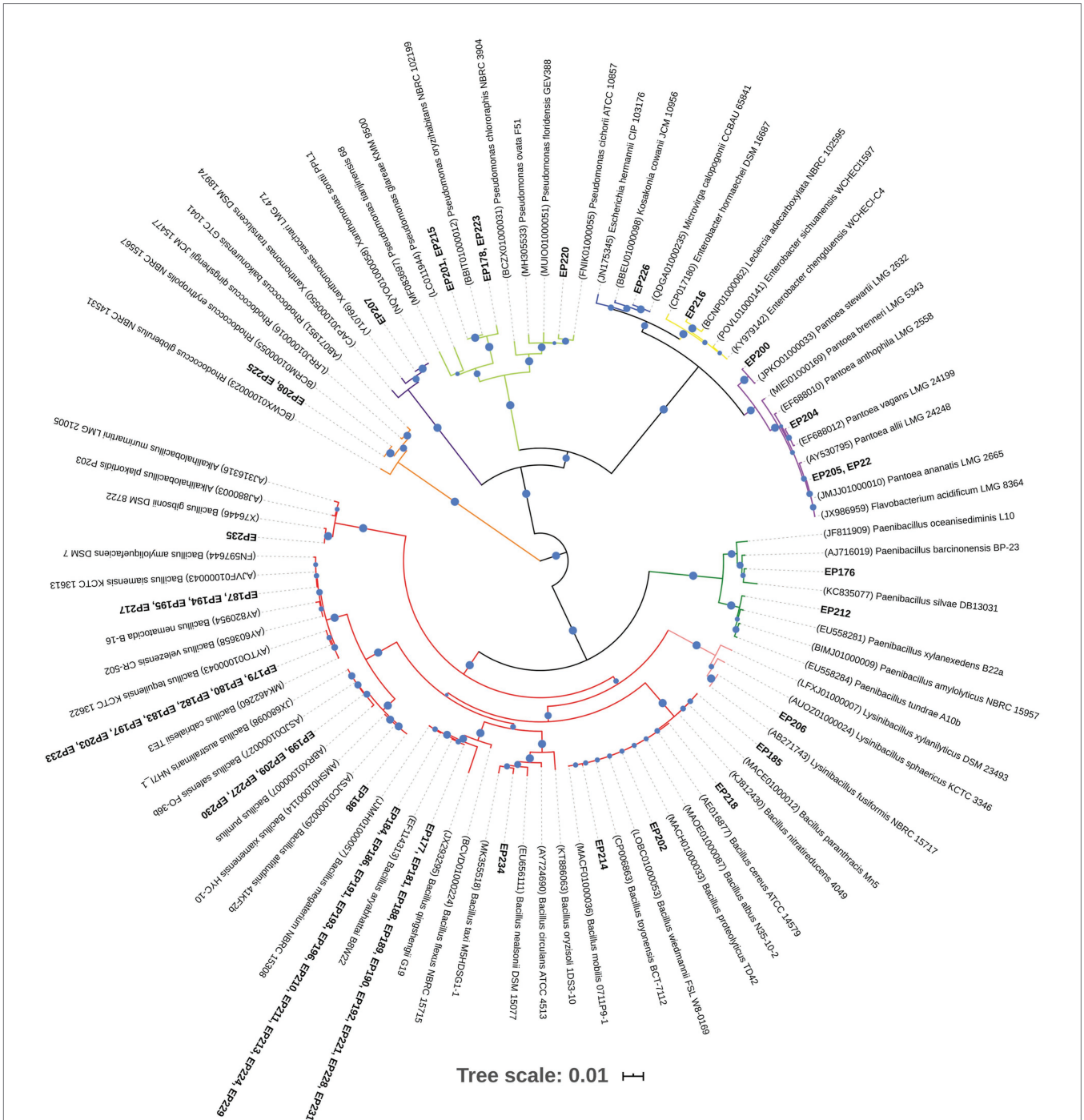

FIGURE 1 | Neighbor-joining phylogenetic tree based on partial 16S rRNA sequences of endophytic bacteria isolated from *Passiflora incarnata* leaves and reference sequences from EzBioCloud. The branch colors indicate different bacterial genera. Only bootstrap values equal and greater than 60% are displayed as circles with increasing size up to 100%. Accession numbers from references sequences are in parentheses.

of the positive strains were placed in the intermediate potential group and largely associated with the *Bacillus* genus (**Supplementary Figure S2**).

Regarding IAA production, 44 isolates (75.8%) were able to synthesize IAA-like molecules when grown in a liquid medium supplemented with tryptophan. The IAA concentrations detected varied from 1.01 to 6.04 μg/ml. The values calculated for all isolates are shown in **Supplementary Table S2**. All strains belonging to *Pseudomonas*, *Pantoea* and *Paenibacillus* produced IAA-like compounds, but *Bacillus* was the genus with

the highest number of positive strains. *Xanthomonas*, *Leclercia*, and *Rhodococcus* had one each positive strain for this test. The two *Paenibacillus* strains produced a mean of 5.35 µg/ml, the highest value among all genera. Nevertheless, EP229 (associated with *Bacillus*) was the strain that exhibited the highest IAA value (6.04 µg/ml).

Siderophore production was screened by using the CAS agar medium. Most of the endophytic strains (77.6%) formed orange halos around the bacterial colony, indicating that chelating agents capable of capturing the iron were secreted. Positive strains were mostly associated with *Bacillus*, followed by *Pseudomonas* (5) and *Pantoea* (4) strains. Members of *Xanthomonas*, *Leclercia*, *Rhodococcus*, and *Microvirga* were represented by only one positive strain.

Screening of PGP Traits by PCR

Endophytic bacteria were evaluated by harboring genes related to plant growth promotion using a genotypic approach. The results obtained from this approach are presented in **Figure 2** (**Supplementary Table S2**). The amplification of the *nifH* gene was performed to confirm the diazotrophic potential. A fragment (~371 bp) from the *nifH* gene was amplified only in the EP220 strain, which was closely related to *P. cichorii*. The BLASTX analysis showed that the deduced sequence from this strain shared 86% identity with a nitrogenase iron protein from *Insolitispirillum peregrinum*. This result is the first report of the presence of the *nifH* gene from a *P. cichorii* strain.

The *AcPho* gene was detected in nine strains. Conserved domains related to acid phosphatase enzyme were detected from amplified sequences. Strains carrying *AcPho* sequences were exclusively associated with the *Bacillus* genus, likely because the primer design was addressed for *Bacillus thuringiensis* strains (Raddadi et al., 2008).

Partial amplification of the *ipdC* gene was a success in 16 endophytic strains. Conserved domains related to the IPA decarboxylase enzyme were detected by the BLASTX analysis. Most strains carrying *ipdC* sequences were associated with the *Bacillus* genus. The *Rhodococcus* and *Paenibacillus* genera had only one representative in the genotypic approach.

However, *asb* gene was partially amplified in four strains (EP185, EP202, EP214, and EP218), which were associated with *Bacillus*. The BLASTX analysis detected conserved domains related to siderophore synthesis proteins, such as Aerobactin. Interestingly, an unspecific fragment of approximately 1,000 bp (**Supplementary Figure S3**) was amplified in 15 strains: 13 belonging to *Bacillus* and the

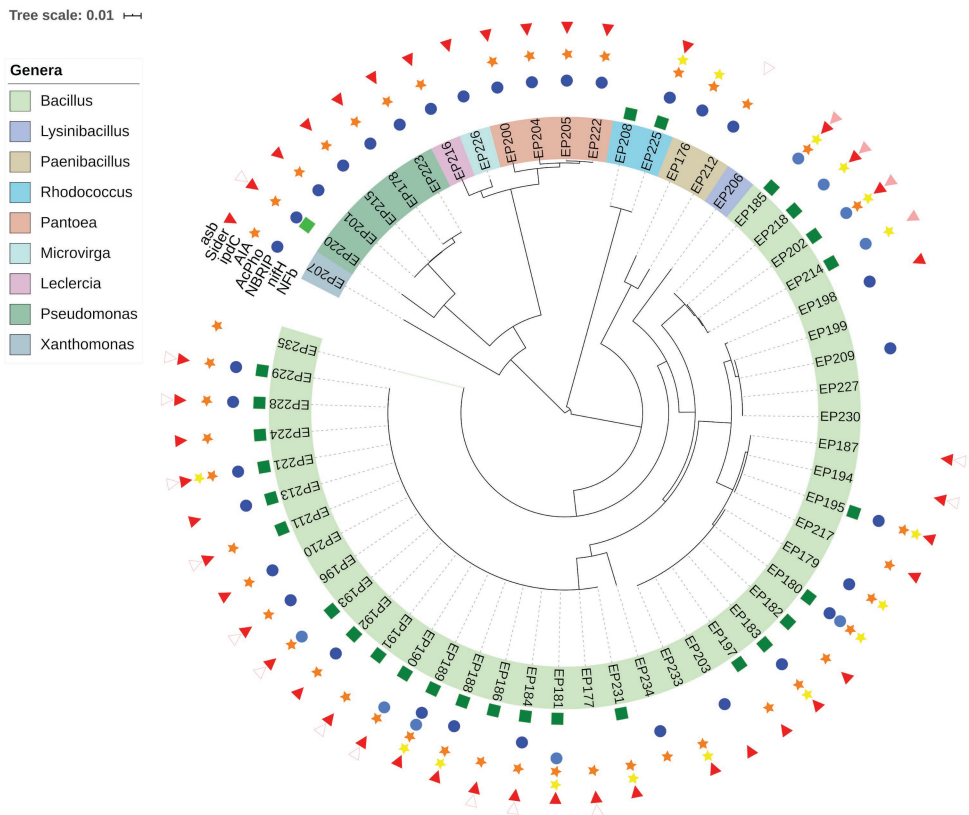

FIGURE 2 | Diversity of PGP traits among endophytic bacteria according to their taxonomic affiliations inferred from phylogenetic analysis of 16S rRNA gene sequences. Growth on a N-free media (■); detection of the *nifH* gene(■); formation of halo on a NBRIP medium (●);detection of the *AcPho* gene (●); IAA-like compound production (★); detection of the *ipdC* gene (★); formation of orange halo on a CAS Agar (▼); detection of the *asb* gene (▼); and unspecific amplification of a gene involved iron metabolism (*tatA*; ▽).

other two to *Paenibacillus* and *Pseudomonas*. The sequencing and analysis of this unspecific fragment determined that it possessed conserved domains related to the TatA/TatE subunit of the translocase A protein, which transports proteins across bacterial cytoplasmatic membrane.

The Dominant Groups Exhibited PGP Traits

The strains belonging to the genera *Bacillus*, *Pseudomonas*, *Pantoea*, *Rhodococcus*, and *Paenibacillus* account to ~93% of the total endophytic bacteria retrieved from *P. incarnata* leaves in the vegetative stage. The plant growth-promoting trait abundance was evaluated on the five most abundant members (genera) mentioned before. Based on the biochemical tests (**Figure 3A**), the phosphates solubilizing ability varied from 44% in *Bacillus* and 55% in *Rhodococcus* to 100% in *Pseudomonas*, *Pantoea*, and *Paenibacillus* strains, while IAA-like compounds were detected in 50% of *Rhodococcus*, 73.2% of *Bacillus*, and 100% of *Pseudomonas*, *Pantoea*, and *Paenibacillus* strains. Siderophore production was exhibited in 100% of *Pseudomonas* and *Pantoea*, 78% of *Bacillus*, and 50% of *Rhodococcus* strains, while only 50% of *Rhodococcus* and 60% of *Bacillus* strains have grown forming a sub-surface pellicle in the NFb medium. Regarding the PCR-based approach (**Figure 3B**), the *nifH* gene was only detected in one out of *Pseudomonas* strains (EP220). None of the other genera had representatives carrying this gene. Only in the *Bacillus* strains, the *asb* and *AcPho* sequences were amplified. Unlikely, the *ipdC* gene was more frequently encountered among tested strains since it was detected in 34.1% of *Bacillus*, 50% of *Rhodococcus*, and 50% of *Paenibacillus* strains.

Additionally, the frequency of strains with one or more PGP traits tested by both phenotypic and genotypic approaches was analyzed (**Figure 4**). The results showed that 11 strains constituted the largest functional group. They showed the phenotypic potential for phosphates solubilization, IAA synthesis and siderophore production, followed by six strains with phenotypic potential for nitrogen fixation, IAA, and siderophore production, and five isolates with phenotypic potential for all PGP traits and genotypic potential for IAA production. Interestingly, two isolates exhibited genotypic and phenotypic potential for tree PGP traits.

Improved Germination in Cape Gooseberry Seeds

Based on results from biochemical PGP tests, nine endophytic strains were selected for testing their effect on germination percentage and speed and vigor index in Cape gooseberry seeds. All isolates increased the germination percentage by 6–29%, compared with the control. The EP222 (associated with *Pantoea ananatis*; 97.9%), EP184 (*B. megaterium*), and EP216 (*Leclercia adecarboxylata*; 93.8%) strains produced the highest germination percentages and were significantly different ($p < 0.05$) from non-inoculated seeds (66.7%). These strains reached the mentioned above germination percentages in just 10 days, and they also exhibited the highest GSIs (**Figure 5A**). The vigor index was increased

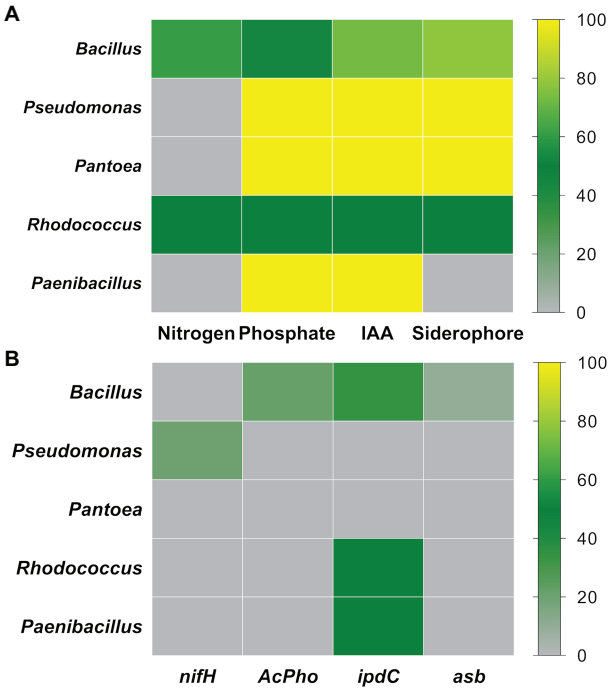

FIGURE 3 | Relative abundance of PGP strains in the five most dominant genera: **(A)** PGP activities tested by biochemical assays and **(B)** PGP activities detected by PCR-based approach.

in 2.7–52.7% by the strains EP222, EP184, EP229, EP215, EP223, and EP216 in comparison with the control treatment (**Figure 5B**). The strains EP222, EP184, and EP216 significantly increased germination parameters compared with control, which suggested that it could be used as an effective inoculant in Cape gooseberry seeds.

Plant Growth Promotion in Cape Gooseberry Plants

The results showed that the treatment with selected strains boosted the Cape gooseberry growth (**Figure 6**). Inoculation with strain EP216 exhibited the best results about the shoot and root lengths, increasing it by 55.4 and 24.5% compared with the control. Concerning to shoot and root dry matter, treatment with strain EP216 significantly improved these parameters compared with the control treatment, followed by strains EP215 and EP178. The individuals treated with strain EP184 also increased the shoot and root dry matter by 52.7 and 24.5%, respectively. All treatments showed increased phenotypic parameters in comparison with control, except the strains EP229 and EP220. The a and b chlorophyll levels were significantly higher in plants inoculated with EP216 than in control (**Supplementary Table S3**). The plants treated with strains EP184, EP223, and EP229 also showed higher chlorophyll levels than the control treatment. For the nutritional parameters measured in plant aboveground parts, the inoculation of isolates EP178, EP216, EP229, EP220, and

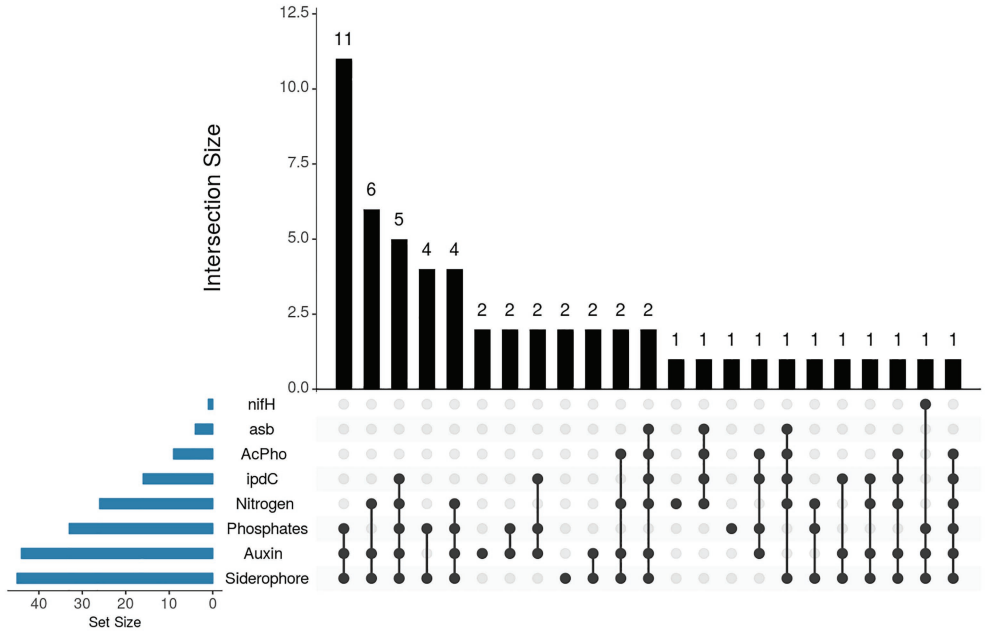

FIGURE 4 | UpSet plot of PGP traits detected by biochemical assays and by PCR. The bar chart on the left indicates the total number of isolates that exhibit each PGP trait. The upper bar chart indicates the intersection size between sets of isolates with one or more PGP traits. Dark connected dots indicate which PGP trait is considered for each intersection.

EP201 showed nitrogen, phosphorus, potassium, calcium, copper, iron, manganese, and sodium levels higher than the control.

DISCUSSION

Plants can recruit beneficial microbes from the environment as response to a particular unfavorable condition (Liu et al., 2020). Nutritional stress that passionflowers face when growing in poor soils and/or without application of fertilizer can promote recruitment and accumulation of microorganisms with the capacity to cope with nutritional needs. Also, the occurrence of microorganisms with the potential to facilitate the acquisition of essential nutrients or modulate the level of hormones within plants might be substantial in the early growth stages. This study revealed that most endophytic bacteria retrieved in the vegetative stage of passionflower possess multiple PGP traits. The phenotypic and genotypic approaches were carried out to access these functional traits (Raddadi et al., 2008). Combining these approaches allowed us to confirm the potential attributed by one, complement the result between both, or increase detection coverage when ones failed to reveal the PGP trait.

The phylogenetic analysis of 16S rRNA gene sequences allowed taxonomically categorize endophytic isolates and revealed bacterial diversity of genera. In the case of the EP178 and EP223 strains, a further phylogeny analysis suggested that they may belong to a new species of *Pseudomonas*. Phylogenetic affiliations for *Bacillus* isolates were difficult because the 16S rRNA gene has low phylogenetic resolution and weak discriminatory power for some taxonomic groups (Ash et al., 1991; Janda and Abbott, 2017), so the use of another taxonomic marker is recommended. Endophytic isolates were mainly associated with *Bacillus* and *Pseudomonas*. The dominance of these genera was already reported in other medicinal plants (Miller et al., 2012; Rhoden et al., 2015). Coincidentally, members of *Bacillus* and *Pseudomonas* have been extensively reported as plant growth enhancers (McSpadden Gardener, 2004; Mercado-Blanco and Bakker, 2007; Govindasamy et al., 2010; Ferreira et al., 2019), suggesting what could be the ecological role of these dominant groups in the vegetative stage of *P. incarnata*. The next more abundant genus was *Pantoea*, which has already been reported in medicinal plants such as *Hypericum perforatum* and *Ziziphora capitate* (Egamberdieva et al., 2017); even this genus was the most found in six *Eucallyptus* species (Procópio et al., 2009). Although usually known as a plant pathogen, some studies reported *Pantoea* strains with plant growth-promoting capabilities (Andreolli et al., 2016; Chen et al., 2017). Likewise, several members of the less represented genera (*Lysinibacillus*, *Microvirga*, *Xanthomonas*, and *Leclercia*) in this study have been described previously as both endophytes, and plant growth promoters (Shahzad et al., 2017; Walitang et al., 2017; Shabanamol et al., 2018), reinforcing the hypothesis that bacterial endophytes naturally occurring in the vegetative stage of *P. incarnata* may have a crucial role in vegetative development of plant host.

Microbes often use two mechanisms to support the plant growth directly (Santoyo et al., 2016): (1) facilitating the mobilization and uptake of soil deficient nutrients (Van der Heijden et al., 2008) and (2) modulating the level of

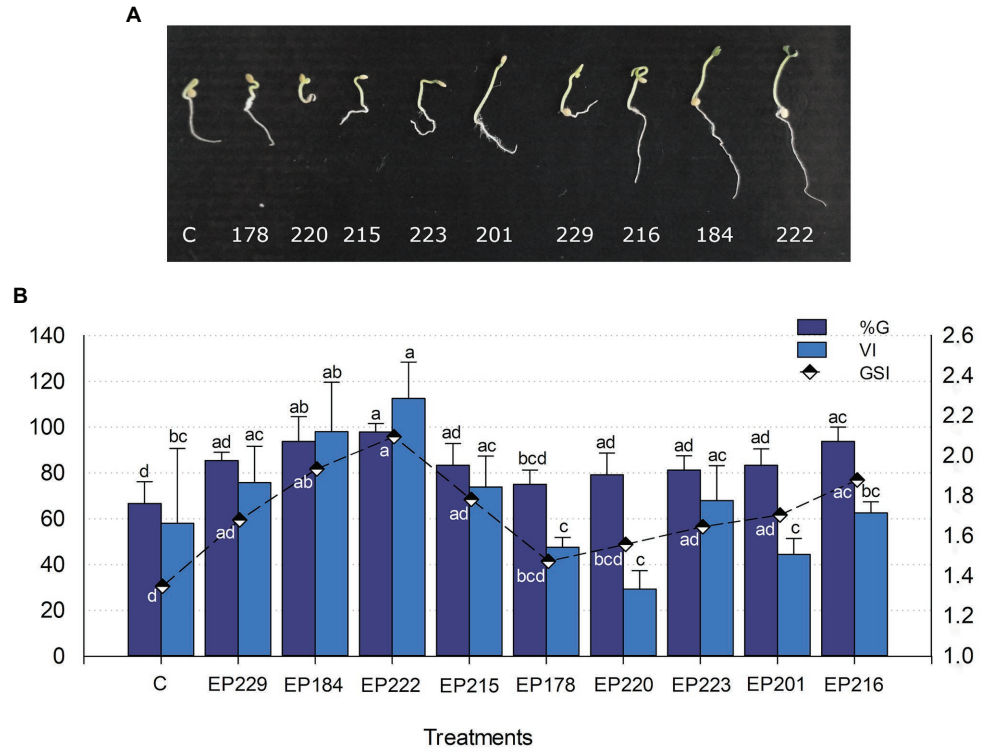

FIGURE 5 | Effect of bacterial strains isolated from *P. incarnata* on the Cape gooseberry germination: **(A)** Representative pictures on sprouted seeds at 10 days and **(B)** Bar chart of germination percentage (%G) and vigor index (VI) exhibited by each bacterial strain. The vigor index (VI) is graphed with black and white colored rhombuses. Values represent the arithmetic mean ± SD. Treatments with different letters, within each tested parameter, are significantly different according to the Tukey statistical test ($p < 0.05$).

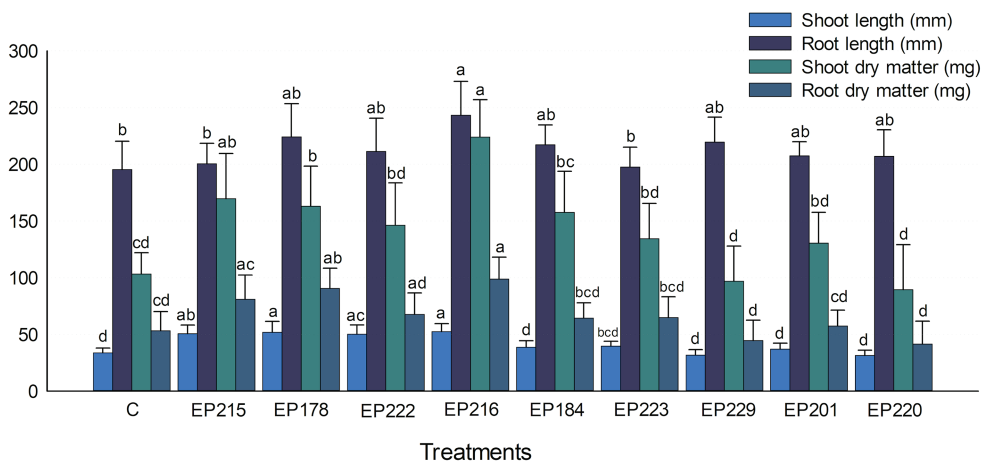

FIGURE 6 | Effect of bacterial inoculants isolated from *P. incarnata* on the Cape gooseberry growth. Values represent the arithmetic mean ± SD. Treatments with different letters, within each tested parameter, are significantly different according to the Tukey statistical test ($p < 0.05$).

hormones in plants (Verbon and Liberman, 2016). In this study, the potential of isolates to mobilize essential nutrients (N, P, and Fe) and synthesize phytohormones (auxins) was accessed. Most strains reported in this study exhibited PGP traits in biochemical and/or genetic assays. Nitrogen is present abundantly in the environment in its diatomic form (N_2), limiting its absorption for plants. Many strains grown in the NFb medium, forming a sub-surface pellicle, and they were

mostly associated with the *Bacillus* genus. A previous study reported endophytic *Bacillus* strains isolated from the *Lolium perenne* rhizosphere, which showed their diazotrophic activity (Castellano-Hinojosa et al., 2016). Although most studies described diazotrophic bacteria from rhizospheric environments, some investigations have reported phyllosphere bacteria associated with the nitrogen fixation (Pati and Chandra, 1993; Desgarennes et al., 2014). Amplification of the *nifH* gene was performed to confirm diazotrophic potential. However, *nifH* sequences were detected in just one strain (EP220). The NFb medium not only allows the retrieval of diazotrophs but also favors the growth of bacteria able to scavenge traces of different nitrogen sources from the atmosphere (Zuluaga et al., 2020).

Phosphorus is an essential nutrient for plant development and growth (Khan et al., 2010). The isolates associated to *Bacillus*, *Pseudomonas*, and *Pantoea* were the most frequently encountered in the phosphate solubilization phenotypic tests. Some studies have shown that the main mechanism of *Pantoea* and *Pseudomonas* to solubilize inorganic phosphate is the secretion of the gluconic acid (Castagno et al., 2011; Oteino et al., 2015). In comparison, *Bacillus* species secrete other organic acids, such as lactic, acetic, succinic, and propionic (Saeid et al., 2018). Taking into account that the solubilization of inorganic phosphate compounds occurs mainly through the secretion of organic acids, changes in the composition of the culture medium may alter the microbial metabolism and affect the rate of solubilization (Nautiyal, 1999), masking the ability of strains for phosphate solubilization. The gene encoding phosphatase enzyme was chosen as a genetic marker since it is involved in the solubilization of various organic phosphates. The *AcPho* gene was amplified using primers designed from *B. thuringiensis* sequences (Raddadi et al., 2008), which favored the detection in *Bacillus* strains and limited it for the less represented groups. *AcPho* sequences were not only detected in strains closely associated with *B. thuringiensis* but also in other taxa (*B. aryabhattai*, *B. tequilensis*, *B. megaterium*, *B. anthracis*, and *B. cereus*), showing its potential as phosphate solubilization functional marker for the *Bacillus* genus. Overall, the combination of the two approaches proved to be complementary, since the formation of solubilizing halo on the NBRIP medium indicated that the bacteria could solubilize inorganic phosphate (Nautiyal, 1999). Meanwhile, the detection of *AcPho* sequences showed the potential to solubilize organic phosphates (Sharma et al., 2013). Various isolates confirmed their ability to solubilize organic and inorganic phosphate compounds, remarkably increasing their potential as plant beneficial inoculants.

The IAA is involved in several processes of plant vegetative development (Spaepen and Vanderleyden, 2011). The phenotypic assay to detect IAA-like compound production was carried out under the same culture conditions for all isolates, without taking into account their wide physiological and taxonomic diversity, which reduced the possibility of offering the specific conditions that each isolate requires to produce maximum IAA amounts (Frankenberger and Arshad, 1995). *Bacillus* was not only the genus with the most IAA-producing number of strains but also comprised the strain (EP229) with the highest value of IAA-like compounds. IAA values similar to this study were found in *Bacillus* isolates from plants at a multi-metal contaminated mine site (Shim et al., 2015). The gene (*ipdC*) chosen for the genotypic approach encodes a key enzyme in the main IAA biosynthetic pathway (IPA) found in plant-associated beneficial bacteria (Spaepen and Vanderleyden, 2011). The primers used to detect the ipdC gene were also designed on sequences belonging to *B. thuringiensis*, which favored its detection in *Bacillus* strains. Lyngwi et al. (2016) have already reported *ipdC* gene sequences in *Bacillus* and *Paenibacillus* species recovered from soils of the sacred groves in India. The *ipdC* sequences were also amplified in isolates belonging to *Rhodococcus*. A study previously demonstrated the ability of some *Rhodococcus* strains to synthesize IAA (Vandeputte et al., 2005). The isolates that produce IAA-like substances and harbor *ipdC* gene sequences could synthesize the IAA through the IPA pathway. However, the microbial IAA can be produced by other metabolic pathways, such as AMI or IAOx/IAN, which can occur and be expressed together with the IPA pathway (Duca et al., 2014).

Iron is the fourth most abundant element in the earth's crust, but in aerobic (oxidant) conditions and neutral pH, it is almost insoluble for plants (Schwab and Lindsay, 1983). Under conditions of iron stress, microorganisms can produce low-molecular-mass compounds with high affinity for ferric ion, termed siderophores. Most of the tested strains secreted Fe (III) chelating agents when sequestered in the complex HDTMA-Fe (III)-CAS on the medium Blue Agar. This PGP trait was the most common among all identified genera as the method developed by Schwyn and Neilands (1987) did no limit the detection of a single molecule. Only *Lysinibacillus* and *Paenibacillus* strains did not exhibit siderophores-producing ability. Various studies previously reported siderophore production in *Bacillus*, *Pseudomonas*, and *Pantoea* strains (Loaces et al., 2011; Andreolli et al., 2016; Tchakounté et al., 2018). The *asb* gene was used as a genetic marker to characterize siderophore production because it commonly occurs in *Bacillus* species (Koppisch et al., 2008). However, this was amplified in just four *Bacillus* strains, likely because there is a wide structural diversity of siderophores described (Hider and Kong, 2010). On the other hand, a non-specific fragment related to the TatA/TatE subunit of the translocase A protein was amplified in several strains. Curiously, this protein is involved in the mechanism of the reception and translocation of an iron (III) reductase (Lechowicz and Krawczyk-Balska, 2015), so it is closely related to extracellular iron metabolism.

The treatment with the selected bacteria increased the germination rate of Cape gooseberry seeds, which often range 85–90% after 15 days of incubation (Fischer et al., 2005). The use of film-coating has already shown its potential to increase the germination rate of *P. peruviana* until 97% (Campos et al., 2015). However, this strategy must be carefully used as it may compromise the water and gas availability. In our study, the immersion of Cape gooseberry seeds in bacterial suspensions improved the germination rate and timing in 10 days. Some studies have reported PGP bacteria to positively influence seed germination synthesizing

phytohormones (Delshadi et al., 2017). The bacteria used in the germination test showed potential for the synthesis of one of the main phytohormones (indole acetic acid) associated with vegetative development. The results from pot experiments supported the capability of the *P. incarnata* endophytic strains to promote plant growth. They have previously shown their potential to solubilize phosphates, synthesize IAA, and produce siderophores in genetic and biochemical assays. But, the detection of PGP traits by assays *in vitro* is not conclusive to determinate the effect of a candidate strain on the plant growth promotion, since that bacterial performance depends on environmental conditions and plant-microbe interactions (Smyth et al., 2011). However, selected strains were able to improve agronomic parameters in Cape gooseberry seedlings, suggesting that they might have used mechanisms exhibited *in vitro* to stimulate plant development and growth *in vivo*. The used endophytic strains as probiotic and protective agents for crops have gained relevance as they possess traits associated to improvement and supporting of plant development and health. In addition, they intrinsically have the capability of access to a restricted environment, the endosphere. The boosting effects of selected strains were exhibited in a plant species different than native, suggesting their versatility for colonizing other environments. These characteristics become them in promising candidates for agriculture systems (Farrar et al., 2014).

The function and structure of plant-associated microbiomes are shaped by host and environmental factors (Trivedi et al., 2020). However, a theory denominated "Cry for Help" hypothesize that a plant can attract beneficial microbes from the environment to cope with particular stresses (Liu and Brettell, 2019). This recruitment might also be associated to physiological needs that a plant exhibits during its development. The uptake of essential nutrients (such as N, P, K, and S) and the auxin synthesis are substantially higher in the early stages of plant development (Ramanathan and Krishnamoorthy, 1973; Ljung et al., 2001; Arunachalam and Chavan, 2018). Thus, the recruitment of bacteria capable meet these physiological needs (Carvalhais et al., 2013) may be favored during the passionflower vegetative development. Vendan et al. (2010) also found endophytic PGP bacteria mainly in the early stages of the ginseng life cycle. A study reported the dominance of IAA-producing rhizobacteria in the rosette (early) canola development stage (Farina et al., 2012). On the other hand, various studies have described PGP activities in microorganisms isolated from medicinal plants (Ansary et al., 2018; Li et al., 2018; Huang et al., 2019; Aeron et al., 2020). As in the food industry, pharmacological companies require that medicinal plant culture not includes chemical fertilization. This requirement reflects challenging conditions that plant medicinal culture deals and suggests a possible role of PGP microorganisms in these plants. The physiological needs that passionflower often exhibits in its vegetative stage added to the limited nutritional conditions that this plant faces in the agriculture systems of pharmacological interest which might explain the occurrence of PGP bacteria. However, a study of taxonomic and functional profile of endophytic microbiome could describe more precisely the bacterial group's domaining endophytic environment and reveal roles they playing in the development and growth of plant host.

CONCLUSION

This study reveals the dominance of groups belonging to *Bacillus*, *Pseudomonas*, and *Pantoea* among the bacterial endophytes from passionflower leaves. The contribution of these genera to the promotion of plant-growth and germination is highlighted by their potential to produce IAA, solubilize phosphate, and synthesize siderophores as demonstrated by the present assays using Cape gooseberry as a model. It can be also concluded that the combination of genotypic and phenotypic approaches is effective in revealing plant growth-promoting traits. The occurrence of several culturable PGP strains is probably associated with conditions of the passionflower culture. The strains of bacteria isolated in this study may be used in future projects as beneficial inoculants for agricultural systems.

DATA AVAILABILITY STATEMENT

The datasets presented in this study can be found in online repositories. The names of the repository/repositories and accession number(s) can be found below: Isolate sequences were deposited in GenBank under accession numbers MG778707 to MG778907.

AUTHOR CONTRIBUTIONS

LC-Y and FF-G designed the work and drafted the manuscript. LC-Y and MN conducted experiments *in vitro* and *in vivo*, respectively. MG, DA, and FF-G analyzed and interpreted the results. All authors read and approved the manuscript.

FUNDING

This work was supported by The São Paulo Research Foundation, FAPESP (2015/02395-8). The scholarship to LGCY was provided by the "Programa Nacional de Becas y Créditos Educativos" (PRONABEC), Perú.

ACKNOWLEDGMENTS

We thank Adriana da Silva Santos for assistance with quantitative tests, Rafael Vasconcelos Ribeiro for assistance with chlorophyll measurements, and Yesenia Santa-Cruz Vásquez for collaboration in the assembly of pot experiments.

SUPPLEMENTARY MATERIAL

The Supplementary Material for this article can be found online at: https://www.frontiersin.org/articles/10.3389/fpls.2020.621740/full#supplementary-material

REFERENCES

Aeron, A., Maheshwari, D. K., and Meena, V. S. (2020). Endophytic bacteria promote growth of the medicinal legume *Clitoria ternatea* L. by chemotactic activity. *Arch. Microbiol.* 202, 1049–1058. doi: 10.1007/s00203-020-01815-0

Andreolli, M., Lampis, S., Zapparoli, G., Angelini, E., and Vallini, G. (2016). Diversity of bacterial endophytes in 3- and 15-year-old grapevines of *Vitis vinifera* cv. Corvina and their potential for plant growth promotion and phytopathogen control. *Microbiol. Res.* 183, 42–52. doi: 10.1016/j.micres.2015.11.009

Ansary, W. R., Prince, F. R. K., Haque, E., Sultana, F., West, H. M., Rahman, M., et al. (2018). Endophytic *Bacillus* spp. from medicinal plants inhibit mycelial growth of *Sclerotinia sclerotiorum* and promote plant growth. *Z. Naturforsch. C, J. Biosci.* 73, 247–256. doi: 10.1515/znc-2018-0002

Arunachalam, T., and Chavan, K. M. (2018). Dry matter accumulation and nutrient uptake patterns of onion seed crop. *J. Plant Nutr.* 41, 1879–1889. doi: 10.1080/01904167.2018.1476538

Ash, C., Farrow, J. A., Dorsch, M., Stackebrandt, E., and Collins, M. D. (1991). Comparative analysis of *Bacillus anthracis*, *Bacillus cereus*, and related species on the basis of reverse transcriptase sequencing of 16S rRNA. *Int. J. Syst. Bacteriol.* 41, 343–346. doi: 10.1099/00207713-41-3-343

Baldani, J. I., Baldani, V. L. D., Seldin, L., and Döbereiner, J. (1986). Characterization of *Herbaspirillum seropedicae* gen. nov., sp. nov., a root associated nitrogen fixing bacterium. *Int. J. Syst. Bacteriol.* 136, 86–93.

Bargaz, A., Lyamlouli, K., Chtouki, M., Zeroual, Y., and Dhiba, D. (2018). Soil microbial resources for improving fertilizers efficiency in an integrated plant nutrient management system. *Front. Microbiol.* 9:1606. doi: 10.3389/fmicb.2018.01606

Bharti, N., Sharma, S. K., Saini, S., Verma, A., Nimonkar, Y., and Prakash, O. (2017). "Microbial plant probiotics: problems in application and formulation" in *Probiotics and plant health*. eds. V. Kumar, M. Kumar, S. Sharma and R. Prasad (Singapore: Springer), 317–335.

Björnberg, K., Jonas, E., Marstorp, H., and Tidåker, P. (2015). The role of biotechnology in sustainable agriculture: views and perceptions among key actors in the Swedish food supply chain. *Sustain.* 7, 7512–7529.

Bürgmann, H., Widmer, F., Von Sigler, W., and Zeyer, J. (2004). New molecular screening tools for analysis of free-living diazotrophs in soil. *Appl. Environ. Microbiol.* 70, 240–247. doi: 10.1128/AEM.70.1.240-247.2004

Campos, A., Neto, C. S., Seleguini, A., and Fernandes, P. (2015). Does fruit cooling and seed film coating affect the germination potential of physalis? *Scientia Agropecuaria* 6, 325–328. doi: 10.17268/sci.agropecu.2015.04.09

Carvalhais, L.C., Dennis, P.G., Fan, B., Fedoseyenko, D., Kierul, K., and Becker, A., von Wiren, N. , and Borriss, R. (2013). Linking plant nutritional status to plant-microbe interactions. *PLoS One* 8:e68555. doi: 10.1371/journal.pone.0068555

Castagno, L. N., Estrella, M. J., Sannazzaro, A. I., Grassano, A. E., and Ruiz, O. A. (2011). Phosphate-solubilization mechanism and in vitro plant growth promotion activity mediated by *Pantoea eucalypti* isolated from *Lotus tenuis* rhizosphere in the Salado River Basin (Argentina). *J. Appl. Microbiol.* 110, 1151–1165. doi: 10.1111/j.1365-2672.2011.04968.x

Castellano-Hinojosa, A., Correa-Galeote, D., Palau, J., and Bedmar, E. J. (2016). Isolation of N_2 – fixing rhizobacteria from *Lolium perenne* and evaluating their plant growth promoting traits. *J. Basic Microbiol.* 56, 85–91. doi: 10.1002/jobm.201500247

Chen, C., Xin, K., Liu, H., Cheng, J., Shen, X., Wang, Y., et al. (2017). *Pantoea alhagi*, a novel endophytic bacterium with ability to improve growth and drought tolerance in wheat. *Sci. Rep.* 7:41564. doi: 10.1038/srep41564

Chimwamurombe, P. M., Grönemeyer, J. L., and Reinhold-Hurek, B. (2016). Isolation and characterization of culturable seed-associated bacterial endophytes from gnotobiotically grown Marama bean seedlings. *FEMS Microbiol. Ecol.* 92:fiw083. doi: 10.1093/femsec/fiw083

Compant, S., Clément, C., and Sessitsch, A. (2010). Plant growth-promoting bacteria in the rhizo- and endosphere of plants: their role, colonization, mechanisms involved and prospects for utilization. *Soil Biol. Biochem.* 42, 669–678. doi: 10.1016/j.soilbio.2009.11.024

Crowley, D. E. (2006). "Microbial Siderophores in the plant Rhizosphere" in *Iron nutrition in plants and rhizospheric microorganisms*. eds. L. L. Barton and J. Abadia (Dordrecht: Springer), 169–198.

da Silva, K. J., de Armas, R. D., Soares, C. R., and Ogliari, J. B. (2016). Communities of endophytic microorganisms in different developmental stages from a local variety as well as transgenic and conventional isogenic hybrids of maize. *World J. Microbiol. Biotechnol.* 32:189. doi: 10.1007/s11274-016-2149-6

Delshadi, S., Ebrahimi, M., and Shirmohammadi, E. (2017). Influence of plant-growth-promoting bacteria on germination, growth and nutrients' uptake of *Onobrychis sativa* L. under drought stress. *J. Plant Interact.* 12, 200–208. doi: 10.1080/17429145.2017.1316527

Desgarennes, D., Garrido, E., Torres-Gomez, M. J., Peña-Cabriales, J. J., and Partida-Martinez, L. P. (2014). Diazotrophic potential among bacterial communities associated with wild and cultivated Agave species. *FEMS Microbiol. Ecol.* 90, 844–857. doi: 10.1111/1574-6941.12438

Dhawan, K., Kumar, R., Kumar, S., and Sharma, A. (2001). Correct identification of *Passiflora incarnata* Linn., a promising herbal anxiolytic and sedative. *J. Med. Food* 4, 137–144. doi: 10.1089/109662001753165710

Duca, D., Lorv, J., Patten, C. L., Rose, D., and Glick, B. R. (2014). Indole-3-acetic acid in plant-microbe interactions. *Antonie Van Leeuwenhoek* 106, 85–125. doi: 10.1007/s10482-013-0095-y

Edi-Premono, M., Moawad, M. A., and Vleck, P. L. G. (1996). Effect of phosphate solubilizing Pseudomonas putida on the growth of maize and its survival in the rhizosphere. *Indones. J. Crop Sci.* 11, 13–23.

Eevers, N., Gielen, M., Sánchez-López, A., Jaspers, S., White, J. C., Vangronsveld, J., et al. (2015). Optimization of isolation and cultivation of bacterial endophytes through addition of plant extract to nutrient media. *Microb. Biotechnol.* 8, 707–715. doi: 10.1111/1751-7915.12291

Egamberdieva, D., Wirth, S., Behrendt, U., Ahmad, P., and Berg, G. (2017). Antimicrobial activity of medicinal plants correlates with the proportion of antagonistic Endophytes. *Front. Microbiol.* 8:199. doi: 10.3389/fmicb.2017.00199

El-Sawah, M. M. A., Hauka, F. I. A., and El-Rafey, H. H. (1993). Study on some enzymes cleaving phosphorus from organic substrates in soil. *J. Agric. Sci.* 18, 2775–2785.

Farina, R. A., Beneduzi, A., Ambrosini, A., Campos, S. B., Lisboa, B. B., Wendisch, V., et al. (2012). Diversity of plant growth-promoting rhizobacteria communities associated with the stages of canola growth. *Appl. Soil Ecol.* 55, 44–52. doi: 10.1016/j.apsoil.2011.12.011

Farrar, K., Bryant, D., and Cope-Selby, N. (2014). Understanding and engineering beneficial plant-microbe interactions: plant growth promotion in energy crops. *Plant Biotechnol. J.* 12, 1193–1206. doi: 10.1111/pbi.12279

Felsenstein, J. (1985). Confidence limits on phylogenies: an approach using the bootstrap. *Evolution* 39, 783–791. doi: 10.1111/j.1558-5646.1985.tb00420.x

Ferreira, C. M. H., Soares, H. M. V. M., and Soares, E. V. (2019). Promising bacterial genera for agricultural practices: an insight on plant growth-promoting properties and microbial safety aspects. *Sci. Total Environ.* 682, 779–799. doi: 10.1016/j.scitotenv.2019.04.225

Fischer, G., Miranda, D., Piedrahíta, W., and Romero, J. (2005). *Avances en cultivo, poscosecha y exportación de la uchuva (Physalis peruviana L.) en Colombia*. Bogotá: Unibiblos, Universidad Nacional de Colombia.

Frankenberger, W. T. J., and Arshad, M. (1995). *Phytohormones in soil: Microbial production and function*. New York: Marcel Dekker Inc.

Fuentes, V., Lemes, C., and Rodríguez, C. (2000). Instructivo Técnico del cultivo de *Passiflora incarnata* L. *Rev. Cubana Plant. Med.* 5, 118–122.

Glick, B. R. (2014). Bacteria with ACC deaminase can promote plant growth and help to feed the world. *Microbiol. Res.* 169, 30–39. doi: 10.1016/j.micres.2013.09.009

Goulart, M. C., Cueva-Yesquén, L. G., Hidalgo Martinez, K. J., Attili-Angelis, D., and Fantinatti-Garboggini, F. (2019). Comparison of specific endophytic bacterial communities in different developmental stages of *Passiflora incarnata* using culture-dependent and culture-independent analysis. *MicrobiologyOpen* 8:e896. doi: 10.1002/mbo3.896

Govindasamy, V., Senthilkumar, M., Magheshwaran, V., Kumar, U., Bose, P., Sharma, V., et al. (2010). "*Bacillus* and *Paenibacillus* spp.: potential PGPR for sustainable agriculture" in *Plant growth and health promoting bacteria*. ed. D. Maheshwari (Springer Heidelberg), 333–364.

Gupta, G., Panwar, J., Akhtar, M. S., and Jha, P. N. (2012). "Endophytic nitrogen-fixing bacteria as biofertilizer" in *Sustainable agriculture reviews. Vol. 11*. ed. E. Lichtfouse (Dordrecht: Springer).

Hall, T. (1999). BioEdit: a user-friendly biological sequence alignment editor and analysis program for Windows 95/98/NT. *Nucleic Acids Symp. Ser.* 41, 95–98.

Hardoim, P. R., van Overbeek, L. S., Berg, G., Pirttilä, A. M., Compant, S., Campisano, A., et al. (2015). The hidden world within plants: ecological and evolutionary considerations for defining functioning of microbial Endophytes. *Microbiol. Mol. Biol. Rev.* 79, 293–320. doi: 10.1128/MMBR.00050-14

Hider, R. C., and Kong, X. (2010). Chemistry and biology of siderophores. *Nat. Prod. Rep.* 27, 637–657. doi: 10.1039/b906679a

Huang, C. M., Chen, W. C., Lin, S. H., Wang, Y. N., and Shen, F. T. (2019). Exploration of root-associated bacteria from the medicinal plant *Platycodon grandiflorum*. *Microbes Environ.* 34, 413–420. doi: 10.1264/jsme2.ME19030

Hussein, K. A., and Joo, J. H. (2014). Potential of siderophore production by bacteria isolated from heavy metal: polluted and rhizosphere soils. *Curr. Microbiol.* 68, 717–723. doi: 10.1007/s00284-014-0530-y

Janda, J. M., and Abbott, S. L. (2017). 16S rRNA gene sequencing for bacterial identification in the diagnostic laboratory: pluses, perils, and pitfalls. *J. Clin. Microbiol.* 45, 2761–2764. doi: 10.1128/JCM.01228-07

Khan, A., and Mathelier, A. (2017). Intervene: a tool for intersection and visualization of multiple gene or genomic region sets. *BMC Bioinform.* 18:287. doi: 10.1186/s12859-017-1708-7

Khan, M. S., Zaidi, A., Ahemad, M., Oves, M., and Wani, P. A. (2010). Plant growth promotion by phosphate solubilizing fungi – current perspective. *Arch. Agron. Soil Sci.* 56, 73–98. doi: 10.1080/03650340902806469

Koppisch, A. T., Dhungana, S., Hill, K. K., Boukhalfa, H., Heine, H. S., Colip, L. A., et al. (2008). Petrobactin is produced by both pathogenic and nonpathogenic isolates of the *Bacillus cereus* group of bacteria. *Biometals* 21, 581–589. doi: 10.1007/s10534-008-9144-9

Kumar, A., Singh, S., Gaurav, A. K., Srivastava, S., and Verma, J. P. (2020). Plant growth-promoting bacteria: biological tools for the mitigation of salinity stress in plants. *Front. Microbiol.* 11:1216. doi: 10.3389/fmicb.2020.01216

Lane, D. J. (1991). "16S/23S rRNA sequencing" in: *Nucleic acid techniques in bacterial systematics*." eds. E. Stackebrandt and M. Goodfellow (Chichester, UK: John Wiley and Sons), 115–175.

Lechowicz, J., and Krawczyk-Balska, A. (2015). An update on the transport and metabolism of iron in *Listeria monocytogenes*: the role of proteins involved in pathogenicity. *Biometals* 28, 587–603. doi: 10.1007/s10534-015-9849-5

Letunic, I., and Bork, P. (2016). Interactive tree of life (iTOL) v3: an online tool for the display and annotation of phylogenetic and other trees. *Nucleic Acids Res.* 44, W242–W245. doi: 10.1093/nar/gkw290

Li, L., Mohamad, O. A. A., Ma, J., Friel, A. D., Su, Y., Wang, Y., et al. (2018). Synergistic plant-microbe interactions between endophytic bacterial communities and the medicinal plant *Glycyrrhiza uralensis* F. *Antonie Van Leeuwenhoek* 111, 1735–1748. doi: 10.1007/s10482-018-1062-4

Liu, H., and Brettell, L. E. (2019). Plant defense by VOC-induced microbial priming. *Trends Plant Sci.* 24, 187–189. doi: 10.1016/j.tplants.2019.01.008

Liu, H., Brettell, L. E., Qiu, Z., and Singh, B. K. (2020). Microbiome-mediated stress resistance in plants. *Trends Plant Sci.* 25, 733–743. doi: 10.1016/j.tplants.2020.03.014

Ljung, K., Bhalerao, R. P., and Sandberg, G. (2001). Sites and homeostatic control of auxin biosynthesis in Arabidopsis during vegetative growth. *Plant J.* 28, 465–474. doi: 10.1046/j.1365-313x.2001.01173.x

Loaces, I., Ferrando, L., and Scavino, A. F. (2011). Dynamics, diversity and function of endophytic siderophore-producing bacteria in rice. *Microb. Ecol.* 61, 606–618. doi: 10.1007/s00248-010-9780-9

López-Arredondo, D. L., Leyva-González, M. A., Alatorre-Cobos, F., and Herrera-Estrella, L. (2013). Biotechnology of nutrient uptake and assimilation in plants. *Int. J. Dev. Biol.* 57, 595–610. doi: 10.1387/ijdb.130268lh

Lyngwi, N. A., Nongkhlaw, M., Kalita, D., and Joshi, S. R. (2016). Bioprospecting of plant growth promoting bacilli and related genera prevalent in soils of pristine sacred groves: biochemical and molecular approach. *PLoS One* 11:e0152951. doi: 10.1371/journal.pone.0152951

Maguire, J. D. (1962). Speeds of germination-aid selection and evaluation for seedling emergence and vigor. *Crop Sci.* 2, 176–177.

McCully, M. E. (2001). Niches for bacterial endophytes in crop plants: a plant biologist's view. *Aust. J. Plant Physiol.* 28, 983–990. doi: 10.1071/PP01101

McSpadden Gardener, B. B. (2004). Ecology of *Bacillus* and *Paenibacillus* spp. in agricultural systems. *Phytopathology* 94, 1252–1258. doi: 10.1094/PHYTO.2004.94.11.1252

Mehta, S., and Nautiyal, C. S. (2001). An efficient method for qualitative screening of phosphate-solubilizing bacteria. *Curr. Microbiol.* 43, 51–56. doi: 10.1007/s002840010259

Mercado-Blanco, J., and Bakker, P. A. (2007). Interactions between plants and beneficial *Pseudomonas* spp.: exploiting bacterial traits for crop protection. *Antonie Van Leeuwenhoek* 92, 367–389. doi: 10.1007/s10482-007-9167-1

Miller, K. I., Qing, C., Sze, D. M., Roufogalis, B. D., and Neilan, B. A. (2012). Culturable endophytes of medicinal plants and the genetic basis for their bioactivity. *Microb. Ecol.* 64, 431–449. doi: 10.1007/s00248-012-0044-8

Miroddi, M., Calapai, G., Navarra, M., Minciullo, P. L., and Gangemi, S. (2013). *Passiflora incarnata* L.: ethnopharmacology, clinical application, safety and evaluation of clinical trials. *J. Ethnopharmacol.* 150, 791–804. doi: 10.1016/j.jep.2013.09.047

Nautiyal, C. S. (1999). An efficient microbiological growth medium for screening phosphate solubilizing microorganisms. *FEMS Microbiol. Lett.* 170, 265–270. doi: 10.1111/j.1574-6968.1999.tb13383.x

Oteino, N., Lally, R. D., Kiwanuka, S., Lloyd, A., Ryan, D., Germaine, K. J., et al. (2015). Plant growth promotion induced by phosphate solubilizing endophytic *Pseudomonas* isolates. *Front. Microbiol.* 6:745. doi: 10.3389/fmicb.2015.00745

Pati, B. R., and Chandra, A. K. (1993). Diazotrophic bacterial population and other associated organisms on the phyllosphere of some crop plants. *Zentralbl. Mikrobiol.* 148, 392–402.

Procópio, R. E., Araújo, W. L., Maccheroni, W. Jr., and Azevedo, J. L. (2009). Characterization of an endophytic bacterial community associated with Eucalyptus spp. *Genet. Mol. Res.* 8, 1408–1422. doi: 10.4238/vol8-4gmr691

Puente, L., Pinto-Muñoz, C. A., Castro, E. S., and Cortes, M. (2011). *Physalis peruviana* Linnaeus, the multiple properties of a highly functional fruit: a review. *Food Res. Int.* 44, 1733–1740. doi: 10.1016/j.foodres.2010.09.034

Raddadi, N., Cherif, A., Boudabous, A., and Daffonchio, D. (2008). Screening of plant growth-promoting traits of *Bacillus thuringiensis*. *Ann. Microbiol.* 58, 47–52. doi: 10.1007/BF03179444

Ramanathan, K. M., and Krishnamoorthy, K. K. (1973). Nutrient uptake by paddy during the main three stages of growth. *Plant Soil* 39:29. doi: 10.1007/BF00018042

Rashid, M. I., Mujawar, L. H., Shahzad, T., Almeelbi, T., Ismail, I. M., and Oves, M. (2016). Bacteria and fungi can contribute to nutrients bioavailability and aggregate formation in degraded soils. *Microbiol. Res.* 183, 26–41. doi: 10.1016/j.micres.2015.11.007

Rhoden, S. A., Garcia, A., Santos Silva, M. C., Azevedo, J. L., and Pamphile, J. A. (2015). Phylogenetic analysis of endophytic bacterial isolates from leaves of the medicinal plant *Trichilia elegans* A. Juss. (Meliaceae). *Genet. Mol. Res.* 14, 1515–1525. doi: 10.4238/2015

Saeid, A., Prochownik, E., and Dobrowolska-Iwanek, J. (2018). Phosphorus solubilization by Bacillus species. *Molecules* 23:2897. doi: 10.3390/molecules23112897

Santoyo, G., Moreno-Hagelsieb, G., del Orozco-Mosqueda, M. C., and Glick, B. R. (2016). Plant growth-promoting bacterial endophytes. *Microbiol. Res.* 183, 92–99. doi: 10.1016/j.micres.2015.11.008

Schwab, A. B., and Lindsay, W. L. (1983). Effect of redox on solubility and availability of iron. *Soil Sci. Soc. Am. J.* 47, 201–205.

Schwyn, B., and Neilands, J. B. (1987). Universal chemical assay for the detection and determination of siderophores. *Anal. Biochem.* 160, 47–56. doi: 10.1016/0003-2697(87)90612-9

Seghers, D., Wittebolle, L., Top, E. M., Verstraete, W., and Siciliano, S. D. (2004). Impact of agricultural practices on the *Zea mays* L. endophytic community. *Appl. Environ. Microbiol.* 70, 1475–1482. doi: 10.1128/aem.70.3.1475-1482.2004

Shabanamol, S., Divya, K., George, T. K., Rishad, K. S., Sreekumar, T. S., and Jisha, M. S. (2018). Characterization and in planta nitrogen fixation of plant growth promoting endophytic diazotrophic Lysinibacillus sphaericus isolated from rice (*Oryza sativa*). *Physiol. Mol. Plant Pathol.* 102, 46–54. doi: 10.1016/j.pmpp.2017.11.003

Shahzad, R., Waqas, M., Khan, A. L., Al-Hosni, K., Kang, S. M., Seo, C. W., et al. (2017). Indoleacetic acid production and plant growth promoting potential of bacterial endophytes isolated from rice (*Oryza sativa* L.) seeds. *Acta Biol. Hung.* 68, 175–186. doi: 10.1556/018.68.2017.2.5

Sharma, S. B., Sayyed, R. Z., Trivedi, M. H., and Gobi, T. A. (2013). Phosphate solubilizing microbes: sustainable approach for managing phosphorus deficiency in agricultural soils. *Springerplus* 2:587. doi: 10.1186/2193-1801-2-587

Shim, J., Kim, J. W., Shea, P. J., and Oh, B. T. (2015). IAA production by Bacillus sp. JH 2-2 promotes Indian mustard growth in the presence of hexavalent chromium. *J. Basic Microbiol.* 55, 652–658. doi: 10.1002/jobm.201400311

Silva Filho, G. N., and Vidor, C. (2000). Solubilização de fosfato por microrganismos na presença de fontes de carbono. *Rev. Bras. Cienc. Solo.* 24, 311–319. doi: 10.1590/S0100-06832000000200008

Smyth, E. M., McCarthy, J., Nevin, R., Khan, M. R., Dow, J. M., O'Gara, F., et al. (2011). *In vitro* analyses are not reliable predictors of the plant growth promotion capability of bacteria; a *Pseudomonas fluorescens* strain that promotes the growth and yield of wheat. *J. Appl. Microbiol.* 111, 683–692. doi: 10.1111/j.1365-2672.2011.05079.x

Spaepen, S., and Vanderleyden, J. (2011). Auxin and plant-microbe interactions. *Cold Spring Harb. Perspect. Biol.* 3:a001438. doi: 10.1101/cshperspect.a001438

Tamura, K., Stecher, G., Peterson, D., Filipski, A., and Kumar, S. (2013). MEGA6: molecular evolutionary genetics analysis version 6.0. *Mol. Biol. Evol.* 30, 2725–2729. doi: 10.1093/molbev/mst197

Tang, Y. W., and Bonner, J. (1948). The enzymatic inactivation of indole acetic acid; the physiology of the enzyme. *Am. J. Bot.* 35, 570–578. doi: 10.1002/j.1537-2197.1948.tb08123.x.

Tchakounté, G. V. T., Berger, B., Patz, S., Fankem, H., and Ruppel, S. (2018). Community structure and plant growth-promoting potential of cultivable bacteria isolated from Cameroon soil. *Microbiol. Res.* 214, 47–59. doi: 10.1016/j.micres.2018.05.008

Thompson, J. D., Higgins, D. G., and Gibson, T. J. (1994). CLUSTAL W: improving the sensitivity of progressive multiple sequence alignment through sequence weighting, position-specific gap penalties and weight matrix choice. *Nucleic Acids Res.* 22, 4673–4680.

Trivedi, P., Leach, J. E., Tringe, S. G., Sa, T., and Singh, B. K. (2020). Plant-microbiome interactions: from community assembly to plant health. *Nat. Rev. Microbiol.* 18, 607–621. doi: 10.1038/s41579-020-0412-1

Uroz, S., Courty, P. E., and Oger, P. (2019). Plant Symbionts are engineers of the plant-associated microbiome. *Trends Plant Sci.* 24, 905–916. doi: 10.1016/j.tplants.2019.06.008

Vandeputte, O., Oden, S., Mol, A., Vereecke, D., and Goethals, K., El Jaziri, M., and Prinsen, E. (2005). Biosynthesis of auxin by the gram-positive phytopathogen *Rhodococcus fascians* is controlled by compounds specific to infected plant tissues. *Appl. Environ. Microbiol.* 71, 1169–1177. doi: 10.1128/AEM.71.3.1169-1177.2005

Van der Heijden, M.G., and Bardgett, R.D., van Straalen, N.M. (2008). The unseen majority: soil microbes as drivers of plant diversity and productivity in terrestrial ecosystems. *Ecol. Lett.* 11, 296–310. doi: 10.1111/j.1461-0248.2007.01139.x

Van Overbeek, L., and Van Elsas, J. D. (2008). Effects of plant genotype and growth stage on the structure of bacterial communities associated with potato (*Solanum tuberosum* L.). *FEMS Microbiol. Ecol.* 64, 283–296. doi: 10.1111/j.1574-6941.2008.00469.x

Van Soolingen, D., de Haas, P. E., Hermans, P. W., Groenen, P. M., and van Embden, J. D. (1993). Comparison of various repetitive DNA elements as genetic markers for strain differentiation and epidemiology of *Mycobacterium tuberculosis*. *J. Clin. Microbiol.* 31, 1987–1995. doi: 10.1128/JCM.31.8.1987-1995.1993

Vendan, R. T., Yu, Y. J., Lee, S. H., and Rhee, Y. H. (2010). Diversity of endophytic bacteria in ginseng and their potential for plant growth promotion. *J. Microbiol.* 48, 559–565. doi: 10.1007/s12275-010-0082-1

Verbon, E. H., and Liberman, L. M. (2016). Beneficial microbes affect endogenous mechanisms controlling root development. *Trends Plant Sci.* 21, 218–229. doi: 10.1016/j.tplants.2016.01.013

Walitang, D. I., Kim, K., Madhaiyan, M., Kim, Y. K., Kang, Y., and Sa, T. (2017). Characterizing endophytic competence and plant growth promotion of bacterial endophytes inhabiting the seed endosphere of rice. *BMC Microbiol.* 17:209. doi: 10.1186/s12866-017-1117-0

Woo, S. L., and Pepe, O. (2018). Microbial consortia: promising probiotics as plant biostimulants for sustainable agriculture. *Front. Plant Sci.* 9:1801. doi: 10.3389/fpls.2018.01801

Yoon, S. H., Ha, S. M., Kwon, S., Lim, J., Kim, Y., Seo, H., et al. (2017). Introducing EzBioCloud: a taxonomically united database of 16S rRNA gene sequences and whole-genome assemblies. *Int. J. Syst. Evol. Microbiol.* 67, 1613–1617. doi: 10.1099/ijsem.0.001755

Zehr, J. P., and McReynolds, L. A. (1989). Use of degenerate oligonucleotides for amplification of the *nifH* gene from the marine cyanobacterium *Trichodesmium thiebautii*. *Appl. Environ. Microbiol.* 55, 2522–2526. doi: 10.1128/AEM.55.10.2522-2526.1989

Zhao, L. X., Xu, L. H., and Jiang, C. L. (2012). Methods for the study of endophytic microorganisms from traditional Chinese medicine plants. *Methods Enzymol.* 517, 3–21. doi: 10.1016/B978-0-12-404634-4.00001-2

Zuluaga, M. Y. A., Lima Milani, K. M., Azeredo Gonçalves, L. S., and Martinez de Oliveira, A. L. (2020). Diversity and plant growth-promoting functions of diazotrophic/N-scavenging bacteria isolated from the soils and rhizospheres of two species of *Solanum*. *PLoS One* 15:e0227422. doi: 10.1371/journal.pone.0227422

Conflict of Interest: The authors declare that the research was conducted in the absence of any commercial or financial relationships that could be construed as a potential conflict of interest.

frontiers in Plant Science

ORIGINAL RESEARCH
published: 03 February 2021
doi: 10.3389/fpls.2020.634819

Bacillus subtilis SL18r Induces Tomato Resistance Against *Botrytis cinerea*, Involving Activation of Long Non-coding RNA, MSTRG18363, to Decoy miR1918

Cheng Zhou[1,2], Jingjing Zhu[2], Nana Qian[2], Jiansheng Guo[4] and Congsheng Yan[3]**

[1] Jiangsu Provincial Key Lab of Solid Organic Waste Utilization, Jiangsu Collaborative Innovation Center of Solid Organic Wastes, Educational Ministry Engineering Center of Resource-Saving Fertilizers, Nanjing Agricultural University, Nanjing, China, [2] Key Lab of Bio-Organic Fertilizer Creation, Ministry of Agriculture and Rural Affairs, Anhui Science and Technology University, Bengbu, China, [3] Institute of Horticulture, Anhui Academy of Agricultural Sciences, Hefei, China, [4] School of Medicine, Zhejiang University, Hangzhou, China

OPEN ACCESS

Edited by:
Jianfei Wang, Anhui University of Science and Technology, China

Reviewed by:
Lai-sheng Meng, Jiangsu Normal University, China
Huini Xu, Kunming University of Science and Technology, China
Xudong Sun, Kunming Institute of Botany, Chinese Academy of Sciences, China

***Correspondence:**
Cheng Zhou
zhoucheng@njau.edu.cn
Congsheng Yan
yancs1979@outlook.com

Specialty section:
This article was submitted to Plant Symbiotic Interactions, a section of the journal Frontiers in Plant Science

Received: *29 November 2020*
Accepted: *30 December 2020*
Published: *03 February 2021*

Citation:
Zhou C, Zhu J, Qian N, Guo J and Yan C (2021) Bacillus subtilis SL18r Induces Tomato Resistance Against Botrytis cinerea, Involving Activation of Long Non-coding RNA, MSTRG18363, to Decoy miR1918. Front. Plant Sci. 11:634819. doi: 10.3389/fpls.2020.634819

Mounting evidence has indicated that beneficial rhizobacteria can suppress foliar pathogen invasion via elicitation of induced systemic resistance (ISR). However, it remains elusive whether long non-coding RNAs (lncRNAs) are involved in the mediation of the rhizobacteria-primed ISR processes in plants. Herein, we demonstrated the ability of the rhizobacterial strain *Bacillus subtilis* SL18r to trigger ISR in tomato plants against the foliar pathogen *Botrytis cinerea*. Comparative transcriptome analysis was conducted to screen differentially expressed lncRNAs (DELs) between the non-inoculated and SL18r-inoculated plants. Among these DELs, four variants of MSTRG18363 possessed conserved binding sites for miR1918, which negatively regulates immune systems in tomato plants. The expression of MSTRG18363 in tomato leaves was significantly induced by SL18r inoculation. The transcription of MSTRG18363 was negatively correlated with the expression of miR1918, but displayed a positive correlation with the transcription of the RING-H2 finger gene *SlATL20* (a target gene of miR1918). Moreover, MSTRG18363-overexpressing plants exhibited the enhanced disease resistance, reduction of miR1918 transcripts, and marked increases of *SlATL20* expression. However, the SL18r-induced disease resistance was largely impaired in the MSTRG18363-silenced plants. VIGS-mediated *SlATL20* silencing also greatly weakened the SL18r-induced disease resistance. Collectively, our results suggested that induction of MSTRG18363 expression in tomato plants by SL18r was conducive to promoting the decoy of miR1918 and regulating the expression of *SlATL20*, thereby provoking the ISR responses against foliar pathogen infection.

Keywords: beneficial rhizobacteria, induced systemic resistance, long non-coding RNA, *Botrytis cinerea*, comparative transcriptome

INTRODUCTION

In plants, a series of intricate strategies has been evolved to defend against pathogenic bacteria, fungi and virus. Besides physical and chemical defense, plants develop sophisticatedly inducible immune systems that can be quickly evoked by pathogen-derived elicitors. The inducible defense responses are tightly controlled by several hormone such as salicylic acid (SA) and jasmonic acid (JA) (De Vos et al., 2006; Pozo and Azcón-Aguilar, 2007; Asselbergh et al., 2008). Apart from basal immune systems that can be stimulated at the pathogen-infected sites, a primed defense strategy has also been developed by plants, in which defense responses have not been activated for increasing plant's resistance, but is attributable to quicker induction of defense-related signaling pathways upon exposure to the attacks of pathogens (Bostock, 2005). In contrast to constitutive defense, initiation of priming defense exhibits less fitness costs of disease resistance in plants (van Hulten et al., 2006).

Well-studied examples of inducible defenses in plants are the activated systemic acquired resistance (SAR) by necrosis-inducing pathogen infection (Grant and Lamb, 2006). Initiation of SAR is required for locally and systemically increasing SA synthesis in plants, which result in transcriptional changes of a variety of pathogenesis-related (PR) proteins (Maleck et al., 2000; Molinari et al., 2014). The regulatory protein NPR1 is essential for transducing the SA signals in *Arabidopsis* (Ding et al., 2018). Overexpression of the *nahG* gene encoding a putative salicylate hydroxylase (SA-degrading enzyme) in transgenic plants fails to initiate SAR and activating the transcription of PR-related genes (Yang et al., 2004). The other example of the induced plant resistance is inducible systemic resistance (ISR), which can be effectively elicited by beneficial rhizobacteria strains (Lugtenberg and Kamilova, 2009). In contrast to SAR, initiation of the ISR responses is closely related to the stimulation of the JA- and ET-dependent pathways, involving upregulation of the expression of defensin 1.2 (*PDF1.2*) (De Vleesschauwer et al., 2008; Takishita et al., 2018). However, the SA-related signaling pathways can be triggered in plants exposed to several PGPR strains (Yan et al., 2002; Ryu et al., 2003). Rhizobacteria strain *B. subtilis* FB17 has been reported to activate both the SA- and ABA-related pathways to prevent the stomata-mediated entering routes of foliar pathogen into *Arabidopsis* plants (Kumar et al., 2012). *Bacillus cereus* AR156 can provoke ISR of *Arabidopsis* plants against pathogenic bacteria via stimulation of the JA-/ET- and SA-related pathways (Nie et al., 2017).

In nature, plant roots can recognize a myriad of microbe-derived elicitors for successful establishment of ISR. Bacteria-derived signals such as lipopolysaccharides, volatile organic compounds (VOCs), siderophores and cyclic lipopeptides have been identified to stimulate ISR responses in plants (Ongena et al., 2007; Aznar and Dellagi, 2015; Tahir et al., 2017). For example, the VOCs released by rhizobacterial strain *B. subtilis* GB03 can trigger the ISR responses in *Arabidopsis* plants via the ET-dependent pathways (Sharifi and Ryu, 2016). Cyclic lipopeptides from *B. subtilis* can provoke ISR by triggering the SA- and JA-dependent pathways (Ongena et al., 2007). MicroRNAs (miRNAs) have recently been demonstrated to participate in the mediation of rhizobacteria-mediated ISR processes in plants. *B. cereus* AR156 can effectively provoke the ISR responses in *Arabidopsis* plants against pathogenic bacteria via repression of miR825 and miR825* (Niu et al., 2016). *Bacillus amyloliquefaciens* FZB42 inhibits the expression of miR846 to elicit the ISR responses via the JA-related pathway (Xie et al., 2018). It is increasingly evidenced that long non-coding RNAs (lncRNAs) can mediate plant defense responses against pathogen infection by decoying miRNAs. In tomato plants, Slylnc0195 regulates the expression of class III HD-Zip TF genes by decoying miR166 in the yellow leaf curl virus-infected tomato plants (Wang et al., 2015). LncRNA39026 induces tomato resistance against *Phytophthora infestans* via promoting the decoy of miR168a and the transcription of PR-related genes (Hou et al., 2020). LncRNA23468 modulate the expression of NBS-LRR genes in the *P. infestans*-infected tomato by decoying miR482b (Jing et al., 2019). Despite the critical roles of lncRNAs in plant immunity, the functions of lncRNAs in the rhizobacteria-induced ISR remain sparsely explored.

Aiming at dissecting the ISR responses in tomato plants, we explored the mechanisms underpinning beneficial rhizobacteria *Bacillus subtilis* SL18r elicited ISR at the lncRNA level. To identify tomato lncRNAs that mediated the ISR responses provoked by *B. subtilis* SL18r, we sequenced lncRNA species by high-throughput sequencing and found that the transcription levels of MSTRG18363 were evidently induced in tomato leaves by root inoculation with *B. subtilis* SL18r. Upon exposure to *Botrytis cinerea*, the SL18r-inoculated plants had higher levels of MSTRG18363 expression than the control plants. Compared with the wild-type (WT) plants, the MSTRG18363-overexpressing plants exhibited the enhanced resistance of transgenic tomato plants to *B. cinerea*. However, virus-mediated silencing of MSTRG18363 largely weakened the SL18r-induced resistance against the invasion of *B. cinerea*. Furthermore, we further demonstrated that overexpression of MSTRG18363 in transgenic tomato plants markedly suppressed the expression of miR1918, a negative regulator of plant immunity. These findings indicated that the MSTRG18363-mediated decoy of miR1918 contributed to the SL18r-induced ISR in tomato plants.

MATERIALS AND METHODS

Bacterial Inoculation and Pathogen Infection Assays

Bacillus subtilis SL18r isolated from tomato rhizospheric soils was identified by sequencing of 16S rRNA genes (GenBank No. MW269558). *B. subtilis* SL18r was cultured for 16 h at 30°C and then centrifuged at 8,000 × *g*, followed by resuspension in sterile 0.05 M phosphate buffered saline (PBS) solution (pH 7.2). Finally, sterilized (autoclaved) soil was poured with cell suspensions of SL18r at the indicated concentrations, and the sterilized (autoclaved) soil treated with the PBS solution were used as the control. For preparing the inoculum of *Botrytis cinerea*, the fungal pathogen was cultured for 2 weeks and spore suspensions were then prepared with the solution containing 0.01 M KH_2PO_4 and

6.67 mM glucose to a density of 2×10^5 spores ml^{-1} (Curvers et al., 2010).

After 3 days (d) of bacterial inoculation, tomato plants were used to perform *in vivo* and *in vitro* assays of pathogen inoculation as reported by El Oirdi et al. (2011) with minor modifications: *in vitro* tests (pathogenicity tests on detached leaves), in which 5 μl droplet of spore suspension was inoculated on one side of the midvein of detached leaves and incubated in moist petri dishes at 23°C and *in vivo* tests (whole-plant inoculation), in which the uniform plants were selected and sprayed with spore suspension, and then cultivated at 23°C with 90% relative humidity (14 h day/10 h night cycle). At 5 days post infection (dpi), lesion diameters of detached leaves and disease index were measured as described recently by Jing et al. (2019). In addition, the transcription of *B. cinerea* actin gene (*BcActin*) was quantified for measuring the biomass of *B. cinerea* in leaves, and the tomato actin gene (*SlActin*) was used as a control as reported recently by Hu et al. (2018). The ratio of *BcActin* to *SlActin* was used to evaluate relative biomass of *B. cinerea*.

RNA-Sequencing (RNA-Seq)

To perform RNA-Seq, 7-day-old tomato seedlings were initially cultivated in soil for 3 weeks and were then poured with cell suspension of SL18r at a final density of 1×10^8 CFU g^{-1} soil for 3 days, and tomato plants poured with the PBS solution were used as the control. Subsequently, the control and inoculated leaves were sprayed with 2×10^5 spore ml^{-1} spore suspension of *B. cinerea*. At 0, 24, and 48 h post infection, the control and inoculated leaves were used to construct the RNA-Seq libraries. Total RNAs were isolated from leaf samples using the TRIzol reagents (Invitrogen, United States). The obtained RNA samples were applied to construct RNA-Seq libraries through the Illumina Hiseq 4000 platform. Raw sequencing data were submitted to the NCBI Sequence Read Archive (SRA) database (No. PRJNA679081). Finally, the clean reads were mapped to a reference tomato genome iTAGv2.3 as described previously by Trapnell et al. (2009). Comparative analyses between the RNA-Seq libraries of the control and inoculated plants were applied to identify differentially expressed lncRNAs (DELs). The expression of lncRNAs was determined by the normalized read counts using Cufflinks. The DELs were identified using R package DEGseq with $\log_2$ (fold change) $\geq$1.0 and a false discovery rate (FDR) adjusted $P \leq 0.05$ (Anders and Huber, 2010).

Construction of MSTRG18363-, Mutated MSTRG18363-, and miR1918-Overexpressing Plasmids

The sequences of four MSTRG18363 variants were obtained by RNA-Seq in this study (**Supplementary Figure 1**). The MSTRG18363 variants were amplified by PCR, and positive clones were sequenced. The MSTRG18363 sequences were digested and ligated into the plant binary vector pCAMBIA1300. An artificially synthesized form of MSTRG18363 (asf-MSTRG18363, consensus sequence of four MSTRG18363 variants; **Supplementary Figure 2**) was also inserted into the plant binary vector pCAMBIA1300. Furthermore, a mutated lncRNA23468 carrying six base mutation paring with miR1918 (masf-MSTRG18363; **Supplementary Figure 3**) was artificially synthesized by Tsingke Biotech (Nanjing, China) and cloned into the pCAMBIA1300. Moreover, genomic DNA from tomato plants was used as the template to amplify the precursor sequence of miR1918 (miRBase accession: MI0008353) by polymerase chain reaction (PCR). The amplified products were sequenced and cloned into the pCAMBIA1300. The constructed plasmids were introduced into *Agrobacterium tumefaciens* strain GV3101. Subsequently, *A. tumefaciens* harboring the recombinant plasmids was transformed into tomato plants as reported previously by Sharma et al. (2009). To further screen the transgene, genomic DNA from primary transformants (T0) was used as the template to amplify the NPT-II gene (Porebski et al., 1997). The primers used for the construction of recombinant plasmids are listed in **Supplementary Table 1**.

Virus-Induced Gene Silencing

To develop a virus-mediated gene silencing (VIGS) system for tomato, the virus vectors (pTRV1 and pTRV2) were applied in our experiments. The VIGS systems were carried out as reported previously by Liu et al. (2002). In the VIGS systems, cDNA fragment of phytoene desaturase gene (PDS) from tomato plants were inserted into the pTRV2. In addition, to construct the VIGS system for silencing other target genes, the corresponding cDNA fragments were inserted into the pTRV2, respectively. All the vectors including the pTRV1 and recombinant pTRV2 were introduced into *A. tumefaciens* strain GV3101. *A. tumefaciens* harboring the pTRV1 or pTRV2-derived plasmids were mixed in a volume ratio of 1:1. Subsequently, the mixture was infiltrated into 7-day-old tomato cotyledons. Finally, these treated plants were cultured for 3 weeks at 21°C. The primers used for the construction of TRV-based recombinant plasmids are supplemented in **Supplementary Table 1**.

3, 3′-Diaminobenzidine (DAB) and Trypan Blue Staining

For *in vivo* localization of H_2O_2, DAB staining was carried out to analyze the accumulation of H_2O_2 in leaves as described previously by Lee et al. (2002). Leaf tissues were immersed in the DAB staining solution (pH 3.0; 1 mg L^{-1} of DAB, 0.05% v/v Tween 20) and vacuum-filtrated for 5 min. Then, the stained leaves were incubated at room temperature in the dark for 4 h, followed by bleaching with destaining solution (acetic acid: ethanol: glycerol, 1:1:1) for 12 h. For detection of cell death, trypan blue staining was carried out according to the method (Jiang et al., 2018). Briefly, pathogen-infected leaves were incubated in 100 ml of staining solution (80 mg of trypan blue, 20 ml of sterile distilled water, 20 ml of lactic acid, 20 ml of glycerol and 20 ml of phenol) at room temperature in the dark for 30 min. Then, the stained leaves were bleached with destaining solution (acetic acid: ethanol, 1:3) for 6 h.

Quantitative Real-Time (qPCR) Analysis

The transcription of lncRNAs, miRNAs and target genes was examined using qPCR analyses. The miRNA Universal

SYBR qPCR Master Mix (Vazyme Biotech, Nanjing) was applied to conduct qPCR reactions of miRNAs. The qPCR reactions of lncRNAs and target genes were conducted using the SYBR Premix Ex TaqTM II kit (TaKaRa, Japan). All the reactions were conducted using an ABI 7500 PCR machine according to the method (Zhou et al., 2016; Meng et al., 2020). The *SlActin* gene was used as a control to normalize gene expression using the $2^{-\Delta\Delta CT}$ method. The primers used for qPCR reactions are supplemented in **Supplementary Table 1**.

Statistical Analysis

The data were statistically analyzed by the IBM SPSS software. The data represented the means ± SD from three biological repeats. Significant difference between different experimental groups was analyzed using Tukey's *post hoc* ($^{*}P < 0.05$, $^{**}P < 0.01$; ns, not significant) or Duncan's multiple range tests (different letters indicated statistically different at $P < 0.05$) for one way ANOVA.

RESULTS

Bacillus subtilis SL18r Increased Tomato Resistance Against *B. cinerea* Infection

To examine whether rhizo-inoculation with *B. subtilis* SL18r enhanced the ability of tomato plants to withstand the invasion of *B. cinerea*, pot experiments were conducted (**Figure 1A**). Seven-day-old tomato seedlings were firstly cultured in soil for 3 weeks and were then poured with cell suspension of SL18r at the different concentrations of 4×10^6, 2×10^7, and 1×10^8 CFU g^{-1} of soil for 3 days, respectively, and tomato plants treated with the PBS solution were used as the control. Subsequently, 5 μl of 2×10^5 spore ml^{-1} spore suspension of *B. cinerea* were inoculated on the detached leaves. As shown in **Figure 1B**, the inoculation with SL18r at the density of 4×10^6 CFU g^{-1} soil could not suppress *B. cinerea* infection at 5 dpi. In contrast, higher inoculum dosage of SL18r at the density of 2×10^7 or 1×10^8 CFU g^{-1} soil distinctly reduced necrotic spots and lesion diameters on the detached leaves. DAB staining showed that the production of H_2O_2 were notably less in leaves of tomato plants treated with higher inoculum dosage of SL18r compared with the controls (**Figure 1C**). Trypan blue staining displayed more cell death in the control leaves compared with the inoculated leaves (**Figure 1D**). In the whole-plant inoculation tests, the control and inoculated plants were sprayed with 2×10^5 spore ml^{-1} spore suspension of *B. cinerea* on the leaf surface for 5 days. As shown in **Figure 1E**, higher inoculum dosage of SL18r significantly lowered disease index in tomato plants compared with the controls. In line with the reduced disease occurrence, the SL18r-inoculated leaves displayed lower the expression of *BcActin* than the control leaves (**Figure 1F**). Our findings indicated that the increased disease resistance of plants conferred by SL18r was dependent on its inoculum dose.

Identification of Differentially Expressed LncRNAs

To unravel the molecular responses of SL18r-inoculated plants to *B. cinerea* infection, RNA-Seq was conducted for comparative analyses of the lncRNA expression profiles between the control and inoculated plants. Tomato plants were inoculated with SL18r for 3 days. After 0, 24, and 48 h of pathogen infection, leaf samples were used for the extraction of total RNAs to perform RNA-Seq (**Figure 2A**). Compared with the controls, a total of 55, 34, and 15 lncRNAs as differentially expressed lncRNAs (DELs) in the inoculated plants were screened with a FDR-adjusted $P < 0.05$ and fold change >1.0 or <-1.0), including 34, 14, and 10 upregulated DELs, and 20, 21, and 5 downregulated DELs, respectively (**Figures 2B–E** and **Supplementary Table 2**). Among these DELs, a total of 6 upregulated DELs were commonly expressed in the inoculated plants at different pathogen-infected times (**Figures 2F,G**), which included MSTRG14877.1, MSTRG19536.1, and four alternatively spliced forms of MSTRG18363. In accordance to this, qPCR analyses showed that the SL18r-inoculated plants exhibited significantly higher transcription of MSTRG14877.1, MSTRG19536.1 and four variants of MSTRG18363 (which could not be distinguished by qPCR) as compared to the controls (**Figures 2H–J**).

Activation of MSTRG18363 Expression Was Required for *B. subtilis* S18r-Induced Disease Resistance

To explore the functions of MSTRG18363 in the responses of tomato leaves to the invasion of *B. cinerea*, the pCAMBIA1300-MSTRG18363 plasmids were transformed into tomato plants. Compared with the wide-type (WT) plants, four MSTRG18363 variants and an artificially synthesized form of MSTRG18363 (asf-MSTRG18363, consensus sequence of four MSTRG18363 variants; **Supplementary Figure 1**) were highly transcribed in transgenic plants (**Figure 3A**). In *in vitro* assays, after 5 days of *B. cinerea* infection, the WT plants displayed more serious disease symptoms with larger lesion diameters than all the transgenic plants (**Figures 3B,C**). In *in vivo* assays, these plants were infected by *B. cinerea* for 5 days. The SL18r-inoculated plants displayed significantly lower disease index than the controls (**Figure 3D**). Accordantly, the expression of *BcActin* was markedly less in the SL18r-inoculated leaves than the control leaves (**Figure 3E**). In addition, tomato plants overexpressed asf-MSTRG18363 also exhibited stronger resistance against *B. cinerea* compared with the WT plants (**Figures 3B–E**).

Furthermore, the VIGS system was developed to silence the expression of MSTRG18363 for analyzing its roles in the SL18r-induced disease resistance. Compared with the *TRV::00* leaves, the tomato *PDS* gene was considerably suppressed in the *TRV::PDS* leaves, showing the photo-leaching symptoms (**Figure 4A**). Moreover, the cDNA fragment of MSTRG18363 was inserted into the TRV2 plasmids (*TRV::MSTRG18363*), and the *TRV::00* plants were used as the controls. After 3 weeks of VIGS treatment, these plants were subjected to

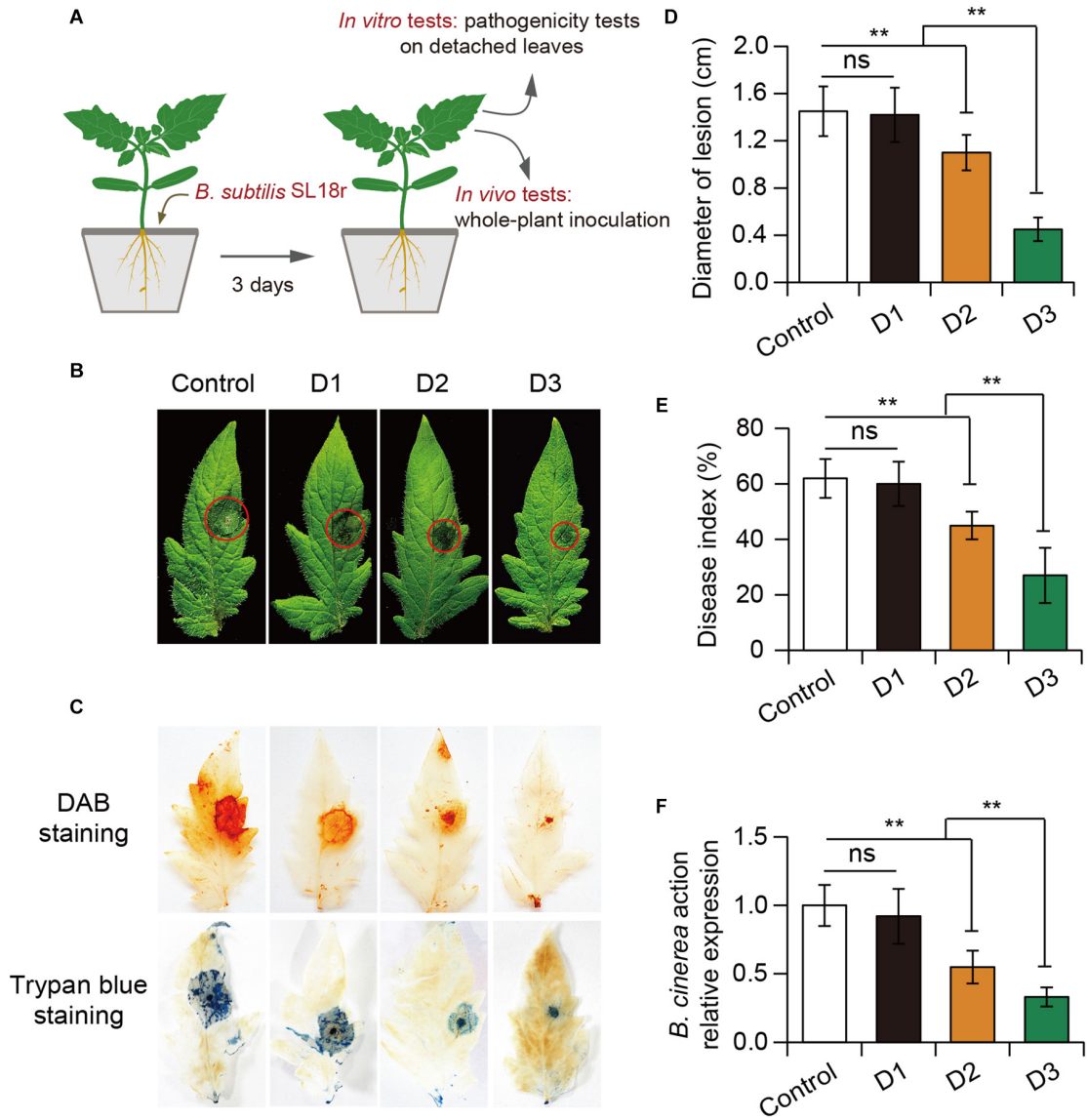

FIGURE 1 | Soil inoculation with *Bacillus subtilis* SL18r increased tomato resistance against the invasion of *Botrytis cinerea*. **(A)** Seven-day-old tomato seedlings were initially cultivated in soil for 3 weeks and were then exposed to different doses of SL18r (D1: 4×10^6, D2: 2×10^7, and D3: 1×10^8 CFU g^{-1} of soil). After 3 days of culture, both the control and inoculated plants were used to perform *in vitro* and *in vivo* assays. **(B)** Phenotypes of detached leaves from both the control and inoculated plants at 5 dpi. Diaminobenzidine (DAB) and trypan blue staining **(C)** and lesion diameters **(D)** of the detached leaves. Moreover, in the whole-plant inoculation tests, the collected spore suspension of *B. cinerea* was applied to spray the leaves. Disease index **(E)** and *B. cinerea* actin gene expression **(F)** of the control and inoculated plants was detected at 5 dpi. Significant difference was analyzed using Tukey's *post hoc* (**$P < 0.01$; ns, not significant).

treatment with SL18r for 3 days. The transcription levels of MSTRG18363 were observably lower in the *TRV::MSTRG18363* leaves than the *TRV::00* leaves (**Figure 4B**). However, the *TRV::00* plants displayed no phenotypic discrepancy with the *TRV::MSTRG18363* plants (**Figure 4A**). After 5 days of pathogen infection, the *TRV::00* leaves exhibited higher expression of MSTRG18363 than the *TRV::MSTRG18363* leaves (**Figure 4B**). At 5 dpi, detached leaves of the *TRV::MSTRG18363* plants exhibited more serious disease symptoms and larger lesion diameters than the *TRV::00* plants (**Figures 4C,D**). In *in vivo* assays, the *TRV::MSTRG18363* plants displayed higher disease index than the *TRV::00* plants (**Figure 4E**). Our data suggested that induction of MSTRG18363 expression by SL18r resulted in stronger resistance of tomato plants against *B. cinerea* infection.

MSTRG18363 as a miRNA Decoy to Suppress the Expression of miR1918

As shown in **Figure 5A**, the binding site of miR1918 by MSTRG18363 was predicted using psRNATarget. To examine whether miR1918 and MSTRG18363 affected the responses of tomato plants to *B. cinerea* infection, their transcripts were

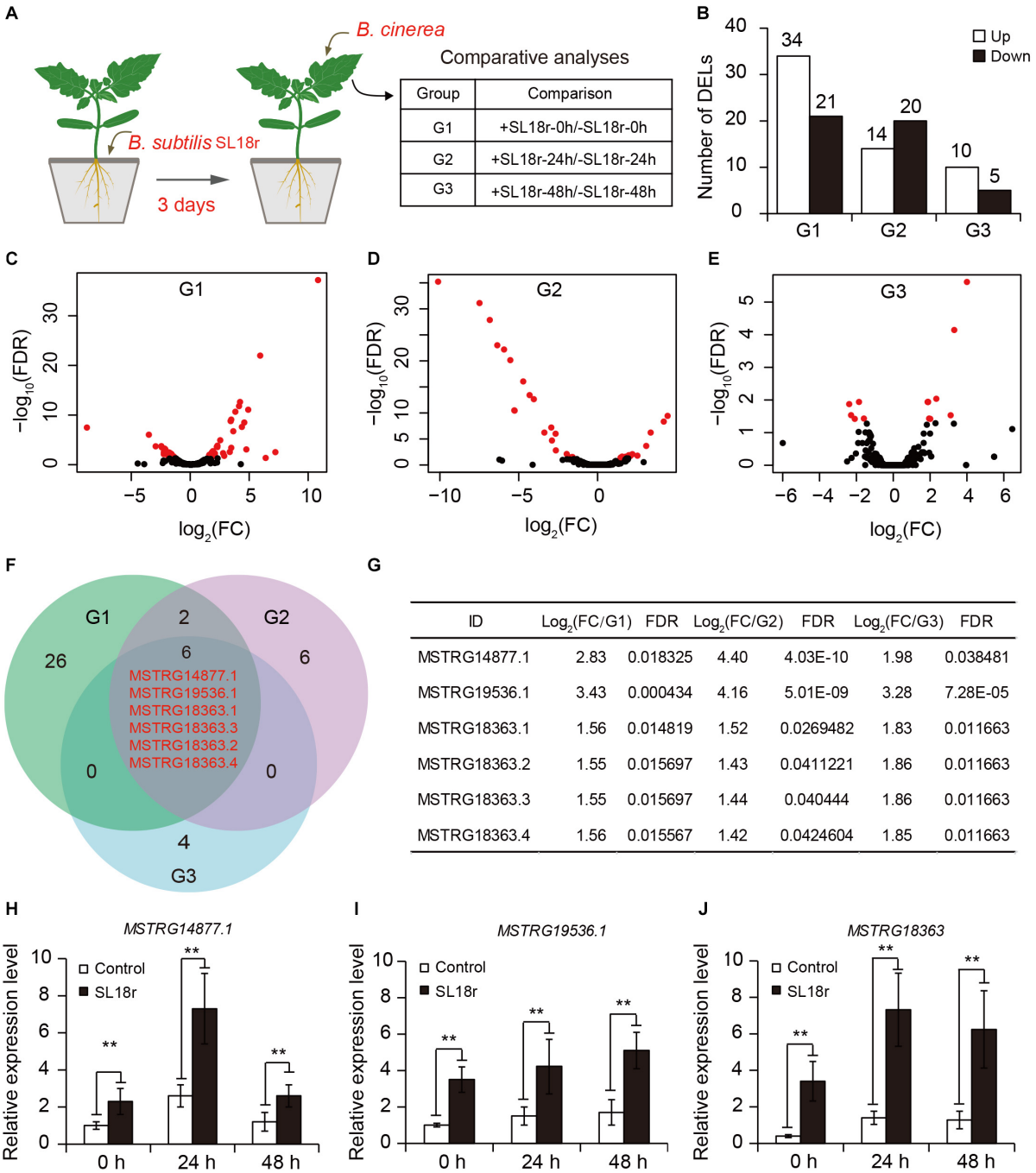

ID	Log_2(FC/G1)	FDR	Log_2(FC/G2)	FDR	Log_2(FC/G3)	FDR
MSTRG14877.1	2.83	0.018325	4.40	4.03E-10	1.98	0.038481
MSTRG19536.1	3.43	0.000434	4.16	5.01E-09	3.28	7.28E-05
MSTRG18363.1	1.56	0.014819	1.52	0.0269482	1.83	0.011663
MSTRG18363.2	1.55	0.015697	1.43	0.0411221	1.86	0.011663
MSTRG18363.3	1.55	0.015697	1.44	0.040444	1.86	0.011663
MSTRG18363.4	1.56	0.015567	1.42	0.0424604	1.85	0.011663

FIGURE 2 | Identification of differentially expressed lncRNAs (DELs) between the control and SL18r-inoculated plants. **(A)** Seven-day-old tomato seedlings were initially cultivated in soil for 3 weeks and were then treated without (−SL18r) or with SL18r (+SL18r) at the final density of 1×10^8 CFU g^{-1} of soil for 3 days. Then, the leaves were sprayed with 2×10^5 spore mL^{-1} of spore suspension of *Botrytis cinerea* and were used to conduct RNA-Seq. **(B)** Number of DELs. **(C–E)** Volcano plot of DELs. Red points represented the DELs. **(F)** Venn diagram of upregulated DELs among different experimental groups. G1, +SL18r-0h/-SL18r-0h; G2, +SL18r-24h/-SL18r-24h; G3, +SL18r-48h/ -SL18r-48h. **(G)** The expression profiles of the shared DELs among different experiment groups. **(H–J)** qPCR analyses of the shared DELs. Significant difference was analyzed using Tukey's *post hoc* (**$P < 0.01$).

quantified in the pathogen-infected leaves. The transcription levels of miR1918 were markedly increased in the non-inoculated (control) leaves at 48 h post infection (hpi), whereas the expression of MSTRG18363 was significantly reduced (**Figures 5B,C**). However, the opposite trends were observed for the expression of miR1918 and MSTRG18363 in the leaves of the SL18r-inoculated plants (**Figures 5D,E**). Moreover, the recombinant plasmid pCAMBIA1300-miR1918

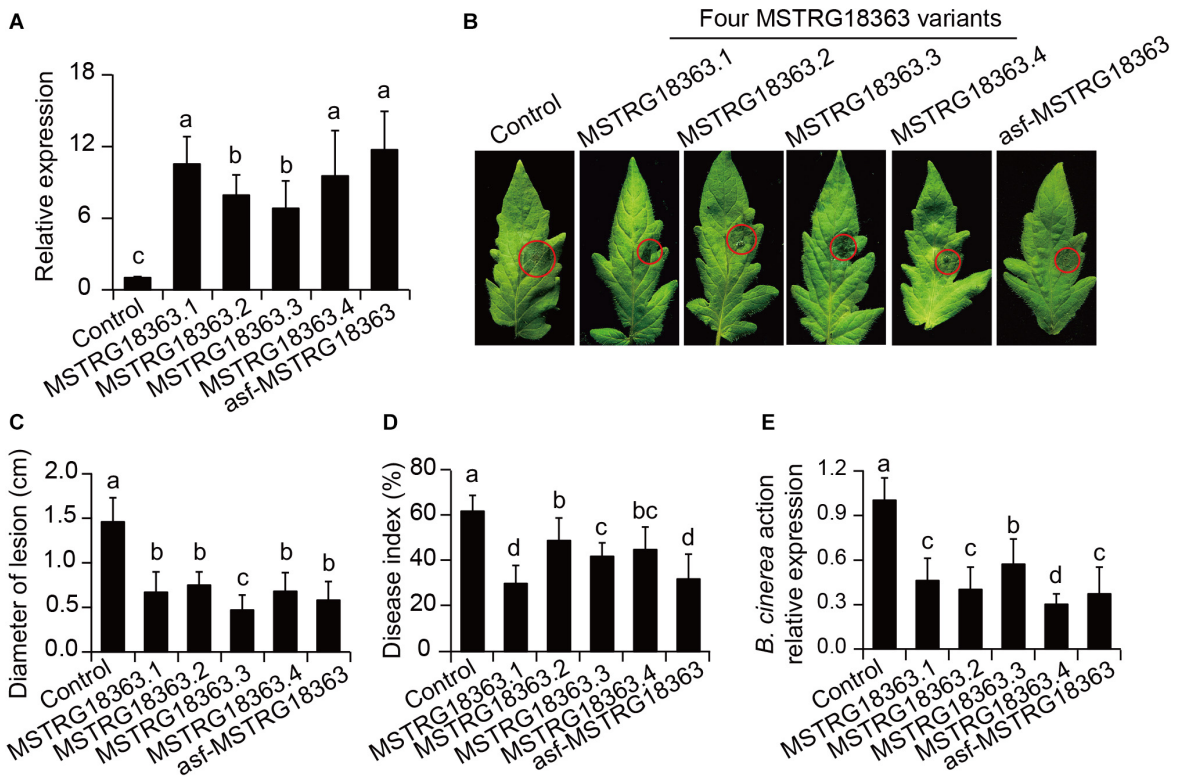

FIGURE 3 | Overexpression of four MSTRG18363 variants and artificially synthesized form of MSTRG18363 (asf-MSTRG18363, consensus sequence of four MSTRG18363 variants) increased the ability of transgenic tomato plants to inhibit the infection of *Botrytis cinerea.* Four-week-old tomato plants were used to perform *in vitro* (pathogenicity tests on detached leaves) and *in vivo* (whole plant inoculation tests) assays. **(A)** qPCR analyses of MSTRG18363 expression in transgenic tomato plants. Phenotypes **(B)** and lesion diameters **(C)** of detached leaves from the MSTRG18363-overexpressing plants at 5 dpi. In the whole-plant inoculation tests, the leaves were sprayed with 2×10^5 spore mL^{-1} spore suspension of *B. cinerea*. Disease index **(D)** and the expression of *BcActin* **(E)** were analyzed at 5 dpi. Different letters represented significant difference using Duncan's multiple range tests at $P < 0.05$ for one way ANOVA.

was introduced into tomato plants. Compared with the wide-type (WT) plants, two independent miR1918-overexpressing lines (OE-miR1918#3 and #7) exhibited higher expression levels of miR1918 (**Figure 5F**). Detached leaves from both the WT and miR1918-overexpressing lines were subjected to the infection of *B. cinerea* for 5 days. The leaves from two miR1918-overexpressing lines displayed more serious disease symptoms than those of the controls (**Figure 5G**). Lesion diameters were also larger in the leaves of the miR1918-overexpressing lines than the controls (**Figure 5H**). In the whole-plant inoculation tests, disease index and abundance of *B. cinerea* was markedly higher in the two miR1918-overexpressing lines than the WT plants (**Figures 5I,J**).

To explore whether MSTRG18363 functioned by pairing with miR1918, base mutation was introduced into the paired sites of MSTRG18363 with miR1918 (mMSTRG18363) (**Figure 6A**). The transcription levels of miR1918 were investigated in the leaves of tomato plants that overexpressed MSTRG18363 by qPCR analyses. Overexpression of asf-MSTRG18363 reduced the transcription of miR1918 in tomato plants compared with the controls (**Figure 6B**). The regulation between MSTRG18363 and miR1918 was further analyzed by the transient expression system of *Nicotiana benthamiana*. The *Agrobacterium* strain harboring pCAMBIA1300-miR1918 was injected into leaf cells, which led to marked increases in the expression of miR1918 at 72 h compared with the controls. Then, the *Agrobacterium* strains carrying pCAMBIA1300-asf-MSTRG18363 and -masf-MSTRG18363 were injected into the leaves that overexpressed miR1918. As shown in **Figure 6C**, the expression of miR1918 was notably decreased after the introduction of asf-MSTRG18363, but was not found for masf-MSTRG18363. The expression of miR1918 was also less in the asf-MSTRG18363-overexpressing lines than the controls (**Figure 6A**). However, overexpression of masf-MSTRG18363 in tomato plants did not reduce the expression of miR1918 (**Figure 6A**). Furthermore, asf-MSTRG18363-overexpressing lines exhibited the increased transcription of the target gene *SlATL20* (Solyc01g095820 encoding a RING-H2 finger protein ATL20-like) of miR1918 (Luan et al., 2016). These results indicated that MSTRG18363 may function as a ceRNA for decoying miR1918 in tomato plants.

The VIGS system was further applied to explore the function of the target gene *SlATL20* of miR1918 in tomato plants. At 3 weeks after infiltration, the gene transcript abundance was greatly repressed in the leaves of *TRV::SlATL20* plants (**Figure 6D**). As shown in **Figure 6E**, more severe disease symptoms were observed in the *TRV::SlATL20* plants compared

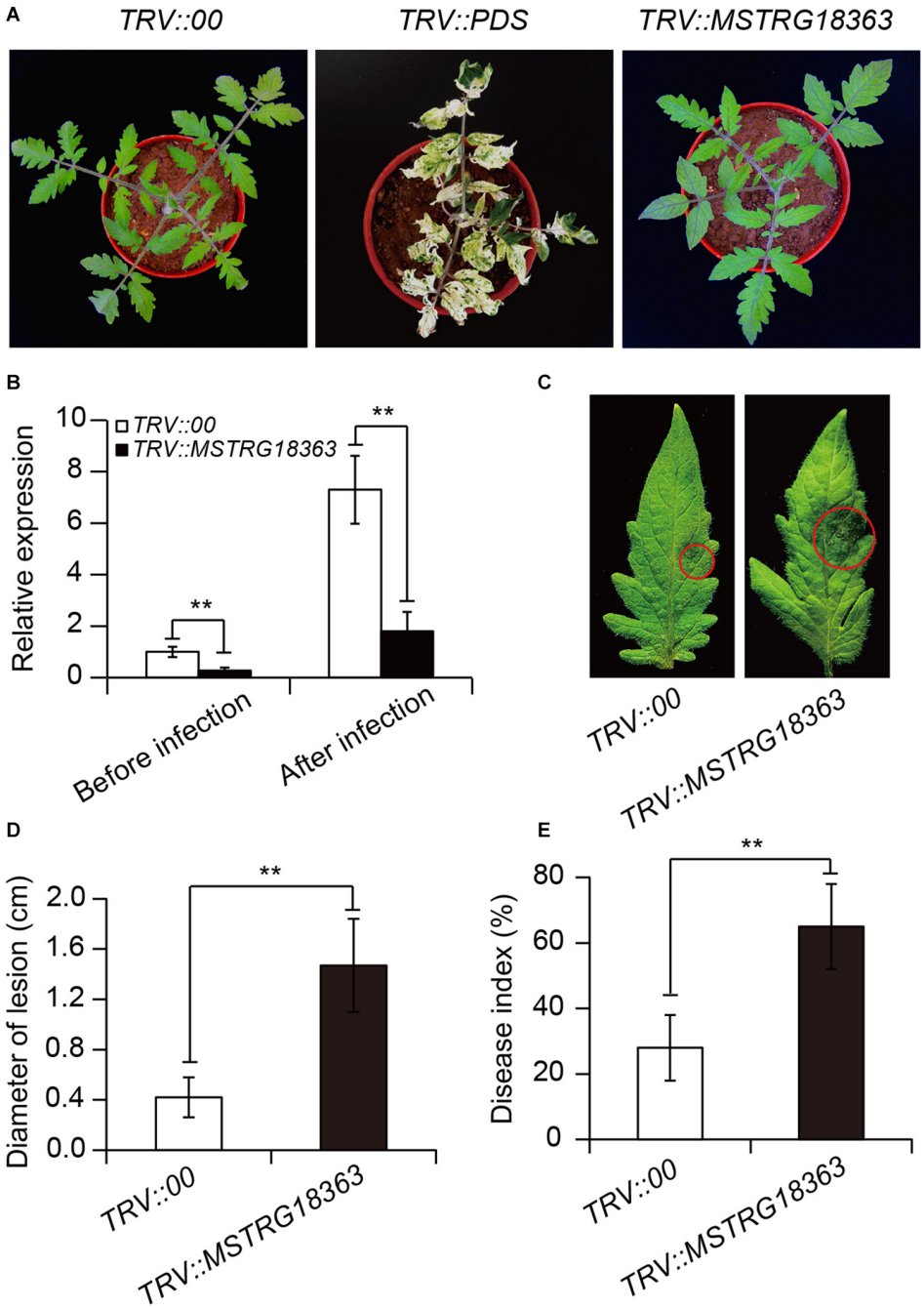

FIGURE 4 | Silencing of MSTRG18363 largely weakened the SL18r-induced tomato resistance against the invasion of *Botrytis cinerea*. **(A)** Phenotype of tomato plants treated with *TRV::00*, *TRV::PDS* or *TRV::MSTRG18363* after 3 weeks of culture. **(B)** The expression of MSTRG18363 in both the leaves *TRV::00* and *TRV::MSTRG18363* tomato in the presence of SL18r before or after 5 days of *B. cinerea* infection. Phenotypes **(C)** and lesion diameters **(D)** of detached leaves from both the *TRV::00* and *TRV::MSTRG18363* plants at 5 dpi. In the whole-plant inoculation tests, the leaves were sprayed with 2×10^5 spore mL^{-1} of spore suspension of *B. cinerea*. **(E)** Disease index of the *TRV::00* and *TRV::MSTRG18363* plants was detected at 5 dpi. Significant difference was analyzed using Tukey's *post hoc* (**$P < 0.01$).

with the controls at 5 dpi (**Figure 6E**). The silenced plants had larger lesion diameters, higher disease index and more abundance of *B. cinerea* compared with the controls (**Figures 6F–H**). Furthermore, the SL18r-induced disease resistance was largely weakened in the *TRV::SlATL20* plants, as reflected by *in vivo* and *in vitro* assays of pathogen infection, which was similar to the observation for the miR1918-overexpressing lines (**Figures 6E–H**).

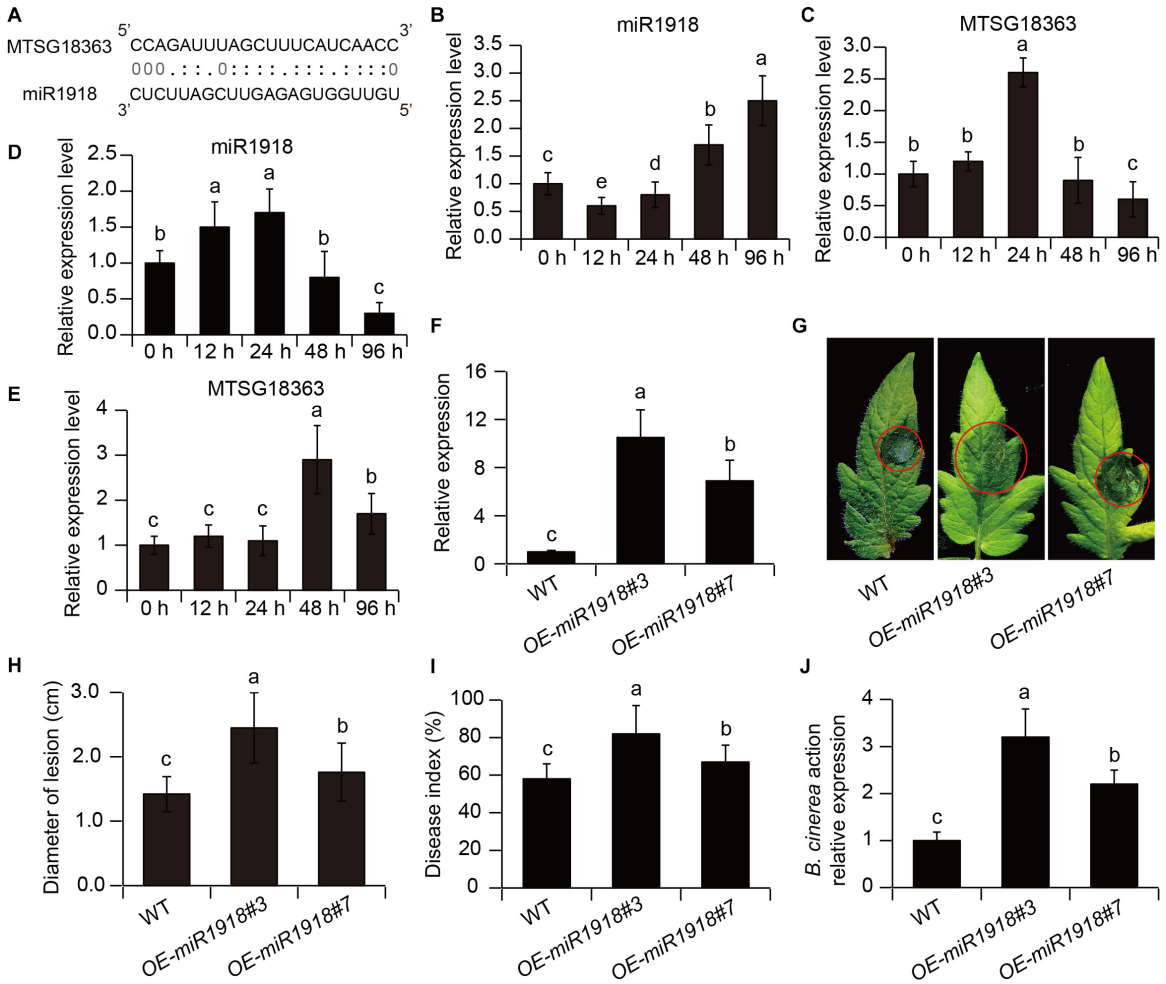

FIGURE 5 | MSTRG18363 decoyed miR1918 in tomato plants. **(A)** Predicted base-pairing interactions between miR1918 and the binding site of MSTRG18363. The expression profiles of miR1918 and MSTRG18363 in both the control **(B,C)** and SL18r-inoculated **(D,E)** plants at different time points of pathogen infection. **(F)** The transcription of miR1918 in leaves of two independent miR1918-overexpressing tomato lines. **(G)** Phenotypes and **(H)** lesion diameters of detached leaves from the two independent transgenic lines at 5 dpi. Moreover, in the whole-plant inoculation tests, **(I)** disease index and **(J)** *Botrytis cinerea* actin gene expression of the control and transgenic lines was detected at 5 dpi. Different letters represented significant difference using Duncan's multiple range tests at $P < 0.05$ for one way ANOVA.

DISCUSSION

The molecular mechanisms underlying the PGPR-mediated ISR responses have recently been investigated extensively in many plant species such as tomato (Yan et al., 2002), *Arabidopsis* (Verhagen et al., 2004) and melon (García-Gutiérrez et al., 2013). The ISR processes involving several regulatory components have been well explored (Van Wees et al., 2008; Banks et al., 2012; Timmermann et al., 2019), but the roles of lncRNAs in the PGPR-induced ISR responses remain elusive so far. It is increasingly evidenced that lncRNAs can act as positive regulators of plant innate immunity: pathogen infection induces the expression of several miRNAs to suppress plant defense responses; meanwhile, a healthy plant is able to activate the lncRNA-mediated defense responses for decoying these negative regulators of defense systems (Jing et al., 2019; Hou et al., 2020; Jiang et al., 2020). In this study, beneficial rhizobacteria strain *B. subtilis* SL18r elevated the ability of tomato plants to inhibit the invasion of *B. cinerea*. Our results demonstrated that the SL18r-induced expression of MSTRG18363 conferred the increased host disease resistance via decoying miR1918, indicating that the PGPR-mediated ISR was closely associated with activation of lncRNA-mediated defense pathways.

Many studies have shown that LncRNAs can modulate the transcription of target genes *in cis* or *in trans* (Mercer and Mattick, 2013), and function as molecular scaffolds for recruiting the chromatin-modifying complexes (Fan et al., 2015; Holoch and Moazed, 2015). LncRNAs has also been reported to act as important regulators that bind to miRNA by the eTM sites in the sequences of lncRNAs and further inhibit the interactions between miRNA and its target mRNA, thereby enhancing the transcription of the target genes (Jing et al., 2019;

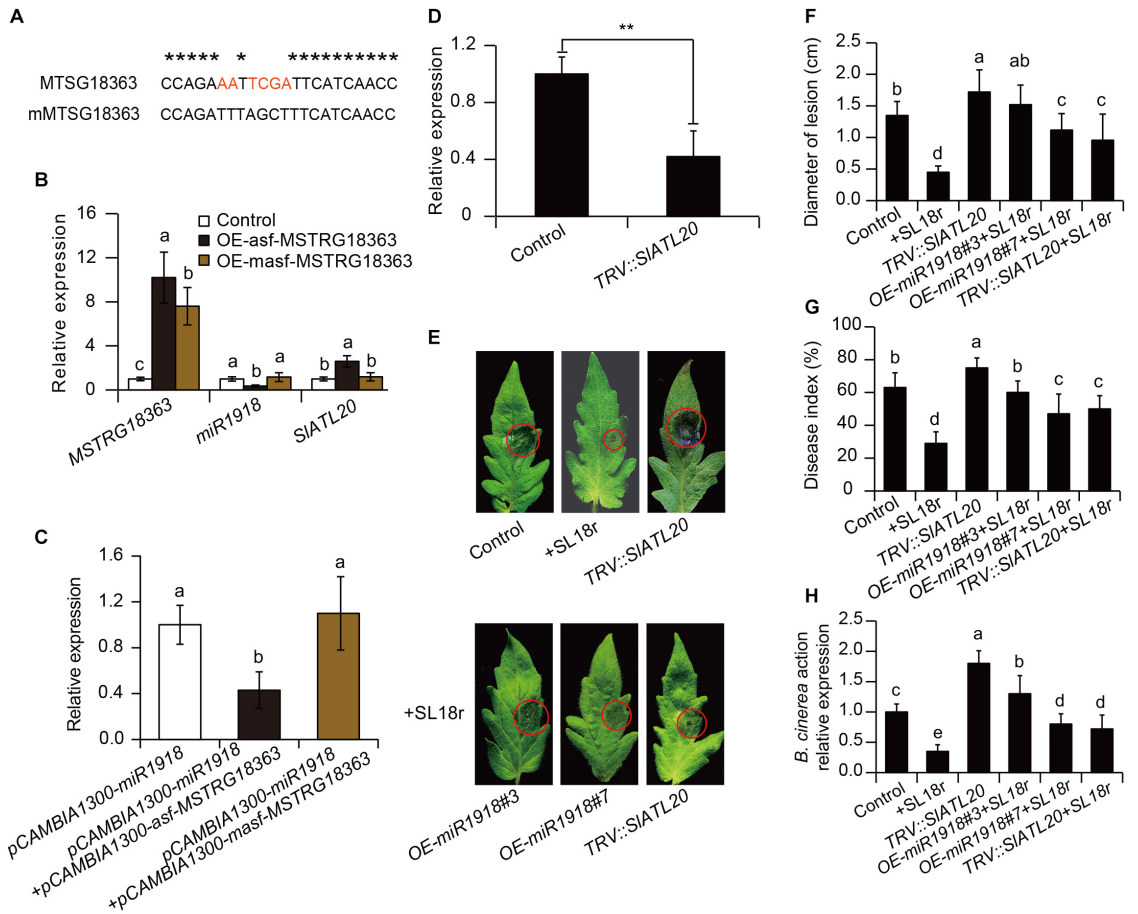

FIGURE 6 | *Bacillus subtilis* SL18r-induced expression of MSTRG18363 functioned to mediate the *SlATL20* gene by decoying miR1918. **(A)** Predicted base-pairing interactions between miR1918 and the binding site of MSTRG18363 with the designed base mutation. Red letters indicated mutated bases. **(B)** qPCR analysis of MSTRG18363, miR1918 and *SlATL20* in the control, OE-asf-MSTRG18363, and OE-masf-MSTRG18363 tomato plants. **(C)** MSTRG18363 suppressed the expression of miR1918 in *Nicotiana* systems. The transcription of the miR1918 after the *Agrobacterium* strain harboring pCAMBIA1300-asf-MSTRG18363 and -masf- MSTRG18363 were introduced into the tobacco leaves that overexpressed miR1918. **(D)** The transcription of *SlATL20* in both the *TRV::00* and *TRV::SlATL20* tomato leaves. **(E)** Phenotypes of detached leaves from the *TRV::00*, SL18r-inoculated and *TRV::SlATL20* plants, and from the miR1918-overexpressing lines and *TRV::SlATL20* plants inoculated with SL18r at 5 dpi. **(F)** Lesion diameters of the detached leaves. Moreover, in the whole-plant inoculation tests, the leaves were sprayed with 2×10^5 spore mL^{-1} spore suspension of *Botrytis cinerea*. **(G)** Disease index and **(H)** *B. cinerea* actin gene expression of above the plants was detected at 5 dpi. Different letters represented significant difference using Duncan's multiple range tests at $P < 0.05$ for one way ANOVA. Significant difference was analyzed using Tukey's *post hoc* (**$P < 0.01$) or Duncan's multiple range tests (different letters indicated statistically different at $P < 0.05$) for one way ANOVA.

Hou et al., 2020). IPS1 contains the eTM site to target the phosphate starvation-induced miR399 and thus increases the transcription of *PHO2* in *Arabidopsis* plants, thereby controlling the phosphate homeostasis (Ajmera et al., 2018). Similarly, PDIL1 can suppress the miR399-mediated *MtPHO2* degradation to control the P deficiency responses in *Medicago truncatula* (Wang et al., 2017). MLNC3.2 and MLNC4.6 can decoy the miR156a to inhibit the degradation of *SPL2-like* and *SPL33* genes in apple fruit, thereby regulating the light-induced anthocyanin biosynthesis (Yang et al., 2019). Overexpression of lncRNA23468 and lncRNA39026 in tomato plants reduces the expression of miR482b and miR168a, respectively (Jing et al., 2019; Hou et al., 2020), which contribute to the increased resistance of plants to *P. infestans*. However, it remains unclear whether the lncRNA-mediated pathways are involved in the PGPR-induced ISR responses. In this study, we examined which of the DELs between the control and SL18r-inoculated plants were likely involved in mediating the ISR responses. We further focused on the investigation of these DELs that potentially targeted miRNAs, which were involved in negative regulation of plant defense. Moreover, it was observed that four MSTRG18363 variants contained potential sites for binding to miR1918. The expression of MSTRG18363 was negatively related to the accumulation of miR1918 in the pathogen-infected leaves. Therefore, the interactions of MSTRG18363 with miR1918 may participate in the SL18r-mediated ISR processes in tomato plants.

It has previously been indicated that miR1918 negatively regulates plant defense systems in tomato plants (Luan et al., 2016). In tomato plants, miR1918 is present in target region of a putative RING finger gene *SlATL20* belonging to the zinc

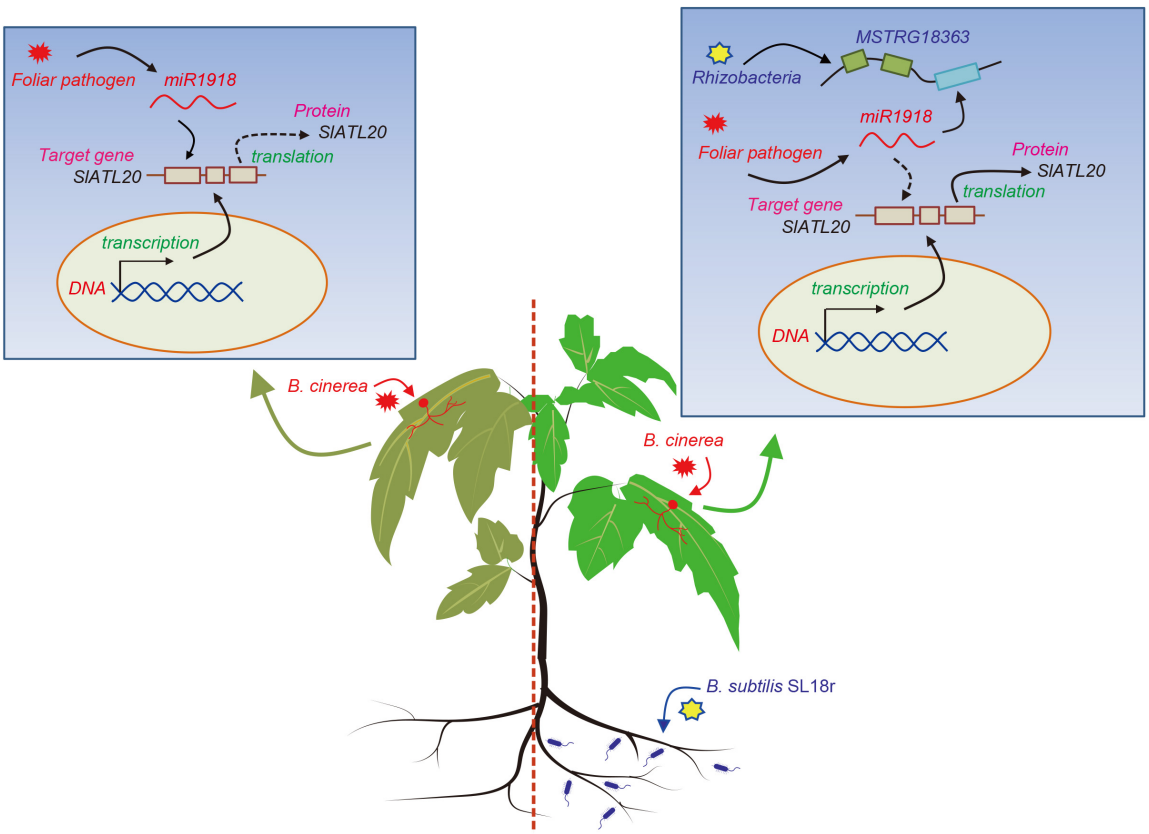

FIGURE 7 | A proposed model was illustrated for *Bacillus subtilis* SL18r-induced ISR. When tomato plants were infected by the foliar pathogen *Botrytis cinerea,* the expression of miR1918 was considerably increased. However, high-level transcription of miR1918 suppressed the expression of the target gene *SlATL20* and further negatively regulated plant immune systems. Upon exposure to *B. subtilis* SL18r, the expression of MSTRG18363 was greatly stimulated in the leaves of tomato plants. Subsequently, the *B. cinerea*-initiated miR1918 was quickly decoyed by MSTRG18363, which prevented the miR1918-mediated inhibition of *SlATL20* transcripts. This contributed to the increased resistance of SL18r-inoculated plants against *B. cinerea* infection.

finger-coding family genes, which can mediate the growth and development, and stress adaption of plants (Zeng et al., 2006; Matthews et al., 2009; Luan et al., 2016). Several RING finger proteins are closely related to the mediation of plant ubiquitination, which is responsible for plant defense against abiotic and biotic stresses. For example, the transcription of *RFP1*, encoding a RING finger protein-coding gene from *Vitis pseudoreticulata,* is greatly induced in *V. pseudoreticulata* plants by the grapevine powdery mildew *Uncinula necator* (Van Wees et al., 2008). *Arabidopsis* plants overexpressing *VpRFP1* displays the increased resistance against *Arabidopsis* powdery mildew *Golovinomyces cichoracearum* and *Pseudomonas syringae* pv. *tomato* DC3000 (Yu et al., 2011). In *V. pseudoreticulata*, the RING finger protein gene *EIRP1* has been reported to regulate plant defense responses via promoting the proteolysis of VpWRKY11 (Yu et al., 2013). Furthermore, overexpression of *CaRING1* encoding a putative E3 ubiquitin ligase markedly enhances the resistance of *Arabidopsis* plant to *P. syringae* pv *tomato* and *Hyaloperonospora arabidopsidis* (Lee et al., 2011). Our findings revealed that the expression of miR1918 was negatively correlated with the expression of *SlATL20* and that there were more serious disease symptoms in the miR1918-overexpressing plants, indicating that miR1918 was involved in the silencing of *SlATL20*. Furthermore, silencing of *SlATL20* resulted in the increased susceptibility of tomato plants to *B. cinerea* infection. Therefore, we speculated that MSTRG18363 activated the ISR responses by regulation of miR1918-mediated plant ubiquitination. To confirm this hypothesis, the impacts of MSTRG18363-overexpression on disease resistance were assessed. Overexpression of MSTRG18363 reduced the expression of miR1918 and enhanced disease resistance in transgenic tomato plants, while silencing of MSTRG18363 increased the transcription levels of miR1918 and reduced disease resistance in the SL18r-inoculated plants. These observations were in concert with our conclusion that MSTRG18363 were positively involved in priming plants from *B. cinerea* infection via decoying miR1918.

CONCLUSION

In summary, previous studies exploring the mechanisms of PGPR-induced ISR have been focused on the functions of protein regulators, miRNAs, JA-, and SA-signaling

pathways, yet the involvement of lncRNAs in the rhizobacteria-primed ISR processes has not been investigated so far. Our data demonstrated that beneficial rhizobacteria strain *B. subtilis* SL18r was able to increase the resistance of tomato plants against the invasion of *B. cinerea* via the MSTRG18363-mediated decoy of miR1918, thereby contributing to efficient activation of ISR. As shown in **Figure 7**, a new model was proposed for illustrating the mechanisms of the SL18r-mediated disease resistance, in which pathogen infection induced a marked increase in miR1918 transcripts and thus inhibited the expression of *SIATL20* (the target gene of miR1918), leading to the reduced disease resistance. Upon infection in a primed state, the expression of the pathogen-initiated miR1918 was quickly quenched. The rhizobacteria-induced host resistance against foliar pathogens was in such an effective manner that did not require for activating a series of pathogenesis-related proteins and best fitted plant growth.

DATA AVAILABILITY STATEMENT

The datasets presented in this study can be found in online repositories. The names of the repository/repositories and accession number(s) can be found in the article/**Supplementary Material**.

AUTHOR CONTRIBUTIONS

CY and CZ conceptualized the research, responsible for the funding acquisition, and did the supervision. JZ and NQ conducted the investigation and formal analysis. CZ and JZ conducted the experiments. CZ, JZ, and NQ analyzed the results. CY, JG, and CZ wrote the original draft. JZ, JG, and NQ reviewed and edited the manuscript. All authors contributed to the article and approved the submitted version.

FUNDING

This research was funded by the Outstanding Talent Cultivation Program in Colleges and Universities of Education Department of Anhui Province (gxypZD2020038), Undergraduate Innovation and Entrepreneurship Training Program of Anhui Province (S201910879190), Key R&D Program Projects of Anhui Province (202004a06020003), Natural Science Foundation of the Anhui Science and Technology Committee (1908085QC110), Natural Science Foundation of Education Department of Anhui Province (KJ2018ZD051), Research Foundation of Key Laboratory of Bio-organic Fertilizer Creation of Ministry of Agriculture and Rural Affairs (BOFA202012), and National Natural Science Foundation of China (31600210).

ACKNOWLEDGMENTS

We are grateful to Prof. Jian Zhu for the revision of the English language in the manuscript.

SUPPLEMENTARY MATERIAL

The Supplementary Material for this article can be found online at: https://www.frontiersin.org/articles/10.3389/fpls.2020.634819/full#supplementary-material

Supplementary Figure 1 | Sequence analyses of four MSTRG18363 variants.

Supplementary Figure 2 | Consensus sequence of four MSTRG18363 variants (*asf-MSTRG18363*).

Supplementary Figure 3 | Mutated sequence of asf-MSTRG18363 (*masf-MSTRG18363*).

Supplementary Table 1 | Primers used in this study.

Supplementary Table 2 | Up-regulated and down-regulated differentially expressed lncRNAs (DELs) in the SL18r-inoculated plants compared with the non-inoculated (control) plants.

REFERENCES

Ajmera, I., Shi, J., Giri, J., Wu, P., Stekel, D. J., Lu, C., et al. (2018). Regulatory feedback response mechanisms to phosphate starvation in rice. *NPJ Syst. Biol. Appl*. 4:4.

Anders, S., and Huber, W. (2010). Differential expression analysis for sequence count data. *Genome Biol*. 11:R106.

Asselbergh, B., De Vleesschauwer, D., and Hofte, M. (2008). Global switches and fine-tuning: ABA modulates plant pathogen defense. *Mol. Plant Microbe Interact*. 21, 709–719. doi: 10.1094/mpmi-21-6-0709

Aznar, A., Dellagi, A. (2015). New insights into the role of siderophores as triggers of plant immunity: what can we learn from animals? J. Exp. Bot. 66, 3001-3010.

Banks, I. R., Zhang, Y., Wiggins, B. E., Heck, G. R., and Ivashuta, S. (2012). RNA decoys: an emerging component of plant regulatory networks? *Plant Signal. Behav*. 7, 1188–1193. doi: 10.4161/psb.21299

Bostock, R.M. (2005). Signal crosstalk and induced resistance: straddling the line between cost and benefit. *Annu. Rev. Phytopathol*. 43, 545–580.

Curvers, K., Seifi, H., Mouille, G., de Rycke, R., Asselbergh, B., Van Hecke, A., et al. (2010). Abscisic acid deficiency causes changes in cuticle permeability and pectin composition that influence tomato resistance to *Botrytis cinerea*. *Plant Physiol*. 154, 847–860. doi: 10.1104/pp.110.158972

De Vleesschauwer, D., Djavaheri, M., Bakker, P.A.H.M., and Hoefte, M. (2008). *Pseudomonas fluorescens* WCS374r-induced systemic resistance in rice against *Magnaporthe oryzae* is based on pseudobactin mediated priming for a salicylic acid-repressible multifaceted defense response. *Plant Physiol*. 148, 1996–2012.

De Vos, M., Van Zaanen, W., Koornneef, A., Korzelius, J. P., Dicke, M., Van Loon, L. C., et al. (2006). Herbivore-induced resistance against microbial pathogens in *Arabidopsis*. *Plant Physiol*. 142, 352–363. doi: 10.1104/pp.106.083907

Ding, Y., Sun, T., Ao, K., Peng, Y., Zhang, Y., Li, X., et al. (2018). Opposite roles of salicylic acid receptors NPR1 and NPR3/NPR4 in transcriptional regulation of plant immunity. *Cell* 173, 1454–1467.

El Oirdi, M., Abd El Rahman, T., Rigano, L., El Hadrami, A., Rodriguez, M. C., Daayf, F., et al. (2011). *Botrytis cinerea* manipulates the antagonistic effects between immune pathways to promote disease development in tomato. *Plant Cell* 23, 2405–2421. doi: 10.1105/tpc.111.083394

Fan, J., Xing, Y., Wen, X., Jia, R., Ni, H., He, J., et al. (2015). Long non-coding RNA ROR decoys gene-specific histone methylation to promote tumorigenesis. *Genome Biol*. 16:139.

García-Gutiérrez, L., Zeriouh, H., Romero, D., Cubero, J., de Vicente, A., and Pérez-García, A. (2013). The antagonistic strain *Bacillus subtilis* UMAF6639 also confers protection to melon plants against cucurbit powdery mildew by activation of jasmonate- and salicylic acid-dependent defence responses. *Microb. Biotechnol.* 6, 264–274. doi: 10.1111/1751-7915.12028

Grant, M., and Lamb, C. (2006). Systemic immunity. *Curr. Opin. Plant Biol.* 9, 414–420.

Holoch, D., and Moazed, D. (2015). RNA-mediated epigenetic regulation of gene expression. *Nat. Rev. Genet.* 16, 71–84. doi: 10.1038/nrg3863

Hou, X., Cui, J., Liu, W., Jiang, N., Zhou, X., Qi, H., et al. (2020). LncRNA39026 enhances tomato resistance to *Phytophthora infestans* by decoying miR168a and inducing PR gene expression. *Phytopathology* 110, 873–880.

Hu, Z., Shao, S., Zheng, C., Sun, Z., Shi, J., Yu, J., et al. (2018). Induction of systemic resistance in tomato against *Botrytis cinerea* by N-decanoyl-homoserine lactone via jasmonic acid signaling. *Planta* 247, 1217–1227. doi: 10.1007/s00425-018-2860-7

Jiang, N., Cui, J., Hou, X., Yang, G., Xiao, Y., Han, L., et al. (2020). Sl-lncRNA15492 interacts with Sl-miR482a and affects *Solanum lycopersicum* immunity against *Phytophthora infestans*. *Plant J.* 103, 1561-1574.

Jiang, N., Meng, J., Cui, J., Sun, G., and Luan, Y. (2018). Function identification of miR482b, a negative regulator during tomato resistance to *Phytophthora infestans*. *Hortic. Res.* 5:9.

Jing, N., Cui, J., Shi, Y., Yang, G., Zhou, X., Hou, X., et al. (2019). Tomato lncRNA23468 functions as a competing endogenous RNA to modulate NBS-LRR genes by decoying miR482b in the tomato-*Phytophthora infestans* interaction. *Hortic. Res.* 6:28.

Kumar, A., Lakshmanan, V., Caplan, J., Powell, D., Czymmek, K., Levia, D., et al. (2012). Rhizobacteria *Bacillus subtilis* restricts foliar pathogen entry through stomata. *Plant J.* 72, 694–706. doi: 10.1111/j.1365-313x.2012.05116.x

Lee, B., Lee, H., Xiong, L., and Zhu, J. (2002). A mitochondrial complex I defect impairs cold-regulated nuclear gene expression. *Plant Cell* 14, 1235–1251.

Lee, D., Choi, H., and Wang, B. (2011). The pepper E3 ubiquitin ligase RING1 gene, CaRING1, is required for cell death and the salicylic acid-dependent defense response. *Plant Physiol.* 156, 2011–2015. doi: 10.1104/pp.111.177568

Liu, Y., Schiff, M., and Dinesh-Kumar, S. (2002). Virus-induced gene silencing in tomato. *Plant J.* 31, 777–786.

Luan, Y., Cui, J., Wang, W., and Meng, J. (2016). MiR1918 enhances tomato sensitivity to *Phytophthora infestans* infection. *Sci. Rep.* 6:35858.

Lugtenberg, B., and Kamilova, F. (2009). Plant-growth-promoting rhizobacteria. *Annu. Rev. Microbiol.* 63, 541–556.

Maleck, K., Levine, A., Eulgem, T., Morgan, A., Schmid, J., Lawton, K. A., et al. (2000). The transcriptome of *Arabidopsis thaliana* during systemic acquired resistance. *Nat. Genet.* 26, 403–410. doi: 10.1038/82521

Matthews, J., Bhati, M., Lehtomaki, E., Mansfield, R., Cubeddu, L., and Mackay, J. (2009). It takes two to tango: the structure and function of LIM, RING, PHD and MYND domains. *Curr. Pharm. Des.* 15, 3681–3696.

Meng, L. S., Wei, Z. Q., Cao, X. Y., Tong, C., Lv, M. J., Yu, F., et al. (2020). Cytosolic invertase mediated root growth is feedback-regulated by a glucose-dependent signaling loop. *Plant Physiol.* 184, 895–908. doi: 10.1104/pp.20.00778

Mercer, T.R., and Mattick, J.S. (2013). Structure and function of long noncoding RNAs in epigenetic regulation. *Nat. Struct. Mol. Biol.* 20, 300-307.

Molinari, S., Fanelli, E., and Leonetti, P. (2014). Expression of tomato salicylic acid (SA)-responsive pathogenesis-related genes in Mi-1-mediated and SA-induced resistance to root-knot nematodes. *Mol. Plant Pathol.* 15, 255–264. doi: 10.1111/mpp.12085

Nie, P., Li, X., Wang, S., Guo, J., Zhao, H., and Niu, D. (2017). Induced systemic resistance against *Botrytis cinerea* by *Bacillus cereus* AR156 through a JA/ET- and NPR1-dependent signaling pathway and activates PAMP-triggered immunity in *Arabidopsis*. *Front. Plant Sci.* 8:238. doi: 10.3389/fpls.2017.00238

Niu, D., Xia, J., Jiang, C., Qi, B., Ling, X., Lin, S., et al. (2016). Bacillus cereus AR156 primes induced systemic resistance by suppressing miR825/825* and activating defense-related genes in *Arabidopsis*. *J. Integr. Plant Biol.* 58, 426–439. doi: 10.1111/jipb.12446

Ongena, M., Jourdan, E., Adam, A., Paquot, M., Brans, A., Joris, B., et al. (2007). Surfactin and fengycin lipopeptides of *Bacillus subtilis* as elicitors of induced systemic resistance in plants. *Environ. Microbiol.* 9, 1084–1090.

Porebski, S., Bailey, L. G., and Baurn, B. R. (1997). Modification of a CTAB DNA extraction protocol for plants containing high polysaccharide and polyphenol components. *Plant Mol. Biol. Rep.* 15, 8–15. doi: 10.1007/bf02772108

Pozo, M.J., and Azcón-Aguilar, C. (2007). Unraveling mycorrhiza-induced resistance. *Curr. Opin. Plant Biol.* 10, 393–398.

Ryu, C.M., Hu, C.H., Reddy, M.S., and Kloepper, J.W. (2003). Different signaling pathways of induced resistance by rhizobacteria in *Arabidopsis thaliana* against two pathovars of *Pseudomonas syringae*. *New Phytol.* 160, 413–420.

Sharifi, R., and Ryu, C. M. (2016). Are bacterial volatile compounds poisonous odors to a fungal pathogen *Botrytis cinerea*, alarm signals to *Arabidopsis* seedlings for eliciting induced resistance, or both? *Front. Microbiol.* 7:196. doi: 10.3389/fmicb.2016.00196

Sharma, M.K., Solanke, A.U., Jani, D., Singh, Y., and Sharma, A.K. (2009). A simple and efficient *Agrobacterium*-mediated procedure for transformation of tomato. *J. Biosci.* 34, 423–433.

Tahir, H. A. S., Gu, Q., Wu, H., Raza, W., Safdar, A., Huang, Z., et al. (2017). Effect of volatile compounds produced by *Ralstonia solanacearum* on plant growth promoting and systemic resistance inducing potential of *Bacillus* volatiles. *BMC Plant Biol.* 17:133. doi: 10.1186/s12870-017-1083-6

Takishita, Y., Charron, J. B., and Smith, D. L. (2018). Biocontrol Rhizobacterium *Pseudomonas sp.* 23S induces systemic resistance in tomato (*Solanum lycopersicum* L.) against bacterial canker *Clavibacter michiganensis* subsp. *michiganensis*. *Front. Microbiol.* 9:2119. doi: 10.3389/fmicb.2018.02119

Timmermann, T.; Poupin, M.J.; Vega, A., Urrutia, C.; Ruz, G.A., and González, B. (2019). Gene networks underlying the early regulation of *Paraburkholderia phytofirmans* PsJN induced systemic resistance in *Arabidopsis*. *PLoS One* 14:e0221358. doi: 10.1371/journal.pone.0221358

Trapnell, C., Pachter, L., and Salzberg, S. L. (2009). TopHat: discovering splice junctions with RNA-Seq. *Bioinformatics* 25, 1105–1111. doi: 10.1093/bioinformatics/btp120

van Hulten, M., Pelser, M., Van Loon, L.C., Pieterse, C.M.J., and Ton, J. (2006). Costs and benefits of priming for defense in *Arabidopsis*. *Proc. Natl. Acad. Sci. U.S.A.* 103, 5602–5607.

Van Wees, S. C., Van der Ent, S., and Pieterse, C. M. (2008). Plant immune responses triggered by beneficial microbes. *Curr. Opin. Plant Biol.* 11, 443–448. doi: 10.1016/j.pbi.2008.05.005

Verhagen, B.W., Glazebrook, J., Zhu, T., Chang, H.S., van Loon, L.C., and Pieterse, C.M. (2004). The transcriptome of rhizobacteria-induced systemic resistance in *Arabidopsis*. *Mol. Plant Microbe Interact.* 17, 895-908.

Wang, J., Yu, W., Yang, Y., Li, X., Chen, T., Liu, T., et al. (2015). Genome-wide analysis of tomato long non-coding RNAs and identification as endogenous target mimic for microRNA in response to TYLCV infection. *Sci. Rep.* 5:16946.

Wang, T., Zhao, M., Zhang, X., Liu, M., Yang, C., Chen, Y., et al. (2017). Novel phosphate deficiency-responsive long non-coding RNAs in the legume model plant *Medicago truncatula*. *J. Exp. Bot.* 68, 5937-5948.

Xie, S., Jiang, H., Ding, T., Xu, Q., Chai, W., and Cheng, B. (2018). *Bacillus amyloliquefaciens* FZB42 represses plant miR846 to induce systemic resistance via a jasmonic acid-dependent signalling pathway. *Mol. Plant Pathol.* 19, 1612–1623. doi: 10.1111/mpp.12634

Yan, Z., Reddy, M.S., Ryu, C.M., McInroy, J.A., Wilson, M., Kloepper, J.W. (2002). Induced systemic protection against tomato late blight elicited by plant growth-promoting rhizobacteria. *Phytopathology* 92, 1329–1333.

Yang, T., Ma, H., Zhang, J., Wu, T., Song, T., Tian, J., et al. (2019). Systematic identification of long noncoding RNAs expressed during light-induced anthocyanin accumulation in apple fruit. *Plant J.* 100, 572–590. doi: 10.1111/tpj.14470

Yang, Y.N., Qi, M., and Mei, C.S. (2004). Endogenous salicylic acid protects rice plants from oxidative damage caused by aging as well as biotic and abiotic stress. *Plant J.* 40, 909–919.

Yu, Y., Xu, W., Wang, J., Wang, L., Yao, W., Yang, Y., et al. (2013). The Chinese wild grapevine (*Vitis pseudoreticulata*) E3 ubiquitin ligase *Erysiphe necator*-induced RING finger protein 1 (EIRP1) activates plant defense responses by inducing proteolysis of the VpWRKY11 transcription factor. *New Phytol.* 200, 834–846. doi: 10.1111/nph.12418

Yu, Y., Xu, W., Wang, S., Xu, Y., Li, H., Wang, Y., et al. (2011). VpRFP1, a novel C4C4-type RING finger protein gene from Chinese wild *Vitis pseudoreticulata*,

functions as a transcriptional activator in defense response of grapevine. *J. Exp. Bot.* 62, 5671–5682.

Zeng, L. R., Vega-Sánchez, M. E., Zhu, T., and Wang, G. L. (2006). Ubiquitination-mediated protein degradation and modification: an emerging theme in plant-microbe interactions. *Cell Res.* 16, 413–426. doi: 10.1038/sj.cr.7310053

Zhou, C., Guo, J., Zhu, L., Xiao, X., Xie, Y., Zhu, J., et al. (2016). *Paenibacillus polymyxa* BFKC01 enhances plant iron absorption via improved root systems and activated iron acquisition mechanisms. *Plant Physiol. Biochem.* 105, 162-173.

Conflict of Interest: The authors declare that the research was conducted in the absence of any commercial or financial relationships that could be construed as a potential conflict of interest.

frontiers in Plant Science

ORIGINAL RESEARCH
published: 22 February 2021
doi: 10.3389/fpls.2021.645338

Pseudomonas fluorescens DN16 Enhances Cucumber Defense Responses Against the Necrotrophic Pathogen *Botrytis cinerea* by Regulating Thermospermine Catabolism

*Lin Zhu[1], Nana Qian[1], Yujun Sun[1,2], Xiaoming Lu[1], Haiming Duan[1]*and Lisheng Qian[1,2]**

[1]School of Life and Health Science, Anhui Science and Technology University, Bengbu, China, [2]College of Life science, Anhui Agricultural University, Hefei, China

OPEN ACCESS

Edited by:
Carlos Lucena,
University of Cordoba, Spain

Reviewed by:
Kang Qiao,
Shandong Agricultural University, China
Jie Wang,
Tobacco Research Institute (CAAS), China

***Correspondence:**
Lisheng Qian
qianls@ahstu.edu.cn
Haiming Duan
duanhm@ahstu.edu.cn

Specialty section:
This article was submitted to Plant Symbiotic Interactions, a section of the journal Frontiers in Plant Science

Received: 23 December 2020
Accepted: 25 January 2021
Published: 22 February 2021

Citation:
Zhu L, Qian N, Sun Y, Lu X, Duan H and Qian L (2021) Pseudomonas fluorescens DN16 Enhances Cucumber Defense Responses Against the Necrotrophic Pathogen Botrytis cinerea by Regulating Thermospermine Catabolism. Front. Plant Sci. 12:645338. doi: 10.3389/fpls.2021.645338

Plants can naturally interact with beneficial rhizobacteria to mediate defense responses against foliar pathogen infection. However, the mechanisms of rhizobacteria-mediated defense enhancement remain rarely clear. In this study, beneficial rhizobacterial strain *Pseudomonas fluorescens* DN16 greatly increased the resistance of cucumber plants against *Botrytis cinerea* infection. RNA-sequencing analyses showed that several polyamine-associated genes including a thermospermine (TSpm) synthase gene (*CsACL5*) and polyamine catabolic genes (*CsPAO1*, *CsPAO5*, and *CsCuAO1*) were notably induced by DN16. The associations of TSpm metabolic pathways with the DN16-mediated cucumber defense responses were further investigated. The inoculated plants exhibited the increased leaf TSpm levels compared with the controls. Accordantly, overexpression of *CsACL5* in cucumber plants markedly increased leaf TSpm levels and enhanced defense against *B. cinerea* infection. The functions of TSpm catabolism in the DN16-mediated defense responses of cucumber plants to *B. cinerea* were further investigated by pharmacological approaches. Upon exposure to pathogen infection, the changes of leaf TSpm levels were positively related to the enhanced activities of polyamine catabolic enzymes including polyamine oxidases (PAOs) and copper amine oxidases (CuAOs), which paralleled the transcription of several defense-related genes such as pathogenesis-related protein 1 (*CsPR1*) and defensin-like protein 1 (*CsDLP1*). However, the inhibited activities of polyamine catabolic enzymes abolished the DN16-induced cucumber defense against *B. cinerea* infection. This was in line with the impaired expression of defense-related genes in the inoculated plants challenged by *B. cinerea*. Collectively, our findings unraveled a pivotal role of TSpm catabolism in the regulation of the rhizobacteria-primed defense states by mediating the immune responses in cucumber plants after *B. cinerea* infection.

Keywords: thermospermine oxidation, defense response, *Botrytis cinerea*, rhizobacteria, polyamine

INTRODUCTION

Plants as sessile organisms inevitably suffer from biotic and abiotic stresses. Unlike animals, plants cannot avoid these stressful factors, which seriously impact plant growth and development, and the biomass of agricultural crops. During long-term evolution, a series of highly complicated and coordinated strategies has been developed to tolerate various biotic stresses, involving activation of signaling cascades that results in a wide range of stress responses. These adaptive stress responses have well been manifested by diverse biochemical and physiological alterations, such as the biosynthesis of terpenes, pathogenesis-related proteins, and polyamines (PAs; Walters, 2003; van Loon et al., 2006; Block et al., 2019).

Polyamines including putrescine (Put), spermidine (Spd), spermine (Spm), and thermospermine (TSpm) are widely found in diverse plant species, which are important for plant physiological and metabolic processes (Shi and Chan, 2014). The Put can be synthesized *via* the catalysis of the ornithine decarboxylase and arginine decarboxylase. Subsequently, the Spd synthase promotes the conversion of Put into Spd. The Spd can be successively converted into both the Spm and TSpm by the Spm and TSpm synthase, respectively (Fuell et al., 2010; Kim et al., 2014). The TSpm exists in the whole plant kingdom, whereas the Spm is only found in diverse angiosperms (Takano et al., 2012). In *Arabidopsis*, the xylem-specific *ACL5* gene is essential for the synthesis of TSpm, which participates in the regulation of vascular development by hindering the premature death of xylem elements (Kakehi et al., 2018). The functions of TSpm have been found to be associated with the modulation of diverse processes such as cell wall patterning, cell death, and xylem cell morphology (Muñiz et al., 2008; Shinohara et al., 2019; Vuosku et al., 2019). Furthermore, high-level TSpm contributes to enhancing the tolerance of *Arabidopsis* plants to *Pseudomonas viridiflava*, whereas the *acl5* mutants deficient in the synthesis of TSpm exhibit the increased sensitivity to the pathogen attacks compared with the wild type (WT) plants (Marina et al., 2013). Accordantly, silencing of *GhACL5* reduces the levels of TSpm in cotton, thereby increasing the susceptibility to *Verticillium dahlia* (Mo et al., 2015a).

In plants, the catabolism of cellular PAs can be modulated by the PA oxidases (PAOs) and copper amine oxidases (CuAOs) under abiotic and biotic stress conditions (Cona et al., 2006; Wang et al., 2009). In many cases, biotic stress can induce the synthesis of PA synthesis and further trigger its catabolism (Angelini et al., 2010). Microbial pathogens have also been shown to induce the synthesis and oxidation of PAs in the tobacco leaf apoplast (Marina et al., 2008). Upon exposure to biotic stress, the metabolic homeostasis of PA participates in regulating defense responses in plants (Takahashi et al., 2004; Gonzalez et al., 2011). Spm can function as a key signaling molecule that provokes defense responses in both the virus- and *P. viridiflava*-infected plants (Gonzalez et al., 2011). However, high-level Spd can enhance the susceptibility of tomato plants to *Botrytis cinerea* by attenuating the ET-mediated signaling pathways (Nambeesan et al., 2012). PAOs can catalyze the conversion of Spd and Spm into 1,3-diaminopropane, H_2O_2, and the corresponding aldehyde (Rea et al., 2002). In *Arabidopsis*, several PAOs promote the back conversion of Spm to Put, accompanied by generating 3-aminopropanal and H_2O_2 (Moschou et al., 2008). Many studies have indicated that the oxidation of PAs can impact cell-wall maturation, lignification and reinforce cell wall, leading to the increased resistance against pathogen infection (Cona et al., 2006). Overexpression of the *PAO* genes in tobacco plants induces systemic acquired resistance and enhances the cell-wall-based defenses, conferring the increased resistance against bacterial and fungal pathogens (Moschou et al., 2009). It is increasingly evidenced that the oxidation of PAs in plants by PAOs and CuAOs is correlated with plant disease resistance (Hatmi et al., 2014, 2015). Repression of the PAO and CuAO activities in the stressed-treated grapevine leaves abolishes the activation of defense systems against *B. cinerea* infection.

It has previously been indicated that interaction of plant roots with soil microorganisms can mediate plant growth and development, and adaptive responses under adverse environments (Nadeem et al., 2014; Fahad et al., 2015). Several rhizobacteria strains establish mutualistic relationships with the hosts to benefit two parties (Zhou et al., 2019). Beneficial bacteria habituated in plant rhizosphere are frequently called as plant growth promoting rhizobacteria (PGPR), which help the host inhibit phytopathogens, promote plant growth and survive under adverse conditions (Lugtenberg and Kamilova, 2009). Many studies have reported that several PGPR strains can augment the levels of PAs in host plants by upregulating the expression of PA biosynthetic genes or direct secretion of PAs, which confers the enhanced abiotic stress tolerance in plants (Zhou et al., 2016; Sen et al., 2018). However, it remains elusive whether rhizobacteria can mediate the metabolic pathways of PAs in plants and how its metabolic alterations are correlated with host immune responses.

In this study, inoculation with *P. fluorescens* DN16 increased leaf TSpm levels in cucumber plants, which were positively associated with the transcription levels of *CsACL5*, as evidenced by the RNA-sequencing data. We further assessed the impacts of DN16 on the levels of TSpm and the activities of PA catabolic enzymes. A pharmacological approach was also applied to assess the roles of DN16-mediated TSpm catabolism in the regulation of cucumber resistance against *B. cinerea* infection.

MATERIALS AND METHODS

Plant Materials and Microbial Culture

Seeds of the cucumber (*Cucumis sativus* L.) inbred line NK23 were sterilized with 0.1% $HgCl_2$ followed by rinsing with sterile water and were then cultured in 1/2 MS medium. Seven-day-old cucumber seedlings were transferred into sterile soil and placed in a plant growth chamber at 16-h day (25°C)/8-h night (23°C) cycle.

The bacterial strain tested in this study was *P. fluorescens* DN16, which was isolated from the rhizospheric soil of 2-month-old cucumber plants. DN16 was cultured in liquid potato dextrose agar (PDA) medium at 28°C. The cultures

were centrifuged at 6000 rpm for 5 min and resuspended in sterile PBS solution (0.02 M, pH 7.2). The collected cells were then adjusted to the concentration of 1×10^8 CFU ml^{-1} for next experiments.

For assays of pathogen infection, the foliar pathogen *B. cinerea* was cultured on PDA agar medium at 28°C for 2 weeks. Spore suspensions of *B. cinerea* were harvested with the solution (0.05 M KH_2PO_4 and 6 mM glucose) and 0.01% (v/v) Tween 20, adjusting to 2×10^5 spores ml^{-1} (Curvers et al., 2010).

Generation of Transgenic Cucumber Plants

To construct *CsACL5*-overexpressing vector, cDNA sequence of *CsACL5* was amplified and ligated into the pMD18-T vector (Takara, Japan). After sequencing, the cDNA sequence of *CsACL5* was digested and introduced into the plant binary vector pCAMBIA1300. To generate RNAi-*CsACL5* vector, the cDNA fragment of *CsACL5* was amplified and inserted into the intermediated vector pHANNIBAL with the sense direction by digestion of XhoI and EcoRI and antisense direction by digestion of HindIII and XbaI, respectively. Subsequently, the pHANNIBA-*CsACL5* vector was digested by NotI and ligated into the pART27 to form the recombinant plasmid RNAi-*CsACL5*. *Agrobacterium tumefaciens* EHA105 harboring the above constructed plasmids were transformed into cucumber plants as described by Wang et al. (2014).

Pathogen Infection Tests

Assays of *P. fluorescens* DN16-induced disease resistance were carried out, in which 7-day-old cucumber seedlings grown in 1/2 MS media were transferred into plastic pots containing sterile soils and grown for 4 weeks. Then, cell suspensions of DN16 were collected and poured into the soil (5×10^7 CFU g^{-1} soil), and the control treatments were inoculated with sterile PBS solution (0.02 M, pH 7.2) for 5 days. Then, the control and inoculated plants were subjected to *in vitro* and *in vivo* pathogen infection assays (El Oirdi et al., 2011). For *in vitro* tests, 5 μl spore suspensions of *B. cinerea* were dipped on detached leaves. At 5 days post infection (dpi), lesion diameters were determined. For *in vivo* tests, the leaves were sprayed with *B. cinerea* and placed in growth chamber at 100% relative humidity. At 7 dpi, disease index was evaluated as described recently by Jing et al. (2019). Moreover, the ratio of *BcActin* to *CsActin* was calculated for determining the biomass of *B. cinerea* as reported by Hu et al. (2018).

Histochemical Detection and Determination of Fv/Fm

In vivo localization of dead cells and H_2O_2 were detected in cucumber leaves using trypan blue and diaminobenzidine (DAB) staining, respectively (Daudi and O'Brien, 2012; Tian et al., 2018). To analyze pathogen-induced cell death, leaf tissues separated from both the pathogen-infected control and inoculated plants were incubated in the trypan blue staining solution for 45 min, followed by rinsing with distilled water five times and bleaching with 75% ethanol. To observe the production of H_2O_2, harvested leaves were immediately immersed in the DAB staining solution for 6 h, followed by bleaching with 75% ethanol. In addition, the values of Fv/Fm were determined by a Portable Photosynthesis System CIRAS-2.

Analyses of RNA Sequencing and Quantitative Real-Time PCR

Five-week-old cucumber plants grown in sterile soils were inoculated with or without DN16 at the density of 5×10^7 CFU g^{-1} soil for 5 days, and the control and inoculated leaves were then sprayed with spore suspension of *B. cinerea* (2×10^5 spore ml^{-1}). Universal RNA Extraction Kit (Takara, Japan) was applied to isolate total RNAs from the control and inoculated leaves at different time points post pathogen infection. The quality and concentration of RNA samples were spectrophotometericaly detected and the contaminated DNA was digested. To conduct RNA-Seq analyses, these RNA samples from the leaves at 0, 24, and 48 hpi were used to construct cDNA libraries, and three biological replicates were carried out. Low-quality and adapter sequences were then removed from raw data that were deposited in the NCBI SRA database (no. PRJNA686802), and were then aligned to the database.[1] Compared with the controls, several DEGs were screened from the leaves of DN16-inoculated plants at a cutoff of FDR value <0.05 and $\left|\log_2 \text{ratio} \geq 1.5\right|$, and were enriched by the GO terms and KEGG pathways (Zhang et al., 2016). Furthermore, quantitative PCR (qPCR) analyses were conducted with at least three biological replicates. qPCR reactions were performed with the SYBR Premix Ex TaqTM II kit (TaKaRa, Japan) in an ABI7500 machine. Gene expression in cucumber leaves was analyzed by qPCR and the *CsActin* gene was used as an internal control for normalizing their transcription (Yang et al., 2019). Gene expression was analyzed using the $2^{-\Delta\Delta Ct}$ method. The information of primers was shown in **Supplementary Table S1**.

Determination of PAs

The content of PAs was quantified by HPLC as reported previously by Mo et al. (2015b). Briefly, leaf tissues (0.5 g) were ground and mixed in 10 ml of ice-cold 5% perchloric acid for 1 h, and then centrifuged at 12000 rpm for 15 min at 4°C. The supernatants (0.5 ml) were mixed with 1 ml of 2 N NaOH and 7 μl of benzoyl chloride, followed by reacting for 30 min at 37°C. After that, 1.5 ml of saturated NaCl and diethyl ether was added into the mixture and was then centrifuged for 10 min at 1000 rpm. One milliliter of organic solvent phase was collected and dissolved in 100 μl of methanol and filtered by 0.22 μm microfiltration membrane. Finally, the methanol solution was detected by HPLC as reported by Mo et al. (2015b).

Analyses of PAO and CuAO Activities and Pharmacological Treatments

Assays of leaf PAO and CuAO activities were carried out as reported previously by Hatmi et al. (2015). Leaf tissues (0.5 g)

[1]http://cucurbitgenomics.org

was homogenized in 1 ml of 0.25 M phosphate buffer solution, and then centrifuged at 12000 rpm for 5 min at 4°C. The supernatants were used to detect the activities of PAOs and CuAOs as described previously by Cona et al. (2006). In addition, to inhibit the activities of PA catabolic enzymes, the leaves of whole plants were pretreated with the CuAO inhibitor aminoguanidine (AG, 5 mM) or the PAO inhibitor β-hydroxyehtylhydrazine (HEH, 10 mM). After 3 days of treatments, these plants were subjected to foliar treatment with spore suspension of *B. cinerea* (2×10^5 spore ml^{-1}).

Statistical Analysis

The data were analyzed with SPSS software, and all the data were indicated as the means ± SD from three biological repeats and analyzed statistically using Duncan's multiple range tests ($p < 0.05$).

RESULTS

P. fluorescens DN16 Induces Cucumber Resistance Against *B. cinerea* Infection

To examine whether *P. fluorescens* DN16-induced systemic resistance (ISR) was effective against the foliar pathogen *B. cinerea*, 5-week-old cucumber plants grown in sterile soils were treated with cell suspension of DN16 for 5 days, followed by challenging with *B. cinerea*. In the detached leaf tests, leaves of non-inoculated (control) plants exhibited larger lesion diameters and necrotic tissues at 5 dpi (**Figure 1A**). In contrast, leaves of DN16-inoculated plants displayed disease-resistant phenotypes, as reflected by smaller lesion diameters (**Figures 1A,B**). In addition, the inoculated plants had higher proportions of fewer small lesions (lesion diameter < 5 mm) than the controls (**Figure 1C**).

The production of H_2O_2 and cell death in the leaves was further examined by DAB and trypan blue staining, respectively. As shown in **Figure 1A**, the leaves of the inoculated plants accumulated lower H_2O_2 levels than those of the controls. The inoculated leaves also exhibited markedly less cell death than the control leaves. In the whole-plant inoculation assays, both the control and inoculated leaves were treated with *B. cinerea*. At 7 dpi, the inoculated plants had lower disease index than the controls (**Figure 1D**). Moreover, qPCR analyses showed that the inoculated leaves had lower *BcActin* transcripts than the controls at 3 and 7 dpi (**Figure 1E**), which was in accordance to the observed reduction of disease occurrence.

To rule out the probability that the DN16-induced disease resistance was resulted from direct impacts of DN16 on *B. cinerea*, potentially transferring of root-inoculated bacteria into leaf tissues was evaluated by culturing leaf extracts from the DN16-inoculated plants onto selective KB agar plates. However, DN16 was not detected in the inoculated leaves (data not shown). In combination with the inability of DN16 to antagonize the growth of *B. cinerea*, our data indicated that the DN16-induced systemic resistance was not attributable to microbial antagonism but rather activation of the defense systems of plant itself.

Transcriptome Analyses of the DN16-Inoculated Plants Infected by *B. cinerea*

To unravel the molecular mechanisms of DN16-mediated ISR in cucumber plants, DEGs were identified by comparing analyses of the control and inoculated plants, which were markedly induced by DN16. Herein, 5-week-old cucumber plants cultivated in the sterile soils were treated with DN16 for 5 days, a total of 933 DEGs were screened, including 284 downregulated and 649 upregulated DEGs (**Supplementary Table S2**). KEGG pathway enrichment analysis revealed a total of 20 enriched pathways, involving metabolic pathways, biosynthesis of secondary metabolites, phenylpropanoid biosynthesis, and other pathways (**Figure 2A**). GO enrichment analysis for these DEGs was categorized into biological process, cell component, and molecular function (**Figure 2B**). The enriched DEGs were assigned to multiple processes, such as metabolic processes, cellular process, and biological regulation, and the majority of the enriched DEGs belonged to the metabolic process.

After 5 days of inoculation, the cucumber plants were subjected to foliar treatment with *B. cinerea*. A total of 681 and 519 DEGs were screened at 24 (**Supplementary Table S3**) and 48 hpi (**Supplementary Table S4**), respectively, which were distinctly induced in the pathogen-infected plants colonized by DN16. As shown in **Figure 2C**, Venn diagram revealed that 34 upregulated DEGs were shared in the DN16-inoculated plants, which was likely related to the DN16-mediated disease resistance (**Supplementary Table S5**). Among these shared DEGs, the expression of a thermospermine synthase *ACL5* gene (*CsACL5*) was induced by DN16. Moreover, 54 upregulated DEGs were significantly enriched in the inoculated plants at 24 and 48 hpi. Among these DEGs, several pathogen defense-related genes including pathogenesis-related protein 1 (*CsPR1*), defensin-like protein 1 (*CsDLP1*), and PA catabolic genes including polyamine oxidase 1 (*CsPAO1*), polyamine oxidase 5 (*CsPAO5*), and copper amine oxidase 1 (*CsCuAO1*) were significantly enriched in the pathogen-infected plants colonized by DN16 (**Figure 2D**). qPCR analyses showed that these PA-related genes were significantly affected in the inoculated plants, which was in line with the data of RNA-Seq (**Supplementary Table S6**).

Induction of *CsACL5* by DN16 Contributed to Increased Disease Resistance

As shown in **Figure 3A**, compared with the controls, the cucumber plants exhibited a marked increase of leaf TSpm levels after 3 days of DN16 inoculation. The levels of TSpm were gradually decreased in the inoculated leaves followed by the time delay of pathogen infection. After 3 days of pathogen infection, the inoculated plants displayed no marked discrepancy with the controls (**Figure 3B**). As mentioned above, RNA-Seq data revealed that the inoculation with DN16 induced a remarkable elevation of *CsACL5* transcripts in the cucumber leaves. To verify whether upregulation of *CsACL5* contributed to the improved host resistance against *B. cinerea*, the WT plants were transformed with *CsACL5* driven by the CaMV 35S promoter. Two independent T2 lines (ACL5ox-L2 and -L8)

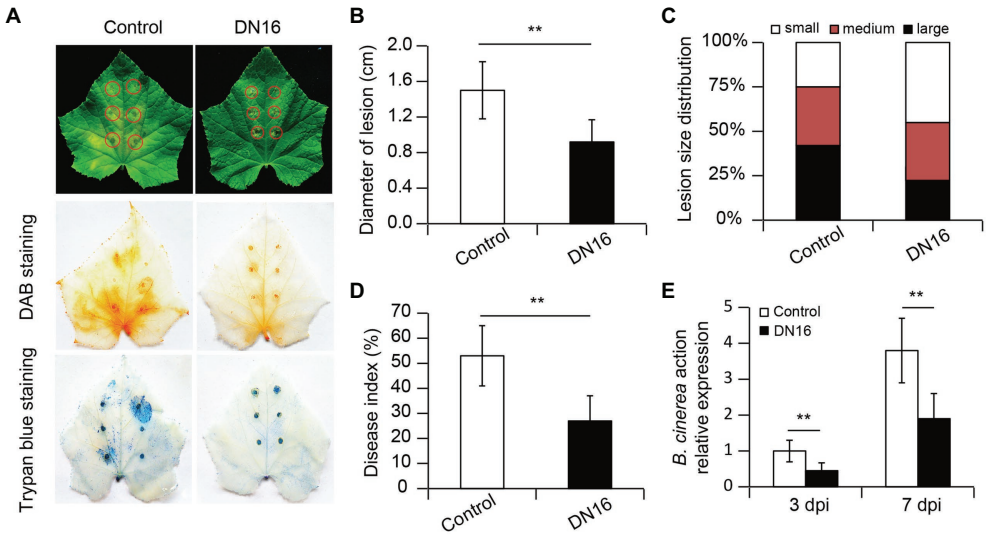

FIGURE 1 | Effects of *Pseudomonas fluorescens* DN16 inoculation on the resistance of cucumber plants against *Botrytis cinerea*. Five-week-old cucumber plants were treated with or without DN16 for 5 days. Then, these plants were challenged with the foliar pathogen *B. cinerea*. **(A)** Lesion symptoms of detached leaves at 5 days post infection (dpi), and diaminobenzidine (DAB) and trypan blue staining of pathogen-infected leaves. **(B)** Lesion diameters of detached leaves. **(C)** Lesion distribution: small (LD < 5 mm), medium (5 mm < LD < 10 mm), and large (LD > 10 mm). **(D)** Both the control and inoculated leaves were sprayed with *B. cinerea* for 7 days, and disease index was calculated. **(E)** Relative expression of *BcActin* was examined at 3 and 7 dpi, respectively. The data represented the means ± SD from three biological repeats and significant differences were examined by student's *t*-test at $^{**}p < 0.01$.

were used in this study, which exhibited exceedingly high expression of *CsACL5* (**Figure 3C**). Accordantly, the two 35S::*CsACL5* lines had higher leaf TSpm levels than the WT plants (**Figure 3D**). We further assessed the impacts of *CsACL5* overexpression on disease resistance. At 7 dpi, the 35S::*CsACL5* lines exhibited a notable reduction in disease index compared with the WT plants (**Figure 3E**). The 35S::*CsACL5* lines also displayed less photosynthetic damages than the WT plants upon exposure to pathogen infection, as reflected by higher values of ΦPSII in the transgenic lines (**Figure 3F**). qPCR analyses revealed that the transcription of *BcActin* was markedly lower in the leaves of the 35S::*CsACL5* lines than the WT plants (**Figure 3G**). Consistently, in the detached leaf pathogen tests, overexpression of *CsACL5* enhanced cucumber resistance against *B. cinerea* infection, displaying smaller lesion diameters (**Figures 3H,I**). These findings implied that high-level transcription of *CsACL5* conferred the increased disease resistance in cucumber plants.

To further ascertain whether induction of *CsACL5* transcripts in cucumber plants by DN16 was responsible for the DN16-mediated disease resistance, the RNAi-*CsACL5* vector was introduced into the WT plants. qPCR analyses revealed a marked decrease in the transcription of *CsACL5* of approximate 60% in two *CsACL5*-silenced lines (ACL5s-L3 and -L5) compared with the WT plants (**Figure 4A**). Consistently, leaf TSpm levels were significantly reduced in the *CsACL5*-silenced lines compared with the WT plants (**Figure 4B**). The inoculation with DN16 was not able to considerably augment the levels of TSpm in the leaves of the *CsACL5*-silenced lines (**Figure 4B**). Furthermore, we examined the effects of *CsACL5* silencing on the DN16-mediated ISR. As shown in **Figure 4C**, silencing of *CsACL5* greatly weakened the DN16-induced cucumber resistance against *B. cinerea* infection. At 7 dpi, the *CsACL5*-silenced lines displayed the increased disease index compared with the WT plants. qPCR analyses showed that the expression of *BcActin* was distinctly less in the leaves of the *CsACL5*-silenced lines than the WT plants (**Figure 4D**). Accordantly, detached leaves of the *CsACL5*-silenced lines exhibited more serious necrotic tissues and larger lesion diameters than the WT plants at 5 dpi (**Figures 4E,F**). Additionally, the WT plants had lower proportions of fewer small lesions (lesion diameter < 5 mm) than the *CsACL5*-silenced lines (**Figure 4G**).

PA Catabolism Is Essential for DN16-Induced Resistance Against *B. cinerea*

Pathogen-mediated activation of defense responses is concomitant with the stimulated oxidation of cellular PAs in plants (Hatmi et al., 2014, 2015). The increased disease resistance is positively associated with the promoted PA catabolism in the pathogen-infected plants. In this study, the RNA-Seq data mentioned above showed that the transcription of PA catabolic genes (*CsPAO1*, *CsPAO5*, and *CsCuAO1*) was remarkably upregulated in the pathogen-infected leaves, but their expression was observably higher in the inoculated leaves. Furthermore, the PAO activities were measured in both the pathogen-infected control and inoculated leaves in the presence or absence of DN16. Before pathogen infection, there were no significant differences in the PAO and CuAO activities between the control and inoculated plants (**Figure 5A**). Upon exposure to *B. cinerea* infection, the activities of PAOs and CuAOs were progressively elevated followed by the time

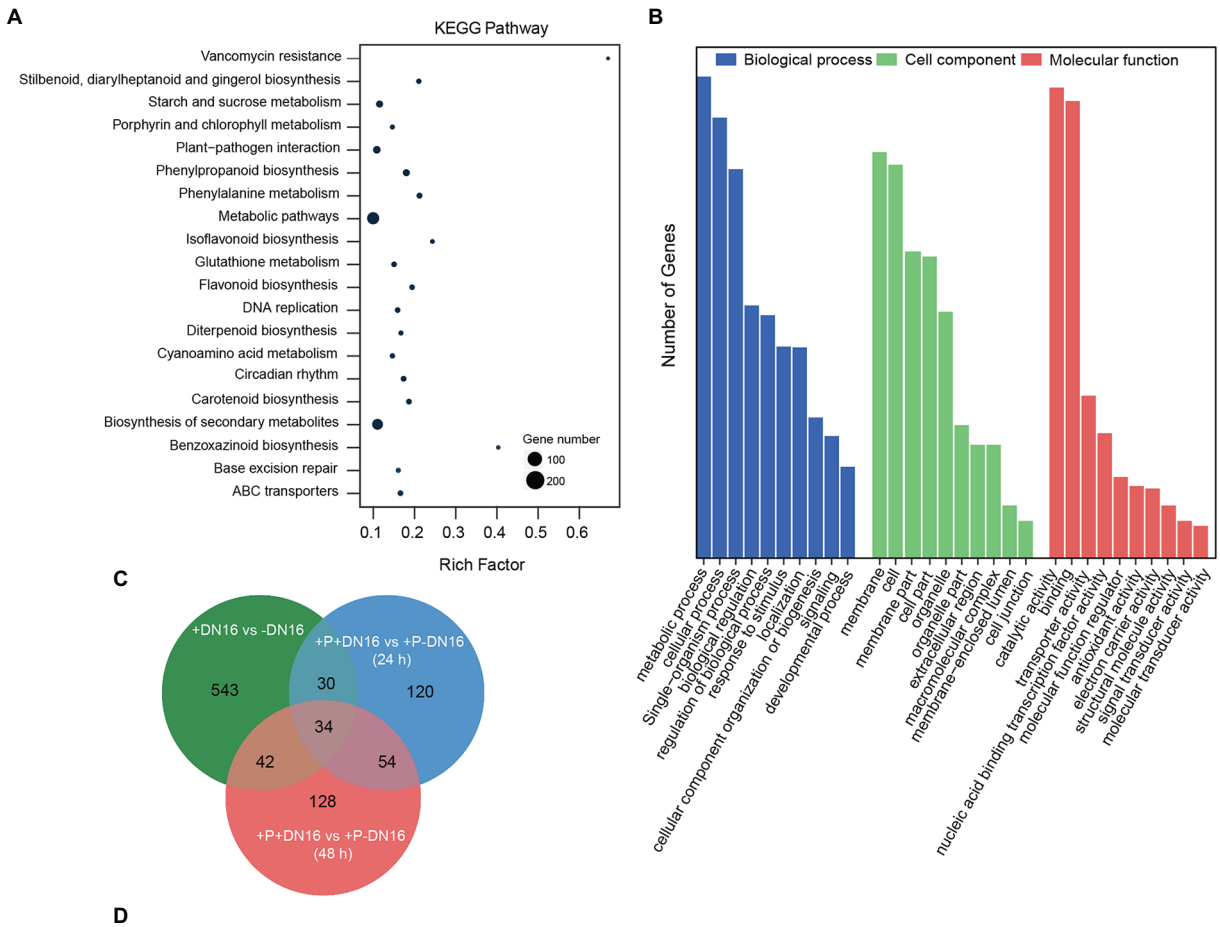

D

ID	Annotation	+DN16 vs –DN16 [Log_2(Fold change)]	+P+DN16 vs +P-DN16 (24h) [Log_2(Fold change)]	+P+DN16 vs +P-DN16 (48h) [Log_2(Fold change)]
Csa3G147770	Thermospermine synthase ACAULIS5 (*ACL5*)	5.28	6.09	5.12
Csa7G426460	Polyamine oxidase 1 (*PAO1*)	ns	3.03	2.03
Csa2G000460	Polyamine oxidase 5 (*PAO5*)	ns	2.08	1.75
Csa1G004100	Copper amine oxidase 1 (*CuAO1*)	ns	2.04	3.01

FIGURE 2 | Identification of differentially expressed genes (DEGs) in cucumber plants in response to *P. fluorescens* DN16 and/or *B. cinerea*. Five-week-old cucumber plants were treated with or without DN16 for 5 days. Then, both the control and inoculated leaves were sprayed with *B. cinerea*. The leaves at 0, 24, and 48 dpi were harvested for the RNA-Seq analyses. **(A)** KEGG pathway and **(B)** GO enrichment analyses of DEGs at 0 dpi. **(C)** Venn diagrams of shared DEGs among different experimental groups. **(D)** Expression profiles of four polyamines (PA)-related genes (*CsACL5*, *CsPAO1*, *CsPAO5*, and *CsCuAO1*) in both the control and inoculated leaves challenged with or without *B. cinerea* infection.

delay of pathogen infection. However, the inoculated plants had higher PA catabolic enzymatic activities than the controls (**Figure 5B**).

We further examined whether the oxidation of TSpm was involved in the DN16-induced cucumber resistance against *B. cinerea*. For this purpose, both the control and inoculated

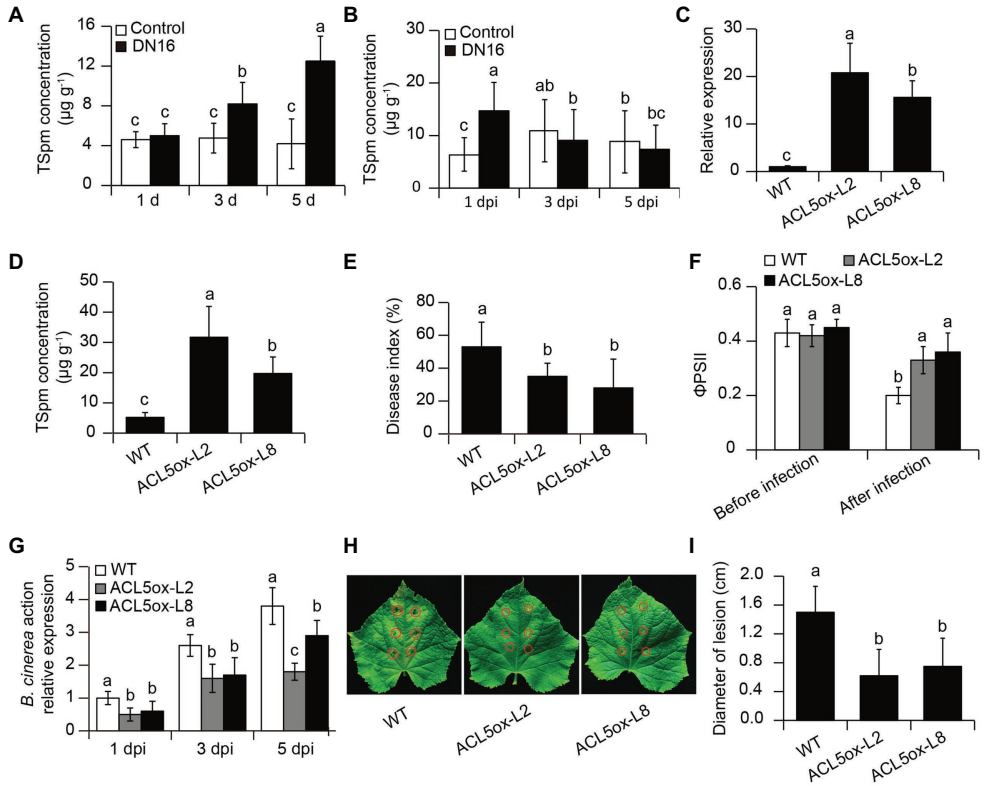

FIGURE 3 | The contribution of thermospermine (TSpm) to *P. fluorescens* DN16-induced defense against *B. cinerea* infection. Five-week-old cucumber plants were treated with or without DN16, followed by *B. cinerea* infection. **(A)** After 1, 3, and 5 days of inoculation, the levels of TSpm were quantified in both the control and inoculated leaves. **(B)** The levels of TSpm in the control and inoculated leaves at 1, 3, and 5 dpi. **(C)** The expression of *CsACL5* and **(D)** leaf TSpm levels in both the wild type (WT) and two transgenic lines (ACL5ox-L2 and -L8). Five-week-old cucumber plants were treated with *B. cinerea*, and disease index **(E)**, ΦPSII **(F)**, and the expression of *BcActin* **(G)** were determined, respectively. **(H)** Lesion symptoms and **(I)** diameters of detached leaves at 5 dpi. The data represented the means ± SD from three biological repeats and different letters indicated significant differences using Duncan's multiple range tests ($p < 0.05$).

plants were pre-treated with the PAO inhibitor HEH for 3 days, and were then infected with *B. cinerea*. The disease-resistant ability of plants was evaluated by observing the necrosis on the pathogen-infected leaves at 5 dpi. As shown in **Figure 6A**, the inoculation with DN16 enhanced leaf resistance against *B. cinerea* infection. The diameters of necrotic lesion were significantly smaller in the DN16-inoculated leaves than the controls (**Figure 6B**). However, foliar treatment with HEH resulted in the increased necrotic lesions. Accordantly, HEH treatment fully abrogated the DN16-induced disease resistance, displaying higher disease index (**Figure 6C**). Overexpression of *CsACL5* also failed to the increased disease resistance of cucumber plants pre-treated with HEH. Moreover, qPCR analyses showed that the transcription levels of *BcActin* were remarkably higher in the HEH-treated leaves than the control leaves. Our findings suggested a pivotal role of TSpm oxidation in mediating the defense of cucumber plants against *B. cinerea* infection.

The PAO-mediated oxidation of TSpm is associated with the production of Put, which can be further oxidized by CuAOs. This indicated that the DN16-induced resistance to *B. cinerea* was likely resulted from the CuAO-mediated Put oxidation. As shown in **Figures 6A–D**, the function of CuAOs in the DNA16-mediated ISR was verified by the data that the CuAO inhibitor AG abrogated the DN16-induced cucumber resistance against pathogen infection. Similarly, overexpression of *CsACL5* could not increase the resistance of cucumber plants against pathogen invasion when the plants were pre-treated with AG. In addition, pre-treatment with the AG or HEH failed to considerably elevate the transcription of defense-related genes including *CsPR1* and *CsDLP1* in both the DN16-inoculated and *CsACL5*-overexpressing plants after pathogen infection (**Figures 6E,F**). Therefore, these data indicated that the DN16-mediated enhancement of defense responses was closely related to the PAO- and CuAO-mediated oxidation of PAs.

DISCUSSION

The present study showed that beneficial rhizobacterial strain *P. fluorescens* DN16 remarkably stimulated the synthesis of TSpm and its catabolism with obvious ramifications for the interactions between the foliar pathogen *B. cinerea* and cucumber plants. Specifically, the DN16-inoculated plants accumulated higher leaf TSpm levels than the controls. The transcription levels of the

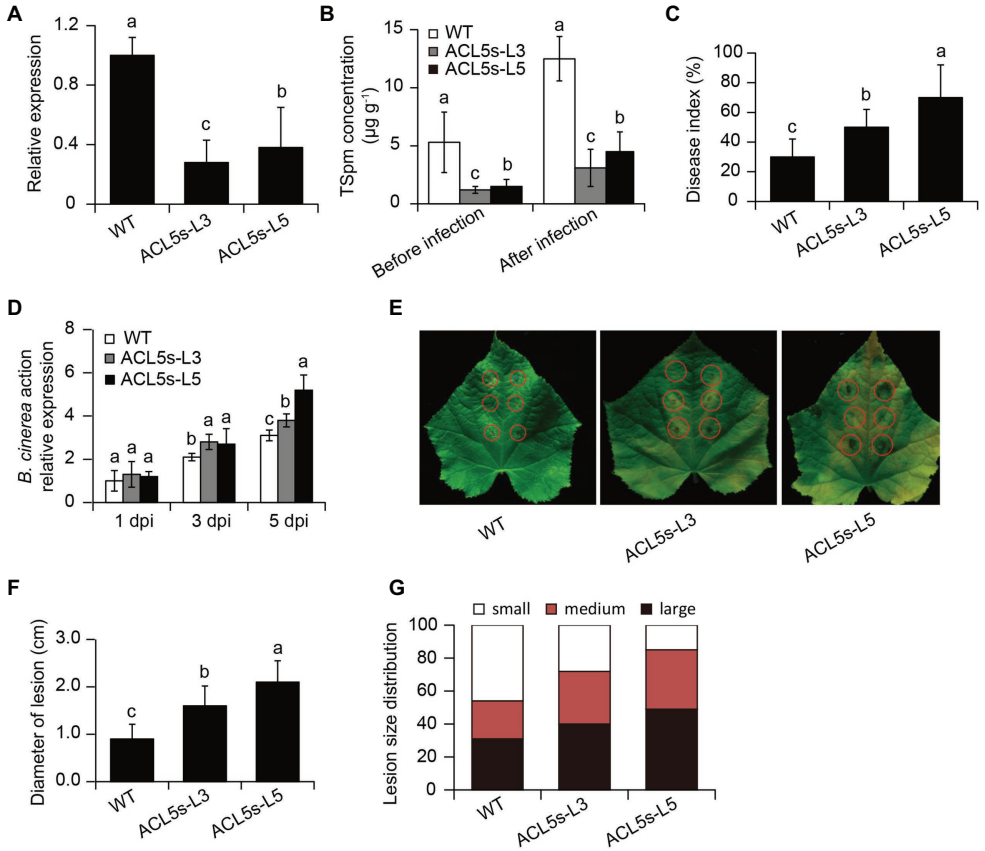

FIGURE 4 | Silencing of *CsACL5* increased the susceptibility of cucumber plants to *B. cinerea* infection. **(A)** The expression of *CsACL5* in both the WT and two transgenic leaves (ACL5s-L3 and -L5). **(B)** Leaf TSpm content in both the WT and two transgenic lines before pathogen infection or after 5 days of pathogen infection. Five-week-old WT and transgenic lines were sprayed with *B. cinerea*, and **(C)** disease index and **(D)** the expression of *BcActin* were calculated at 1, 3, and 5 dpi, respectively. **(E)** Lesion symptoms, **(F)** diameters, and **(G)** size distribution of detached leaves at 5 dpi. The data represented the means ± SD from three biological repeats and different letters indicated significant differences Duncan's multiple range tests ($p < 0.05$).

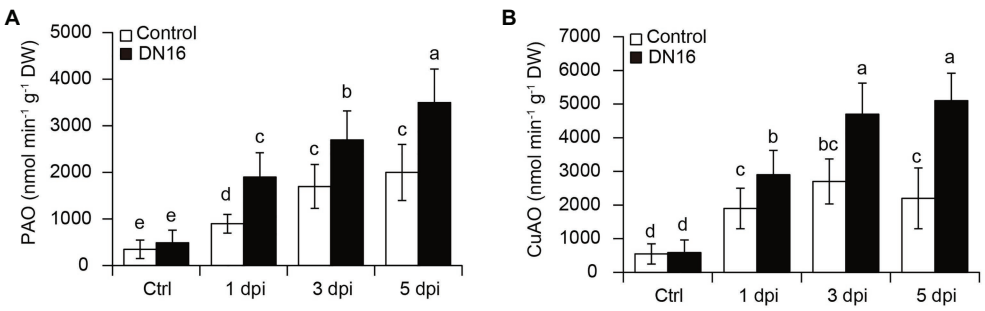

FIGURE 5 | Changes of copper amine oxidase (CuAO) and polyamine oxidase (PAO) activities in both the control and DN16-inoculated leaves in response to *B. cinerea* infection. Detached leaves were treated with *B. cinerea* at the indicated times. **(A)** The activities of PAOs and **(B)** CuAOs were quantified in both the non-pathogen- (Ctrl) and pathogen-infected leaves in the absence or presence of DN16. The data represented the means ± SD from three biological repeats and different letters indicated significant differences using Duncan's multiple range tests ($p < 0.05$).

CsACL5 gene, encoding a putative TSpm synthase, were notably induced in the cucumber plants colonized by DN16. The increased TSpm level was positively correlated with upregulation of *CsACL5* transcripts in the leaves of the inoculated plants. Suppression of *B. cinerea* infection in the inoculated plants with higher level of TSpm implied that this tetraamine conferred the enhanced host resistance against this pathogen. This hypothesis was further favored by the increased tolerance to *B. cinerea* displayed by

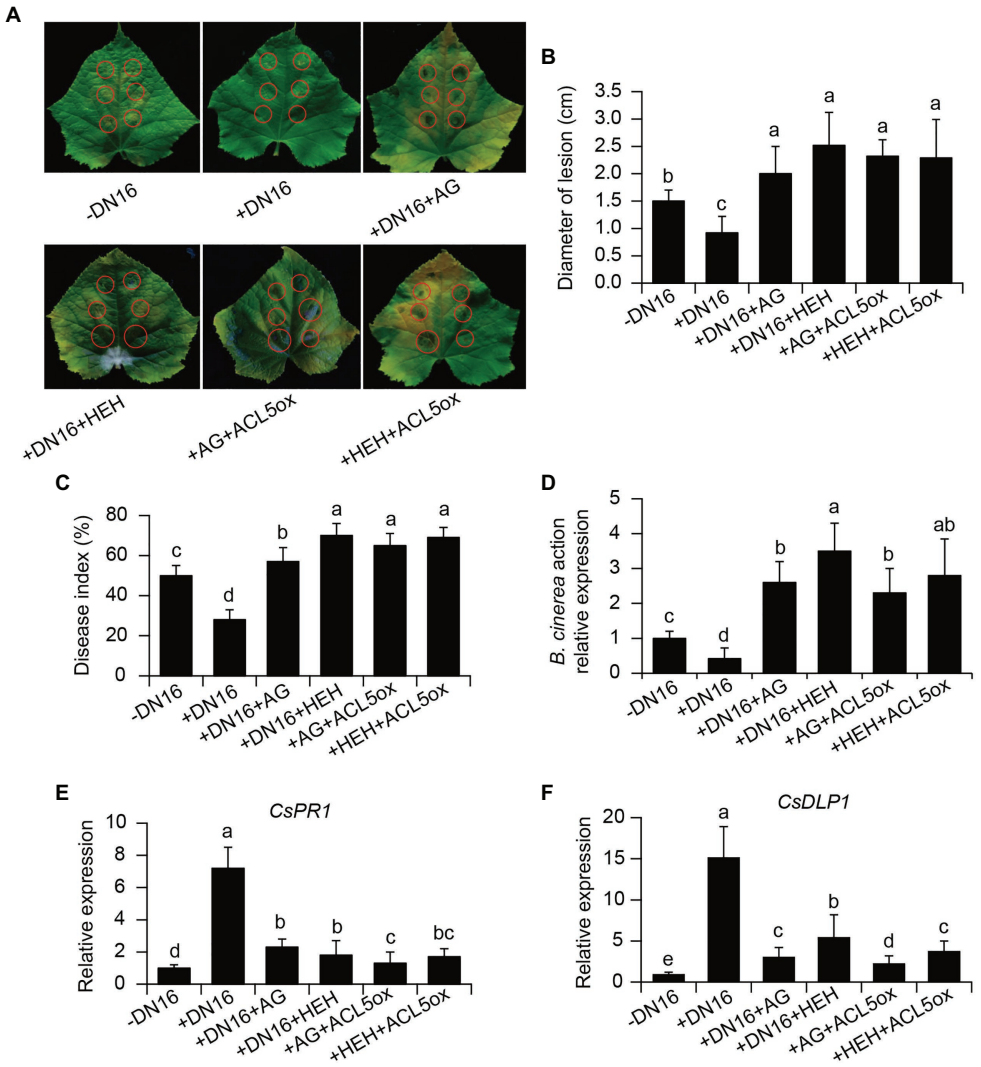

FIGURE 6 | Effects of PA oxidation on the DN16-induced defense against *B. cinerea*. The control, inoculated, and *ACL5*-overexpressing plants were pre-treated with aminoguanidine (AG) or β-hydroxyehtylhydrazine (HEH) for 24 h. These plants were then subjected to *B. cinerea* infection. **(A)** Lesion symptoms and **(B)** diameters of detached leaves at 5 dpi. Disease index **(C)**, the expression of *BcActin* **(D)**, *CsPR1* **(E)**, and *CsDLP1* **(F)** were determined in cucumber plants at 7 dpi. Control, –DN16; DN16-inoculated plants, +DN16; DN16-inoculated plants treated with AG (+DN16+AG) or HEH (+DN16+HEH); *ACL5*-overexpressing plants treated with AG (+AG+ACL5ox) or HEH (+HEH+ACL5ox). The data represented the means ± SD from three biological repeats and different letters indicated significant differences using Duncan's multiple range tests ($p < 0.05$).

the *CsACL5*-overexpressing lines. Moreover, the inoculated plants also displayed higher transcription of PA catabolic genes than the controls. Repression of the PAO and CuAO activities distinctly abrogated the DN16-mediated ISR in cucumber plants, indicating that the abilities of PA catabolic enzymes to oxidize TSpm were responsible for the TSpm-mediated defense responses in the DN16-inoculated plants. Our findings were in accordance with the data of a previous study, in which the PAO-mediated TSpm catabolism participates in modifying *Arabidopsis* defense against *B. cinerea* infection (Marina et al., 2013).

Thermospermine is a major type of PAs widely present in plant kingdom known to induce defense responses in plants (Jiménez-Bremont et al., 2014). TSpm exogenously supplied can enhance the resistance of *Arabidopsis* plants against *P. viridiflava*, which is also similar to the observation for *Arabidopsis* plants ectopically expressing *AtACL5* (Marina et al., 2013). Mount evidence has indicated that genetic manipulation of *ACL5* homologous genes or the increased TSpm levels can enhance defense responses in plants (Sagor et al., 2012; Mo et al., 2015a). Silencing of *GhACL5* reduces the levels of TSpm and increases the susceptibility of plants to *V. dahlia*. In this study, it was worth noting that the transcription levels of *CsACL5* were markedly increased in the DN16-inoculated plants. Consistently, the inoculated plants accumulated more leaf TSpm content than the controls. Similarly, overexpression of *GhACL5* can increase the levels of TSpm in *Arabidopsis* plants

(Mo et al., 2015a). We further verified whether the DN16-induced expression of *CsACL5* contributed to the increased disease resistance in cucumber plants. Our results showed that overexpression of *CsACL5* in cucumber plants led to higher accumulation of TSpm and stronger resistance to *B. cinerea*. Conversely, silencing of *CsACL5* abolished the DN16-induced resistance of plants to *B. cinerea* infection. Collectively, these results indicated that the expression levels of *CsACL5* were positively associated with the disease-resistant ability of cucumber plants to *B. cinerea* infection.

It has recently been indicated that overexpression of *AtACL5* lead to no obvious changes of the TSpm levels in *Arabidopsis* plants compared with the controls, but enhances disease resistance, which is primarily attributable to activation of *PAOs* that can mediate the catabolism of TSpm (Marina et al., 2013). Interestingly, upon exposure to pathogen infection, there was no marked discrepancy in the leaf TSpm levels between the control and DN16-inoculated plants challenged with *B. cinerea* in spite of higher TSpm levels in the inoculated plants without pathogen infection. This finding prompted us to speculate that the attacks of *B. cinerea* may trigger the expression of several genes involved in the PA catabolism, thereby promoting the catabolism of TSpm. The enhanced transcription of *CsPAO1*, *CsPAO5*, and *CsCuAO1* displayed by the pathogen-infected plants inoculated with DN16 implied that reduction of leaf TSpm levels in the inoculated plants were resulted from the enhanced activities of PA catabolic enzymes, probably participating in adjusting dynamic homeostasis of TSpm. Similar results were also observed in *Arabidopsis* plants, in which overexpression of *AtACL5* significantly upregulates the expression levels of several *PAO* genes including *PAO1*, *3*, and *5*, indicating that these PAOs play important roles in controlling the level of TSpm (Marina et al., 2013).

Either abiotic stress or and *B. cinerea* infection can also enhance the activities of PAOs and defense responses in grapevine leaves (Hussain et al., 2011; Hatmi et al., 2014, 2015). Yoda et al. (2009) have shown that the tobacco mosaic virus (TMV)-infected tobacco plants display the augmented PAO activities with higher production of apoplastic H_2O_2 through the PA oxidation-related pathways. The PA oxidation further contributes to the enhanced defense responses of tobacco plants against TMV infection. Apoplastic PA oxidation has previously been shown to participate in plant defense against microbial pathogens (Marina et al., 2008). Gonzalez et al. (2011) have demonstrated that the increased *Arabidopsis* resistance to *P. viridiflava* regulated by Spm is at least partially dependent on the activities of PAOs. In this study, the inoculation with DN16 failed to increase the resistance of cucumber plants against *B. cinerea* infection after treatment with the PAO or CuAO inhibitor, indicating that the PAO- and CuAO-mediated TSpm catabolism was essential for the DN16-induced resistance against *B. cinerea* infection. In fact, either beneficial rhizobacteria or pathogens can induce priming in plants, which has been shown to effectively provoke defense responses. A faster and stronger activation of defense responses frequently occurs in the primed plants after subsequent invasion of pathogens (Heil and Bostock, 2002; Van der Ent et al., 2009; Romera et al., 2019). Previously, volatile organic compounds can be released by caterpillar-infested plants for inducing priming protective effects for earlier and stronger activation of subsequent defenses rather than to induce a direct activation of defense responses (Ton et al., 2006). Our data revealed that the inoculation with DN16 did not largely impact the expression of most defense-related genes, but the induced defense responses were markedly enhanced in the inoculated plants infected by *B. cinerea*. However, the priming effects were fully abolished in the inoculated plants treated with the PAO or CuAO inhibitor. These results confirmed that the TSpm-mediated priming was a more valid defense strategy, involving the DN16-induced cucumber resistance against *B. cinerea*.

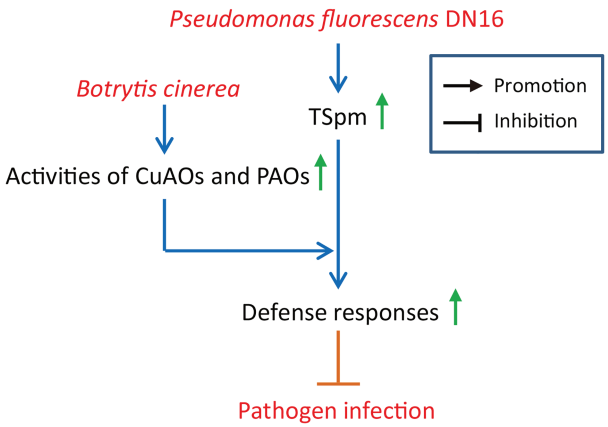

FIGURE 7 | A proposed model for illustrating the functions of TSpm oxidation in the rhizobacteria-mediated cucumber resistance against *B. cinerea*. *Pseudomonas fluorescens* DN16 increased leaf TSpm levels in cucumber plants, but did not trigger the expression of pathogenesis-related genes, conferring a primed state of enhanced defense in cucumber plants. Upon exposure to *B. cinerea*, the catabolism of TSpm was quickly activated, involving the stimulation of the CuAO and PAO activities. This further contributed to the increased host resistance against pathogen infection.

CONCLUSION

Our study has unraveled an important role of beneficial rhizobacterial strains as a part of cucumber immune systems against *B. cinerea*. To our knowledge, these findings provide novel evidence for the tripartite interactions between rhizobacteria, plants, and foliar pathogen. Herein, a model was provided for the DN16-induced cucumber resistance against *B. cinerea* (**Figure 7**), whereby the biosynthesis of TSpm is substantially induced by DN16, resulting in higher leaf TSpm levels. Upon exposure to *B. cinerea* infection, the PAO and CuAO activities can be quickly activated to promote the catabolism of TSpm in the inoculated plants, thereby effectively provoking defense responses.

DATA AVAILABILITY STATEMENT

The datasets presented in this study can be found in online repositories. The names of the repository/repositories and accession number(s) can be found in the article/**Supplementary Material**.

AUTHOR CONTRIBUTIONS

LQ and HD: conceptualization and supervision. LZ, NQ, and YS: investigation and formal analysis. LQ and LZ: funding acquisition. LZ and NQ: experiments. LZ, NQ, and XL: analysis of results. LZ, LQ, and XL: writing original draft. HD, YS, NQ, and LZ: review and editing. All authors contributed to the article and approved the submitted version.

FUNDING

This research was funded by the Natural Science Foundation of the Anhui Science and Technology Committee (1908085QC110), the National Undergraduate Training Program for Innovation and Entrepreneurship (201910879073), the Open Funds of the Anhui Province Key Laboratory of Farmland Ecological Conservation and Pollution Prevention (KLFECPP201802), the School-enterprise Cooperation Projects (ZHEP2019001), and the Natural Science Foundation of Education Department of Anhui province (KJ2020A0067).

SUPPLEMENTARY MATERIAL

The Supplementary Material for this article can be found online at: https://www.frontiersin.org/articles/10.3389/fpls.2021.645338/full#supplementary-material

REFERENCES

Angelini, R., Cona, A., Federico, R., Fincato, P., Tavladoraki, P., and Tisi, A. (2010). Plant amine oxidases "on the move": an update. *Plant Physiol. Biochem.* 48, 560–564. doi: 10.1016/j.plaphy.2010.02.001

Block, A. K., Vaughan, M. M., Schmelz, E. A., and Christensen, S. A. (2019). Biosynthesis and function of terpenoid defense compounds in maize (*Zea mays*). *Planta* 249, 21–30. doi: 10.1007/s00425-018-2999-2

Cona, A., Rea, G., Angelini, R., Federico, R., and Tavladoraki, P. (2006). Functions of amine oxidases in plant development and defence. *Trends Plant Sci.* 11, 80–88. doi: 10.1016/j.tplants.2005.12.009

Curvers, K., Seifi, H., Mouille, G., de Rycke, R., Asselbergh, B., Van Hecke, A., et al. (2010). Abscisic acid deficiency causes changes in cuticle permeability and pectin composition that influence tomato resistance to *Botrytis cinerea*. *Plant Physiol.* 154, 847–860. doi: 10.1104/pp.110.158972

Daudi, A., and O'Brien, J. A. (2012). Detection of hydrogen peroxide by DAB staining in *Arabidopsis* leaves. *Bio Protoc.* 2:e263. doi: 10.21769/BioProtoc.263

El Oirdi, M., Abd El Rahman, T., Rigano, L., El Hadrami, A., Rodriguez, M. C., Daayf, F., et al. (2011). *Botrytis cinerea* manipulates the antagonistic effects between immune pathways to promote disease development in tomato. *Plant Cell* 23, 2405–2421. doi: 10.1105/tpc.111.083394

Fahad, S., Hussain, S., Bano, A., Saud, S., Hassan, S., Shan, D., et al. (2015). Potential role of phytohormones and plant growth-promoting rhizobacteria in abiotic stresses: consequences for changing environment. *Environ. Sci. Pollut. Res. Int.* 22, 4907–4921. doi: 10.1007/s11356-014-3754-2

Fuell, C., Elliott, K. A., Hanfrey, C. C., Franceschetti, M., and Michael, A. J. (2010). Polyamine biosynthetic diversity in plants and algae. *Plant Physiol. Biochem.* 48, 513–520. doi: 10.1016/j.plaphy.2010.02.008

Gonzalez, M. E., Marco, F., Minguet, E. G., Carrasco-Sorli, P., Blazquez, M. A., Carbonell, J., et al. (2011). Perturbation of spermine synthase gene expression and transcript profiling provide new insights on the role of the tetraamine spermine in *Arabidopsis* defense against *Pseudomonas viridiflava*. *Plant Physiol.* 156, 2266–2277. doi: 10.1104/pp.110.171413

Hatmi, S., Gruau, C., Trotel-Aziz, P., Villaume, S., Rabenoelina, F., Baillieul, F., et al. (2015). Drought stress tolerance in grapevine involves activation of polyamine oxidation contributing to improved immune response and low susceptibility to *Botrytis cinerea*. *J. Exp. Bot.* 66, 775–787. doi: 10.1093/jxb/eru436

Hatmi, S., Trotel-Aziz, P., Villaume, S., Couderchet, M., Clément, C., and Aziz, A. (2014). Osmotic stress-induced polyamine oxidation mediates defence responses and reduces stress-enhanced grapevine susceptibility to *Botrytis cinerea*. *J. Exp. Bot.* 65, 75–88. doi: 10.1093/jxb/ert351

Heil, M., and Bostock, R. M. (2002). Induced systemic resistance (ISR) against pathogens in the context of induced plant defences. *Ann. Bot.* 89, 503–512. doi: 10.1093/aob/mcf076

Hu, Z., Shao, S., Zheng, C., Sun, Z., Shi, J., Yu, J., et al. (2018). Induction of systemic resistance in tomato against *Botrytis cinerea* by N-decanoyl-homoserine lactone via jasmonic acid signaling. *Planta* 247, 1217–1227. doi: 10.1007/s00425-018-2860-7

Hussain, S. S., Ali, M., Ahmad, M., and Siddique, K. H. (2011). Polyamines: natural and engineered abiotic and biotic stress tolerance in plants. *Biotechnol. Adv.* 29, 300–311. doi: 10.1016/j.biotechadv.2011.01.003

Jiménez-Bremont, J. F., Marina, M., Guerrero-González Mde, L., Rossi, F. R., Sánchez-Rangel, D., Rodríguez-Kessler, M., et al. (2014). Physiological and molecular implications of plant polyamine metabolism during biotic interactions. *Front. Plant Sci.* 5:95. doi: 10.3389/fpls.2014.00095

Jing, N., Cui, J., Shi, Y., Yang, G., Zhou, X., Hou, X., et al. (2019). Tomato lncRNA23468 functions as a competing endogenous RNA to modulate NBS-LRR genes by decoying miR482b in the tomato-Phytophthora infestans interaction. *Hortic. Res.* 6:28. doi: 10.1038/s41438-018-0096-0

Kakehi, J., Kuwashiro, Y., Niitsu, M., and Takahashi, T. (2018). Thermospermine is required for stem elongation in *Arabidopsis thaliana*. *Plant Cell Physiol.* 49, 1342–1349. doi: 10.1093/pcp/pcn109

Kim, D. W., Watanabe, K., Murayama, C., Izawa, S., Niitsu, M., Michael, A. J., et al. (2014). Polyamine oxidase5 regulates *Arabidopsis* growth through thermospermine oxidase activity. *Plant Physiol.* 165, 1575–1590. doi: 10.1104/pp.114.242610

Lugtenberg, B., and Kamilova, F. (2009). Plant-growth-promoting rhizobacteria. *Annu. Rev. Microbiol.* 63, 541–556. doi: 10.1146/annurev.micro.62.081307.162918

Marina, M., Maiale, S. J., Rossi, F. R., Romero, M. F., Rivas, E. I., Gárriz, A., et al. (2008). Apoplastic polyamine oxidation plays different roles in local responses of tobacco to infection by the necrotrophic fungus *Sclerotinia sclerotiorum* and the biotrophic bacterium *Pseudomonas viridiflava*. *Plant Physiol.* 147, 2164–2178. doi: 10.1104/pp.108.122614

Marina, M., Sirera, F. V., Rambla, J. L., Gonzalez, M. E., Blázquez, M. A., Carbonell, J., et al. (2013). Thermospermine catabolism increases *Arabidopsis thaliana* resistance to *Pseudomonas viridiflava*. *J. Exp. Bot.* 64, 1393–1402. doi: 10.1093/jxb/ert012

Mo, H., Wang, X., Zhang, Y., Yang, J., and Ma, Z. (2015a). Cotton ACAULIS5 is involved in stem elongation and the plant defense response to *Verticillium dahliae* through thermospermine alteration. *Plant Cell Rep.* 34, 1975–1985. doi: 10.1007/s00299-015-1844-3

Mo, H., Wang, X., Zhang, Y., Zhang, G., Zhang, J., and Ma, Z. (2015b). Cotton polyamine oxidase is required for spermine and camalexin signalling in the defence response to *Verticillium dahliae*. *Plant J.* 83, 962–975. doi: 10.1111/tpj.12941

Moschou, P. N., Sanmartin, M., Andriopoulou, A. H., Rojo, E., SanchezSerrano, J. J., and Roubelakis-Angelakis, K. A. (2008). Bridging the gap between plant and mammalian polyamine catabolism: a novel peroxisomal polyamine oxidase responsible for a full back-conversion pathway in *Arabidopsis*. *Plant Physiol.* 147, 1845–1857. doi: 10.1104/pp.108.123802

Moschou, P. N., Sarris, P. F., Skandalis, N., Andriopoulou, A. H., Paschalidis, K. A., Panopoulos, N. J., et al. (2009). Engineered polyamine catabolism preinduces tolerance of tobacco to bacteria and oomycetes. *Plant Physiol.* 149, 1970–1981. doi: 10.1104/pp.108.134932

Muñiz, L., Minguet, E. G., Singh, S. K., Pesquet, E., Vera-Sirera, F., Moreau-Courtois, C. L., et al. (2008). ACAULIS5 controls *Arabidopsis* xylem

specification through the prevention of premature cell death. *Development* 135, 2573–2582. doi: 10.1242/dev.019349

Nadeem, S. M., Ahmad, M., Zahir, Z. A., Javaid, A., and Ashraf, M. (2014). The role of mycorrhizae and plant growth promoting rhizobacteria (PGPR) in improving crop productivity under stressful environments. *Biotechnol. Adv.* 32, 429–448. doi: 10.1016/j.biotechadv.2013.12.005

Nambeesan, S., AbuQamar, S., Laluk, K., Mattoo, A. K., Mickelbart, M. V., Ferruzzi, M. G., et al. (2012). Polyamines attenuate ethylene-mediated defense responses to abrogate resistance to *Botrytis cinerea* in tomato. *Plant Physiol.* 158, 1034–1045. doi: 10.1104/pp.111.188698

Rea, G., Metoui, O., Infantino, A., Federico, R., and Angelini, R. (2002). Copper amine oxidase expression in defense responses to wounding and *Ascochyta rabiei* invasion. *Plant Physiol.* 128, 865–875. doi: 10.1104/pp.010646

Romera, F. J., García, M. J., Lucena, C., Martínez-Medina, A., Aparicio, M. A., Ramos, J., et al. (2019). Induced systemic resistance (ISR) and Fe deficiency responses in dicot plants. *Front. Plant Sci.* 10:287. doi: 10.3389/fpls.2019.00287

Sagor, G. H., Takahashi, H., Niitsu, M., Takahashi, Y., Berberich, T., and Kusano, T. (2012). Exogenous thermospermine has an activity to induce a subset of the defense genes and restrict cucumber mosaic virus multiplication in *Arabidopsis thaliana*. *Plant Cell Rep.* 31, 1227–1232. doi: 10.1007/s00299-012-1243-y

Sen, S., Ghosh, D., and Mohapatra, S. (2018). Modulation of polyamine biosynthesis in *Arabidopsis thaliana* by a drought mitigating *Pseudomonas putida* strain. *Plant Physiol. Biochem.* 129, 180–188. doi: 10.1016/j.plaphy.2018.05.034

Shi, H., and Chan, Z. (2014). Improvement of plant abiotic stress tolerance through modulation of the polyamine pathway. *J. Integr. Plant Biol.* 56, 114–121. doi: 10.1111/jipb.12128

Shinohara, S., Okamoto, T., Motose, H., and Takahashi, T. (2019). Salt hypersensitivity is associated with excessive xylem development in a thermospermine-deficient mutant of *Arabidopsis thaliana*. *Plant J.* 100, 374–383. doi: 10.1111/tpj.14448

Takahashi, Y., Uehara, Y., Berberich, T., Ito, A., Saitoh, H., Miyazaki, A., et al. (2004). A subset of hypersensitive response marker genes, including HSR203J, is the downstream target of a spermine signal transduction pathway in tobacco. *Plant J.* 40, 586–595. doi: 10.1111/j.1365-313X.2004.02234.x

Takano, A., Kakehi, J., and Takahashi, T. (2012). Thermospermine is not a minor polyamine in the plant kingdom. *Plant Cell Physiol.* 53, 606–616. doi: 10.1093/pcp/pcs019

Tian, X., Song, L., Wang, Y., Jin, W., Tong, F., and Wu, F. (2018). miR394 acts as a negative regulator of *Arabidopsis* resistance to *B. cinerea* infection by targeting LCR. *Front. Plant Sci.* 9:903. doi: 10.3389/fpls.2018.00903

Ton, J., D'Alessandro, M., Jourdie, V., Jakab, G., Karlen, D., Held, M., et al. (2006). Priming by airborne signals boosts direct and indirect resistance in maize. *Plant J.* 49, 16–26. doi: 10.1111/j.1365-313X.2006.02935.x

Van der Ent, S., Van Wees, S. C., and Pieterse, C. M. (2009). Jasmonate signaling in plant interactions with resistance-inducing beneficial microbes. *Phytochemistry* 70, 1581–1588. doi: 10.1016/j.phytochem.2009.06.009

van Loon, L. C., Rep, M., and Pieterse, C. M. (2006). Significance of inducible defense-related proteins in infected plants. *Annu. Rev. Phytopathol.* 44, 135–162. doi: 10.1146/annurev.phyto.44.070505.143425

Vuosku, J., Muilu-Mäkelä, R., Avia, K., Suokas, M., Kestilä, J., Läärä, E., et al. (2019). Thermospermine synthase (ACL5) and diamine oxidase (DAO) expression is needed for zygotic embryogenesis and vascular development in scots pine. *Front. Plant Sci.* 10:1600. doi: 10.3389/fpls.2019.01600

Walters, D. R. (2003). Polyamines and plant disease. *Phytochemistry* 64, 97–107. doi: 10.1016/S0031-9422(03)00329-7

Wang, W., Paschalidis, K., Feng, J. C., Song, J., and Liu, J. H. (2009). Polyamine catabolism in plants: a universal process with diverse functions. *Front. Plant Sci.* 10:561. doi: 10.3389/fpls.2019.00561

Wang, H., Sui, X., Guo, J., Wang, Z., Cheng, J., Ma, S., et al. (2014). Antisense suppression of cucumber (*Cucumis sativus* L.) sucrose synthase 3 (CsSUS3) reduces hypoxic stress tolerance. *Plant Cell Environ.* 37, 795–810. doi: 10.1111/pce.12200

Yang, S., Wen, C., Liu, B., Cai, Y., Xue, S., Bartholomew, E. S., et al. (2019). A CsTu-TS1 regulatory module promotes fruit tubercule formation in cucumber. *Plant Biotechnol. J.* 17, 289–301. doi: 10.1111/pbi.12977

Yoda, H., Fujimura, K., Takahashi, H., Munemura, I., Uchimiya, H., and Sano, H. (2009). Polyamines as a common source of hydrogen peroxide in host and nonhost hypersensitive response during pathogen infection. *Plant Mol. Biol.* 70, 103–112. doi: 10.1007/s11103-009-9459-0

Zhang, W., Zhang, H., Qi, F., and Jian, G. (2016). Generation of transcriptome profiling and gene functional analysis in *Gossypium hirsutum* upon *Verticillium dahliae* infection. *Biochem. Biophys. Res. Commun.* 473, 879–885. doi: 10.1016/j.bbrc.2016.03.143

Zhou, C., Ma, Z., Zhu, L., Xiao, X., Xie, Y., Zhu, J., et al. (2016). Rhizobacterial strain *Bacillus megaterium* BOFC15 induces cellular polyamine changes that improve plant growth and drought resistance. *Int. J. Mol. Sci.* 17:976. doi: 10.3390/ijms17060976

Zhou, C., Zhu, L., Guo, J., Xiao, X., Ma, Z., and Wang, J. (2019). *Bacillus subtilis* STU6 ameliorates iron deficiency in tomato by enhancement of polyamine-mediated iron remobilization. *J. Agric. Food Chem.* 67, 320–330. doi: 10.1021/acs.jafc.8b05851

Conflict of Interest: The authors declare that the research was conducted in the absence of any commercial or financial relationships that could be construed as a potential conflict of interest.

frontiers in Plant Science

ORIGINAL RESEARCH
published: 23 March 2021
doi: 10.3389/fpls.2021.647372

Interactive Effects of Mycorrhizae, Soil Phosphorus, and Light on Growth and Induction and Priming of Defense in *Plantago lanceolata*

*Laiye Qu[1,2], Minggang Wang[3,4] and Arjen Biere[4]**

[1]State Key Laboratory of Urban and Regional Ecology, Research Center for Eco-Environmental Science, Chinese Academy of Sciences, Beijing, China, [2]College of Resources and Environment, University of Chinese Academy of Sciences, Beijing, China, [3]College of Forestry, Beijing Forestry University, Beijing, China, [4]Department of Terrestrial Ecology, Netherlands Institute of Ecology (NIOO-KNAW), Wageningen, Netherlands

OPEN ACCESS

Edited by:
Jianfei Wang,
Anhui University of Science and Technology, China

Reviewed by:
Wang Jie,
Fujian Agriculture and Forestry University, China
Xiancan Zhu,
Anhui Normal University, China

***Correspondence:**
Arjen Biere
a.biere@nioo.knaw.nl

Specialty section:
This article was submitted to Plant Symbiotic Interactions, a section of the journal Frontiers in Plant Science

Received: 29 December 2020
Accepted: 26 February 2021
Published: 23 March 2021

Citation:
Qu L, Wang M and Biere A (2021) Interactive Effects of Mycorrhizae, Soil Phosphorus, and Light on Growth and Induction and Priming of Defense in Plantago lanceolata. Front. Plant Sci. 12:647372. doi: 10.3389/fpls.2021.647372

Increasing demands to reduce fertilizer and pesticide input in agriculture has triggered interest in arbuscular mycorrhizal fungi (AMF) that can enhance plant growth and confer mycorrhiza-induced resistance (MIR). MIR can be based on a variety of mechanisms, including induction of defense compounds, and sensitization of the plant's immune system (priming) for enhanced defense against later arriving pests or pathogens signaled through jasmonic acid (JA). However, growth and resistance benefits of AMF highly depend on environmental conditions. Low soil P and non-limiting light conditions are expected to enhance MIR, as these conditions favor AMF colonization and because of observed positive cross-talk between the plant's phosphate starvation response (PSR) and JA-dependent immunity. We therefore tested growth and resistance benefits of the AMF *Funneliformis mosseae* in *Plantago lanceolata* plants grown under different levels of soil P and light intensity. Resistance benefits were assessed in bioassays with the leaf chewing herbivore *Mamestra brassicae*. Half of the plants were induced by jasmonic acid prior to the bioassays to specifically test whether AMF primed plants for JA-signaled defense under different abiotic conditions. AMF reduced biomass production but contrary to prediction, this reduction was not strongest under conditions considered least optimal for carbon-for-nutrient trade (low light, high soil P). JA application induced resistance to *M. brassicae*, but its extent was independent of soil P and light conditions. Strikingly, in younger plants, JA-induced resistance was annulled by AMF under high resource conditions (high soil P, ample light), indicating that AMF did not prime but repressed JA-induced defense responses. In older plants, low soil P and light enhanced susceptibility to *M. brassicae* due to enhanced leaf nitrogen levels and reduced leaf levels of the defense metabolite catalpol. By contrast, in younger plants, low soil P enhanced resistance. Our results highlight that defense priming by AMF is not ubiquitous and calls for studies revealing the causes of the increasingly observed repression of JA-mediated defense by AMF. Our study further shows that in our system abiotic factors are significant modulators

of defense responses, but more strongly so by directly modulating leaf quality than by modulating the effects of beneficial microbes on resistance.

Keywords: defense priming, *Funneliformis mosseae*, induced systemic resistance, iridoid glycosides, *Mamestra brassicae*, mycorrhiza-induced resistance, shading, soil phosphorus

INTRODUCTION

The use of beneficial microbes such as arbuscular mycorrhizal fungi (AMF) is considered a promising way to meet the increasing demand to reduce fertilizer and pesticide use in agriculture and horticulture (Choudhary et al., 2016). AMF form symbioses with over 80% of the land plants, trading mineral nutrients, and especially phosphorus, for carbon sources with their host plants (Smith and Read, 2008). Under a range of conditions, AMF can provide benefits to plants in the form of e.g., growth promotion, enhancement of abiotic and biotic stress tolerance, enhanced pollinator service, and enhancement of tolerance and defense against particular groups of pathogens and herbivores (Bennett et al., 2006; Pozo and Azcon-Aguilar, 2007; Gehring and Bennett, 2009; Hartley and Gange, 2009; Koricheva et al., 2009; Vannette and Hunter, 2009; Jung et al., 2012; Biere and Bennett, 2013; Tao et al., 2016).

The systemic enhancement of resistance against above- and belowground pathogens and insect herbiores by AMF is referred to as "mycorrhiza-induced resistance" (MIR). Several mechanisms underlying MIR have been identified (Cameron et al., 2013). Most prominently, AMF have been shown to sensitize the immune system of their host plants, resulting in a primed state (Conrath et al., 2015; Mauch-Mani et al., 2017). This allows mycorrhizal plants to respond faster and/or stronger when they are challenged by later arriving herbivores and pathogens that are signaled by the plant through the plant hormones jasmonic acid (JA) and ethylene (ET; Pozo and Azcon-Aguilar, 2007; Jung et al., 2012; Song et al., 2013), notably necrotrophic pathogens and generalist chewing leaf herbivores. Priming prepares plants for future attack without directly activating costly defenses (Martinez-Medina et al., 2016). JA-dependent priming forms the basis of induced systemic resistance (ISR) triggered by a variety of beneficial soil microbes (Van Wees et al., 2008; Zamioudis and Pieterse, 2012; Pieterse et al., 2014; Miozzi et al., 2019; Yu et al., 2019; Nishad et al., 2020). In addition to priming of JA-signaled defenses, MIR can also be simply mediated by induction of different classes of defense metabolites that has been widely observed in response to AMF colonization (e.g., Andrade et al., 2013; Vannette et al., 2013; Shrivastava et al., 2015).

Although mycorrhiza-induced resistance has been shown in many systems, it is not a ubiquitously observed phenomenon. For instance, priming of JA-dependent proteinaceous defenses by AMF has been elegantly demonstrated in cultivated tomato (Song et al., 2013), but mixed results have been obtained for wild solanaceous species (Minton et al., 2016). Moreover, even when AMF trigger defense responses, this does not necessarily result in enhanced resistance. This is because AMF colonization commonly results in a diverse set of phenotypic changes in their host plants, that each can contribute to either enhanced resistance or to enhanced susceptibility to a particular pest or pathogen. For instance, AMF colonization results in a strong reprogramming of the root and shoot metabolome (Kaur and Suseela, 2020), that often not only encompassess the induction of defense metabolites, but also results in an enhancement of the nutritional status of root and shoot tissues. Likewise, the set of distinct morphological and physiological changes that are induced by AMF colonization includes alterations in phenology, size, apparency, availability, palatability, and digestibility of plant tissues, that each can either enhance or reduce the plant's resistance to pathogens and pests (Bennett et al., 2006).

Moreover, both the extent of AMF-induced growth promotion and the extent of MIR have been shown to strongly depend on the abiotic environmental context. This context dependency has been identified as one of the major problems in the application of beneficial microbes to enhance crop resistance and production (Barber et al., 2013). Much of the current research is therefore focused on understanding such context dependency (Koricheva et al., 2009; Hoeksema et al., 2010; Johnson et al., 2015; Pozo et al., 2015). Two of the environmental factors that have been identified as important drivers of context-dependency in both the mycorrhizal growth response (MGR, the percent growth benefit incurred by AMF compared to non-mycorrhizal, NM, plants) and in MIR are the availability of soil phosphorus (Johnson et al., 2015) and light (Konvalinkova and Jansa, 2016).

Optimal trade principles predict that plant growth will most strongly benefit from symbiosis with AMF under conditions of low soil phosphorus supply, when plants gain optimal benefit from the P provided by the fungal partner, and under conditions of ample light, entailing minimal costs for the plant to provide carbon sources in the form of hexoses and fatty acids in return to the fungus (Hoeksema et al., 2010; Johnson, 2010). Indeed, in an elegant series of grassland experiments, Johnson et al. (2015) showed that mutualisms between *Andropogon gerardii* and AMF arose in P-limited but not in N-limited systems, and that shading generated less mutualistic interactions, resulting in reduced plant and fungal biomass. These results are corroborated by several experimental studies showing that the growth benefit of AMF is strongly reduced, or even becomes negative, under increasing levels of soil P (Hetrick et al., 1983), as well as under conditions of shading (reviewed by Konvalinkova and Jansa, 2016). Accordingly, plants have evolved active mechanisms to reduce colonization by AMF under such unfavorable conditions for trade. The AM symbiosis is tightly regulated and integrated with the plant's Pi status through a complex signaling network, involving phytohormones, micro-RNAs, and secreted peptides (Vierheilig et al., 2000; Nagy et al., 2009; Mueller and Harrison, 2019) in a process known as autoregulation of mycorrhization (AOM). In this process, Pi acts systemically to repress the expression of symbiotic genes,

such as genes involved in the production of strigolactones, important in the initial plant-AMF dialog, and symbiosis-associated phosphate transporters (Breuillin et al., 2010), resulting in lower AMF colonization and functionality at high soil phosphate and high internal plant Pi levels (Nagy et al., 2009; Smith and Smith, 2011; Gosling et al., 2013). Similarly, low light levels (shading) commonly result in lower levels of AMF colonization (reviewed by Konvalinkova and Jansa, 2016).

Not only plant growth, but also MIR is expected to be affected by soil P and light availability, for two reasons. First, as explained above, plants will tend to reduce colonization rates by AMF under conditions of high soil P and shading, which may reduce the extent to which MIR can be activated. Second, recent studies show that soil P can be an important driver of plant immunity. Phosphate deficiency activates the phosphate starvation response (PSR) in plants (Morcuende et al., 2007; Bustos et al., 2010; Rouached et al., 2010; Chiou and Lin, 2011). Recent studies have shown strong cross-talk between the signaling pathways involved in PSR and immunity. High expression of the master transcriptional regulators of PSR in *Arabidopsis thaliana*, *PSR 1 (PHR1)*, and *PHR1-LIKE 1 (PHL1)* enhances the expression of jasmonic acid (JA)-inducible genes associated with defense against generalist leaf chewing insect herbivores and necrotrophic pathogens, but directly represses salicylic acid (SA)-inducible genes, associated with defense against biotrophic pathogens and sap-sucking or cell-feeding insects (Castrillo et al., 2017). This pattern is confirmed by bioassays with insect herbivores and plant pathogens. Several plant species, including *A. thaliana*, tomato, and tobacco, were shown to induce the JA pathway and enhance defense against a generalist leaf chewing insect herbivore when they experienced deficiency in inorganic phosphate (Pi; Khan et al., 2016), a response that was attenuated in JA- as well as PSR-signaling mutants (Khan et al., 2016). By contrast, functional PSR signaling was shown to be associated with enhanced susceptibility to a bacterial and an oomycete pathogen in *A. thaliana* (Castrillo et al., 2017). This is in agreement with earlier studies showing that several transcription factors co-regulate both PSR and immunity (Baek et al., 2017). For instance, *WRKY75* not only activates transcription of PSR genes (Devaiah et al., 2007), but also increases the transcript levels of marker genes of the JA defense signaling pathway, whereas it decreases the expression of marker genes of the SA defense signaling pathway (Schmiesing et al., 2016), or by AMF-mediated recruitment of ISR-inducing rhizobacteria (Cameron et al., 2013).

Collectively, these studies suggest that low soil phosphate may contribute to enhanced plant resistance to leaf chewing herbivores either through enhanced JA immune signaling or through enhanced functional association with ISR-inducing beneficial microbes. However, only few studies have studied interactions between MIR and soil P to test whether low soil P can indeed enhance MIR. In support of this idea, AMF did not induce resistance to charcoal rot in soybean under high soil P conditions, but incurred a more than 5-fold reduction in disease severity under low soil P, that more than compensated the 2.5-fold increase in susceptibility caused by low P in the absence of AMF (Spagnoletti et al., 2018). By contrast, in susceptible wheat, AMF reduced mildew severity independent of soil P, despite its lower colonization rate at high soil P, and low P itself reduced mildew severity as well (Mustafa et al., 2016). Even fewer studies have considered interactions between soil P and MIR with respect to resistance against insect herbivory. Wang et al. (2020) observed that low soil P resulted in higher AMF colonization and lower aphid infestation, but combinatory effects were not tested. Furthermore, as far as we know, no studies have investigated how the effects of soil P on MIR depend on the availability of carbohydrates, as affected by the availability of light for photosynthesis. Like high soil P, low light conditions are expected to hamper plant colonization by resistance-inducing AMF, and may also limit C-resources for the production of defense metabolites upon activation of defenses. Low light conditions may thus counteract the positive effects of low P on MIR.

In this paper, we study the interactive effects of AMF, soil P, and light intensity on plant growth and MIR against a generalist leaf chewing insect herbivore. We grew plants of ribwort plantain (*Plantago lanceolata*) under a factorial combination of light and soil P conditions in the presence or absence of the AM fungus *Funneliformis mosseae*. Subsequently, we used bioassays with caterpillars of the generalist leaf chewing insect herbivore *Mamestra brassicae* to test effects of light, soil P, and AMF on resistance. To specifically test whether AMF can prime plants for JA-dependent defenses and whether such effects are modulated by soil P and light, we challenged half of the plants with leaf application of JA prior to the bioassays. In addition, we measured a set of leaf biochemical and morphological leaf traits of bioassay plants to enable us to associate changes in resistance with changes in leaf traits.

Of specific interest are a class of carbon-based terpenoid defense metabolites produced by *P. lanceolata*, known as iridoid glycosides (IGs), that commonly deter generalist chewing insect herbivores (Puttick and Bowers, 1988; Harvey et al., 2005; Reudler et al., 2011), but can also reduce the performance of fungal pathogens (Marak et al., 2002a; Biere et al., 2004) and AMF (De Deyn et al., 2009). IGs in *P. lanceolata* can be induced by a wide range of organisms, including not only generalist and specialist insect herbivores (e.g., Bowers and Stamp, 1993; Darrow and Bowers, 1999; Fuchs and Bowers, 2004; Quintero and Bowers, 2011, 2012), but also pathogens (Marak et al., 2002b) and AMF (Gange and West, 1994; Bennett et al., 2009; Schweiger et al., 2014a; Wang et al., 2015). Based on stoichiometric principles, production of C-based secondary metabolites such as IGs is expected to be reduced under low light, high nutrient conditions (Fajer et al., 1992) and this is supported for IGs in *P. lanceolata* by a number of studies (Fajer et al., 1992; Darrow and Bowers, 1999; Jarzomski et al., 2000; Tamura, 2001; Marak et al., 2003; Miehe-Steier et al., 2015; Pankoke et al., 2015). This could be an additional reason for lower induction or priming of these defenses in response to AMF under low light and high soil P conditions. We examine whether induction or priming of these compounds by AMF is involved in MIR and whether the extent of induction or priming is dependent on soil P and light conditions. Furthermore, given the strong changes in plant defense strategies and

responsiveness to induction during ontogeny (Van Dam et al., 2001; Boege and Marquis, 2005; Barton and Koricheva, 2010; Miller et al., 2014), we study whether these effects change with plant age.

We address the following specific questions: (1) Are root colonization rates and effects of the AM fungus *F. mosseae* on growth of *P. lanceolata* affected by light and soil P conditions? (2) Are effects of AMF on induction and priming of JA-signaled plant defenses in *P. lanceolata* against the generalist insect herbivore *M. brassicae* affected by light and soil P? (3) Which biochemical and morphological leaf traits changes are associated with the effects of AMF, light, and P on resistance? We hypothesize that the beneficial effect of AMF on plant growth is highest under conditions optimal for trade (high light, low soil P) and lowest under shading and high soil P, and that the extent of induction or priming of defense is similarly strongest under low soil P and high light conditions.

MATERIALS AND METHODS

Plant Materials and Growing Conditions

Ribwort plantain (*Plantago lanceolata* L.) is a rosette-forming, self-incompatible, wind pollinated, perennial herb. It has a worldwide distribution and is commonly used in studies of plant-AM fungus interactions and plant defense (e.g., Gange and West, 1994; Bennett et al., 2009; De Deyn et al., 2009; Pankoke et al., 2015; Wang et al., 2015). The major defense metabolites produced by *P. lanceolata* are the IGs aucubin and catalpol. Like glucosinolates, IGs form a dual defense system, in which vacuole-stored IGs are activated by membrane-bound beta-glucosidases upon damage (Pankoke et al., 2013). Seeds of *P. lanceolata* were obtained from Cruydthoeck (Assen, Netherlands), a supplier of seeds collected from wild plant populations. Seeds were surface-sterilized in a 1% sodium hypochlorite solution for 15 min, rinsed with demineralized water, and germinated on moistened glass beads in a growth cabinet at 20°C and a 16 h photoperiod for 12 days. Seedlings were individually transplanted into 10 cm× 10 cm× 11 cm plastic pots filled with 675 g of a 1:1 (v:v) mixture of sterilized sand (particle size 0.75–1.5 mm) and Sorbix (an inert absorbent, Imerys Industrial Minerals, Fur, Denmark). Pots were placed in 15 × 15 × 7 containers to allow re-absorption of drained water by plants and to prevent contamination of soil biota contained within the drainage water between pots. Plants were grown in a climate-controlled greenhouse at Netherlands Institute of Ecology at 22 ± 2°C and a 16 h photoperiod. Natural daylight was automatically supplemented with light from 400-W metal halide lamps when natural light levels dropped below 225 μmol $m^{-1}s^{-1}$ photon flux density.

AMF, Soil P, and Light Treatments

A factorial combination of two AMF treatments (M), two soil phosphorus treatments (P), and two light treatments (L) was applied. As source of AM fungal inoculum, we used *F. mosseae* BEG 198 (Symbiom Ltd., Lanskroun, Czech Republic). This species forms symbioses with many plant species including *P. lanceolata* (Karasawa et al., 2012; Orlowska et al., 2012; Wang et al., 2015). Fifteen grams of inoculum (granules containing hyphae, spores, and substrate) were mixed into pots assigned to the mycorrhizal inoculation treatment (M+) before seedling transplantation. Pots assigned to the non-mycorrhizal inoculation treatment (M−) received 15 g of sterilized *F. mosseae* inoculum. Because AMF usually perform better in a non-sterile background, 30 ml of a microbial wash was added to all (mycorrhizal and non-mycorrhizal) pots before seedling transplantation. Soil used to obtain a microbial wash originated from a grassland on loamy sand soil in a nature restoration area (Renkum, Netherlands, N 52°00'9", E 5°45'8") that contained 1.45 g total N kg^{-1} and 0.25 g P_2O_5 kg^{-1} soil (Hannula et al., 2017). The microbial wash was obtained by adding 20 kg of soil to 20 L of demineralized water, stirring overnight, and filtering through successively smaller filters (200, 75, 45, and 20 μm) to remove any resident mycorrhizal hyphae and spores, but retaining a microbial background population. Soil phosphorus was applied to experimental pots in the form of bonemeal containing 16% of P_2O_5 (Ecostyle B.V., Oosterwolde, Netherlands). Before seedling transplantation, 1 g of bonemeal was mixed into pots assigned to the high soil phosphorus treatment (P+), whereas 0.1 g was added to pots of the low soil phosphorus treatment (P-), corresponding to ca. 105 and 10.5 mg of organically bound P per kg soil, respectively. Shading treatments were applied to groups of 16 plants (four plants from each of the four combinations of AMF and soil P treatment) that were placed together in 100 cm × 70 cm flats. Half of the flats were covered with a light shade cloth that reduced light levels by only 15% (high light, L+), as measured with a Licor Quantum Sensor LI-190SA (Licor, Bad Homburg, Germany). The cloth was mounted 50 cm above pot level, covering both the top and the sides of the flats. The other half of the flats was covered with shade cloth that reduced light levels by 50% (low light, L-). In total, 24 flats were used, that were grouped into 12 blocks, each block consisting of one group of L+ plants and one group of L-plants. In total, 480 plants were grown (12 blocks × 2 M × 2 P × 2 L treatments × 5 replicates per block). Positions of blocks within the greenhouse were rearranged weekly to avoid effects of any spatial differences in light conditions within the greenhouse. Plants received 0.5 strength Hoagland nutrient solution (Hoagland and Arnon, 1950) without any phosphate (KH_2PO_4) once a week (increasing from 20 ml. in week 2 to 80 ml. in week 10), as well as additional water to maintain soil moisture levels at around 16%. A total of 192 plants were harvested to monitor growth, biomass allocation, and shoot and root morphology and biochemistry across four time points during plant development ("sequential harvests," 3, 6, 9, and 12 weeks after seedling transplantation). The remaining 288 plants were used to test plant resistance against the generalist leaf chewing herbivore, *M. brassicae*, at two time points during development ("bioassays," 7 and 10 weeks after seedling transplantation).

Sequential Harvests

At each of the four sequential harvests, 48 plants (one from each treatment combination from 3 to 6 of the blocks) were harvested. Plants were separated into roots, caudex, leaves, and (at the fourth harvest, when half of the plants had initiated flowering) inflorescences. Roots were thoroughly rinsed to remove all particles of soil substrate. Root and shoot fractions were then oven dried at 60°C for 48 h to measure their dry weights and the root mass fraction (RMF, root dry weight divided by total dry weight). The MGR was calculated as 100 × (M-NM)/NM (Cavagnaro et al., 2003), where M and NM are the dry weights of mycorrhizal and non-mycorrhizal plants, respectively. AMF colonization was quantified at two time points, 6 and 9 weeks after inoculation with *F. mosseae*. A weighed subsample of fresh root material, <1 mm in diameter, was taken, cut in 1.5 cm pieces, cleared in 10% KOH for 20 min. at 90°C, rinsed, stained in a 5% Parker Blue ink–vinegar solution for 15 min. at 90°C, washed, and destained in a 1:1:1 solution of lactic acid, glycerol, and 1% HCL (Vierheilig et al., 1998). AM colonization was recorded according to the magnified intersections method (McGonigle et al., 1990). The incidence of AM structures (hyphae, arbuscules, and vesicles) was scored at a total of 120 intersections to calculate the incidence (%) of each structure over the total number of intersections and the total percentage of root colonization.

Bioassays

At two time points, 7 and 10 weeks after seedling transplantation, bioassays were performed ("Bio1" and "Bio2," respectively) to test plant resistance against the generalist leaf chewing herbivore *M. brassicae*. For each of the bioassays, 144 plants were used (18 per treatment combination, maximum two per treatment combination per block).

Insect Rearing

The cabbage moth [*M. brassicae* (Noctuidae, Lepidoptera)] is a polyphagous chewing insect herbivore whose caterpillar larvae feed on a broad range of host plant species in the Palearctic (Rojas et al., 2000). Insect eggs were obtained from the Laboratory of Entomology, Wageningen University, Netherlands. Caterpillars were grown on artificial diet (Singh et al., 1983) until they reached L3 and starved for 12 h prior to the bioassays.

JA Treatment

In response to generalist leaf chewing herbivores, such as *M. brassicae*, plants generally activate primarily the JA signaling pathway, resulting in the downstream activation of defenses that are effective to these biotic challenges. JA application to plants is often used to mimic the activation of the JA pathway following attack by generalist chewing insect herbivores (Dicke and Hilker, 2003). To test whether mycorrhizae can prime plants for a faster or stronger response to a biotic challenge that triggers the JA signaling pathway, half of the plants (nine per treatment combination) were challenged by application of JA 48 h. prior to initiating the bioassays. A pipette was used to apply 0.5 ml of a 9.5 mM solution of JA dissolved in 0.1% triton to the sixth (Bio1) or ninth (Bio2) youngest fully expanded leaf of plants assigned to the JA treatment. The solution was dispersed across the leaf by gently spreading it over the leaf surface using gloves. The other half of the plants, serving as control, similarly received 0.5 ml of a 0.1% triton solution. Lower performance of bioassay caterpillars on JA-induced plants with AMF than on JA-induced plants without AMF would indicate *priming* of JA-signaled defenses by AMF. Lower performance of bioassay caterpillars on control plants (not treated with JA) with AMF than on control plants without AMF would indicate *induction* of defenses by AMF.

Bioassays

After measuring their initial fresh weight (CFW1), one freshly molted (Bio1) or 2nd day (Bio2) L3 caterpillar was put in a clip cage (5 cm diameter) mounted on the 3rd (Bio1) or 6th (Bio2) youngest leaf of each plant, representing a leaf of intermediate age on plants from these time points, respectively. After 24 (Bio1) or 48 h (Bio2), caterpillars were taken off the plants, re-weighed (CFW2), and dried at 60°C for 48 h to measure their dry weights (CDW2) and dry matter content (CDMC = CDW2/CFW2). Fourteen of the 288 caterpillars died or were lost during the experiment and were excluded from analysis. Leaves used for the bioassays were then removed from the plant, and scanned to estimate the amount of remaining leaf area (LA) and leaf area eaten (dLA) using WINFOLIA (Regent Instruments Inc., Quebec, Canada). In cases where caterpillars fed from leaf margins rather than chewing holes, accurate estimation of the leaf area eaten depends on the ability to reconstruct the leaf margin. This was not possible in 14 of the 288 samples and these data were excluded from analysis. The remains of the leaves were then dried at 60°C for 48 h to measure their dry weights (LDW). For each plant, leaf dry weight eaten (dLDW) was estimated as dLA × LDW/LA. From these data, caterpillar relative growth rate, (RGR, g dw caterpillar. g dw^{-1} caterpillar. day^{-1}), was calculated as dCDW/(avgCDW × t), where dCDW is the dry weight increase of caterpillars during the entire feeding period, calculated as CDW2 − (CFW1 × CDMC), avgCDW is the average dry weight of caterpillars during the feeding period, calculated as 0.5 × (CDW2 + (CFW1 × CDMC), and t is the duration of the bioassay (1 or 2 days for Bio1 and Bio2, respectively). Similarly, relative consumption rate (RCR, g dw leaf eaten. g dw^{-1} caterpillar. Day^{-1}) was calculated as dLDW/(avgCDW × t). The efficiency of conversion of ingested food (ECI), a measure for how efficient caterpillars can convert leaf material into caterpillar mass, was calculated as ECI = RGR/RCR (Scriber and Slansky, 1981).

Leaf Chemical Analyses

From each of the plants used in the bioassays, one leaf, viz. the next younger leaf than the one used for the bioassay (i.e., the 2nd and 5th youngest fully expanded leaf for Bio1 and Bio2, respectively), was harvested simultaneously with the bioassay leaf to analyze leaf morphological traits and primary and secondary metabolites. This enabled us to correlate variation in caterpillar growth parameters with variation in leaf morphological and biochemical traits at the individual

plant level. After measuring leaf fresh weight leaves were spread out on a glass plate to scan total leaf area using an Epson Perfection V850 pro scanner. Leaf area was estimated from the images using WinFOLIA software (Regent Instruments Inc., Quebec, Canada). Thereafter, leaves were dried for 48 h. in a stove at 40°C to estimate leaf dry weight and calculate specific leaf area (SLA, leaf area per unit leaf dry weight) and leaf dry matter content (LDMC, leaf dry weight divided by leaf fresh weight). Dried leaves were ground to a fine powder using a Retsch mill ball (Retsch GmbH, Haan, Germany). Shoot total nitrogen and carbon concentrations were measured based on 1 mg of ground leaf sample using a Flash EA1112 elemental analyzer (Thermo Fisher Scientific Inc., Waltham, MA, United States). To determine shoot phosphorus concentrations, 3 mg of ground leaf sample was ignited at 550°C for 30 min in a muffle furnace, then extracted with 10 ml of 2.5% potassium persulfate, and measured with an Auto-Analyzer (Seal QuAAtro SFA system; Murphy and Riley, 1962). To determine leaf concentrations of the two IGs aucubin and catalpol, 25 mg of ground leaf sample was extracted by shaking overnight in 10 ml 70% methanol, filtered over Whatman #4 filter paper, readjusted to 10 ml, diluted 10x with milliQ water, and analyzed by HPLC following Marak et al. (2002b) using geniposide as internal standard. Leaf N, P, C, and IG concentrations were expressed as % of leaf dry weight.

Statistical Analyses

Sequential harvest data (shoot, root, and total dry weight, RMF), were analyzed using generalized linear mixed models (procedure MIXED, SAS v. 9.2, SAS Institute, Cary, NC). The factors Time (T), Light (L), AMF (M), and soil P (P) and their interactions were entered as fixed factors. Block and block × light were entered as random factors. As the experimental set-up followed a split plot design, the whole-plot factor (light) was tested against the whole-plot error term block × light, whereas the other factors were tested against the pooled residual error term. Separate analyses per time point were performed for closer inspection of L, M, and P effects at each of the different time points. Dry weights were log-transformed prior to analysis to meet assumptions of normality of the distribution of residuals and homogeneity of variances. Similar models were used to test effects of light, soil P, and their interaction on root colonization by AMF, for 3- and 6-week old plants, separately.

Bioassay data (RGR, RCR, ECI, SLA, LDMC, and leaf biochemical traits) were also analyzed using generalized linear mixed models with the factors light (L), AMF (M), soil P (P), and jasmonic acid (J) and their interactions as fixed factors and block and block × light as random factors. Leaf IG concentrations were square-root transformed to meet assumptions of normality of the distribution of residuals and homogeneity of variances. In addition, forward stepwise multiple regressions (inclusion/removal criterion $p < 0.10$) were performed to identify leaf traits significantly associated with variation in caterpillar RGR, RCR, and ECI among plants (procedure REG, SAS v. 9.2, SAS Institute, Cary, NC).

RESULTS

Effects of AMF, Light, and Soil P on Root Colonization by *Funneliformis mosseae*

Root colonization by *F. mosseae* after 6 weeks of growth was high (55.0%) and independent of light or soil phosphorus treatment (**Figure 1**; **Supplementary Table S1**). After 9 weeks of growth, root colonization levels were overall much lower (32.4%), and, contrary to expectation, were significantly higher under high soil P (38.1%) than under low soil P (26.6%; $p < 0.05$) but, as expected, marginally lower under low light (27.8%) than under high light conditions (36.9%; $p = 0.058$). At both points in time, no vesicles and only few arbuscules were observed (1.7 and 2.4% in weeks 6 and 9, respectively), independent of light, soil P, or their interaction (all $p > 0.10$). No colonization was observed in non-inoculated plants.

Effects of AMF, Light, and Soil P on Root and Shoot Biomass

Total dry weight of plants was overall enhanced by soil P and light, but reduced by the presence of AMF (**Figure 2A**; **Table 1**). The strength of these effects varied over time (**Table 1**: TxL, $p < 0.05$; TxP, $p < 0.001$; TxM, $p < 0.01$). The MGR (the percent difference in plant dry weight of AMF plants compared to non-mycorrhizal plants), averaged across light and soil P treatments, was significantly negative from week 6, when the growth reduction was strongest (33%), but the extent of this

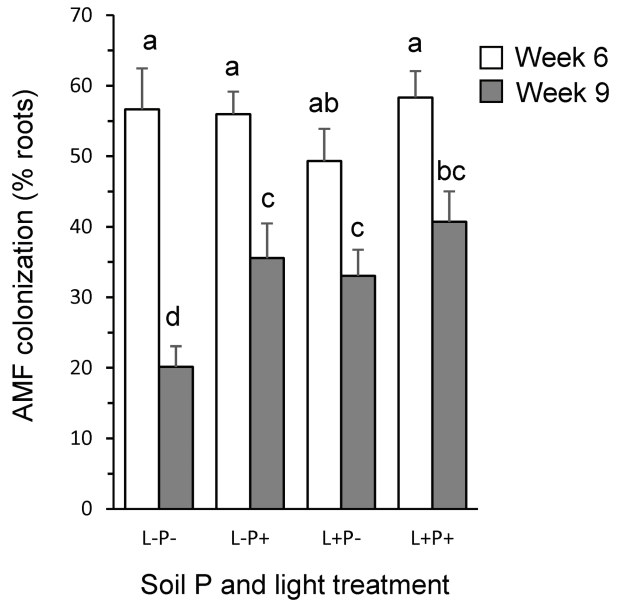

FIGURE 1 | Percent of *P. lanceolata* roots colonized by the mycorrhizal fungus *F. mosseae* for plants grown under four combinations of light intensity (L–: low light; L+: high light) and soil phosphorus treatments (P–: low soil P; P+: high soil P). Open bars: 6 weeks after seedling tansplantation; gray bars: 9 weeks after seedling transplantation. Bars that do not share the same letter are significantly different from each other (*post hoc* tests using LS means, $p < 0.05$).

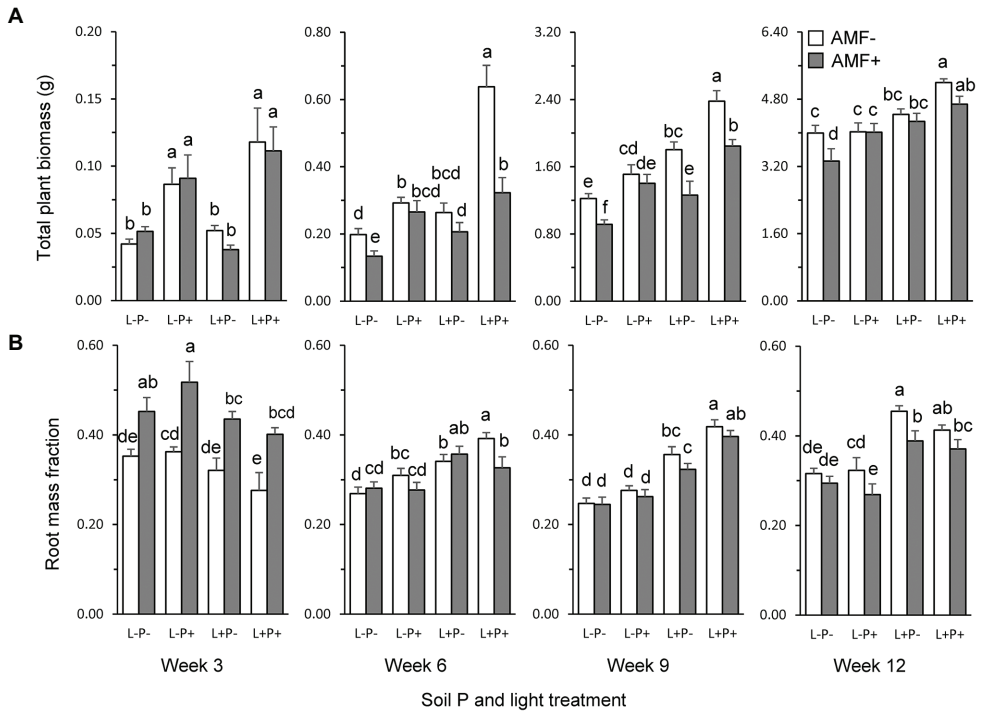

FIGURE 2 | (A) Total plant dry weight, and **(B)** RMF (root biomass/total biomass) of *P. lanceolata* plants at four time points during growth (panels from left to right: 3, 6, 9, and 12 weeks after seedling transplantation). Each panel displays results for plants grown under four different combinations of light intensity (L-: low light; L+: high light) and soil phosphorus treatment (P-: low soil P; P+: high soil P). Open bars: non-mycorrhizal plants; gray bars: plants inoculated with the AMF *F. mosseae*. Bars within panels that do not share the same letter are significantly different from each other (*post hoc* tests using LS means, $p < 0.05$).

reduction declined afterward (**Supplementary Table S2**). By contrast, high soil P enhanced total dry weight, but the extent of this enhancement also steadily declined over time (**Figure 2A**, averaged across light and AMF treatments: +122, +89, + 37, and +12%, in weeks 3, 6, 9, and 12, respectively). Similarly, high light enhanced total dry weight from week 9, (**Figure 2A**), and the extent of enhancement declined from +61% to +45 and +21% in weeks 6, 9, and 12, respectively.

Contrary to expectation, AMF inoculation was not least beneficial for plant dry weight production under conditions considered most unfavorable for trade, i.e., low light and high soil P (**Figure 2A**). In fact, the combination of low light and high P was the only condition under which we did not observe a negative, but an overall neutral MGR (**Supplementary Table S2**). The reduction in total biomass by AMF was on average stronger under high than under low light conditions (**Table 1**: LxM, $p < 0.05$; **Figure 2A**; **Supplementary Table S2**). Furthermore, we observed a more complex interaction (**Table 1**, TxLxPxM, $p < 0.05$) indicating that the interactive effects of light and soil P on the MGR varied over time.

Both shoots and roots contributed to the response of total plant biomass to AMF, but the two plant tissues strongly differed in the temporal dynamics of their responses (**Table 1**). Overall, shoot biomass was reduced by AMF up to week 9, but no longer at final harvest (**Supplementary Figure S1A**; **Supplementary Table S2**). By contrast, root biomass was initially enhanced by AMF, but reduced by AMF from week 6 onwards (**Supplementary Figure S1B**; **Supplementary Table S2**). Effects of AMF on the RMF therefore shifted from positive to negative over the course of time (**Figure 2B**; **Table 1**: TxM, $p < 0.001$; **Supplementary Table S2**).

Roots and shoots also differed in the temporal dynamics of their responses to light and soil P (**Table 1**). Shoot biomass initially responded positively to both soil P and light, but was only enhanced by higher P at final harvest (**Supplementary Figure S1A**). By contrast, root biomass was initially only enhanced by higher P, but at final harvest only by light availability (**Supplementary Figure S1B**). As a result, at final harvest, shoot biomass was more strongly determined by soil P, whereas root biomass was more strongly determined by light, i.e., tissue growth was most strongly limited by the resources in the other compartment (**Supplementary Figure S1**).

Effects of JA, AMF, Light, and Soil P on Caterpillar Performance

First Bioassay

In the first bioassay (7-week old plants), application of JA 2 days before the bioassay reduced the RCR of *M. brassicae* caterpillars by on average 6.1% ($p < 0.05$, **Table 2; Figure 3A**), indicating that there was JA-induced resistance. However, the extent of JA-induced resistance was independent of soil P and light (LxP and LxJ interactions, $p > 0.4$, **Table 2**). As hypothesized,

TABLE 1 | General Linear Mixed Models of the effects of time (T), light intensity (L), soil phosphorus (P), and Arbuscular Mycorrhizal Fungi (AMF; M), on growth and morphological traits of *Plantago lanceolata:* total, shoot and root dry weight and root mass fraction (RMF, root weight/total weight).

Source	df	Total DW	Shoot DW	Root DW	RMF
		F	F	F	F
T	3, 138	**0.5*****	**2623.7*****	**1601.8*****	**25.0*****
L	1, 11	**50.6*****	**21.9*****	**100.6*****	**67.7*****
P	1, 138	**148.6*****	**135.4*****	**109.5*****	2.6
M	1, 138	**27.1*****	**33.1*****	**14.3*****	1.9
TxL	3, 138	**3.5***	2.1^{+}	**15.7*****	**33.7*****
TxP	3, 138	**14.4*****	**13.5*****	**10.9*****	**3.9***
TxM	3, 138	**4.4****	**3.6***	**12.3*****	**29.1*****
LxP	1, 138	2.9^{+}	**4.5***	0.6	1.6
LxM	1, 138	**4.1***	2.4	2.6	0.9
PxM	1, 138	0.4	0.5	0.0	0.3
TxLxP	3, 138	0.8	2.0	0.1	**3.0***
TxLxM	3, 138	0.8	0.7	0.4	0.0
TxPxM	3, 138	0.6	0.4	1.2	1.7
LxPxM	1, 138	0.8	0.6	0.3	0.0
TxLxPxM	3, 138	**3.2***	**3.7***	2.5^{+}	0.8

Time represents the age of plants, 3, 6, 9, or 12 weeks after seedling transplantation. AMF represents inoculation with Funneliformis mosseae. Values are F-values. Values in bold indicate significant effects ($p < 0.05$).

$^{+}p < 0.10$.

$^{*}p < 0.05$.

$^{**}p < 0.01$.

$^{***}p < 0.001$.

df, degrees of freedom; denominator degrees of freedom are 11 for effects of light and 138 for the other factors. RMF, Root mass fraction.

the effect of JA depended on the presence of AMF (JxM interaction, $p < 0.05$, **Table 2**), but the direction of this interaction was unexpected. In the absence of AMF, JA significantly decreased RCR by on average 14.0% ($p = 0.02$), whereas in the presence of AMF, JA did not affect the RCR of caterpillars ($p > 0.6$; **Figure 3A**). Similarly, in the absence of a prior JA-stimulus, AMF reduced caterpillar RCR by 13.5% ($p = 0.02$), indicating AMF-induced resistance, whereas after a prior JA stimulus, AMF did not affect caterpillar RCR ($p > 0.6$). When the interactions between AMF and JA effects were studied separately under each of the four abiotic conditions (i.e., combinations of light and soil P), a significant interaction was only observed under high light and high soil P [$F(1,24) = 11.0$, $p = 0.003$] and not under the three other treatment combinations. However, the three-way interactions between JA, AMF, and light (**Table 2**, $p = 0.08$), or between JA, AMF, and soil P (**Table 2**, $p = 0.09$) were only marginally significant. Therefore, we can only conclude that there is a tendency that the strength of the AMF-induced suppression of the JA response depends on the abiotic conditions, and further studies are needed to support this observation. In conclusion, at the timescale of the experiment, JA-induced resistance was independent of soil P and light, and AMF did not prime plants for a JA-mediated response against *M. brassicae* feeding but, on the contrary, antagonized the JA-response of plants to these caterpillars, and this response tended to by most strongly expressed under high soil P and light conditions.

Caterpillar RCR was also directly affected by soil P levels (**Table 2**: $p < 0.01$); RCR of caterpillars was on average 12.6% lower on plants grown under low soil P than on under high soil P, indicating that plants grown under low soil P were more resistant to caterpillar feeding. Light did not directly affect caterpillar RCR (**Table 2**).

The RGR of caterpillars (**Supplementary Figure S2A**), which is the product of the RCR and the ECI, was only affected by JA application (7.0% reduction, $p < 0.05$, **Table 2**) and was independent of the presence or absence of AMF. This was due to the fact that the negative effects of AMF on the RCR of caterpillars feeding on plants that had not been treated with JA were partly offset by positive effects of AMF on the efficiency with which these caterpillars could convert the ingested leaf material into caterpillar mass (ECI) under these conditions (**Supplementary Figure S2B**; **Table 2**, JxM, $p < 0.05$).

Second Bioassay

Results for the second bioassay (10-week old plants) were qualitatively different from those of the first bioassay. Like in the first bioassay, JA application reduced caterpillar RCR, on average by 14.3% ($p < 0.01$, **Table 3; Figure 3B**), and the extent of JA-induced resistance was independent of soil P and light conditions (**Table 3**). However, in this bioassay, there was no interaction between JA and AMF effects (**Table 3**), indicating that the fungus did not prime, nor repress, JA-responses. There were also no interactions between effects of AMF and light or soil P (**Table 3**). Surprisingly, in contrast to the first bioassay, lower levels of soil P resulted in a significant 13.9% enhancement, not reduction, of caterpillar RCR (**Figure 3B**; **Table 3**, $p < 0.05$). Similarly, lower light levels resulted in a 12.5% enhancement of caterpillar RCR (**Figure 3B**; **Table 3**, $p < 0.05$).

Like in the first bioassay, caterpillar RGR was only reduced by JA application (**Supplementary Figure S2C**, 11.5% reduction; **Table 3**, $p < 0.05$), so effects of light and soil P on RCR did not translate into differences in RGR. AMF enhanced the ECI under low soil P (+17.2%), but not under high soil P (−8.6%; **Supplementary Figure S2D**), resulting in a significant interaction between AMF and soil P effects on ECI (**Table 3**, $p < 0.05$).

Plant Traits Potentially Mediating Treatment Effects on Caterpillar Performance

Effects of JA, AMF, Light, and Soil P on Leaf Biochemistry and Morphology

Leaf biochemistry was strongly affected by AMF, soil P, and light treatments. In 7-week old plants (**Figures 4A–C**; **Table 2**), leaf P and N concentrations were reduced under high light and, surprisingly, also under high soil P conditions (**Figures 4A**,**B**; **Table 2**, all $p < 0.01$). By contrast, AMF enhanced leaf P under high light and high soil P conditions, but reduced leaf P under low light and low soil P conditions, basically buffering variation in leaf P under the various light and soil P conditions (**Figure 4A**; **Table 2**: LxM and PxM, $p < 0.01$). Application of

TABLE 2 | General Linear Mixed Models of the effects of light intensity (L), soil phosphorus (P), jasmonic acid treatment (J), and AMF (M), on leaf traits *P. lanceolata* plants and on growth and consumption parameters of *Mamestra brassicae* caterpillars feeding on these plants.

Source	Ndf	Caterpillar traits			Leaf traits					
		RGR	RCR	ECI	Leaf P	Leaf N	Aucubin	Catalpol	SLA	LDMC
		F	F	F	F	F	F	F	F	F
L	1	1.4	0.1	0.3	**35.5*****	**17.0****	2.4	0.1	**6.5***	**30.7*****
P	1	2.4	**10.0****	2.1	**95.7*****	**35.2*****	0.6	**6.1***	**10.5****	**48.4*****
J	1	**5.0***	2.2	0.0	**6.2***	**7.5****	1.4	1.9	1.6	0.4
M	1	1.3	1.7	0.7	2.8^{+}	2.3	2.5	0.4	**14.9*****	0.7
LxP	1	1.6	0.0	1.0	0.0	1.7	0.7	0.4	0.5	3.8^{+}
LxJ	1	0.0	0.4	0.1	0.6	0.1	0.1	0.0	0.6	0.4
PxJ	1	0.0	0.7	1.5	**7.7****	0.1	1.9	0.6	0.0	0.3
LxM	1	0.2	1.3	0.9	**12.4*****	**4.6***	0.7	0.0	0.2	3.3^{+}
PxM	1	0.0	0.5	0.9	**9.8****	**4.9***	0.3	0.4	0.5	**6.1***
JxM	1	0.1	**4.0***	**4.8***	0.1	1.0	0.0	0.0	0.2	0.1
LxPxJ	1	0.1	0.5	0.2	0.0	0.0	1.5	0.0	0.3	0.4
LxPxM	1	1.6	0.0	1.0	1.0	0.0	0.1	0.1	1.6	0.1
LxJxM	1	1.6	3.1^{+}	0.0	1.0	0.0	0.3	0.0	0.2	0.0
PxJxM	1	0.3	2.9^{+}	0.3	1.0	1.4	0.6	1.8	0.9	2.6
LxPxJxM	1	0.6	0.0	0.7	0.7	0.4	0.1	0.3	0.3	0.9

Data for bioassay 1 (7-week old plants). Values are F-values. Values in bold indicate significant effects ($p < 0.05$).
$^{+}p < 0.10$.
$^{*}p < 0.05$.
$^{**}p < 0.01$.
$^{***}p < 0.001$.
Ndf, numerator degrees of freedom. Denominator degrees of freedom (Dnf) are eight for effects of light. Dnf for other factors are: 111 for RGR, 98 for RCR and RCR, 67 for leaf N and P, 112 for leaf aucubin and catalpol, SLA, and LDMC. RGR, relative growth rate; RCR, relative consumption rate; ECI, efficiency of conversion of ingested food; leaf N, leaf nitrogen concentration; leaf P, leaf phosphorus concentration; SLA, specific leaf area; and LDMC, leaf dry matter content (% dry weight).

JA 3 days before leaf metabolite assessment slightly reduced leaf N (**Figure 4B**) but enhanced leaf P under low soil P conditions (**Figure 4A**; **Table 2**: PxJ, $p < 0.01$). High light and soil P both enhanced LDMC (**Supplementary Figure S3A**) and reduced SLA (**Supplementary Figure S3B**), changes that are commonly associated with reductions in leaf palatability. By contrast, AMF enhanced SLA (**Supplementary Figure S3B**), and had variable effects on LDMC, depending on soil P (**Table 2**). Unexpectedly, AMF and JA treatments did not affect leaf levels of the defense metabolites catalpol (**Figure 4C**) or aucubin (**Supplementary Figure S3C**; **Table 2**). By contrast, high soil P did increase leaf levels of catalpol (**Figure 4C**; **Table 2**).

In 10-week old plants (**Figures 4D–F**; **Table 3**), high light conditions continued to reduce leaf N and P concentrations (**Figures 4D**,**E**; **Table 3**, all $p < 0.01$), but high soil P conditions enhanced leaf P, especially in mycorrhizal plants. Indeed, at this later stage of the interaction, AMF enhanced leaf P under a wide range of conditions, but again most strongly under high soil P (**Figure 4D**; **Table 3**: PxM, $p < 0.01$). As observed for 7-week old plants, high light and soil P conditions enhanced LDMC and reduced SLA in 10-week old plants as well (**Supplementary Figures S3D**,**E**; **Table 3**: all $p < 0.001$) whereas, conversely, AMF reduced LDMC and enhanced SLA especially under low soil P conditions, both expected to result in higher leaf palatability. As observed in 6-week old plants, AMF did not affect leaf levels of the defense metabolites catalpol or aucubin (**Table 3**) but high soil P increased levels of catalpol (**Figure 4F**; **Table 3**), In addition, high light induced higher levels of both catalpol and aucubin (**Figure 4F**; **Supplementary Figure S3F**; **Table 3**). JA application 4 days prior to leaf metabolite assessment did not induce any changes in the measured metabolites and traits in 10-week old plants (**Table 3**).

Associations Between Plant Traits and Caterpillar Performance

In the first bioassay, leaf traits explained 9.9% of the variation in RCR (**Table 4**: $p < 0.01$). High RCR was associated with low leaf P (**Figure 5A**; **Table 4**: $p < 0.01$). This could partly explain why caterpillar RCR was enhanced by the high soil P treatment in the first bioassay, which resulted in a reduction of leaf P concentrations by on average 27.8% (**Figure 4A**). Leaf P was also the only leaf trait explaining a significant proportion of the variation in RGR (3.2%, $p < 0.05$); higher RGR was associated with lower leaf P. None of the leaf traits could explain a significant part of variation in ECI (5.1%, $p = 0.09$).

In the second bioassay, leaf traits explained 10.2% of the variation in RCR (**Table 4**: $p < 0.01$). High RCR was associated with low leaf concentrations of the defense chemical catalpol (**Figure 5B**; **Table 4**: $p < 0.05$) and high leaf N (**Figure 5C**; **Table 4**: $p < 0.01$). This could partly explain why caterpillar RCR was reduced by high light and high soil P conditions, which resulted in increases in leaf catalpol levels by on average 43.7 and 80.2%, respectively (**Figure 4F**). In addition, the 15.2% lower levels of leaf *N* under high light conditions (**Figure 4E**) could have contributed to the lower caterpillar

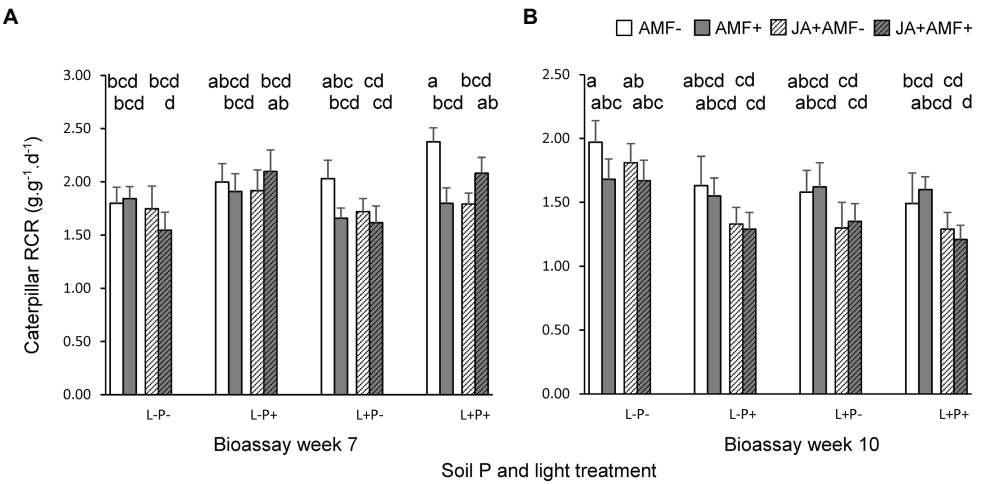

FIGURE 3 | Relative consumption rates (RCRs; amount of leaf mass eaten per unit caterpillar weight per day) of *M. brassicae* caterpillars feeding on *P. lanceolata* during two bioassays, performed when plants were **(A)** 7 weeks old (left panel), and **(B)** 10 weeks old (right panel). Each panel displays results for plants grown under four combinations of light intensity (L-: low light; L+: high light) and soil phosphorus treatments (P-: low soil P; P+: high soil P). In addition, plants had either be challenged by leaf application of jasmonic acid (JA) 48 h. prior to the bioassay (hatched bars) or not (non-hatched bars) and plants had either been inoculated with the AMF *F. mosseae* (bars with gray background) or not (white background). Bars within panels that do not share the same letter are significantly different from each other (*post hoc* tests using LS means, $p < 0.05$). The top row of letters refers to bars that display treatments without AMF, the second row of letters to those with AMF.

TABLE 3 | General Linear Mixed Models of the effects of light intensity (L), soil phosphorus (P), jasmonic acid treatment (J), and AMF (M), on leaf traits *P. lanceolata* plants and on growth and consumption parameters of *M. brassicae* caterpillars feeding on these plants.

Source	Ndf	Caterpillar traits			Leaf traits					
		RGR	RCR	ECI	Leaf P	Leaf N	Aucubin	Catalpol	SLA	LDMC
		F	F	F	F	F	F	F	F	F
L	1	1.6	**5.1***	0.4	**15.3****	**48.9*****	**8.0***	**7.2***	**100.7*****	**118.1*****
P	1	0.8	**5.8***	3.8^{+}	**22.4*****	0.5	3.4+	**6.3***	**22.4*****	**10.9****
J	1	**4.6***	**8.1****	0.3	1.3	0.3	0.0	0.1	3.4^{+}	1.1
M	1	0.1	0.5	0.7	**66.8*****	1.0	0.6	1.0	**28.7*****	**16.8*****
LxP	1	1.6	2.6	0.0	1.1	**4.3***	0.0	1.0	**8.3****	2.8^{+}
LxJ	1	0.1	0.4	0.0	**9.0****	1.6	0.9	0.3	1.1	0.2
PxJ	1	0.1	0.5	1.3	0.4	0.7	0.5	1.5	0.0	0.5
LxM	1	0.0	1.0	1.2	0.0	0.7	0.3	0.0	0.8	0.0
PxM	1	2.2	0.1	**6.0***	**11.3****	**7.9****	1.5	1.1	**9.2****	**5.4***
JxM	1	0.1	0.0	0.2	1.7	0.2	0.0	0.2	0.3	1.7
LxPxJ	1	0.0	0.3	0.3	1.6	0.0	0.4	0.2	3.1^{+}	1.6
LxPxM	1	0.2	0.3	0.1	0.3	0.9	0.0	0.3	3.1^{+}	0.1
LxJxM	1	0.8	0.3	0.1	**6.3***	2.2	0.5	0.3	2.7	0.0
PxJxM	1	0.4	0.2	0.0	0.3	0.1	0.1	0.0	0.1	0.0
LxPxJxM	1	1.1	0.0	1.0	1.0	0.3	0.0	0.2	**6.8***	2.3

Data for bioassay 2 (10-week old plants). Values are F-values. Values in bold indicate significant effects ($p < 0.05$).

$^{+}p < 0.10$.

$^{*}p < 0.05$.

$^{**}p < 0.01$.

$^{***}p < 0.001$.

Ndf, numerator degrees of freedom. Denominator degrees of freedom (Dnf) are 11 for effects of light. Dnf for other factors are: 93 for RGR, RCR, and ECI, and 106 for the other traits. RGR, relative growth rate; RCR, relative consumption rate; ECI, efficiency of conversion of ingested food; leaf N, leaf nitrogen concentration; leaf P, leaf phosphorus concentration; SLA, specific leaf area; LDMC, leaf dry matter content (% dry weight).

RCR under these conditions. Leaf traits did not explain a significant proportion of the variation in ECI in the second bioassay and only 3.5% of the variation in RGR (**Table 4**: $p < 0.05$). As observed for RCR, high RGR was associated with low leaf concentrations of catalpol (**Table 4**). JA application did not affect leaf N, or leaf catalpol in the

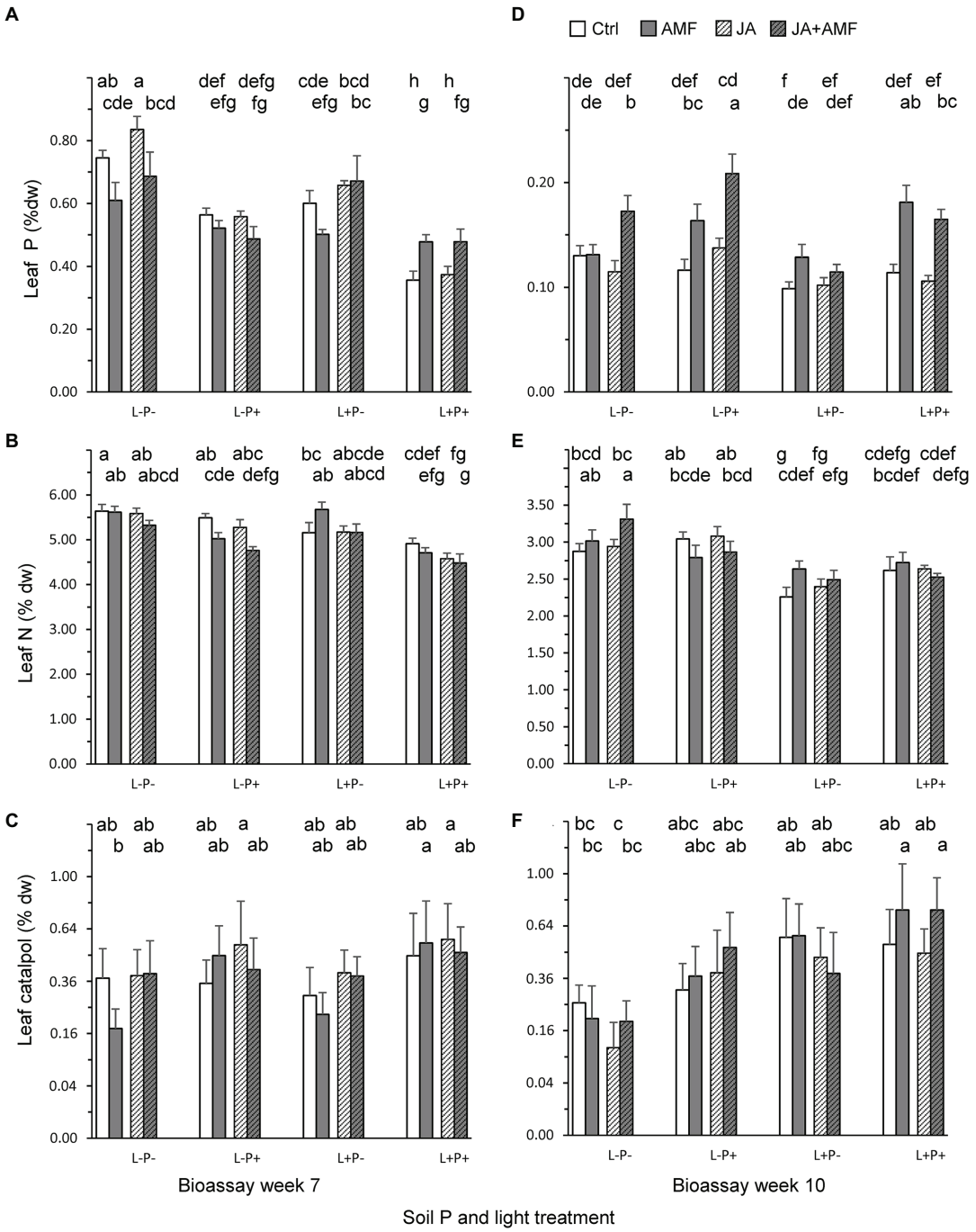

FIGURE 4 | Leaf concentrations of primary and secondary metabolites in *P. lanceolata* plants at the time of two bioassays, when plants were 7 (left panels) and 10 weeks (right panels) old. **(A,D)** Leaf phosphorus; **(B,E)** Leaf nitrogen; **(C,F)** Leaf catalpol. Each panel displays results for plants grown under four combinations of light intensity (L-: low light; L+: high light) and soil phosphorus treatments (P-: low soil P; P+: high soil P). In addition, plants had either be challenged by leaf application of jasmonic acid (JA) 48 h. prior to the bioassay (hatched bars) or not (non-hatched bars) and plants had either been inoculated with the arbuscular mycorrhizal fungus (AMF) *F. mosseae* (bars with gray background) or not (white background). Bars within panels that do not share the same letter are significantly different from each other (*post hoc* tests using LS means, $p < 0.05$). The top row of letters refers to bars that display treatments without AMF, the second row of letters to those with AMF.

second bioassay, hence JA-induced resistance to *M. brassicae* was mediated by plant traits not measured in the current experiment.

Strikingly, SLA and LDMC, that are often strongly associated with insect performance on host plants (Schoonhoven et al., 2005), were strongly affected by light, soil P, and AMF

TABLE 4 | Forward multiple regressions of *P. lanceolata* leaf traits on growth and consumption parameters of caterpillars of *M. brassicae* feeding on these plants.

Source	Bioassay 1			Bioassay 2		
	RGR	RCR	ECI	RGR	RCR	ECI
Specific leaf area (SLA)	-	-	-	-	-	-
Leaf dry matter content (LDMC)	-	-	-	-	-	-
Leaf N concentration	-	-	-	-	**+0.21****	-
Leaf P concentration	**−0.22***	**−0.31****	+0.16	-	-	-
Leaf aucubin concentration	-	-	-	-	-	-
Leaf catalpol concentration	-	-	-	**−0.18***	**−0.20***	-
Model R^2 (%)	4.7	9.9	2.6	3.2	10.2	-
F-value	**4.6***	**10.2****	2.5	**4.3***	**7.3*****	-
df	1,93	1,93	1,93	1,129	2,128	-

Values are standard partial regression coefficients. Data for bioassays 1 and 2 (7- and 10-week old plants, respectively). Model fit (100 × R^2), F-tests, and their degrees of freedom (df) are indicated at the bottom. Values in bold indicate significant effects ($p < 0.05$).

$^{*}p < 0.05$.

$^{**}p < 0.01$.

$^{***}p < 0.001$.

RGR, relative growth rate; RCR, relative consumption rate; and ECI, efficiency of conversion of ingested food.

(**Supplementary Figure S3**), but played no significant role in explaining variation in caterpillar relative consumption or growth rates (**Table 4**), and therefore did not appear to mediate effects of AMF, light, or soil P on caterpillar performance.

DISCUSSION

Three main conclusions arise from our study. First, The MGR varied significantly among abiotic conditions and plant ontogenetic stages. However, AMF did not benefit plant growth under any of these abiotic conditions and, contrary to our hypothesis, the association with AMF was not least beneficial for plant growth under a combination of low light and high soil phosphorus conditions, that is usually considered least optimal for trade between the two symbionts. Second, in both of the bioassays, JA induced resistance, but the extent of this induction was independent of light and soil phosphorus conditions. Moreover, AMF inoculation did not prime plants for a stronger jasmonic acid-mediated defense response. On the contrary, as indicated by the caterpillar leaf consumption rates, jasmonic acid application induced resistance in non-mycorrhizal plants, but not in mycorrhizal plants during the first bioassay. This suggests that AMF inoculation suppressed rather than primed the JA-induced defense response of plants at this stage. This modulation of the JA-induced defense response by AMF was only observed under conditions of high resource supply (high light and soil P). However, since the impact of abiotic factors on this interaction was statistically only marginally significant, evidence for significant modulation of the impact of AMF on plant resistance by soil P or light in this system awaits further study. Third, in this experiment, AMF did not affect leaf concentrations of an important class of defense metabolites in *P. lanceolata*, the iridoid glycosides aucubin and catalpol, under any of the soil P or light conditions. AMF inoculation did affect many other leaf traits, including leaf N and P, SLA and leaf dry matter content in a light-, soil P-, and plant age-specific manner. But in spite of these induced changes, AMF did not affect caterpillar consumption and growth other than through suppression of the JA-priming response in younger plants. By contrast, high light and soil P levels reduced the RCR of caterpillars feeding on older plants and these effects were associated with a reduction in leaf nitrogen concentrations and an increase in the leaf concentrations of the defense chemical catalpol in plants grown under these conditions. Abiotic factors were thus important determinants of plant resistance to insect feeding, but these effects appeared to be more strongly mediated by modulating leaf quality than by modulating AMF-induced resistance.

Effects of AMF, Light, and Soil P on Growth and Biomass Allocation

Functionality of the mycorrhizal symbiosis generally depends on its abiotic and biotic context and consequently, the outcome of plant-AMF interactions can range from mutualism to parasitism (Hoeksema et al., 2010). In our study, inoculation of *P. lanceolata* plants with a strain of the AM fungus *F. mosseae* overall reduced the total biomass of *P. lanceolata* plants, i.e., the MGR was overall negative. This may be related to the fact that we observed substantial rates of root colonization by the fungus, but a relatively low incidence of arbuscules (around 2%) under all environmental conditions tested, indicating a limited functionality of the symbiosis in terms of P-for-C trade. Similar negative MGR values have been reported in *P. lanceolata* following inoculation with another strain of *G. mosseae* (Wang et al., 2015). However, in general, effects of AMF inoculation in *P. lanceolata* have been shown to range from negative to positive (e.g., Ayres et al., 2006; Zaller et al., 2011; Karasawa et al., 2012; Pankoke et al., 2015).

The extent of growth reduction by AMF strongly varied with the age of the plants. However, the effects of light and soil P on MGR were inconsistent over time and generally did not

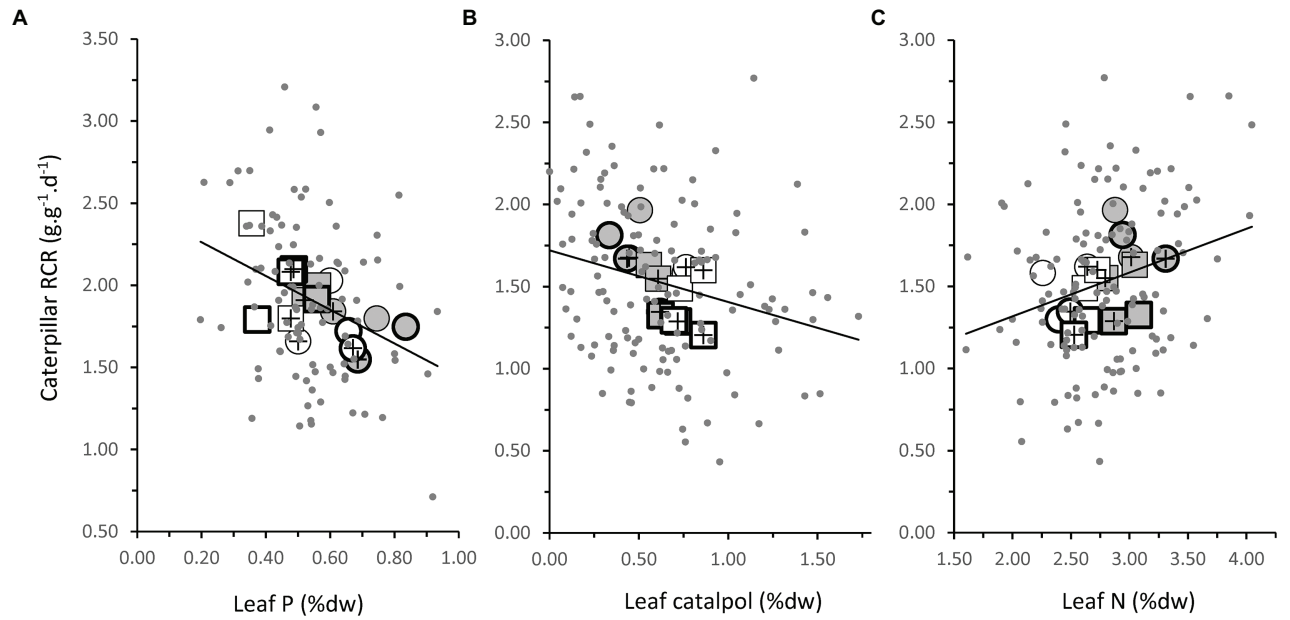

FIGURE 5 | Relationship between leaf traits of *P. lanceolata* plants and the RCR of caterpillars of *M. brassicae* feeding on them. **(A)** Leaf phosphorus concentration at the time of bioassay 1; **(B)** Leaf catalpol at the time of bioassay 2; and **(C)** Leaf nitrogen concentration at the time of bioassay 2. Gray dots represent data points for individual plants. Symbols represent treatment means. Closed symbols: plants grown under low light; open symbols: high light. Circles: plants grown under low soil phosphate; squares: high soil phosphate. Symbols with a plus sign: plants inoculated with AMF; no plus sign: without AMF. Thick symbols: plants challenged by jasmonic acid application 48 h. prior to bioassays, thin symbols: no jasmonic acid application. Lines are slopes from linear regressions (all $p < 0.05$). Note that the values along the leaf catalpol axis are square-root transformed values.

follow predictions from stoichiometry- and trade-based principles (Hoeksema et al., 2010; Johnson, 2010). In particular, MGR did not appear to be lowest under conditions considered to be least optimal for symbiotic trade (low light and high soil P). In fact, this was the only condition under which MGR was consistently neutral during the entire growth period. The absence of a consistent reduction in MGR under high soil P and low light conditions contradicts most other published studies (Johnson, 2010; Konvalinkova and Jansa, 2016). For instance, MGR can shift from positive to neutral at higher soil P (Hetrick et al., 1983) and studies on effect of light availability generally show that the growth benefit of AMF is reduced or becomes negative under shading conditions (Konvalinkova and Jansa, 2016). However, closer inspection of the review by Konvalinkova and Jansa (2016) reveals an interesting pattern. In host-AMF combinations for which an overall positive MGR is observed, shading generally results in a reduction of the MGR. However, in host-AMF combinations for which an overall negative MGR is observed, shading generally does not further reduce MGR (see e.g., Reinhard et al., 1993; Olsson et al., 2010; Grman, 2012). The mechanism underlying the lack of shade-induced reductions in MGR in plants experiencing negative MGR is unknown, but it could simply reflect the fact that whereas all plants experience their lowest MGR under low light conditions, some plant species benefit from AMF under more favorable light conditions, whereas others fail to benefit, resulting in an apparent lack of light responsiveness of MGR. It is unknown whether a similar pattern occurs in plants grown under high soil P.

Growth depressions (negative MGR) have traditionally been viewed as the result of excessive carbon use by AMF, i.e., high allocation of carbon to the fungus relative to the available C-resources under conditions where carbon resources are scarce relative to nutrients, such as under shading and high soil P conditions (Johnson, 2010). Since the discovery that the extent of negative MGR does not necessarily increase with the amount of root colonization or C-drain by the fungus (Li et al., 2008; Grace et al., 2009), a second explanation has been put forward based on nutrient limitation (Smith and Smith, 2011). AM plants can take up nutrients through two different pathways. One is the direct pathway by which plants acquire nutrients from the rhizosphere through their own roots. The other is the mycorrhizal pathway in which the AM fungal partner transfers nutrients to the plant taken up through the extra-radical mycelial network. AMF suppress uptake of P by the plant through its direct pathway. Hence, negative MGR may not only occur in cases of excessive fungal carbon demand, but also when in AM plants the delivery of P through the mycorrhizal is functional, but insufficient to compensate for the reduced uptake of P through the plant's direct pathway (Smith and Smith, 2012). In those cases, AM plants may suffer P-deficiency resulting in growth depression, for instance under low light conditions when only low amounts of assimilates are available for the fungus. Our experiments were not designed to discriminate between these two mechanisms. However, it is interesting that, despite negative MGR values, leaf P concentrations

were still similar or higher in mycorrhizal compared to non-mycorrhizal plants. In seven-week old plants, leaf P concentrations were on average similar between mycorrhizal and non-mycorrhizal plants, although they were less responsive to variation in light and soil P in mycorrhizal plants. In 10-week old plants, leaf P concentrations were even higher in mycorrhizal plants than in non-mycorrhizal plants, despite negative MGR. This suggests that the negative MGR in our study was unlikely to be caused by P-deficiency due to a lack of compensation for reduced P acquisition *via* the plant's own direct P-uptake pathway by mycorrhizal P delivery.

The extent of the negative MGR diminished over time as plants grew older. At final harvest, MGR was overall close to zero and only remained significantly negative under the lowest resource condition (low light and low soil P). The decline in the extent of negative MGR was accompanied by a decline in AMF root colonization over time, indicating that the production of new fungal structures did not keep up with root growth and the turnover of existing structures. However, the decline in colonization rate was not strongest under the conditions predicted to be least optimal for trade. Instead, the decline was strongest under the lowest resource supply condition (low light, low soil P; 2.8 fold) and weakest under the highest resource supply condition (high light, high soil P; 1.4 fold). As the RGRs of roots under these conditions were similar, this might indicate that there was differential regulation of the AMF by the plant's complex feedback mechanism known as AOM under these conditions (Vierheilig et al., 2000; Nagy et al., 2009; Mueller and Harrison, 2019). However, despite the fact that the decline in colonization rate was strongest under the lowest resource condition, a negative MGR still persisted under these conditions at final harvest. This indicates that the AMF association was maintained even under the least beneficial conditions. This is a well-known phenomenon. For instance, AMF are usually not eliminated from roots even under very low light intensities (Schubert et al., 1992; Olsson et al., 2010), which has led to the speculation that root colonization by AMF is maintained as an investment for potentially more beneficial trade in the future (Landis and Fraser, 2008; Walder and van der Heijden, 2015; Konvalinkova and Jansa, 2016). Similarly, AMF in common mycorrhizal networks preferentially allocate nutrients to non-shaded plants, but still supply shaded hosts with nutrients and maintain a high colonization in these plants, which has led to the speculation that AMF maintain association with less rewarding hosts to retain "bargaining power" (Fellbaum et al., 2014; Zheng et al., 2015).

Effects of JA, AMF, Light, and Soil P on Defense Induction and Priming

Induction

Unexpectedly, AMF inoculation did not result in the induction of the most commonly studied defense metabolites in *P. lanceolata*, the iridoid glycosides aucubin and catalpol, under any of the experimental conditions. Induction in response to AMF has been commonly reported for catalpol (Gange and West, 1994; Schweiger et al., 2014a; Wang et al., 2015). However, induction of these compounds by AMF has also been shown to vary among AM fungal species. In a single experiment, Bennett et al. (2009) showed that among three fungal species tested, induction of IGs ranged from non-significant by *Glomus* "white" to a significant 1.4 and 3.5 fold increases by *Archaeospora trappei* and *Scutellospora calospora*, respectively. Also other studies have reported no effect of AMF inoculation on leaf IG concentrations in *P. lanceolata* (Fontana et al., 2009).

Since IGs were not induced by AMF inoculation in our study, the question to what extent the induction of these defense chemicals by AMF is dependent on light and soil P conditions awaits future studies. We could only test how the constitutive production of these metabolites varied with light and soil P conditions. Based on stoichiometric principles, production of C-based secondary metabolites such as IGs is expected to be reduced under low light, high nutrient conditions (Fajer et al., 1992). Our study showed that in older plants the production of both aucubin and catalpol was indeed reduced under low light conditions, in agreement with earlier studies (Tamura, 2001; Miehe-Steier et al., 2015). However, in contrast to earlier studies that confirmed a lower production of IGs under high nutrient conditions (Fajer et al., 1992; Darrow and Bowers, 1999; Jarzomski et al., 2000; Marak et al., 2003; Pankoke et al., 2015), we observed higher levels of catalpol under high soil P conditions. It is unknown whether the effect of nutrient limitation on IG production depends on the type of nutrient limitation. As in many of these studies it is unknown what nutrient was limiting growth, it is possible that most of them assessed effects of N- rather than P-limitation that we studied. Further, it should be noted that effect of nutrient limitation on the constitutive production of IGs is not necessarily a good predictor of its effect on the induction of these defense chemicals. For instance, Darrow and Bowers (1999) showed that constitutive levels of IGs were lower at high nutrient level, but the extent of induction by herbivores was independent of nutrient level.

Priming

Application of JA to systemic leaves, 24 h prior to the bioassays, significantly reduced the RCRs of caterpillar, during both bioassays. This indicates that plants experienced JA-induced resistance to *M. brassicae*. However, contrary to predictions based on the observation that activation of the PSR can co-activate JA-dependent immunity (Khan et al., 2016; Castrillo et al., 2017); the observed JA-induced resistance was independent of soil P. Our experiments do not allow us to disentangle whether this was due to a lack of induction of PSR or lack of co-activation of JA-dependent resistance. Importantly, our results indicate that, at the timescale studied in the experiment, AMF did not prime plants for a JA-mediated defense response against *M. brassicae* feeding. On the contrary, AMF antagonized the JA-mediated defense response during the first bioassays. In the absence of AMF inoculation, JA significantly reduced the RCR of caterpillars. But whereas we expected an even stronger reduction in the presence of AMF in the case of priming, we actually observed that JA application did no longer reduce caterpillar RCR in plants inoculated with AMF. This raises the question why we did not observe mycorrhizal priming

for enhanced defense in our study. Priming is a dynamic process and assessing priming effects at only one point in time, in our case 48 h after challenge, may not capture the event (Martinez-Medina et al., 2016), or the concentration of JA applied may not have been appropriate. However, it is also possible that priming truly did not occur in the study system of *P. lanceolata* and the particular strain of *F. mosseae* that we used, under the environmental conditions that we tested. Despite convincing evidence for mycorrhizal priming in study systems such as tomato (Song et al., 2013), variable results have been reported in others. For instance, Minton et al. (2016) tested mycorrhizal priming of defense in response to the chewing herbivore *Manduca sexta* in two wild *Solanum* species following JA-application to plants that had or had not been pre-inoculated with the AM fungus *Rhizophagus irregularis*. In both plant species JA reduced caterpillar mass, but AMF did not induce, nor prime plant defenses in terms of reduced caterpillar weight gain in response to JA application. Interestingly, at the underlying molecular level, the AM fungus did modulate JA-induced gene expression. But whereas it primed the JA-induced transcription of one of the genes for protein-based chemical defenses (peroxidase), it repressed another (polyphenol oxidase) and did not affect the JA-induced transcriptional response to a third one (proteinase inhibitor) in *Solanum dulcamara*. Moreover, it did not affect any of these in the annual *Solanum ptycanthum*. This indicates, first, that modulation of the JA-induced responses by a single AM strain can differ among plant species and, second, that modulation of JA-responses by AMF at the transcriptional level may range from priming to repression and that it may not translate into defense responses at the phenotypic level.

Our results are in agreement with several earlier studies showing that AMF might not only fail to prime plants for defense but even repress the plant's defense response to herbivory. Barber (2013) showed that inoculation of cucumber with the AM fungus *R. irregularis* did not affect the amount of leaf feeding by the generalist leaf chewing insect herbivore *Spodoptera exigua* in the absence of prior damage, and actually enhanced feeding after prior damage. Earlier studies in *P. lanceolata* have also yielded mixed results. Wang et al. (2015) showed that in plants that were not inoculated with AMF, the RGR of caterpillars of *S. exigua* decreased with time after prior herbivory by conspecifics, indicating a progressive build-up of induced defense. Inoculation of plants with the AM fungus *F. mosseae* also decreased caterpillar RGR, indicating AMF-induced resistance. However, in plants inoculated with *F.mosseae,* no further induction of defense occurred in response to herbivory, suggesting that AMF did not prime, but suppress, the induction of defense in response to herbivory. This nicely matched with the build-up of one of the defense chemicals, the iridoid glycoside catalpol, in response to previous herbivory in non-inoculated plants, but not in plants inoculated by *F. mosseae*. A very similar response had been observed by Bennett et al. (2009) for the AM fungus *Scutellospora calospora*. In the absence of previous herbivory, this AM fungus induced iridoid glycosides in *P. lanceolata* plants. In non-mycorrhizal plants, previous herbivory by the specialist leaf chewing herbivore *Junonia coenia* also induced iridoid glycosides. However, in plants inoculated with the AM fungus, no further increase in leaf concentrations of these defense chemicals were observed in response to previous herbivory. This suggests that the AM fungus itself induced defense, but that it suppressed defense induction by herbivory. These results could suggest that the processes of induction and priming are interconnected, and that plants already expressing induced defenses in response to AMF are less prone to activate priming (ISR), but by contrast may suppress further induction. However, this is not supported by the pattern observed for other AMF tested by Bennett et al. (2009). For instance, even though the AMF strain "*Glomus white*" itself did not induce iridoid glycosides in *P. lanceolata*, it completely suppressed the strong induction of iridoid glycosides in response to herbivory that was observed in non-mycorrhizal plants (Bennett et al., 2009), like we observed in our study. These studies indicate that whereas priming of defenses may occur in some study systems, opposite patterns may be found in others and our study is not an exception. This may be one of the reasons that a growing number of studies is observing AMF-induced susceptibility (Bernaola et al., 2018; Frew et al., 2018; Real-Santillán et al., 2019) even against insect herbivores that are assumed to be signalled through JA, and calls for future studies examining factors that underlie variation in the extent to which AMF prime their host plants for defense or not.

Our expectation was that the extent to which AMF prime plants for enhanced JA-mediated defense would be affected by light and soil P conditions for several reasons. Firstly, soil phosphate and light are expected to impact AMF colonization rates and functionality. Secondly, there are strong interconnections between the regulation of the PSR and immunity. Finally, the production of defense chemicals following the activation of downstream defense genes will eventually require the availability of sufficient amounts of the resources needed. We observed that the modulation of the JA-induced defense response by AMF during the first bioassay indeed only occurred under one combination of environmental conditions, viz. under the highest resource supply (high light and soil P). Although this suggests that the ability of AMF to modulate the plant's response to a JA challenge indeed depends on soil P and light, statistical analyses indicated that this dependence on abiotic conditions was only marginally significant. Further studies are therefore required to confirm this environmental dependence. In any case, the results suggest that the AMF-induced suppression of defense activation in response to herbivory was unlikely to be driven by low availability of carbon or nutrient resources, as it did not specifically occur under low resource conditions. The AMF colonization data show that the highest level of AMF proliferation was maintained under high resource conditions. This might suggest that the stronger AMF-induced suppression of defense activation under high resource conditions could be related to higher levels of colonization under these conditions. However, at the time of the first bioassay, when these effects were observed, AMF colonization levels were still overall high, making this explanation less likely.

Leaf Traits Mediating Effects of JA, AMF, Light, and Soil P on Defense

Two leaf traits were major determinants of caterpillar relative leaf consumption rates in older plants. Leaf consumption rates were positively correlated with leaf N and negatively with leaf catalpol concentrations. These results are in line with a plethora of studies showing that caterpillars of generalist herbivores preferentially feed on leaves with a high nutritional value (low C/N ratio) and low levels of defense metabolites (e.g., Coley et al., 2006). This may explain why caterpillars had higher leaf consumption rates on plants grown under low light and low soil P during the second bioassay. As commonly observed (Poorter et al., 2019), low light conditions resulted in a larger proportion of biomass allocated to leaves (lower RMF), a larger leaf area per unit leaf mass (SLA), higher leaf concentrations of N and P, and in a lower leaf dry matter content (LDMC) and lower leaf concentrations of the C-based defense metabolites aucubin and catalpol in these plants. Similarly, low soil P conditions resulted in increased leaf N and lower leaf catalpol concentrations in older plants. Thus, these two leaf traits may well have mediated the higher susceptibility of plants to caterpillar feeding when grown under low light and low soil P. Traits mediating the lower consumption rates on plants that had been treated with JA could not be identified. Clearly, this was not mediated by increases in the measured defense metabolites aucubin or catalpol. Although the first committed steps in the biosynthesis of these iridoid glycosides can be upregulated in response to JA (Biere, unpublished results), JA application in our experiment did not result in higher levels of these defense metabolites 3–4 days after treatment, in agreement with observations from previous experiments (Sutter and Mueller, 2011; Schweiger et al., 2014b).

Interestingly, AMF strengthened some of the leaf responses to low light in older plants including the increases in SLA and leaf P and decreases in RMF and LDMC. These results corroborate findings from earlier studies showing that under light deprivation AMF can enhance adaptation to low light conditions by increasing SLA and reducing RMF (Konvalinkova et al., 2015), as commonly observed in AM plants (Pankoke et al., 2015; Tomczak et al., 2016). However, unlike light deprivation, AMF did not enhance leaf N, or reduce leaf catalpol concentrations in older plants, the only two traits that affected caterpillar consumption rates in older plants in our study. This explains why, unlike light and soil P, AMF did not directly affect plant susceptibility to caterpillar feeding in our experiments.

Although AMF inoculation did not affect the leaf consumption rates of caterpillars on older plants, it did affect another aspect of caterpillar performance. AMF increased the caterpillar's efficiency of converting ingested food into caterpillar biomass (ECI) under low, but not under high soil P conditions, i.e., AMF increased leaf quality for caterpillars under low soil P conditions. Interestingly, exactly under these conditions AMF enhanced SLA and reduced LDMC (the latter indicating increased leaf water content). Increases in SLA and leaf water content commonly enhance performance of insect herbivores (Schoonhoven et al., 2005). Furthermore, studies in the congener *Plantago major* revealed that inoculation with the AM fungus *R. irregularis* similarly resulted in a higher SLA and water content (Tomczak et al., 2016) and in an increase in biomass of caterpillars of *M. brassicae* feeding on mycorrhizal plants. Therefore, we hypothesized that modulation of these traits by AMF under low soil P could offer an explanation for the AMF-induced increase in caterpillar ECI under these conditions. However, in our analyses of trait associations with caterpillar performance, we could not show a significant impact of either SLA or LDMC on ECI, hence other, unmeasured, traits may have been responsible for this AMF-induced effect. Also, in our study, the positive effect of AMF on ECI did not translate into a positive effect on caterpillar RGR, indicating that the positive effect on ECI was partly offset by a reduced consumption rate.

The traits explaining effects of treatments on caterpillar consumption rates in young plants differed from those in older plants. In contrast to older plants, low soil P in younger plants was associated with lower caterpillar leaf consumption rates. However, in younger plants, this was not mediated by increased leaf N, or by reduced leaf catalpol concentrations under these conditions. Surprisingly, and in contrast to older plants, younger non-mycorrhizal plants grown under low P showed elevated leaf P concentrations, a response that was buffered in mycorrhizal plants, and high leaf P was associated with lower leaf consumption rates. This result is currently unexplained, but might indicate a highly activated PSR associated with enhanced immunity in younger plants. In general, our results depict a very dynamic interplay of trait modulation by AMF and environmental factors. The effects and relative importance of the different abiotic and biotic conditions that act as modulators of leaf morphological and biochemical traits involved in herbivore resistance varied over the course of time and stage of the plant-AMF symbiosis. This further adds to temporal variation in plant resistance on top of the already present common ontogenetic changes in resistance strategies during ontogeny (Van Dam et al., 2001; Boege and Marquis, 2005; Barton and Koricheva, 2010; Miller et al., 2014).

Conclusion

We did not find support for our hypothesis that the benefits of AMF for plant growth are reduced under conditions considered unfavorable for trade, i.e., high soil P and low light. We speculate that this may be a general pattern for plants already experiencing an overall negative MGR even at higher light and lower soil P conditions. Furthermore, soil P and light affected the plant's resistance to a leaf chewing insect herbivore, but these effects were more strongly mediated by direct changes in leaf primary and secondary metabolites than by their modulating effects on mycorrhiza-induced resistance. Finally, our study adds to the growing number of studies reporting that priming of JA-dependent defenses by mycorrhizae may occur in some systems, but that repression of JA-dependent defenses may occur in other systems. In our system, such repression seems to be most strongly

expressed under high resource (light, soil P) conditions, but significant modulation of repression by environmental factors awaits confirmation by future studies.

DATA AVAILABILITY STATEMENT

The datasets generated for this study are available on request to the corresponding author. Data are available in the Dryad repository (https://doi.org/10.5061/dryad.wm37pvmmp).

AUTHOR CONTRIBUTIONS

AB and LQ conceived and analyzed the experiments and wrote the manuscript. LQ, MW, and AB performed the experiments. All authors contributed to the article and approved the submitted version.

FUNDING

This research was supported by grants from the China Exchange Program JRP530-5CDP28 to AB and LQ, and by the China Scholarship Council (No. 201404910206) to LQ. This is NIOO publication no. 7165.

ACKNOWLEDGMENTS

We thank Ciska Raaijmakers and Iris Chardon for the chemical analyses.

SUPPLEMENTARY MATERIAL

The Supplementary Material for this article can be found online at: https://www.frontiersin.org/articles/10.3389/fpls.2021.647372/full#supplementary-material

REFERENCES

Andrade, S. A. L., Malik, S., Sawaya, A., Bottcher, A., and Mazzafera, P. (2013). Association with arbuscular mycorrhizal fungi influences alkaloid synthesis and accumulation in *Catharanthus roseus* and *Nicotiana tabacum* plants. *Acta Physiol. Plant.* 35, 867–880. doi: 10.1007/s11738-012-1130-8

Ayres, R. L., Gange, A. C., and Aplin, D. M. (2006). Interactions between arbuscular mycorrhizal fungi and intraspecific competition affect size, and size inequality, of *Plantago lanceolata* L. *J. Ecol.* 94, 285–294. doi: 10.1111/j.1365-2745.2006.01103.x

Baek, D., Chun, H. J., Yun, D. -J., and Kim, M. C. (2017). Cross-talk between phosphate starvation and other environmental stress signaling pathways in plants. *Mol. Cell* 40, 697–705. doi: 10.14348/molcells.2017.0192

Barber, N. A. (2013). Arbuscular mycorrhizal fungi are necessary for the induced response to herbivores by *Cucumis sativus*. *J. Plant Ecol.* 6, 171–176. doi: 10.1093/jpe/rts026

Barber, N. A., Kiers, E. T., Hazzard, R. V., and Adler, L. S. (2013). Context-dependency of arbuscular mycorrhizal fungi on plant-insect interactions in an agroecosystem. *Front. Plant Sci.* 4:338. doi: 10.3389/fpls.2013.00338

Barton, K. E., and Koricheva, J. (2010). The ontogeny of plant defense and herbivory: characterizing general patterns using meta-analysis. *Am. Nat.* 175, 481–493. doi: 10.1086/650722

Bennett, A. E., Alers-Garcia, J., and Bever, J. D. (2006). Three-way interactions among mutualistic mycorrhizal fungi, plants, and plant enemies: hypotheses and synthesis. *Am. Nat.* 167, 141–152. doi: 10.1086/499379

Bennett, A. E., Bever, J. D., and Bowers, M. D. (2009). Arbuscular mycorrhizal fungal species suppress inducible plant responses and alter defensive strategies following herbivory. *Oecologia* 160, 771–779. doi: 10.1007/s00442-009-1338-5

Bernaola, L., Cosme, M., Schneider, R. W., and Stout, M. (2018). Belowground inoculation with arbuscular mycorrhizal fungi increases local and systemic susceptibility of rice plants to different pest organisms. *Front. Plant Sci.* 9:747. doi: 10.3389/fpls.2018.00747

Biere, A., and Bennett, E. A. (2013). Three-way interactions between plants, microbes and insects. *Funct. Ecol.* 27, 567–573. doi: 10.1111/1365-2435.12100

Biere, A., Marak, H. B., and van Damme, J. M. M. (2004). Plant chemical defense against herbivores and pathogens: generalized defense or trade-offs? *Oecologia* 140, 430–441. doi: 10.1007/s00442-004-1603-6

Boege, K., and Marquis, R. J. (2005). Facing herbivory as you grow up: the ontogeny of resistance in plants. *Trends Ecol. Evol.* 20, 441–448. doi: 10.1016/j.tree.2005.05.001

Bowers, M. D., and Stamp, N. E. (1993). Effects of plant age, genotype, and herbivory on *Plantago* performance and chemistry. *Ecology* 74, 1778–1791. doi: 10.2307/1939936

Breuillin, F., Schramm, J., Hajirezaei, M., Ahkami, A., Favre, P., Druege, U., et al. (2010). Phosphate systemically inhibits development of arbuscular mycorrhiza in *Petunia hybrida* and represses genes involved in mycorrhizal functioning. *Plant J.* 64, 1002–1017. doi: 10.1111/j.1365-313X.2010.04385.x

Bustos, R., Castrillo, G., Linhares, F., Puga, M. I., Rubio, V., Perez-Perez, J., et al. (2010). A central regulatory system largely controls transcriptional activation and repression responses to phosphate starvation in *Arabidopsis*. *PLoS Genet.* 6:e1001102. doi: 10.1371/journal.pgen.1001102

Cameron, D. D., Neal, A. L., van Wees, S. C., and Ton, J. (2013). Mycorrhiza-induced resistance: more than the sum of its parts? *Trends Plant Sci.* 18, 539–545. doi: 10.1016/j.tplants.2013.06.004

Castrillo, G., Teixeira, P. J., Paredes, S. H., Law, T. F., de Lorenzo, L., Feltcher, M. E., et al. (2017). Root microbiota drive direct integration of phosphate stress and immunity. *Nature* 543, 513–518. doi: 10.1038/nature21417

Cavagnaro, T. R., Smith, F. A., Ayling, S. M., and Smith, S. E. (2003). Growth and phosphorus nutrition of a Paris-type arbuscular mycorrhizal symbiosis. *New Phytol.* 157, 127–134. doi: 10.1046/j.1469-8137.2003.00654.x

Chiou, T. -J., and Lin, S. -I. (2011). Signaling network in sensing phosphate availability in plants. *Annu. Rev. Plant Biol.* 62, 185–206. doi: 10.1146/annurev-arplant-042110-103849

Choudhary, D. K., Varma, A., and Tuteja, N. (2016). *Plant-microbe interaction: An approach to sustainable agriculture. Singapore: springer.*

Coley, P. D., Bateman, M. L., and Kursar, T. A. (2006). The effects of plant quality on caterpillar growth and defense against natural enemies. *Oikos* 115, 219–228. doi: 10.1111/j.2006.0030-1299.14928.x

Conrath, U., Beckers, G. J. M., Langenbach, C. J. G., and Jaskiewicz, M. R. (2015). Priming for enhanced defense. *Annu. Rev. Phytopathol.* 53, 97–119. doi: 10.1146/annurev-phyto-080614-120132

Darrow, K., and Bowers, M. D. (1999). Effects of herbivore damage and nutrient level on induction of iridoid glycosides in *Plantago lanceolata*. *J. Chem. Ecol.* 25, 1427–1440. doi: 10.1023/A:1020991229072

De Deyn, G. B., Biere, A., van der Putten, W. H., Wagenaar, R., and Klironomos, J. N. (2009). Chemical defense, mycorrhizal colonization and growth responses in *Plantago lanceolata* L. *Oecologia* 160, 433–442. doi: 10.1007/s00442-009-1312-2

Devaiah, B. N., Karthikeyan, A. S., and Raghothama, K. G. (2007). WRKY75 transcription factor is a modulator of phosphate acquisition and root development in *Arabidopsis*. *Plant Physiol.* 143, 1789–1801. doi: 10.1104/pp.106.093971

Dicke, M., and Hilker, M. (2003). Induced plant defences: from molecular biology to evolutionary ecology. *Basic Appl. Ecol.* 4, 3–14. doi: 10.1078/1439-1791-00129

Fajer, E. D., Bowers, M. D., and Bazzaz, F. A. (1992). The effect of nutrients and enriched CO2 environments on production of carbon-based allelochemicals in *Plantago*—a test of the carbon nutrient balance hypothesis. *Am. Nat.* 140, 707–723. doi: 10.1086/285436

Fellbaum, C. R., Mensah, J. A., Cloos, A. J., Strahan, G. E., Pfeffer, P. E., Kiers, E. T., et al. (2014). Fungal nutrient allocation in common mycorrhizal networks is regulated by the carbon source strength of individual host plants. *New Phytol.* 203, 646–656. doi: 10.1111/nph.12827

Fontana, A., Reichelt, M., Hempel, S., Gershenzon, J., and Unsicker, S. B. (2009). The effects of arbuscular mycorrhizal fungi on direct and indirect defense metabolites of *Plantago lanceolata* L. *J. Chem. Ecol.* 35, 833–843. doi: 10.1007/s10886-009-9654-0

Frew, A., Powell, J. R., Glauser, G., Bennett, A. E., and Johnson, S. N. (2018). Mycorrhizal fungi enhance nutrient uptake but disarm defences in plant roots, promoting plant-parasitic nematode populations. *Soil Biol. Biochem.* 126, 123–132. doi: 10.1016/j.soilbio.2018.08.019

Fuchs, A., and Bowers, M. D. (2004). Patterns of iridoid glycoside production and induction in *Plantago lanceolata* and the importance of plant age. *J. Chem. Ecol.* 30, 1723–1741. doi: 10.1023/B:JOEC.0000042398.13765.83

Gange, A. C., and West, H. M. (1994). Interactions between arbuscular mycorrhizal fungi and foliar-feeding insects in *Plantago lanceolata*. *New Phytol.* 128, 79–87. doi: 10.1111/j.1469-8137.1994.tb03989.x

Gehring, C., and Bennett, A. (2009). Mycorrhizal fungal-plant-insect interactions: the importance of a community approach. *Environ. Entomol.* 38, 93–102. doi: 10.1603/022.038.0111

Gosling, P., Mead, A., Proctor, M., Hammond, J., and Bending, G. D. (2013). Contrasting arbuscular mycorrhizal communities colonising different host plants show a similar response to a soil phosphorus concentration gradient. *New Phytol.* 198, 546–556. doi: 10.1111/nph.12169

Grace, E. J., Cotsaftis, O., Tester, M., Smith, F. A., and Smith, S. E. (2009). Arbuscular mycorrhizal inhibition of growth in barley cannot be attributed to extent of colonization, fungal phosphorus uptake or effects on expression of plant phosphate transporter genes. *New Phytol.* 181, 938–949. doi: 10.1111/j.1469-8137.2008.02720.x

Grman, E. (2012). Plant species differ in their ability to reduce allocation to non-beneficial arbuscular mycorrhizal fungi. *Ecology* 93, 711–718. doi: 10.1890/11-1358.1

Hannula, S. E., Morrien, E., de Hollander, M., van der Putten, W. H., van Veen, J. A., and de Boer, W. (2017). Shifts in rhizosphere fungal community during secondary succession following abandonment from agriculture. *ISME J.* 11, 2294–2304. doi: 10.1038/ismej.2017.90

Hartley, S. E., and Gange, A. C. (2009). Impacts of plant symbiotic fungi on insect herbivores: mutualism in a multitrophic context. *Annu. Rev. Entomol.* 54, 323–342. doi: 10.1146/annurev.ento.54.110807.090614

Harvey, J. A., Van Nouhuys, S., and Biere, A. (2005). Effects of quantitative variation in allelochemicals in *Plantago lanceolata* on development of a generalist and a specialist herbivore and their endoparasitoids. *J. Chem. Ecol.* 31, 287–302. doi: 10.1007/s10886-005-1341-1

Hetrick, D. B. A., Kitt, D. G., and Wilson, G. T. (1983). The influence of phosphorus fertilization, drought, fungal species, and nonsterile soil on mycorrhizal growth response in tall grass prairie plants. *Can. J. Bot.* 64, 1199–1203. doi: 10.1139/b86-162

Hoagland, D. R., and Arnon, D. I. (1950). *The water culture method for growing plants without soil*, California Agricultural Experiment Station Circular 347. Berkeley: University of California, 1–32.

Hoeksema, J. D., Chaudhary, V. B., Gehring, C. A., Johnson, N. C., Karst, J., Koide, R. T., et al. (2010). A meta-analysis of context-dependency in plant response to inoculation with mycorrhizal fungi. *Ecol. Lett.* 13, 394–407. doi: 10.1111/j.1461-0248.2009.01430.x

Jarzomski, C. M., Stamp, N. E., and Bowers, M. D. (2000). Effects of plant phenology, nutrients and herbivory on growth and defensive chemistry of plantain, *Plantago lanceolata*. *Oikos* 88, 371–379. doi: 10.1034/j.1600-0706.2000.880216.x

Johnson, N. C. (2010). Tansley review: resource stoichiometry elucidates the structure and function of arbuscular mycorrhizas across scales. *New Phytol.* 185, 631–647. doi: 10.1111/j.1469-8137.2009.03110.x

Johnson, N. C., Wilson, G. W. T., Wilson, J. A., Miller, R. M., and Bowker, M. A. (2015). Mycorrhizal phenotypes and the law of the minimum. *New Phytol.* 205, 1473–1484. doi: 10.1111/nph.13172

Jung, S. C., Martinez-Medina, A., Lopez-Raez, J. A., and Pozo, M. J. (2012). Mycorrhiza-induced resistance and priming of plant defenses. *J. Chem. Ecol.* 38, 651–664. doi: 10.1007/s10886-012-0134-6

Karasawa, T., Hodge, A., and Fitter, A. H. (2012). Growth, respiration and nutrient acquisition by the arbuscular mycorrhizal fungus *Glomus mosseae* and its host plant *Plantago lanceolata* in cooled soil. *Plant Cell Environ.* 35, 819–828. doi: 10.1111/j.1365-3040.2011.02455.x

Kaur, S., and Suseela, V. (2020). Unraveling arbuscular mycorrhiza-induced changes in plant primary and secondary metabolome. *Meta* 10:335. doi: 10.3390/metabo10080335

Khan, G. A., Vogiatzaki, E., Glauser, G., and Poirier, Y. (2016). Phosphate deficiency induces the jasmonate pathway and enhances resistance to insect herbivory. *Plant Physiol.* 171, 632–644. doi: 10.1104/pp.16.00278

Konvalinkova, T., and Jansa, J. (2016). Lights off for arbuscular mycorrhiza: on its symbiotic functioning under light deprivation. *Front. Plant Sci.* 7:782. doi: 10.3389/fpls.2016.00782

Konvalinkova, T., Püschel, D., Janouskova, M., Gryndler, M., and Jansa, J. (2015). Duration and intensity of shade differentially affects mycorrhizal growth and phosphorus uptake responses of *Medicago truncatula*. *Front. Plant Sci.* 6:65. doi: 10.3389/fpls.2015.00065

Koricheva, J., Gange, A. C., and Jones, T. (2009). Effects of mycorrhizal fungi on insect herbivores: a meta-analysis. *Ecology* 90, 2088–2097. doi: 10.1890/08-1555.1

Landis, F. C., and Fraser, L. H. (2008). A new model of carbon and phosphorus transfers in arbuscular mycorrhizas. *New Phytol.* 177, 466–479. doi: 10.1111/j.1469-8137.2007.02268.x

Li, H.-Y., Smith, F. A., Dickson, S., Holloway, R. E., and Smith, S. E. (2008). Plant growth depressions in arbuscular mycorrhizal symbiosis: not just caused by carbon drain? *New Phytol.* 178, 852–862. doi: 10.1111/j.1469-8137.2008.02410.x

Marak, H. B., Biere, A., and van Damme, J. M. M. (2002a). Two herbivore-deterrent iridoid glycosides reduce the in-vitro growth of a specialist but not of a generalist pathogenic fungus of *Plantago lanceolata* L. *Chemoecology* 12, 185–192. doi: 10.1007/PL00012667

Marak, H. B., Biere, A., and Van Damme, J. M. M. (2002b). Systemic, genotype-specific induction of two herbivore-deterrent iridoid glycosides in *Plantago lanceolata* L. in response to fungal infection by *Diaporthe adunca* (rob.) Niessel. *J. Chem. Ecol.* 28, 2429–2448. doi: 10.1023/A:1021475800765

Marak, H. B., Biere, A., and Van Damme, J. M. M. (2003). Fitness costs of chemical defense in *Plantago lanceolata* L.: effects of nutrient and competition stress. *Evolution* 57, 2519–2530. doi: 10.1111/j.0014-3820.2003.tb01496.x

Martinez-Medina, A., Flors, V., Heil, M., Mauch-Mani, B., Pieterse, C. M. J., Pozo, M. J., et al. (2016). Recognizing plant defense priming. *Trends Plant Sci.* 21, 818–822. doi: 10.1016/j.tplants.2016.07.009

Mauch-Mani, B., Baccelli, I., Luna, E., and Flors, V. (2017). Defense priming: an adaptive part of induced resistance. *Annu. Rev. Plant Biol.* 68, 485–512. doi: 10.1146/annurev-arplant-042916-041132

McGonigle, T. P., Miller, M. H., Evans, D. G., Fairchild, G. L., and Swan, J. A. (1990). A new method which gives an objective measure of colonization of roots by vesicular arbuscular mycorrhizal fungi. *New Phytol.* 115, 495–501. doi: 10.1111/j.1469-8137.1990.tb00476.x

Miehe-Steier, A., Roscher, C., Reichelt, M., Gershenzon, J., and Unsicker, S. B. (2015). Light and nutrient dependent responses in secondary metabolites of *Plantago lanceolata* offspring are due to phenotypic plasticity in experimental grasslands. *PLoS One* 10:e0136073 doi: 10.1371/journal.pone.0136073

Miller, R. E., Gleadow, R. M., and Cavagnaro, T. R. (2014). Age versus stage: does ontogeny modify the effect of phosphorus and arbuscular mycorrhizas on above- and below-ground defence in forage sorghum? *Plant Cell Environ.* 37, 929–942. doi: 10.1111/pce.12209

Minton, M. M., Barber, N. A., and Gordon, L. L. (2016). Effects of arbuscular mycorrhizal fungi on herbivory defense in two *Solanum* (Solanaceae) species. *Plant Ecol. Evol.* 149, 157–164. doi: 10.5091/plecevo.2016.1176

Miozzi, L., Vaira, A. M., Catoni, M., Fiorilli, V., Accotto, G. P., and Lanfranco, L. (2019). Arbuscular mycorrhizal symbiosis: plant friend or foe in the fight against viruses? *Front. Microbiol.* 10:1238. doi: 10.3389/fmicb.2019.01238

Morcuende, R., Bari, R., Gibon, Y., Zheng, W., Pant, B. D., Bläsing, O., et al. (2007). Genome-wide reprogramming of metabolism and regulatory networks of *Arabidopsis* in response to phosphorus. *Plant Cell Environ.* 30, 85–112. doi: 10.1111/j.1365-3040.2006.01608.x

Mueller, L. M., and Harrison, M. J. (2019). Phytohormones, miRNAs, and peptide signals integrate plant phosphorus status with arbuscular mycorrhizal symbiosis. *Curr. Opin. Plant Biol.* 50, 132–139. doi: 10.1016/j.pbi.2019.05.004

Murphy, J., and Riley, J. P. (1962). A modified single solution method for determination of phosphate in natural waters. *Anal. Chim. Acta* 27, 31–36. doi: 10.1016/S0003-2670(00)88444-5

Mustafa, G., Randoux, B., Tisserant, B., Fontaine, J., Magnin-Robert, M., Sahraoui, A. L. -H., et al. (2016). Phosphorus supply, arbuscular mycorrhizal fungal species, and plant genotype impact on the protective efficacy of mycorrhizal inoculation against wheat powdery mildew. *Mycorrhiza* 26, 685–697. doi: 10.1007/s00572-016-0698-z

Nagy, R., Drissner, D., Amrhein, N., Jakobsen, I., and Bucher, M. (2009). Mycorrhizal phosphate uptake pathway in tomato is phosphorus-repressible and transcriptionally regulated. *New Phytol.* 181, 950–959. doi: 10.1111/j.1469-8137.2008.02721.x

Nishad, R., Ahmed, T., Rahman, V. J., and Kareem, A. (2020). Modulation of plant defense system in response to microbial interactions. *Front. Microbiol.* 11:1298. doi: 10.3389/fmicb.2020.01298

Olsson, P. A., Rahm, J., and Aliasgharzad, N. (2010). Carbon dynamics in mycorrhizal symbioses is linked to carbon costs and phosphorus benefits. *FEMS Microbiol. Ecol.* 72, 125–131. doi: 10.1111/j.1574-6941.2009.00833.x

Orlowska, E., Godzik, B., and Turnau, K. (2012). Effect of different arbuscular mycorrhizal fungal isolates on growth and arsenic accumulation in *Plantago lanceolata* L. *Environ. Pollut.* 168, 121–130. doi: 10.1016/j.envpol.2012.04.026

Pankoke, H., Buschmann, T., and Mueller, C. (2013). Role of plant beta-glucosidases in the dual defense system of iridoid glycosides and their hydrolyzing enzymes in *Plantago lanceolata* and *Plantago major*. *Phytochemistry* 94, 99–107. doi: 10.1016/j.phytochem.2013.04.016

Pankoke, H., Hopfner, I., Matuszak, A., Beyschlag, W., and Mueller, C. (2015). The effects of mineral nitrogen limitation, competition, arbuscular mycorrhiza, and their respective interactions, on morphological and chemical plant traits of *Plantago lanceolata*. *Phytochemistry* 118, 149–161. doi: 10.1016/j.phytochem.2015.07.014

Pieterse, C. M. J., Zamioudis, C., Berendsen, R. L., Weller, D. M., Van Wees, S. C. M., and Bakker, P. (2014). Induced systemic resistance by beneficial microbes. *Annu. Rev. Phytopathol.* 52, 347–375. doi: 10.1146/annurev-phyto-082712-102340

Poorter, H., Niinemets, U., Ntagkas, N., Siebenkas, A., Maenpaa, M., Matsubara, S., et al. (2019). Tansley review: a meta-analysis of plant responses to light intensity for 70 traits ranging from molecules to whole plant performance. *New Phytol.* 223, 1073–1105. doi: 10.1111/nph.15754

Pozo, M. J., and Azcon-Aguilar, C. (2007). Unraveling mycorrhiza-induced resistance. *Curr. Opin. Plant Biol.* 10, 393–398. doi: 10.1016/j.pbi.2007.05.004

Pozo, M. J., Lopez-Raez, J. A., Azcon-Aguilar, C., and Garcia-Garrido, J. M. (2015). Phytohormones as integrators of environmental signals in the regulation of mycorrhizal symbioses. *New Phytol.* 205, 1431–1436. doi: 10.1111/nph.13252

Puttick, G. M., and Bowers, M. D. (1988). Effect of qualitative and quantitative variation in allelochemicals on generalist insects: iridoid glycosides and the southern army worm. *J. Chem. Ecol.* 14, 335–351. doi: 10.1007/BF01022550

Quintero, C., and Bowers, M. D. (2011). Plant induced defenses depend more on plant age than previous history of damage: implications for plant-herbivore interactions. *J. Chem. Ecol.* 37, 992–1001. doi: 10.1007/s10886-011-0007-4

Quintero, C., and Bowers, M. D. (2012). Changes in plant chemical defenses and nutritional quality as a function of ontogeny in *Plantago lanceolata* (Plantaginaceae). *Oecologia* 168, 471–481. doi: 10.1007/s00442-011-2114-x

Real-Santillán, R. O., del-Val, E., Cruz-Ortega, R., Contreras-Cornejo, H. A., González-Esquivel, C. E., and Larsen, J. (2019). Increased maize growth and P uptake promoted by arbuscular mycorrhizal fungi coincide with higher foliar herbivory and larval biomass of the fall armyworm *Spodoptera frugiperda*. *Mycorrhiza* 29, 615–622. doi: 10.1007/s00572-019-00920-3

Reinhard, S., Martin, P., and Marschner, H. (1993). Interactions in the tripartite symbiosis of pea (*Pisum sativum* L) Glomus and rhizobium under non-limiting phosphorus supply. *J. Plant Physiol.* 141, 7–11. doi: 10.1016/S0176-1617(11)80844-8

Reudler, J. H., Biere, A., Harvey, J. A., and van Nouhuys, S. (2011). Differential performance of a specialist and two generalist herbivores and their parasitoids on *Plantago lanceolata*. *J. Chem. Ecol.* 37, 765–778. doi: 10.1007/s10886-011-9983-7

Rojas, J. C., Wyatt, T. D., and Birch, M. C. (2000). Flight and oviposition behavior toward different host plant species by the cabbage moth, *Mamestra brassicae* (L.) (Lepidoptera: Noctuidae). *J. Insect Behav.* 13, 247–254. doi: 10.1023/A:1007792332046

Rouached, H., Arpat, A. B., and Poirier, Y. (2010). Regulation of phosphate starvation responses in plants: signaling players and cross-talks. *Mol. Plant* 3, 288–299. doi: 10.1093/mp/ssp120

Schmiesing, A., Emonet, A., Gouhier-Darimont, C., and Reymond, P. (2016). Arabidopsis MYC transcription factors are the target of hormonal salicylic acid/jasmonic acid cross talk in response to *Pieris brassicae* egg extract. *Plant Physiol.* 170, 2432–2443. doi: 10.1104/pp.16.00031

Schoonhoven, L. M., van Loon, J. J., and Dicke, M. (2005). *Insect-plant biology*. Oxford: Oxford University Press.

Schubert, A., Wyss, P., and Wiemken, A. (1992). Occurrence of trehalose in vesicular-arbuscular mycorrhizal fungi and in mycorrhizal roots. *J. Plant Physiol.* 140, 41–45. doi: 10.1016/S0176-1617(11)81054-0

Schweiger, R., Baier, M. C., Persicke, M., and Muller, C. (2014a). High specificity in plant leaf metabolic responses to arbuscular mycorrhiza. *Nat. Comm.* 5:3886. doi: 10.1038/ncomms4886

Schweiger, R., Heise, A. M., Persicke, M., and Mueller, C. (2014b). Interactions between the jasmonic and salicylic acid pathway modulate the plant metabolome and affect herbivores of different feeding types. *Plant Cell Environ.* 37, 1574–1585. doi: 10.1111/pce.12257

Scriber, J. M., and Slansky, F. Jr. (1981). The nutritional ecology of immature insects. *Annu. Rev. Entomol.* 26, 183–211. doi: 10.1146/annurev.en.26.010181.001151

Shrivastava, G., Ownley, B. H., Auge, R. M., Toler, H., Dee, M., Vu, A., et al. (2015). Colonization by arbuscular mycorrhizal and endophytic fungi enhanced terpene production in tomato plants and their defense against a herbivorous insect. *Symbiosis* 65, 65–74. doi: 10.1007/s13199-015-0319-1

Singh, P., Unnithan, G. C., and Delobel, A. G. L. (1983). An artificial diet for sorghum shootfly larvae. *Entomol. Exp. Appl.* 33, 122–124. doi: 10.1111/j.1570-7458.1983.tb03245.x

Smith, S. E., and Read, D. J. (2008). *Mycorrhizal Symbiosis*. *3rd Edn*. London: Academic Press.

Smith, S. E., and Smith, F. A. (2011). Roles of arbuscular mycorrhizas in plant nutrition and growth: new paradigms from cellular to ecosystem scales. *Annu. Rev. Plant Biol.* 62, 227–250. doi: 10.1146/annurev-arplant-042110-103846

Smith, S. E., and Smith, F. A. (2012). Fresh perspectives on the roles of arbuscular mycorrhizal fungi in plant nutrition and growth. *Mycologia* 104, 1–13. doi: 10.3852/11-229

Song, Y. Y., Ye, M., Li, C. Y., Wang, R. L., Wei, X. C., Luo, S. M., et al. (2013). Priming of anti-herbivore defense in tomato by arbuscular mycorrhizal fungus and involvement of the jasmonate pathway. *J. Chem. Ecol.* 39, 1036–1044. doi: 10.1007/s10886-013-0312-1

Spagnoletti, F. N., Leiva, M., Chiocchio, V., and Lavado, R. S. (2018). Phosphorus fertilization reduces the severity of charcoal rot (*Macrophomina phaseolina*) and the arbuscular mycorrhizal protection in soybean. *J. Plant Nutr. Soil Sci.* 181, 855–860. doi: 10.1002/jpln.201700569

Sutter, R., and Mueller, C. (2011). Mining for treatment-specific and general changes in target compounds and metabolic fingerprints in response to herbivory and phytohormones in *Plantago lanceolata*. *New Phytol.* 191, 1069–1082. doi: 10.1111/j.1469-8137.2011.03768.x

Tamura, Y. (2001). Effects of temperature, shade, and nitrogen application on the growth and accumulation of bioactive compounds in cultivars of *Plantago lanceolata* L. *Jpn. J. Crop Sci.* 70, 548–553. doi: 10.1626/jcs.70.548

Tao, L. L., Ahmad, A., de Roode, J. C., and Hunter, M. D. (2016). Arbuscular mycorrhizal fungi affect plant tolerance and chemical defences to herbivory through different mechanisms. *J. Ecol.* 104, 561–571. doi: 10.1111/1365-2745.12535

Tomczak, V. V., Schweiger, R., and Mueller, C. (2016). Effects of arbuscular mycorrhiza on plant chemistry and the development and behavior of a generalist herbivore. *J. Chem. Ecol.* 42, 1247–1258. doi: 10.1007/s10886-016-0785-9

Van Dam, N. M., Horn, M., Mares, M., and Baldwin, I. T. (2001). Ontogeny constrains systemic protease inhibitor response in *Nicotiana attenuata*. *J. Chem. Ecol.* 27, 547–568. doi: 10.1023/a:1010341022761

Van Wees, S. C. M., Van der Ent, S., and Pieterse, C. M. J. (2008). Plant immune responses triggered by beneficial microbes. *Curr. Opin. Plant Biol.* 11, 443–448. doi: 10.1016/j.pbi.2008.05.005

Vannette, R. L., and Hunter, M. D. (2009). Mycorrhizal fungi as mediators of defence against insect pests in agricultural systems. *Agric. For. Entomol.* 11, 351–358. doi: 10.1111/j.1461-9563.2009.00445.x

Vannette, R. L., Hunter, M. D., and Rasmann, S. (2013). Arbuscular mycorrhizal fungi alter above- and below-ground chemical defense expression differentially among *Asclepias* species. *Front. Plant Sci.* 4:361. doi: 10.3389/fpls.2013.00361

Vierheilig, H., Coughlan, A. P., Wyss, U., and Piché, Y. (1998). Ink and vinegar, a simple staining technique for arbuscular-mycorrhizal fungi. *Appl. Environ. Microbiol.* 64, 5004–5007. doi: 10.1128/AEM.64.12.5004-5007.1998

Vierheilig, H., Garcia-Garrido, J. M., Wyss, U., and Piché, Y. (2000). Systemic suppression of mycorrhizal colonization of barley roots already colonized by AM fungi. *Soil Biol. Biochem.* 32, 589–595. doi: 10.1016/S0038-0717(99)00155-8

Walder, F., and van der Heijden, M. G. A. (2015). Regulation of resource exchange in the arbuscular mycorrhizal symbiosis. *Nat. Plants* 1:15159. doi: 10.1038/nplants.2015.159

Wang, M. G., Bezemer, T. M., van der Putten, W. H., and Biere, A. (2015). Effects of the timing of herbivory on plant defense induction and insect performance in ribwort plantain (*Plantago lanceolata* L.) depend on plant mycorrhizal status. *J. Chem. Ecol.* 41, 1006–1017. doi: 10.1007/s10886-015-0644-0

Wang, C., Tian, B., Yu, Z., and Ding, J. (2020). Effect of different combinations of phosphorus and nitrogen fertilization on arbuscular mycorrhizal fungi and aphids in wheat. *Insects* 11:365. doi: 10.3390/insects11060365

Yu, K., Pieterse, C. M. J., Bakker, P. A. H. M., and Berendsen, R. L. (2019). Beneficial microbes going underground of root immunity. *Plant Cell Environ.* 42, 2860–2870. doi: 10.1111/pce.13632

Zaller, J. G., Frank, T., and Drapela, T. (2011). Soil sand content can alter effects of different taxa of mycorrhizal fungi on plant biomass production of grassland species. *Eur. J. Soil Biol.* 47, 175–181. doi: 10.1016/j.ejsobi.2011.03.001

Zamioudis, C., and Pieterse, C. M. J. (2012). Modulation of host immunity by beneficial microbes. *Mol. Plant-Microbe Interact.* 25, 139–150. doi: 10.1094/MPMI-06-11-0179

Zheng, C. Y., Ji, B. M., Zhang, J. L., Zhang, F. S., and Bever, J. D. (2015). Shading decreases plant carbon preferential allocation towards the most beneficial mycorrhizal mutualist. *New Phytol.* 205, 361–368. doi: 10.1111/nph.13025

Conflict of Interest: The authors declare that the research was conducted in the absence of any commercial or financial relationships that could be construed as a potential conflict of interest.

frontiers in Plant Science

ORIGINAL RESEARCH
published: 14 April 2021
doi: 10.3389/fpls.2021.644597

Bacillus circulans GN03 Alters the Microbiota, Promotes Cotton Seedling Growth and Disease Resistance, and Increases the Expression of Phytohormone Synthesis and Disease Resistance-Related Genes

Lijun Qin[1,2†], Peidong Tian[1†], Qunyao Cui[1], Shuping Hu[1], Wei Jian[1], Chengjian Xie[1], Xingyong Yang[1] and Hong Shen[2,3]**

[1] College of Life Sciences, Chongqing Normal University, Chongqing, China, [2] Biological Science Research Center, Southwest University, Chongqing, China, [3] College of Resources and Environment Science, Southwest University, Chongqing, China

OPEN ACCESS

Edited by:
Jianfei Wang,
Anhui University of Science and Technology, China

Reviewed by:
Christos Zamioudis,
Democritus University of Thrace, Greece
Li Xue,
Zhejiang Normal University, China
Xingang Zhou,
Northeast Agricultural University, China

***Correspondence:**
Xingyong Yang
yangxy94@swu.edu.cn
Hong Shen
shenhong@swu.edu.cn

† These authors have contributed equally to this work

Specialty section:
This article was submitted to Plant Symbiotic Interactions, a section of the journal Frontiers in Plant Science

Received: 21 December 2020
Accepted: 23 March 2021
Published: 14 April 2021

Citation:
Qin L, Tian P, Cui Q, Hu S, Jian W, Xie C, Yang X and Shen H (2021) Bacillus circulans GN03 Alters the Microbiota, Promotes Cotton Seedling Growth and Disease Resistance, and Increases the Expression of Phytohormone Synthesis and Disease Resistance-Related Genes. Front. Plant Sci. 12:644597. doi: 10.3389/fpls.2021.644597

Plant growth-promoting bacteria (PGPB) are components of the plant rhizosphere that promote plant growth and/or inhibit pathogen activity. To explore the cotton seedlings response to *Bacillus circulans* GN03 with high efficiency of plant growth promotion and disease resistance, a pot experiment was carried out, in which inoculations levels of GN03 were set at 10^4 and 10^8 cfu·mL^{-1}. The results showed that GN03 inoculation remarkably enhanced growth promotion as well as disease resistance of cotton seedlings. GN03 inoculation altered the microbiota in and around the plant roots, led to a significant accumulation of growth-related hormones (indole acetic acid, gibberellic acid, and brassinosteroid) and disease resistance-related hormones (salicylic acid and jasmonic acid) in cotton seedlings, as determined with ELISA, up-regulated the expression of phytohormone synthesis-related genes (*EDS1*, *AOC1*, *BES1*, and *GA20ox*), auxin transporter gene (*Aux1*), and disease-resistance genes (*NPR1* and *PR1*). Comparative genomic analyses was performed between GN03 and four similar species, with regards to phenotype, biochemical characteristics, and gene function. This study provides valuable information for applying the PGPB alternative, GN03, as a plant growth and disease-resistance promoting fertilizer.

Keywords: *Bacillus circulans*, upland cotton (*Gossypium hirsutum* L.), disease resistance, growth-promoting, phytohormones synthesis, rhizosphere and endophytic microbiota

INTRODUCTION

In recent years, there has been considerable interest in plant growth-promoting bacteria (PGPB), which are free-living bacteria in the surrounding rhizosphere or in plant. PGPB can improve plant nutrient uptake, enhance plant growth and yield (Lugtenberg and Kamilova, 2009; Hassan et al., 2019), induce resistance against pathogens in plants, and aggressively colonize the root rhizosphere

(Lugtenberg and Kamilova, 2009; Emmanuel and Babalola, 2020). The effect of PGPB is primarily explained by their ability to secrete metabolites (Mahmood and Kataoka, 2020) that are able to: (a) stimulate plant growth by inducing the production and release of plant growth regulators or phytohormones such as indole acetic acid (IAA) and gibberellic acid (GA); (b) enhance asymbiotic N_2-fixation; (c) solubilize inorganic phosphate and mineralize organic phosphate and/or other nutrients; and (d) resist, tolerate, or compete with detrimental microorganisms (Lugtenberg and Kamilova, 2009; Ramakrishna et al., 2019). PGPB also indirectly promote plant growth by improving the diversity of the rhizosphere microbiome and entering inside the roots to trigger induced systemic resistance (ISR), thereby further antagonizing soil borne pathogens (Araujo et al., 2019; Dahmani et al., 2020).

At present, more than 20 species and genera of PGPB strains, including *Agrobacterium*, *Azospirillum*, *Azotobacter*, *Bacillus*, *Burkholderia*, *Enterobacter*, *Klebsiella*, and *Pseudomonas,* have been identified (Aloo et al., 2019). Among them, *Bacillus* is an important genus that can form long-lived, stress tolerant spores existing inside or outside the plant roots under adverse environmental conditions (Gadhave et al., 2018). It has strong saprophytic ability and competitiveness and is capable of secreting metabolites that stimulate plant growth and prevent pathogen infection (Qiao et al., 2017; Aloo et al., 2019; Hashem et al., 2019). Some studies have reported that three principal plant-associated bacteria, *Bacillus cereus*, *Bacillus subtilis* and *Bacillus amyloliquefaciens*, are colonizers of both the in- and outside of plant roots during the growth stage and can improve nutrient utilization, vegetative growth, flowering and fruit ripening, as well as resistance to diseases, insect pests, and environmental stress (Lugtenberg and Kamilova, 2009; Gadhave et al., 2018). However, these studies did not examine the impact of these bacteria on the rhizosphere and endophytic microflora (Qiao et al., 2017); thus, there remains a disconnect between the theoretical research and the practical application of PGPB (Ramakrishna et al., 2019; Alka et al., 2020). For example, the application of a fertilizer with the incorporation of PGPB reportedly showed inconsistent results between laboratory and field applications (Parnell et al., 2016). Currently, limited information is available on the intrinsic relationship between the bacteria and the soil rhizosphere habitat (soil depth, temperature, pH, and intra-species relationships) (Ahemad and Kibret, 2014), further implying that there is a gap in understanding the mechanistic interaction between PGPB and their host plants. In view of this, it is important to determine the impact of these *Bacillus* spp. inoculants on the native microbial community, to effectively apply the theory in field. The potential application of *Bacillus* in the production of a few crops, such as soybean, wheat, and rice (Khatri et al., 2020; Lee et al., 2020; Wang et al., 2020), and its effects on the growth promotion and disease resistance enhancement of upland cotton (*Gossypium hirsutum* L.) are rarely reported.

Upland cotton is an important cultivated oil and fiber crop worldwide; however, it is prone to the attack by the soil-borne hemibiotrophic fungus *Verticillium dahliae* associated with Verticillium wilt (Zhang et al., 2013). As microsclerotia, a dormant survival structure formed by *V. dahliae*, can exist in the soil for a long time, Verticillium wilt is considered the most destructive disease of cotton and is extremely difficult to control (Wang et al., 2016; Zhang et al., 2017a). Breeding of upland cotton varieties with disease resistance is limited by more variation in *V. dahliae* strains and the lack of *V. dahliae* resistant germplasm in upland cotton (Zhang et al., 2017a, 2021). Some chemicals, such as benomyl and acibenzolar-*S*-methyl, seem to work for Verticillium wilt, but they are not environment friendly (Goicoechea, 2009). Therefore, application of PGPB to control this disease is a safer and better alternative to protect upland cotton from Verticillium wilt (Hasan et al., 2020). Accordingly, beneficial PGPB with inhibitory action against *V. dahliae* are a promising biocontrol agent for the control of cotton Verticillium wilt. To date, some researchers have isolated multiple strains with biocontrol activities against *V. dahliae* from *Bacillus*, *Enterobacter*, *Paenibacillus*, *Pseudomonas*, *Serratia,* and *Streptomyces* genera (Erdogan and Benlioglu, 2010; Zhang et al., 2018; Cheng et al., 2020; Hasan et al., 2020; Sherzad and Canming, 2020; Tao et al., 2020; Zhang et al., 2020).

Bacillus circulans was first isolated and described in 1890 by Jordon. It is a Gram-positive bacterium (Nakamura and Swezey, 1983) with the ability to secrete polysaccharide degrading enzymes such as β-1,3 and β-1,6 glucanases, β-1,3 and β-1,4-glucanases, α-l,3-glucanases, amylase, chitinase, and xylanase (Tanaka and Watanabe, 1995). Several studies have shown that the *B. circulans* strain has the ability to promote plant growth and can be developed as a biological fertilizer (Mehta et al., 2010, 2015; Bokhari et al., 2019).

In this study, upland cotton seedlings were applied as the experimental host plant to investigate the plant growth-promoting mechanism and disease-resistance effect of *B. circulans* GN03 isolated from purple soil. Furthermore, we provided a full overview of the properties attributed by the GN03, and performed its comparative genomic analysis with four other *B. circulans* strains. The results of this study provide useful information for promoting sustainable agricultural practices for improving the soil environment and crop yield while also providing a basis for more in-depth microbial species interaction research.

MATERIALS AND METHODS

Bacterial Strain

The GN03 strain was isolated from the root surface of pakchoi cabbage (*Brassica chinensis*) grown in purple soil in an agricultural field in the Beibei District (30°26′12″ N, 106°26′25″ E), Chongqing, China (Shen et al., 2018). Bacterial suspensions were obtained by culturing cells in 50 mL of LB medium (10 g tryptone, 5 g yeast extract, and 10 g $NaCl{\cdot}L^{-1}$) in 300 mL flasks on a rotary shaker (150 rpm) at 37°C for 12 h. Scanning electron microscopy was used for morphological observations (Golding et al., 2016). The spore staining, Gram staining, and biochemical characteristics were evaluated according to Mehnaz et al. (2010).

Molecular Identification

After culturing GN03 in LB medium for 48 h (37°C, 150 rpm), the bacterial cells were collected by centrifugation (4,500 × *g* for 5 min at 4°C). To preliminarily confirm the strain of bacteria isolated, PCR (94°C for 10 min followed by 34 cycles at 94°C for 30 s, 56°C for 30 s, and 72°C for 90 s, with a final extension at 72°C for 10 min) was performed with universal 16S primers 27F (5′-AGAGTTTGATCCTGGCTCAG-3′) and 1492R (5′-TACGGTTACCTTGTTACGACTT-3′). The PCR products were sequenced by BGI (Shenzhen, China), and the resultant sequences were compared with those hosted on the GenBank database using BLAST. Genomic DNA was isolated from the cell pellets with a Bacteria DNA Kit (OMEGA) according to the manufacturer's instructions, and quantified using TBS-380 fluorometer (BioSystems, CA).

Evaluation of Growth Promotion and Disease Resistance in Cotton Seedlings

Bacteria were resuspended and diluted in deionized water (0 cfu·mL^{-1} for the Mock group, 10^4 cfu·mL^{-1} for the C1 group and 10^8 cfu·mL^{-1} for the C2 group). Upland cotton (*G. hirsutum* 'Yumian-1') seeds kindly provided by Dr. Zhengsheng Zhang (Southwest University, China), underwent surface sterilization with 20% (v/v) H_2O_2 for 2 min, and were then individually sown into plastic pots (12 cm diameter and 16 cm height). The soil was collected at 0–15 cm depth from the campus (30°36′45″N, 106°17′59″E, 261 m above sea level) of Chongqing Normal University, China. After being sieved (<1 mm) and air-dried, the soil contained 17.19 ± 0.62 g·kg^{-1} organic matter, 40.76 ± 2.86, 70.19 ± 2.01, and 93.84 ± 10.91 mg·kg^{-1} available nitrogen, phosphorus, and potassium, 0.78 ± 0.05, 1.02 ± 0.12, and 17.21 ± 0.38g·kg^{-1} total nitrogen, phosphorus, and potassium, respectively. Once two cotyledons started to unfold, 5 mL GN03 or an equal volume of deionized water was inoculated in rhizosphere (**Supplementary Table 1**). After 7 days, the plants were re-inoculated using the same method and concentration as in the initial inoculations. Throughout the experimental period, cotton seedlings were randomly placed in greenhouse conditions, wherein the average day/night period, daytime light intensity, temperature, and humidity were 12.5/11.5 h, 2,000–4,000 lux, 16–30°C and 50–80%, respectively. Twenty-three days after the second inoculation, indicators, including phenotypic data, hormone levels, gene expression, and microbial diversity, were measured. Three independent tests with 30 plants per replicate were performed.

The virulent defoliating *V. dahliae* strain V991, stored at −80°C, was first isolated from cotton originated in Xinjiang, China, and reactivated on potato dextrose agar (PDA, 200 g·L^{-1} potato, 20 g·L^{-1} dextrose, and 18 g·L^{-1} agar) medium at 25°C. After growing on PDA medium at 25°C for 7 days, mycelia were collected and cultured in potato dextrose broth (PDB, 200 g·L^{-1} potato and 20 g·L^{-1} dextrose) medium for 7 days at 25°C with constant shaking (150 rpm). Once the cotton seedlings presented with two true-leaves, they were inoculated with 5 mL GN03 suspensions (0, 10^4, and 10^8 cfu·mL^{-1}, respectively) poured into the soil surrounding the roots. After 24 h, the pre-treated seedlings were inoculated with the V991 strain by injecting 10 mL spore suspensions (10^7 conidia·mL^{-1}) into the soil around the roots, and control seedlings were inoculated with an equal volume of sterile distilled water (Zhou et al., 2013). The disease index was calculated by assessing 30 individual plants per treatment and repeated three times with the following formula: disease index = Σ (number of disease leaves × disease grade)/(total number of leaves × 4) × 100. The disease grade was classified as follows: 0 (no symptoms), 1 (>0–25% yellowing or wilting leaves), 2 (25–50% yellowing or wilting leaves), 3 (50–75% yellowing or wilting leaves), and 4 (75–100% yellowing or wilting leaves) (Luo et al., 2020). The assessment was performed every 3 days for 21 days post inoculation (dpi) V991.

Evaluation of Hormone Levels, Growth, and Disease Resistance-Related Gene Expression

The contents of IAA, GA, brassinosteroid (BR), salicylic acid (SA), and jasmonic acid (JA) in cotton leaves were measured using the corresponding ELISA Kits (Shanghai Preferred Biotechnology, China), with minimum detection concentration of less than 0.1 nM and accuracy of more than 99%. To determine the expression of genes related to growth and disease resistance, RNA was extracted from cotton roots using a MiniBEST plant RNA Extraction Kit (TaKaRa, Japan) and a RT reagent Kit for Perfect Real Time (TaKaRa) was used to obtain cDNA. *Ghhistone3* (the gene of *G. hirsutum* histone 3) was used as the reference gene in the quantitative reverse transcription-PCR (RT-qPCR). The expression of growth-promoting and disease resistance-related genes in the cotton root was measured in 10 μL PCR reactions containing 5 μL SYBR Green Real-time PCR Master Mix (Bio-Rad, Hercules, CA, United States), 1 μL root cDNA, 2 μL ultrapure water, and 1 μL each of the 10 μM forward and reverse primers (**Supplementary Table 2**). The following RT-qPCR protocol was used in a CFX96 instrument (Bio-Rad): 94°C for 2 min followed by 39 cycles of 94°C for 5 s and 60°C for 30 s, then 95°C for 5 s, 65°C for 5 s, and 95°C for 5 s.

Assessing the Rhizosphere and Endophytic Microbiota

The cotton roots with rhizosphere soils were placed in 0.02 M phosphate-buffered saline (pH 6.8) and incubated at 180 rpm for 20 min. After taking out the plant roots, the suspension was centrifuged at 12,000 × *g* for 10 min to collect the sediment containing the rhizosphere soil samples. The sediment was rinsed with 70% ethanol for 2 min and then with sterile water (5 times), whereas the removed cotton roots from the previous step were analyzed for endophytic microbial content. Total microbial genomic DNA was extracted from both the cotton roots and the rhizosphere soil samples using the DNeasy PowerSoil Kit (Qiagen, Hilden, Germany), following the manufacturer's instructions, and stored at −20°C for further analysis.

PCR amplification of the bacterial 16S rRNA genes V3–V4 region was performed using the forward primer 38F (5′-ACTCCTACGGGAGGCAGCA-3′) and the reverse primer 806R (5′-GGACTACHVGGGTWTCTAAT-3′) (Xu et al., 2016).

PCR amplicons were purified with Agencourt AMPure Beads (Beckman Coulter, Brea, CA, United States) and quantified using the PicoGreen dsDNA Assay Kit (Invitrogen, Carlsbad, CA, United States). After the individual quantification step, amplicons were pooled in equal amounts, and paired-end 2 × 300 bp sequencing was performed using the Illumina MiSeq platform with MiSeq Reagent Kit v3 at Shanghai Personal Biotechnology (China). The data were analyzed on the free online Majorbio Cloud Platform[1]. Operational taxonomic units (OTUs) were clustered at 97% similarity; rarefaction curves (Kemp and Aller, 2004) were prepared using a reasonable amount of sequencing data (**Supplementary Figure 1**), which produced a flat curve meaning that the amount of sequencing data was large enough to reflect the vast majority of microbial diversity information in the sample. The unclassified bacterial phyla were not applied to analyses. In addition, reads representing chloroplasts were removed prior to further analyses as chloroplasts are abundant in cotton roots.

Whole Genome Sequencing and Comparative Genome Analysis

The genome was sequenced by Genedenovo (Guangzhou, China) using a combination of the PacBio RS II system (Menlo Park, CA, United States) and Illumina sequencing platforms (San Diego, CA, United States). The GN03 gene model identified by Glimmer V3 was got by the *Ab initio* prediction method (Delcher et al., 2007). Then, all gene models were blasted against the non-redundant (NR)[2], SwissProt[3], KEGG[4], and COG[5] databases for functional annotation using the BLASTp module. In addition, tRNAs were identified using tRNAscan-SE (v1.23[6]) and rRNAs were determined using RNAmmer (v1.2[7]).

Comparative genomic analysis was carried out by comparing the genome sequence of the GN03 strain with that of four other *B. circulans* stains (**Supplementary Table 3**). Among them, PK3-109 and PK3-138 strains were isolated from plant root endophytes that grow in the Thar Desert, India (Bokhari et al., 2019); RIT379 strain was isolated from the internal stem tissue of *Costus igneus*, which grows in Puerto Rico (Polter et al., 2015); and a model strain NCTC2610[8]. PK3-109 strain has been shown to produce IAA and exopolysaccharide, and to increase the total fresh weight of *Arabidopsis thaliana* under conditions of salt stress (Bokhari et al., 2019).

Statistical Analysis

Biochemical and physiological measurements were evaluated using an analysis of variance (ANOVA) followed by Dunnett's *post hoc* test using the Statistical Package for the Social Sciences, v22.0 (SPSS, Chicago, IL, United States). Means among treatments were considered significantly different when the probability (p-value) was less than 0.05. All data in the tables and figures are presented as the mean ± SE (standard error). Values were compared using a one-way ANOVA least significant difference (LSD) test, or a non-parametric Kruskal–Wallis test when the data were not normally distributed. The Bray–Curtis dissimilarity metric and analysis of similarities (ANOSIM) with 999 permutations were performed when comparing groups.

Data Deposition

16S rDNA amplicon raw sequencing data were deposited in the NCBI Short Read Archive (SRA) BioProject PRJNA631145 under the accession numbers SRR11735611-SRR11735637. The *B. circulans* GN03 genome was deposited under accession numbers CP053315 and CP053316 (the latter is for the plasmid).

RESULTS

Morphological, Biochemical and Molecular Characteristics of GN03

Bacterial characterization of the GN03 strain revealed that it formed white round micro-bulge colonies with a small diameter and neat edges. The cells were rod-shaped and approximately 2 μm long. After fission, the daughter cells separated to form single cells (**Figure 1A**). GN03 presented as Gram-positive bacterium with oval-shaped mid-spores and capsular hypertrophy (**Supplementary Figure 2**). Biochemical characterization of GN03 revealed that it produced catalase and nitrate reductase. However, it did not produce phenylalanine deaminase or cytochrome oxidase c, neither degraded tryptophan to produce hydrazine, or use citrate as its sole carbon source. Sugar fermentation tests of GN03 resulted in the production of acid, but not gas. Fermentation of glucose by GN03 resulted in the production of acidic compounds as well as acetyl-methyl-methanol. Furthermore, GN03 was able to hydrolyze starch and liquefy gelatin (**Supplementary Table 4**). The characteristics of the GN03 strain conformed to the general characteristics of *B. circulans* (Buchanan et al., 1994). Sequencing of 16S rDNA and analysis via NCBI BLAST also revealed GN03 to be a strain of *B. circulans* with the genome characteristics of GN03, similar to the average *B. circulans* genomes recorded by the NCBI. Hence, the complete taxonomic descriptor is: *Firmicutes*, *Bacilli*, *Bacillales*, *Bacillaceae*, *Bacillus*, *B. circulans* GN03.

Effect of GN03 on Cotton Seedling Growth and Disease Resistance

To explore the plant growth-promoting effect of GN03, each cotton seedling was inoculated with various concentrations of GN03, ranging from 0 cfu·mL^{-1} as the control (Mock), 10^4 cfu·mL^{-1} (C1), to 10^8 cfu·mL^{-1} (C2). The evaluated phenotypic characteristics of cotton significantly improved with the increase in inoculation concentration (C2 > C1 > Mock; **Figure 1B**). Compared to the Mock group, the C2 group exhibited significantly increased stem length, leaf area, root length, stem width, and leaf number by 85.91, 98.45, 38.42, 22.22,

[1]http://www.majorbio.com
[2]https://ftp.ncbi.nih.gov/blast/db/
[3]http://uniprot.org
[4]http://www.genome.jp/kegg/
[5]http://www.ncbi.nlm.nih.gov/COG
[6]http://lowelab.ucsc.edu/tRNAscan-SE
[7]http://www.cbs.dtu.dk/services/RNAmmer
[8]https://www.ncbi.nlm.nih.gov/biosample/?term=circulans%20NCTC2610

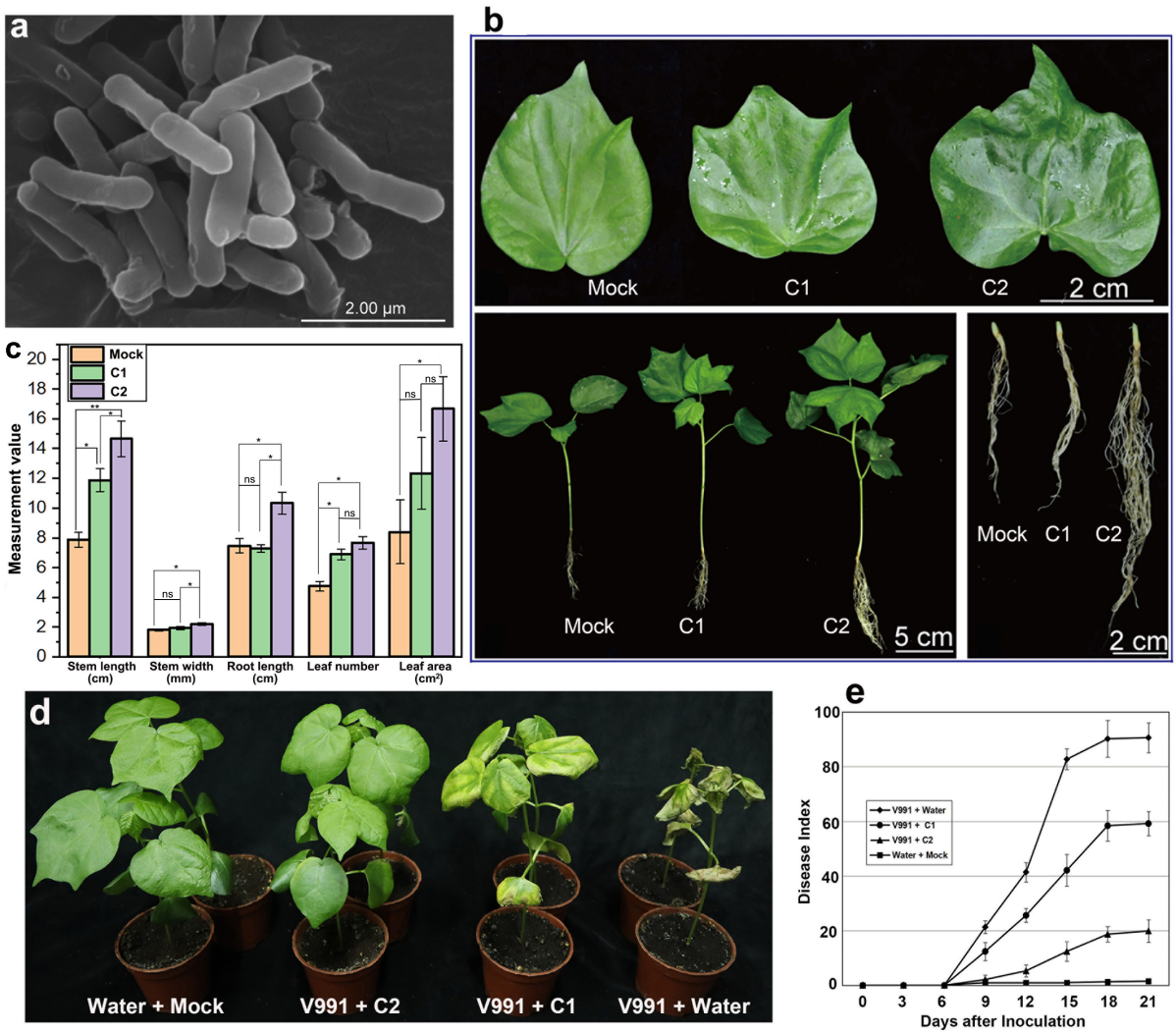

FIGURE 1 | Morphological characteristics and phenotypic changes in cotton seedling 30 days after inoculation of GN03. **(a)** Scanning electron microscopic image of the bacterial cell after culture for 16 h at 37°C. **(b)** The phenotype of the leaf, whole plant and root in cotton seedlings 30 days after inoculation of GN03. **(c)** The biomass of cotton seedlings. Leaf area is measured as the area of the third leaf from the top bud. Statistical significance was evaluated by one-way ANOVA and LSD *post hoc* test (*$p < 0.05$, **$p < 0.01$; ns, not significant, $n = 30$). **(d)** Disease symptoms of cotton plants pre-treated with different concentrations of GN03 (0, 10^4, and 10^8 cfu/mL) following inoculation with *V. dahliae* strain V991 at 18 dpi. **(e)** Disease indexes of the GN03-pre-treated cotton were determined from 3 to 21 dpi. Values are means ± SD; $n = 30$.

and 61.47%, respectively (**Figure 1C**). Overall, GN03 inoculation promoted cotton seedling growth in a dose-dependent manner.

After pouring different concentrations (0, 10^4, and 10^8 cfu·mL^{-1}) of GN03 suspensions into the soil surrounding the roots of the cotton seedling, the seedlings were inoculated with V991 spore suspensions. Different responses to the V991 infection were observed in pre-treated and control seedlings, and the symptoms of wilt and etiolation were much more severe in the control than the pre-treated seedlings at 21 dpi (Mock + V991 > C1 + V991 > C2 + V991; **Figure 1D**). The disease index increased with prolonged dpi, but disease development was slower in the pre-treated seedlings. At 21 dpi, compared to the Mock + V991 group, the C1 + V991 and C2 + V991 groups exhibited significantly increased Verticillium wilt resistance, and the disease indexes were 90.6, 59.2, and 19.9% for the Mock + V991, C1 + V991, and C2 + V991 groups, respectively (**Figure 1E**). These results indicated that GN03 inoculation enhanced the disease resistance of cotton seedlings.

Changes in Phytohormones and the Expression of Disease Resistance-Related Genes After GN03 Inoculation

Bacillus association boosts plant growth and immunity to adversity by regulating growth and stress response genes, proteins, plant hormones, and related metabolites (Radhakrishnan et al., 2017; Afzal et al., 2019;

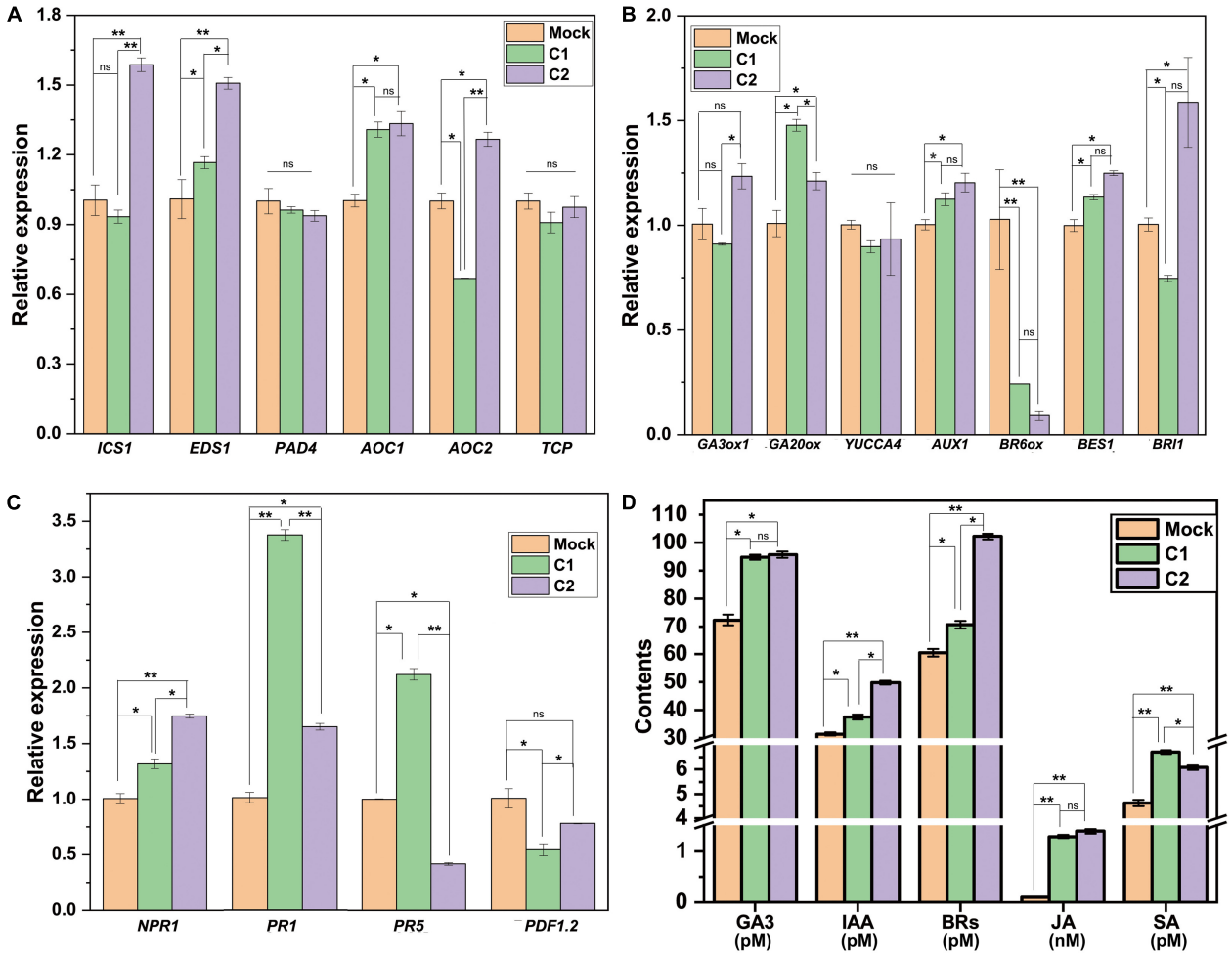

FIGURE 2 | Changes in cotton hormones and related gene expression 30 days after GN03 inoculation. Relative expression of **(A)** SA and JA synthesis-related gene, **(B)** IAA, GA, BR synthesis-related genes, and **(C)** disease resistance-related genes, assessed with RT-qPCR. **(D)** Hormone content of cotton leaves. In the graphs, mean values with SD are indicated; statistical significance was evaluated by one-way ANOVA and LSD *post hoc* test (*$p < 0.05$, **$p < 0.01$; ns, not significant, $n = 5$).

Hashem et al., 2019). Accordingly, in cotton seedling roots, the expression of SA, JA, BRs, and GA synthesis-related genes (*EDS1*, *AOC1*, *BES1*, and *GA20ox*), auxin transporter gene (*AUX1*), and disease resistance-related genes (*NPR1* and *PR1*) was significantly increased (**Figures 2A–C**). The changes in plant hormone levels in the seedlings were consistent with the expression of genes related to phytohormone synthesis. Compared to those in the Mock group, the level of IAA, GA, BR, JA, and SA were increased by 19.4, 31.1, 16.6, 28.6, and 44.9% in the C1 group, and that were significantly increased by 58.9, 32.4, 68.7, 38.7, and 31.3% in the C2 group, respectively (**Figure 2D**).

Rhizosphere Microbiota Changes After GN03 Inoculation

Thirty days after inoculation, rhizosphere soil samples from each group were extracted to assess the microbial communities based on 16S rDNA amplicon sequencing. The richness and diversity of bacterial species were evaluated using the Chao1 and Shannon indices (Shannon, 1948; Chao, 1984). The results showed no significantly difference between the rhizosphere sample groups (**Supplementary Table 5A**). Nevertheless, the PCoA (Ramette, 2007) suggested that the microbiota could be divided into two distinct clusters based on the presence or absence of inoculation (**Figure 3A**). A network diagram (Faust and Raes, 2012) of species association showed very complex bacterial relationships in the rhizosphere, wherein the bacterial species promoted as well as inhibited each other (**Supplementary Figure 3**). This indicated that the rhizosphere microbiota was large in number and complex in composition, and that the microbial equilibrium in the rhizosphere would not be easily disrupted, thereby retaining a strong ability to recover.

With regards to rhizosphere bacterial composition at the phylum level (**Figure 3B**), the top three phyla were Proteobacteria, Actinomycetes, and Bacteroides. The relative proportion of Proteobacteria was approximately 50–60%. In the C2 group, the proportion of Spirochaetes was decreased by 5.05% but that of Actinobacteria was increased by 11.01%. At the

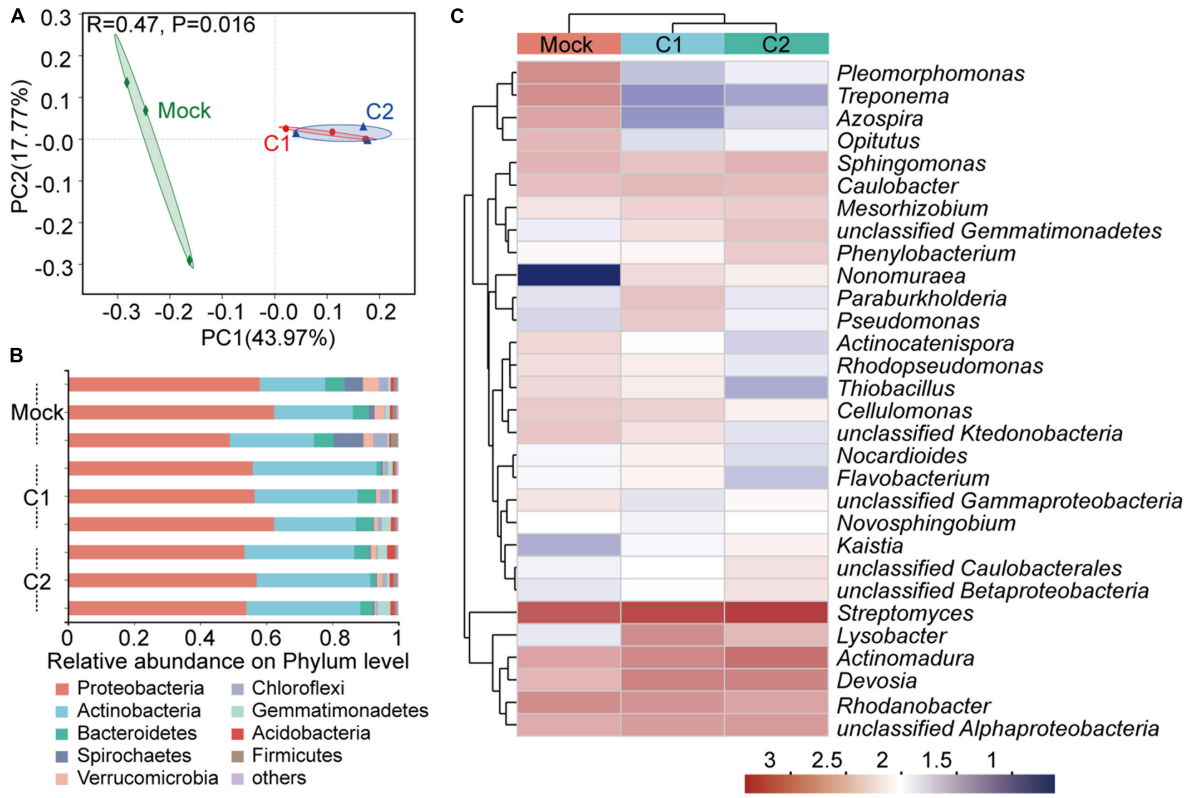

FIGURE 3 | Bacterial community of the rhizosphere 30 days after GN03 inoculation. **(A)** PCoA plot based on the structure of the microbial community. Mock, green diamonds; C1, red circle; and C2, blue triangles. Variation in communities was based on Bray–Curtis distances and an ANOSIM test with 999 permutations. **(B)** Relative abundance of bacterial phyla in different samples. **(C)** Heatmap showing the relative abundance of the dominant taxa with respect to treatment. Hierarchical cluster analysis was based on Bray–Curtis distances using a complete-linkage method. Each sample was measured in triplicate.

genus level, the proportions of *Lysobacter* and *Herbaspirillum*, which have important biocontrol activities and nitrogen fixation abilities (Chubatsu et al., 2012; Exposito et al., 2015), were increased in the rhizosphere after inoculation, while those of *Geobacter*, *Curvibacter*, and *Methylocysti*, which have repair functions (Baani and Liesack, 2008; Gulay et al., 2018), were reduced (**Figure 3C** and **Supplementary Figure 4A**).

Endophytic Microbiota Changes After GN03 Inoculation

The cotton seedlings root samples after GN03 inoculation 30 days from each group were extracted to assess the microbial communities. Corresponding to the rhizosphere results, the microbial diversity in plant roots showed the following changes: (1) species richness and diversity increased after inoculation (**Figure 4A** and **Supplementary Table 5B**); (2) each treatment formed a separate cluster in the PCoA (**Figure 4B**); and (3) the structure of the network diagram was very simple, with only *Dechloromonas* being negatively correlated to the 25 other genera and all others positively correlated to the top 50 genera (**Figure 4D**). This suggested that the root microbiota was more sensitive to GN03 inoculation than the rhizosphere microbiota. Furthermore, functional prediction also confirmed this result. PICRUSt2 software (Douglas et al., 2019) analysis showed that the clusters of orthologous groups (COG) of protein function did not change significantly in the rhizosphere. However, in post-inoculation plant roots, amino acid transport and metabolism were the most abundant functions, followed by energy production. Furthermore, fatty acid metabolism, the pentose phosphate pathway, and biosynthesis of neomycin, kanamycin, and gentamicin increased following GN03 inoculation, while plant apoptosis and plant disease were inhibited. Further testing was performed to identify the bacteria responsible for this functional change.

The top bacterial species at the phylum level of roots, were similar to those in the rhizosphere (**Figure 4C**). However, their relative abundances varied greatly. For example, the relative proportion of Proteobacteria reached 97.46% within roots, whereas it was 52.63% in the rhizosphere. It should be noted that, as the inoculation concentration increased, the relative proportion of Proteobacteria gradually decreased to 81.94%. In the C2 group, the proportions of Actinobacteria and Bacteroidetes were increased by 7.65 and 6.87%, respectively. At genus level, the proportion of many genera increased after GN03 inoculation, especially in the C1 samples (**Figure 4E** and **Supplementary Figure 4B**), including *Rhizobium*, a bacterium that forms a symbiotic relationship with plant roots and

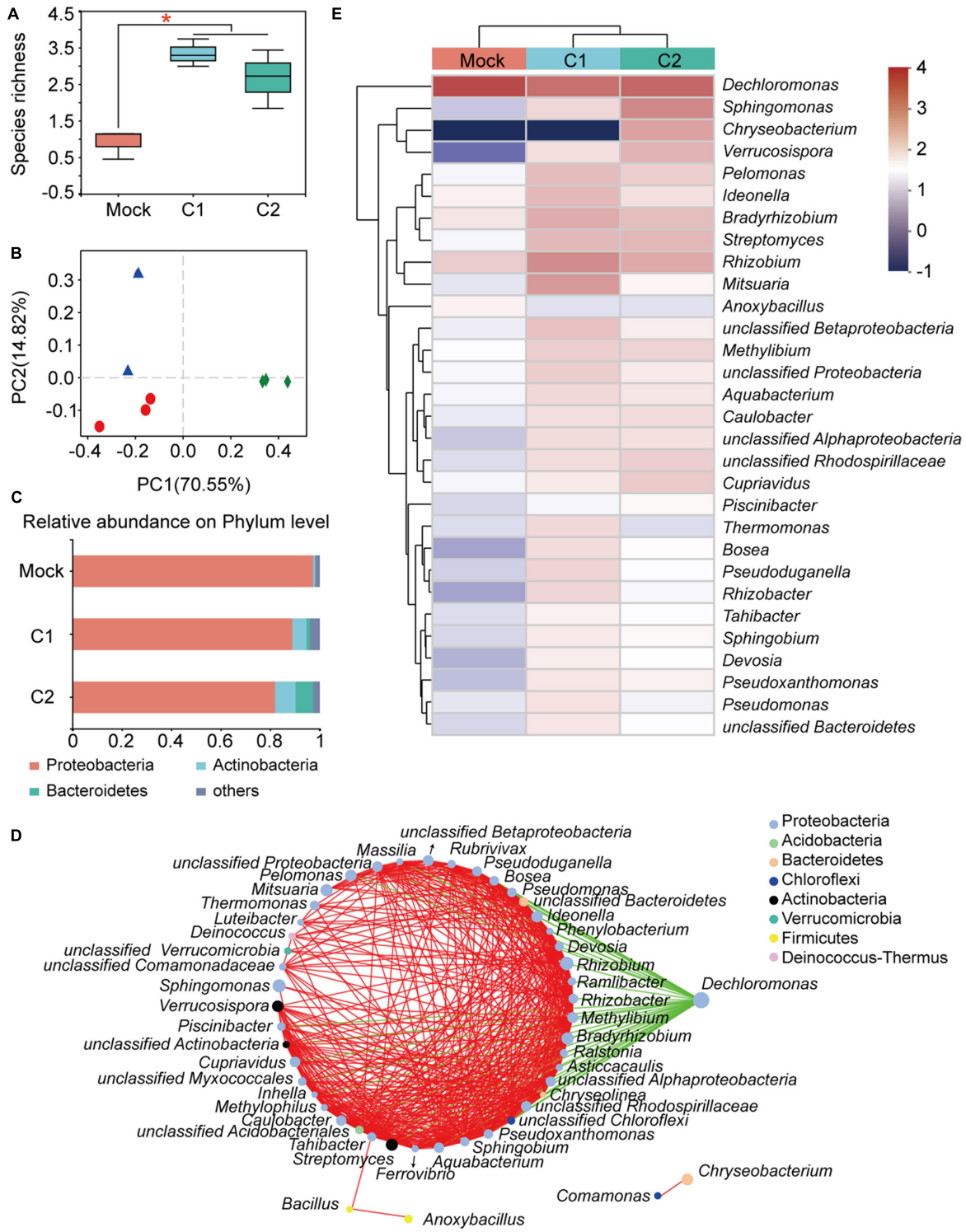

FIGURE 4 | Bacterial community of cotton roots 30 days after GN03 inoculation. **(A)** Boxplot of species richness (number of OTUs) by Shannon index. The asterisk (*) indicates a significant difference (one-way ANOVA, LSD *post hoc* test, $p < 0.05$, see **Supplementary Table 5B**). **(B)** PCoA plot based on the structure of the microbial community. Each symbol represents a sample. Mock, green diamonds; C1, red circle; and C2, blue triangles. **(C)** Relative abundance of bacterial phyla in each group. Each value is the mean of three measurements. **(D)** Network correlation between plant root bacteria. The nodes on the left side of the ring are positively correlated at all instances (red lines) and the green lines indicate negative correlations between the genera. **(E)** Heatmap showing the relative abundance of the top 30 dominant taxa at the genus level in cotton roots.

is able to fix nitrogen (Zilli et al., 2020), *Rubrivivax*, a photosynthetic bacterium (Mekala et al., 2019), *Actinomadura*, a bacterium with potential use in new antibiotics (Lazzarini et al., 2000), and *Labrys*, a bacterium capable of chlorobenzene and fluoride biodegradation (Amorim et al., 2014). These results indicated that GN03 regulated the changes in the rhizosphere and endophytic microbiota. After inoculation, the microbial community had a huge change and showed some regularities.

Comparative Genomic Analysis of GN03

The above findings have so far demonstrated that GN03 inoculation can promote cotton seedlings growth, change the microbiota in and around the plant roots, increase phytohormones in cotton seedlings, up-regulate the expression of phytohormone synthesis and disease-resistance related genes. Then, we conducted a genome-wide sequencing analysis followed by a comparative genome analysis. The complete genome sequence of GN03 was deposited in the GenBank database (chromosome and plasmid accession numbers CP053315 and CP053316, respectively). An illustration of the genomic structure of the GN03 chromosome is shown in **Figure 5A**, and that of the plasmid is shown in **Figure 5B**. The total genome length was 5,217,129 bp. The mean average GC content was 35.64%, which was similar to the average GC content across *B. circulans* genomes (length, 5.09 Mbp; mean GC content, 35.5%) recorded by the NCBI. Of interest, GN03 contained a plasmid that was 0.18 Mbp long with a mean GC content of 31.62%. Multiple databases (Nr, COG, KEGG, Swiss-Prot, GO, and CAZy) were integrated to annotate gene function through sequence alignment.

The GN03 genome included clusters of the following: *de novo* amino acid synthesis and metabolic pathways, *de novo* sugar synthesis and metabolism (such as starch, sucrose, and other polysaccharide metabolism), and *de novo* lipid synthesis (such as saturated fatty acids and unsaturated fatty acids synthesis) and metabolism. It also contained gene clusters for folic acid synthesis and for porphyrin, chlorophyll, butyric acid, biotin, inositol phosphate, sulfur, and methane metabolism. GN03 could effectively degrade naphthalene, xylene, ethylbenzene, nitrotoluene, chlorobenzene, and chlorocyclohexane. The genome also contained a comprehensive DNA repair system that could act as a DNA protectant. The functions of plasmid genes were mainly focused on DNA replication, mismatch repair, and phosphonate metabolism. In addition, we predicted the presence of genes that confer resistance by producing antibiotics (streptomycin, surfactin, penicillin, novobiocin, and cephalosporin) and other genes, such as *gabD, opuC* and *opuA* and *proX, proV,* and *proW*, against stress. These results indicated that GN03 was capable of pathogen resistance and pollutant degradation.

We selected four *B. circulans* reference strains with or without growth-promoting function (**Supplementary Table 3**) and performed a comparative genomic analysis. To identify homologous genes and specific gene families among the five bacterial species, homologous genes were identified using multiple databases (with an *E*-value < 1e-7) and the numbers of genes and gene families were analyzed using a Venn diagram (**Figure 6A**). Functional annotation data were obtained from multiple databases. The following top three KEGG pathways were shared among all strains: secondary metabolite biosynthesis, ribosome biosynthesis, and aminoacyl-tRNA biosynthesis. The collinear and the molecular evolutionary tree analysis of GN03 with four reference strains (**Figures 6B,C**) showed that the GN03 strain is most closely matched to the PK3-109 strain, which has also been reported to promote plant growth (Bokhari et al., 2019).

DISCUSSION

GN03 Inoculation Promoted Cotton Seedling Growth and Accumulation of Growth- Related Phytohormones

Plant roots can anchor and absorb nutrients and water in the soil. Lateral roots and root hairs are closely related to nutrient and water use efficiency. Many PGPB strains are known to promote the increase of lateral roots and the formation of root hairs (Zamioudis et al., 2013; Luo et al., 2019). GN03 is a soil-borne bacterium with positive effects on plant growth (Shen et al., 2018). In this study, The GN03 promoted the growth of cotton seedlings, which may be achieved by increasing the length and number of lateral roots (**Figures 1B,C**) resulting in cotton seedlings with a larger root surface in contact with the soil, thus boosting plants to absorb more nutrients and water. Accordingly, the GN03-treated cotton seedlings showed obvious increases stem length and width, leaf number and area during growth, especially in the C2 group (**Figures 1B,C**).

The improving effect of PGPB on plant growth is mainly reflected in the production of hormones or the induction of hormone signals (Egamberdieva et al., 2017). Phytohormones, such as IAA, GA, and BRs, can regulate various cellular processes and plant responses to biotic and abiotic stresses with a very low concentration (Ciura and Kruk, 2018). Auxins play an essential role in plant developmental process ranging from the cell division, and cell elongation to morphogenesis (Felten et al., 2009). Brassinosteroids are capable of executing diverse functions in plant growth, development, and stress tolerance (Banerjee and Roychoudhury, 2018). Gibberellins play an indispensable role in stem elongation, leaf expansion, and plant development, while GA deficit results in plant dwarfism (Ciura and Kruk, 2018). In our study, GN03 inoculation led to accumulation of growth-related hormones (IAA, GA, and BRs), as determined with ELISA, in the cotton leaves. Compared to those in the Mock group, the level of IAA, GA, and BR were increased by 19.4, 31.1, and 16.6% in the C1 group, and that were significantly increased by 58.9, 32.4, and 68.7% in the C2 group, respectively (**Figure 2D**). Accordingly, compared to those in the Mock group, the expression of IAA, BRs, and GA synthesis-related genes (*AUX1*, *BES1*, and *GA20ox*) was significantly increased in cotton seedling roots (**Figure 2B**). Phytohormones can be transported to different parts of the plant by different sophisticated transporter molecules through the vascular system in plant (Lacombe and Achard, 2016). These hormones may include endogenous hormones produced by the plant and the exogenous hormones

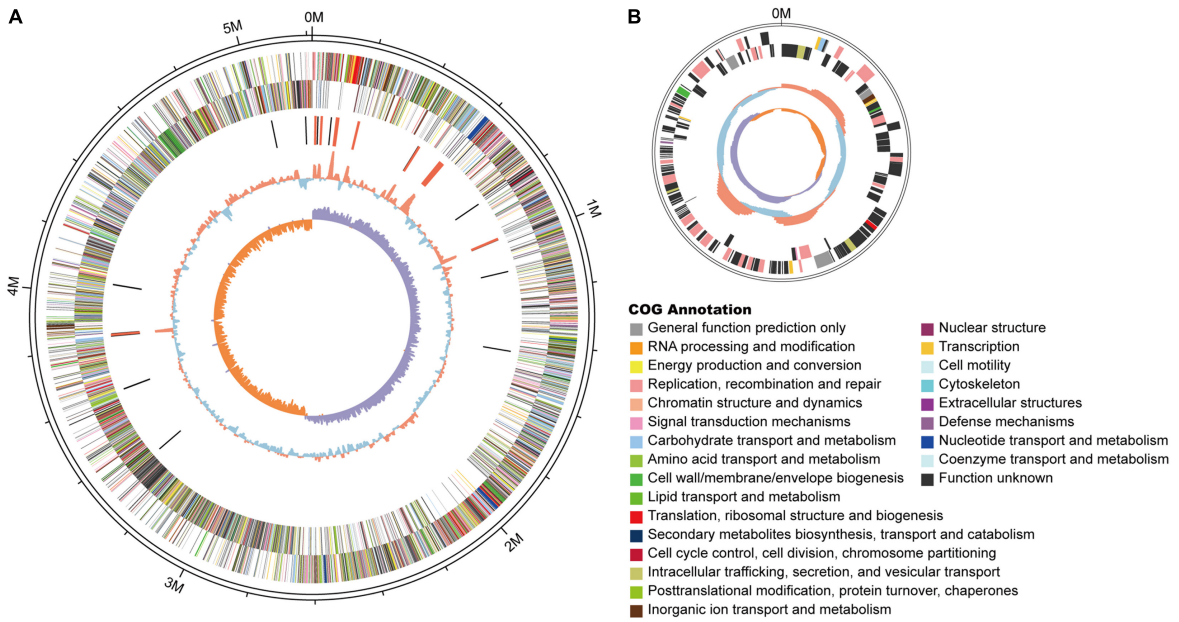

FIGURE 5 | Schematic of the complete GN03 genome. GN03 chromosome **(A)** and plasmid **(B)**. Rings represent the following features labeled from the outside to the center, where the outermost circle represents the scale in bp: the first ring represents positive strand genes and the second ring represents negative strand genes. Each color patch represents a COG functional classification. The third ring represents ncRNA (black indicates tRNA, red indicates rRNA). The fourth ring represents the GC content (red indicates GC content above the mean, blue indicates GC content below the mean). The innermost ring shows the GC skew (GC skew = [GC]/[G + C]; purple means greater than 0, orange means less than 0). Circos v0.62 (http://circos.ca/) software was used to draw the genomic circle map.

produced by rhizosphere and endophytic microbes (Backer et al., 2018). Hence, this may also be the reason for the total amount of hormones accumulated in the leaves.

GN03 Inoculation Promoted Cotton Seedling Disease Resistance and the Expressing of Disease Resistance-Related Genes

The plant hormones JA and SA play key roles in the response of the plant to *V. dahliae* infection (Glazebrook, 2005; Zhang et al., 2017b). Consistently, we observed significant differences in JA and SA levels (**Figure 2D**) and changes in the expression of both JA and SA synthetic genes (*EDS1* and *AOC1*, respectively) and disease resistance-related genes (*NPR1* and *PR1*) after inoculation with the GN03 strain. Meanwhile, disease assessment after GN03 pre-treatment revealed significantly increased cotton disease resistance to *V. dahliae* (**Figures 1D,E**). We, therefore, presume that this resistance is mediated by GN03-regulating hormones signaling pathways. However, further molecular and genetic evidence is needed to elucidate the resistance mechanisms. Controlling Verticillium wilt is challenging, since the pathogen *V. dahliae* can survive for many years in the soil in dormant survival structure (microsclerotia) forms, which germinate to produce hyphae approximal to the root exudates of a suitable host (Inderbitzin et al., 2011; Inderbitzin and Subbarao, 2014; Luo et al., 2014; Daayf, 2015; Shaban et al., 2018). Some bacteria, collectively known as PGPB, can be effective when applied as fertilizers. This is of great significance for the development of more environment friendly agricultural practices. Moreover, biological control agents are eco-friendly strategies with great promise for controlling Verticillium wilt in cotton (Markakis et al., 2016; Zhang et al., 2021). *B. circulans* GN03 can promote upland cotton seedling growth and significantly reduce the incidence of Verticillium wilt. To our knowledge, this study is the first to investigate the growth promotion of *B. circulans* in cotton and application of *B. circulans* cells to reduce disease incidence.

Several beneficial bacteria and non-pathogenic rhizobacteria can also cause activation of the SA/JA pathway and lead to hormonal changes (Olanrewaju et al., 2017). After inoculation, the abundance of bacteria showed additional beneficial function in the roots, especially in the C1 group, though the C2 group showed a stronger growth promotion effect than C1. The expression levels of hormone-related genes (endogenous hormones) in plant roots support the theory that plants can reduce their growth to invest in disease resistance. This implies that the activation of plant growth and defense against potential pathogens are opposing processes in that the onset of one often leads to the inhibition of the other (Zhu et al., 2013; Huot et al., 2014).

To infect cotton roots favorably, *V. dahliae* can selectively steer the local microbiome by its effector proteins, and increasing reports have shown that the microbiome inside and outside a plant plays an crucial role in its health (Snelders et al., 2020). *Bacillus* species can produce some antibiotics, which can directly strangle the growth of the pathogen or induce systemic resistance in plants (Hasan et al., 2020). In our study, it was found that GN03 possess antibiotics (streptomycin, surfactin,

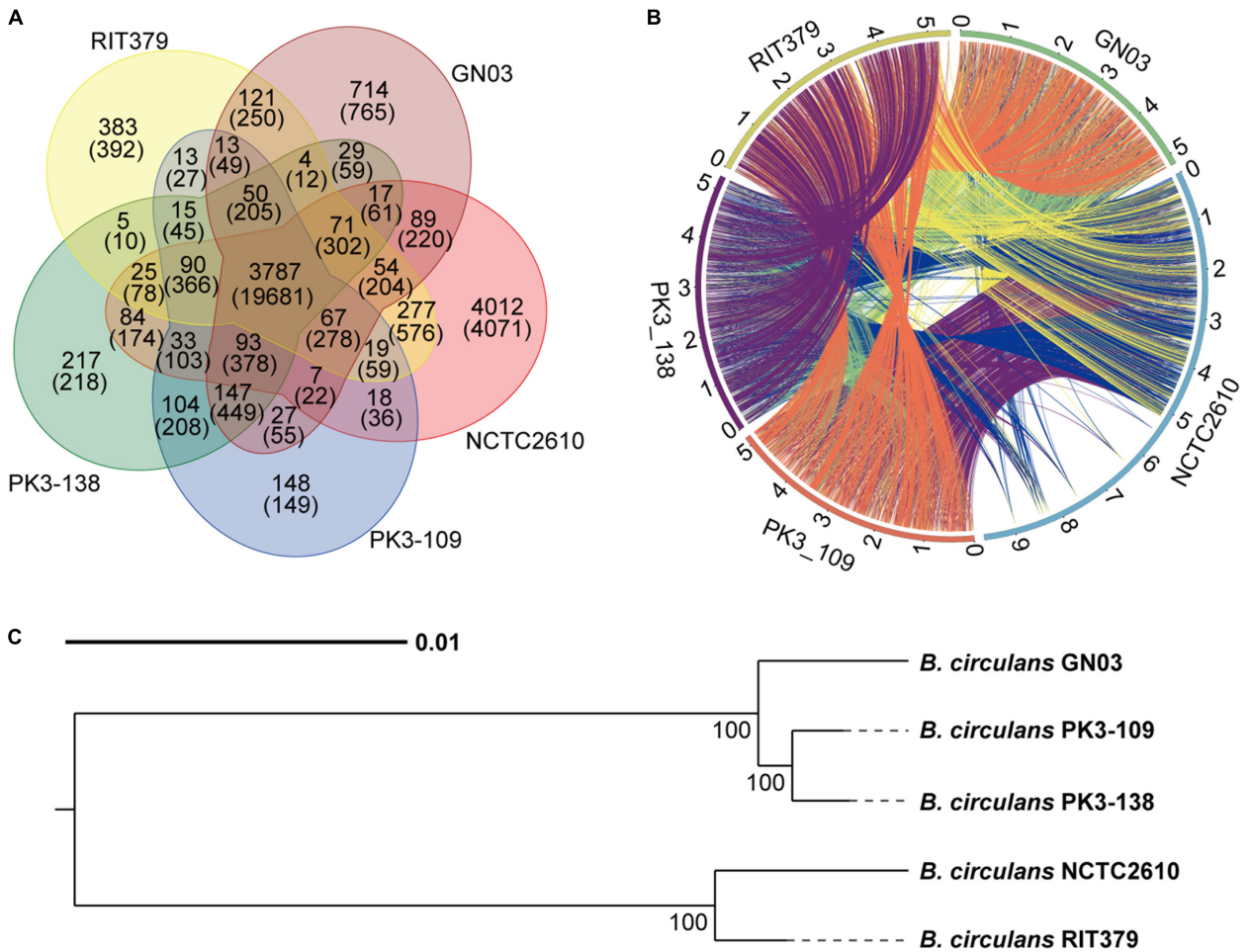

FIGURE 6 | Comparative genomic analysis of GN03 with other four *Bacillus* stains. **(A)** Venn diagram showing the number of genes in all five strains. In BLAST alignment, gene pairs with *E*-values less than 1e-7 are considered to be homologous. OrthoMCL was used to group the homologous genes into the same families. The upper number represents the number of gene families and the lower number represents the number of genes. **(B)** The collinear circos diagram of the five bacterial strains. The outermost circle represents the genomic sequences of the five bacteria. For example, green in the upper right corner represents the genomic sequence of GN03 bacteria. Every two strains are connected by a line representing a collinear area between the two bacteria. **(C)** Phylogenetic tree of the five strains. The tree was built using a single copy homologous gene using the neighbor joining method with a bootstrap value of 1,000. Unit: nucleotide substitution rate.

penicillin, novobiocin, and cephalosporin) encoding genes and other genes, such as *gabD, opuC* and *opuA* and *proX, proV,* and *proW*, against stress. In addition, GN03 inoculation altered the microbiota in and around the plant roots and the expressing of disease resistance-related genes. Finally, the co-production of these antibiotics producing genes and the changes in cotton seedlings after GN03 inoculation may be form a amassing role against *V. dahliae*.

GN03 Inoculation Changed the Rhizosphere and Endophytic Bacterial Composition

Within the complex soil environment, many biotic and abiotic factors affect the colonization of PGPB. As colonization can be enhanced by multiple inoculations (Benizri et al., 2001; Coy et al., 2014), we tested different inoculation concentrations (C1 and C2), with greater inoculation concentration showing better beneficial effects. Furthermore, it was previously shown that rhizosphere microorganisms can recover after being temporarily affected by PGPB inoculation (Qiao et al., 2017). Our study confirmed that there were no significant differences in rhizosphere, while various plant indicators showed significant differences. We speculate that GN03 exerted a high ecological effect, which significantly influenced other bacterial changes within 30 days, such as increase in the levels of *Lysobacter, Rubrivivax,* and *Rhizobium* that are beneficial in promoting plant growth and enhancing disease resistance. Interestingly, obvious change of *Bacillus* or Firmicutes in the cotton seedling roots was found, while that was not found around the cotton seedling roots (**Supplementary Figure 5**). This may be due to (1) the time interval of detection is too long (30 days after inoculation); (2) microbial competition in a wide diversity of niches (Snelders et al., 2020). The dynamic changes of bacterial

composition (especially beneficial bacteria including *Bacillus*) discovered in the 30-day period after inoculation need to be further investigated in future research.

Activation of defense against potential pathogens may inhibit growth activation, whereas the abundance of beneficial bacteria results in either the generation or stimulated-release of growth hormones (Backer et al., 2018). In general, plants in the C1 group did not show excessive growth promotion or inhibition which indicates that GN03 concentration is crucial to achieve optimal growth promotion effects.

Genome Analysis of GN03 Promoting Plant Growth and Disease Resistance

Our study demonstrated that GN03 promoted plant growth by regulating the rhizosphere and endophytic microbiota, together with the expression of plant hormones. To further understand the underlying mechanism, we conducted a genome-wide sequencing analysis, followed by a comparative genome analysis, to elucidate this growth promoting effect. Various genes of interest were found to be involved in the potential growth promoting and disease-resistance effects observed with GN03 inoculation. Inorganic phosphate uptake in some beneficial bacteria may be promoted by high-affinity phosphate transport systems regulated altogether by *PstB, PstC, PstA,* and *PstS; PhnC, PhnE,* and *PhnD* (Liu et al., 2016), and the genes *cysC, cysI, cysJ, cysH,* and *cysN,* responsible for H_2S biosynthesis (Dooley et al., 2013). Of note, some of the *trp* cluster genes (*trpA, trpB, trpD,* and *trpC*) involved in tryptophan biosynthesis might be involved in multiple biological processes, including plant hormone biosynthesis (Gupta et al., 2014). The *speB* and *speE* genes encode agmatinase and spermidine synthase to catalyze the transformation of amino acids into plant growth-promoting compounds (Cassan et al., 2009). Furthermore, *gabD* is responsible for the production of pest/disease inhibiting γ-aminobutyric acid (Gupta et al., 2014). Autoinducer-2 (*luxS*) is a small molecule, produced by a number of bacterial species, that is implicated in the regulation of biofilm formation, motility, and the production of virulence factors. It has been reported to act directly through quorum sensing or indirectly through modulation of cellular metabolism (Reading and Sperandio, 2006). Lastly, the heat-shock protein genes *dnaK* and *groEL* could aid the survival of GN03 in harsh environments (Guazzaroni et al., 2013), whereas *opuC* and *opuA* and *proX, proV,* and *proW* might be involved in protecting plants against oxidative stress (Gupta et al., 2014).

In conclusion, the GN03 strain of *B. circulans* has been shown to improve plant growth and disease resistance, but the exact underlying mechanism is unclear. In fact, to our knowledge, very little work has been done on the synergistic relationship of plant root microbiota and *B. circulans*. This study showed that the application of *B. circulans* GN03 in cotton seedlings can regulate the microbiota in and around the plant roots, promote cotton seedling growth and disease resistance, induce the production of phytohormones such as IAA, GA, and SA, and up-regulate the expression of phytohormone synthesis-related genes (*EDS1*, *AOC1*, *AUX1*, *BES1*, and *GA20ox*) and disease-resistance genes (*NPR1* and *PR1*).

DATA AVAILABILITY STATEMENT

16S rDNA amplicon raw sequencing data were deposited in the NCBI Short Read Archive (SRA) BioProject PRJNA631145 under the accession numbers SRR11735611–SRR11735637. The *B. circulans* GN03 genome was deposited under accession numbers CP053315 and CP053316 (the latter is for the plasmid).

AUTHOR CONTRIBUTIONS

LQ designed and performed the experiments. XY conducted the experiments. QC and WJ performed cotton growth measurements. SH, PT, and CX performed RNA extraction, RT-qPCR, and assisted in bioinformatics data analysis. LQ, PT, and QC analyzed the data, wrote the original draft of the manuscript, and performed the lab work. LQ, PT, and XY reviewed and edited the manuscript. XY obtained the funding. All authors read and approved the final manuscript.

FUNDING

This work was supported by the Basic Research and Frontier Exploration Foundation of Chongqing (cstc2017jcyjBX00078).

SUPPLEMENTARY MATERIAL

The Supplementary Material for this article can be found online at: https://www.frontiersin.org/articles/10.3389/fpls.2021.644597/full#supplementary-material

REFERENCES

Afzal, I., Shinwari, Z. K., Sikandar, S., and Shahzad, S. (2019). Plant beneficial endophytic bacteria: mechanisms, diversity, host range and genetic determinants. *Microbiol. Res.* 221, 36–49. doi: 10.1016/j.micres.2019.02.001

Ahemad, M., and Kibret, M. (2014). Mechanisms and applications of plant growth promoting rhizobacteria: current perspective. *J. King Saud Univ. Sci.* 26, 1–20. doi: 10.1016/j.jksus.2013.05.001

Alka, S., Shahir, S., Ibrahim, N., Chai, T. T., Bahari, Z. M., and Abd Manan, F. (2020). The role of plant growth promoting bacteria on arsenic removal: a review of existing perspectives. *Environ. Technol. Inno.* 17:100602. doi: 10.1016/j.eti.2020.100602

Aloo, B. N., Makumba, B. A., and Mbega, E. R. (2019). The potential of Bacilli rhizobacteria for sustainable crop production and environmental sustainability. *Microbiol. Res.* 219, 26–39. doi: 10.1016/j.micres.2018.10.011

Amorim, C. L., Moreira, I. S., Maia, A. S., Tiritan, M. E., and Castro, P. M. L. (2014). Biodegradation of ofloxacin, norfloxacin, and ciprofloxacin as single and mixed substrates by Labrys portucalensis F11. *Appl. Microbiol. Biotechnol.* 98, 3181–3190. doi: 10.1007/s00253-013-5333-8

Araujo, R., Dunlap, C., Barnett, S., Barnett, S., and Franco, C. M. M. (2019). Decoding wheat endosphere–rhizosphere microbiomes in Rhizoctonia solani infested soils challenged by Streptomyces biocontrol agents. *Front. Plant Sci.* 10:1038. doi: 10.3389/fpls.2019.01038

Baani, M., and Liesack, W. (2008). Two isozymes of particulate methane monooxygenase with different methane oxidation kinetics are found in Methylocystis sp strain SCZ. *Proc. Nat. Acad. Sci. U.S.A.* 105, 10203–10208. doi: 10.1073/pnas.0702643105

Backer, R., Rokem, J. S., Ilangumaran, G., Lamont, J., Praslickova, D., Ricci, E., et al. (2018). Plant growth-promoting rhizobacteria: context, mechanisms of action, and roadmap to commercialization of biostimulants for sustainable agriculture. *Front. Plant Sci.* 9:1473. doi: 10.3389/fpls.2018.01473

Banerjee, A., and Roychoudhury, A. (2018). Interactions of brassinosteroids with major phytohormones: antagonistic effects. *J. Plant Growth Regul.* 37, 1025–1032. doi: 10.1007/s00344-018-9828-5

Benizri, E., Baudoin, E., and Guckert, A. (2001). Root colonization by inoculated plant growth-promoting rhizobacteria. *Biocontrol. Sci. Technol.* 11, 557–574. doi: 10.1080/09583150120076120

Bokhari, A., Essack, M., Lafi, F. F., Andres-Barrao, C., Jalal, R., Alamoudi, S., et al. (2019). Bioprospecting desert plant Bacillus endophytic strains for their potential to enhance plant stress tolerance. *Sci. Rep.* 9:18154. doi: 10.1038/s41598-019-54685-y

Buchanan, R., Gibbons, N., and Cowan, S. (1994). *Bergey's Manual of Determinative Bacteriology*, 9th Edn. Philadelphia: Williams & Wilkins.

Cassan, F., Maiale, S., Masciarelli, O., Vidal, A., Luna, V., and Ruiz, O. (2009). Cadaverine production by *Azospirillum brasilense* and its possible role in plant growth promotion and osmotic stress mitigation. *Eur. J. Soil Biol.* 45, 12–19. doi: 10.1016/j.ejsobi.2008.08.003

Chao, A. (1984). Nonparametric-estimation of the number of classes in a population. *Scand. J. Stat.* 11, 265–270.

Cheng, F. F., Li, G., Peng, Y. J., Wang, A. Y., and Zhu, J. B. (2020). Mixed bacterial fermentation can control the growth and development of Verticillium dahliae. *Biotechnol. Biotech. Eq.* 34, 58–69. doi: 10.1080/13102818.2020.1713023

Chubatsu, L. S., Monteiro, R. A., de Souza, E. M., Schuler de Oliveira, M. A., Yates, M. G., Wassem, R., et al. (2012). Nitrogen fixation control in Herbaspirillum seropedicae. *Plant Soil* 356, 197–207. doi: 10.1007/s11104-011-0819-6

Ciura, J., and Kruk, J. (2018). Phytohormones as targets for improving plant productivity and stress tolerance. *J. Plant Physiol.* 229, 32–40. doi: 10.1016/j.jplph.2018.06.013

Coy, R. M., Held, D. W., and Kloepper, J. W. (2014). Rhizobacterial inoculants increase root and shoot growth in 'Tifway' hybrid bermudagrass. *J. Environ. Horticult.* 32, 149–154. doi: 10.24266/0738-2898.32.3.149

Daayf, F. (2015). Verticillium wilts in crop plants: pathogen invasion and host defence responses. *Can. J. Plant Pathol.* 37, 8–20. doi: 10.1080/07060661.2014.989908

Dahmani, M. A., Desrut, A., Moumen, B., Verdon, J., Mermouri, L., Kacem, M., et al. (2020). Unearthing the plant growth-promoting traits of Bacillus megaterium RmBm31, an endophytic bacterium isolated from root nodules of Retama monosperma. *Front. Plant Sci.* 11:124. doi: 10.3389/fpls.2020.00124

Delcher, A. L., Bratke, K. A., Powers, E. C., and Salzberg, S. L. (2007). Identifying bacterial genes and endosymbiont DNA with Glimmer. *Bioinformatics* 23, 673–679. doi: 10.1093/bioinformatics/btm009

Dooley, F. D., Nair, S. P., and Ward, P. D. (2013). Increased growth and germination success in plants following hydrogen sulfide administration. *PLoS One* 8:e0062048. doi: 10.1371/journal.pone.0062048

Douglas, G. M., Maffei, V. J., Zaneveld, J., Yurgel, S. N., Brown, J. R., Taylor, C. M., et al. (2019). PICRUSt2: an improved and extensible approach for metagenome inference. *BioRxiv [Preprint]* doi: 10.1101/672295

Egamberdieva, D., Wirth, S. J., Alqarawi, A. A., Abd Allah, E. F., and Hashem, A. (2017). Phytohormones and beneficial microbes: essential components for plants to balance stress and fitness. *Front. Microbiol.* 8:2104. doi: 10.3389/fmicb.2017.02104

Emmanuel, O. C., and Babalola, O. O. (2020). Productivity and quality of horticultural crops through co-inoculation of *arbuscular mycorrhizal* fungi and plant growth promoting bacteria. *Microbiol. Res.* 239:126569. doi: 10.1016/j.micres.2020.126569

Erdogan, O., and Benlioglu, K. (2010). Biological control of Verticillium wilt on cotton by the use of fluorescent *Pseudomonas* spp. under field conditions. *Biol. Control* 53, 39–45. doi: 10.1016/j.biocontrol.2009.11.011

Exposito, R. G., Postma, J., Raaijmakers, J. M., and De Bruijn, I. (2015). Diversity and activity of Lysobacter species from disease suppressive soils. *Front. Microbiol.* 6:1255. doi: 10.3389/fmicb.2015.01243

Faust, K., and Raes, J. (2012). Microbial interactions: from networks to models. *Nat. Rev. Microbiol.* 10, 538–550. doi: 10.1038/nrmicro2832

Felten, J., Kohler, A., Morin, E., Bhalerao, R. P., Palme, K., Martin, F., et al. (2009). The ectomycorrhizal fungus Laccaria bicolor stimulates lateral root formation in poplar and Arabidopsis through auxin transport and signaling. *Plant Physiol.* 151, 1991–2005. doi: 10.1104/pp.109.147231

Gadhave, K. R., Devlin, P. F., Ebertz, A., Ross, A., and Gange, A. C. (2018). Soil inoculation with Bacillus spp. Modifies root endophytic bacterial diversity, evenness, and community composition in a context-specific manner. *Microb. Ecol.* 76, 741–750. doi: 10.1007/s00248-018-1160-x

Glazebrook, J. (2005). Contrasting mechanisms of defense against biotrophic and necrotrophic pathogens. *Annu. Rev. Phytopathol.* 43, 205–227. doi: 10.1146/annurev.phyto.43.040204.135923

Goicoechea, N. (2009). To what extent are soil amendments useful to control Verticillium wilt? *Pest Manage. Sci.* 65, 831–839. doi: 10.1002/ps.1774

Golding, C. G., Lamboo, L. L., Beniac, D. R., and Booth, T. F. (2016). The scanning electron microscope in microbiology and diagnosis of infectious disease. *Sci. Rep.* 6:26516. doi: 10.1038/srep26516

Guazzaroni, M.-E., Morgante, V., Mirete, S., and Gonzalez-Pastor, J. E. (2013). Novel acid resistance genes from the metagenome of the Tinto River, an extremely acidic environment. *Environ. Microbiol.* 15, 1088–1102. doi: 10.1111/1462-2920.12021

Gulay, A., Cekic, Y., Musovic, S., Albrechtsen, H.-J., and Smets, B. F. (2018). Diversity of iron oxidizers in groundwater-fed rapid sand filters: evidence of Fe(II)-dependent growth by *Curvibacter* and *Undibacterium* spp. *Front. Microbiol.* 9:2808. doi: 10.3389/fmicb.2018.02808

Gupta, A., Gopal, M., Thomas, G. V., Manikandan, V., Gajewski, J., Thomas, G., et al. (2014). Whole genome sequencing and analysis of plant growth promoting bacteria isolated from the rhizosphere of plantation crops coconut, cocoa and arecanut. *PLoS One* 9:e0104259. doi: 10.1371/journal.pone.0104259

Hasan, N., Farzand, A., Heng, Z., Khan, I. U., Moosa, A., Zubair, M., et al. (2020). Antagonistic potential of novel endophytic Bacillus strains and mediation of plant defense against Verticillium wilt in upland cotton. *Plants (Basel, Switzerland)* 9:1438. doi: 10.3390/plants9111438

Hashem, A., Tabassum, B., and Abd Allah, E. F. (2019). Bacillus subtilis: a plant-growth promoting rhizobacterium that also impacts biotic stress. *Saudi J. Biol. Sci.* 26, 1291–1297. doi: 10.1016/j.sjbs.2019.05.004

Hassan, M. K., McInroy, J. A., and Kloepper, J. W. (2019). The interactions of rhizodeposits with plant growth-promoting rhizobacteria in the rhizosphere: a review. *Agriculture* 9:142. doi: 10.3390/agriculture9070142

Huot, B., Yao, J., Montgomery, B. L., and He, S. Y. (2014). Growth-defense tradeoffs in plants: a balancing act to optimize fitness. *Mol. Plant* 7, 1267–1287. doi: 10.1093/mp/ssu049

Inderbitzin, P., Bostock, R. M., Davis, R. M., Usami, T., Platt, H. W., and Subbarao, K. V. (2011). Phylogenetics and taxonomy of the fungal vascular wilt pathogen Verticillium, with the descriptions of five new species. *PLoS One* 6:e28341. doi: 10.1371/journal.pone.0028341

Inderbitzin, P., and Subbarao, K. V. (2014). Verticillium systematics and evolution: how confusion impedes Verticillium wilt management and how to resolve it. *Phytopathology* 104, 564–574. doi: 10.1094/phyto-11-13-0315-ia

Kemp, P. F., and Aller, J. Y. (2004). Bacterial diversity in aquatic and other environments: what 16S rDNA libraries can tell us. *FEMS Microbiol. Ecol.* 47, 161–177. doi: 10.1016/s0168-6496(03)00257-5

Khatri, S., Sharma, R. K., and Shridhar, V. (2020). Influence of cadmium-tolerant and plant growth-promoting rhizobacteria on cadmium accumulation and growth response of wheat seedlings under mountain ecosystem. *Agric. Res.* 9, 56–65. doi: 10.1007/s40003-019-00407-9

Lacombe, B., and Achard, P. (2016). Long-distance transport of phytohormones through the plant vascular system. *Curr. Opin. Plant Biol.* 34, 1–8. doi: 10.1016/j.pbi.2016.06.007

Lazzarini, A., Cavaletti, L., Toppo, G., and Marinelli, F. (2000). Rare genera of actinomycetes as potential producers of new antibiotics. *Int. J. Gen. Mol. Microbiol.* 78, 399–405. doi: 10.1023/a:1010287600557

Lee, S., Trinh, C. S., Lee, W. J., Jeong, C. Y., Truong, H. A., Chung, N., et al. (2020). Bacillus subtilis strain L1 promotes nitrate reductase activity in *Arabidopsis* and

elicits enhanced growth performance in *Arabidopsis*, lettuce, and wheat. *J. Plant Res.* 133, 231–244. doi: 10.1007/s10265-019-01160-4

Liu, W., Wang, Q., Hou, J., Tu, C., Luo, Y., and Christie, P. (2016). Whole genome analysis of halotolerant and alkalotolerant plant growth-promoting rhizobacterium Klebsiella sp D5A. *Sci. Rep.* 6:26710. doi: 10.1038/srep26710

Lugtenberg, B., and Kamilova, F. (2009). Plant-growth-promoting rhizobacteria. *Annu. Rev. Microbiol.* 63, 541–556. doi: 10.1146/annurev.micro.62.081307.162918

Luo, X., Tian, T., Tan, X., Zheng, Y., Xie, C., Xu, Y., et al. (2020). VdNPS, a nonribosomal peptide synthetase, is involved in regulating virulence in Verticillium dahliae. *Phytopathology* 110, 1398–1409. doi: 10.1094/phyto-02-20-0031-r

Luo, X., Xie, C., Dong, J., Yang, X., and Sui, A. (2014). Interactions between Verticillium dahliae and its host: vegetative growth, pathogenicity, plant immunity. *Appl. Microbiol. Biotechnol.* 98, 6921–6932. doi: 10.1007/s00253-014-5863-8

Luo, Y., Wang, F., Huang, Y., Zhou, M., Gao, J., Yan, T., et al. (2019). Sphingomonas sp. Cra20 increases plant growth rate and alters rhizosphere microbial community structure of *Arabidopsis* thaliana under drought stress. *Front. Microbiol.* 10:1221. doi: 10.3389/fmicb.2019.01221

Mahmood, A., and Kataoka, R. (2020). Metabolite profiling reveals a complex response of plants to application of plant growth-promoting endophytic bacteria. *Microbiol. Res.* 234:126421. doi: 10.1016/j.micres.2020.126421

Markakis, E. A., Tjamos, S. E., Antoniou, P. P., Paplomatas, E. J., and Tjamos, E. C. (2016). Biological control of Verticillium wilt of olive by Paenibacillus alvei, strain K165. *BioControl* 61, 293–303. doi: 10.1007/s10526-015-9669-0

Mehnaz, S., Baig, D. N., and Lazarovits, G. (2010). Genetic and phenotypic diversity of plant growth promoting rhizobacteria isolated from sugarcane plants growing in Pakistan. *J. Microbiol. Biotechnol.* 20, 1614–1623. doi: 10.4014/jmb.1005.05014

Mehta, P., Chauhan, A., Mahajan, R., Mahajan, P. K., and Shirkot, C. K. (2010). Strain of Bacillus *circulans* isolated from apple rhizosphere showing plant growth promoting potential. *Curr. Sci.* 98, 538–542.

Mehta, P., Walia, A., Kulshrestha, S., Chauhan, A., and Shirkot, C. K. (2015). Efficiency of plant growth-promoting P-solubilizing Bacillus *circulans* CB7 for enhancement of tomato growth under net house conditions. *J. Basic Microbiol.* 55, 33–44. doi: 10.1002/jobm.201300562

Mekala, L. P., Mohammed, M., Chinthalapati, S., and Chinthalapati, V. R. (2019).). Pyomelanin production: insights into the incomplete aerobic L-phenylalanine catabolism of a photosynthetic bacterium, *Rubrivivax benzoatilyticus* JA2. *Int. J. Biol. Macromol.* 126, 755–764. doi: 10.1016/j.ijbiomac.2018.12.142

Nakamura, L. K., and Swezey, J. (1983). Taxonomy of Bacillus-circulans Jordan 1890 - base composition and reassociation of deoxyribonucleic-acid. *Int. J. Syst. Bacteriol.* 33, 46–52. doi: 10.1099/00207713-33-1-46

Olanrewaju, O. S., Glick, B. R., and Babalola, O. O. (2017). Mechanisms of action of plant growth promoting bacteria. *World J. Microbiol. Biotechnol.* 33:197. doi: 10.1007/s11274-017-2364-9

Parnell, J. J., Berka, R., Young, H. A., Sturino, J. M., Kang, Y. W., Barnhart, D. M., et al. (2016). From the Lab to the farm: an industrial perspective of plant beneficial microorganisms. *Front. Plant Sci.* 7:1110. doi: 10.3389/fpls.2016.01110

Polter, S. J., Caraballo, A. A., Lee, Y. P., Eng, W. W. H., Gan, H. M., Wheatley, M. S., et al. (2015). Isolation, identification, whole-genome sequencing, and annotation of four *Bacillus* species, B.*anthracis* RIT375, B.*circulans* RIT379, B. *altitudinis* RIT380, and B. *megaterium* RIT381, from internal stem tissue of the insulin plant Costus igneus. *Genome Announ* 3, e00847–15. doi: 10.1128/genomeA.00847-15

Qiao, J., Yu, X., Liang, X., Liu, Y., Borriss, R., and Liu, Y. (2017). Addition of plant-growth-promoting Bacillus subtilis PTS-394 on tomato rhizosphere has no durable impact on composition of root microbiome. *BMC Microbiol.* 17:131. doi: 10.1186/s12866-017-1039-x

Radhakrishnan, R., Hashem, A., and Abd Allah, E. F. (2017). Bacillus: a biological tool for crop improvement through bio-molecular changes in adverse environments. *Front. Physiol.* 8:667. doi: 10.3389/fphys.2017.00667

Ramakrishna, W., Yadav, R., and Li, K. (2019). Plant growth promoting bacteria in agriculture: two sides of a coin. *Appl. Soil Ecol.* 138, 10–18. doi: 10.1016/j.apsoil.2019.02.019

Ramette, A. (2007). Multivariate analyses in microbial ecology. *FEMS Microbiol. Ecol.* 62, 142–160. doi: 10.1111/j.1574-6941.2007.00375.x

Reading, N. C., and Sperandio, V. (2006). Quorum sensing: the many languages of bacteria. *FEMS Microbiol. Lett.* 254, 1–11. doi: 10.1111/j.1574-6968.2005.00001.x

Shaban, M., Miao, Y., Ullah, A., Khan, A. Q., Menghwar, H., Khan, A. H., et al. (2018). Physiological and molecular mechanism of defense in cotton against Verticillium dahliae. *Plant Physiol. Biochem.* 125, 193–204. doi: 10.1016/j.plaphy.2018.02.011

Shannon, C. E. (1948). A mathematical theory of communication. *Bell Sys. Tech. J.* 27, 623–656. doi: 10.1002/j.1538-7305.1948.tb00917.x

Shen, H., Wu, B., Li, H. H., Liu, Y. Q., Wu, X. W., and Yang, X. Y. (2018). Screening of plant growth-promoting bacteria from purple soil and growth promoting effects of its complex microbial inoculant on ginger germchit (in Chinese). *China Veget* 6, 54–59.

Sherzad, Z., and Canming, T. (2020). A new strain of *Bacillus velezens* is as a bioagent against *Verticillium dahliae* in cotton: isolation and molecular identification. *Egypt. J. Biol. Pest Control* 30:118. doi: 10.1186/s41938-020-00308-y

Snelders, N. C., Rovenich, H., Petti, G. C., Rocafort, M., van den Berg, G. C. M., Vorholt, J. A., et al. (2020). Microbiome manipulation by a soil-borne fungal plant pathogen using effector proteins. *Nat. Plants* 6:1365. doi: 10.1038/s41477-020-00799-5

Tanaka, H., and Watanabe, T. (1995). Glucanases and chitinases of Bacillus *circulans* WL-12. *J. Ind. Microbiol.* 14, 478–483. doi: 10.1007/BF01573962

Tao, X. Y., Zhang, H. L., Gao, M. T., Li, M. L., Zhao, T., and Guan, X. Y. (2020). *Pseudomonas* species isolated via high-throughput screening significantly protect cotton plants against Verticillium wilt. *AMB Express* 10:193. doi: 10.1186/s13568-020-01132-1

Wang, J., Li, R., Zhang, H., Wei, G., and Li, Z. (2020). Beneficial bacteria activate nutrients and promote wheat growth under conditions of reduced fertilizer application. *BMC Microbiol.* 20:38. doi: 10.1186/s12866-020-1708-z

Wang, Y., Liang, C., Wu, S., Zhang, X., Tang, J., Jian, G., et al. (2016). Significant improvement of cotton Verticillium wilt resistance by manipulating the expression of Gastrodia antifungal proteins. *Mol. Plant* 9, 1436–1439. doi: 10.1016/j.molp.2016.06.013

Xu, N., Tan, G., Wang, H., and Gai, X. (2016). Effect of biochar additions to soil on nitrogen leaching, microbial biomass and bacterial community structure. *Eur. J. Soil Biol.* 74, 1–8. doi: 10.1016/j.ejsobi.2016.02.004

Zamioudis, C., Mastranesti, P., Dhonukshe, P., Blilou, I., and Pieterse, C. M. J. (2013). Unraveling root developmental programs initiated by beneficial *Pseudomonas* spp. bacteria. *Plant Physiol.* 162, 304–318. doi: 10.1104/pp.112.212597

Zhang, F., Li, X. L., Zhu, S. J., Ojaghian, M. R., and Zhang, J. Z. (2018). Biocontrol potential of *Paenibacillus polymyxa* against Verticillium dahliae infecting cotton plants. *Biol. Control* 127, 70–77. doi: 10.1016/j.biocontrol.2018.08.021

Zhang, J., Yu, X., Zhang, C., Zhang, Q., Sun, Y., Zhu, H., et al. (2021). Pectin lyase enhances cotton resistance to Verticillium wilt by inducing cell apoptosis of Verticillium dahliae. *J. Hazard. Mater.* 404:124029. doi: 10.1016/j.jhazmat.2020.124029

Zhang, L., Ni, H., Du, X., Wang, S., Ma, X.-W., Nürnberger, T., et al. (2017a). The Verticillium-specific protein VdSCP7 localizes to the plant nucleus and modulates immunity to fungal infections. *New Phytol.* 215, 368–381. doi: 10.1111/nph.14537

Zhang, L., Tao, Y., Zhao, S., Yin, X., Chen, J., Wang, M., et al. (2020). A novel peroxiredoxin from the antagonistic endophytic bacterium *Enterobacter* sp. V1 contributes to cotton resistance against Verticillium dahliae. *Plant Soil* 454, 395–409. doi: 10.1007/s11104-020-04661-7

Zhang, W., Corwin, J. A., Copeland, D., Feusier, J., Eshbaugh, R., Chen, F., et al. (2017b). Plastic transcriptomes stabilize immunity to pathogen diversity: the jasmonic acid and salicylic acid networks within the *Arabidopsis*/Botrytis pathosystem. *Plant Cell* 29, 2727–2752. doi: 10.1105/tpc.17.00348

Zhang, Y., Wang, X. F., Ding, Z. G., Ma, Q., Zhang, G. R., Zhang, S. L., et al. (2013). Transcriptome profiling of *Gossypium barbadense* inoculated with Verticillium dahliae provides a resource for cotton improvement. *BMC Genomics* 14:637. doi: 10.1186/1471-2164-14-637

Zhou, L., Zhao, J., Guo, W., and Zhang, T. (2013). Functional analysis of autophagy genes via Agrobacterium-mediated transformation in the vascular wilt fungus

Verticillium dahliae. *J. Genet. Genom.* 40, 421–431. doi: 10.1016/j.jgg.2013.04.006

Zhu, Y., Du, B., Qian, J., Zou, B., and Hua, J. (2013). Disease resistance gene-induced growth inhibition is enhanced by rcd1 independent of defense activation in *Arabidopsis*. *Plant Physiol.* 161, 2005–2013. doi: 10.1104/pp.112.213363

Zilli, J. E., Simoes-Araujo, J. L., Marie Rouws, L. F., and de Barros Soares, L. H. (2020). Draft genome sequence of *Bradyrhizobium elkanii* BR 2003, an efficient rhizobium strain for cajanus, canavalia, crotalaria, and indigofera. *Microbiol. Resour. Announc.* 9:e01565–19. doi: 10.1128/mra.01565-19

Conflict of Interest: The authors declare that the research was conducted in the absence of any commercial or financial relationships that could be construed as a potential conflict of interest.

frontiers in Plant Science

REVIEW
published: 30 June 2021
doi: 10.3389/fpls.2021.701152

Orchid Reintroduction Based on Seed Germination-Promoting Mycorrhizal Fungi Derived From Protocorms or Seedlings

Da-Ke Zhao[1], Marc-André Selosse[2,3], Limin Wu[4], Yan Luo[5], Shi-Cheng Shao[5] and Yong-Ling Ruan[6]**

[1] Biocontrol Engineering Research Center of Plant Disease and Pest, Biocontrol Engineering Research Center of Crop Disease and Pest, School of Ecology and Environmental Science, Yunnan University, Kunming, China, [2] Département Systématique et Evolution, UMR 7205 ISYEB, Muséum National d'Histoire Naturelle, Paris, France, [3] Faculty of Biology, University of Gdansk, Gdansk, Poland, [4] Agriculture and Food, Commonwealth Scientific and Industrial Research Organisation, Canberra, ACT, Australia, [5] Gardening and Horticulture Department, Xishuangbanna Tropical Botanical Garden, Chinese Academy of Sciences, Mengla, China, [6] Australia-China Research Centre for Crop Improvement, School of Environmental and Life Sciences, The University of Newcastle, Callaghan, NSW, Australia*

OPEN ACCESS

Edited by:
Carlos Lucena, University of Cordoba, Spain

Reviewed by:
Songjun Zeng, South China Botanical Garden, Chinese Academy of Sciences, China
Hironori Kaminaka, Tottori University, Japan

***Correspondence:**
Shi-Cheng Shao
shaoshicheng@xtbg.org.cn
Yong-Ling Ruan
yong-ling.ruan@newcastle.edu.au

Specialty section:
This article was submitted to Plant Symbiotic Interactions, a section of the journal Frontiers in Plant Science

Received: *27 April 2021*
Accepted: *04 June 2021*
Published: *30 June 2021*

Citation:
Zhao D-K, Selosse M-A, Wu L, Luo Y, Shao S-C and Ruan Y-L (2021) Orchid Reintroduction Based on Seed Germination-Promoting Mycorrhizal Fungi Derived From Protocorms or Seedlings. Front. Plant Sci. 12:701152. doi: 10.3389/fpls.2021.701152

Orchids are among the most endangered in the plant kingdom. Lack of endosperm in their seeds renders orchids to depend on nutrients provided by orchid mycorrhizal fungi (OMF) for seed germination and seedling formation in the wild. OMF that parasitize in germination seeds is an essential element for orchid seedling formation, which can also help orchid reintroduction. Considering the limitations of the previous orchid reintroduction technology based on seed germination-promoting OMF (sgOMF) sourced from orchid roots, an innovative approach is proposed here in which orchid seeds are directly co-sown with sgOMF carrying ecological specificity from protocorms/seedlings. Based on this principle, an integrative and practical procedure concerning related ecological factors is further raised for re-constructing long-term and self-sustained orchid populations. We believe that this new approach will benefit the reintroduction of endangered orchids in nature.

Keywords: symbiosis, seed germination, reintroduction, orchid mycorrhizal fungi, orchid conservation

ORCHID REINTRODUCTION AND CONSERVATION: A GLOBAL URGENCY

Orchidaceae is the second largest family of flowering plants after Asteraceae (Chase et al., 2015; Givnish et al., 2015; Willis, 2017), with a total of 29,199 species identified (Govaerts et al., 2017). They are tremendously valuable for biodiversity, conservation, and the production of a wide range of medicinal compounds, healthy food, and ornamental plants (Willis, 2017; Hinsley et al., 2018). Moreover, they are popular flagships for habitat conservation. However, orchids are currently among the most threatened flowering plants, with many species on the verge of extinction in the wild due to over-collection, loss of habitats, or climate change (Liu et al., 2015; Gale et al., 2018; Hinsley et al., 2018; Wang et al., 2019). Furthermore, most orchids require specialized habitats and are usually in small populations with a high dependence on pollinators, symbiotic germination fungi, and host trees for epiphytic species, further making them particularly vulnerable to extinction

(Roberts and Dixon, 2008; Selosse, 2014; Fay et al., 2015; Rasmussen et al., 2015; Keppel et al., 2016; Fay, 2018; Gale et al., 2018).

Retrospectively, few orchid species have been domesticated and cultivated on a large scale, except for these with high values in ornamental horticulture (e.g., in the genera *Cymbidium*, *Phalaenopsis,* and *Cattleya*), medicine (several *Dendrobium* and *Gastrodia* spp.) or food industries (e.g., *Vanilla fragrans*). Consequently, a large portion of orchids still grows in their natural habitats. All orchids have been included in their entirety in Appendices I and II of the Convention on International Trade in Endangered Species of Wild Fauna and Flora (CITES) in 2017 to ban illegal trade (Gale et al., 2018; Hinsley et al., 2018). Based upon the assessments of 1770 orchid species worldwide in 2021 by Global International Union for Conservation of Nature (IUCN) for Red Lists of Threatened Species, nearly a half (46.5%) of orchid species are under one of the three threat categories, namely, vulnerable, endangered, and critically endangered (IUCN, 2021). Clearly, the majority of orchids are facing extinction threats, which demands urgent attention and targeted conservation actions such as reintroduction (Roberts and Dixon, 2008; Rasmussen et al., 2015). Reintroduction means the controlled placement of plant individuals of an endangered species into its natural habitat or managed ecological area to re-establish populations in the wild.

REINTRODUCTION AS A PRIORITY FOR EFFICIENT ORCHID CONSERVATION

Ex situ and *in situ* conservation, together with reintroduction, are the main methods for the conservation of threatened plant species (Oldfield, 2009). For plants deprived of their original natural habitats, *ex situ* conservation in botanic gardens may be the only way for their survival in short to medium terms (Ren et al., 2014). Of the 350,699 categorized plant species, 105,634 or 30% are held in the living collections of the global botanic garden network, indicating a significant effort in *ex situ* conservation (Mounce et al., 2017). Botanic gardens are, however, are concentrated on temperate regions and a majority of the collected species is kept in the northern hemisphere (Mounce et al., 2017). It implies that a large number of orchids is beyond *ex situ* conservation, mostly growing in tropical and subtropical areas with high genetic diversity (Givnish et al., 2015).

In contrast to *ex situ* conservation, *in situ* conservation is considered to be more effective for sustainable biodiversity conservation. The procedure is, however, complex and multifaceted. It involves both the maintenance and management of the protected areas and actions required at the species and population levels. So far, species-level measures have only been undertaken for a very small percentage of threatened plants by a few countries, and with limited success (Heywood, 2015). Indeed, it is difficult to carry out efficient *in situ* conservation for most of the endangered orchids due to the vast number of species involved and their broad geographic distributions.

Reintroduction of individual plants to their natural habitats, as an essential and effective measure to protect endangered species, has become increasingly important for species conservation worldwide, especially for plants facing extinction such as many orchid species (Oldfield, 2009; Godefroid et al., 2011). Plants from *ex situ* conservation can be linked to *in situ* conservation via reintroduction. In other words, reintroduction could bridge the gap between conservation theories and practices (Gale et al., 2018). As a consequence, reintroduction programs represent a better choice for orchid protection (Zeng et al., 2012; Wu et al., 2014).

SEED GERMINATION PROMOTING ORCHID MYCORRHIZAL FUNGI (sgOMF) PLAY KEY ROLES IN THE ORCHID REINTRODUCTION

Orchid conservationists have long been trying to develop ways to reintroduce endangered orchids (Swarts and Dixon, 2009; Johnson, 2011). The current strategies of orchid reintroduction primarily focus on restoration-friendly cultivation, translocation of individual plants, or transplantation of *in vitro* cultured seedlings (Zeng et al., 2012; Wu et al., 2014). However, these approaches have often been proven to be insufficient and ineffective for *in situ* protection of some critically endangered orchid species, because of the poor survival rate of the seedlings produced *in vitro* or the low genetic diversity of the reintroduced plants (Liu et al., 2010; Shao et al., 2017; Hinsley et al., 2018; Sathiyadash et al., 2020).

Due to the lack of endosperm (Yeung, 2017; Zhang et al., 2017; Yeh et al., 2019), the germination of nearly all orchid seeds relies on the specific fungal partner in the wild (Bruns and Read, 2000; Bidartondo and Read, 2008; Merckx et al., 2009; Swarts and Dixon, 2009; Dearnaley et al., 2012; McCormick et al., 2018; Shao et al., 2019). To this end, the seed germination-promoting fungi, predominantly residing in the protocorm of the germinating seeds are known to play a key role in realizing *in situ* orchid seed germination and seedling formation (Selosse et al., 2017). Seed germination-promoting fungi generally belong to orchid mycorrhizal fungi (OMF) characterized by the formation of pelotons, inside the cells of orchid roots or germinating seeds (Jacquemyn et al., 2017). Therefore, we focus on sgOMF for orchid reintroduction.

In broad term, OMF could colonize orchid roots (root-originated OMF, rOMF) or seeds (seed-originated OMF, sOMF) at distinctive development stages as illustrated in **Figure 1A** (Peterson et al., 2004; Smith and Read, 2008; Yeh et al., 2019; Favre Godal et al., 2020; Sathiyadash et al., 2020). Theoretically, sgOMF could be potentially identified from sOMF or rOMF (**Figure 1**). There may be more than one OMF species colonized at a given germinating stage (Bidartondo and Read, 2008; Stöckel et al., 2014; Shao et al., 2017, 2019; Meng et al., 2019a). These sgOMF are saprotrophic and/or endophytic in non-orchid plants (Selosse and Martos, 2014; Weiß et al.,

Abbreviations: OMF, Orchid mycorrhizal fungi; sgOMF, Seed germination-promoting orchid mycorrhizal fungi; rOMF, Root-originated OMF; sOMF, Seed-originated OMF; SSR, Simple sequence repeats.

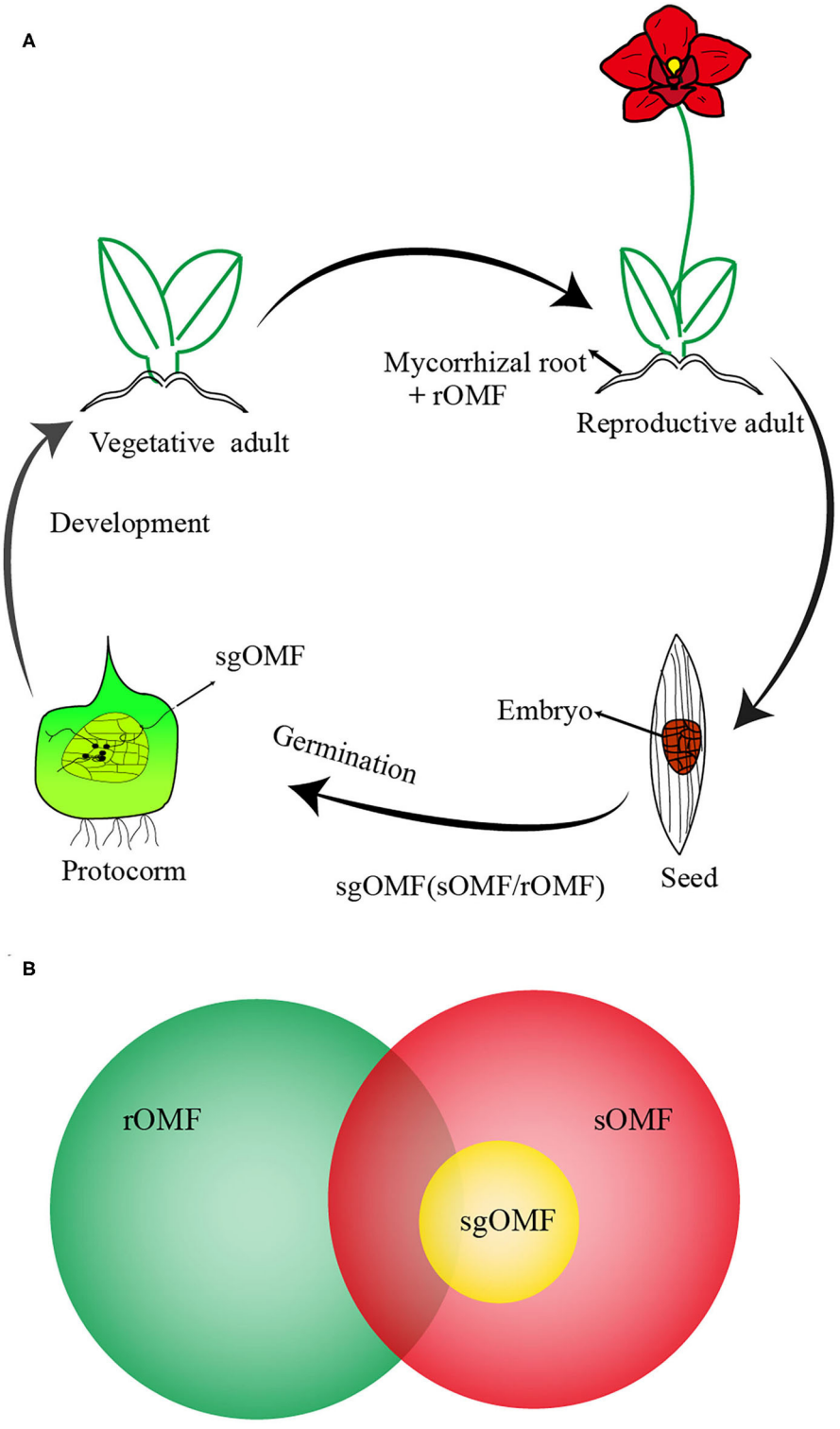

FIGURE 1 | A schematic presentation on the role of rOMF, sOMF, and sgOMF in orchid life cycle and their relationship. **(A)** A flow chart on orchid life cycle from seed germination to adult plants with positions of rOMF and sOMF in the life cycle indicated. Due to the lack of endosperm, orchid seed germination requires the establishment of symbiosis with seed germination-promoting OMF (sgOMF), mostly found in the protocorm of the germinating seeds (sOMF). Vegetative adults can develop into the reproductive stage and undergo mycorrhization with root-originated OMF (rOMF). **(B)** A schematic diagram on the relationship among rOMF, sOMF, and sgOMF. Both rOMF and sOMF originate from saprophytic or ectomycorrhizal fungi. Here, sgOMF is the subset of sOMF capable of promoting orchid seed germination *in situ*. rOMF strains are often different but could be similar to sOMF (see text for more details).

2016), or concurrently ectomycorrhizal (typical for terrestrial or mycoheterotrophic orchids).

At the genus level, sgOMF generally belong to the polyphyletic "rhizoctonia" aggregate that includes Tulasnellaceae, Ceratobasidiaceae, and Serendipitaceae (Dearnaley et al., 2012; Rasmussen and Rasmussen, 2014; Rasmussen et al., 2015). Some other genera are reported to be involved in symbiotic germination as well, including *Mycena* (Xu and Guo, 1989), *Helicogloea* (Kottke et al., 2010), *Thanatephorus* (Sebastian et al., 2014), and *Fusarium* (Jiang et al., 2019). Beyond saprobic fungi, some mycoheterotrophic orchid species display symbiosis with *Tomentella, Russula, Tuber,* or other fungi (Selosse et al., 2004; Julou et al., 2005; Abadie et al., 2006; Bidartondo and Read, 2008; Fochi et al., 2017; Shao et al., 2017).

It was believed that sgOMF generally come from rOMF (e.g., Rasmussen, 1995). Yet, although this may apply to many terrestrial orchids from temperate regions, the general validity of this hypothesis deserves a close examination. At the species level, sgOMF may or may not be identical to those from the corresponding adult roots (McCormick and Jacquemyn, 2014; Meng et al., 2019c). Even for the same fungal species, the isolates from adult roots often fail to promote seed germination *in situ*, while that fungi from protocorms can (Zelmer and Currah, 1997). The underlying mechanism for this disparity remains to be elucidated (Douhan et al., 2011; Johnson et al., 2012).

The mycorrhizal specificity associated with an orchid *in situ* seed symbiotic germination is often so restrictive that seeds from many orchids do not germinate or develop without their compatible fungal symbiont (Rasmussen, 1995; Bruns and Read, 2000; Merckx et al., 2009; Tesitelova et al., 2012; Davis et al., 2015; Fay, 2018). Even if seed germination is triggered by close relatives of the target fungus, the orchid seedling may not survive beyond the early developmental stages, which probably explains why some protocorms succeed in germination but fail in further seedling growth. The exact cause of this extreme level of fungal specificity under *in situ* symbiotic germination is yet to be examined. Nevertheless, coevolution might play a role in this phenomenon: once an appropriate fungus had been recruited. The orchid may have fine-tuned its physiology to adapt to this fungus, thereby making the plants incapable of host-jumping for distantly related fungi (Bidartondo and Bruns, 2002), especially under *in situ* conditions (Masuhara and Katsuya, 1994; Perkins et al., 1995).

Some sOMF and rOMF can promote orchid seed germination under controlled laboratory conditions, i.e., *in vitro*, thereby exhibiting potential specificity (Smith and Read, 2008; Rasmussen et al., 2015; Jacquemyn et al., 2017; Shao et al., 2019; Sathiyadash et al., 2020). If those isolates exhibiting potential specificity can successfully stimulate orchid seed symbiotic germination and survival under *in situ* conditions, they are considered to have ecological specificity. Mycorrhizal roots are historically the major source for identifying fungi that could be used for orchid symbiotic seed germination, since it is much easier to access rOMF than sOMF from protocorms or germinating seeds. The latter are difficult to be detected under natural conditions (Perkins et al., 1995; Zelmer and Currah, 1997; Steinfort et al., 2010; Herrera et al., 2017; Jiang et al., 2019). Potential specificity may also be possessed by some endophytic or even soil fungi (Jusaitis and Sorensen, 1993; Vujanovic and Vujanovic, 2007; Jiang et al., 2019). However, the effects of rOMF isolates with potential specificity have rarely been evaluated in natural environments or *in situ*. Among those tested, few of them showing ecological specificity in the wild where the natural factors are uncontrollable and much more complex and variable than those *in vitro* (Meng et al., 2019c).

While sgOMF may exist among the rOMF (Masuhara and Katsuya, 1994; Bidartondo and Read, 2008; Stöckel et al., 2014), the isolates from adult roots do not always display the ability to promote seed germination. For example, among the *Ceratobasidium cornigerum* recovered from the field-grown adult roots and the protocorms of *Spiranthes lacera* at the same site, only the strain from the protocorm, promoted seed germination and seedling development (Zelmer and Currah, 1997). Furthermore, even if the isolate from adult roots promotes *in vitro* germination and seedling formation, it could fail to work in the field (Batty et al., 2006).

Due to the lack of or lower chance of finding sgOMF from roots, the effective way is to isolate sgOMF from the protocorms or germinating seeds either occurred naturally or induced using *in* or *ex situ* baiting. This method allows simultaneous baiting for mycorrhizal fungi that promote orchid seed germination *in situ* or *ex situ* from soil or bark (Shao et al., 2017). Symbiotic fungal diversity is sometimes lower in protocorms and seedlings than that in the adult roots (Bidartondo and Read, 2008; Zi et al., 2014). The sOMF usually consist of few fungal strains per germinating seed or seedling and in most cases display a high degree of species-specificity (Masuhara and Katsuya, 1994; Rasmussen and Rasmussen, 2014). However, one should not overlook the possibility that multiple sgOMF species may colonize protocorms or seedlings (Perkins et al., 1995; Bidartondo and Read, 2008; Tesitelova et al., 2012; Stöckel et al., 2014; Meng et al., 2019a; Shao et al., 2019, 2020). Therefore, candidate sgOMF should be firstly evaluated for their potential specificity for seed germination *in vitro* (Masuhara and Katsuya, 1994; Jacquemyn et al., 2017).

LIMITATIONS OF THE CURRENT ORCHID REINTRODUCTION RELYING ON rOMF

The concept of using rOMF to promote orchid seed germination was proposed by Bernard in the early 1900's (Selosse et al., 2017) and elaborated later by others including Warcup and Clements in the 1970's and 1980's (Clements et al., 1986). Rasmussen (1995) and Zettler (1997) then suggested the application of rOMF in orchid reintroduction about 20 years ago. There are several preliminary reintroduction reports with rOMF for some green terrestrial orchids including *Spiranthes magnicamporum* (Anderson, 1991), *Spiranthes brevilabris* (Stewart et al., 2003), *Dactylorhiza hatagirea* (Aggarwal and Zettler, 2010), and *Dactylorhiza praetermissa* (Mckendrick, 1995), two epiphytic orchids *Epidendrum nocturnum* (Zettler et al., 2007) and *Vanda coerulea* (Aggarwal et al., 2012) (**Table 1**). Despite the progress and the role that rOMF play in nutrient uptake from soil

TABLE 1 | Key orchid reintroduction cases based upon OMF.

Taxa	OMF	OMF origin	Specificity	Materials for reintroduction	Supervision period	References
Spiranthes magnicamporum	*Epulorhiza repens*	Roots	Potential specificity	Seedling	Flowering after planted on calcarious sand 15 months later	Anderson, 1991
Dactylorhizapraetermissa	*Unidentified fungus*	Roots	Potential specificity	Seedlings	Flowering after 2 or 3 years	Mckendrick, 1995
Spiranthes brevilabris	*Epulorhiza repens*	Roots	Potential specificity	Seedlings	Flowering after planted 6 months later	Stewart et al., 2003
Epidendrumnocturnum	*Epulorhiza repens*	Roots of *Spiranthes brevilabris*	Potential specificity	Seedlings	Not mentioned	Zettler et al., 2007
Dactylorhiza hatagirea	*Ceratobasidium* sp.	Roots	Potential specificity	Seedlings	Individuals without flowering after 2 years later	Aggarwal and Zettler, 2010
Vanda coerulea	*Thanatephorus cucumeris*	Roots	Ecological specificity	Seedlings	Individuals after 1 year	Aggarwal et al., 2012
Dendrobium devonianum	*Tulasnella* sp.	Protocorms	Ecological specificity	Co-sowing seeds and *tulasnella* sp.	Seedlings after 3 month	Shao et al., 2017
Dendrobium aphyllum	*Tulasnella calospora*	Protocorms	Ecological specificity	Co-sowing seeds and *tulasnella calospora*	Seedlings after 3 month	Shao et al., 2018
Dendrobium nobile	*Tulasnella* sp.	Protocorms	Ecological specificity	Co-sowing seeds and *tulasnella* sp.	Seedlings after 3 month	Shao et al., 2018

(Dearnaley et al., 2012) and vegetative dormancy (McCormick et al., 2018), there are several major limitations of the rOMF-based reintroduction.

Firstly, based on available information, this method hardly led to the re-establishment of a self-sustainable population for critically endangered orchids (Scade et al., 2006). The success of long-term reintroduction can only be achieved if self-sustained populations are established that do not require further human intervention (Scade et al., 2006; Reiter et al., 2016). Orchid mycorrhizal associations are essential for rebuilding self-sustainable wild populations (Scade et al., 2006; Liu et al., 2010; Reiter et al., 2016). Noteworthily, it is the sgOMF from sOMF, but not rOMF, often promote *in situ* seed germination and the subsequent survival and adaption to the natural habitats (Batty et al., 2006; Shao et al., 2017). In other words, sgOMF can be selected among fungi colonizing protocorms (Shao et al., 2017, 2018), whereas the rOMF in many cases lack the ecological specificity required and fail to help the rebuilding of self-sustained orchid populations.

Some rOMF strains promote seed germination and plantlet formation under laboratory conditions, thereby exhibiting potential specificity (Steinfort et al., 2010; Herrera et al., 2017; Jiang et al., 2019). Some of those individuals even reach the reproductive stage after being transplanted from *in vitro* environment to the field (Mckendrick, 1995; Stewart et al., 2003). However, and although this was rarely checked, rOMF may not possess suitable inoculum of sgOMF from protocorms and may lack ecological specificity.

Secondly, there is a risk of a failure in identifying any sgOMF from adult orchid roots. For example, all rOMF isolates (*Tulasnella* spp.) failed to sustain seedling growth *in vitro* both in the epiphytic *Dendrobium exile* and terrestrial *Arundina graminifolia* (Meng et al., 2019b,c). Overall, the limitations and challenges outlined above make rOMF approach impractical for *in situ* orchid reintroduction (Reiter et al., 2016).

It is clear that although the application of rOMF contributed to reintroduction in the past and may continue to do so in the future, it has several inherent limitations that prompt efforts to develop new approaches. Moreover, the specificities of epiphytic orchids, both in terms of ecology and fungal partners (Martos et al., 2012), call for re-thinking the protocols inherited from the study of North-American and European terrestrial orchids.

TARGETING sgOMF FROM PROTOCORMS AND GERMINATING SEED FOR SUCCESSFUL *IN SITU* ORCHID REINTRODUCTION

Under field conditions, sOMF often promote symbiotic seed germination *in situ*, resulting in the development of plantlets (Masuhara and Katsuya, 1994; Perkins et al., 1995; Smith and Read, 2008; Sathiyadash et al., 2020) (**Figure 1**), thereby contributing to the rebuilding the orchid populations in the wild. Due to the ecological specificity displayed by sOMF for the symbiotic germination of the target orchid (Perkins et al., 1995; Shao et al., 2017, 2018; Meng et al., 2019c), orchid reintroduction based on sOMF is a natural way compared to that of rOMF. By co-sowing orchid seeds with germination-enhancing sgOMF carrying ecological specificity (see below), the resultant plantlets could serve as not only orchid individuals but also inoculum in the surroundings of the target orchid as a germination

promoting- mycobiont for continuous orchid germination (Batty et al., 2006; Reiter et al., 2016). It thereby helps to re-establish self-sustainable populations for critically endangered orchids, particularly for those orchids whose *ex situ* conservation should be conducted in the wild.

Protocorms and seedlings simultaneously associate with multiple OMF in the wild (Shao et al., 2019, 2020). However, co-cultures with two or three sgOMF did not increase protocorm formation and seedling establishment. Rather it often resulted in lower germination percentages compared with that of monocultures for *D. nobile* (Shao et al., 2020). While it seems easy to just perform direct sowing of orchid seeds into their natural habitats for reintroduction, this practice typically leads to sporadic and unstable seedling emergence, owing to the low probability of encountering the target sgOMF in the environment (Jacquemyn et al., 2007; Jersakova and Malinova, 2007; Zi et al., 2014; Shao et al., 2017; Yang et al., 2017).

The concept to use sgOMF carrying ecological specificity for orchid rehabilitation was raised 25 years ago (Perkins et al., 1995). Two decades later, the application of sgOMF from sOMF in orchid restoration finally came into reality for the epiphytic orchid *Dendrobium devonianum* (Shao et al., 2017). Using packaged seed mixed with symbiotic fungus *Tulasnella* sp. isolated from protocorms, an efficient reintroduction was conducted, which resulted in the construction of a natural population of this endangered orchid (Shao et al., 2017). With improved methods, the other two threatened orchid species *Dendrobium aphyllum* and *D. nobile* have also been successfully reintroduced to the wild, as well as the restoration of another field population of *D. devonianum* (Shao et al., 2018).

Since epiphytes account for ∼70% of all the orchid species (Peterson et al., 2004; Zotz, 2013) and previous reintroduction activities largely focused on terrestrial orchids (Anderson, 1991; Mckendrick, 1995; Stewart et al., 2003; Aggarwal and Zettler, 2010), the co-sowing practice to construct populations for these epiphytic species (Shao et al., 2017, 2018) represents a promising direction and tool in orchid population establishment. Based on the success in the reintroduction of the three epiphytic orchids (Shao et al., 2017, 2018) as discussed above, it is now the time for the application of sgOMF carrying ecological specificity to be tested on other genera. We presume that it will be an effective way to achieve orchid reintroduction *in situ*.

In contrast to the use of rOMF to produce seedlings *ex situ,* the reintroduction of the three *Dendrobium* spp. was based on a novel approach where orchid seeds were directly germinated *in situ* with the resultant seedlings fully developed into fertile adult plants (Shao et al., 2017, 2018) (**Table 1**). As nearly all the orchids that naturally germinate are accompanied with sgOMF with ecological specificity, the sOMF-based approach could be broadly applicable for the efficient reintroduction and even natural cultivation of endangered orchidaceae species. One should bear in mind that regardless the rOMF- or sOMF- based studies, there have been no reports on long term analyses over 5 years to check the status of reintroduction if the plantlets emerged from seeds. Thus, monitoring the seedling recruitment over two generations is needed to further verify the result of orchid reintroduction with sOMF (**Table 1**), especially when reintroducing to sites where the orchids disappeared long time ago. We described the key steps involved in this procedure exploiting sgOMF isolated from protocorms or germinating seeds.

ISOLATION OF sgOMF FROM PROTOCORMS OR GERMINATING SEEDS WITH POTENTIAL SPECIFICITY

To realize *in situ* orchid reintroduction, it is essential to identify sgOMF carrying ecological specificity for initiating symbiotic seed germination *in situ*. As mentioned before, sgOMF isolated from protocorms or seedlings typically promote seed germination not only *in vitro* but also in the wild, thus showing both potential and ecological specificity (Shao et al., 2017, 2018). The isolates are first verified for potential specificity in laboratories (Zi et al., 2014; Shao et al., 2017, 2019; Meng et al., 2019c) (**Figure 2**). Yet, sgOMF exhibiting potential specificity does not necessarily carry ecological specificity; as that if they could stimulate *in situ* seed germination remains unclear. Thus, further screening is required.

APPRAISAL OF ECOLOGICAL SPECIFICITY OF sgOMF FROM PROTOCORMS OR GERMINATING SEED

After having isolated sgOMF with potential specificity, their *in situ* co-culture with orchid seeds are conducted to screen for sgOMF capable of promoting seed germination in natural habitats, i.e., carrying ecological specificity (**Figure 2**). The procedure is supposed to be easily carried out by blending orchid seeds with mycelium and subsequently transferring the mixture to the wild. In reality, however, it faces great challenges due to the high complexity of orchid seed germination *in situ* (Rasmussen et al., 2015). Hence, innovative and comprehensive measures are needed to design an efficient, reliable, and practical program. Based on our experience in conjunction with considerations of other factors (Shao et al., 2017, 2018), we summarized below the key conditions influencing *in situ* symbiotic germination.

For epiphytic orchids, maintaining moisture is crucial for achieving *in situ* seed germination. Previously, orchid seeds were placed on organic substances such as sphagnum moss or bark for germination (Arditti, 1967), which often results in a disappointing outcome largely because of the dry microenvironment surrounding the seeds. To circumvent this problem, paper packets containing a mixture of orchid seeds and fungal hyphae were attached to tree trunks and then wrapped with biodegradable plastic film to retain moisture for producing seedling *in situ* (Shao et al., 2017). Further supplement of sphagnum moss in paper packets increased the germination rate of *D. devonianum* to 9.4% (Shao et al., 2018), as compared to only 0.9∼1.4 % without the inclusion of the moss (Shao et al., 2017). We consider that this 10-fold increment in the germination rate is primarily owing to the much-improved moisture retention during early germination. Moreover, instead of using nylon net packets in primary reintroduction studies, which could physically block late seedling growth (Shao et al.,

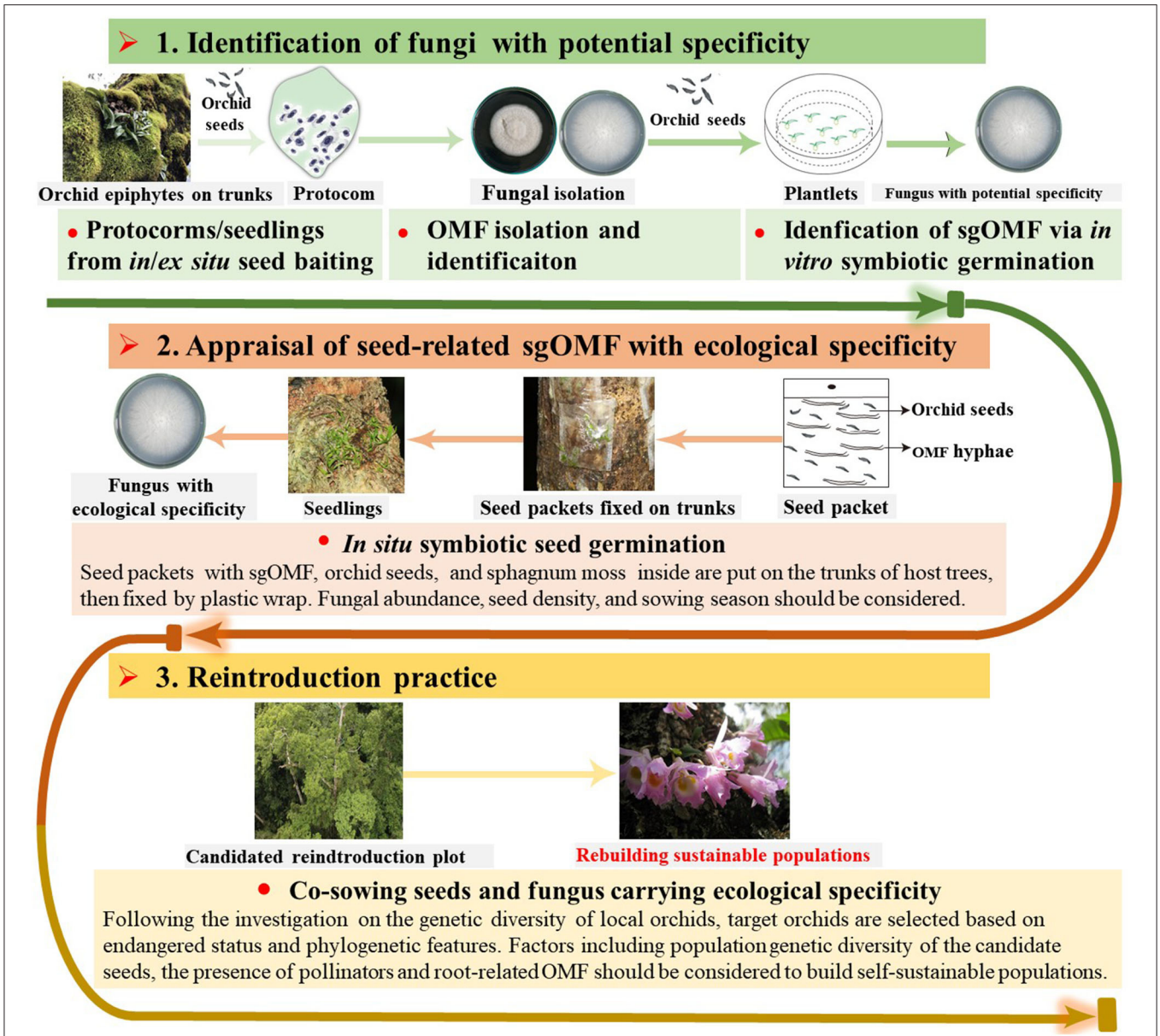

FIGURE 2 | A procedure for *in situ* orchid reintroduction through direct co-sowing with sgOMF. The protocol consists of three key steps: (i) Identification of fungal strains with potential specificity isolated from protocorms or germinating seeds using symbiotic germination *in vitro*; (ii) Screening for sgOMF carrying ecological specificity through seed-fungus co-sowing *in situ*, and (iii) Reintroduction. More specifically, *in* or *ex situ* seed baiting is recommended to develop protocorms and germinating seeds slightly beyond the protorm stage, from which sgOMF candidates are isolated. All isolates are screened for their efficiency in promoting seed germination *in vitro* in laboratories, leading to the identification of sgOMF with potential specificity. To further identify sgOMF carrying ecological specificity, paper bags containing sgOMF candidates, orchid seeds, and sphagnum moss are placed on the trunks of host trees under *in situ* conditions. With the successful identification sgOM exhibiting ecological specificity, reintroduction can proceed (see text for more details).

2017, 2018), the paper packets did not constrain seedling emergence. The seedlings can grow readily by enlarging the holes punctured in the wrap, allowing the plantlets to develop naturally without the need for other management intervention (Shao et al., 2018).

Sowing time is another important factor impacting germination *in situ* as it relates to air temperature and humidity (Shao et al., 2017, 2018). *In situ* seed germination and the subsequent formation of protocorm-like bodies and seedlings correlate with the humidity as well as the temperature of the microhabitats across seasons (Shao et al., 2017, 2018; Yang et al., 2017). Therefore, knowledge on the local timing of natural seed dispersal and their germination of the target orchid is required to determine sowing time.

The density of the fungal patch could also affect orchid seed germination (McCormick et al., 2012, 2018; Favre Godal et al., 2020). The mixture with enough pre-grown fungal hyphae with orchid seeds keeps the dominance of sgOMF, preventing the invasion of competitors (Shao et al., 2017). In practice, fungal mycelium mixed with agar was blended into powder and used at the ratio of 1.0 mg powder to 50 seeds per paper bag based on our successful co-sowing experience. The viability of using the blended fungal powder for seed germination has been verified in our hands both *in vitro* and *in situ*. The number of seeds and the amount of powder are controllable and adjustable in each packet that can be easily preserved in the fridge for later reintroduction (Shao et al., 2017, 2018).

The interactions between the host trees for the majority of epiphytic orchids and candidate sgOMF carrying ecological specificity should also be taken into account (Martos et al., 2012; Fay et al., 2015; Rasmussen and Rasmussen, 2018). The sgOMF are susceptible to changes in moisture, pH, and organic amendments in the microhabitat provided by the host trees (McCormick et al., 2012; McCormick and Jacquemyn, 2014; Shao et al., 2018). For example, the percentage of germination of three tested *Dendrobium* species with sgOMF on the host tree *Bauhinia purpurea* was higher than that on the *Citrus maxima* and *Camellia assamica* (Shao et al., 2018).

We recognize that some orchids potentially utilize a variety of opportunistic mycorrhizal partners to induce seed germination (Waud et al., 2017). Thus, the possibility of requiring more than two strains simultaneously for *in situ* seed germination cannot be ruled out. In any case, it is necessary to experimentally identify the optimal fungus or fungal combination for seed germination leading to the re-establishment of a self-sustainable population. Following the co-sowing practice, calibrated with the aforementioned key factors, the sgOMF carrying ecological specificity in enhancing *in situ* germination are identified.

REINTRODUCTION WITH sgOMF CARRYING ECOLOGICAL SPECIFICITY

With the identification of sgOMF *in situ*, reintroduction can be conducted in the wild (**Figure 2**). The rich genetic diversity of the founder population increases the chance of successful plant colonization (Crawford and Whitney, 2010) and the functionality of the ecosystem (Prieto et al., 2015). Thus, for a given target orchid species to be reintroduced, the seeds for co-sowing with sgOMF are ideally chosen from the population with the richest genetic diversity based on assessments such as simple sequence repeats (SSR) (Zotz, 2013). A mix of several populations for one target species of origin may improve the chances of local adaptation at the recipient site. To this end, a minimum of 50–200 individuals is required to establish an effective and self-sustainable population for out-crossing species such as the majority of orchids (Reiter et al., 2016). Further, it is necessary to monitor over a long period of time to determine the sustainability of the rebuilt populations. Given the complex process involved in the re-establishment of orchid (Rasmussen et al., 2015; Shao et al., 2017), other factors including availability of pollinators (Heywood, 2015) and local rOMF (Dearnaley et al., 2012; McCormick et al., 2018) should also be taken into account for successful reintroduction (**Figure 2**).

CONCLUDING REMARKS AND FUTURE PERSPECTIVES

We illustrated here the application of sgOMF selected from sOMF in the orchid reintroduction. Through performing *in situ* co-sowing with sgOMF carrying ecological specificity, coupled with other relevant measures as discussed, it is feasible to achieve an effective and self-sustained population establishment of endangered orchids in the wild. This approach rectifies the shortcomings of the current methods based on rOMF in the genus *Dendrobium* and should be now tested in more species and regions. The reintroduction of epiphytic orchids is still in its infancy, and many factors in the described protocol can be optimized further or adapted to other species. We call for more applications and updating of our method as we deeply believe that this integrated protocol provides a valuable basis for the reintroduction and protection of threatened orchid species worldwide. This could contribute to the global efforts in orchid reintroduction and realization of *in situ* restorations of threatened orchid populations in the long run.

AUTHOR CONTRIBUTIONS

D-KZ, S-CS, and Y-LR conceived the project. LW, YL, D-KZ, S-CS, M-AS, and Y-LR analyzed the selected references. D-KZ, S-CS, M-AS, and Y-LR wrote the manuscript with inputs from all authors. All authors read and approved the final manuscript.

FUNDING

The work in the authors' laboratories was supported in part by the Australian Research Council (DP180103834), the National Natural Science Foundation of China (31960082, 31600440, and 31400021), and West Light Talent Program of the Chinese Academy of Sciences (Grant No. E1XB011B01). M-AS is currently funded by the Polish National Science Centre (Maestro7-NZ project entitled Orchidomics) and the Fondation de France.

REFERENCES

Abadie, J. C., Puttsepp, U., Gebauer, G., Faccio, A., Bonfante, P., and Selosse, M. A. (2006). *Cephalanthera longifolia* (Neottieae, Orchidaceae) is mixotrophic: a comparative study between green and nonphotosynthetic individuals. *Can. J. Bot.* 84, 1462–1477. doi: 10.1139/b06-101

Aggarwal, S., Nirmala, C., Beri, S., Rastogi, S., and Adholeya, A. (2012). *In vitro* symbiotic seed germination and molecular characterization of associated endophytic fungi in a commercially important and endangered

Indian orchid *Vanda coerulea* Griff. ex Lindl. *Eur. J. Environ. Sci.* 2, 33–42. doi: 10.14712/23361964.2015.36

Aggarwal, S., and Zettler, L. W. (2010). Reintroduction of an endangered terrestrial orchid, *Dactylorhiza hatagirea* (D. Don). Soo, assisted by symbiotic seed germination-first report from the Indian subcontinent. *Nat. Sci.* 8, 139–145.

Anderson, A. B. (1991). Symbiotic and asymbiotic germination and growth of *Spiranthes magnicamporum* (Orchidaceae). *Lindreyana* 6, 183–186.

Arditti, J. (1967). Factors affecting the germination of orchid seed. *Bot. Rev.* 33, 1–97. doi: 10.1007/BF02858656

Batty, A. L., Brundrett, M. C., Dixon, K. W., and Sivasithamparam, K. (2006). *In situ* symbiotic seed germination and propagation of terrestrial orchid seedlings for establishment at field sites. *Aust. J. Bot.* 54, 375–381. doi: 10.1071/BT04024

Bidartondo, M., and Bruns, T. (2002). Fine-level mycorrhizal specificity in the Monotropoideae (Ericaceae): specificity for fungal species groups. *Mol. Ecol.* 11, 557–569. doi: 10.1046/j.0962-1083.2001.01443.x

Bidartondo, M. I., and Read, D. J. (2008). Fungal specificity bottlenecks during orchid germination and development. *Mol. Ecol.* 17, 3707–3716. doi: 10.1111/j.1365-294X.2008.03848.x

Bruns, T. D., and Read, D. J. (2000). *In vitro* germination of nonphotosynthetic, myco-heterotrophic plants stimulated by fungi isolated from the adult plants. *New Phytol.* 148, 335–342. doi: 10.1046/j.1469-8137.2000.00766.x

Chase, M. W., Cameron, K. M., Freudenstein, J. V., Pridgeon, A. M., Salazar, G., Van den Berg, C, et al. (2015). An updated classification of Orchidaceae. *Bot. J. Linn. Soc.* 177, 151–174. doi: 10.1111/boj.12234

Clements, M., Muir, H., and Cribb, P. (1986). A preliminary report on the symbiotic germination of European terrestrial orchids. *Kew Bull.* 41, 437–445. doi: 10.2307/4102957

Crawford, K., and Whitney, K. (2010). Population genetic diversity influences colonization success. *Mol. Ecol.* 19, 1253–1263. doi: 10.1111/j.1365-294X.2010.04550.x

Davis, B. J., Phillips, R. D., Wright, M., Linde, C. C., and Dixon, K. W. (2015). Continent-wide distribution in mycorrhizal fungi: implications for the biogeography of specialized orchids. *Ann. Bot.* 116, 413–421. doi: 10.1093/aob/mcv084

Dearnaley, J. D. W., Martos, F., and Selosse, M. A. (2012). "Orchid mycorrhizas: mol ecol, physiology, evolution and conservation aspects," in *Fungal Associations. The Mycota*, ed B. Hock (Berlin, Heidelberg: Springer), 207–230. doi: 10.1007/978-3-642-30826-0_12

Douhan, G. W., Vincenot, L., Gryta, H., and Selosse, M. A. (2011). Population genetics of ectomycorrhizal fungi: from current knowledge to emerging directions. *Fungal Biol.* 115, 569–597. doi: 10.1016/j.funbio.2011.03.005

Favre Godal, Q., Gourguillon, L., Riffault Valois, L., Urbain, A., Lordel Madeleine, S., Gindro, K., et al. (2020). Orchids and their mycorrhizal fungi: an insufficiently explored relationship. *Mycorrhiza* 30, 5–22. doi: 10.1007/s00572-020-00934-2

Fay, M. F. (2018). Orchid conservation: how can we meet the challenges in the twenty-first century? *Bot. Stud.* 59:16. doi: 10.1186/s40529-018-0232-z

Fay, M. F., Pailler, T., and Dixon, K. W. (2015). Orchid conservation: making the links. *Ann. Bot.* 116, 377–379. doi: 10.1093/aob/mcv142

Fochi, V., Chitarra, W., Kohler, A., Voyron, S., Singan, V. R., Lindquist, E. A., et al. (2017). Fungal and plant gene expression in the *Tulasnella calospora–Serapias vomeracea* symbiosis provides clues about nitrogen pathways in orchid mycorrhizas. *New Phytol.* 213, 365–379. doi: 10.1111/nph.14279

Gale, S. W., Fischer, G. A., Cribb, P. J., and Fay, M. F. (2018). Orchid conservation: bridging the gap between science and practice. *Bot. J. Linn. Soc.* 186, 425–434. doi: 10.1093/botlinnean/boy003

Givnish, T. J., Spalink, D., Ames, M., Lyon, S. P., Hunter, S. J., Zuluaga, A., et al. (2015). Orchid phylogenomics and multiple drivers of their extraordinary diversification. *P. Roy. Soc. B-Biol. Sci.* 282, 2108–2111. doi: 10.1098/rspb.2015.1553

Godefroid, S., Piazza, C., Rossi, G., Buord, S., Stevens, A. D., Aguraiuja, R., et al. (2011). How successful are plant species reintroductions? *Biol. Conserv.* 144, 672–682. doi: 10.1016/j.biocon.2010.10.003

Govaerts, R., Bernet, P., Kratochvil, K., Gerlach, G., Carr, G., Alrich, P., et al. (2017). *World checklist of orchidaceae*. Facilitated by the Royal Botanic Gardens, Kew.

Herrera, H., Valadares, R., Contreras, D., Bashan, Y., and Arriagada, C. (2017). Mycorrhizal compatibility and symbiotic seed germination of orchids from the coastal range and Andes in south central Chile. *Mycorrhiza* 27, 175–188. doi: 10.1007/s00572-016-0733-0

Heywood, V. H. (2015). *In situ* conservation of plant species–an unattainable goal? *Isr. J. Plant Sci.* 63, 211–231. doi: 10.1080/07929978.2015.1035605

Hinsley, A., De Boer, H. J., Fay, M. F., Gale, S. W., Gardiner, L. M., Gunasekara, R. S., et al. (2018). A review of the trade in orchids and its implications for conservation. *Bot. J. Linn. Soc.* 186, 435–455. doi: 10.1093/botlinnean/box083

IUCN (2021). *The IUCN red list of threatened species, Version 2021-1*. Available online at: www.iucnredlist.org

Jacquemyn, H., Brys, R., Vandepitte, K., Honnay, O., Roldan Ruiz, I., and Wiegand, T. (2007). A spatially explicit analysis of seedling recruitment in the terrestrial orchid *Orchis purpurea*. *New Phytol.* 176, 448–459. doi: 10.1111/j.1469-8137.2007.02179.x

Jacquemyn, H., Duffy, K. J., and Selosse, M. A. (2017). "Biogeography of orchid mycorrhizas," in *Biogeography of Mycorrhizal Symbiosis*, ed L. Tedersoo (Cham: Springer International), 159–177. doi: 10.1007/978-3-319-56363-3_8

Jersakova, J., and Malinova, T. (2007). Spatial aspects of seed dispersal and seedling recruitment in orchids. *New Phytol.* 176, 237–241. doi: 10.1111/j.1469-8137.2007.02223.x

Jiang, J., Zhang, K., Cheng, S., Nie, Q., Zhou, S. X., Chen, Q., et al. (2019). *Fusarium oxysporum* KB-3 from *Bletilla striata*: an orchid mycorrhizal fungus. *Mycorrhiza* 29, 531–540. doi: 10.1007/s00572-019-00904-3

Johnson, D., Martin, F., Cairney, J. W. G., and Anderson, I. C. (2012). The importance of individuals: intraspecific diversity of mycorrhizal plants and fungi in ecosystems. *New Phytol.* 194, 614–628. doi: 10.1111/j.1469-8137.2012.04087.x

Johnson, T. R. (2011). *Developing a Model of Orchid Seed Germination: In Vitro Studies of the Threatened Florida Species Bletia purpurea*. Florida: University of Florida Press.

Julou, T., Burghardt, B., Gebauer, G., Berveiller, D., Damesin, C., and Selosse, M. A. (2005). Mixotrophy in orchids: insights from a comparative study of green individuals and nonphotosynthetic individuals of *Cephalanthera damasonium*. *New Phytol.* 166, 639–653. doi: 10.1111/j.1469-8137.2005.01364.x

Jusaitis, M., and Sorensen, B. (1993). Germination of *Pterostylis arenicola* - an endangered greenhood orchid from south Australia. *Sch. Disp.* 11, 18–22.

Keppel, G., Gillespie, T. W., Ormerod, P., and Fricker, G. A. (2016). Habitat diversity predicts orchid diversity in the tropical south-west Pacific. *J. Biogeogr.* 43, 2332–2342. doi: 10.1111/jbi.12805

Kottke, I., Pablo Suarez, J., Herrera, P., Cruz, D., Bauer, R., Haug, I., et al. (2010). Atractiellomycetes belonging to the 'rust' lineage (Pucciniomycotina) form mycorrhizae with terrestrial and epiphytic neotropical orchids. *P. Roy. Soc. B-Biol. Sci.* 277, 1289–1298. doi: 10.1098/rspb.2009.1884

Liu, H., Luo, Y. B., and Liu, H. X. (2010). Studies of mycorrhizal fungi of Chinese orchids and their role in orchid conservation in China—a review. *Bot. Rev.* 76, 241–262. doi: 10.1007/s12229-010-9045-9

Liu, Q., Chen, J., Corlett, R. T., Fan, X. L., Yu, D. L., Yang, H. P., et al. (2015). Orchid conservation in the biodiversity hotspot of southwestern China. *Conserv. Biol.* 29, 1563–1572. doi: 10.1111/cobi.12584

Martos, F., Munoz, F., Pailler, T., Kottke, I., Gonneau, C., and Selosse, M. A. (2012). The role of epiphytism in architecture and evolutionary constraint within mycorrhizal networks of tropical orchids. *Mol. Ecol.* 21, 5098–5109. doi: 10.1111/j.1365-294X.2012.05692.x

Masuhara, G., and Katsuya, K. (1994). *In situ* and *in vitro* specificity between Rhizoctonia spp. and Spiranthes sinensis (Persoon). Ames, var. Amoena (M. bieberstein). hara (Orchidaceae). *New Phytol.* 127, 711–718. doi: 10.1111/j.1469-8137.1994.tb02974.x

McCormick, M. K., and Jacquemyn, H. (2014). What constrains the distribution of orchid populations? *New Phytol.* 202, 392–400. doi: 10.1111/nph.12639

McCormick, M. K., Lee Taylor, D., Juhaszova, K., Burnett, R. K., Jr., Whigham, D. F., and O'Neill, J. P. (2012). Limitations on orchid recruitment: not a simple picture. *Mol. Ecol.* 21, 1511–1523. doi: 10.1111/j.1365-294X.2012.05468.x

McCormick, M. K., Whigham, D. F., and Canchani Viruet, A. (2018). Mycorrhizal fungi affect orchid distribution and population dynamics. *New Phytol.* 219, 1207–1215. doi: 10.1111/nph.15223

Mckendrick, S. L. (1995). The effects of herbivory and vegetation on laboratory-raised *Dactylorhiza praetermissa* (Orchidaceae) planted into grassland in southern England. *Biol. Conserv.* 73, 215–220. doi: 10.1016/0006-3207(94)00111-3

Meng, Y. Y., Fan, X. L., Zhou, L. R., Shao, S. C., Liu, Q., Selosse, M. A., et al. (2019a). Symbiotic fungi undergo a taxonomic and functional bottleneck during orchid seeds germination: a case study on *Dendrobium moniliforme*. *Symbiosis* 79, 1–8. doi: 10.1007/s13199-019-00647-x

Meng, Y. Y., Shao, S. C., Liu, S. J., and Gao, J. Y. (2019b). Do the fungi associated with roots of adult plants support seed germination? A case study on Dendrobium exile (Orchidaceae). *Glob. Ecol. Conserv*. 17:E00582. doi: 10.1016/j.gecco.2019.e00582

Meng, Y. Y., Zhang, W. L., Selosse, M. A., and Gao, J. Y. (2019c). Are fungi from adult orchid roots the best symbionts at germination? A case study. *Mycorrhiza* 29, 541–547. doi: 10.1007/s00572-019-00907-0

Merckx, V., Bidartondo, M. I., and Hynson, N. A. (2009). Myco-heterotrophy: when fungi host plants. *Ann. Bot.* 104, 1255–1261. doi: 10.1093/aob/mcp235

Mounce, R., Smith, P., and Brockington, S. (2017). *Ex situ* conservation of plant diversity in the world's botanic gardens. *Nat. Plants* 3, 795–802. doi: 10.1038/s41477-017-0019-3

Oldfield, S. F. (2009). Botanic gardens and the conservation of tree species. *Trends Plant Sci.* 14, 581–583. doi: 10.1016/j.tplants.2009.08.013

Perkins, A., Masuhara, G., and McGee, P. (1995). Specificity of the associations between *Microtis parviflora* (Orchidaceae) and its mycorrhizal fungi. *Aust. J. Bot.* 43, 85–91. doi: 10.1071/BT9950085

Peterson, R. L., Massicotte, H. B., and Melville, L. H. (2004). *Mycorrhizas: Anatomy and Cell Biology*. Ottawa, Canada: National Research Council Research Press.

Prieto, I., Violle, C., Barre, P., Durand, J. L., Ghesquiere, M., and Litrico, I. (2015). Complementary effects of species and genetic diversity on productivity and stability of sown grasslands. *Nat. Plants* 1, 1–5. doi: 10.1038/nplants.2015.33

Rasmussen, H. N. (1995). *Terrestrial Orchids, From Seed to Mycotrophic Plant*. Cambridge: Cambridge University Press. doi: 10.1017/CBO9780511525452

Rasmussen, H. N., Dixon, K. W., Jersáková J., and Těšitelová T. (2015). Germination and seedling establishment in orchids: a complex of requirements. *Ann. Bot.* 116, 391–402. doi: 10.1093/aob/mcv087

Rasmussen, H. N., and Rasmussen, F. N. (2014). Seedling mycorrhiza: a discussion of origin and evolution in orchidaceae. *Bot. J. Linn. Soc.* 175, 313–327. doi: 10.1111/boj.12170

Rasmussen, H. N., and Rasmussen, F. N. (2018). The epiphytic habitat on a living host: reflections on the orchid–tree relationship. *Bot. J. Linn. Soc.* 186, 456–472. doi: 10.1093/botlinnean/box085

Reiter, N., Whitfield, J., Pollard, G., Bedggood, W., Argall, M., Dixon, K., et al. (2016). Orchid re-introductions: an evaluation of success and ecological considerations using key comparative studies from Australia. *Plant Ecol.* 217, 81–95. doi: 10.1007/s11258-015-0561-x

Ren, H., Jian, S., Liu, H., Zhang, Q. M., and Lu, H. F. (2014). Advances in the reintroduction of rare and endangered wild plant species. *Sci. China Life Sci.* 57, 603–609. doi: 10.1007/s11427-014-4658-6

Roberts, D. L., and Dixon, K. W. (2008). Orchids. *Curr. Biol.* 18, R325–R329. doi: 10.1016/j.cub.2008.02.026

Sathiyadash, K., Muthukumar, T., Karthikeyan, V., and Rajendran, K. (2020). "Orchid mycorrhizal fungi: structure, function, and diversity," in *Orchid Biology: Recent Trends and Challenges*, eds S. Khasim, S. Hegde, M. González-Arnao, and K. Thammasiri (Singapore: Springer), 239–280. doi: 10.1007/978-981-32-9456-1_13

Scade, A., Brundrett, M. C., Batty, A. L., Dixon, K. W., and Sivasithamparam, K. (2006). Survival of transplanted terrestrial orchid seedlings in urban bushland habitats with high or low weed cover. *Aust. J. Bot.* 54, 383–389. doi: 10.1071/BT04025

Sebastian, F., Vanesa, S., Eduardo, F., Graciela, T., and Silvana, S. (2014). Symbiotic seed germination and protocorm development of *Aa achalensis* Schltr., a terrestrial orchid endemic from Argentina. *Mycorrhiza* 24, 35–43. doi: 10.1007/s00572-013-0510-2

Selosse, M. A. (2014). The latest news from biological interactions in orchids: in love, head to toe. *New Phytol.* 202, 337–340. doi: 10.1111/nph.12769

Selosse, M. A., Faccio, A., Scappaticci, G., and Bonfante, P. (2004). Chlorophyllous and achlorophyllous specimens of *Epipactis microphylla* (Neottieae, Orchidaceae) are associated with ectomycorrhizal Septomycetes, including truffles. *Microb. Ecol.* 47, 416–426. doi: 10.1007/s00248-003-2034-3

Selosse, M. A., and Martos, F. (2014). Do chlorophyllous orchids heterotrophically use mycorrhizal fungal carbon? *Trends Plant Sci.* 19, 683–685. doi: 10.1016/j.tplants.2014.09.005

Selosse, M. A., Minasiewicz, J., and Boullard, B. (2017). An annotated translation of Noel Bernard's 1899 article 'on the germination of *Neottia nidus-avis*. *Mycorrhiza* 27, 611–618. doi: 10.1007/s00572-017-0774-z

Shao, S. C., Burgess, K. S., Cruse Sanders, J. M., Liu, Q., Fan, X. L., and Gao, J. (2017). Using *in situ* symbiotic seed germination to restore over-collected medicinal orchids in southwest China. *Front. Plant Sci.* 8:888. doi: 10.3389/fpls.2017.00888

Shao, S. C., Mohandass, D., and Gao, J. Y. (2018). *In situ* symbiotic seed germination in *Dendrobium* spp. (Orchidaceae): implications for orchid restoration. *Cah. Soc. Fr. Orch.* 9, 36–46.

Shao, S. C., Wang, Q. X., Beng, K., Zhao, D. K., and Jacquemyn, H. (2020). Fungi isolated from host protocorms accelerate symbiotic seed germination in an endangered orchid species (*Dendrobium chrysotoxum*) from southern China. *Mycorrhiza* 30, 529–539. doi: 10.1007/s00572-020-00964-w

Shao, S. C., Xi, H. P., and Mohandass, D. (2019). Symbiotic mycorrhizal fungi isolated via *ex situ* seed baiting induce seed germination of *Dendrobium catenatum* Lindl. (Orchidaceae). *Appl. Ecol. Environ. Res.* 17, 9753–9771. doi: 10.15666/aeer/1704_97539771

Smith, S. E., and Read, D. J. (2008). *Mycorrhizal Symbiosis*. London: Academic Press.

Steinfort, U., Verdugo, G., Besoain, X., and Cisternas, M. A. (2010). Mycorrhizal association and symbiotic germination of the terrestrial orchid *Bipinnula fimbriata* (Poepp.) Johnst (Orchidaceae). *Flora* 205, 811–817. doi: 10.1016/j.flora.2010.01.005

Stewart, S. L., Zettler, L. W., Minso, J., and Brown, P. M. (2003). Symbiotic germination and reintroduction of *Spiranthes brevilabris* Lindley, an endangered orchid native to Florida. *Selbyana* 24, 64–70. doi: 10.2307/41750957

Stöckel, M., Těšitelová, T., Jersáková, J., Bidartondo, M. I., and Gebauer, G. (2014). Carbon and nitrogen gain during the growth of orchid seedlings in nature. *New Phytol.* 202, 606–615. doi: 10.1111/nph.12688

Swarts, N. D., and Dixon, K. W. (2009). Terrestrial orchid conservation in the age of extinction. *Ann. Bot.* 104, 543–556. doi: 10.1093/aob/mcp025

Tesitelova, T., Tesitel, J., Jersakova, J., Rihova, G., and Selosse, M. A. (2012). Symbiotic germination capability of four *Epipactis* species (Orchidaceae) is broader than expected from adult ecology. *Am. J. Bot.* 99, 1020–1032. doi: 10.3732/ajb.1100503

Vujanovic, V., and Vujanovic, J. (2007). Mycovitality and mycoheterotrophy: where lies dormancy in terrestrial orchid and plants with minute seeds? *Symbiosis* 44, 93–99.

Wang, Q. X., Shao, S. C., Su,Y., Hu X, Shen, Y., and Zhao, D. K. (2019). A novel case of autogamy and cleistogamy in *Dendrobium wangliangii*: a rare orchid distributed in the dry-hot valley. *Ecol. Evol.* 9, 12906–12914. doi: 10.1002/ece3.5772

Waud, M., Brys, R., Van Landuyt, W., Lievens, B., and Jacquemyn, H. (2017). Mycorrhizal specificity does not limit the distribution of an endangered orchid species. *Mol. Ecol.* 26, 1687–1701. doi: 10.1111/mec.14014

Weiβ, M., Waller, F., Zuccaro, A., and Selosse, M. A. (2016). Sebacinales - one thousand and one interactions with land plants. *New Phytol.* 211, 20–40. doi: 10.1111/nph.13977

Willis, K. J. (2017). State of the world's plants report-2017. Royal Botanic Gardens, Kew.

Wu, K. L., Zeng, S. J., Lin, D. N., Teixeira da Silva, J. A., Bu, Z. Y., Zhang, J. X., et al. (2014). *In vitro* propagation and reintroduction of the endangered *Renanthera imschootiana* Rolfe. *PLoS ONE* 9:e110033. doi: 10.1371/journal.pone.0110033

Xu, J. T., and Guo, S. X. (1989). Fungus associated with nutrition of seed germination of *Gastrodia elata-Mycena osmundicola* Lange. *Acta Mycol. Sinica* 8, 221–226.

Yang, F. S., Sun, A. H., Zhu, J., Downing, J., Song, X. Q., and Liu, H. (2017). Impacts of host trees and sowing conditions on germination success and a simple *ex situ* approach to generate symbiotic seedlings of a rare epiphytic orchid endemic to Hainan island, China. *Bot. Rev.* 83, 74–86. doi: 10.1007/s12229-017-9178-1

Yeh, C. M., Chung, K., Liang, C. K., and Tsai, W. C. (2019). New insights into the symbiotic relationship between orchids and fungi. *Appl Sci* 9:585. doi: 10.3390/app9030585

Yeung, E. C. (2017). A perspective on orchid seed and protocorm development. *Bot. Stud.* 58:33. doi: 10.1186/s40529-017-0188-4

Zelmer, C., and Currah, R. (1997). Symbiotic germination of *Spiranthes lacera* (Orchidaceae). with a naturally occurring endophyte. *Lindleyana* 12, 142–148.

Zeng, S. J., Wu, K., da Silva, J. A. T., Zhang, J., Chen, Z., Xia, N., et al. (2012). Asymbiotic seed germination, seedling development and reintroduction of *Paphiopedilum wardii* Sumerh., an endangered terrestrial orchid. *Sci. Hortic.* 138, 198–209. doi: 10.1016/j.scienta.2012.02.026

Zettler, L. W. (1997). Terrestrial orchid conservation by symbiotic seed germination: techniques and perspectives. *Selbyana* 18, 188–194.

Zettler, L. W., Poulter, S. B., McDonald, K. I., and Stewart, S. L. (2007). Conservation-driven propagation of an epiphytic orchid (*Epidendrum nocturnum*) with a mycorrhizal fungus. *HortScience* 42, 135–139. doi: 10.21273/HORTSCI.42.1.135

Zhang, G. Q., Liu, K. W., Li, Z., Lohaus, R., Hsiao, Y. Y., Niu, S. C., et al. (2017). The *Apostasia* genome and the evolution of orchids. *Nature* 549, 379–383. doi: 10.1038/nature23897

Zi, X. M., Sheng, C. L., Goodale, U. M., Shao, S. C., and Gao, J. Y. (2014). *In situ* seed baiting to isolate germination-enhancing fungi for an epiphytic orchid, *Dendrobium aphyllum* (Orchidaceae). *Mycorrhiza* 24, 487–499. doi: 10.1007/s00572-014-0565-8

Zotz, G. (2013). The systematic distribution of vascular epiphytes–a critical update. *Bot. J. Linn. Soc.* 171, 453–481. doi: 10.1111/boj.12010

Disclaimer: The authors alone are responsible for the content and functionality of these materials.

Conflict of Interest: The authors declare that the research was conducted in the absence of any commercial or financial relationships that could be construed as a potential conflict of interest.

frontiers in Plant Science

ORIGINAL RESEARCH
published: 26 July 2021
doi: 10.3389/fpls.2021.640789

Coupling Between the Responses of Plants, Soil, and Microorganisms Following Grazing Exclusion in an Overgrazed Grassland

Zhen Wang[1†], Xiliang Li[1†], Baoming Ji[2], Paul C. Struik[3], Ke Jin[1] and Shiming Tang[4*]*

[1] National Agricultural Experimental Station for Soil Quality, Institute of Grassland Research, Chinese Academy of Agricultural Sciences, Ministry of Agriculture, Hohhot, China, [2] The College of Forestry, Beijing Forestry University, Beijing, China, [3] Centre for Crop Systems Analysis, Department of Plant Sciences, Wageningen University & Research, Wageningen, Netherlands, [4] Department of Ecology, School of Ecology and Environment, Inner Mongolia University, Hohhot, China

OPEN ACCESS

Edited by:
Sabine Dagmar Zimmermann, Délégation Languedoc Roussillon (CNRS), France

Reviewed by:
Fan Wu, Chinese Academy of Sciences (CAS), China
Xavier Le Roux, INRAE, France

***Correspondence:**
Ke Jin
jinke@caas.cn
Shiming Tang
tangsm001@126.com

[†] These authors have contributed equally to this work

Specialty section:
This article was submitted to Plant Symbiotic Interactions, a section of the journal Frontiers in Plant Science

Received: 12 December 2020
Accepted: 06 July 2021
Published: 26 July 2021

Citation:
Wang Z, Li X, Ji B, Struik PC, Jin K and Tang S (2021) Coupling Between the Responses of Plants, Soil, and Microorganisms Following Grazing Exclusion in an Overgrazed Grassland. Front. Plant Sci. 12:640789. doi: 10.3389/fpls.2021.640789

Grazing exclusion is an effective management practice to restore grassland ecosystem functioning. However, little is known about the role of soil microbial communities in regulating grassland ecosystem functioning during long-term ecosystem restorations. We evaluated the recovery of a degraded semiarid grassland ecosystem in northern China by investigating plant and soil characteristics and the role of soil microbial communities in ecosystem functioning after 22 years of grazing exclusion. Grazing exclusion significantly increased the alpha diversity and changed the community structure of bacteria, but did not significantly affect the alpha diversity or community structure of fungi. The higher abundance of copiotrophic *Proteobacteria* and *Bacteroidetes* with grazing exclusion was due to the higher carbon and nutrient concentrations in the soil, whereas the high abundance of *Acidobacteria* in overgrazed soils was likely an adaptation to the poor environmental conditions. Bacteria of the *Sphingomonadaceae* family were associated with C cycling under grazing exclusion. Bacteria of the *Nitrospiraceae* family, and especially of the *Nitrospira* genus, played an important role in changes to the N cycle under long-term exclusion of grazing. Quantitative PCR further revealed that grazing exclusion significantly increased the abundance of nitrogen fixing bacteria (*nifH*), ammonia oxidizers (AOA and AOB), and denitrifying bacteria (*nirK* and *nosZ*1). Denitrifying enzyme activity (DEA) was positively correlated with abundance of denitrifying bacteria. The increase in DEA under grazing exclusion suggests that the dependence of DEA on the availability of NO_3^- produced is due to the combined activity of ammonia oxidizers and denitrifiers. Our findings indicate that decades-long grazing exclusion can trigger changes in the soil bacterial diversity and composition, thus modulating the restoration of grassland ecosystem functions, carbon sequestration and soil fertility.

Keywords: overgrazing, grazing exclusion, bacteria, fungi, community structure

INTRODUCTION

Livestock grazing is a common grassland management practice with far-ranging societal and environmental impacts. However, the effect of grazing on grassland ecosystem functioning primarily depends on the initial grazing intensity (Bardgett and Wardle, 2003). Overgrazing has been found to cause degradation of grassland ecosystem functioning and to reduce both plant productivity and soil fertility, resulting in nutrient depleted initial systems (Bardgett and Wardle, 2003; Chartier et al., 2013; Li et al., 2016; Yang et al., 2019). Grazing exclusion is an effective grassland management practice aimed at preventing grassland degradation and maintaining grassland ecosystem functions (Wang et al., 2018). Grazing exclusion can promote plant productivity (Deng et al., 2014), species diversity (Wu et al., 2014), soil fertility (Raiesi and Riahi, 2014), and soil microbial activity (Owen et al., 2015). Previous studies reported that approximately 20 years of grazing exclusion would be appropriate for restoring the degraded grasslands in northern China in terms of productivity and C and N storage (Qiu et al., 2013). Microbes are important contributors to the structure and functioning of ecosystems (Buyer et al., 2010); they drive nutrient transport and cycling in the soil (Wang Z. et al., 2019). However, there is not much literature reporting on the cumulative effects of long-term continuous overgrazing on the soil microbial community, and the role of the soil microbial community in the temporal progression of recovery from overgrazing remains unclear.

Grazing exclusion can have multiple effects on interactions among the soil microbiome, plant community and soil properties (Yang et al., 2018; Zhang X. et al., 2019). The plant community is an important driver during ecosystem restoration, affecting soil physicochemical properties by altering the input of litter, soil turnover of roots, and root exudation (Fry et al., 2016). In turn, the change in soil physicochemical properties influences the microbial communities (Liu et al., 2018). Microbes may, therefore, impact the growth of the plants in the sward because microbes can drive the transformation of organic substrates and the release of mineral elements during the process of ecosystem restoration (Wang Z. et al., 2019). However, we do not know the extent to which changes in the soil microbial community affect the impact of the grazing exclusion on plant growth and soil physicochemical properties.

On the other hand, soil microbial communities play an important role in biogeochemical processes, especially the N cycle. Microbes can support the N cycle via many of the critical processes, including nitrogen fixation, assimilation, nitrification and denitrification (Yang et al., 2013). Although grazing can strongly influence these N processes and related microbial groups (Patra et al., 2005; Xu et al., 2008; Xie et al., 2014), the effects of grazing on N cycling and microbial groups depend on its intensity (Bardgett and Wardle, 2003). Grazing exclusion eliminates the intake of livestock, which often leads to an increase in soil C and N storage, mainly due to the accumulation of plant litter on the soil surface (Wang Z. et al., 2019). The high soil N content under grazing exclusion increased soil ammonia availability, and substantially impacted the activity and communities of ammonia oxidizers (e.g., AOA, ammonia-oxidizing archaea; AOB, ammonia-oxidizing bacterial) (Lou et al., 2011). As a result of the change in nitrification [ammonium (NH_4^+) is converted to nitrite (NO_2^-) and then to nitrate (NO_3^-)], there is a change in the soil N cycle (Philippot et al., 2011).

Moreover, appropriate restoration (approximately 20 years of grazing exclusion) reduces soil compaction by avoiding animal trampling, which results in increased soil aeration and water-holding capacity (Kauffman et al., 2004; Blagodatsky and Smith, 2012). The denitrification activities of bacteria are suppressed in the presence of either NO_3^- or NO_2^- when animal trampling is avoided due to the changes in soil aeration (Hayatsu et al., 2008), which are linked to nitrite reductase and nitrous oxide reductase encoded by *nirK*, *nirS*, and *nosZ*1 (Pan et al., 2016). Therefore, further research is needed to investigate the mechanisms behind the influence of ecosystem rehabilitation on soil microbial community structure and function, especially related to the N cycle.

In this study, we investigate the long-term impact of grazing exclusion on the structure and functioning of soil microbial communities during ecosystem recovery. Considering the water-limited and oligotrophic environmental conditions in the semi-arid steppe (Pan et al., 2016; Wang Z. et al., 2019), the objectives of the current study were to analyze (1) which main environmental factors drive the shift of soil microbiome (bacterial or fungal community) during the recovery of a degraded ecosystem after the release of grazing pressure; and (2) whether the changes in the composition of soil microbial communities play a large role in the recovery of the biogeochemical function.

MATERIALS AND METHODS

Study Area

The field experiment was carried out at the Inner Mongolia Grassland Ecosystem Research Station (N 43°35′30″ to 43°35′42″, E 116°42′20″ to 116°42′35″, **Figure 1**), which represents the semiarid steppe ecosystem. The long-term mean annual precipitation (1953–2009) was 335 mm, with more than 70% of precipitation falling during the growing season (May−August). The mean annual temperature is 0.4°C, ranging from the lowest monthly average temperature of −21.4°C in January to the highest of 18.0°C in July. The soil is classified as Calcic Chernozems (IUSS Working Group WRB, 2006), with similar physiochemical properties of chestnuts and calcic chernozems in a previous study (Steffens et al., 2008). The basic soil properties of the study areas were found to comprise 17.3% clay, 34.8% silt and 47.9% sand by using the hydrometer method (Kettler et al., 2001), the soil organic carbon (SOC) was 21.10 g kg^{-1} assessed using dichromate oxidation (Nelson and Sommers, 1982) and soil total nitrogen (TN) content was 1.85 g kg^{-1} assessed using an automatic Kjeldahl instrument (Kjeltec 8400, FOSS Corporation, Denmark).

Experimental Design and Sampling

To explore the role of grazing exclusion on grassland ecosystem function, we compared the soil community in grazed plots

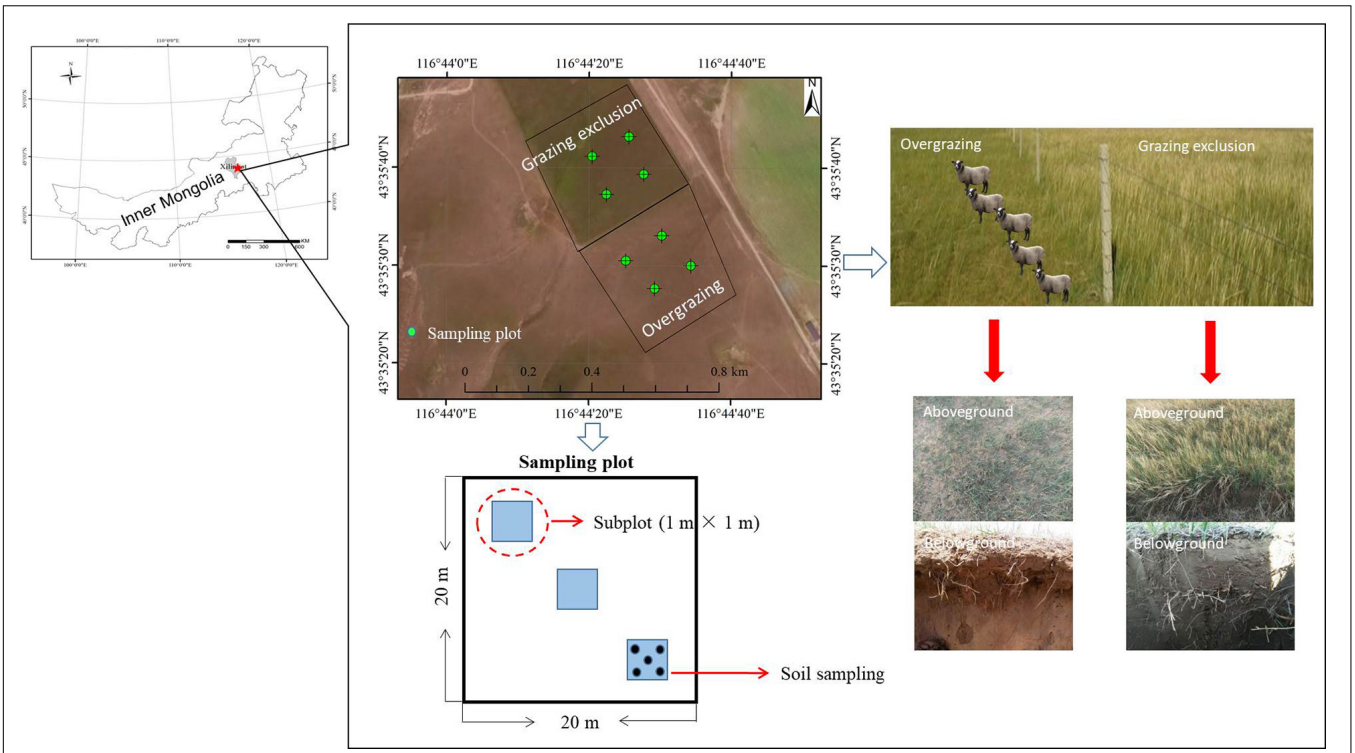

FIGURE 1 | Effect of overgrazing and grazing exclusion on the semiarid steppe.

where grazing had been eliminated for 22 years. Our study was established as a pair of large-scale plots which involved pseudo-replication limited in space-for-time substitution. However, this challenge is surmountable as has been reported in previous ecological studies (Walker et al., 2010; Blois et al., 2013; Lü et al., 2015). Grazing and grazing exclusion plots had similar soil types, topographies, altitudes, slope gradients and slope aspects (**Supplementary Table 1**). The grazed plots were located adjacent to the grazing exclusion (or restoration) plots, and had been grazed year-round for more than 30 years. Grazing begins in early-June and ends in early-October. The stocking rate in the grazing plots was approximately 3 sheep ha^{-1} y^{-1}, which was two times higher than the local stocking rate of 1.5 sheep ha^{-1} y^{-1} (Li et al., 2015). The dominant plant species in the grazing site were *Stipa grandis* (grass), *Artemisia frigida,* (forb), and *Cleistogenes polyphylla* (grass) (**Supplementary Table 2** and **Supplementary Figure 1**), while the grazing exclusion site was dominated by *Leymus chinensis* (grass) and *Stipa grandis* (grass) after 22 years of restoration (**Supplementary Figure 1**). Bare soil increased by 24.25% under overgrazing in our study.

Four 20 m × 20 m plots were randomly established at each site, using a paired sampling method within the overgrazed and grazing exclusion treatments (**Figure 1**). The two sites were never fertilized or mowed during the management. The plots were randomly assigned within 200 m of each other. Three 1 m × 1 m subplots were established along a transect within each plot for investigation and sampling in mid-August 2018. In the middle of August during peak biomass, we measured vegetation ground coverage, aboveground net primary productivity (ANPP), plant height, and species richness (SR). All aboveground plant materials were harvested to the ground surface (including living aboveground biomass, standing litter, and ground litter) in the quadrat (1 m × 1 m). We separated plant aboveground tissue (living aboveground biomass) from standing litter of the previous year and litter on the ground. We used the Shannon—Wiener index ($H = -\Sigma P_i \ln P_i$) and plant species richness to estimate the diversity of the plant communities, where P_i is the ratio of the coverage of each species to the coverage of all species. Harvested biomass was determined by drying the aboveground tissues at 65°C for 48 h (Wang et al., 2014). Aboveground net primary productivity (ANPP) was calculated as the sum of the aboveground biomass for all plant species (Wang et al., 2016). Soil bulk density (BD) was measured by using the USDA (1972) method. Five soil cores (3.5 cm in diameter) were extracted and segmented in depth increments of 0–5, 5–10, 10–15, and 15–20 cm. The core was composited at different depth increments, air-dried, then ground until passable through a 2-mm screen. Soil samples were collected from the top 20 cm of the soil profile as soil cores (3.5 cm in diameter). Five soil cores were collected from each subplot after removing aboveground biomass, and then a total of 15 soil cores (five each from three subplots) were combined to make one composite sample. We eliminated roots, stones, litter, and debris from each soil sample by using a 2-mm sieve, before field storage and transport to the laboratory on ice in a cooler. The composite soil samples were divided into three subsamples. The first subsample was air dried

for physicochemical analysis. The second subsample was stored at 4°C to determine soil NH_4^+ and NO_3^- concentrations and transported to the laboratory for immediate analysis, as well as for microbial C and N biomass determination. The third subsample was stored at −80°C for DNA extraction.

Analysis of Soil Physicochemical Properties

Soil water content (SW) of each composite soil sample was measured by weighing before and after drying at 105°C for 24 h. Soil pH was determined by shaking a soil/water suspension (1:1 weight/vol, DI water) for 30 min (Fierer et al., 2006). Soil organic carbon (SOC) was measured using dichromate oxidation (Nelson and Sommers, 1982). The total nitrogen content (TN) was determined using an automatic Kjeldahl instrument (Kjeltec 8400, FOSS Corporation, Denmark). The NH_4^+ and NO_3^- concentrations in the soil subsamples were determined by digestion with 2 mol L^{-1} KCl at a 1:3 ratio (w:v) and analyzed by a flow injection analyzer (FIAstar 5000, FOSS Analytical, Höganäs, Sweden). Soil available phosphorus (AP) was measured using the Kelowna method as described by Van Lierop (1988) using a solid to liquid ratio of 1:5. The soil total phosphorus concentration (TP) in the extracting solution was measured using an Astoria auto-analyzer (Clackamas, OR, United States).

Soil Microbial Biomass and Enzymatic Activities

We used a fumigation extraction method to measure the soil microbial C and N biomass (Vance et al., 1987). We fumigated 25 g of the oven-dry equivalent of field-moist at 25.8°C for 24 h with $CHCl_3$. The soil was added to 100 ml of 0.5 M potassium sulfate, shaken at 200 rpm for 1 h, and then filtered (0.2 μm) after removing the fumigant. An additional 25 g of non-fumigated soil was simultaneously extracted. The soil organic carbon (SOC) and soil total nitrogen (TN) contents of the extracts were measured using a Liqui TOCII analyzer (Elementar Analyses system, Hanau, Germany).

Urease activity was measured using a urea solution as the substrate and incubation at 37°C for 24 h (a spectrophotometer was employed to determine the NH_4^+-N concentration at 578 nm) (Nannipieri et al., 1980). Nitrate reductase activity was determined using KNO_3 solution as the substrate and incubation at 25°C for 24 h (a spectrophotometer was employed to determine the NO_2^- concentration at 520 nm) (Daniel and Curran, 1981).

The potential nitrification rate (PNR) was assessed according to the procedures described in Kurola et al. (2005). Twenty mL of phosphate buffered saline (PBS) solution was added as substrate to 5 g of fresh soil in a 50 mL centrifuge tube with 1 mmol L^{-1} $(NH_4)_2SO_4$ (100 ppm N), and then the centrifuge tubes were placed at room temperature in the dark for 24 h. Eight grams NaCl, 0.2 g KCl, 0.2 g Na_2HPO_4 and 0.2 g NaH_2PO_4 were mixed in about 800 mL of water as PBS solution (pH = 7.1). To inhibit nitrite oxidation, potassium chlorate (at a final concentration of 10 mmol L^{-1}) was then added to the centrifuge tubes. After incubation, 5 mL of 2 mol L^{-1} KCl was added to the tubes to extract NO_2-N. After centrifugation, the sulfonamide and naphthalene oxalamide were used as reagents to analyze the optical density of the supernatant by the presence of NO_2-N at 545 nm.

Soil denitrifying enzyme activity (DEA) was measured according to the method of Hart et al. (1994). A fresh soil sample (equivalent to 15 g dry soil) was added to a 250 ml plasma flask with a 100 mL solution of 1.5 mM $(NH_4)_2SO_4$ (100 ppm N) and 1 mM phosphate buffer (pH = 7.2). The flask was incubated at room temperature with continuously stirring (180 rpm). Samples were extracted at 2, 4, 8, 12, and 24 h during incubation. The concentrations of NO_2^- and NO_3^- were measured in the samples by using a continuous flow analyzer. The DEA rate was calculated based on the slope of the regression of NO_2^- plus NO_3^- concentration against time.

Soil DNA Extraction and Sequencing

Before sequencing the 16S rRNA and internal transcribed spacer (ITS) gene sequences, all soil composite samples (0.5 g) were processed for DNA extraction with the FAST DNA Spin Kit for Soil (MP Biomedicals, Santa Ana, CA, United States) according to the manufacturer's instructions. Two separate DNA extractions from 0.5 g of soil were then merged together for polymerase chain reaction (PCR) amplification. The bacterial PCR primers were 515F (5′-GTGCCAGCMGCCGCGGTAA-3′) and 806R (5′-GGACTACHVGGGTWTCTAAT-3′) with the target 16S V4 region (Zheng et al., 2018). The fungal ITS1 region was amplified using the primers ITS5-1737F (5′-GGAAGTAAAAGTCGTAACAAGG-3′) and ITS2-2043R (5′-GCTGCGTTCTTCATCGATGC-3′) (Bellemain et al., 2010). Both sets of primers contained a 6-bp error-correcting barcode (8 – 4 for overgrazing and 4 for grazing exclusion) that was unique to each sample for the identification of individual samples in mixture Illumina HiSeq sequencing runs (Novogene Bioinformatics Technology Co., Ltd., Beijing, China). PCR amplicons were further purified with a DNA purification kit (BioFlux, Japan), and the concentrations were determined using spectrometry (NanoDrop-1000, United States). Amplicons from different samples were then mixed and purified with Qiagen Gel Extraction Kit (Qiagen, Germany) to achieve equal mass concentrations in the final mixture, and sent to Novogene Co., Ltd., Tianjing, China, for sequencing library construction and pair-end sequencing using the Illumina HiSeq sequencing system (Illumina, United States). All amplicon sequencing data have been deposited in the NCBI SRA under the accession number PRJNA695426 (bacteria) and PRJNA695427 (fungi). After sequencing, 250 bp paired-end reads were generated and assigned to samples based on their unique barcode sequence, followed by cutting off the barcode and primer sequence. Paired-end reads were merged using FLASH (V1.2.7) (Magoč and Salzberg, 2011). Quality filtering (Bokulich et al., 2013) was performed to obtain only the high-quality clean tags according to the QIIME quality control process (V1.7.0) (Caporaso et al., 2010). Chimera sequences were removed by comparing with the reference database (Gold database) using the UCHIME algorithm (Edgar, 2013). Sequences with ≥97% similarity were assigned to the same operational taxonomic unit (OTU). The SILVA (bacteria) and UNITE (fungi) databases were used to assign

taxonomic information to each OTU representative sequence. OTU abundance information was normalized using a standard sequence number corresponding to the sample with the least number of sequences (44,254 for bacteria and 37,223 for fungi) and used for subsequent analysis of alpha diversity and beta diversity (**Supplementary Figure 2**).

Real-Time Quantitative PCR

We quantified the amount of the target sequence in genomic DNA by using real-time quantitative PCR. After the quality control, nitrogen-fixing genes were quantified using different primers. The primer pairs and thermal-cycling conditions of real-time quantitative PCR are described in detail in **Supplementary Table 3**. The total bacterial community was quantified using the 16S rRNA gene (34lF/534R). The total fungal community was quantified using the ITS gene (ITS4/ITS5). The abundances of nitrogen-fixing (*nifH*), nitrification (AOA and AOB), and denitrification genes (*nirK*, *nirS,* and *nosZ*1) were obtained for subsequent comparative analysis. The amplification of PCR products was monitored by measuring specific fluorescence signals using the dsDNA-specific fluorescent dye SYBR Green I (measured after the extension phase). The inhibition tests were performed when we ran the qPCR assay. We conducted an inhibition test to determine whether samples were amplified with the same efficiency as the standard. In the qPCR inhibition test, each sample to be tested was spiked with a standard. The Ct value of the spiked sample was then compared with the Ct value of the pure standard. The percent inhibition (or actual % efficiency) was calculated according to the following formula: $1 - [(\text{Ct sample} - \text{Ct standard})/\text{Ct standard}] \times 100$. In our study, a calculated inhibition of 1–2% was observed in some samples and was accepted without dilution. All quantitative PCR reactions were performed in triplicate with an ABI 7900 system. We added Bovine Serum Albumin (BSA) (10 mg/mL) to these PCR reaction mixes to reduce the inhibitory effects of co-extracted polyphenolic soil compounds. Briefly, 10 μL of reaction mixes contained 5 μL Power qPCR PreMix (GENEray, GK8020) and primers, 1 μL BSA, 1 μL 20×-diluted DNA template (1.2–5.0 ng) and 3 μL Milli-Q water. We analyzed the products from quantitative PCR reactions, and only accepted one specific peak of each target sequence in the dissociation curves. A standard curve of DNA copies was created using the concentration on the *X*-axis (in copies/μL of 10-folded dilution series) and CT value on the *Y*-axis (Greilhuber et al., 2005). Every dot represents a CT value from duplication of standard DNA. We performed a linear regression and obtained the logarithm equation from each standard curve. The equation $\text{Eff} = [10^{(-1/slope)} - 1]$ was used to calculate the amplification efficiencies, which resulted in the following values: bacterial 16S rRNA 90%, fungal ITS 91%, *nifH* 92%, AOA-*amoA* 93%, AOB-*amoA* 85%, *nirK* 87%, *nirS* 98%, and *nosZ*1 99%.

Statistical Analysis

Prior to statistical analysis, plant characteristic data in the three 1 m × 1 m subplots were averaged. All of the statistical analyses were conducted using R software (Version 3.2.4) (R Core Team, 2016). Univariate analysis of variance (ANOVA) was used to examine the effects of grazing exclusion on plant characteristics (ANPP and diversity), soil physicochemical metrics (SOC, TN, TP, NH_4^+, NO_3^-, and AP), soil enzymatic activities (urease, nitrate reductase, potential nitrification rate, and denitrifying enzyme activity), soil microbial characteristics (C and N biomass, and diversity), bacterial 16S rRNA, abundance, fungal ITS abundance, and N cycle functional genes (*nifH*, AOA-*amoA*, AOB-*amoA*, *nirK*, *nirS,* and *nosZ*1). A suite of alpha diversity indices, including number of OTUs, Chao1, Shannon–Wiener, Simpson, ACE, and good-coverage, were calculated for analyzing species diversity with QIIME, and visualized with R software. Significance tests were based on Tukey's honestly significant difference (HSD) between any two compared objects. Statistical significance was defined as *P*-values in the Tukey's HSD corrected with the Benjamini-Hochberg false discovery rate.

Additionally, PERMANOVA was used to examine the effects of grazing exclusion on soil bacterial and fungal community compositions based on weighted UniFrac distances. The weighted UniFrac distances were employed to assess whether two communities were different using the QIIME software (Version 1.7.0). A principal coordinate analysis (PCoA) was used to assess the differences in the structures of microbial communities among different grazing treatments based on weighted UniFrac metric matrices using the VEGAN package (Oksanen et al., 2013) in R software (R Core Team, 2016). The relative abundances of different taxa in the bacterial and fungal community compositions between grazing and grazing exclusion were also determined by PERMANOVA using the VEGAN package in R software. The effects of grazing exclusion on the statistical difference between the relative abundance of bacterial and fungal taxa were analyzed using STAMP software. Significance tests were based on unpaired Student's *t*-tests to identify differences between any two compared objects.

Pearson's correlation analyses were conducted to identify the environmental factors accounting for the patterns of microbial alpha diversity (number of OTUs, Chao1, Shannon–Wiener, Simpson, ACE, and good-coverage) and the gene abundances associated with N fixation (*nifH*), nitrification (AOA-*amoA* and AOB-*amoA*) and denitrification (*nirK*, *nirS,* and *nosZ*). Heat maps were generated to show the relationships between the relative abundances of different taxa in soil microbial community compositions (bacterial/fungal) and environmental variables (plant characteristics and soil chemical properties) and microbial C and N biomass. The heat maps were generated in R.3.2.4 using the pheatmap package and the correlation analysis was carried out using the psych package of R.3.2.4. A multivariate regression trees (MRT) analysis was carried out to identify the most important biotic and abiotic factors for bacterial and fungal community composition using the mvpart package (De'Ath, 2002). Stepwise multiple linear analyses were used to examine the relationships between the gene abundances associated with N fixation (*nifH*), nitrification (AOA-*amoA* and AOB-*amoA*), denitrification (*nirK*, *nirS* and *nosZ*1), and soil properties (SW, pH, NH_4^+, NO_3^-, SOC, and TN).

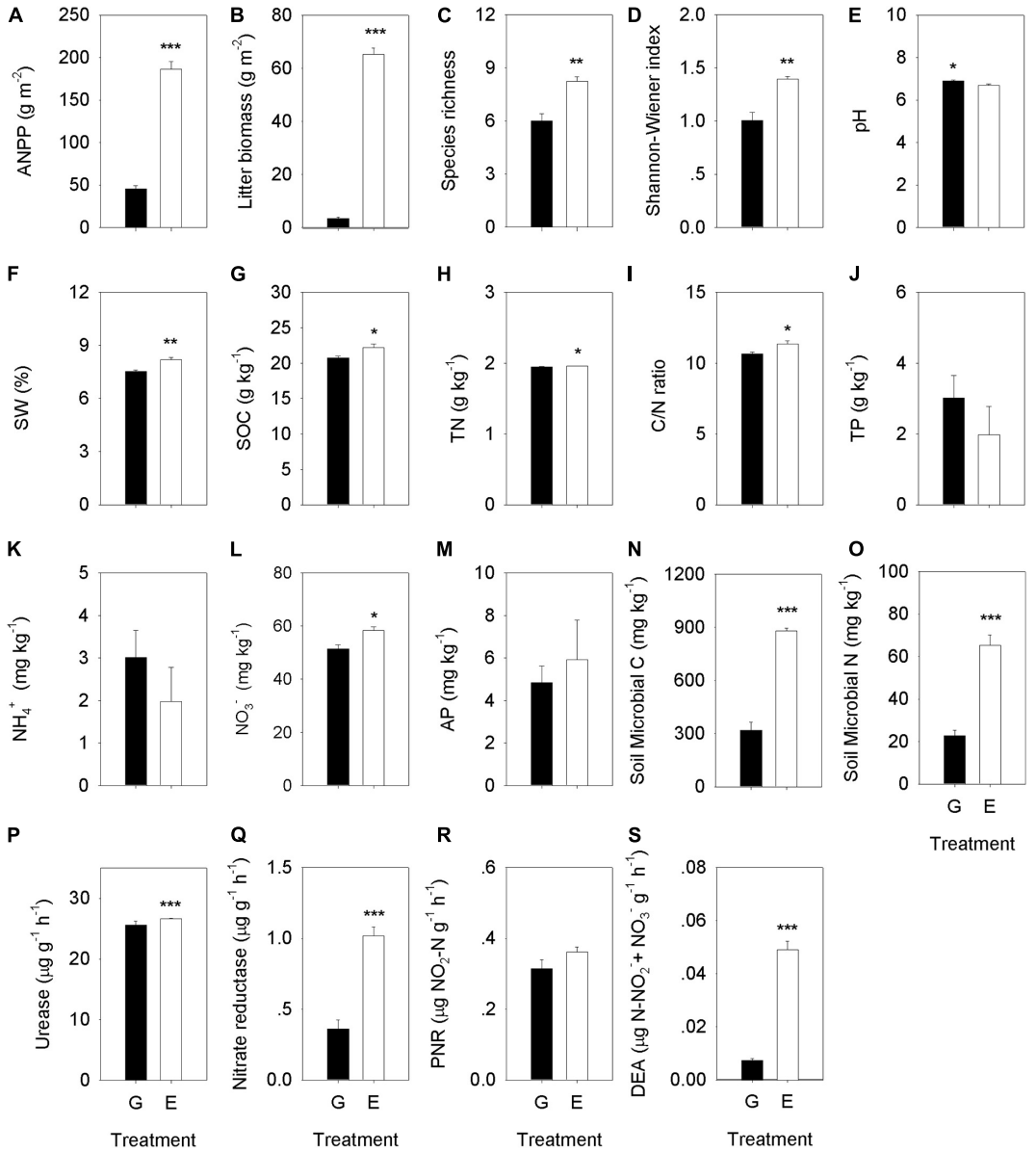

FIGURE 2 | Comparison analysis of the plant community characteristics, soil properties, soil microbial C and N, and soil enzyme activities between the overgrazing and grazing exclusion treatments. Plant community characteristics include **(A)** ANPP, **(B)** litter biomass, **(C)** species richness, and **(D)** Shannon–Wiener index. Soil properties include **(E)** soil pH value, **(F)** soil water content (SW), **(G)** soil organic carbon content (SOC), **(H)** soil total nitrogen content (TN), **(I)** soil C/N ratio, **(J)** soil total phosphorus content (TP), **(K)** soil NH_4^+ content, **(L)** soil NO_3^- content, and **(M)** soil available phosphorus content (AP). Soil microbial biomass include **(N)** microbial C, and **(O)** microbial N. Soil enzyme activities include: **(P)** urease (UR), **(Q)** Nitrate reductase (NR), **(R)** the potential nitrification rate (PNR), and **(S)** soil denitrifying enzyme activity (DEA). G, overgrazing; E, grazing exclusion. Values represent the mean ± standard error (n = 4). Significance levels are indicated as: $^*P < 0.05$, $^{**}P < 0.01$, and $^{***}P < 0.001$.

RESULTS

The Effect of Grazing Exclusion on Plant, Soil, and Microbial Activity

Grazing exclusion significantly changed plant community composition and increased plant species biomass ($P < 0.05$), including *Leymus chinensis* ($P < 0.001$), *Stipa grandis* ($P < 0.001$), *Achnatherum sibiricum* ($P = 0.006$), and *Agropyron cristatum* ($P < 0.001$) (**Supplementary Figure 1**), ANPP ($P < 0.001$), species richness ($P = 0.003$) and the Shannon−Wiener index ($P = 0.003$) (**Figure 2** and **Supplementary Table 4**). Moreover, there was a significantly positive effect of long-term grazing exclusion to soil physicochemical characteristics (**Figure 2**). Grazing exclusion significantly increased SW ($P = 0.007$), SOC ($P = 0.043$), TN ($P = 0.006$), soil C/N ratio ($P = 0.048$), NO_3^- ($P = 0.014$), nitrate reductase activity ($P = 0.003$), and

DEA ($P < 0.001$) (**Figure 2** and **Supplementary Table 4**). Grazing exclusion significantly reduced soil BD at different depth increments, including 0–5 ($P = 0.007$), 5–10 ($P < 0.001$), 10–15 ($P = 0.035$), and 15–20 cm ($P = 0.041$) (**Supplementary Figure 3**).

Effect of Grazing Exclusion on Microbial Biomass and Composition

Grazing exclusion significantly increased soil microbial biomass C ($P < 0.001$) and N ($P < 0.001$) (**Figure 2** and **Supplementary Table 4**). Bacterial alpha diversity was higher in grazing exclusion soils than in overgrazed ones, including higher OTU richness ($P = 0.035$), and higher values for the H' ($P = 0.039$), Chao1 ($P = 0.039$), and ACE diversity ($P = 0.029$) (**Table 1**). However, there were no significant differences in the fungal alpha diversity index between the overgrazing and the grazing exclusion soils (**Table 1**).

The change of relative abundances in bacterial groups revealed shifts in dominant taxa between overgrazing and grazing exclusion ($P < 0.05$, **Figure 3**). The dominant bacterial phyla in the overgrazing and grazing exclusion included *Acidobacteria* (29.13% vs. 18.54%), *Proteobacteria* (22.53% vs. 25.97%), *Verrucomicrobia* (10.57% vs. 12.21%), *Actinobacteria* (10.59% vs. 12.86%), *Gemmatimonadetes* (10.33% vs. 8.51%), *Bacteroidetes* (2.63% vs. 5.80%), *Planctomycetes* (4.95% vs. 3.81%), and *Firmicutes* (4.49% vs. 3.17%; **Figure 3A**). *Acidobacteria* ($P < 0.001$) and *Planctomycetes* ($P < 0.001$) showed greater relative abundance in the overgrazed soils, while *Proteobacteria* ($P = 0.034$), *Actinobacteria* ($P < 0.001$), *Bacteroidetes* ($P = 0.005$), and *Firmicutes* ($P = 0.034$) showed greater abundance in grazing exclusion soils ($P < 0.05$; **Figure 3A**). Grazing exclusion significantly increased the relative abundance of *Betaproteobacteria* ($P = 0.001$) and *Deltaproteobacteria* ($P = 0.015$) (**Supplementary Figure 4**). Compared with overgrazing, grazing exclusion significantly increased the relative abundance of some families, including *Gaiellaceae*, *Solirubrobacteraceae*, *Nocardioidaceae*, and *Conexibacteraceae* (all belonging to the phylum *Actinobacteria*), *Sphingomonadaceae*, *Rhodobiaceae, Polyangiaceae*, *Sinobacteraceae*, and *Haliangiaceae* (all belonging to the phylum *Proteobacteria*), and *Nitrospiraceae* (phylum *Nitrospirae*), but significantly decreased the relative abundance of *mb2424* (phylum *Acidobacteria*) ($P < 0.05$; **Supplementary Figure 5**). Grazing exclusion significantly increased the abundance of some genera, such as *Mycobacterium* (phylum *Actinobacteria*), *Afifella*, *Sphingomonas*, and *Lysobacter* (all belonging to the phylum *Proteobacteria*), and *Nitrospira* (phylum *Nitrospirae*) ($P < 0.05$; **Supplementary Figure 6**).

Compared with overgrazing, grazing exclusion significantly increased the abundance of *Basidiomycota* ($P = 0.039$; **Figure 3B**). Grazing exclusion significantly increased the relative abundance of some families, including *Lasiosphaeriaceae* and *Herpotrichiellaceae* (phylum *Ascomycota*), as well as *Auriscalpiaceae* (phylum *Basidiomycota*) ($P < 0.05$; **Supplementary Figure 7**). The PCoA ordination revealed differences in bacterial communities, which showed a clear separation between overgrazing and grazing exclusion along the first PCoA 1 axis ($P < 0.05$, **Figure 4A**). No difference was found for the fungal community (**Figure 4B**).

Associations of Bacterial and Fungal Diversity With Soil and Plant Properties

In this study, plant characteristics (SR, ANPP, and litter biomass) and soil properties (SOC, C/N ratio, and NO_3^-) were positively related to the alpha diversity indices of the soil bacterial community (the number of OTUs, H', Chao1 and ACE) ($P < 0.05$, **Supplementary Table 5**). For bacterial communities, significant correlations based on heat map analyses were found between soil or plant characteristics and bacterial taxa (except *Chloroflexi*) (**Figure 5A**). For fungal communities, no significant relationship was found between environmental factors (except SW) and fungal taxa (**Figure 5B**). MRT analysis was used to explain the relative effects of plant and soil properties on the bacterial and fungal community composition from all samples (**Figures 5C,D**). A visual tree in the MRT analysis showed two splits in the bacterial community based on plant and soil properties (**Figure 5C**; cross-validated relative error 1.27 and 0.742, respectively), whereas fungal community composition showed three splits in a visual tree (**Figure 5D**; cross-validated relative error 1.16 and 0.510, respectively). SOC was the major factor affecting soil bacterial community composition and explained 70.47% of the variation (**Figure 5C**). SW and SOC together explained 91.66% of the variation in fungal community composition (**Figure 5D**), and we found that SW (which explained 81.70%) was the key factor affecting changes in the fungal community composition.

Effect of Grazing Exclusion on the Abundances of Microbial Groups

A significant difference between overgrazed and grazing exclusion soils was found for bacterial 16S rRNA gene copy numbers and six key functional N gene families (nitrification, denitrification and N fixation) ($P < 0.05$; **Figure 6**). The grazing exclusion significantly increased the bacterial 16S rRNA gene copy numbers and *nifH* gene abundance ($P = 0.003$; **Figure 6**). For nitrification genes, the abundances of AOA-*amoA* ($P < 0.001$) and AOB-*amoA* ($P = 0.014$) both increased in the grazing exclusion soils (**Figure 6**). For denitrification genes, the grazing exclusion significantly increased the abundance of the *nirK* ($P = 0.007$) and *nosZ*1 ($P = 0.008$) genes (**Figure 6**). Soil physicochemical characteristics (SOC, TN and NO_3^-) increased linearly with the gene abundances of the N cycle (*nifH*, AOA, AOB, *nirK*, and *nosZ*) ($P < 0.05$, **Figure 7**). Soil microbial biomass (C and N) showed a linear and positive correlation with gene abundances of the N cycle (*nifH*, AOA, AOB, *nirK*, and *nosZ*) ($P < 0.05$, **Figure 7**). The soil enzyme activities (NR and DEA) also indicated a positive, linear relationship with the N cycle gene abundances (*nifH*, AOA, AOB, *nirK*, and *nosZ*) ($P < 0.05$, **Figure 7**). Stepwise multiple regression analyses showed that the abundance or relative abundance of six key functional N gene families could be explained by the four soil physicochemical factors, namely, SW, SOC, soil TN content, and soil NO_3^- content (**Table 2**). SW and SOC together

TABLE 1 | The comparison of the alpha diversity of bacteria and fungi between overgrazing and grazing exclusion.

	Bacteria			Fungi		
	Overgrazing	**Grazing exclusion**	***P*-value**	**Overgrazing**	**Grazing exclusion**	***P*-value**
OTU richness	**3990.00 ± 25.16**	**4193.25 ± 69.07**	**0.0348**	1302.00 ± 78.21	12 19.25 ± 114.87	0.5733
H′	**9.77 ± 0.07**	**10.00 ± 0.06**	**0.0385**	7.84 ± 0.38	7.12 ± 0.59	0.3402
Simpson	0.99 ± 0.01	0.99 ± 0.01	0.5370	0.98 ± 0.01	0.94 ± 0.02	0.1681
Chao1	**5027.81 ± 184.58**	**5649.88 ± 107.16**	**0.0269**	1752.88 ± 128.81	1627.63 ± 114.34	0.4345
ACE	**5224.60 ± 110.94**	**5661.46 ± 105.73**	**0.0292**	1795.70 ± 114.77	1719.43 ± 127.36	0.6722
Goods_coverage	0.97 ± 0.01	0.96 ± 0.01	0.0528	0.97 ± 0.01	0.97 ± 0.01	0.7329

Results reported as the mean ± standard error (n = 4). P < 0.05 values in bold indicates significant differences between grazing and grazing exclusion. H′, Shannon–Wiener diversity.

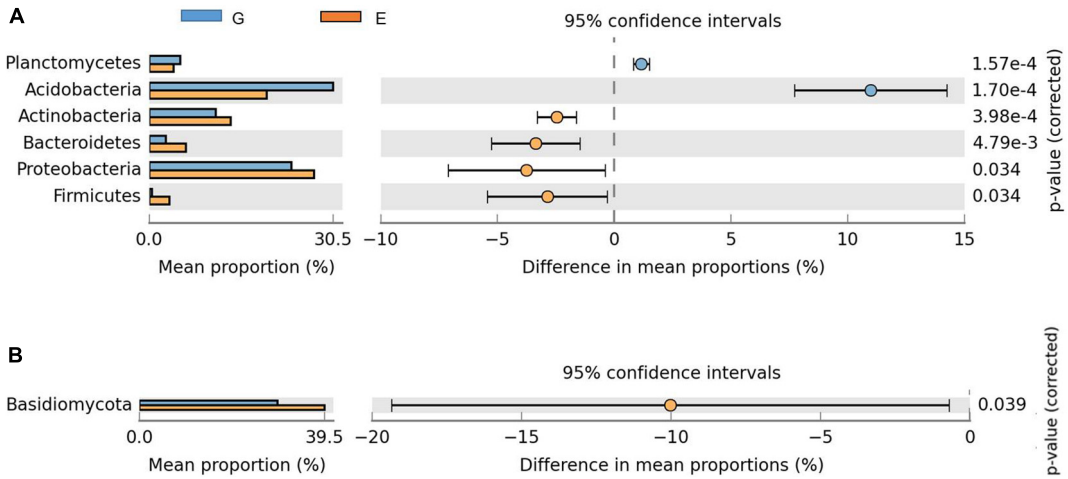

FIGURE 3 | Comparison of phyla with significant differences between the overgrazing and grazing exclusion treatments. The data were visualized using STAMP (error bars represent Welch's t-interval). **(A)** Bacteria, **(B)** fungi. Bars on the left represent the proportion of each phylum abundance (bacterial and fungal) in the treatments. Bacterial abundance differences with a *q*-value of <0.05 were considered to be significant. *Q*-values were determined using the Benjamini-Hochberg adjustment for *p*-values.

accounted for 98% of the spatial variation in the *nifH* gene ($P < 0.001$; **Table 2**). SW explained 53% of the spatial variation in the abundance of AOA genes ($P = 0.025$; **Table 2**). TN alone explained 58% of the abundance of AOB genes ($P = 0.017$; **Table 2**). Soil NO_3^- content alone explained 83% of the spatial variation in the gene abundance of *nirK* ($P < 0.001$), whereas NO_3^- alone explained 52% of the spatial variation in the gene abundance of *nirS* ($P = 0.026$; **Table 2**). Both SW and TN content were responsible for 92% of the spatial variation in the abundance of *nosZ*1 ($P < 0.001$; **Table 2**).

DISCUSSION

Grazing Exclusion Altered Bacterial Diversity

Our results revealed that bacterial alpha diversity (i.e., OTU richness, H', Chao1, and ACE) significantly increased in response to grazing exclusion (**Table 1**), which was consistent with previous findings that both the H' and ACE indices of soil bacterial diversity significantly increased with recovery age (Wu et al., 2014; Zhang et al., 2018). The observed positive relationship between soil nutrient content (i.e., SOC and NO_3^-) and bacterial alpha diversity in our study supported previous findings (Cheng et al., 2016; Wang et al., 2018). Additionally, bacterial alpha diversity was not directly associated with plant diversity in a previous study (Millard and Singh, 2010), but in our study plant diversity had a positive relationship with bacterial alpha diversity (**Supplementary Table 5**). Our results suggested that the management practice of grazing exclusion (appropriate restoration) increased bacterial alpha diversity and are consistent with a recent study on semiarid grasslands (Zhang et al., 2018), in which bacterial alpha diversity was higher after 25 years of grazing exclusion than in other sites (0, 10, and 35 years of grazing exclusion). We attributed this to the fact that the nutrients required by soil bacteria are usually obtained from plant litter, release of root exudates and root decay of live plants (Tang et al., 2020). High plant species diversity increased plant community production, which was related with greater litter accumulation on the soil surface and enhanced C inputs to soil (Buyer et al., 2010). Our results further showed that the effect of plant diversity on soil nutrient concentration also impacted

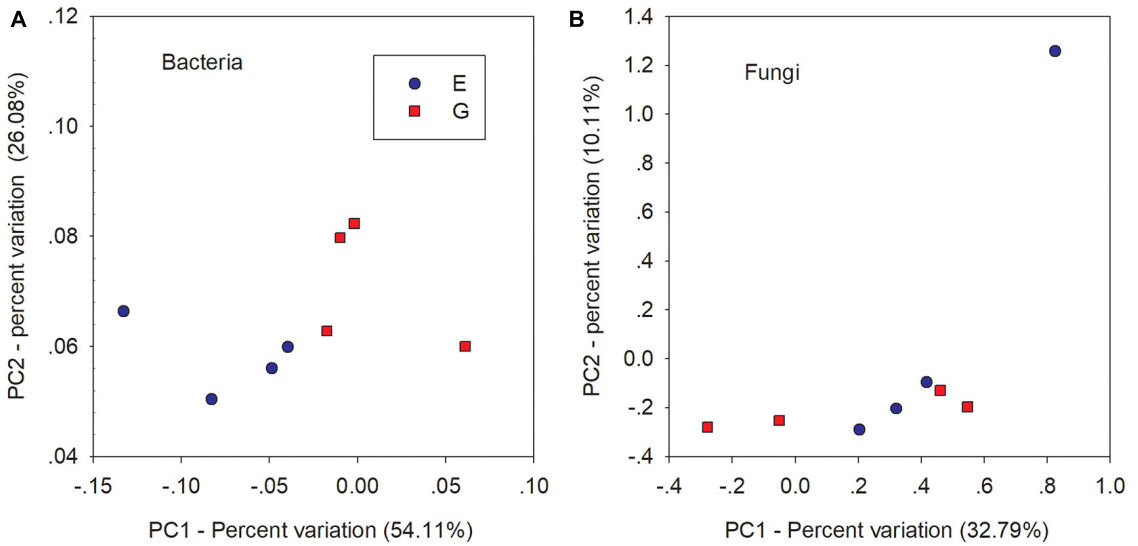

FIGURE 4 | Principal Coordinates Analysis **(**PCoA) of bacteria **(A)** and fungi **(B)** dissimilarity based on weighted UniFrac distance matrix between overgrazing (red squares) and grazing exclusion (blue circles).

soil bacterial diversity among soil bacteria taxa (**Figures 3**, **5**). High plant diversity may contribute to greater diversity of plant-derived resources (El Moujahid et al., 2017), and provide more opportunities for soil microbes to specialize in different resources (Kinkel et al., 2011). Thus, changes in bacterial alpha diversity were closely associated with plant diversity (i.e., species richness and Shannon–Wiener index). The relationship between the diversities of plant species (above-ground) and soil bacteria (below-ground) is a key point of the ecosystem biodiversity (Yang et al., 2020).

Grazing Exclusion Changed Bacterial Community Composition

With regard to the effects of grazing exclusion on the microbial community composition, we observed that different microbial taxa exhibited different behaviors. A previous study showed that intensive grazing increased the relative abundances of *Proteobacteria*, *Bacteroidetes* and *Firmicutes* (Patra et al., 2005; Xun et al., 2018; Zhang et al., 2020b). However, in our study, the relative abundances of *Actinobacteria*, *Proteobacteria*, *Firmicutes,* and *Bacteroidetes* increased under grazing exclusion by increasing soil carbon. These induced changes of grazing exclusion in bacterial taxa are consistent with previous studies (Cheng et al., 2016; Wang et al., 2018).

There are some possible explanations for the changes in bacterial community diversity and composition due to grazing exclusion. First, direct effects of avoiding animal trampling under grazing exclusion on soil carbon have been associated with increased soil air permeability (Wang Z. et al., 2019). Indirect carbon storage induced under grazing exclusion via plant litter accumulation has been demonstrated in the Loess Plateau (Cui et al., 2019). The increased abundances of bacterial taxa are for copiotrophic groups under grazing exclusion, which are generally fast-growing and positively linked to SOC concentration (Leff et al., 2015; Zhang et al., 2018). Thus, the increase in SOC after 22 years of grazing exclusion resulted in a shift in the bacterial community from oligotrophic groups to copiotrophic groups, characterized by decreases in *Acidobacteria* phyla abundances and increased abundances in the *Actinobacteria* phylum and the *Bacteroidetes* phylum, and the *Betaproteobacteria* and *Deltaproteobacteria* class (**Figure 4**; **Supplementary Figure 3**).

Although a previous study showed that grazing increased the relative abundance of both the *Firmicutes* and *Bacteroidetes* phyla through livestock dung, such results were observed under moderate grazing (Zhang et al., 2020b). Compared to grazing exclusion and moderate grazing, the limited amount of herbage under overgrazing may cause livestock to consume more energy while foraging and this might result in reduced quantities of palatable, high-quality and highly productive grasses, such as *Leymus chinensis*, *Stipa grandis,* and *Melissilus ruthenicus* (L.) Peschkova (**Supplementary Figure 1** and **Supplementary Table 1**). Overgrazing decelerated nutrient cycling by the dominance of nutrient-poor or chemically defensive species (e.g., *Salsola collina* and *Tribulus terrestris*) with low litter quality (Bai et al., 2012). Under nutrient-deficient conditions, low-quality litter decreased nutrient concentration and root biomass, which often affects the amount of C-rich substrates exuded into the rhizosphere (McNaughton, 1985). Thus, microbial activity and the use of stored nutrients were inhibited under overgrazing. As a result, overgrazing accelerated the loss of soil nutrients, and consequently reduced SOC concentration. Both the *Firmicutes* and *Bacteroidetes* phyla consisted of copiotrophic bacteria (Leff et al., 2015), which are fast growing and positively correlated with SOC concentration, thus, explaining the reductions in the relative abundance of *Bacteroidetes* and *Firmicutes* under overgrazing.

Additionally, the heat map analyses also showed that the change in the relative abundances of main bacterial phyla was

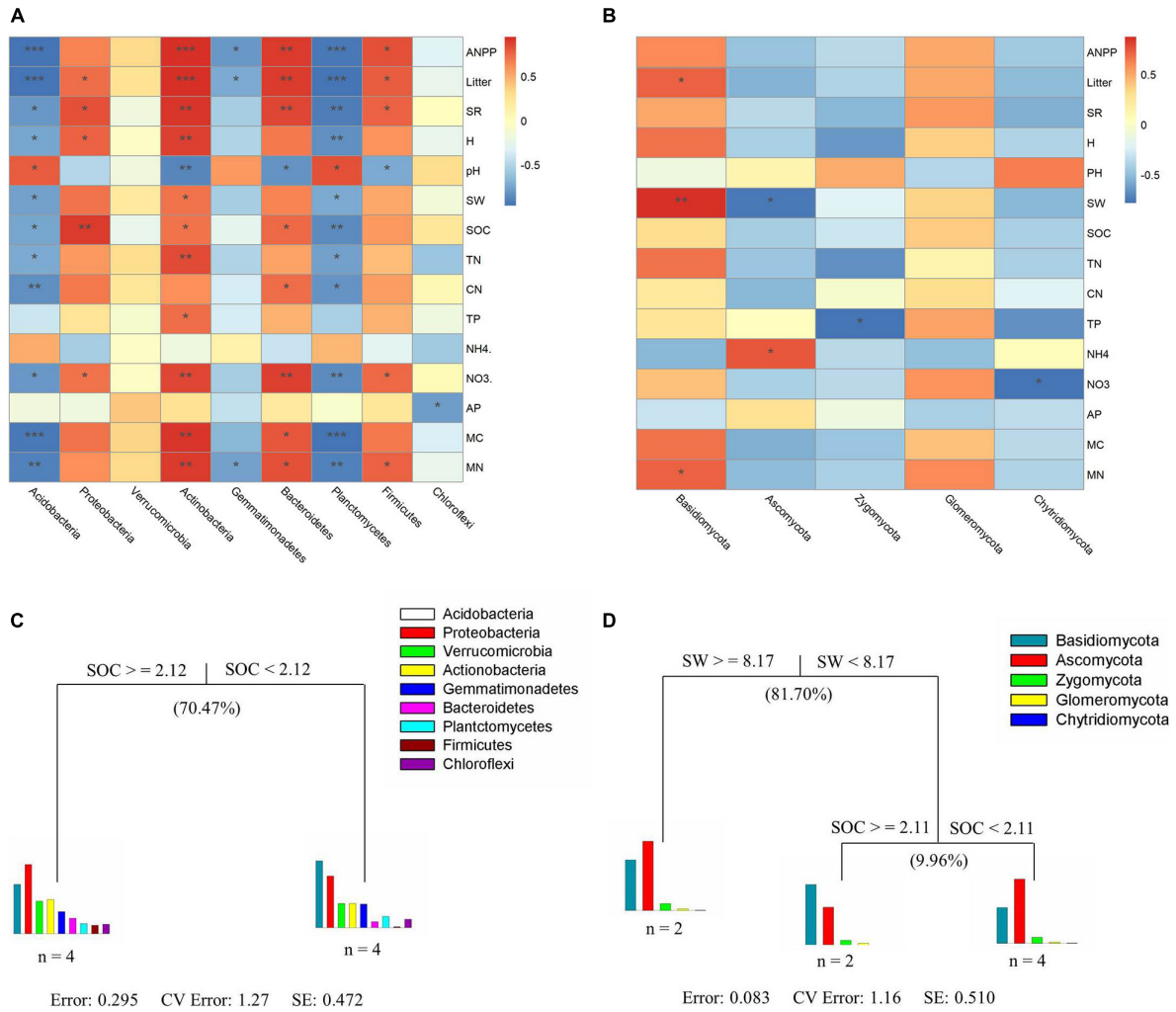

FIGURE 5 | Correlations between biotic and abiotic factors and dominant bacterial and fungal phyla **(A,B)**. Multivariate regression tree analysis of environmental factors on the patterns of soil bacterial **(C)** and fungal **(D)** community composition. The number of soil samples included in the analysis is shown under the bar plots. Plant community characteristics include the ANPP, litter (litter biomass), SR (species richness), and *H* (Shannon–Wiener index). Soil properties include the pH (soil pH value), soil water content (SW), SOC (soil organic carbon content), TN (soil total nitrogen content), CN (soil C/N ratio), TP (soil total phosphorus content), NH4 (soil NH_4^+ content), NO3 (soil NO_3^- content), and AP (soil available phosphorus content). Soil microbial variables include the MC (microbial C) and MN (microbial N). Significance levels in heat maps analysis are indicated as: $^*P < 0.05$, $^{**}P < 0.01$, and $^{***}P < 0.001$.

related to plant characteristics, soil properties and soil microbial biomass (**Figure 5**). For example, the *Actinobacteria* phylum can promote plant growth by making nutrients/substrates (e.g., phosphorus and nitrogen) available to host plants and producing various plant hormones to prevent plant infections (Liu et al., 2017). The *Proteobacteria* phylum can accumulate soil N content to promote plant growth because many N-fixing bacteria belong to the *Proteobacteria* phylum (Spain et al., 2009). The negative correlation between the abundance of the *Acidobacteria* phylum and other parameters (plant characteristics, soil properties, and soil microbial biomass) is due to the fact that the *Acidobacteria* phylum contains microbes that usually grow rapidly in a nutritionally poor environment (Koyama et al., 2014). Moreover, the increased abundance of the *Proteobacteria* family (*Sphingomonadaceae*, *Sinobacteraceae*, *Haliangiaceae*, *Polyangiaceae*, and *Rhodobiaceae*), the *Actinobacteria* family (*Gaiellaceae*, *Solirubrobacteraceae*, *Streptomycetaceae*, and *Conexibacteraceae*), and the decreased abundance of the *Acidobacteria* family (*mb2424*) under grazing exclusion, also led to the change in bacterial community composition (**Supplementary Table 4**).

Lack of Fungal Response Under Grazing Exclusion

Unlike diversity and composition of the bacterial community, fungal community composition did not significantly differ between overgrazing and grazing exclusion (Patra et al., 2005), suggesting that the bacterial community may develop faster than the fungal community (**Figure 5**). Our results are consistent

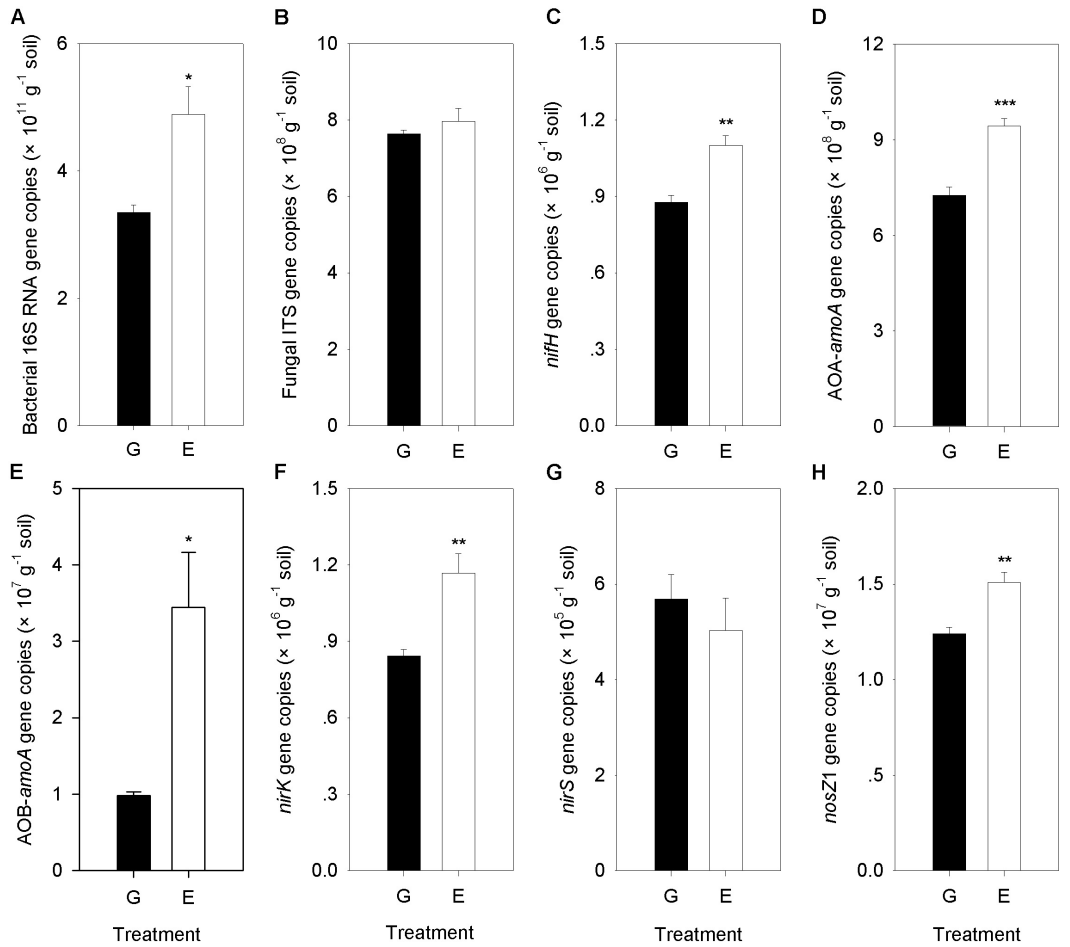

FIGURE 6 | Comparison of Bacterial 16S RNA gene, Fungal ITS gene and the N cycling gene abundances (*nifH*, AOA-*amoA*, AOB-*amoA*, *nirK*, *nirS*, and *nosZ*1) between overgrazing and grazing exclusion. G, overgrazing; E, grazing exclusion. Values represent the mean ± standard error ($n = 4$). Significance levels are indicated as: $^{*}P < 0.05$, $^{**}P < 0.01$, and $^{***}P < 0.001$. Bacterial 16S RNA gene copies **(A)**, Fungal ITS gene copies **(B)**, nifH gene copies **(C)**, AOA-amoA gene copies **(D)**, AOB-amoA gene copies **(E)**, nirK gene copies **(F)**, nirS gene copies **(G)**, and nosZ1 gene copies **(H)**.

with a previous study conducted by Brown and Jumpponen (2015), who found that the fungal community did not respond to succession age, while the bacterial community strongly responded, as determined by a phylogenetic diversity analysis. Bacteria have a more diverse physiology than fungi, thus they successfully colonize during the grassland ecosystem restoration (Zhang et al., 2018). Compared to bacteria, fungi are more dependent on C and N sources. Fungi may not have many available niches before accumulating enough organic matter in the succession process (Prewitt et al., 2014). Additionally, MRT analysis showed that SW was a key factor affecting the change in fungal community composition based on the MRT analysis. Our results are in accordance with recent studies (Tedersoo et al., 2014), in which water availability affected plant community productivity, and subsequently impacted the quantity and quality of the input of plant residues supporting the soil fungal community. Grazing exclusion enhanced the relative abundance of the *Basidiomycota* phyla (saprotroph) (**Figure 3B**), which was likely due to the relatively higher SW, MN, litter biomass, SOC, and plant biomass under grazing exclusion (Yang et al., 2018).

Bacterial Response Under Grazing Exclusion

Removal of grazing elicited changes in soil microbial community structure that led to improved biogeochemical functions and higher soil fertility. The change in bacterial phyla may be due to increased soil C and N substrates by litter accumulation (Zeng et al., 2017), which is in agreement with the higher litter biomass, OC, and TN contents detected in our study (**Figure 2**). The increase in the relative abundance of the family *Sphingomonadaceae* may improve the oxygen availability and may change the soil physical environment (e.g., decreased soil bulk diversity) by avoiding animal trampling (Wang Z. et al., 2019). As a result, grazing exclusion increased the SOC, which is associated with greater litter input into soil. The MRT analysis also identified SOC as the predominant factor driving the change

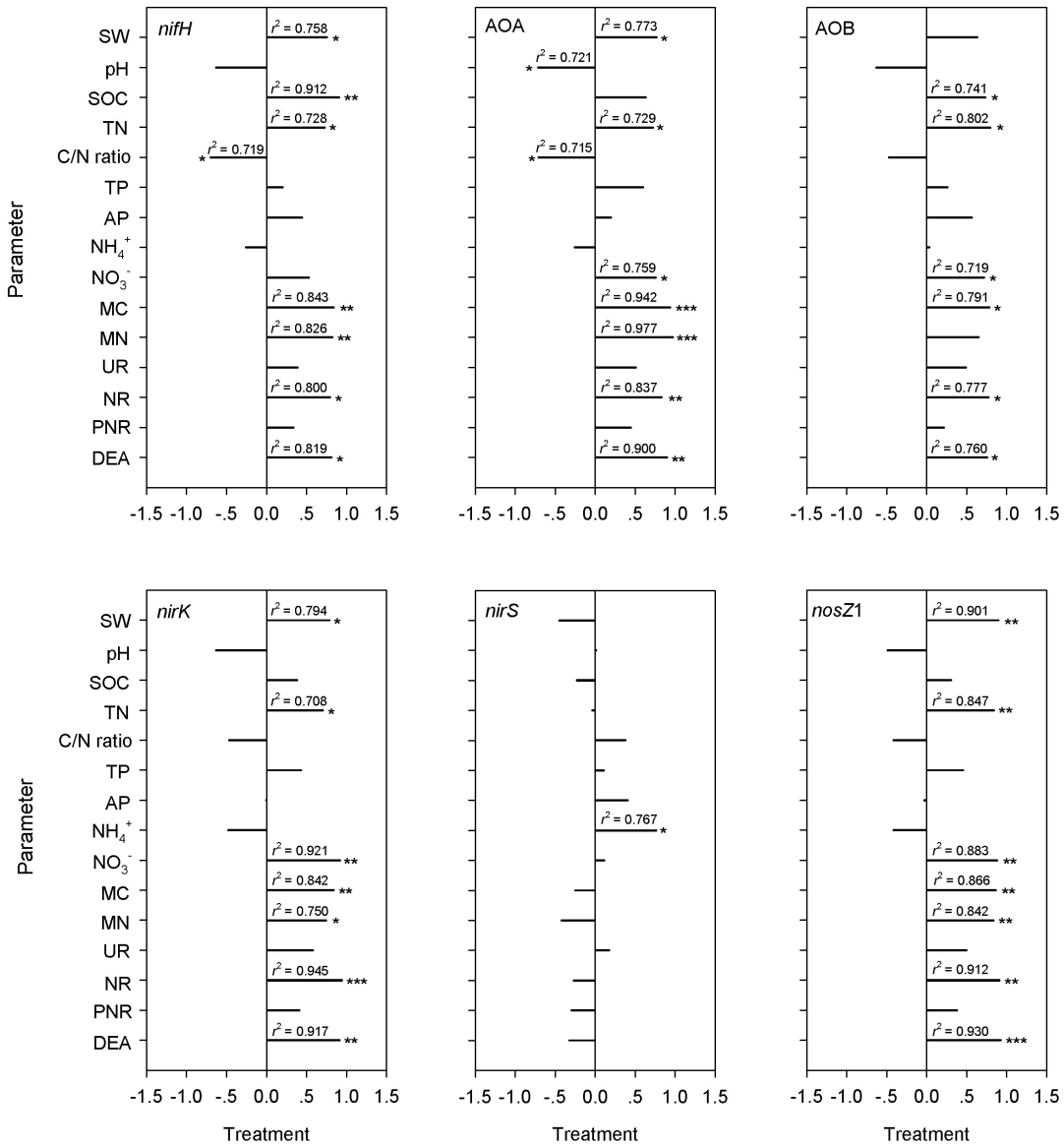

FIGURE 7 | Pearson correlation coefficients between N cycling gene abundances (*nifH*, AOA-*amoA*, AOB-*amoA*, *nirK*, *nirS*, and *nosZ*1) and biotic and abiotic factors. The correlations were derived for SW, water/moisture content of soil samples; pH, soil pH value; SOC, soil organic content of the soil samples; TN, total nitrogen concentration of soil samples; C/N ratio, (soil C/N ratio); TP, total phosphorus content of soil samples; AP, available phosphorus content of soil; NH_4^+, soil NH_4^+ content; NO_3^-, soil NO_3^- content; MC, soil microbial C; MN, soil microbial N; UN, urease; NR, nitrate reductase; PNR, the potential nitrification rate; DEA, soil denitrifying enzyme activity. Significance levels are indicated as: $^*P < 0.05$, $^{**}P < 0.01$, and $^{***}P < 0.001$.

in the composition of the soil bacterial community. Therefore, changes in the composition of specific microbial groups likely played an important role in the recovery of the biogeochemical functions as it is supported by the strengthened relationship between microbial phylogenetic composition and soil fertility since the release from the exclusion of grazing.

The changes in the abundance of N cycle functional genes provided a glimpse of the functional potentials of microbial communities under grazing exclusion. We observed a dramatic increase in *nifH* gene abundance with the grassland ecosystem recovery, which was related to plant and soil properties. Previous studies showed that *nifH* genes primarily from aerobic and facultatively anaerobic organisms, which belong to three bacterial phyla (*Proteobacteria*, *Firmicutes,* and *Actinobacteria*) (Gaby and Buckley, 2014). The higher relative abundance of *Proteobacteria*, *Firmicutes,* and *Actinobacteria* led to an increase in the abundance of *nifH* genes due to the increased soil fertility under grazing exclusion (Meyer et al., 2013). Additionally, our results are consistent with those of a previous study (Poly et al., 2001), in which the increase in the soil C/N ratio drove N fixation under grazing exclusion. Moreover, potential acidity is related to pH, a well-established factor affecting the diversity of microbial

TABLE 2 | Stepwise multiple regression analysis of the relationships between independent variables and gene abundance of *nifH*, AOA, AOB, *nirK*, *nirS*, and *nosZ*1.

Functional genes	Results	R^2	*F*	*P*
nifH	$y = 0.717 \times (SOC) + 0.438 \times (SW) - 2.07$	0.98	177.27	<0.001
AOA	$y = 0.773 \times (SW) - 1.01$	0.53	8.88	0.025
AOB	$y = 0.802 \times (TN) - 3.28$	0.58	10.84	0.017
nirK	$y = 0.921 \times (NO_3^-) - 1.23$	0.83	33.69	<0.001
nirS	$y = 0.061 \times (NO_3^-) + 0.38$	0.52	8.59	0.026
*nosZ*1	$y = 0.556 \times (SW) + 0.498 \times (TN) - 6.88$	0.92	39.58	<0.001

SW, soil water content; SOC, soil organic carbon content; TN, soil total nitrogen content; NO_3^-, soil NO_3^- content.

communities (Jesus et al., 2009), which also increased *nifH* gene abundance under grazing exclusion.

For the nitrifier communities, the abundance of AOA was much greater than that of AOB in our study. Our results agree with those of a recent study, in which AOA played a major role in the nitrification of acidic soils (Zhang et al., 2012). Additionally, AOA rather than AOB is favored in the low-fertility and low-nitrogen environments in this semiarid grassland (**Figure 2**), which is in line with observations in other ecosystems (Shrewsbury et al., 2016; Assémien et al., 2017). Grazing exclusion increased the abundance of nitrification genes (AOA and AOB) in soils, reflecting a response to remove the grazing trampling. Nitrification genes in grazing exclusion grassland soils increased (**Figure 6**), which might be attributed to the removal of grazing trampling that promotes the oxygen-requiring nitrification process (Pan et al., 2016). In our study, SW was correlated with changes in the abundance of the AOA gene (**Table 2**). This agreed with a previous study in the Inner Mongolia Steppe (Xie et al., 2014; Ding et al., 2015), in which AOA gene abundance rapidly responded to the water content. The recovery of the soil NO_3^- content is tightly related to changes in the gene abundance of AOB (**Table 2**), which was associated with the abundance of *Nitrospiraceae* (**Supplementary Figure 5**). Our results agree with the findings of Wang J. et al. (2019), who reported that the abundance of AOB was correlated with *Nitrospira* abundance. Effectively, grazing exclusion increased the abundance of nitrification genes.

Interestingly, grazing exclusion did not change PNR but increased the abundance of the AOA and AOB communities, suggesting the PNR was not necessarily associated with the abundance of ammonia-oxidizers in our study (Yin et al., 2019). Le Roux et al. (2013) showed that the correlations between the abundance of ammonia oxidizers (AOA and AOB) and PNR were weak in grasslands. Our results are consistent with previous studies (Nicol et al., 2008; Yin et al., 2019), in which the activities of ammonia-oxidizers were related with enzyme function rather than with the abundance of functional genes.

For the denitrifier communities, the gene abundances (*nirK* and *nosZ*1) showed positive relationships with DEA, which was associated with the general enhancement of substrates (e.g., NO_3^-). Our results are in line with a previous study, which indicated that DEA can predict the change in denitrifier (*nirK*) abundance (Morales et al., 2010; Attard et al., 2011; Zhang X. et al., 2019). The higher DEA in our grazing exclusion soils suggested that ammonia oxidizers (higher AOA and AOB abundances under grazing exclusion) provided substrates (e.g., NO_3^-) to denitrifiers (*nirK* and *nosZ*1), and DEA relies on the availability of NO_3^- production.

The increased abundance of *nirK* observed under grazing exclusion supports the findings of previous studies, in which the nitrate reducer communities increased during the ecological recovery of the grassland (Song et al., 2019). Consistent with this interpretation (Ding et al., 2015), the SW, soil nutrients (e.g., NO_3^-) and oxygen were the most important factors mediating the gene abundances of denitrifiers. Grazing exclusion significantly increased the abundance of the *nirK* gene, but no changes were observed in the abundance of the *nirS* gene (**Figure 6**), which was inconsistent with the findings of a previous study in a semiarid steppe (Pan et al., 2016). Our results are consistent with the observations of a recent study in Tibetan alpine meadows (Xie et al., 2014), in which the different responses of the abundances of *nirK*- and *nirS*-nitrite reducers to grazing intensity were attributed to niche differentiation between these two groups of denitrifiers for different ecosystems (Assémien et al., 2019). Additionally, nitrate reductase activity was determined by *nirK*, and there was a positive relationship between enzyme activities and the changes in gene abundances of denitrifier genes (Barrena et al., 2017).

CONCLUSION

Grazing exclusion in the semiarid steppe caused significant changes in soil properties, bacterial diversity and community structure, but there were no significant alterations in fungal diversity and community structure. The diversity and structure of the bacterial community indicated a positive linear relationship with plant and soil functioning during restoration of these grassland ecosystems. Our results clearly demonstrated a positive relationship between the abundances of denitrifying functional genes (*nirK* and *nosZ*1) and DEA during restoration of grassland ecosystems. Our results suggest that grazing exclusion can initiate changes in the soil bacterial community that facilitate the recovery of ecosystem functions in grasslands.

DATA AVAILABILITY STATEMENT

All amplicon sequencing data have been deposited in the NCBI SRA under the accession numbers SRR13612594-SRR13612601 (bacteria) and SRR13612480-SRR13612487 (fungi).

AUTHOR CONTRIBUTIONS

ZW, KJ, BJ, XL, and ST conceived and designed the research. ZW, XL, KJ, and ST conducted the experiment. ZW, BJ and PS analyzed and interpreted the data. ZW, KJ, BJ, and ST wrote the

manuscript. All authors discussed and approved the final version of the manuscript.

FUNDING

This work was supported by the National Natural Science Foundation of China (42077054, 32071681, and 31770542) and Natural Science Foundation of Inner Mongolia, China (2019MS03001 and 2019MS03002). This work was also supported by the Central Public-Interest Scientific Institution Basal Research Fund (1610332020005) and Science and Technology Development Center project (KJZXYZ202001).

ACKNOWLEDGMENTS

We thank Jianjun Chen and Xiangjun Yun for help setting up the experiment and collecting the soil samples. We also thank LetPub (www.letpub.com) for its linguistic assistance during the preparation of the manuscript.

SUPPLEMENTARY MATERIAL

The Supplementary Material for this article can be found online at: https://www.frontiersin.org/articles/10.3389/fpls.2021.640789/full#supplementary-material

REFERENCES

Assémien, F. L., Cantarel, A. A. M., Florio, A., Lerondelle, C., Pommier, T., Gonnety, J. T., et al. (2019). Different groups of nitrite-reducers and N_2O-reducers have distinct ecological niches and functional roles in West African cultivated soils. *Soil Biol. Biochem.* 129, 39–47. doi: 10.1016/j.soilbio.2018.11.003

Assémien, F. L., Pommier, T., Gonnety, J. T., Gervaix, J., and Le Roux, X. (2017). Adaptation of soil nitrifiers to very low nitrogen level jeopardizes the efficiency of chemical fertilization in West African moist savannas. *Sci. Rep.* 7:10275. doi: 10.1038/s41598-017-10185-5

Attard, E., Recous, S., Chabbi, A., Berranger, C. D., Guillaumaud, N., Labreuche, J., et al. (2011). Soil environmental conditions rather than denitrifier abundance and diversity drive potential denitrification after changes in land uses. *Global Change Biol.* 17, 1975–1989. doi: 10.1111/j.1365-2486.2010.02340.x

Bai, Y. F., Wu, J. G., Clark, C. M., Pan, Q. M., Zhang, L. X., Chen, S. P., et al. (2012). Grazing alters ecosystem functioning and C:N:P stoichiometry of grasslands along a regional precipitation gradient. *J. Appl. Ecol.* 49, 1204–1215. doi: 10.1111/j.1365-2664.2012.02205.x

Bardgett, R. D., and Wardle, D. A. (2003). Herbivore-mediated linkages between aboveground and belowground communities. *Ecology* 84, 2258–2268. doi: 10.1890/02-0274

Barrena, I., Menéndez, S., Correa-Galeote, D., Vega-Mas, I., Bedmar, E. J., González-Murua, C., et al. (2017). Soil water content modulates the effect of the nitrification inhibitor 3, 4-dimethylpyrazole phosphate (DMPP) on nitrifying and denitrifying bacteria. *Geoderma* 303, 1–8. doi: 10.1016/j.geoderma.2017.04.022

Bellemain, E., Carlsen, T., Brochmann, C., Coissac, E., Taberlet, P., and Kauserud, H. (2010). ITS as an environmental DNA barcode for fungi: an in silico approach reveals potential PCR biases. *BMC Microbiol.* 10:189. doi: 10.1186/1471-2180-10-189

Blagodatsky, S., and Smith, P. (2012). Soil physics meets soil biology: towards better mechanistic prediction of greenhouse gas emissions from soil. *Soil Biol. Biochem.* 47, 78–92. doi: 10.1016/j.soilbio.2011.12.015

Blois, J. L., Williams, J. W., Fitzpatrick, M. C., Jackson, S. T., and Ferrier, S. (2013). Space can substitute for time in predicting climate change effects on biodiversity. *Proc. Natl. Acad. Sci. U.S.A.* 110, 9374–9379. doi: 10.1073/pnas.1220228110

Bokulich, N. A., Subramanian, S., Faith, J. J., Gevers, D., Gordon, J. I., Knight, R., et al. (2013). Quality-filtering vastly improves diversity estimates from Illumina amplicon sequencing. *Nat. Methods* 10, 57–59. doi: 10.1038/nmeth.2276

Brown, S. P., and Jumpponen, A. (2015). Phylogenetic diversity analyses reveal disparity between fungal and bacterial communities during microbial primary succession. *Soil Biol. Biochem.* 89, 52–60. doi: 10.1016/j.soilbio.2015.06.025

Buyer, J. S., Zuberer, D. A., Nichols, K. A., and Franzluebbers, A. J. (2010). Soil microbial community function, structure, and glomalin in response to tall fescue endophyte infection. *Plant Soil* 339, 401–412. doi: 10.1007/s11104-010-0592-y

Caporaso, J. G., Kuczynski, J., Stombaugh, J., Bittinger, K., Bushman, F. D., and Knight, R. (2010). QIIME allows analysis of high-throughput community sequencing data. *Nat. Methods* 7, 335–336.

Chartier, M. P., Rostagno, C. M., and Videla, L. S. (2013). Selective erosion of clay, organic carbon and total nitrogen in grazed semi-arid rangelands of northeastern Patagonia, Argentina. *J. Arid Environ.* 88, 43–49. doi: 10.1016/j.jaridenv.2012.08.011

Cheng, J., Jin, G., Wei, L., and Jing, Z. (2016). Long-term grazing exclusion effects on vegetation characteristics, soil properties and bacterial communities in the semi-arid grasslands of China. *Ecol. Eng.* 97, 170–178. doi: 10.1016/j.ecoleng.2016.09.003

Cui, Y., Fang, L., Guo, X., Han, F., Ju, W., Ye, L., et al. (2019). Natural grasslands as the optimal pattern of vegetation restoration in arid and semi-arid regions: evidence from nutrient limitation of soil microbes. *Sci. Total Environ.* 648, 388–397. doi: 10.1016/j.scitotenv.2018.08.173

Daniel, R. M., and Curran, M. P. (1981). A method for the determination of nitrate reductase. *J. Biochem. Biophys. Methods* 4, 131–132.

De'Ath, G. (2002). Multivariate regression trees: a new technique for modeling species environment relationships. *Ecology* 83, 1105–1117. doi: 10.1890/0012-9658(2002)083[1105:MRTANT]2.0.CO;2

Deng, L., Zhang, Z. N., and Shangguan, Z. P. (2014). Long-term fencing effects on plant diversity and soil properties in China. *Soil Till. Res.* 137, 7–15. doi: 10.1016/j.still.2013.11.002

Ding, K., Zhong, L., Xin, X. P., Xu, Z. H., Kang, X. M., Liu, W. J., et al. (2015). Effect of grazing on the abundance of functional genes associated with N cycling in three types of grassland in Inner Mongolia. *J. Soils Sediments* 15, 683–693. doi: 10.1007/s11368-014-1016-z

Edgar, R. C. (2013). UPARSE: highly accurate OTU sequences from microbial amplicon reads. *Nat. Methods* 10, 996–998. doi: 10.1038/nmeth.2604

El Moujahid, L., Le Roux, X., Michalet, S., Bellvert, F., Weigelt, A., and Poly, F. (2017). Effect of plant diversity on the diversity of soil organic compounds. *PLoS One* 12:e0170494. doi: 10.1371/journal.pone.0170494

Fierer, N., Colman, B. P., Schimel, J. P., and Jackson, R. B. (2006). Predicting the temperature dependence of microbial respiration in soil: a continental-scale analysis. *Glob. Biogeochem. Cycles* 20:GB3026.

Fry, E. L., Manning, P., Macdonald, C., Hasegawa, S., De Palma, A., Power, S. A., et al. (2016). Shifts in microbial communities do not explain the response of grassland ecosystem function to plant functional composition and rainfall change. *Soil Biol. Biochem.* 92, 199–210. doi: 10.1016/j.soilbio.2015.10.006

Gaby, J., and Buckley, D. (2014). A comprehensive aligned nifH gene database: a multipurpose tool for studies of nitrogen-fixing bacteria. *Database* 2014:bau001. doi: 10.1093/database/bau001

Greilhuber, J., Dolezel, J., Lysak, M. A., and Bennett, M. D. (2005). The origin, evolution and proposed stabilization of the terms 'genome size' and 'C-value' to describe nuclear DNA contents. *Ann. Bot.* 95, 255–260. doi: 10.1093/aob/mci019

Hart, S. C., Stark, J. M., Davidson, E. A., and Firestone, M. K. (1994). "Nitrogen mineralization, immobilization, and nitrification," in *Methods of Soil Analysis:*

II. Microbiological and Biochemical Properties, ed. R. W. Weaver (Madison, WI: SSSA), 985–1018. doi: 10.2136/sssabookser5.2.c42

Hayatsu, M., Tago, K., and Saito, M. (2008). Various players in the nitrogen cycle: diversity and functions of the microorganisms involved in nitrification and denitrification. *Soil Sci. Plant Nutr.* 54, 33–45. doi: 10.1111/j.1747-0765.2007.00195.x

Jesus, E. D., Marsh, T. L., Tiedje, J. M., and Moreira, F. M. D. (2009). Changes in land use alter the structure of bacterial communities in western Amazon soils. *ISME J.* 3, 1004–1011. doi: 10.1038/ismej.2009.47

Kauffman, J. B., Thorpe, A. S., and Brookshire, E. N. J. (2004). Livestock exclusion and belowground ecosystem responses in riparian meadows of eastern Oregon. *Ecol. Appl.* 14, 1671–1679. doi: 10.1890/03-5083

Kettler, T. A., Doran, J. W., and Gibert, T. L. (2001). Simplified method for soil particle-size determination to accompany soil-quality analyses. *Soil Sci. Soc. Am. J.* 65, 849–852. doi: 10.2136/sssaj2001.653849x

Kinkel, L. L., Bakker, M. G., and Schlatter, D. C. (2011). A coevolutionary framework for managing disease-suppressive soils. *Annu. Rev. Phytopathol.* 49, 47–67. doi: 10.1146/annurev-phyto-072910-095232

Koyama, A., Wallenstein, M. D., Simpson, R. T., and Moore, J. C. (2014). Soil bacterial community composition altered by increased nutrient availability in Arctic tundra soils. *Front. Microbiol.* 5:516. doi: 10.3389/fmicb.2014.00516

Kurola, J., Salkinoja-Salonen, M., Aarnio, T., Hultman, J., and Romantschuk, M. (2005). Activity, diversity and population size of ammonia-oxidising bacteria in oil-contaminated landfarming soil. *FEMS Microbiol. Lett.* 250, 33–38. doi: 10.1016/j.femsle.2005.06.057

Leff, J. W., Jones, S. E., Prober, S. M., Barberán, A., Borer, E. T., Firn, J. L., et al. (2015). Consistent responses of soil microbial communities to elevated nutrient inputs in grasslands across the globe. *Proc. Natl. Acad. Sci. U.S.A.* 112, 10967–10972. doi: 10.1073/pnas.1508382112

Le Roux, J. J., Sumner, P. D., Lorentz, S. A. and, Germishuyse, T., (2013). Connectivity 705 aspects in sediment migration modelling using the Soil and Water Assessment 706 Tool. *Geosciences* 3, 112.

Li, X., Wu, Z., Liu, Z., Hou, X., Badgery, W., and Guo, H. (2015). Contrasting effects of long-term grazing and clipping on plant morphological plasticity: evidence from a rhizomatous grass. *PLoS One* 10:e0141055. doi: 10.1371/journal.pone.0141055

Li, Y., Wang, S., Jiang, L., Zhang, L., Cui, S., Meng, F., et al. (2016). Changes of soil microbial community under different degraded gradients of alpine meadow. *Agric. Ecosyst. Environ.* 222, 213–222. doi: 10.1016/j.agee.2016.02.020

Liu, H., Carvalhais, L. C., Crawford, M., Singh, E., Dennis, P. G., Pieterse, C. M. J., et al. (2017). Inner plant values: diversity, colonization and benefits from endophytic bacteria. *Front. Microbiol.* 8:2552. doi: 10.3389/fmicb.2017.02552

Liu, S. B., Zamanian, K., Schleuss, P. M., Zarebanadkouki, M., and Kuzyakov, Y. (2018). Degradation of Tibetan grasslands: consequences for carbon and nutrient cycles. *Agri. Ecosystem Environ.* 252, 93–104. doi: 10.1016/j.agee.2017.10.011

Lou, Y. L., Liang, W. J., Xu, M. G., He, X. H., Wang, Y. D., and Zhao, K. (2011). Straw coverage alleviates seasonal variability of the topsoil microbial biomass and activity. *Catena* 86, 117–120. doi: 10.1016/j.catena.2011.03.006

Lü, X. T., Freschet, G. T., Kazakou, E., Wang, Z. W., Zhou, L. S., and Han, X. G. (2015). Contrasting responses in leaf nutrient-use strategies of two dominant grass species along a 30-yr temperate steppe grazing exclusion chronosequence. *Plant Soil* 387, 69–79. doi: 10.1007/s11104-014-2282-7

Magoč, T., and Salzberg, S. L. (2011). FLASH: fast length adjustment of short reads to improve genome assemblies. *Bioinformatics* 27, 2957–2963. doi: 10.1093/bioinformatics/btr507

McNaughton, S. J. (1985). Ecology of a grazing ecosystem: the Serengeti. *Ecol. Monogr.* 55, 259–294. doi: 10.2307/1942578

Meyer, A., Focks, A., Radl, V., Keil, D., Welzl, G., Schoning, I., et al. (2013). Different land use intensities in grassland ecosystems drive ecology of microbial communities involved in nitrogen turnover in soil. *PLoS One* 8:e73536. doi: 10.1371/journal.pone.0073536

Millard, P., and Singh, B. K. (2010). Does grassland vegetation drive soil microbial diversity? *Nutr. Cycl. Agroecosyst.* 88, 147–158. doi: 10.1007/s10705-009-9314-3

Morales, S. E., Cosart, T., and Holben, W. E. (2010). Bacterial gene abundances as indicators of greenhouse gas emission in soils. *ISME J.* 4, 799–808. doi: 10.1038/ismej.2010.8

Nannipieri, P., Ceccanti, B., Cervelli, S., and Matarese, E. (1980). Extraction of phosphatase, urease, proteases, organic carbon and nitrogen from soil. *Soil Sci. Soc. Am. J.* 44, 1011–1016. doi: 10.2136/sssaj1980.03615995004400050028x

Nelson, D., and Sommers, L. E. (1982). "Total carbon, organic carbon and organic matter," in *Methods of Soil Analysis. Part 2: Chemical and Microbiological Properties*, ed. A. L. Page (Madison, WI: SSSA).

Nicol, G. W., Leininger, S., Schleper, C., and Prosser, J. I. (2008). The influence of soil pH on the diversity, abundance and transcriptional activity of ammonia oxidizing archaea and bacteria. *Environ. Microbiol.* 10, 2966–2978. doi: 10.1111/j.1462-2920.2008.01701.x

Oksanen, J., Blanchet, F. G., Kindt, R., Legendre, P., Minchin, P. R., O'Hara, R. B., et al. (2013). *Vegan: Community Ecology Package.* R Package Version 2.0-10.

Owen, D., Williams, A. P., Griffith, G. W., and Withers, P. J. A. (2015). Use of commercial bio-inoculants to increase agricultural production through improved phosphrous acquisition. *Appl. Soil Ecol.* 86, 41–54. doi: 10.1016/j.apsoil.2014.09.012

Pan, H., Li, Y., Guan, X., Li, J., Xu, X., Liu, J., et al. (2016). Management practices have a major impact on nitrifier and denitrifier communities in a semiarid grassland ecosystem. *J. Soils Sediments* 16, 896–908. doi: 10.1007/s11368-015-1321-1

Patra, A. K., Abbadie, L., Clays-Josserand, A., Degrange, V., Grayston, S. J., Loiseau, P., et al. (2005). Effects of grazing on microbial functional groups involved in soil dynamics. *Ecol. Monogr.* 75, 65–80. doi: 10.1890/03-0837

Philippot, L., Andert, J., Jones, C. M., Bru, D., and Hallin, S. (2011). Importance of denitrifiers lacking the genes encoding the nitrous oxide reductase for N_2O emissions from soil. *Glob. Chang. Biol.* 17, 1497–1504. doi: 10.1111/j.1365-2486.2010.02334.x

Poly, F., Ranjard, L., Nazaret, S., Gourbière, F., and Monrozier, L. J. (2001). Comparison of nifH gene pools in soils and soil microenvironments with contrasting properties. *Appl. Environ. Microbiol.* 67, 2255–2262. doi: 10.1128/aem.67.5.2255-2262.2001

Prewitt, L., Kang, Y. M., Kakumanu, M. L., and Williams, M. (2014). Fungal and bacterial community succession differs for three wood types during decay in a forest soil. *Microb. Ecol.* 68, 212–221. doi: 10.1007/s00248-014-0396-3

Qiu, L., Wei, X., Zhang, X., and Cheng, J. (2013). Ecosystem carbon and nitrogen accumulation after grazing exclusion in semiarid grassland. *PLoS One* 8:e55433. doi: 10.1371/journal.pone.0055433

R Core Team (2016). *R: A Language and Environment for Statistical Computing*. Vienna: R Development Core Team.

Raiesi, F., and Riahi, M. (2014). The influence of grazing exclosure on soil C stocks and dynamics, and ecological indicators in upland arid and semi-arid rangelands. *Ecol. Indic.* 41, 145–154. doi: 10.1016/j.ecolind.2014.01.040

Shrewsbury, L. H., Smith, J. L., Huggins, D. R., Carpenter-Boggs, L., and Reardon, C. L. (2016). Denitrifier abundance has a greater influence on denitrification rates at larger landscape scales but is a lesser driver than environmental variables. *Soil Biol. Biochem.* 103, 221–231. doi: 10.1016/j.soilbio.2016.08.016

Song, Z., Wang, J., Liu, G., and Zhang, C. (2019). Changes in nitrogen functional genes in soil profiles of grassland under long-term grazing prohibition in a semiarid area. *Sci. Total Environ.* 673, 92–101. doi: 10.1016/j.scitotenv.2019.04.026

Spain, A. M., Krumholz, L. R., and Elshahed, M. S. (2009). Abundance, composition, diversity and novelty of soil *Proteobacteria*. *ISME J.* 3, 992–1000. doi: 10.1038/ismej.2009.43

Steffens, M., Koelbl, A., Totsch, E. K. U., and Kögel-Knabner, I. (2008). Grazing effects on soil chemical and physical properties in a semiarid steppe of Inner Mongolia (PR China). *Geoderma* 143, 63–72. doi: 10.1016/j.geoderma.2007.09.004

Tang, H., Nolte, S., Jensen, K., Yang, Z., Wu, J., and Muller, P. (2020). Grazing mediates soil microbial activity and litter decomposition in salt marshes. *Sci. Total Environ.* 720:137559. doi: 10.1016/j.scitotenv.2020.137559

Tedersoo, L., Bahram, M., Põlme, S., Kõljalg, U., Yorou, N. S., Wijesundera, R., et al. (2014). Global diversity and geography of soil fungi. *Science* 346:1078. doi: 10.1126/science.1256688

Van Lierop, W. (1988). Determination of available phosphorus in acid and calcareous soils with the Kelowna multiple-element extractant. *Soil Sci.* 146, 284–291. doi: 10.1097/00010694-198810000-00009

Vance, E. D., Brookes, P. C., and Jenkinson, D. (1987). An extraction method for measuring microbial biomass carbon. *Soil Biol. Biochem.* 19, 703–707. doi: 10.1016/0038-0717(87)90052-6

Walker, L. R., Wardle, D. A., Bardgett, R. D., and Clarkson, B. D. (2010). The use of chronosequences in studies of ecological succession and soil development. *J. Ecol.* 98, 725–736. doi: 10.1111/j.1365-2745.2010.01664.x

Wang, J., Wang, J., Rhodes, G., He, J., and Ge, Y. (2019). Adaptive responses of comammox *Nitrospira* and canonical ammonia oxidizers to long-term fertilizations: implications for the relative contributions of different ammonia oxidizers to soil nitrogen cycling. *Sci. Total Environ.* 668, 224–233. doi: 10.1016/j.scitotenv.2019.02.427

Wang, L., Gan, Y., Wiesmeier, M., Zhao, G., Zhang, R., Han, G., et al. (2018). Grazing exclusion—an effective approach for naturally restoring degraded grasslands in Northern China. *Land Degrad. Dev.* 29, 4439–4456. doi: 10.1002/ldr.3191

Wang, Z., Hou, X., Schellenberg, M. P., Qin, Y., Yun, X., Wei, Z., et al. (2014). Different responses of plant species to deferment of sheep grazing in a desert steppe of Inner Mongolia, China. *Rangeland J.* 36, 583–592. doi: 10.1071/rj13115

Wang, Z., Ji, L., Hou, X., and Schellenberg, M. P. (2016). Soil respiration in semiarid temperate grasslands under various land management. *PLoS One* 11:e0147987. doi: 10.1371/journal.pone.0147987

Wang, Z., Zhang, Q., Staley, C., Gao, H., Ishii, S., Wei, X., et al. (2019). Impact of long-term grazing exclusion on soil microbial community composition and nutrient availability. *Biol. Fertil. Soils* 55, 121–134. doi: 10.1007/s00374-018-01336-5

Wu, X., Li, Z., Fu, B., Zhou, W., Liu, H., and Liu, G. (2014). Restoration of ecosystem carbon and nitrogen storage and microbial biomass after grazing exclusion in semi-arid grasslands of Inner Mongolia. *Ecol. Eng.* 73, 395–403. doi: 10.1016/j.ecoleng.2014.09.077

Xie, Z., Le Roux, X., Wang, C., Gu, Z., An, M., Nan, H., et al. (2014). Identifying response groups of soil nitrifiers and denitrifiers to grazing and associated soil environmental drivers in Tibetan alpine meadows. *Soil Biol. Biochem.* 77, 88–99.

Xu, Y., Wan, S., Cheng, W., and Li, L. (2008). Impacts of grazing intensity on denitrification and N_2O production in a semi-arid grassland ecosystem. *Biogeochemistry* 88, 103–115. doi: 10.1007/s10533-008-9197-4

Xun, W., Yan, R., Ren, Y., Jin, D., Xiong, W., Zhang, G., et al. (2018). Grazing-induced microbiome alterations drive soil organic carbon turnover and productivity in meadow steppe. *Microbiome* 6:170.

Yang, F., Niu, K., Collins, C. G., Yan, X., Ji, Y., Ling, N., et al. (2019). Grazing practices affect the soil microbial community composition in a Tibetan alpine meadow. *Land Degrad. Dev.* 39, 49–59. doi: 10.1002/ldr.3189

Yang, F., Wu, J., Zhang, D., Chen, Q., Zhang, Q., and Cheng, X. (2018). Soil bacterial community composition and diversity in relation to edaphic properties and plant traits in grasslands of southern China. *Appl. Soil Ecol.* 128, 43–53. doi: 10.1016/j.apsoil.2018.04.001

Yang, K., Luo, S., Hu, L., Chen, B., Xie, Z., Ma, B., et al. (2020). Responses of soil ammonia-oxidizing bacteria and archaea diversity to N, P and NP fertilization: relationships with soil environmental variables and plant community diversity. *Soil Biol. Biochem.* 145:107795. doi: 10.1016/j.soilbio.2020.107795

Yang, Y. F., Wu, L. W., Lin, Q. Y., Yuan, M. T., Xu, D. P., Yu, H., et al. (2013). Responses of the functional structure of soil microbial community to livestock grazing in the Tibetan alpine grassland. *Glob. Change Biol.* 19, 637–648. doi: 10.1111/gcb.12065

Yin, M., Gao, X., Tenuta, M., Kuang, W., Gui, D., and Zeng, F. (2019). Manure application increased denitrifying gene abundance in a drip-irrigated cotton field. *PeerJ* 7:e7894. doi: 10.7717/peerj.7894

Zeng, Q. C., An, S. S., and Liu, Y. (2017). Soil bacterial community response to vegetation succession after fencing in the grassland of China. *Sci. Total Environ.* 609, 2–10. doi: 10.1016/j.scitotenv.2017.07.102

Zhang, C., Li, J., Wang, J., Liu, G., Wang, G., Guo, L., et al. (2019). Decreased temporary turnover of bacterial communities along soil depth gradient during a 35-year grazing exclusion period in a semiarid grassland. *Geoderma* 351, 49–58. doi: 10.1016/j.geoderma.2019.05.010

Zhang, C., Liu, G. B., Song, Z. L., Wang, J., and Guo, L. (2018). Interactions of soil bacteria and fungi with plants during long-term grazing exclusion in semiarid grasslands. *Soil Biol. Biochem.* 124, 47–58. doi: 10.1016/j.soilbio.2018.05.026

Zhang, L. M., Hu, H. W., Shen, J. P., and He, J. Z. (2012). Ammonia-oxidizing archaea have more important role than ammonia-oxidizing bacteria in ammonia oxidation of strongly acidic soils. *ISME J.* 6, 1032–1045. doi: 10.1038/ismej.2011.168

Zhang, X., Johnston, E. R., Wang, Y., Yu, Q., Tian, D., Wang, Z., et al. (2019). Distinct drivers of core and accessory components of soil microbial community functional diversity under environmental changes. *mSystems* 4:e00374-19.

Zhang, Y., Gao, X., Hao, X., Alexander, T. W., Shi, X., Jin, L., et al. (2020a). Heavy grazing over 64 years reduced soil bacterial diversity in the foothills of the Rocky Mountains, Canada. *Appl. Soil Ecol.* 147:103361. doi: 10.1016/j.apsoil.2019.09.011

Zhang, Y., Xin, X., Li, R., Xun, W., Zhang, R., Li, L., et al. (2020b). Heavy grazing reduces the diversity of soil microbial communities in meadow grassland under long-term grazing. *Research Square* [Preprint] doi: 10.21203/rs.3.rs-129099/v1

Zheng, W., Zhao, Z., Gong, Q., Zhai, B., and Li, Z. (2018). Responses of fungal–bacterial community and network to organic inputs vary among different spatial habitats in soil. *Soil Biol. Biochem.* 125, 54–63. doi: 10.1016/j.soilbio.2018.06.029

Conflict of Interest: The authors declare that the research was conducted in the absence of any commercial or financial relationships that could be construed as a potential conflict of interest.

Publisher's Note: All claims expressed in this article are solely those of the authors and do not necessarily represent those of their affiliated organizations, or those of the publisher, the editors and the reviewers. Any product that may be evaluated in this article, or claim that may be made by its manufacturer, is not guaranteed or endorsed by the publisher.

frontiers in Plant Science

ORIGINAL RESEARCH
published: 09 August 2021
doi: 10.3389/fpls.2021.700446

Transcriptome and Biochemical Analysis Jointly Reveal the Effects of *Bacillus cereus* AR156 on Postharvest Strawberry Gray Mold and Fruit Quality

Yi-Yang Yu[1,2,3†], Guo-Xia Dou[4†], Xing-Xing Sun[5†], Lin Chen[1,2,3], Ying Zheng[1,2,3], Hong-Mei Xiao[4], Yun-Peng Wang[6], Hong-Yang Li[5], Jian-Hua Guo[1,2,3*] and Chun-Hao Jiang[1,2,3*]*

[1] Department of Plant Pathology, College of Plant Protection, Nanjing Agricultural University, Nanjing, China, [2] Key Laboratory of Monitoring and Management of Crop Diseases and Pest Insects, Ministry of Agriculture, Nanjing, China, [3] Engineering Center of Bioresource Pesticides in Jiangsu Province, Nanjing, China, [4] Key Laboratory of Quality and Safety Risk Assessment in Agricultural Products Preservation (Nanjing), Ministry of Agriculture, College of Food Science and Technology, Nanjing Agricultural University, Nanjing, China, [5] Jiangsu Coastal Area Institute of Agricultural Science, Yancheng, China, [6] Jiangsu Provincial Key Construction Laboratory of Probiotics Preparation, College of Life Science and Food Engineering, Huaiyin Institute of Technology, Huai'an, China

Postharvest strawberry is susceptible to gray mold disease caused by *Botrytis cinerea*, which seriously damage the storage capacity of fruits. Biological control has been implicated as an effective and safe method to suppress plant disease. The aim of this study is to evaluate the postharvest disease control ability of *Bacillus cereus* AR156 and explore the response of strawberry fruit to this biocontrol microorganism. *Bacillus cereus* AR156 treatment significantly suppressed gray mold disease and postponed the strawberry senescence during storage. The bacterium pretreatment remarkably enhanced the reactive oxygen-scavenging and defense-related activities of enzymes. The promotion on the expression of the encoding-genes was confirmed by quantitative real-time PCR (qRT-PCR) that significantly increased the expression of the marker genes of salicylic acid (SA) signaling pathway, such as *PR1*, *PR2,* and *PR5*, instead of that of the jasmonic acid (JA)/ethylene (ET) pathway, which was also shown. Moreover, through transcriptome profiling, about 6,781 differentially expressed genes (DEGS) in strawberry upon AR156 treatment were identified. The gene ontology (GO) classification and Kyoto Encyclopedia of Genes and Genomes (KEGG) pathway enrichment indicated that AR156 altered the transcription of numerous transcription factors and genes involved in the SA-related plant disease resistance, metabolism, and biosynthesis of benzoxazinoids and flavonoids. This study offered a non-antagonistic *Bacillus* as a method for postharvest strawberry storage and disease control, and further revealed that the biocontrol effects were arisen from the induction of host responses on the transcription level and subsequent resistance-related substance accumulation.

Keywords: strawberry, gray mold, biological control, *Bacillus cereus* AR156, induced systemic resistance (ISR), transcriptome profiling

OPEN ACCESS

Edited by:
Carlos Lucena,
University of Córdoba, Spain

Reviewed by:
Isabel María López-Lara,
National Autonomous University of Mexico, Mexico
Santiago Signorelli,
Universidad de la República, Uruguay

***Correspondence:**
Chun-Hao Jiang
chjiang@njau.edu.cn
Jian-Hua Guo
jhguo@njau.edu.cn
Hong-Yang Li
yclhy@sina.com

† These authors have contributed equally to this work

Specialty section:
This article was submitted to Plant Symbiotic Interactions, a section of the journal Frontiers in Plant Science

Received: *26 April 2021*
Accepted: *28 June 2021*
Published: *09 August 2021*

Citation:
Yu Y-Y, Dou G-X, Sun X-X, Chen L, Zheng Y, Xiao H-M, Wang Y-P, Li H-Y, Guo J-H and Jiang C-H (2021) Transcriptome and Biochemical Analysis Jointly Reveal the Effects of Bacillus cereus AR156 on Postharvest Strawberry Gray Mold and Fruit Quality. Front. Plant Sci. 12:700446. doi: 10.3389/fpls.2021.700446

INTRODUCTION

Strawberry (*Fragaria x ananassa* Duch.) is a popular fruit worldwide, and it is well known for its nutritional compositions and unique flavor. Postharvest strawberry easily suffers from infection of pathogenic microorganisms as well as the primary metabolism that leads to fruit rot and senescence, which finally results in the deterioration of fruit quality and waste of natural resources. The estimated loss of postharvest fruits is as high as 40–50% (Alkan and Fortes, 2015). Despite many other factors, fungal pathogens is the primary reason for the significant fruit losses during storage (Marín et al., 2017), and gray mold disease caused by *Botrytis cinerea* is the main fungal disease that threatens the storage of postharvest strawberries (Shao et al., 2013). Strawberries are frequently exposed to pathogenic microbes. Large doses of chemicals are required to prevent and control strawberry gray mold, which can easily lead to pathogen resistance and concerns on food safety and environment (Droby, 2005; Grabke and Stammler, 2015). How to safely and effectively control postharvest diseases and retard the decay has become an impending task.

Application of yeasts, filamentous fungi, and bacteria has become an effective means for the biocontrol of postharvest fungal diseases (Dukare et al., 2019). For instance, antagonistic yeasts are widely used for controlling postharvest diseases due to their simple nutritional requirements, extreme environmental tolerance, no toxic residues, and broad-spectrum of antibacterial properties (Spadaro and Gullino, 2010). *Bacillus* has been known as a safe and ecofriendly agent to control plant diseases. *Bacillus amyloliquefaciens* FZB42 has been shown to both repress the accumulation of tobacco mosaic virus and control lettuce bottom rot caused by *Rhizoctonia solani* by induced systemic resistance (ISR) (Chowdhury et al., 2015). The use of *Bacillus cereus* NRKT in vineyards contributed to the increase in the resveratrol content in berry skins by upregulating the gene expression of stilbene synthase, and is able to protect grape berries against fungal diseases (Aoki et al., 2017). In postharvest diseases, *Bacillus subtilis* CPA-8 inhibited the growth of fungal pathogens, including *B. cinerea*, *Monilinia laxa*, *Penicillium digitatum*, *in vitro*, and effectively reduced disease incidence of apple gray mold and stone fruit brown rot (Yánez-Mendizábal et al., 2011). *Bacillus pumilus* B19 reduced the size of gray mold lesion on apple caused by *Botrrytismali* (Jamalizadeh et al., 2010). *B. cereus* AR156 has also been reported to reduce the disease incidence of peach soft rot and loquat anthracnose rot, respectively, by inducing fruit resistance-related enzyme activities (Wang et al., 2013, 2014).

Bacillus control plant diseases through a variety of mechanisms, among which, the ability to activate ISR provides the host with long term and broad spectrum resistance to various diseases. Previously, it was found that *Pseudomonas fluorescens* WCS417r-triggered ISR-promoted plant resistance against the leaf pathogen, *Pseudomonas syringae* pv. *tomato* and the root pathogen, *Fusarium oxysporum* f. sp. *raphani* through jasmonic acid (JA) signaling pathway (Pieterse et al., 1998). Recently, Niu et al. (2011, 2012) showed that salicylic acid (SA) and JA/ethylene (ET)-dependent signaling pathways are both involved in *B. cereus* AR156-triggered resistance in *Arabidopsis thaliana* and tomato. Transcription factors (TFs), such as WRKY11 and WRKY70, also played an important role in the AR156-triggered ISR by regulating the transcription of resistance-related genes downstream of the two signaling pathways (Jiang et al., 2016b). The AR156 triggers plant immunity through host recognition of bacterial-secreted extracellular polysaccharides and other microbe-associated molecular patterns (MAMPs); however, the plant receptors for these MAMPs are still unclear (Jiang et al., 2016a). Studies on postharvest diseases have also revealed the remarkable role of defense-related enzymes in the process of microorganism-induced fruit disease resistance. The biocontrol yeast, *Hanseniaspora uvarum* reduced postharvest grape berry gray mold disease by increasing the activities of grape antioxidant enzymes, such as peroxidase (POD), superoxide dismutase (SOD), catalase (CAT), phenylalanine ammonia lyase (PAL), ascorbate peroxidase (APX), and polyphenoloxidase (PPO) (Cai et al., 2015).

In the recent years, with the advent of the post-genome era, omics technologies, such as transcriptomics, proteomics, and metabolomics, are experiencing rapid development. Transcriptome sequencing is a powerful tool for high-throughput research that helps reveal the differences in gene expression of the same organism in different growth periods and environments. Rao et al. (2019) combined targeted metabolome, the second-generation RNA sequencing (RNA-seq), and full-length transcriptome to explore the association between gene expression and polyphenol concentration in different developing stages of olive. Chen et al. (2019) analyzed the transcriptome of postharvest African Pride during cracking, and found that starch degradation and cell wall polysaccharide metabolism are closely related to fruit ripening and cracking. However, there are still few studies on its application in postharvest strawberry.

In this study, we found that *B. cereus* AR156 could improve the resistance of postharvest strawberry to gray mold and increase the storage capacity. In order to acquire a comprehensive understanding on the effect of AR156 treatment on strawberry fruit, we explored the resistance induced by AR156 from multiple perspectives. We first tested the effect of AR156 on the disease resistance and senescence-related enzyme activities of postharvest strawberry fruits. Quantitative real-time PCR (qRT-PCR) was used to verify the consistency of the expression of some of the defense-related enzyme encoding genes by promoting the enzyme activity and disease-resistant phenotype. Besides, to obtain more comprehensive information, we also identified 6781 differentially expressed genes (DEGs) induced by AR156 through comparative transcriptome, and the RNA-seq result was analyzed.

MATERIALS AND METHODS

Plant Material and Strain Growth Condition

The strawberry (Benihoppe) used in this study was picked in Suoshi Ecological Garden, Jiangning District, Nanjing City, Jiangsu Province. Fruits with the same maturity and with no

mechanical or pest damage were selected and shipped to the laboratory within 2 h. The *B. cereus* AR156, the plant growth-promoting rhizobacteria (PGPR) strain, was routinely cultured in Luria-Bertani medium (LB medium, 10 g of tryptone, 5 g of yeast extract, 10 g of NaCl per liter, and pH adjusted to 7.2). The strain was streaked out from −80°C freezer and incubated at 28°C. Single colony was picked out from the plate and inoculated into a shaking test tube with 5 ml LB for ∼16 h. The culture was then inoculated (1:100 v/v) into a flask with 500 ml LB medium. The culture was grown under shaking condition at 28°C for 24 h, and then centrifuged at 4°C, 5000 rpm for 10 min. Cells were collected and suspended with sterilized water to 5×10^7 CFU·ml^{-1}. *B. cinerea* BC1301 (Jiang et al., 2018a) was stored on potato dextrose agar (PDA, 200 g of potato, 18 g of glucose, 15 g of agar per liter) at 4°C. The strain was activated on PDA agar and cultured at 25°C for 7 days in dark. The mycelium was then scraped and dissolved in a sterile physiological saline (8.5 g/l NaCl). Spore was freshly prepared by filtering the sample against 8 layers of gauze and adjusted to 1×10^5 spores·ml^{-1} using a hemocytometer.

Antagonism Assay

The fungal mycelium stored at 4°C was placed on a PDA plate and cultured at 25°C. A sterile perforator was used to make fungal hyphae disk along the outer edge of the colony to obtain active growing hyphae. The fungal disk was transferred to the center of WA (5 g of peptone, 10 g of glucose, 3 g of beef extract, 5 g of NaCl, 15 g of agar per liter, pH was adjusted to 7.2) plate. Ten microliters of biocontrol bacteria suspension and water was dropped at the same distance from the fungal disk on the sterile filter paper disk. The antagonism plate was cultured in a 25°C incubator, and the growth of the fungus was observed. The antagonism diameter was recorded. This assay was repeated three times.

Detection of Bacterial Effect on Gray Mold

Strawberry fruit was soaked in 0.001% sodium hypochlorite solution for 10 s and air-dried for 1 h. A 3 mm × 3 mm wound was created at the center of the fruit with a sterilized inoculating needle and air-dried. In the six AR156 treatments, the wound was treated with 50 μl 5×10^7 CFU·ml^{-1} *B. cereus* AR156 cell suspension at 2 h, 6, 12, 18, 24, and 36 h, respectively, before inoculation of 50 μl 1×10^5 spores·ml^{-1} *B. cinerea* spore suspension. The control was treated with 50 μl of water 24 h before inoculation with 50 μl 1×10^5 spores·ml^{-1}*B. cinerea* spore suspension. After treatment, the strawberry fruit was air-dried and placed in a container sealed with plastic film, and stored in an incubator at 20°C and relative humidity (RH) of 95%. The lesion diameter (in cm) on the strawberry fruit was observed every day and recorded whenever appropriate. Each treatment had three parallels, and each parallel contained 10 fruits. The experiment was repeated.

To verify the role of SA-signaling pathway in the process of disease suppression, the strawberry was sprayed with 0.3 mm 2-aminoindan-2-phosphonic acid (AIP) or paclobutrazol (PAC), respectively, before the wounds were created, and the samples were then air-dried after 1 h of incubation in room temperature. The disease control method is followed as above. *B. cereus* AR156 cell suspension was applied 24 h before the inoculation of the pathogen.

Detection of Bacterial Effect on the Quality of Strawberry Fruit Stored at Low Temperature

Strawberry fruits with the same maturity and intact surface were selected and randomly divided into two groups of 300 each. Each group is then evenly divided into three parallels. Treatment group was evenly sprayed with 5×10^7 CFU·ml^{-1} AR156 cell suspension (containing 0.001% Tween 20); control group was treated with 0.001% Tween 20 water solution. The surface of strawberry was air-dried. Samples were then placed in plastic baskets, covered with modified atmosphere bags to ensure internal air circulation, stored in a cold storage at 2 ± 1°C, and examined every 3–5 days to detect the quality-related indicators of the fruit. The specific methods are described in the sections below.

Measurement of Soluble Solids

A WYT-4 handheld sugar meter (Shanghai Precision & Scientific Instrument Co., Ltd., Shanghai, China) was used for soluble solids measurement. Ten fruits were measured for each treatment.

Measurement of Fruit pH

Fruit samples measuring 2 cm were gently taken from the fruit with a knife and ground. Samples were then removed to a flask, fixed to 100 ml of water, mixed thoroughly, and incubated for 20 min. The ground samples were filtered through four layers of gauze. Filtrate pH was measured at room temperature with a PHS-3C pH meter (Shanghai Precision & Scientific Instrument Co., Ltd., Shanghai, China). The test was repeated three times.

Measurement of Fruit Color

A Px.44-2132 colorimeter (Beijing Zhuochuan Electronic Science and Technology Co., Ltd., Beijing, China) was used to measure the surface color of fruit. The results were represented as L*, a*, and b*, representing brightness, red and green, and yellow and blue, respectively. Symmetrical part at the center of the fruit was selected for measurement. Each treatment had three parallels, and each parallel contained 10 fruits.

Measurement of Vitamin C

Vitamin C was determined using an ultraviolet spectrophotometry (Nano Drop ND1000, Thermo Fisher Scientific, Inc., United States) following the Tillman's method described by Santos et al. (2016) according to the following equations:

$$F = \text{Mass of vitamin C used in the tritation (mg)} / \text{Volume of Tillman's solution used in titration (ml)}$$

$$\text{Vitamin C content (mg per 100 ml)} = V \times F \times 100/A.$$

Measurement of the Relative Content of Fruit Flavonoids and Anthocyanins

Two grams of fruit tissue was ground thoroughly in 2 ml of 1% pre-chilled HCL–methanol solution. Samples were washed with 5 ml of HCL–methanol solution, incubated on ice for 20 min, and centrifuged at 4°C, 10,000 rpm, for 10 min. The absorbance at 325, 530, and 600 nm, respectively, of the supernatant was measured. The absorbance value of each gram of tissue at a wavelength of 325 nm represented the relative content of flavonoids; the difference between the absorbance values at wavelengths of 530 and 600 nm, respectively, represented the relative content of anthocyanins (U):

$$U = (OD_{530} - OD_{600}) \cdot g^{-1}.$$

Detection of Bacterial Effect on Defense-Related Enzymes in Strawberry Fruit

The wound on the strawberry was created as described earlier. The four treatments are listed below. (1) Control treatment: 50 μl sterilized H_2O was inoculated to the wound, 24 h later, another 50 μl sterilized H_2O was applied to the wound; (2) AR156 treatment: 50 μl of 5×10^7 CFU·ml^{-1}*B. cereus* AR156 culture dilution was inoculated to the wound, then 50 μl sterilized H_2O was applied to the wound 24 h later; (3) *B. cinerea* treatment: 50 μl sterilized H_2O was inoculated to the wound, 24 h later, 50 μl 1×10^5 spores·ml^{-1} of *B. cinerea* spore suspension was applied to the wound; (4) AR156 + *B. cinerea* treatment: 50 μl of 5×10^7 CFU·mL^{-1} *B. cereus* AR156 culture dilution was inoculated to the wound, 24 h later, 50 μl of 1×10^5 spores·ml^{-1}*B. cinerea* spore suspension was applied to the wound.

The strawberry fruit was air-dried and placed in a container sealed with a plastic film, and stored in an incubator at 20°C and RH of 95%. The sampling time was 0, 12, 24, 36, 48, 54, 72, and 96 h after inoculation with *B. cinerea*. The wound tissue was cut with a scalpel sterilized with ethanol, frozen in liquid nitrogen, and stored in –80°C ultra low temperature freezer. The crude enzyme extract was prepared following the method described before (Qin et al., 2017). The fruit sample was placed in a liquid nitrogen pre-cooled mortar and ground into powder. Two grams of sample powder was collected in a pre-cooled test tube, and 5 ml of 50 mmol·l^{-1} pH 7.8 phosphate extract buffer [containing 1% polyvinylpolypyrrolidone (PVPP)] was added twice. Samples were vortexed at 4°C, centrifuged at 10,000 rpm for 10 min, and the supernatant was then collected. Each treatment contained three parallels, and the test was repeated two times. The APX, SOD, CAT, PAL, POD, and PPO enzyme activity was measured as described by Wang L. et al. (2019).

RNA Extraction and Gene Expression Analysis

The strawberry fruit was air-dried and placed in a container sealed with a plastic film, and stored in an incubator at 20°C and RH of 95%. The tissue was cut with a scalpel sterilized with ethanol, frozen in liquid nitrogen, and stored in –80°C ultra low temperature freezer. Strawberry fruit samples (0.1 g each), treated according to the requirements of each treatment, were collected and ground into powder in liquid nitrogen. Total RNA was extracted with 1 ml of TRIZOL reagent (Invitrogen, Dalian, China) (Rio et al., 2010) and genomic DNA was removed by treating with RNase-free DNase (Takara, Dalian, China). HiScriptTM Q Select RT SuperMix and 1 μg of total RNA (Vazyme, Nanjing, China) were used for RNA reverse transcription according to the protocol of the manufacturer (37°C/15 min, 85°C/5 s). A constitutively expressed gene (18S rRNA in *Fragaria* x *ananassa*) was the reference gene in the qRT-PCR analysis. The PCR system: 2.5 μl of 10 × RT-PCR Buffer, 2 μl of 2.5 mm dNTP, 0.5 μl of Forward Primer, 0.5 μl of reverse primer, 0.5 μl of 50 × ROX, 1 μl of complementary DNA (cDNA), 0.25 μl of r-Taq, 2.5 μl of 100 × SYBR, and RNase-free dH2O was used to bring the total volume to 25 μl. The amplification procedure: 95°C/3 min + 40 × (95°C/15 s + 60°C/20 s + 72°C/30 s) + 95°C/15 s + 55°C/1 min + 72°C/30 s. The experiment was repeated three times for each treatment. The primers used in this work are shown in **Supplementary Table 1**.

RNA Sequencing and Functional Annotation

The RNA sequencing library of the four treatments was constructed. In the mock treatments, strawberry wound was made as described above and treated with 50 μl of sterile water. One day later, 50 μl of 1×10^5 spores·ml^{-1} *B. cinerea* spore suspension was inoculated. Sample was collected at 0 and 24 h after pathogen treatment in Mock_*B. cinerea*_at 0 h and Mock_*B. cinerea*_at 24 h treatments, respectively. For AR156 treatment, the strawberry wound was first treated with 50 μl of 5×10^7 CFU·ml^{-1}*B. cereus* AR156 cell suspension followed by the same pathogen inoculation procedure in mock treatment. Samples were collected at 0 and 24 h after pathogen treatment in AR156_*B. cinerea*_at 0 h and AR156_*B. cinerea*_at 24 h treatments. Strawberry fruit transcriptome sequencing was completed in Beijing Genomics Institute (BGI), China, using the HiSeqTM 2500 platform. The result has been uploaded to the National Center for Biotechnology Information (NCBI) in FASTQ format (BioProject accessions: PRJNA643674; BioSample accessions: SAMN15423441, SAMN15423442, SAMN15423443, SAMN15423444, SAMN15423445, SAMN15423446, SAMN15423447, SAMN15423448, SAMN15423449, SAMN15423450, SAMN15423451, SAMN15423452).

The data were processed as described by Jiang et al. (2019). Briefly, the clean data were acquired by processing the raw reads by Illumina Pipeline Software, and the adaptors and low-quality reads ($Q < 20$) were removed using Perl scripts. *Denovo* assembly of the transcripts was performed by Trinity method. The summary of the transcriptome assembly can be found in the **Supplementary Data Sheet 1**. Unigenes were then produced by mapping the data back to the contigs of the clean reads. Unigenes with significant

expression were searched against the non-redundant protein sequence database using the NCBI BlastX (*E*-value ≤ 10–5). The blast result was mapped to UniProt, from which GO terms were extracted. Unigenes were further searched against several databases, such as the Swiss-Prot, the KEGG pathway database, and the GO database to acquire the putative function annotation.

Identification of DEGs, TFs, and Plant Disease Resistance Genes

Mapped fragments per kilobase per million (FPKM) was used to represent the expression level of the identified genes. The DESeq R package (1.10.1) was used to analyze the differential gene expression. The DEGs were identified as genes with a log-fold expression change which is greater than 2 or less than –2 using a quality control threshold of false discovery rates (FDR) < 0.001 and a high statistically significant value of $P < 0.05$. The GO enrichment was obtained by enriching and refining the GO annotation acquired above using the GOseq R package using the ELIM method and Kolmogorov–Smirnov test (**Supplementary Data Sheet 2**). The KEGG pathways analysis was performed in KOBAS 2.0 server and enriched by using in-house scripts according to Fisher's exact test. TFs in strawberry fruit were identified by blasting all assembled unigenes against the plant TF database[1] with a threshold *E*-value of 1e-06 (**Supplementary Data Sheet 3**). Plant resistance genes (PRGs) were identified by searching all assembled unigenes in PRG database[2] (**Supplementary Data Sheet 4**).

Data Analysis

The data were analyzed using the statistical software, SPSS 24.0 (IBM SPSS Inc., United States). Differences were compared using the least significant difference (LSD test) (Fisher's protected least significant differences test); the difference of P-value < 0.05 was considered as statistically significant.

RESULTS

B. cereus AR156-Controlled Postharvest Strawberry Gray Mold Caused by *B. cinerea* and Delay Fruit Senescence

The *B. cereus* AR156 has previously been shown to facilitate postharvest storage of peach and loquat fruit (Wang et al., 2013, 2014). At the starting point of this study, we wanted to investigate whether *B. cereus* AR156 has a positive effect on postharvest storage of strawberry fruits. In order to comprehensively understand the impact of AR156 on postharvest strawberry disease, we treated strawberry fruits with AR156 at different time points (2, 6, 12, 18, 24, and 36 h) prior to the inoculation of *B. cinerea* spore. Three days after pathogen treatment, the disease lesion diameter was recorded. The postharvest strawberry in the control treatment showed significant gray mold symptoms (**Figure 1A**) under room temperature storage (25°C). The lesion on strawberry fruits decreased significantly in the AR156 pretreatments (**Figure 1B**). Among all, compared with the control, the AR156 pretreated for 24 h had the most significant effect on disease lesion reduction, indicating the highest inhibitory effect on controlling the gray mold disease (**Figures 1A,B**). *B. cereus* AR156 was known to suppress fungal diseases through direct antagonism (Yu et al., 2017). We carried out an antagonism experiment on a plate to investigate whether it directly inhibits the growth of *B. cinerea*. The result showed that under laboratory condition, *B. cereus* AR156 had no significant ability to antagonize *B. cinerea* (**Supplementary Figure 1**).

We also monitored the effect of AR156 on strawberry storage without pathogen stress by testing the fruit quality indicators. During storage, the L* value, a* value, and b* value of the strawberry underwent significant changes, while AR156 treatment suppressed this trend within the entire 28 days of test (**Figures 2A–C**). The total soluble solids and vitamin C content of the strawberry treated with AR156 were significantly improved compared to the treatment in the first 8 days, but reached consistency with the control in the later period (**Figures 2E,F**). However, the pH and relative contents of flavonoids and anthocyanins of strawberry fruit after AR156 treatment did not show significant difference from those of the control during the storage (**Figures 2D,G,H**).

B. cereus AR156 Raise the Defense-Related Enzymes Activities of Strawberry by Inducing the Expression of Their Encoding Genes

To further explore the mechanism of the improvement of the beneficial bacteria on postharvest storage of strawberries, the effect of AR156 pretreatment on APX, SOD, CAT, PAL, POD, and PPO activities in the strawberry fruit with or without *B. cinerea* inoculation was tested. Pathogen treatment alone increased APX and CAT within 0–24 h. But the activities decreased rapidly afterward, and was lower than or equal to the control after 48 h. On the contrary, AR156 and AR156 + *B. cinerea* treatments could induce sustained enhancement on the activities of the both, within the tested 96 h (**Figures 3A,C**). After 48 h of storage, the APX enzyme activity in the AR156 + *B. cinerea* and AR156 treatment increased by 66.2 and 62.8% compared to the *B. cinerea* treatment, and the CAT activity increased by 56.2 and 51.5%, respectively. Similarly, AR156 and AR156 + *B. cinerea* treatments significantly induced the SOD activity of strawberry fruit than that of *B. cinerea* treatment and control from 24 to 54 h (**Figure 3B**). The AR156 rapidly increases the SOD activity in the early stage of infection. At 36 h, the SOD enzyme activity of the AR156 treatment reached the peak, which increased by 50.1% compared to the *B. cinerea* treatment. The activity of the SOD enzyme in the AR156 treatment showed a decreasing trend after 48 h of incubation; while the activity of the *B. cinerea* in the control treatment

[1] http://plntfdb.bio.uni-potsdam.de

[2] http://prgdb.crg.eu/wiki/Main_Page

FIGURE 1 | Effect of *B. cereus* AR156 on postharvest diseases of strawberry caused by *B. cinerea*. **(A)** Disease symptoms caused by *B. cinerea* infection of strawberry fruit with pretreatment of *B. cereus* AR156 at different times. **(B)** The lesion diameter of *B. cinerea* shown on strawberry fruit. Values were average numbers calculated from twelve different strawberry fruits after challenged with *B. cinerea*. All data were presented as means of three replicates ± SD, and error bars represented as SD for three replicates. Letters above the bars indicated statistically significant differences among treatments [least significant difference (LSD) test, $P < 0.05$]. All experiments were performed three times, and similar results were obtained.

decreased during the entire testing period. *B. cinerea* induced the accumulation of PAL and PPO in the fruit soon after inoculation, but the significant difference from the control disappeared after 48 and 36 h, respectively. Instead, the activities of PAL and PPO, induced by AR156, reached the peak at 36 and 48 h, respectively, and were significantly higher than the control and *B. cinerea* treatment. The PPO enzyme activity in AR156 + *B. cinerea* and AR156 treatments was 61.6 and 56.2% higher compared to *B. cinerea* treatment at 48 h. Both, AR156 and *B. cinerea* could lead to a rapid increase on POD activity in the early stage, but AR156 treatment showed significant higher POD activity than the pathogen treatment and the control after 48 h.

It is rational to speculate that AR156 promoted the activity of these defense-related enzymes by altering the transcription of the coding genes. To verify this hypothesis, we extracted the RNA of strawberry fruits under different treatments at the above time points, and detected the expression of *PAL*, *PPO*, and *CAT*-encoding genes by qRT-PCR. The data showed that the AR156 and AR156 + *B. cinerea* treatments upregulated the expression of *PAL*, *PPO,* and *CAT* at 12 h compared to the control treatment, and the upregulation lasted for a long period during storage (**Figure 4**). We further tested the expression of other defense-related genes, and found that AR156 significantly induced the expression of SA signal pathway-related defense genes, such as *PR1*, *PR2* (*Glu*), *PR5*, while the expression of JA/ET signal pathway marker genes, such as *PDF1* and *JAR1* was not significantly affected. The AR156 and AR156 + *B. cinerea* treatment upregulated the expression of *PR5* at 12 h, and the expression of *PR1* and *PR2* was induced at 36 h compared to the control and *B. cinerea* treatment. *B. cinerea* treatment promoted the expression of *WRKY1* at 54 h, while AR156 + *B. cinerea* treatment was able to induce a stronger expression of *WRKY1* in advance by showing a significant difference on the expression in the control and *B. cinerea* treatments at 36 h. For *NPR1*, the AR156 and AR156 + *B. cinerea* treatments also upregulated the gene expression at 24 h. To further verify the role of SA-signaling pathway in the gray mold resistance induced by AR156, we treated the strawberry with the SA inhibitor, PAC/AIP, before AR156 treatment. The results showed that the control effect of AR156 against gray mold was impaired by PAC/AIP pretreatment (**Figure 5**).

Identification and Functional Annotation of DEGs Upon *B. cereus* AR156 Treatment Revealed Induced Expression of Strawberry Defense-Related Genes in the Process of Strawberry Gray Mold Control

Based on the above results, we found that *B. cereus* could increase the accumulation of defense-related substances in strawberry fruits by modifying the gene transcription, thereby increasing the strawberry resistance to gray mold and slowing down the senescence of fruits during storage. In order to further understand how the genes and regulatory pathways were affected, we compared the transcription of strawberry fruit under AR156 or water treatment at 0 and 24 h after *B. cinerea* inoculation. The heatmap of Pearson's correlation coefficients and principal component analysis (PCA) showed that the transcriptome repeats of each treatment had a high consistency. On the PCA analysis map, repeats of treatments tended to aggregate together, indicating the reliability of the transcriptome data (**Supplementary Figure 2**).

We analyzed the transcription sequencing data and identified DEGs as described in the section "Materials and Methods." At the overall level of gene expression, the transcriptional profiles were consistent within each repeats (**Supplementary Figure 3**). By analyzing the differences among the treatments, we found that the expression of 6,781 genes, in the total of 45,353 genes identified in this study, was affected by the treatments. After

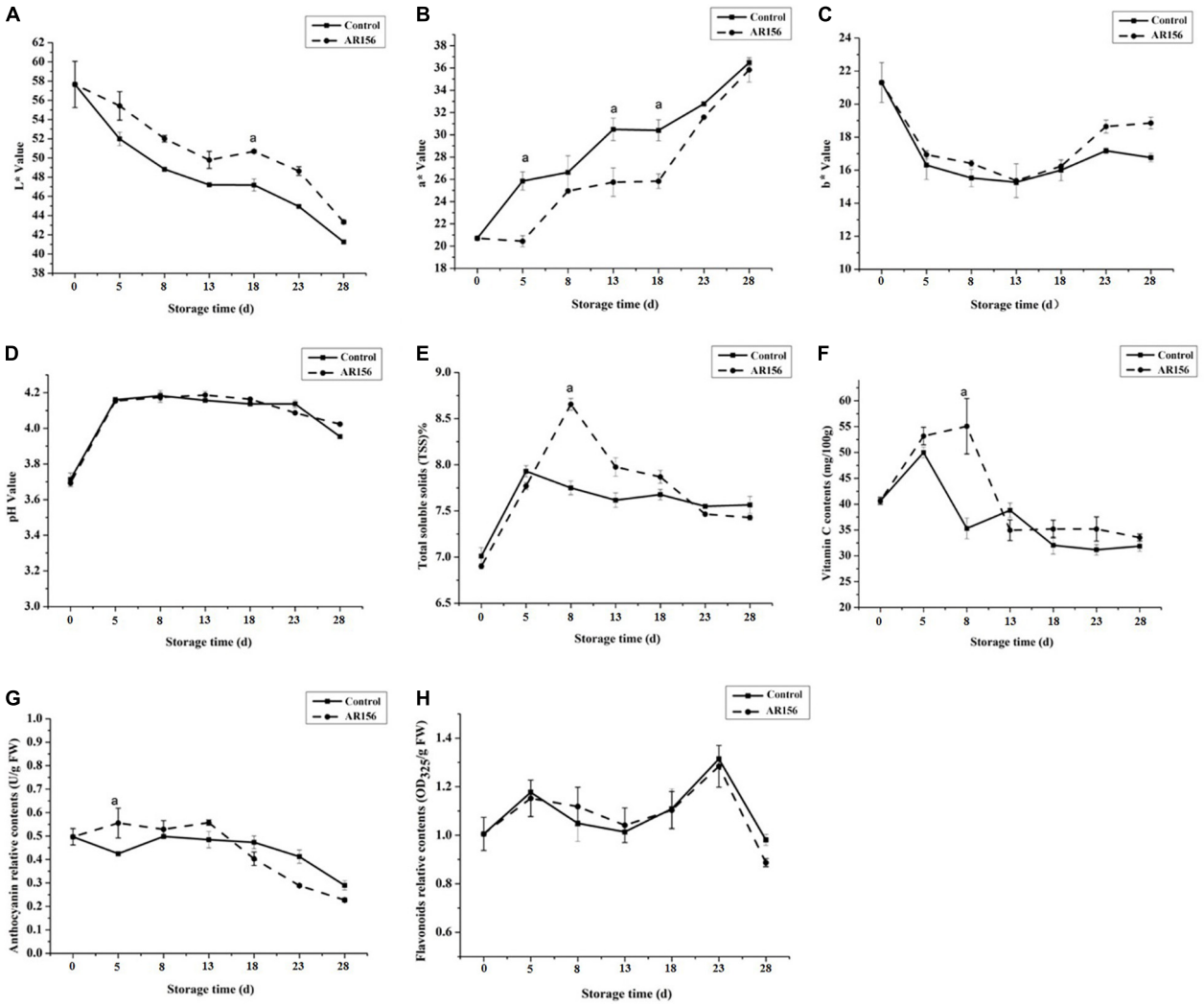

FIGURE 2 | Effect of *B. cereus* AR156 treatment on the quality parameters of strawberry fruits during cold storage at 2 ± 1°C. The fruit quality of strawberry was evaluated in response to *B. cereus* AR156 treatment. Series of fruit quality parameters such as **(A)** L* value, **(B)** a* value, **(C)** b* value, **(D)** pH value, **(E)** total soluble solids, **(F)** vitamin C content, **(G)** anthocyanin relative contents, and **(H)** flavonoids relative contents were detected. All data were presented as means of three replicates ± SD, and error bars represent SD for three replicates. Letters above the bars indicate statistically significant differences among treatments [least significant difference (LSD) test, $P < 0.05$]. All experiments were performed three times, and similar results were obtained.

24 h of pathogen inoculation, AR156 could induce differential expression of 916 genes compared to all other treatments (**Supplementary Figure 3**). Further analysis of DEG revealed that 1,132 genes were upregulated in the AR156 treatment at 24 h compared to the control, and the number of downregulated genes was found to be 403 (**Figures 6A,C**). Comparing the AR156-caused DEG under pathogen and pathogen-free conditions, pretreatment with AR156 for 24 h led to a total of 6,407 DEGs, and the amount of DEGs caused by AR156 after pathogen inoculation was found to be 1,494 (**Figure 6B**). A total of 1,120 DEGs was induced by AR156 pretreatment at both 0 and 24 h, respectively, after pathogen inoculation, and the unique DEGs induced by AR156 was found to be 5,287 at 0 h, and 374 DEGs at 24 h. We also analyzed the magnitude of change in the gene expression. About 1,354 genes were upregulated at 24 h after pathogen inoculation by AR156 pretreatment. Among them, the expression of 124 genes was upregulated over 10-fold; 689 genes were downregulated, and the number of genes with over 10-fold expression was found to be 54 (**Supplementary Figure 4**).

Pathway Enrichment Analysis for DEGs Upon *B. cereus* AR156 Treatment

For further investigation on the changes in the transcription of regulatory pathways and functional units in strawberry caused by AR156, we performed GO and KEGG pathway enrichment analyses with the above transcription data. In the GO analysis, the AR156 caused differential expression of genes, which was divided into three categories including

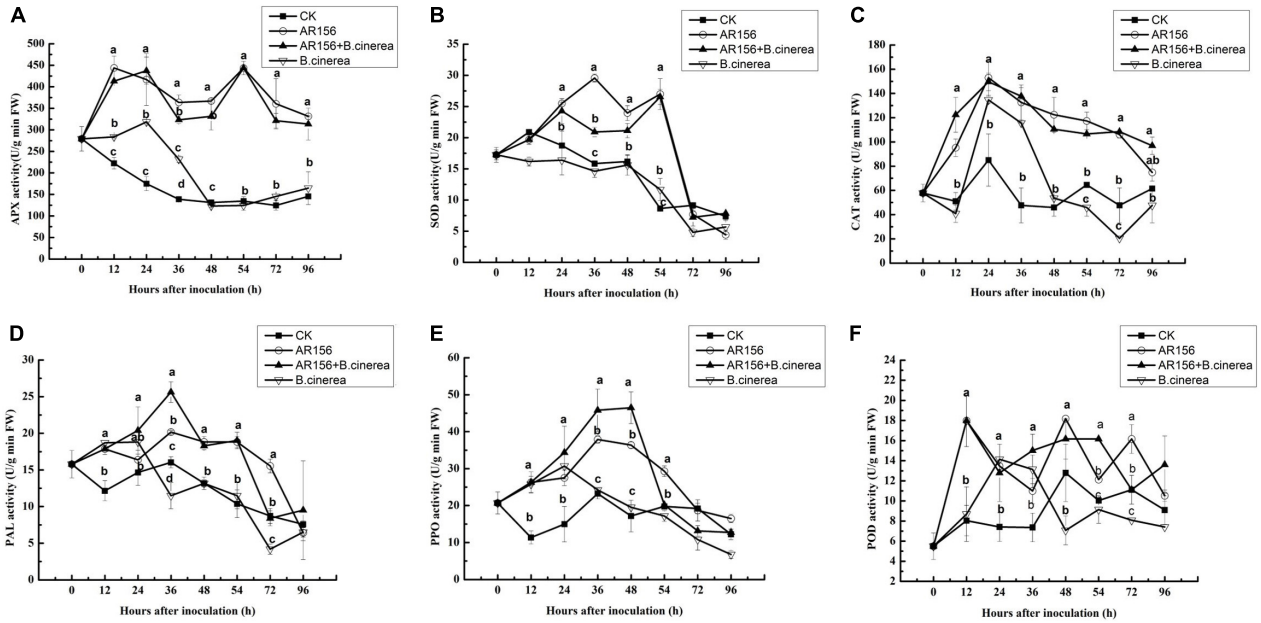

FIGURE 3 | Effect on the activities of defense-related enzymes in the process of controlling postharvest diseases of strawberry by *B. cereus* AR156. Activities of defense-related enzymes in the strawberry pretreated with *B. cereus* AR156, and then were challenged with *B. cinerea*. **(A)** APX, **(B)** SOD, **(C)** CAT, **(D)** PAL, **(E)** PPO, and **(F)** POD. All data were presented as means of three replicates ± SD, and error bars represent SD for three replicates. Letters above the bars indicate statistically significant differences among treatments [least significant difference (LSD) test, $P < 0.05$]. All experiments were performed three times, and similar results were obtained.

biological process, cellular component, and molecular function. The DEGs were more concentrated in the cellular and metabolic processes under the classification of biological process, in the membrane part, cells, organelles, and membranes under cellular component and catalytic activity, binding under molecular function (**Supplementary Figure 5**). Through the enriched GO terms analysis, we found that DEGs were concentrated in intracellular and intracellular parts, cells, cell parts, organelles, and organelle parts (**Supplementary Figure 5**). The proportion of AR156-induced DEG of each category in the GO analysis was similar, regardless of the presence or absence of pathogen. However, the total number of DEGs under pathogenic condition was found to be 444 and 2,218 without the pathogen treatment. Interestingly, in the presence of *B. cinerea*, the AR156-induced DEGs were highly enriched in peptidase-related pathways, including endopeptidase inhibitor activity, peptidase inhibitor activity, endopeptidase regulator activity, peptidase regulator activity, serine-type endopeptidase inhibitor activity, sequence-specific binding, and response to stress pathway (**Supplementary Figure 5**).

In the KEGG pathway enrichment analysis, the AR156 induced DEGs were concentrated in the group of metabolites-related genes (**Supplementary Figure 6**). The enriched KEGG pathway shows that the DEGs induced by AR156 under pathogen-free condition were mainly enriched in ribosome-related genes. The AR156-induced DEGs in the presence of pathogen were mainly enriched in genes related to ribosome biogenesis, glyoxylate, and dicarboxylate metabolism. Moreover, the expression of benzoxazinoid biosynthesis and flavonoid biosynthesis-related genes has also been massively affected (**Supplementary Figure 6**). Further analysis showed that all three DEGs related to flavonoids biosynthesis were upregulated by AR156 treatment, regardless of the presence or absence of the pathogen. However, the effect of AR156 treatment on the gene expression was not consistent among the 16 identified DEGs related to benzoxazinoid biosynthesis (**Supplementary Figure 7**).

Transcription Factors and Plant Disease Resistance Genes Prediction Based on DEGs Provided Potential Regulating Mechanisms of *B. cereus* AR156-Triggered Immunity

Plants activate the transcript of a series of resistance-related genes in the process of resisting diseases, and the regulation of these genes often relies on the involvement of TFs. Therefore, we identified and analyzed TFs that were differentially expressed upon AR156 treatment. In this study, a total of 30 affected families of strawberry transcription factor were identified (**Figure 7A**), among which, NAC, WRKY, ERF, bHLH, and bZIP family transcription factors were widely regulated by *B. cereus* AR156 treatment (**Figure 7B**). Cluster analysis of identified differentially expressed TFs which showed that AR156 treatment could cause transcriptional change in many transcription factor encoding genes without disease infection (0 h after *B. cinerea* treatment) than in the presence of pathogen (24 h after *B. cinerea* treatment) (**Figure 7C**).

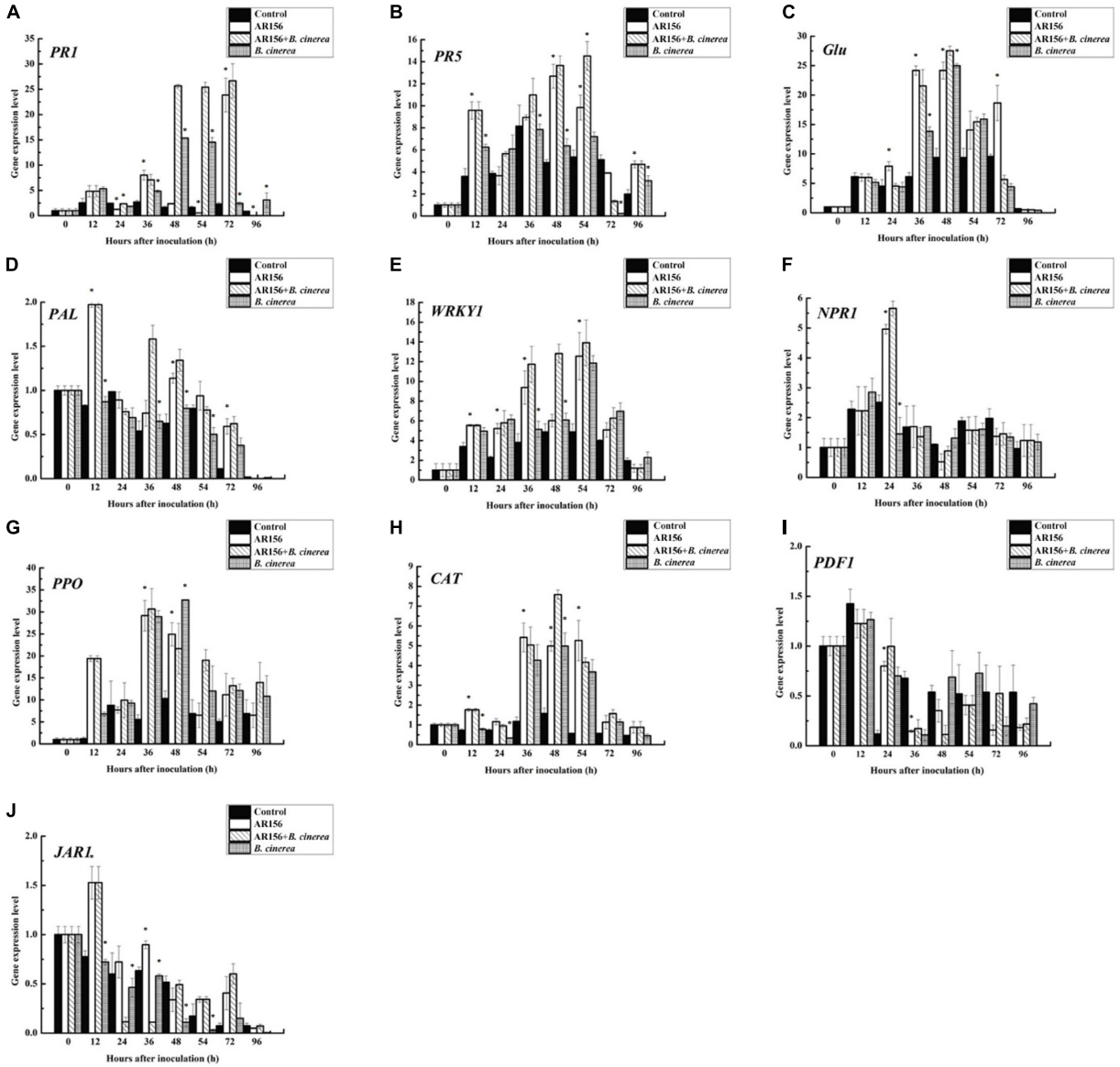

FIGURE 4 | Effects on the expression profiles of defense-related gene in the process of controlling strawberry gray mold by *B. cereus* AR156. The expression of defense-related genes which were involved in SA and JA/ET signaling pathways in response to the interaction between *B. cereus* AR156 and *B. cinerea* were analyzed. Time course of the expression of these genes [**(A)** *PR1*, **(B)** *PR5*, **(C)** *Glu*, **(D)** *PAL*, **(E)** *WRKY1*, **(F)** *NPR1*, **(G)** *PPO*, **(H)** *CAT*, **(I)** *PDF1*, **(J)** *JAR1*] were detected in strawberry pretreated with *B. cereus* AR156 and challenged with *B. cinerea*. Asterisks indicate significant differences ($P < 0.05$) in gene expression caused by AR156 treatment under pathogen or non-pathogen conditions. The expression values of the individual genes were normalized using 18S rRNA coding gene as an internal standard. All experiments were performed three times, and similar results were obtained.

We analyzed the numbers and types of PRGs induced by AR156 in the samples. *B. cereus* AR156 could influence 12 families of PRGs, including CN, CNL, L, N, NL, RLK, RLK-GNK2, RPW8-NL, RLP, Mlo-like, T, and TNL, among which RLP was the most affected (**Figures 7D,E**). In nine of the 12 affected PRG families, there were more significantly upregulated PRGs than the down regulated ones (**Figure 7D**). In terms of the activation of disease-resistance gene transcription, the effect of AR156 treatment was more significant than that of the inoculation time (**Figure 7F**).

DISCUSSION

Postharvest strawberry diseases seriously threaten strawberry production. Biological control using beneficial microorganism is a safe method for postharvest disease control. In this study, we found that *B. cereus* AR156 could suppress strawberry gray mold (**Figure 1**). In addition, the application of AR156 significantly reduced the deterioration of the quality of the strawberry fruit during storage (**Figure 2**). *B. cereus* AR156 has been reported to control a variety of plant diseases, including rice sheath blight,

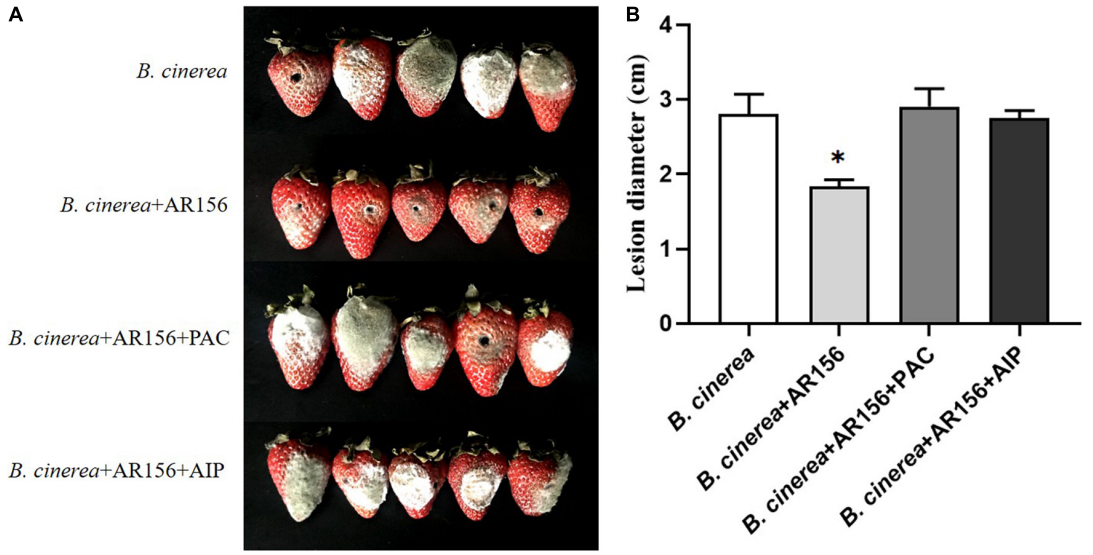

FIGURE 5 | The effect of SA biosynthesis inhibitors on the control effect of AR156 against gray mold. **(A)** Disease symptoms caused by *B. cinerea* infection of strawberry fruit. *B. cereus* AR156 was pretreated 24 h before inoculation with the pathogen, and the strawberries were treated with 0.3 mm PAC or 0.3 mm AIP 1 h before AR156 treatment. **(B)** The lesion diameter of *B. cinerea* shown on the strawberry fruit. Values were average numbers calculated from 12 different strawberry fruits after challenged with *B. cinerea*. Bars were means ± SD. Asterisks indicate statistically significant differences between treatments ($P < 0.05$). The experiment was performed three times, and similar results were obtained.

root-knot nematode disease, and pepper *Ralstonia* wilt (Zhou et al., 2014; Yu et al., 2017; Jiang et al., 2018b). The ability of AR156 to directly antagonize a broad spectrum of pathogenic fungi, such as *R. solani* and *R. solanacearum*, contributes to the control of plant diseases (Yu et al., 2017; Wang N. et al., 2019). However, the result in this study showed that AR156 had no significant inhibition on the growth of *B. cinerea* (**Supplementary Figure 1**), which suggested that the control ability of AR156 against strawberry gray mold did not depend on bacterial antagonism. A series of *B. cereus* AR156 pretreatment at all sequential time points showed positive effect on the postharvest disease control. Among them, pretreatment of AR156 at 24 h before pathogen inoculation was the most effective in controlling strawberry gray mold (**Figure 1**). Based on the results, we hypothesized that *B. cereus* AR156 control postharvest disease by inducing strawberry resistance. The activation of defense may require time to allow the response of the activation of regulatory pathways and accumulation of resistance-related substances. The peak of the resistance induction effect in this study was at 24 h (**Figure 1**).

The quality of strawberry fruit consists of many factors. The color of the fruit directly affects its economic value. Soluble solids including sugar, acids, vitamins, and other nutrients, is an important nutrition and taste indicator of strawberries. During the storage of postharvest strawberry fruits, the AR156 treatment significantly inhibited the changes of strawberry color index, and improved the nutrition of the fruit (**Figure 2**). The changes in the endogenous nutrients of the fruit indicate that AR156 has a wide-ranging effect on the strawberry fruit. In fact, this is consistent with the large amount of DEGs induced by AR156 found under pathogen-free condition in this study. Among all the DEGs, we found that 73 and 668 genes were related to fruit development process and metabolic process, respectively; the differential expression of these genes may be responsible for the change in the storability of strawberry fruits (**Supplementary Figure 5**).

Induced systemic resistance is an important mechanism for beneficial microbes to assist the plants to fight against disease. There have been many reports showing the ability of *Bacillus* to enhance host immunity (Niu et al., 2012; Jiang et al., 2016b). APX, SOD, CAT, and POD are important defense enzymes for ROS metabolism in the plant (Gill and Tuteja, 2010). Damage caused by reactive oxygen species (ROS) is implicated in the process of senescence in the fruit (Tian et al., 2013). In this study, we found that AR156 treatment can significantly promote the enzyme activity of APX, SOD, CAT, and POD in strawberry fruit (**Figure 3**). The promoted enzyme activity coincides with the AR156-induced upregulated expression of coding gene (**Figure 4H**), indicating that AR156 enhances the activity of defense-related enzymes through transcriptional regulation. The increase of ROS metabolism-related enzyme activities may explain the ability of AR156 to retard the senescence of strawberry fruits under storage, which is consistent with the results of the fruit quality indicators (**Figure 2**). The PAL activity was also increased by *B. cereus* AR156 treatment even from the early stage of infection. It has been reported that the phenylalanine ammonium lyase (PAL) pathway is important for SA biosynthesis (Wildermuth et al., 2001). SA is a plant hormone widely involved in plant disease-resistance signal transduction, and PAL has been shown to be involved in plant systemic resistance and disease control through SA. For instance, it was found that acibenzolar-*S*-methyl (ASM) pretreatment of

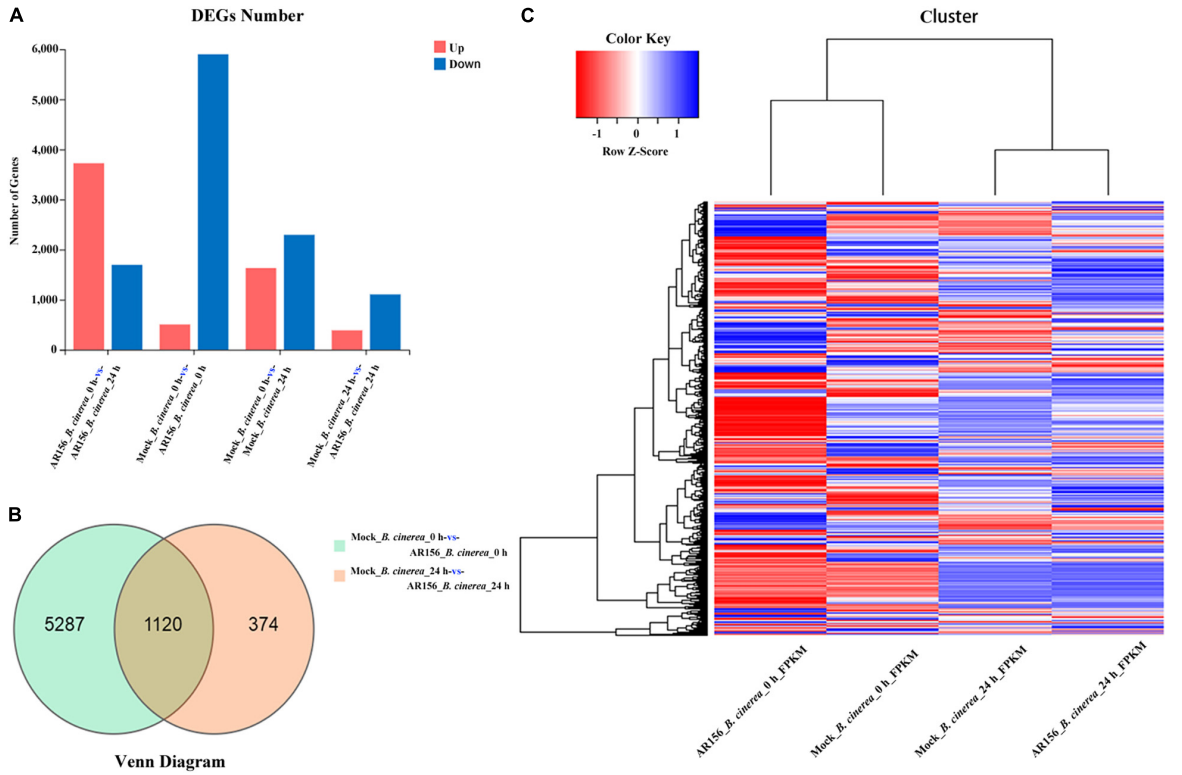

FIGURE 6 | Classification of differentially expressed genes (DEGs) in the fruits of strawberry in response to *B. cereus* AR156 treatment and in combination with *B. cinerea* inoculation. **(A)** Numbers of DEGs in response to *B. cereus* AR156 treatment and in combination with *B. cinerea* inoculation. *X* axis represents DEG numbers *Y* axis represents comparison method between each group. Red color represents upregulated DEGs, blue color represents downregulated DEGs; **(B)** Venn diagram of DEGs in the fruits of strawberry treated by *B. cereus* AR156 treatment and in combination with *B. cinerea* inoculation at different time points; **(C)** Cluster analysis of DEGs in the fruits of strawberry treated by *B. cereus* AR156 treatment and in combination with *B. cinerea* inoculation at different time points based on the expression profiles measured by RNA sequencing (RNA-seq). The color scale in the heat map corresponds to $\log_2{}^{(FPKM)}$ value of genes in each samples.

cucumber plant leaves primed the expression of a phenylalanine ammonia lyse homolog encoding gene, *PAL1*, which activates the SA pathway to protect the entire plant from *Colletotrichum orbiculare* (Cools and Ishii, 2002). The results of this study also showed that the expression of *PAL* gene in AR156-treated strawberry fruits was significantly higher than that of the control at 12 h (**Figure 4**). The changes of these defense-related enzyme activities were consistent with the induced genes expression, further indicating that AR156 affects the disease resistance of fruits by inducing resistance-related enzyme gene expression.

In addition to changes in defense enzymes, fungal infection often causes an accumulation of pathogenesis-related (PR) proteins. PR1, PR2 (Glu), PR5, and PR10 belong to the PR protein families, and are widely used as marker genes for the SA pathway. It has been shown that the infection of the bacterial pathogen, *Xanthomonas campestris* pv. *Vesicatoria,* led to the upregulation of *PR1* expression in pepper leaves (Jin Kim and Kook Hwang, 2000). In this study, *B. cereus* AR156 treatment effectively increased the expression of *PR1*, *PR2* (*Glu*), *PR5* in strawberry fruits from 12 h (**Figure 4**). The induced differential expression lasted at least 54 h, indicating that *B. cereus* AR156 could activate the early upregulation of PR gene expression, and the effect could be present for a long period. NPR1, as a key regulatory protein, controls the signal transduction of the SA-signaling pathway and is essential for activating the expression of PR genes. Overexpression of *AtNPR1* in citrus increases the resistance to citrus canker disease in an expression-depended manner (Zhang et al., 2010). The *NPR1* of strawberry was induced at 24 h after *B. cereus* AR156 inoculation (**Figure 4**), which suggested that the role of NPR1 in the resistance was induced by AR156 by regulating the expression of downstream *PR* genes. PAC and AIP are inhibitors of key enzymes in SA biosynthesis (Zon and Amrhein, 1992; Leon et al., 1995). We found that the ability of AR156 in disease suppression was impaired by the inhibitors treatment (**Figure 5**). Together, these results showed that *B. cereus* AR156 induced an early activation of the defense-related genes expression in strawberry mainly by activating the SA-signaling pathway in the process of controlling postharvest strawberry gray mold. The results of the GO pathway enrichment analysis showed that the AR156-induced biological processes related DEGs, regardless of the presence or absence of pathogens, mainly concentrated on cellular and metabolic processes (**Supplementary Figure 5**). This is consistent with the results of this study which states that AR156 could retard the senescence of strawberries as well as the previous reported ability of AR156 to prolong the storage time of peach and

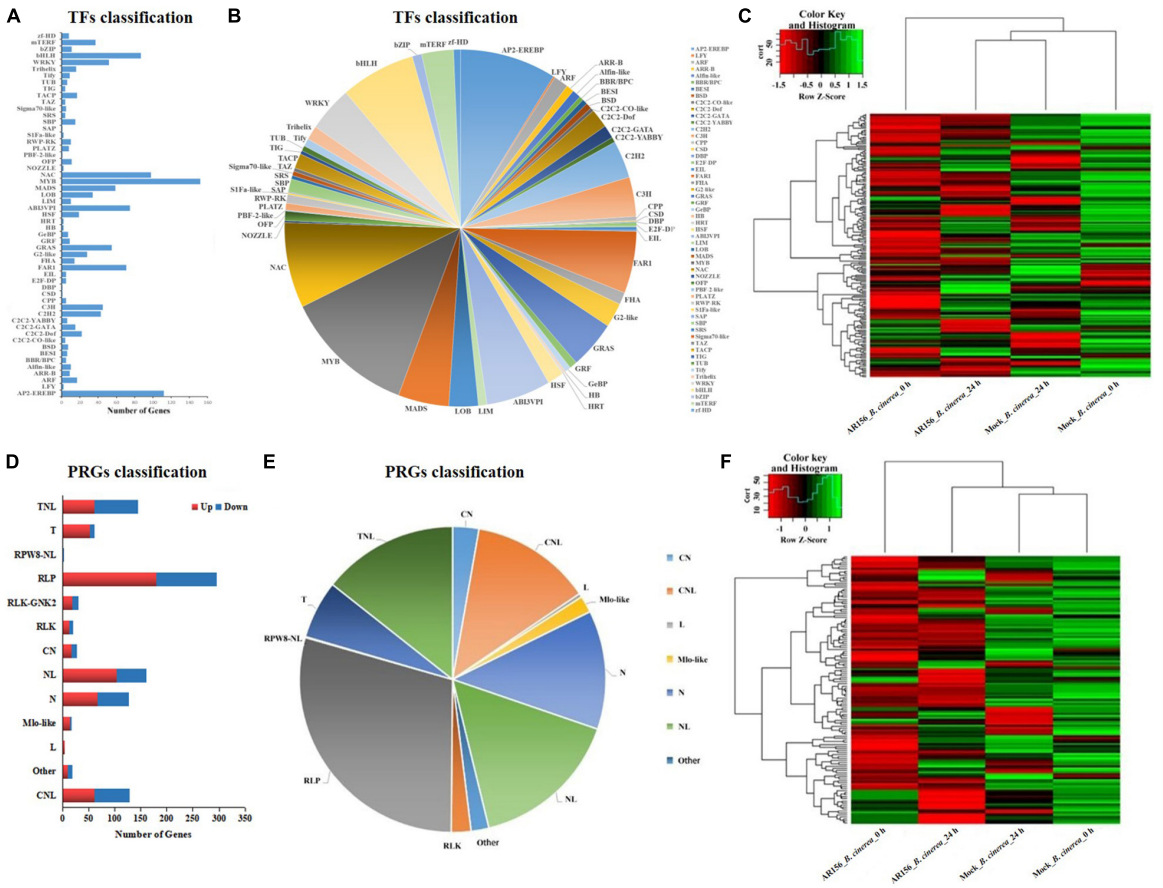

FIGURE 7 | Transcription factors (TFs) and plant disease resistance genes (PRGs) prediction in the differentially expressed genes (DEGs) in response to *B. cereus* AR156 treatment and in combination with *B. cinerea* inoculation. **(A,B)** The classification of DEGs on TFs families in the comparisons of *B. cereus* AR156 pretreatment and mock treatment strawberry fruit, then both challenged with *B. cinerea*. In **(A)**, *X* axis represents the number of TFs, and *Y* axis represents TFs families; **(C)** Cluster analysis of identified differentially expressed TFs in the fruits of strawberry treated by *B. cereus* AR156 treatment and in combination with *B. cinerea* inoculation at different time points based on the expression profiles measured by RNA sequencing (RNA-seq). **(D,E)** Classification of DEGs on PRG families on comparing the strawberry fruits treated by *B. cereus* AR156 pretreatment and mock treatment, then both challenged with *B. cinerea*. In **(D)**, the *X* axis represents the number of PRGs, *Y* axis represents PRG families, and red and blue represent the number of upregulated and downregulated PRGs, respectively; **(F)** Cluster analysis of identified differentially expressed PRGs in the fruits of strawberry treated by *B. cereus* AR156 treatment and in combination with *B. cinerea* inoculation at different time points based on the expression profiles measured by RNA-seq. The color scale in the heat map corresponds to $\log_2^{(FPKM)}$ value of genes in each sample.

loquat fruits under cold storage conditions (Wang et al., 2013, 2014). For cellular component, AR156 can induce a large number of membrane-related DEGs (**Supplementary Figure 5**), which may be related to the pattern recognition of AR156 by the strawberry fruit. Plants can recognize MAMPs produced by beneficial microorganisms, thereby activating immune responses. The extracellular polysaccharide (EPS) produced by *B. cereus* AR156 has been reported as MAMPs with the ability to activate plant resistance to pathogens, but its pattern recognition receptor is still unknown (Jiang et al., 2016a). The membrane-related DEGs identified in this study may have the potential as a pattern recognition receptor, which remains to be tested. For the cellular component, AR156 could induce DEGs related to catalytic activity, which is consistent with the results that AR156 could induce a variety of defense-related enzyme activities (**Figure 3**). The KEGG pathway enrichment analysis showed that besides the metabolism-related DEGs, AR156 had a significant effect on the expression of genes relating to benzoxazinoid and flavonoid biosynthesis in the presence of pathogens (**Supplementary Figure 6**). The expression of all of the three DEGs related to flavonoids biosynthesis was upregulated by AR156 treatment (**Supplementary Figure 7**). Flavonoids are plant polyphenolic secondary metabolic compounds that protect plants from stress by functioning as signaling molecules and as antimicrobial agents. Benzoxazinoids protect plants from insect herbivores by acting as toxins and deterrents of feeding and digestibility. However, the biochemical test of AR156-treated strawberry showed no significant change in flavonoid content during cold storage (**Figure 2**). The discrepancy of gene expression and product may be due to a repressive effect on the metabolism of cold storage condition as the transcriptome sequencing sample was incubated under room temperature.

Transcription factors play key roles in regulating the plant defense against pathogen infection. This study analyzed the effect of AR156 treatment on strawberry transcription factor expression and found that the expression of a large number of MYB, NAC, WRKY, ERF, bHLH, and bZIP family transcription factors were affected. The WRKY family transcription factors are widely involved in the regulatory network of pathogen-induced cellular response processes in various plants. Many of the WRKYs participate in SA-mediated resistance and SA signaling pathways feedback regulation by activating or inhibiting SA responses (Chen et al., 2017). In a study using *Arabidopsis thaliana* as the host, the AR156 could induce the expression of resistance genes related to SA and JA/ET by regulating the expression of WRKY11 and WRKY70 (Jiang et al., 2016b). In consistent with the former study, *B. cereus* AR156 treatment quickly increased the expression of *WRKY1*, which was significantly higher during 36–48 h than in the pathogen treatment (**Figure 4**). The qRT-PCR results, together with the RNA-sequence data, provided evidence for the involvement of transcription factors in the AR156-induced postharvest strawberry disease resistance.

Based on the GO classification and functional annotation of DEGs, the prediction of strawberry resistance genes revealed an alteration on the expression of a large number of unknown PRGs upon AR156 treatment, suggesting the potential participation of PRGs in the AR156-induced disease resistance process. Further exploration of the functions of these unknown PRGs may help us to reveal more detailed mechanism of *B. cereus* AR156-induced disease resistance in strawberry fruits. Plants recognize MAMPs produced by beneficial microorganisms through pattern-recognition receptors (PRRs) to activate immune responses. MAMPs induce the transcription of receptor-like proteins (RLPs), such as LRR-RLKs, wall-associated kinases, and receptor protein kinase in *A. thaliana* (Qutob et al., 2006). We also found that upon AR156 treatment, more RLP-like DEGs were upregulated (180) than downregulated (116) (**Figure 7**). Some of these receptors have the potential to play a role in the recognition of AR156 by strawberries.

DATA AVAILABILITY STATEMENT

The original contributions presented in the study are publicly available. This data can be found here: National Center for Biotechnology Information (NCBI) in FASTQ format (BioProject accessions: PRJNA643674; BioSample accessions: SAMN15423441, SAMN15423442, SAMN15423443, SAMN15423444, SAMN15423445, SAMN15423446, SAMN15423447, SAMN15423448, SAMN15423449, SAMN15423450, SAMN15423451 and SAMN15423452).

AUTHOR CONTRIBUTIONS

Y-YY: writing the original draft, methodology, and data curation. G-XD: project administration, methodology, investigation, and data curation. X-XS: methodology and investigation. LC: investigation. YZ: methodology. H-MX: methodology and supervision. Y-PW: supervision and investigation. H-YL: investigation and writing – review and editing. J-HG: supervision, conceptualization, funding acquisition, and writing – review and editing. C-HJ: software, methodology, formal analysis, and writing – review and editing.

FUNDING

This study was supported by the National Natural Science Foundation of China (31972322 and 31701829), Key Research and Development Projects in Jiangsu Province (BE2020408), Independent Innovation Project of Agricultural Science and Technology in Jiangsu Province [CX(19)2008], the Technical System of Chinese Herbal Medicine Industry (CARS-21), the Opening Project of Key Construction Laboratory of Probiotics in Jiangsu Province (JSYSZJ2019003), and China Postdoctoral Science Foundation (2019M651863).

SUPPLEMENTARY MATERIAL

The Supplementary Material for this article can be found online at: https://www.frontiersin.org/articles/10.3389/fpls.2021.700446/full#supplementary-material

REFERENCES

Alkan, N., and Fortes, A. M. (2015). Insights into molecular and metabolic events associated with fruit response to post-harvest fungal pathogens. *Front. Plant. Sci.* 6:889.

Aoki, T., Aoki, Y., Ishiai, S., Otoguro, M., and Suzuki, S. (2017). Impact of Bacillus cereus NRKT on grape ripe rot disease through resveratrol synthesis in berry skin. *Pest. Manag. Sci.* 73, 174–180. doi: 10.1002/ps.4283

Cai, Z., Yang, R., Xiao, H., Qin, X., and Si, L. (2015). Effect of preharvest application of Hanseniaspora uvarum on postharvest diseases in strawberries. *Postharvest Biol. Technol.* 100, 52–58. doi: 10.1016/j.postharvbio.2014.09.004

Chen, F., Hu, Y., Vannozzi, A., Wu, K., Cai, H., Qin, Y., et al. (2017). The WRKY transcription factor family in model plants and crops. *Crit. Rev. Plant Sci.* 36, 311–335. doi: 10.1080/07352689.2018.1441103

Chen, J., Duan, Y., Hu, Y., Li, W., Sun, D., Hu, H., et al. (2019). Transcriptome analysis of atemoya pericarp elucidates the role of polysaccharide metabolism in fruit ripening and cracking after harvest. *BMC Plant Boil.* 19:219.

Chowdhury, S. P., Uhl, J., Grosch, R., Alquéres, S., Pittroff, S., Dietel, K., et al. (2015). Cyclic lipopeptides of *Bacillus amyloliquefaciens* subsp. plantarum colonizing the lettuce rhizosphere enhance plant defense responses toward the bottom rot pathogen *Rhizoctonia solani*. *Mol. Plant Microbe Interact.* 28, 984–995. doi: 10.1094/mpmi-03-15-0066-r

Cools, H. J., and Ishii, H. (2002). Pre-treatment of cucumber plants with acibenzolar-S-methyl systemically primes a phenylalanine ammonia lyase gene (PAL1) for enhanced expression upon attack with a pathogenic fungus. *Physiol. Mol. Plant Pathol.* 61, 273–280. doi: 10.1006/pmpp.2003.0439

Droby, S. (2005). Improving quality and safety of fresh fruits and vegetables after harvest by the use of biocontrol agents and natural materials. *Acta Horic.* 709, 45–52. doi: 10.17660/actahortic.2006.709.5

Dukare, A. S., Paul, S., Nambi, V. E., Gupta, R. K., and Vishwakarma, R. K. (2019). Exploitation of microbial antagonists for the control of postharvest diseases of fruits: a review. *Crit. Rev. Food Sci. Nutr.* 59, 1498–1513. doi: 10.1080/10408398.2017.1417235

Gill, S. S., and Tuteja, N. (2010). Reactive oxygen species and antioxidant machineryin abiotic stress tolerance in crop plants. *Plant Physiol. Biochem.* 48:909. doi: 10.1016/j.plaphy.2010.08.016

Grabke, A., and Stammler, G. A. (2015). Botrytis cinerea population from a single strawberry field in Germany has a complex fungicide resistance pattern. *Plant Dis.* 99, 1078–1086. doi: 10.1094/pdis-07-14-0710-re

Jamalizadeh, M., Etebarian, H. R., Aminian, H., and Alizadeh, A. (2010). Biological control of Botrytis mali on apple fruit by use of Bacillus bacteria, isolated from the rhizosphere of wheat. *Arch. Phytopathol. Plant Prot.* 43, 1836–1845. doi: 10.1080/03235400902830960

Jiang, C. H., Fan, Z. H., Xie, P., and Guo, J. H. (2016a). Bacillus cereus AR156 extracellular polysaccharides served as a novel micro-associated molecular pattern to induced systemic immunity to Pst DC3000 in Arabidopsis. *Front. Microbiol.* 7:664.

Jiang, C. H., Huang, Z. Y., Xie, P., Gu, C., Li, K., Wang, D. C., et al. (2016b). Transcription factors WRKY70 and WRKY11 served as regulators in rhizobacterium *Bacillus cereus* AR156-induced systemic resistance to *Pseudomonas syringae* pv. tomato DC3000 in Arabidopsis. *J. Exp. Bot.* 67, 157–174.

Jiang, C. H., Liao, M. J., Wang, H. K., Zheng, M. Z., Xu, J. J., and Guo, J. H. (2018a). Bacillus velezensis, a potential and efficient biocontrol agent in control of pepper gray mold caused by Botrytis cinerea. *Biol. Control* 126, 147–157. doi: 10.1016/j.biocontrol.2018.07.017

Jiang, C. H., Xie, P., Li, K., Xie, Y. S., Chen, L. J., Wang, J. S., et al. (2018b). Evaluation of root-knot nematode disease control and plant growth promotion potential of biofertilizer Ning shield on *Trichosanthes kirilowii* in the field. *Braz. J. Microbiol.* 49, 232–239. doi: 10.1016/j.bjm.2017.08.009

Jiang, C., Yao, X., Mi, D., Li, Z., Yang, B., Zheng, Y., et al. (2019). Comparative transcriptome analysis reveals the biocontrol mechanism of Bacillus velezensis F21 against *Fusarium wilt* on watermelon. *Front. Microbiol.* 10:652.

Jin Kim, Y., and Kook Hwang, B. (2000). Pepper gene encoding a basic pathogenesis-related 1 protein is pathogen and ethylene inducible. *Physiol. Plant* 108, 51–60. doi: 10.1034/j.1399-3054.2000.108001051.x

Leon, J., Lawton, M. A., and Raskin, L. (1995). Hydrogen peroxide stimulates salicylic acid biosynthesis in tobacco. *Plant Physiol.* 108, 1637–1678.

Marín, A., Atarés, L., and Chiralt, A. (2017). Improving function of biocontrol agents incorporated in antifungal fruit coatings: a review. *Biocontrol Sci. Technol.* 27, 1220–1241. doi: 10.1080/09583157.2017.1390068

Niu, D. D., Liu, H. X., Jiang, C. H., Wang, Y. P., Wang, Q. Y., Jin, H. L., et al. (2011). The plant growth–promoting rhizobacterium Bacillus cereus AR156 induces systemic resistance in *Arabidopsis thaliana* by simultaneously activating salicylate-and jasmonate/ethylene-dependent signaling pathways. *Mol. Plant Microbe Interact.* 24, 533–542. doi: 10.1094/mpmi-09-10-0213

Niu, D. D., Wang, C. J., Guo, Y. H., Jiang, C. H., Zhang, W. Z., Wang, Y. P., et al. (2012). The plant growth-promoting rhizobacterium Bacillus cereus AR156 induces resistance in tomato with induction and priming of defence response. *Biocontrol Sci. Technol.* 22, 991–1004. doi: 10.1080/09583157.2012.706595

Pieterse, C. M., Van Wees, S. C., Van Pelt, J. A., Knoester, M., Laan, R., Gerrits, H., et al. (1998). A novel signaling pathway controlling induced systemic resistance in Arabidopsis. *Plant Cell* 10, 1571–1580. doi: 10.1105/tpc.10.9.1571

Qin, X., Xiao, H., Cheng, X., Zhou, H., and Si, L. (2017). Hanseniaspora uvarum prolongs shelf life of strawberry via volatile production. *Food Microbiol.* 63, 205–212. doi: 10.1016/j.fm.2016.11.005

Qutob, D., Kemmerling, B., Brunner, F., Küfner, I., Engelhardt, S., Gust, A. A., et al. (2006). Phytotoxicity and innate immune responses induced by Nep1-like proteins. *Plant Cell* 18, 3721–3744. doi: 10.1105/tpc.106.044180

Rao, G., Zhang, J., Liu, X., and Luo, Y. (2019). Identification of putative genes for polyphenol biosynthesis in olive fruits and leaves using full-length transcriptome sequencing. *Food Chem.* 300:125246. doi: 10.1016/j.foodchem.2019.125246

Rio, D. C., Ares, M., Hannon, G. J., and Nilsen, T. W. (2010). Purification of RNA using TRIzol (TRI reagent). *Cold Spring Harb. Protoc.* 2010:pdb.prot 5439.

Santos, D. A., Lima, K. P., Março, P. H., and Valderrama, P. (2016). Vitamin C determination by ultraviolet spectroscopy and multiproduct calibration. *J. Braz. Chem. Soc.* 27, 1912–1917.

Shao, X., Wang, H., Xu, F., and Cheng, S. (2013). Effects and possible mechanisms of tea tree oil vapor treatment on the main disease in postharvest strawberry fruit. *Postharvest Biol. Technol.* 77, 94–101. doi: 10.1016/j.postharvbio.2012.11.010

Spadaro, D., and Gullino, M. L. (2010). Opportunities and constraints in the development of antagonistic yeasts for the control of postharvest diseases of fruit. *Stewart Postharvest Rev.* 3, 1–8. doi: 10.2212/spr.2010.3.7

Tian, S., Qin, G., and Li, B. (2013). Reactive oxygen species involved in regulating fruit senescence and fungal pathogenicity. *Plant Mol. Biol.* 82, 593–602. doi: 10.1007/s11103-013-0035-2

Wang, L., Dou, G., Guo, H., Zhang, Q., Qin, X., Yu, W., et al. (2019). Volatile organic compounds of Hanseniaspora uvarum increase strawberry fruit flavor and defense during cold storage. *Food Sci. Nutr.* 7, 2625–2635. doi: 10.1002/fsn3.1116

Wang, N., Wang, L., Zhu, K., Hou, S., Chen, L., Mi, D., et al. (2019). Plant root exudates are involved in Bacillus cereus AR156 mediated biocontrol against *Ralstonia solanacearum*. *Front. Microbiol.* 10:98.

Wang, X., Wang, L., Wang, J., Jin, P., Liu, H., and Zheng, Y. (2014). Bacillus cereus AR156-induced resistance to *Colletotrichum acutatum* is associated with priming of defense responses in loquat fruit. *PLoS One* 9:e0112494.

Wang, X., Xu, F., Wang, J., Jin, P., and Zheng, Y. (2013). Bacillus cereus AR156 induces resistance against Rhizopus rot through priming of defense responses in peach fruit. *Food Chem.* 136, 400–406. doi: 10.1016/j.foodchem.2012.09.032

Wildermuth, M. C., Dewdney, J., Wu, G., and Ausubel, F. M. (2001). Isochorismate synthase is required to synthesize salicylic acid for plant defence. *Nature* 414, 562–565. doi: 10.1038/35107108

Yánez-Mendizábal, V., Usall, J., Viñas, I., Casals, C., Marín, S., Solsona, C., et al. (2011). Potential of a new strain of *Bacillus subtilis* CPA-8 to control the major postharvest diseases of fruit. *Biocontrol Sci. Technol.* 21, 409–426. doi: 10.1080/09583157.2010.541554

Yu, Y. Y., Jiang, C. H., Wang, C., Chen, L. J., Li, H. Y., and Xu, Q. (2017). An improved strategy for stable biocontrol agents selecting to control rice sheath blight caused by *Rhizoctonia solani*. *Microbiol. Res.* 203, 1–9. doi: 10.1016/j.micres.2017.05.006

Zhang, X., Francis, M. I., Dawson, W. O., Graham, J. H., Orbović, V., Triplett, E. W., et al. (2010). Over-expression of the Arabidopsis NPR1 gene in citrus increases resistance to citrus canker. *Eur. J. Plant Pathol.* 128, 91–100. doi: 10.1007/s10658-010-9633-x

Zhou, D. M., Wang, K. P., Liu, H. X., Gu, C., and Guo, J. H. (2014). Field evaluation of different application methods of the mixture of Bacillus cereus strain AR156 and Bacillus subtilis strain SM21 on pepper growth and disease resistance. *Biocontrol Sci. Technol.* 24, 1451–1468. doi: 10.1080/09583157.2014.945899

Zon, J., and Amrhein, N. (1992). Inhibitors of phenylalanine ammonia-lyase:2-aminoindan-2-phosphonic acid and related compounds. *Eur. J. Org.Chem.* 6, 625–628. doi: 10.1002/jlac.1992199201107

Conflict of Interest: The authors declare that the research was conducted in the absence of any commercial or financial relationships that could be construed as a potential conflict of interest.

Publisher's Note: All claims expressed in this article are solely those of the authors and do not necessarily represent those of their affiliated organizations, or those of the publisher, the editors and the reviewers. Any product that may be evaluated in this article, or claim that may be made by its manufacturer, is not guaranteed or endorsed by the publisher.

frontiers in Plant Science

ORIGINAL RESEARCH
published: 15 October 2021
doi: 10.3389/fpls.2021.649487

Bacillus cereus Improves Performance of Brazilian Green Dwarf Coconut Palms Seedlings With Reduced Chemical Fertilization

Aline Figueiredo Cardoso[1†], Ediane Conceição Alves[1†], Sidney D. Araújo da Costa[1†], Alessandra Jackeline Guedes de Moraes[1†], Dalton Dias da Silva Júnior[2†], Paulo Manoel Pontes Lins[3†] and Gisele Barata da Silva[1†]*

[1] Plant Protection Laboratory, Institute of Agrarian Sciences, Federal Rural University of Amazon (UFRA), Belém, Brazil, [2] Federal University of Amazonas (UFAM), Education, Agriculture and Environment Institute, Humaitá, Brazil, [3] Sococo S.A Agroindústrias da Amazônia, Belém, Brazil

OPEN ACCESS

Edited by:
Sabine Dagmar Zimmermann, Délégation Languedoc Roussillon (CNRS), France

Reviewed by:
Sofia I. A. Pereira, Universidade Católica Portuguesa, Portugal
Christel Baum, University of Rostock, Germany
Brenda Román-Ponce, University of Salamanca, Spain

***Correspondence:**
Gisele Barata da Silva
giselebaratasilva@gmail.com

† These authors have contributed equally to this work

Specialty section:
This article was submitted to Plant Symbiotic Interactions, a section of the journal Frontiers in Plant Science

Received: *04 January 2021*
Accepted: *26 April 2021*
Published: *15 October 2021*

Citation:
Cardoso AF, Alves EC, da Costa SDA, de Moraes AJG, da Silva Júnior DD, Lins PMP and da Silva GB (2021) Bacillus cereus Improves Performance of Brazilian Green Dwarf Coconut Palms Seedlings With Reduced Chemical Fertilization. Front. Plant Sci. 12:649487. doi: 10.3389/fpls.2021.649487

Coconut production in the Amazon requires the knowledge and development of sustainable technologies to alleviate the detrimental effects of inorganic chemical fertilizers and intensive farming practices. In this study, we investigated the effects of plant growth-promoting rhizobacteria (PGPR) isolated from coconut seedlings on nutrient use efficiency (NUE) and physiological mechanisms related to biomass accumulation of seedlings grown with reduced inorganic fertilizer levels. Of the 96 PGPR isolates tested on rice plants, the isolate *Bacillus cereus* (UFRABC40) was selected, as it resulted in the most significant gain in growth variables. In a commercial coconut tree nursery, we subjected seedlings to two treatments, both with seven replications: control 100% NPK chemical fertilizer (CF) and *B. cereus* + 50% NPK CF. The results indicated that the inoculation increased phytohormone levels [190% indole acetic acid (IAA), 31% gibberellic acid GA_3, and 17% gibberellic acid GA_4] and leaf gas exchange [48% by assimilation of CO_2 (*A*), 35% stomatal conductance to water vapor (*gs*), 33% transpiration, and 57% instantaneous carboxylation efficiency] in leaves. Furthermore, growth parameters (shoot, root, and total dry weight, height, and diameter) and macro- and micronutrient levels (95% N, 44% P, 92% K, 103 Ca, 46% Fe, 84% B) were improved. Our results show the potential ability of strain *Bacillus cereus* UFRABC40 to promote the growth performance of coconut seedlings under decreased application of inorganic fertilizers. The application of microbial-based products in coconut seedling production systems improves plants' physiological performance and the efficiency of nutrient use.

Keywords: *Bacillus cereus*, coconut palm, sustainable agriculture, growth promotion, PGPR

INTRODUCTION

The cultivation of coconut trees is of great economic and social importance due to the value generated by coconut production. According to FAO (2018), Indonesia is the world's largest coconut producer, followed by the Philippines, India, Sri Lanka, and Brazil. Production in Brazil occupies an area of 216 hectares, yielding approximately 2 million tons coconuts (IBGE, 2019), 1.5

million of which are obtained from green dwarf and hybrid plants (Sindcoco, 2017). The Amazon region produces 11% of the country's coconut yield; of this, 10% (200,000 tons) comes from the state of Pará. The coconut seedlings are the first stage affecting the productivity of the perennial plant, which has a mean production-life of 40 years. Green dwarf coconut seeds have a low germination rate, and their seedlings have low vigor and quality primarily due to the incidence of leaf spots (Rabelo et al., 2006; Vinodhini and Deshmukh, 2017).

The global demand for food has resulted in large use of CFs to attain maximum agricultural efficiency. According to Wang and Li (2019), only 50% of N from fertilizer is absorbed by crops. Moreover, it has been estimated that up to 7 million tons of P per year will be used in phosphate fertilizers by 2050 (Mogollon et al., 2018). The excessive and incorrect use of fertilizers damages the environment via leaching, runoff, and erosion (Good and Beatty, 2011; Savci, 2012; Conijn et al., 2018). It also leads to changes in the soil's physical, chemical, and microbiological characteristics (Blanco- Blanco-Canqui and Schlegel, 2013). The low efficiency of synthetic fertilizers is related to nutrient loss via leaching and evaporation to the atmosphere (Tilman, 1998; Gyaneshwa et al., 2002). Thus, the efficient use of synthetic fertilizers is important for both productivity and environmental protection (Paungfoo-Lonhienne et al., 2019). Furthermore, technologies that decrease the adverse effects of CFs on soil microbiota while promoting crop growth and productivity should be investigated.

The use of rhizobacteria in plant production can promote growth (Gange and Gadhave, 2018), and some genera such as *Pseudomonas* sp. and *Bacillus* sp. have been shown to promote the growth of coconut seedlings (George et al., 2018). Rhizobacteria can alter anatomical characteristics and improve photosynthetic, hormonal, and nutritional performance (Glick et al., 1999; Lucy et al., 2004; Lwin et al., 2012; Samaniego-Gámez et al., 2016). They also stimulate the synthesis of phytohormones such as indole acetic acid (IAA) and gibberellins that promote root and shoot growth (Pahari and Mishra, 2017). Rhizobacteria also optimize the use of CFs and are considered a sustainable technology (Angulo et al., 2020). They include N_2 fixers, phosphorus, and potassium solubilizers (Bhardwaj et al., 2014). In rice, a 50% reduction in N and P fertilization resulted in better nutrient absorption and chlorophyll content (Naher et al., 2018). Additionally, the use of *Bacillus amyloliquefaciens* combined with 50% CF changed the hormonal behavior of oil palm seedlings in Amazonian climatic conditions, increasing IAA levels by 66%, shoot dry matter by 110%, and root dry matter by 123% and improving macro- and micronutrient uptake (Lima et al., 2020).

Coconut production in the Amazon requires knowledge and sustainable technology development to counteract the negative impacts of CF dependency. Access to the diverse range of microorganisms associated with plants and soil in the Amazon biome may improve bioinoculant production. Bioinoculant production is a process sensitive to both biotic and abiotic factors.

Therefore, this study aimed to evaluate the effects of plant growth-promoting rhizobacteria (PGPR) inoculation on coconut seedlings growth by investigating the physiological and nutritional mechanisms in seedlings grown under low CF conditions.

MATERIALS AND METHODS

The experiment was conducted in a coconut tree seedling nursery, Santa Isabel do Pará-Brazil (1°13′26″ S, 48°02′29″ W).

Isolation of Bacterial Strains

Six soil samples containing roots (100 g) were collected from an 8-year-old dwarf coconut plantation in Brazil. Each sample was divided into portions of 10 g to obtain the isolates. Each soil sample (10 g) was diluted in 50 mL of sterile distilled water and agitated for 30 min. An aliquot of 20 μL was then separated from the original suspension and diluted in 80 μL (10^{-3}). Next, an aliquot of 50 μL was separated from the concentrated suspension and seeded into three 9-mm Petri plates containing 10 mL of culture medium (per liter: g of sucrose, 8 g of hydrolyzed acid casein, 4 g of yeast extract, 2 g of K_2HPO_4, 0.3 g of $MgSO_4$, and 15 g of agar) (Kado and Heskett, 1970). Plates were subsequently incubated at 27°C ± for 12 h. After incubation, colonies with different colors, borders, and morphology in the same plate were isolated and streaked into a new plate containing culture medium (Kado and Heskett, 1970). These plates were incubated for the same time and temperature as described above, followed by bacterial isolate purification. The bacteria were collected in microtubes containing distilled and sterile water and kept at 5°C in a refrigerator.

Selection of Isolates

The selection of growth-promoting isolates was carried out on rice plants, and subsequently, their interaction with coconut seedlings was tested according to the method described by de Castro et al. (2020).

Briefly, rice seeds (10 g) were inoculated with 20 mL of bacterial suspension obtained from the culture growth in liquid medium to 10^8 CFU·mL^{-1} (Kado and Heskett, 1970) and kept under agitation at 114 rpm at 27°C for 24 h (Filippi et al., 2011). The experimental design consisted of 97 treatments (96 rhizobacteria isolates and a control) with three replicates each in a greenhouse. Twenty-one days after germination, plants were evaluated for root and shoot length (LR and LS, respectively) and total biomass (TDM). Analysis of variance was performed for all variables, followed by a comparison of means using the Scott–Knott test ($p < 0.05$). The R40 isolate (**Supplementary Material**) resulted in superior growth parameters compared with all other treatments; therefore, it was subjected to *in vitro* biochemical tests and selected for subsequent testing with green dwarf coconut seedlings from Brazil.

Identification of Bacterial Isolate

The R40 isolate was cultured in culture medium 523 (Kado and Heskett, 1970) for 24 h at 28°C. Two inoculation loops were added to a microtube containing 1 mL of extraction buffer

TABLE 1 | Selection of growth-promoting rhizobacteria in rice, isolated from the rhizosphere of commercially grown green dwarf coconut trees from Santa Isabel, PA, Brazil.

Isolate	LA	LR	TDM	Isolate	CL	RL	TDM
	(cm)		(g)		(cm)		(g)
1	35.53b	16.16d	0.10b	51	35.26b	15.33d	0.07c
2	34.16b	20.00b	0.08c	52	36.28b	15.75d	0.08c
3	34.95b	27.75b	0.09c	53	32.73b	22.56b	0.10b
4	46.03a	13.66e	0.09c	54	31.50b	20.30b	0.10b
5	32.33c	25.91b	0.11b	55	36.35b	20.06b	0.05c
6	37.45b	21.10b	0.16ab	56	31.20b	23.63b	0.13b
7	32.16b	19.33c	0.10b	57	27.90c	20.80b	0.06c
8	33.00b	14.16e	0.09c	58	32.16b	17.93d	0.08c
9	34.6b	19.5c	0.16ab	59	28.16c	18.70d	0.07c
10	32.66b	21.53b	0.07c	60	46.30a	16.60d	0.09c
11	32.06b	21.83b	0.09c	61	28.34c	11.83e	0.09c
12	36.00b	11.00e	0.09c	62	28.13c	18.23d	0.07c
13	32.86b	20.60b	0.12b	63	31.40b	27.13ab	0.09c
14	42.33a	20.00b	0.08c	64	36.20b	23.40b	0.12b
15	41.10a	15.33d	0.12b	65	27.90c	21.13b	0.13b
16	43.00a	25.00b	0.12b	66	35.06b	24.23b	0.11b
17	37.93b	18.90d	0.10b	67	25.10c	14.50e	0.06c
18	43.66a	14.66e	0.10b	68	30.90b	27.03ab	0.13b
19	40.50a	24.53b	0.10b	69	36b	27.8a	0.1b
20	41.50a	20.46b	0.09c	70	29.03bc	22.2b	0.06c
21	32.23b	23.86b	0.15b	71	27.9c	20.8b	0.06c
22	33.70b	20.56b	0.14b	72	29bc	22b	0.09c
23	33.56b	19.26c	0.12b	73	26.8c	17d	0.13b
24	34.23b	20.16b	0.08c	74	22.76c	13.90e	0.10b
25	34.56b	23.90b	0.12b	75	24.90c	13.66e	0.07c
26	35.53b	23.30b	0.14b	76	30.60b	18.26d	0.05c
27	42.83a	16.06d	0.09c	77	28.23c	20.90d	0.13b
28	38.46b	15.03d	0.08c	78	32.63b	18.43d	0.11b
29	32.7b	22.6b	0.01d	79	27.90c	19.50d	0.08c
30	37.5b	18.1d	0.07c	80	27.70c	19.03d	0.06c
31	34.4b	17.9d	0.07c	81	35.16b	25.46b	0.14b
32	36.3b	14.5e	0.08c	82	38.13b	27.83ab	0.17ab
33	35.35b	16.20d	0.07c	83	28.60c	21.53b	0.09c
34	40.76a	13.16e	0.06c	84	35.80b	21.86c	0.15b
35	39.30b	15.03d	0.12b	85	39.40b	24.63b	0.15b
36	36.83b	18.76d	0.13b	86	36.23b	16.26d	0.08 e
37	40.60a	17.23d	0.15b	87	34.70b	19.60d	0.17ab
38	34.20b	22.16b	0.15b	88	31.80b	20.33d	0.16ab
39	35.46b	23.80b	0.17ab	89	32.26b	24.61b	0.14b
40*	49.6a	28.5a	0.19a	90	31.10b	23.36b	0.12b
41	37.33b	21.66b	0.12b	91	27.90c	20.80b	0.07 e
42	45.80a	22.60b	0.13b	92	33.10b	24.54b	0.15b
43	46.23a	21.36 b	0.15b	93	38.13b	16.66d	0.17ab
44	36.20b	19.63b	0.16ab	94	39.56b	17.40d	0.12b
45	36.93b	23.40b	0.14b	95	28.23c	21.80c	0.13b
46	30.90b	21.30b	0.08c	96	36.33b	17.4d	0.12b
47	28.33c	14.83e	0.05c	Control	24.70c	17.86d	0.05 e
48	35.50b	20.63a	0.14b				
49	31.90b	16.53d	0.08c				
50	26.80c	17.06d	0.16ab				

*Same letters indicate no significant difference (SNK test, $p < 0.05$). LR, root length; LA, shoot length (determined with the aid of a millimeter rule); TDM, total biomass (g/weight of dryplant). *Isolate selected as promising for promoting growth in model plants.*

(Tris-HCl 1x). Then, DNA extraction was performed according to the method described by Mariano and Silveira (2005). The R40 isolate was identified using the 16S rDNA region gene and 27F (5′-AGAGTTTGATCMTGGCTCAG-3′) and 1492R (5′ACCTTGTTACGACTT-3′) primers (Lane et al., 1985). The PCR amplification reaction was composed of 1x Master Mix 2x (Promega) (0.05 U μL^{-1} Taq DNA polymerase, 4 mM $MgCl_2$ reaction buffer, 0.4 mM of each DNTP; Promega Corporation, Madison, WI, United States), 10 μM of each primer, and 50 ng DNA. Amplification of the 16S rDNA region was performed in a thermal cycler (MasterCycler Nexus, Eppendorf, Hamburg, Germany) with the following steps: initial denaturation at 94°C for 4 min; 25 cycles of 94°C for 1 min, 55°C for 1 min, and 72°C for 1 min; and a final extension at 72°C for 7 min. Reactions were purified using 5 μL of PCR product plus 2 μL Exo-SAP enzyme (Exonuclease). Samples were purified via a thermal cycler, performed at 37°C for 4 min, followed by an incubation period at 80°C for 1 min to inactivate both enzymes irreversibly. After the purification reaction, sequencing was carried out in an automated sequencer (ABI3730) at the Laboratory of Bioinformatics and Evolutionary Biology, Federal University of Pernambuco (LABBE-UFPE).

DNA sequence analysis and assembly of the R40 isolate contigs were performed using the Staden Package (Staden et al., 1998). The nucleotide sequence of the UFRABC40 bacteria was compared with the isolate sequences available in the National Center for Biotechnology Information (NCBI) database using the BLASTn software[1]. Afterward, all sequences were aligned (MEGA). Bayesian inference (IB) analysis was performed by means of Mr. Bayes v. 3.2.6 (Ronquist et al., 2012) implemented in CIPRES[2] using the best nucleotide replacement model. This was selected according to Aikake's Information Criterion (AIC) through Mr. Modeltest 2.3 (Nylander, 2004) using 1,000,000,000 generations of Markov Chain Monte Carlo (MCMC) with sampling every 1,000 and 10,000 generations. Identification of access and phylogenetic trees was obtained by comparing the selected strain with the reference strains using 29 reference accessions to identify the selected strain (R40). Identifying a bacterial isolate using 16S rRNA was used to identify the strain selected with the strain of greatest homology. Subsequent probabilities were calculated after discarding the first 25% of the generations. All trees obtained from individual genes and concatenated through the IB method were visualized through the Fig Tree 1.4.1 software[3].

[1]https://www.ncbi.nlm.nih.gov

[2]https://www.phylo.org/portal2/home.action

[3]http://tree.bio.ed.ac.uk/software/figtre

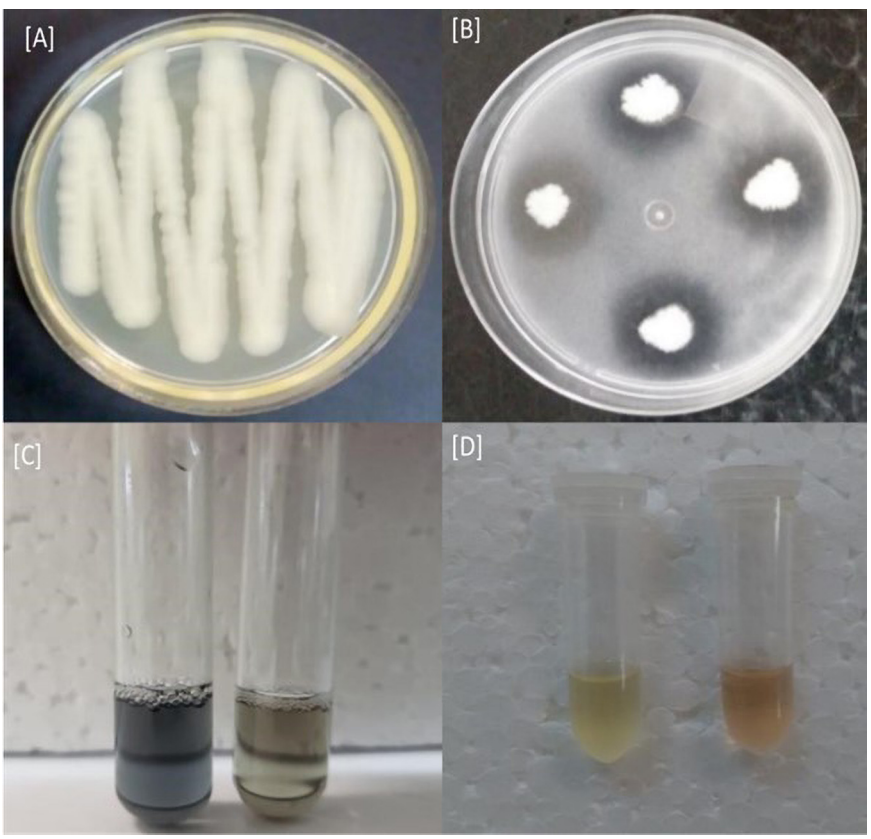

FIGURE 1 | R40 isolate *in vitro* biochemical tests. **(A)** R40 isolate colony in Petri plate, **(B)** phosphate solubilization detection, **(C)** siderophore production, and **(D)** indole acetic acid (IAA) production.

Biochemical Tests

Indole Acetic Acid Production

The R40 isolate was grown in a Luria Bertani (LB) medium under 100 rpm agitation and incubated at 28°C for 78 h. Subsequently, 3 mL of the suspension was centrifuged at 4°C for 10 min at 4,000 rpm (Moustaine et al., 2017). Then, 90 μL of the supernatant and 60 μL of the Salkowski reagent were placed in a microtube and incubated in the dark for 30 min to determine if a change in mean media color occurred (Gordon and Weber, 1951).

Production of Siderophores

The R40 isolate was inoculated into test tubes containing a 10 mL Tryptic Soybean Broth (TSB) (1:10 diluted) medium (3 g in 1,000 mL distilled water) and incubated at 28°C under agitation at 114 rpm for 24 h. Subsequently, tubes containing the bacterial suspension were centrifuged for 10 min at 12,000 rpm. Then, 1 mL of the supernatant was transferred into another tube containing 1 mL of the blue chrome S (BCS) solution. Fifteen minutes after mixing, if siderophores were produced, the dark blue mixture turned yellow (Schwyn and Neilands, 1987).

Phosphate Solubilization

The R40 isolate was grown in an NBRIP growth medium containing 10 g glucose, 2.5 g $Ca_3(PO_4)$, 25 g $MgCl_2W_6H_2O$, 0.25 g $MgSO_4W_7H_2O$, 0.2 g KCl, and 0.1 g $(NH_4)_2SO_4$ (Nautiyal, 1999), at a pH of 7.0, and with the addition of 1.5% agar in triplicate. The plates were incubated for 14 days at 28°C; the presence of a halo was indicative of phosphate solubilization.

Evaluating R40 Isolate Ability to Promote Growth Coconut Seedlings

Coconut Seeds Preparation

In a coconut tree nursery, the coconut seeds were sown in wooden boxes (30 cm high, 2 m wide, and 10 m long) containing coconut fiber and moistened daily for 90 days. The chemical characterization of the coconut fiber substrate (Golden Mix type 4 – AMAFIBRA®) was as follows: 0.086 g kg^{-1} N, 0.264 g kg^{-1} P, 0.580 g kg^{-1} K, 0.128 mg kg^{-1} Ca, 0.447 mg kg^{-1} MgO, 272.86 mg kg^{-1} S, 42.25 mg Na, 0.703 mg L^{-1} B, 0.12 g kg^{-1}, copper Cu, 0.5 mg kg^{-1} Fe, 0.6 mg kg^{-1} Mn, 0.78 mg kg^{-1} Zn, and 92.43% organic matter (OM).

FIGURE 2 | Green dwarf coconut seedlings from Brazil. **(A)** Control coconut seedlings with 100% chemical fertilization and **(B)** coconut seedlings inoculated with *Bacillus cereus* and 50% chemical fertilization.

Coconut Seedling Preparation

Seedlings with 15 cm tall and two leaves were transplanted to polyethylene bags (40 × 40 × 40 cm) containing 7.5 kg/bag of coconut fiber (50% moist). Chemical fertilization was performed 30 days after transplanting (DAT) with 3 g urea, 40 g simple superphosphate (18% P_2O_5), 10 g potassium chloride (60% K_2O), and 5 g magnesium oxide (30% Mg) (Lins and Viégas, 2008).

Evaluation of Coconut Seedling Growth

For the establishment of treatments, the recommendation of commercial fertilization was followed. Thus, the control treatment is characterized as 100% chemical fertilization (CF) and without the use of bioinoculant. The control treatment used standard CF (as described in the previous section) applied at 90 and 150 DAT. The treatment with rhizobacteria comprised inoculation with a suspension of R40 isolate (10^8 CFU) + 50% standard CF at 90 DAT. The bacterial strain was inoculated by applying 300 mL $plant^{-1}$ of a suspension at 10^8 CFU·mL^{-1} through watering at 40 and 70 DAT. Biometrics, gas exchange, hormone levels, and nutrient levels were evaluated at 160 DAT. The experimental design was completely randomized, with 10 replications and 2 treatments.

Biometrics

The following biometric variables were evaluated: shoot, root, and total dry weight, height, and diameter. Additionally, the leaf area was determined from photographs using the APS Assess software version 2.0 (Lamari, 2002).

Leaf Gas Exchange

Gas exchange parameters were estimated using the first physiologically mature, fully expanded leaf, from apex to base, at 3 months of age. The net assimilation of CO_2 (*A*), stomatal conductance to water vapor (*gs*), transpiration rate (*E*), and instantaneous carboxylation efficiency (*A/Ci)* were estimated between 08:00 and 11:00 am using a portable open-flow gas-exchange system (LI6400XT, LI-COR, Lincoln, NE, United States) under an external CO_2 concentration of 400 μmol mol^{-1} of air and artificial photosynthetically active radiation (PAR) of 900 μmol of photons m^{-2} s^{-1}.

Hormone Profile

Indole acetic acid (IAA) and gibberellic acid (GA_3 and GA_4) hormone levels were determined according to Munné-Bosch et al. (2011). For this, 300 mg of fresh tissue from the second leaf of each plant was stored in liquid N. The tissue material was then lyophilized and macerated in liquid N. Then, 40 mg dry mass was weighed, and 400 μL of extraction solvents (methanol:isopropyl alcohol:acetic acid; 20:79:1) was

added. Samples were vortexed four times for 20 s (on ice), sonicated for 5 min, placed on ice for 30 min, and then centrifuged at 13,000 rpm for 10 min at 4°C. After centrifugation, 350 μL of supernatant was removed and transferred to another microtube. Approximately 300 μL of the extract obtained in flasks was added, and 5 μL of the mixture was injected into the NuBioMol LC/MS system (Biomolecule Analysis Center, UFV, Brazil). A chromatography column (Agilent Eclipse; Agilent Technologies, Santa Clara, CA, United States) was used (RRHD, C18 column, 50 mm × 2.1 mm, 1.8 μm) with a flow rate of 0.3 mL min^{-1} coupled to a triple quadrupole QQQ mass spectrometer (Agilent Technologies). Mass spectra were alternately negative/positive operated according to the retention time for each hormone. The generated mass spectra were processed using the MassHunter software to obtain the extracted ion chromatograms (XIC) for each transition and area values, indicating the abundance of each hormone. A curve pattern for each hormone over a concentration range from 0.1 to 300 ng mL^{-1} was used to convert the XIC area values into ng g^{-1} of plant tissue. Molecular mass spectra analysis was conducted using the Skyline software.

Nutritional Content

Leaf samples dried in an oven with forced air circulation at 60°C were ground. The samples were submitted to sulfuric and nitroperchloric digestion. The determination of nitrogen (N) was by distillation in Microdistillator Kjeldhal, phosphorus (P) by visible ultraviolet spectrophotometry (UV-VIS), and

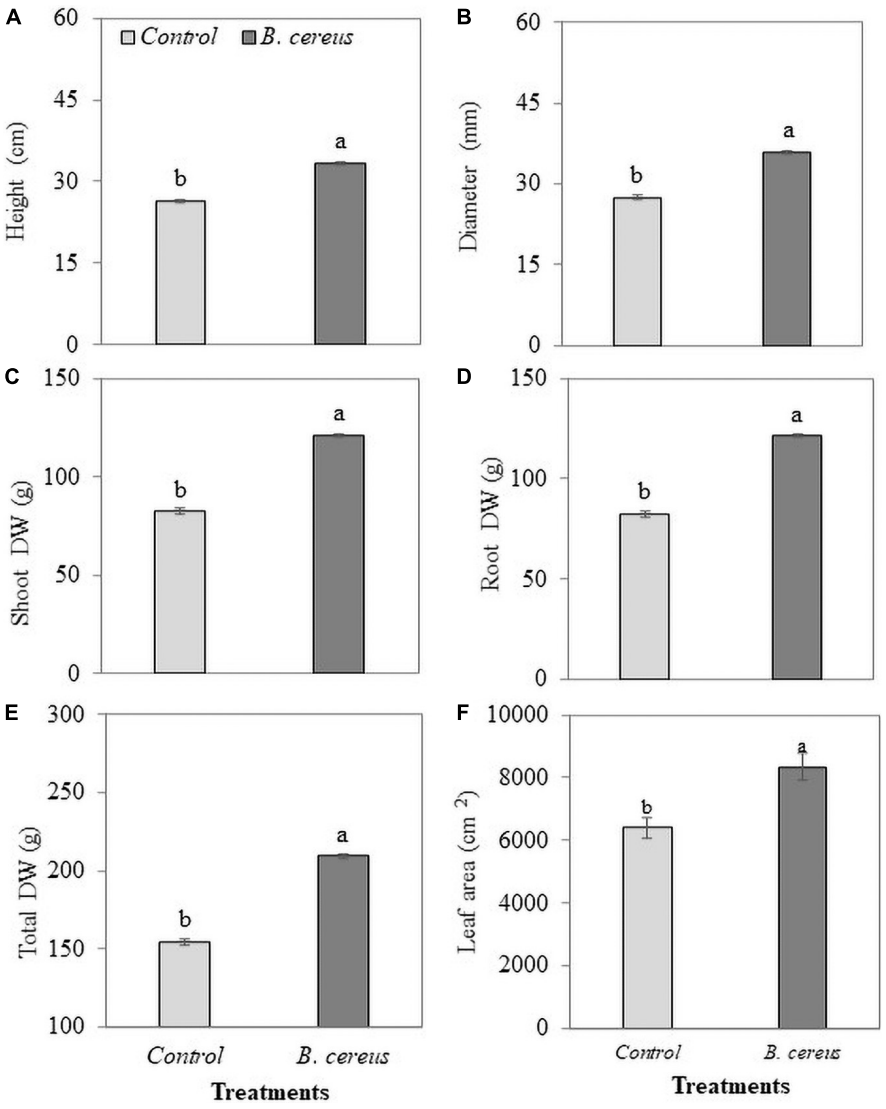

FIGURE 3 | Biometrics of green dwarf coconut seedlings from Brazil (uninoculated and inoculated with *B. cereus*). **(A)** Height, **(B)** stem diameter, **(C)** shoot dry matter, **(D)** root dry matter, **(E)** total dry matter **(E)**, and **(F)** leaf area in plants with 100% chemical fertilization (control) and plants inoculated with *Bacillus cereus* with 50% chemical fertilization. The same letters indicate no significant difference (*t*-test, $p < 0.05$).

potassium (K), calcium (Ca), and iron (Fe) by absorption spectrometry atomic, flame modality (EAA/cham). Analysis of boron (B) was undertaken after dry digestion of the samples using the method described by Azometrinah (Malavolta et al., 1997; Carmo et al., 2000). The nutrient use efficiency (NUE) was estimated from agronomic efficiency, NUE (g DW g^{-1}) = aerial dry weight (g)/plant applied nutrient (g) (Fageria et al., 2008).

Statistical Analysis

Differences among means for treatments were evaluated using the *t*-test ($p < 0.05$). All data were analyzed using the R software (R Core Team, 2017).

RESULTS

Isolate Selection in the Plant Model

The rice plants used as a model for selecting rhizobacteria showed that the R40 isolate was better for root and shoot length variables and total biomass compared with the other treatments (**Table 1**). The isolate R40 increased by 101% shoot length, 60% root length and 280% total biomass in comparation that is seedlings non-bioinoculation. *In vitro* biochemical tests were performed, showing that the R40 isolate was able to solubilize phosphate as proven by the halo formation around the bacterial colonies. There were also reactions indicating siderophore and IAA production when the R40 isolate was exposed to CAS solution and Salkowski's test, respectively (**Figure 1**). Thus, the R40 isolate was selected to evaluate growth promotion in green dwarf coconut seedlings in Brazil under nursery conditions.

Growth-Promotion Coconut Seedlings

The R40 isolate sequence was compared in GenBank using the BLASTn tool. The isolate showed 100% identity with the genus *Bacillus* (ATCC14579T). Based on the construction of the phylogenetic tree from 29 accesses, it was possible to identify the isolate as *B. cereus*. The sequence was deposited in GenBank as *B. cereus* (UFRABC40) with accession number MN393059 (**Supplementary Table 1** and **Supplementary Figure 1**).

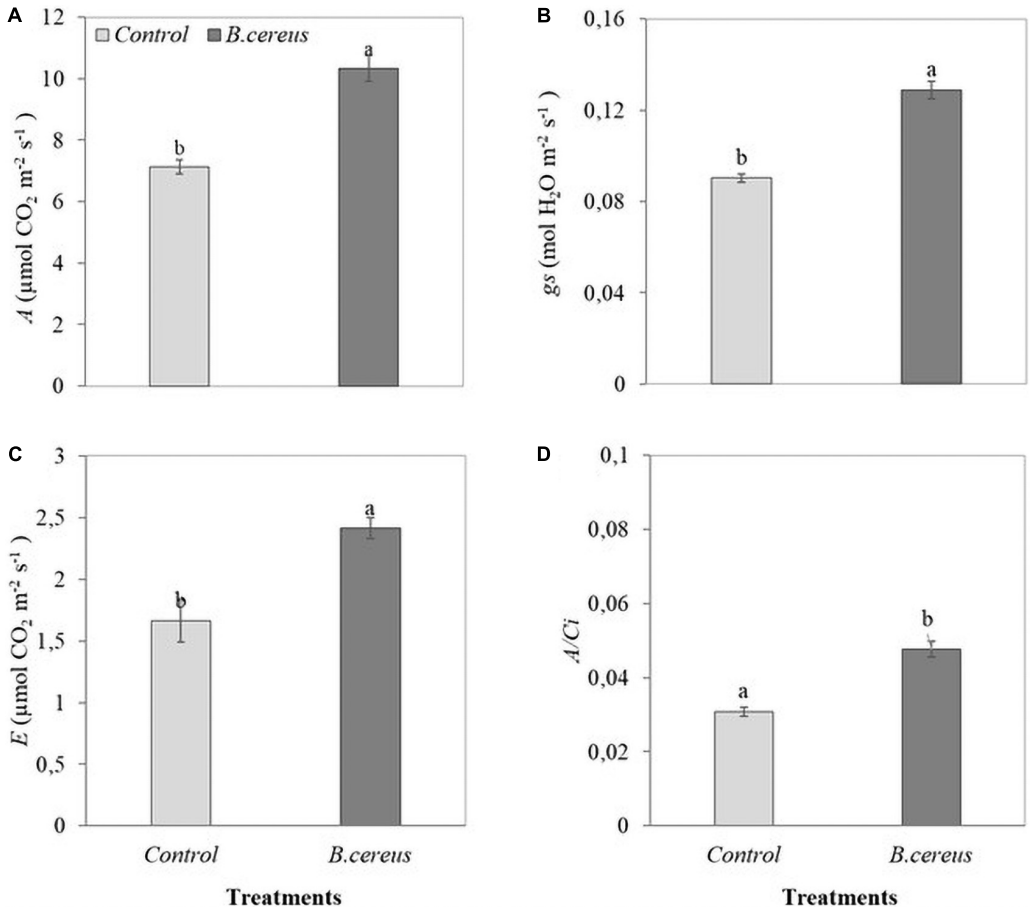

FIGURE 4 | Leaf gas exchange in green dwarf coconut seedlings. **(A)** The net assimilation of CO_2 (*A*), **(B)** stomatal conductance to water vapor (*gs*), **(C)** transpiration (*E*), and instantaneous carboxylation efficiency (*A/Ci*) in plants with 100% chemical fertilization (control) and plants inoculated with *Bacillus cereus* with 50% chemical fertilization. The same letters indicate no significant difference (*t*-test, $p < 0.05$).

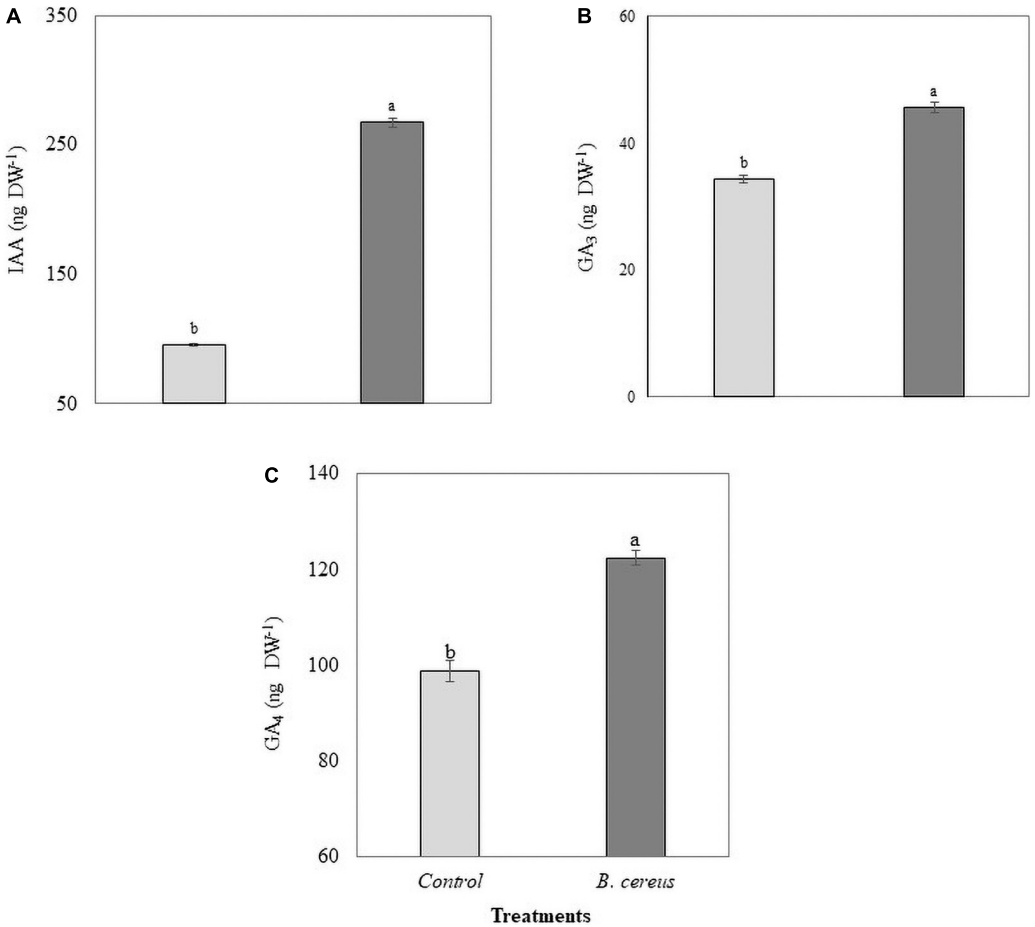

FIGURE 5 | Phytohormone quantification in coconut seedlings. **(A)** Indoleacetic acid (IAA), **(B)** gibberellic acid GA_3, and **(C)** gibberellic acid GA_4 in plants with 100% chemical fertilization (control, T1) and plants inoculated with *Bacillus cereus* with 50% chemical fertilization (T2). The same letters indicate no significant difference (*t*-test, $p < 0.05$).

The inoculation of strain *B. cereus* promoted the growth of coconut seedlings even in the presence of lower levels of chemical fertilizers (**Figure 2**). The application of *B. cereus* significantly increased shoot dry weight (47%), root dry weight (122%), total dry weight (35%), height (26%), and diameter (30%) compared with the control treatment (**Figure 3**).

Gas exchange was also influenced by inoculation with *B. cereus* from the third month of age in Brazilian green dwarf coconut tree seedlings. The nursery trial results indicated a maximum increase of 48% in *A*, 35% in *gs*, 33% in *E*, and 57% in *A/Ci* in plants inoculated with *B. cereus* compared with the uninoculated control (**Figure 4**). *B. cereus* inoculation led to an increase of 190% in IAA, 31% in GA_3, and 17% in GA_4 in coconut seedlings compared with the uninoculated control (**Figure 5**).

The *B. cereus* application significantly increased macronutrients and micronutrients in coconut plants by 95%, 44%, 82%, 103%, 46%, and 84% for N, P, K, Ca, Fe, and B, respectively (**Table 2**), compared with the control. Treatment with *B. cereus* shows greater efficiency in the use of nutrients (**Table 3**).

DISCUSSION

The rhizobacteria *B. cereus* promoted the growth of green dwarf coconut seedlings. Bacterial inoculation induced changes in the metabolism of coconut tree seedlings, by stimulating hormonal modulation, and photosynthetic performance and efficient use of nutrients, which ultimately resulted in a greater growth of coconut tree seedlings. These results may be due to the increase in IAA concentrations derived from the enhanced production by *B. cereus* strain (as shown in **Figure 1**) or due to the regulation of its biosynthesis in the plants (**Figure 5**). Indole acetic acid is responsible for modulating the differentiation and elongation of lateral roots, as well as increasing the number of root hairs, therefore promoting greater nutrient absorption (Costa et al., 2015; Cassán et al., 2020). Combined with the positive effects of IAA, it is possible that bioinoculation has reduced ethylene levels in the roots by the activity of the enzyme 1-aminocyclopropane-1-carboxylic acid (ACC) deaminase. This enzyme regulates ethylene synthesis by cleaving its acid precursor, ACC (Belimov et al., 2004; Siddikee et al., 2011), thus decreasing the negative

TABLE 2 | Nutritional content in the shoots of green dwarf coconut seedlings from Brazil.

Treatments	N	P	K	Ca	Fe	B
	(g/Dry leaf weight)			(mg/Dry leaf weight)		
Control	0.71[b]	0.09[b]	1.28[b]	0.33[b]	10.29[b]	1.21[b]
B. cereus	1.39[a]	0.13[a]	2.33[a]	0.67[a]	15.02[a]	2.23[a]

Control treatment (100% chemical fertilization) and inoculated with Bacillus cereus combined with 50% chemical fertilization. The same letters indicate no significant difference (t-test, $p < 0.05$).

TABLE 3 | Nutrient use efficiency (NUE) of green dwarf coconut seedlings from Brazil.

Treatments	N	P	K	Ca	Fe	B
	NUE (g DW g^{-1})					
Control	8.7[b]	0.7[b]	2.5[b]	107.2[b]	27.5[b]	19.6[b]
B. cereus	25.9[a]	2.0[a]	7.3[a]	320.6[a]	82.1[a]	56.6[a]

Dry weight (DW). Control treatment (100% chemical fertilization) and inoculated with Bacillus cereus combined with 50% chemical fertilization. The same letters indicate no significant difference (t-test, $p < 0.05$).

effects of ethylene on growth and allowing the development of a better root system in inoculated plants (Glick, 2012). *Bacillus cereus* inoculation resulted in the more efficient use of macro- and micronutrients. A significant positive effect on the levels of the seven nutrients evaluated was observed (**Tables 2**, **3**). Recommendations for the use of CFs are based on soil analysis and the mechanisms of macro- and micronutrient loss, such as volatilization, leaching, and adsorption, resulting in low absorption by the plant (Biswas et al., 2000; Ahmad et al., 2019). These root regions have a high influx of available ions, resulting in greater water and nutrient absorption. Root system changes induced by microorganisms improve NUE. This phenomenon has been reported in the interaction between banana and the bacterial strains *Pseudomonas fluorescens* Ps006 and *Bacillus amyloliquefaciens* Bs006 (Gamez et al., 2018) resulting in greater plant biomass. Another mechanism involved in the NUE of biostimulated coconut plants is the mineralization rate of the coconut fiber substrate by bioinoculant enzymatic activity, resulting in increased nutrient availability.

For N, *B. cereus* may make N available from the organic N contained in the coconut fiber via ammonium and nitrite oxidation. This was described by Di Benedetto et al. (2016), who found that *Pseudomonas* and *Bacillus* strains were able to oxidize ammonia to NO_2^- ions (nitrosification) and then to NO_3^- ions (nitrification). In a study with *Triticum aestivum*, the inoculation of *Bacillus megaterium* SNji (BmeSNji) and *Azospirillum brasilense* 65B (Abr65B) provided greater availability of nutrients to plants, such as N, from decomposition of organic matter resulting in greater accumulation of biomass in plants (Nguyen et al., 2019).

Coconut plants inoculated with *B. cereus* also had enhanced K uptake. This might be explained by its ability to produce organic acids that act in the mineralization of K present in the coconut fiber substrate, making K^+ ions available for plant absorption. According to Sheng and He (2006), the *Bacillus edaphicus* NBT strain and its mutants can chelate metals and mobilize K from K-containing minerals using organic acids such as citric, oxalic, tartaric, and succinic.

Solubilization of P by rhizobacteria requires the production of phosphatases and phytases that mineralize the organic material by esters and H_3PO_4 anhydride hydrolysis (Tabatabai, 1994; Nannipieri et al., 2011). In maize, *Pseudomonas plecoglossicida* (PSB5) inoculation increased P production by 18% and its total absorption by 46%. This was due to the increased activity of enzymes such as dehydrogenases and phytases (Kaur and Reddy, 2013). In this study, *B. cereus* was able to solubilize P *in vitro*, and plants inoculated with this strain showed higher levels of P than control ones. As observed *in vitro*, *B. cereus* can produce siderophores, which are low molecular weight iron-chelating compounds with a great affinity and selectivity for binding and forming a Fe complex (III), reducing Fe^{3+} to Fe^{2+} (Hider and Kong, 2010; Fukushima et al., 2013). In mustard, the capacity of *Bacillus* sp. PZ-1 to produce siderophores resulted in higher Fe levels available for the plant (Yu et al., 2017).

Boron is a micronutrient essential for plant growth and development, and coconut plants have high B requirements (Moura et al., 2013). Brazilian Amazonian soils are generally deficient in B, and appropriate CF use is critical to avoid B deficiency. However, the application of excess exogenous B can easily be lethal to plants. Boron is not described as an essential nutrient for PGPR growth; however, in *Arthrobacter nicotinovorans* strain C, phenylboronic acid (PBA) catabolism was demonstrated, releasing B as orthoboric acid [$B(OH)_3$] (Negrete-Raymond et al., 2003). Rhizobacterium-mediated B availability to plants occurs through the production of organic acids in the rhizosphere region, resulting in medium acidification and pH decrease, the latter being the main limiting factor in B availability (Deubel et al., 2000; Turan et al., 2006). Concomitant B uptake by the plant occurs through the mass flow from transpiration (Alpaslan and Gunes, 2001). Therefore, the increased transpiration rate provided by PGPR inoculation can influence B absorption (Mayak et al., 2004; Dodd and Pérez-Alfocea, 2012). In the present study, plants inoculated

with *B. cereus* had almost twice the accumulated B in the shoots and twice the transpiration rate compared with the control. According to our analysis, this may be due to the enzymatic activity of *B. cereus* on the coconut fiber substrate that contained 70.35 ppm of B. The positive relationship between P and B absorption found in plants inoculated with *Bacillus* sp. has been recorded in canola; *Bacillus* improved B and P availability by 37% and 30%, respectively, in native soil (Samreen et al., 2019). These results are like ours, obtained with *B. cereus* coconut seedlings (**Table 2**). The increasing use of CFs especially with NPK and B is rapidly making them polluting agents. When not absorbed by the plants, they are leached and deposited in watercourses, or immobilized and accumulated in the soil. Implementing microbial technology in coconut seedlings tree production systems improves the physiological performance and NUE of plants, reducing the need for CFs.

In this study, the increases in the root system induced by *B. cereus* provided coconut seedlings with a greater possibility of absorption and translocation of nutrients, contributing to a greater growth in the aerial part (Amir et al., 2005). The increase in the aerial part growth and leaf expansion promoted by *B. cereus* can be attributed to the greater synthesis of gibberellins, according to the results obtained in this study (**Figure 3**). Increased active gibberellin concentration in the leaf tissue was stimulated by the activity of *Azospirillum* spp. because this microorganism promoted a significant synthesis and consequent increase in the concentration of this phytohormone (Lucangeli and Bottini, 1997; Piccoli et al., 1997; Cassán et al., 2001). Similar results were observed in alder (*Alnus glutinosa*) plants, where the use of *Bacillus* sp. enhanced the production of several isomers of gibberellins (GA_1, GA_3, GA_4, and GA_{20}) that were responsible for leaf area expansion and increased leaf emission rate (Gutiérrez-Mañero et al., 2001; Chauhan et al., 2015). Larger leaf areas resulted in a higher biomass accumulation in *B. cereus* inoculated plants.

This leaf modulation promoted by the microorganisms led to increased light capture and, consequently, increased CO_2 assimilation. The increased CO_2 input is due to a larger stomatal opening, verified in the present study, allowing greater CO_2 diffusion, and reducing stomatal resistance (Flexas et al., 2012; Zhang et al., 2017). *B. cereus* regulates most of the Rubisco carboxylation, the electron transport rate, and increases the supply of ATP and NADPH molecules for photosynthesis (Shi et al., 2010), increasing carbon fixation and, consequently, increasing carbohydrate production as observed in the improved growth parameters of *B. cereus* inoculated plants.

DATA AVAILABILITY STATEMENT

The datasets presented in this study can be found in online repositories. The names of the repository/repositories and accession number(s) can be found below: https://www.ncbi.nlm.nih.gov/genbank/, MN393059.

AUTHOR CONTRIBUTIONS

AC was present in all study assays and was responsible for fieldwork, statistical analysis of data, interpretation of results, and writing the manuscript. SC was present in all study assays and was responsible for fieldwork. DS, AM, EA, and PL were responsible for statistical analysis, analysis of economic indicators, and interpretation of results and assisted in writing and revising the manuscript. GS was responsible for project management, guiding the students through all stages of the process and also responsible for the verification and monitoring of field data and writing the manuscript. All authors contributed to the article and approved the submitted version.

ACKNOWLEDGMENTS

We thank reviewers for their valuable comments and suggestions. Discussions with Gledson Luiz Salgado de Castro (Universidade Federal Rural da Amazônia, Brazil) were highly valuable in the development of this work. We thank the Federal University of Amazonia and the Plant Protection Laboratory for providing the facilities. We also thank the Amazon Foundation for the Support of Studies and Research of the State of Pará (FAPESPA) and Sococo S/A for their partnership and support, in particular the team from the phytopathology department.

SUPPLEMENTARY MATERIAL

The Supplementary Material for this article can be found online at: https://www.frontiersin.org/articles/10.3389/fpls.2021.649487/full#supplementary-material

Supplementary Figure 1 | Phylogenetic trees analysis of R40 (UFRABC40). Major Bacillus cereus clades and groups are indicated comparing the selected strain with the reference strains.

Supplementary Table 1 | Identification of access and phylogenetic trees obtained by comparing the selected strain (R40) with the reference strains.

REFERENCES

Ahmad, M., Adil, Z., Hussain, A., Mumtaz, M. Z., Nafees, M., Ahmad, I., et al. (2019). Potential of phosphate solubilizing *Bacillus* strains for improving growth and nutrient uptake in mungbean and maize crops. *Pak. J. Agric. Sci.* 56, 283–289. doi: 10.21162/PAKJAS/19.7285

Alpaslan, M., and Gunes, A. (2001). Interactive effects of boron and salinity stress on the growth, membrane permeability and mineral composition of tomato and cucumber plants. *Plant Soil* 236, 123–128. doi: 10.1023/A:1011931831273

Amir, H. G., Shamsuddin, Z. H., Halimi, M. S., Marziah, M. and Ramlan, M. F. (2005). Enhancement in nutrient accumulation and growth of oil palm seedlings caused by PGPR under field nursery conditions. *Commun. Soil Sci. Plant Anal.* 36, 2059–2066. doi: 10.1080/00103620500194270

Angulo, J., Martínez-Salgado, M. M., Ortega-Blu, R., and Fincheira, P. (2020). Combined effects of chemical fertilization and microbial inoculant on nutrient use efficiency and soil quality indicators. *Sci. Agropecu.* 11, 375–380. doi: 10.17268/sci.agropecu.2020.03.09

Belimov, A. A., Dodd, I. C., Hontzeas, N., Theobald, J. C., Safronova, V. I., and Davies, W. J. (2004). Rhizosphere bacteria containing 1-aminocyclopropane-1-carboxylate deaminase increase yield of plants grown in drying soil via both local and systemic hormone signalling. *New Phytol.* 181, 413–423. doi: 10.1111/j.1469-8137.2008.02657.x

Bhardwaj, D., Ansari, M. W., Sahoo, R. K., and Tuteja, N. (2014). Biofertilizers function as key player in sustainable agriculture by improving soil fertility plant tolerance and crop productivity. *Microb. Cell Fact.* 13:66. doi: 10.1186/1475-2859-13-66

Biswas, J. C., Ladha, J. K., and Dazzo, F. B. (2000). Rhizobia inoculation improves nutrient uptake and growth of lowland rice. *Soil Sci. Soc. Am. J.* 64, 1644–1650. doi: 10.2136/sssaj2000.6451644x

Blanco-Canqui, H., and Schlegel, A. J. (2013). Implications of inorganic fertilizer application of irrigated corn on soil properties: lessons learned after 50 years. *J. Environ. Qual.* 42, 861–871. doi: 10.2134/jeq2012.0451

Carmo, C. D. S., de Araujo, W. S., Bernardi, A. D. C., and Saldanha, M. F. C. (2000). *Métodos de Análise de Tecidos Vegetais Utilizados na Embrapa Solos*. Rio de Janeiro: Embrapa Solos-Circular Técnica (INFOTECA-E).

Cassán, F., Bottini, R., Schneider, G., and Piccoli, P. (2001). *Azospirillum brasilense* and *Azospirillum lipoferum* hydrolyze conjugates of GA20 and metabolize the resultant aglycones to GA1 in seedlings of rice dwarf mutants. *Plant Physiol.* 125, 2053–2058. doi: 10.1104/pp.125.4.2053

Cassán, F., Coniglio, A., López, G., Molina, R., Nievas, S., Carlan, C. L., et al. (2020). Everything you must know about *Azospirillum* and its impact on agriculture ans beyond. *Biol. Fertil. Soils* 56, 461–479. doi: 10.1007/s00374-020-01463-y

Chauhan, H., Bagyaraj, D. J., Selvakumar, G., and Sundaram, S. P. (2015). Novel plant growth promoting rhizobacteria—prospects and potential. *Appl. Soil Ecol.* 95, 38–53. doi: 10.1016/j.apsoil.2015.05.011

Conijn, J. G., Bindraban, P. S., Schröder, J. J., and Jongschaap, R. (2018). Can our food system meet food demand within planetary boundaries? *Agric. Ecosyst. Environ.* 251, 244–256. doi: 10.1016/j.agee.2017.06.001

Costa, R. R. G. F., Quirino, G. S. F., Naves, D. C. F., Santos, C. B., and Rocha, A. F. S. (2015). Efficiency of inoculant with *Azospirillum brasilense* on the growth and yield of second-harvest maize. *Pesqui. Agropecu. Trop.* 45, 304–311. doi: 10.1590/1983-40632015v4534593

de Castro, G. L. S., Rêgo, M. C. F., Silvestre, W. V. D., Batista, T. F. V., and da Silva, G. B. (2020). Açaí palm seedling growth promotion by rhizobacteria inoculation. *Braz. J. Microbiol.* 51, 205–216. doi: 10.1007/s42770-019-00159-2

Deubel, A., Gransee, A., and Merbach, W. (2000). Transformation of organic rhizodeposits by rhizoplane bacteria and its influence on the availability of tertiary calcium phosphate. *J. Plant Nutr. Soil Sci.* 163, 387–392. doi: 10.1002/1522-2624(200008)163

Di Benedetto, N. A., Campaniello, D., and Bevilacqua, A. (2016). "Characterization of autochthonous plant growth promoting bacteria in relation to durum wheat nitrogen use efficiency," in *Proceedings of the Plant Biology Europe Congress EPSO/FESPB*, (Prague Czech Republic), 26–30. doi: 10.3934/microbiol.2017.3.413

Dodd, I. C., and Pérez-Alfocea, F. (2012). Microbial amelioration of crop salinity stress. *J. Exp. Bot.* 63, 3415–3428. doi: 10.1093/jxb/ers033

Fageria, N. K., Baligar, V. C., and Li, Y. C. (2008). The role of nutrient efficient plants in improving crop yields in the twenty first century. *J. Plant Nutr.* 31, 1121–1157.

FAO (2018). *Food and Agriculture Data*. Available online at: http://www.fao.org/faostat/es/#rankings/countries_by_commodity_exports (accessed September 16, 2019).

Filippi, M. C. C., Da Silva, G. B., Silva-Lobo, V. L., Côrtes, M. V. C., Moraes, A. J. G., and Prabhu, A. S. (2011). Leaf blast (*Magnaporthe oryzae*) suppression and growth promotion by rhizobacteria on aerobic rice in Brazil. *Biol. Control* 58, 160–166. doi: 10.1016/j.biocontrol.2011.04.016

Flexas, J., Flexas, J., Barbour, M. M., Brendel, O., Cabrera, H. M., Carriquí, M., et al. (2012). Mesophyll diffusion conductance to CO2: an unappreciated central player in photosynthesis. *Plant Sci.* 19, 70–84. doi: 10.1016/j.plantsci.2012.05.009

Fukushima, T., Allred, B. E., Sia, A. K., Nichiporuk, R., Andersen, U. N., and Raymond, K. N. (2013). Gram positive siderophore-shuttle with iron-exchange from Fe-siderophore to apo-siderophore by *Bacillus cereus* YxeB. *Proc. Natl. Acad. Sci. U.S.A.* 110, 13821–13826. doi: 10.1073/pnas.1304235110

Gamez, R., Cardinale, M., Montes, M., Ramirez, S., Schnell, S., and Rodriguez, F. (2018). Screening, plant growth promotion and root colonization pattern of two rhizobacteria (*Pseudomonas fluorescens* Ps006 and *Bacillus amyloliquefaciens* Bs006) on banana cv. Williams (*Musa acuminata* Colla). *Microbiol. Res.* 220, 12–20. doi: 10.1016/j.micres.2018.11.006

Gange, A. C., and Gadhave, K. R. (2018). Plant growth-promoting rhizobacteria promote plant size inequality. *Sci. Rep.* 8:13828. doi: 10.1038/s41598-018312111-z

George, P., Gupta, A., Gopal, M., Thomas, L., and Thomas, G. V. (2018). Systematic screening strategies for identifying elite plant growth promoting rhizobacteria for coconut (*Cocos nucifera* L.). *Int. J. Curr. Microbiol. App. Sci.* 7, 1051–1074. doi: 10.20546/ijcmas.2018.705.130

Glick, B. R. (2012). Plant growth-promoting bacteria: mechanisms and applications. *Scientifica* 2012:963401. doi: 10.6064/2012/963401

Glick, B. R., Patten, C. L., Holguin, G., and Penrose, D. M. (1999). *Biochemical and Genetic Mechanisms Used by Plant Growth Promoting Bacteria*. London: Imperial College Press.

Good, A. G., and Beatty, P. H. (2011). Fertilizing nature: a tragedy of excess in the commons. *PLoS Biol.* 9:e1001124. doi: 10.1371/journal.pbio.1001124

Gordon, S. A., and Weber, R. P. (1951). Colorimetric estimation of indoleacetic acid. *Plant Physiol.* 26, 192–195. doi: 10.1104/pp.26.1.192

Gutiérrez-Mañero, F. J., Ramos-Solano, B., Probanza, A. N., Mehouachi, J. R., Tadeo, F., and Talon, M. (2001). The plant-growth-promoting rhizobacteria *Bacillus pumilus* and *Bacillus licheniformis* produce high amounts of physiologically active gibberellins. *Physiol. Plant.* 111, 206–211. doi: 10.1034/j.1399-3054.2001.1110211.x

Gyaneshwa, P., Kumar, G. N., Parekh, L., and Poole, P. S. (2002). Role of soil microorganisms in improving P nutrition of plants. *Plant Soil* 245, 83–93. doi: 10.1023/A:1020663916259

Hider, R. C., and Kong, X. (2010). Chemistry and biology of siderophores. *Nat. Prod. Rep.* 27, 637–657. doi: 10.1039/b906679a

IBGE (2019). *Indicadores*. Available online at: https://www.ibge.gov.br/estatisticas-novoportal/economicas/agricultura-e pecuaria/92 01-levantamento-sistematico-da-producao-agricola.html?&t=resultado (accessed July 10, 2019).

Kado, C. I., and Heskett, M. G. (1970). Selective media for isolation of Agrobacterium, Corynebacterium, Erwinia, *Pseudomonas* and Xanthomonas. *Phytopathology* 60, 969–979.

Kaur, G., and Reddy, M. S. (2013). Phosphate solubilizing rhizobacteria from an organic farm and their influence on the growth and yield of maize (*Zea mays* L.). *J. Gen. Appl. Microbiol.* 59, 295–303. doi: 10.2323/jgam.59.295

Lamari, L. (2002). *Assess 2.0: Image Analysis Software For Plant Disease Quantification*. Minnesota, MN: St. Paul:APS Press.

Lane, D. J. B., Pace, G. J., Olsen, D. A., Stahl, M. L., Sogin, N., and Pace, R. (1985). Rapid determination of 16S ribosomal RNA sequences for phylogenetic analyses. *Proc. Natl. Acad. Sci. U.S.A.* 82, 6955–6959. doi: 10.1073/pnas.82.20.6955

Lima, J. V., Tinôco, R. S., Olivares, F. L., de Moraes, A. J. G., Chia, G. S., and da Silva, G. B. (2020). Hormonal imbalance triggered by rhizobacteria enhance nutrient use efficiency and biomass in oil palm. *Sci. Hortic.* 264:109161. doi: 10.1016/j.scienta.2019.109161

Lins, P., and Viégas, I. (2008). *Adubação do Coqueiro no Pará*. Belém: Embrapa Amazônia Oriental-Documentos (INFOTECA-E).

Lucangeli, C., and Bottini, R. (1997). Effects of Azospirillum spp on endogenous gibberellin content and growth of maize (*Zea mays* L.) treated with uniconazole. *Symbiosis* 23, 63–72.

Lucy, M., Reed, E., and Glick, B. R. (2004). Applications of free living plant growth promoting rhizobacteria. *Antonie van Leeuwenhoek* 86, 1–25. doi: 10.1023/B:ANTO.0000024903.10757.6e

Lwin, K. M., Myint, M. M., Tar, T., and Aung, W. Z. M. (2012). Isolation of plant hormone (indole-3-acetic acid-IAA) producing rhizobacteria and study on their effects on maize seedling. *Eng. J.* 16, 137–144. doi: 10.4186/ej.2012.16.5.137

Malavolta, E., Vitti, G. C., and Oliveira, S. A. D. (1997). *Avaliação do Estado Nutricional Das Plantas: Princípios e Aplicações*. Piracicaba: Potafos.

Mariano, R. D. L. R., and Silveira, E. D. (2005). *Manual de Práticas em Fitobacteriologia*. Recife: Universidade Federal Rural de Pernambuco.

Mayak, S., Tirosh, T., and Glick, B. R. (2004). Plant growth-promoting bacteria confer resistance in tomato plants to salt stress. *Plant Physiol. Biochem.* 42, 565–572. doi: 10.1016/j.plaphy.2004.05.009

Mogollon, J. M., Beusen, A. H. W., Van Grinsven, H. J. M., Westhoek, H., and Bouwman, A. F. (2018). Future agricultural phosphorus demand according to the shared socioeconomic pathways. *Glob. Environ. Chang.* 50, 149–163. doi: 10.1016/j.gloenvcha.2018.03.007

Moura, J. Z., Prado, R. M., Benvindo, R. N., and Chaves, A. L. (2013). Applying boron to coconut palm plants: effects on the soil, on the plant nutritional status and on productivity boron to coconut palm trees. *J. Soil Sci. Plant Nutr.* 13, 79–85. doi: 10.4067/S0718-95162013005000008

Moustaine, M., Elkahkahi, R., Benbouazza, A., Benkirane, R., and Achbani, E. H. (2017). Effect of plant growth promoting rhizobacterial (PGPR) inoculation on growth in tomato (*Solanum lycopersicum* L.) and characterization for direct PGP abilities in Morocco. *Int. J. Environ. Agric. Biotech.* 2, 590–595. doi: 10.22161/ijeab/2.2.5

Munné-Bosch, S., Oñate, M., Oliveira, P. G., and Garcia, Q. S. (2011). Changes in phytohormones and oxidative stress markers in buried seeds of Vellozia alata. *Flora Morphol. Distrib. Funct. Ecol. Plants* 206, 704–711. doi: 10.1016/j.flora.2010.11.012

Naher, U. A., Panhwar, Q. A., Othman, R., Shamshuddin, J., Ismail, M. R., and Zhou, E. (2018). Proteomic study on growth promotion of PGPR inoculated aerobic rice (*Oryza sativa* L.) cultivar MR219-9. *Pak. J. Bot.* 50, 1843–1852.

Nannipieri, P., Giagnoni, L., Landi, L., and Renella, G. (2011). "Role of phosphatase enzymes in soil," in *Phosphorus in Action: Biological Processes in Soil Phosphorus Cycling, Soil Biology*, Vol. 26, eds E. Bunemann, A. Oberson, and E. Frossard (Heidelberg: Springer), 215–243.

Nautiyal, C. S. (1999). An efficient microbiological growth medium for screening phosphate solubilizing microorganisms. *FEMS Microbiol. Lett.* 170, 265–270. doi: 10.1111/j.1574-6968.1999.tb13383.x

Negrete-Raymond, A. C., Weder, B., and Wackett, L. P. (2003). Catabolism of arylboronic acids by *Arthrobacter nicotinovorans* strain PBA. *Appl. Environ. Microbiol.* 69, 4263–4267. doi: 10.1128/AEM.69.7.4263-4267.2003

Nguyen, M. L., Spaepen, S., du Jardin, P., and Delaplace, P. (2019). Biostimulant effects of rhizobacteria on wheat growth and nutrient uptake depend on nitrogen application and plant development. *Arch. Agron. Soil Sci.* 65, 58–73. doi: 10.1080/03650340.2018.1485074

Nylander, J. A. A. (2004). *MrModeltest v2. Program Distributed by the Author*. Uppsala University: Evolutionary Biology Centre, 575.

Pahari, A., and Mishra, B. B. (2017). Characterization of Siderophore producing rhizobacteria and its effect on growth performance of different vegetables. *Int. J. Curr. Microbiol. Appl. Sci.* 6, 1398–1405. doi: 10.20546/ijcmas.2017.605.152

Paungfoo-Lonhienne, C., Redding, M., Pratt, C., and Wang, W. (2019). Plant growth promoting rhizobacteria increase the efficiency of fertilisers while reducing nitrogen loss. *J. Environ. Manage.* 233, 337–341. doi: 10.1016/j.jenvman.2018.12.052

Piccoli, P., Lucangeli, D., Schneider, G., and Bottini, R. (1997). Hydrolysis of [1717-2H2] gibberellin A20-glucoside and [1717-2H2] gibberellin A20-glucosyl ester by *Azospirillum lipoferum* cultured in a nitrogen-free biotin-based chemically-defined medium. *Plant Growth Regul.* 23, 179–182. doi: 10.1073/pnas.89.17.8045

R Core Team (2017). *R: A Language and Environment for Statistical Computing*. Vienna: R Foundation for Statistical Computing.

Rabelo, T. K., Melo, M. D. V., Loiola, C. M., and Aragão, W. M. (2006). *Germinação de Sementes de Cultivares de Coqueiros. Comunicado Técnico*. Aracaju: Embrapa Tabuleiros Costeiros.

Ronquist, F., Teslenko, M., van de Mark, P., Ayres, D. L., Darling, A., Höhna, S., et al. (2012). MrBayes 3.2: efficient bayesian phylogenetic inference and model choice across a large model space. *Syst. Biol.* 61, 539–542.

Samaniego-Gámez, B. Y., Garruña, R., Tun-Suárez, J. M., Kantun-Can, J., Reyes Ramírez, A., and Cervantes-Díaz, L. (2016). *Bacillus* spp. inoculation improves photosystem II efficiency and enhances photosynthesis in pepper plants. *Chil. J. Agric. Res.* 76, 409–416. doi: 10.4067/S07185839201600040003

Samreen, T., Zahir, Z. A., Naveed, M., and Asghar, M. (2019). Boron tolerant phosphorus solubilizing *Bacillus* spp. MN-54 improved canola growth in alkaline calcareous soils. *Int. J. Agric. Biol.* 21, 538–546. doi: 10.17957/IJAB/15.0926

Savci, S. (2012). Investigation of effect of chemical fertilizers on environment. *Apcbee Procedia* 1, 287–292. doi: 10.1016/j.apcbee.2012.03.047

Schwyn, B., and Neilands, J. B. (1987). Universal chemical assay for the detection and determination of siderophores. *Anal. Biochem.* 160, 47–56. doi: 10.1016/0003-2697(87)90612-9

Sheng, X. F., and He, L. Y. (2006). Solubilization of potassium-bearing minerals by a wild-type strain of *Bacillus* edaphicus and its mutants and increased potassium uptake by wheat. *Can. J. Microbiol.* 52, 66–72. doi: 10.1139/w05-117

Shi, Y., Lou, K., and Li, C. (2010). Growth and photosynthetic efficiency promotion of sugar beet (*Beta vulgaris* L.) by endophytic bacteria. *Photosynth. Res.* 105, 5–13. doi: 10.1007/s11120-010-9547-7

Siddikee, M. A., Glick, B. R., Chauhan, P. S., and Yim, W. S. T. (2011). Enhancement of growth and salt tolerance of red pepper seedlings (*Capsicum annuum* L.) by regulating stress ethylene synthesis with halotolerant bacteria containing 1-aminocyclopropane-1carboxylic acid deaminase activity. *Plant Physiol. Biochem.* 49, 427–434. doi: 10.1016/j.plaphy.2011.01.015

Sindcoco (2017). *Boletim Conjuntural - Importações de Coco Ralado e de Água de Coco. Novembro de 2017; Novembro de 2018*. Available online at: http://www.sindcoco.com.br (accessed Dec 11, 2018).

Staden, R., Beal, K. F., and Bonfield, J. K. (1998). The staden package. *Methods Mol. Biol.* 132, 115–130.

Tabatabai, M. A. (1994). "Soil enzymes," in *Methods of Soil Analysis:Part 2. Microbial and Biochemical Properties, SSSA Book Series 5*, ed. R. W. Weaver (Madison, WI: Soil Science Society of America).

Tilman, D. (1998). The greening of the green revolution. *Nature* 396, 211–212.

Turan, M., Ataoglu, N., and Sahin, F. (2006). Evaluation of the capacity of phosphate solubilizing bacteria and fungi on different forms of phosphorus in liquid culture. *J. Sustain. Agric.* 28, 99–108. doi: 10.1300/J064v28n03_08

Vinodhini, C. C., and Deshmukh, K. V. (2017). An economic analysis of coconut farming in Karur district of Tamil Nadu India. *Int. J. Curr. Microbiol. App. Sci.* 6, 1566–1573. doi: 10.20546/ijcmas.2017.612.176

Wang, Z. H., and Li, S. X. (2019). Chapter three–nitrate N loss by leaching and surface runoff in agricultural land: a global issue. *Adv. Agron.* 156, 159–217.

Yu, S., Teng, C., Bai, X., Liang, J., Song, T., Dong, L., et al. (2017). Optimization of siderophore production by *Bacillus* sp. PZ-1 and its potential enhancement of phytoextration of Pb from soil. *J. Microbiol. Biotechnol.* 27, 1500–1512. doi: 10.4014/jmb.1705.05021

Zhang, K., Liu, Z., and Shan, X. (2017). Physiological properties and chlorophyll biosynthesis in a Pak-choi (*Brassica rapa* L. ssp. chinensis) yellow leaf mutant, pylm. *Acta Physiol. Plant* 39:22. doi: 10.1007/s11738-016-2321-5

Conflict of Interest: The authors declare that the research was conducted in the absence of any commercial or financial relationships that could be construed as a potential conflict of interest.

Publisher's Note: All claims expressed in this article are solely those of the authors and do not necessarily represent those of their affiliated organizations, or those of the publisher, the editors and the reviewers. Any product that may be evaluated in this article, or claim that may be made by its manufacturer, is not guaranteed or endorsed by the publisher.

Advantages of publishing in Frontiers

OPEN ACCESS
Articles are free to read for greatest visibility and readership

FAST PUBLICATION
Around 90 days from submission to decision

HIGH QUALITY PEER-REVIEW
Rigorous, collaborative, and constructive peer-review

TRANSPARENT PEER-REVIEW
Editors and reviewers acknowledged by name on published articles

Frontiers
Avenue du Tribunal-Fédéral 34
1005 Lausanne | Switzerland

Visit us: www.frontiersin.org
Contact us: frontiersin.org/about/contact

REPRODUCIBILITY OF RESEARCH
Support open data and methods to enhance research reproducibility

DIGITAL PUBLISHING
Articles designed for optimal readership across devices

FOLLOW US
@frontiersin

IMPACT METRICS
Advanced article metrics track visibility across digital media

EXTENSIVE PROMOTION
Marketing and promotion of impactful research

LOOP RESEARCH NETWORK
Our network increases your article's readership